

UNIVERSITÉ DU QUÉBEC À MONTRÉAL

STRATÉGIE PAR COUCHE DIFFÉRENTIELLE POUR LA SYNTHÈSE DE
DENDRIMERS

THÈSE
PRÉSENTÉE
COMME EXIGENCE PARTIELLE
DU DOCTORAT EN CHIMIE

PAR
RISHI SHARMA

JUIN 2015

UNIVERSITÉ DU QUÉBEC À MONTRÉAL
Service des bibliothèques

Avertissement

La diffusion de cette thèse se fait dans le respect des droits de son auteur, qui a signé le formulaire *Autorisation de reproduire et de diffuser un travail de recherche de cycles supérieurs* (SDU-522 – Rév.01-2006). Cette autorisation stipule que «conformément à l'article 11 du Règlement no 8 des études de cycles supérieurs, [l'auteur] concède à l'Université du Québec à Montréal une licence non exclusive d'utilisation et de publication de la totalité ou d'une partie importante de [son] travail de recherche pour des fins pédagogiques et non commerciales. Plus précisément, [l'auteur] autorise l'Université du Québec à Montréal à reproduire, diffuser, prêter, distribuer ou vendre des copies de [son] travail de recherche à des fins non commerciales sur quelque support que ce soit, y compris l'Internet. Cette licence et cette autorisation n'entraînent pas une renonciation de [la] part [de l'auteur] à [ses] droits moraux ni à [ses] droits de propriété intellectuelle. Sauf entente contraire, [l'auteur] conserve la liberté de diffuser et de commercialiser ou non ce travail dont [il] possède un exemplaire.»

THIS THESIS IS DEDICATED TO MY PARENTS, MANJU SHARMA AND DR. ASHOK
KUMAR SHARMA; MY WIFE, DR. ANJALI SHARMA; AND MY DAUGHTER
MANYA SHARMA

ACKNOWLEDGEMENTS

When you want something, the entire universe conspires in helping you to achieve it.
Paulo Coelho

Time flies, it seems like yesterday when I entered the premises of chemistry department UQAM. It's hard to believe that such a beautiful journey is coming to an end. I would like to begin by thanking my adviser, Professor René Roy, for providing me an opportunity to work in his group and allowing me to join the great legacy of students and work that have emerged from it. I am indebted to him for the encouragement and the freedom of thought I enjoyed throughout. He has given my career in science a purpose and a meaningful direction. I could not have imagined having a better advisor and mentor for my PhD study.

I am deeply indebted to Dr. Ashok Kakkar from McGill University without whose motivation and encouragement I would not have considered a graduate career in chemistry.

As I look back at this journey from my vantage point that is now, I realize a large part of what I was able to accomplish during this period is due to interaction that I had with some truly remarkable people at UQAM. Among the foremost, is Dr. Rabindra Rej who never loses his patience and always provided his kind ears to my never ending problems. I thank him for the long and fruitful discussions on the problems I was facing during projects and finding their solutions. Big thanks to Dr. Yoann M. Chabre for his continuous support, ideas and consultations on the project. He helped me to initiate my project and shared his valuable secrets of dendrimer synthesis with me. I am especially grateful to Dr. Naresh Kottari for his huge contribution for analysing dendrimers protein interactions with SPR. Tze Chieh Shiao and Dr. Rahul Bagul is highly thanked for their kind support and help in thesis submission. Thanks a lot to all my group members Leila, Chichi, Elham, David, and Melissa for providing such a nice and fun filled environment around.

I sincerely thank Dr. Jerome Claverie and Dr. Steve Bourgault for being part of my thesis committee. They were always very kind to me and have always provided great suggestions regarding the project. I would like to express my deepest appreciation to Dr. Dusica Maysinger and Issan Zhang from Department of Pharmacology and Therapeutics, McGill University for carrying out biological studies of the dendrimers. My special thanks to Dr. Sylvain Canesi for his continuous encouragement. I would like to appreciate his marvelous group, especially Marc-André who was my first neighbour in the lab for 3 years.

My sincere thanks to Dr. Alexandre Arnold and Mr. Vladimir A. Kryuchkov for providing great support for instruments like NMR, DLS and GPC. I am also indebted to Dr. Van Huu Tra for his continuous support and encouragement. My special thanks to Madam Sonia Lachance from administrative department for providing solution of every administrative problem I faced during this period. I would like to thank Mr. Nadim K. Saadeh from McGill university mass spectrometry lab, without his help it would have been a very difficult task.

I wish to thank my wife, Dr. Anjali Sharma, who has stood by me through all my absences, agony and impatience. She helped me with my coursework, proofreading manuscripts and presentations. I am not sure how she maintained such calmness listening all those practice sessions of my presentations. Without her contribution this could have been an impossible task. Thanks to my daughter Manya Sharma (the most cherished result of my PhD) who tried her best distracting me when I was busy writing publications and thesis. I am very sorry for not giving her much attention whenever she wanted to play with me. I would like to express gratitude to my sister Ritu Sharma and my brother in law Dr. Rahul Tugnait for always encouraging me to go for higher studies and pursue my dreams.

A big cheers to my father (Dr. Ashok Sharma) who was always behind me for doing Ph.D. Last but not least, my mother Manju Sharma whose immense sacrifice and contribution cannot be described in words.

TABLE OF CONTENTS

Dedication.....	ii
Acknowledgements.....	iii
Table of Contents.....	v
List of Figures.....	vii
List of Schemes	x
List of Tables.....	xiii
Abstract	xiv
Résumé.....	xvi
List of Abbreviations	xix
Contribution of Authors	xxi
Rights and Permissions	xxiv
CHAPTER 1	1
Introduction and scope of the thesis	1
1.1 Introduction to dendrimers:	1
1.2 Myths and facts about dendrimers:	4
1.3 Applications:.....	5
1.4 Strategies for dendrimer synthesis	13
1.5 Conclusions:.....	48
1.6 Scope of the thesis.....	48
1.7 References:	50
CHAPTER 2	55
“Onion peel” dendrimers: a straightforward synthetic approach towards highly diversified architectures	55
2.1 Introduction:.....	57
2.2 Results and discussion:.....	61
2.2.1 Synthesis	61
2.2.2 Surface plasmon resonance studies	69

2.3 Conclusions:.....	75
2.4 References:	76
CHAPTER 3	81
Highly versatile convergent/divergent “onion peel” strategy toward potent multivalent glycodendrimers	81
3.1 Introduction:.....	83
3.2 Results and discussion:	84
3.3 Conclusions:.....	90
3.4 References:	91
CHAPTER 4	95
A fast track strategy toward highly functionalized dendrimers with different structural layers: “Onion peel approach”	95
4.1 Introduction:.....	97
4.2 Results and Discussion:	99
4.3 Conclusions:.....	112
4.4 References:	113
CHAPTER 5	116
Conclusions and suggestions for future work	116
5.1 Conclusions.....	116
5.2 Suggestions for future work.....	118
APPENDIX A	121
Supporting Information-Chapter 2: “Onion-peel” dendrimers: a straightforward synthetic approach towards highly diversified architectures	121
APPENDIX B.....	192
Supporting information-Chapter 3: Highly versatile convergent/divergent “onion peel” strategy toward potent multivalent glycodendrimers	192
APPENDIX C	253
Supporting information-Chapter 4: A fast track strategy toward highly functionalized dendrimers with different structural layers: “Onion peel approach”	253

LIST OF FIGURES

Figure 1-1 Anatomy of dendrimer.	3
Figure 1-2 Structural representation of SPL 7013, the active component of VivaGel.	4
Figure 1-3 Chemical structures of the most common commercially available dendrimers.	6
Figure 1-4 Representation of applications of dendrimers.	7
Figure 1-5 Structure of dendrimer-Camptothecin conjugate.	8
Figure 1-6 A) The structure of amphiphilic dendrimer and B) schematic illustration of self-assembly of dendrimer upon interaction with siRNA.	9
Figure 1-7 Schematic illustration of gadolinium-loaded dendrimer entrapped gold nanoparticles.	10
Figure 1-8 Dendrimer nanoreactor for catalysis of Cu(I) catalyzed click reaction. ...	12
Figure 1-9 Divergent and convergent methods for dendrimer synthesis.	13
Figure 1-10 Proposed mechanism for CuAAC click reaction.	26
Figure 1-11 Mechanism of radical mediated thiol-ene click reaction.	31
Figure 1-12 Mechanism of radical mediated thiol-yne click reaction.	36
Figure 2-1 Molecular structures of targeted glycodendrimers 1-5.	60
Figure 2-2 Comparison of ^1H NMR spectra (CDCl_3 , 300 MHz) of 6, 15 and 17 with the appearance/disappearance of characteristic signals towards the construction of dodecapropargylated scaffold 17 (observed proton integrations are indicated in italic below each signal.	65
Figure 2-3 Direct comparison of ^1H NMR spectra (in CDCl_3 for top and bottom spectra and in D_2O for middle spectrum, 300 MHz) of 24, 25 and 26 with the appearance/disappearance of characteristic signals towards the construction of tetracosavalent scaffold 26 (observed proton integrations are indicated in italic below each signal and stars in middle spectrum indicates the absence of propargylic signals).	67

- Figure 2-4 Specific region of negative HR-ESI observed (top) and theoretical (bottom) isotopic distributions for 28 exhibiting 12 carboxylic acid functions ($[M-2H]^{2-}$ signal). 68
- Figure 2-5 SPR sensorgrams for the interactions of glycodendrimer 4 (0.306 μ M to 20 μ M) with the surface bound ECA lectin. The binding data are overlaid with the fit (in red) of a 1:1 Langmuir interaction model. 70
- Figure 2-6 Superimposition of glycoclusters 1 (black, 12 sugars) and 4 (black + green + red, 24 sugars) to illustrate their similar composition but different epitopes' density. 72
- Figure 2-7 (a) Sensorgrams obtained by injection of ECA (5 μ M) incubated with different concentrations of glycodendrimer 5 varying from 0.008 μ M (top curve) to 62 μ M (bottom curve) on the surface of immobilized galactoside 31. (b) The inhibitory curve for the glycodendrimer 5. IC_{50} value was extracted from the sigmoidal fit of the inhibition curve. 74
- Figure 4-1 Schematic illustration of accelerated divergent dendrimer synthesis from octadecavalent hypercore 1 *via* onion peel approach using CuAAC and thiol-ene click reactions with AB_3 , AB_5 , and AB_7 monomers giving rise to G(3)-dendrimers containing 108, 180, and 252 end groups respectively. 99
- Figure 4-2 Molecular structures of dendrimers with 108, 180, and 252 end groups at third generation. 105
- Figure 4-3 1H NMR spectrum of 9 (G3-252) (Top) After 5 hours in microwave 50 $^{\circ}C$ indicating 80% conversion, (Bottom) After 7 hours in microwave at 50 $^{\circ}C$ indicating 100% conversion. 108
- Figure 4-4 GPC traces of the dendrimers: (2)G2-54, (4)G2-90, (6)G2-90, and (8)G2-126. 109
- Figure 4-5 Low cytotoxicity of dendrimers in human cells. Dendrimers 3 (G3-108), 5 (G3-180) and 9 (G3-252) were tested in: (A) HepG2 liver carcinoma, (B) U251N glioblastoma and (C) MCF-7 breast adenocarcinoma cells. Increasing concentrations of dendrimers (1 nM – 10 μ M) were incubated with the cells for 24h. Mitochondrial metabolic activity was assessed using the MTT assay. Values are presented as mean percentages \pm S.D relative to untreated controls (set as 100%). The data is reported for six measurements for each concentration. Three independent experiments performed *($p < 0.01$). 111
- Figure 4-6 Concentration-dependent effect of dendrimers on human cell viability. Fluorescence micrograph (A) U251N glioblastoma treated with dendrimers 3, 5,

and **9** (10 μ M, 24h) and labelled with Hoechst 33342 (10 μ M, 10 mins) (scale = 50 μ m). The cytotoxicity of dendrimers **3** (G3-108), **5** (G3-180) and **9** (G3-252) was tested in (B) U251N glioblastoma, (C) HepG2 liver carcinoma, and (D) MCF-7 breast adenocarcinoma cells. Dendrimers in increasing concentrations (up to 10 μ M) were incubated with the cells for 24h. Cell viability was assessed by high-throughput imaging (Operetta, Perkin Elmer) of Hoechst 33342 labelled cells. Values are presented as means \pm S.D relative to untreated controls (set as 100%). The data is reported for three independent experiments performed in six replicates. *($p < 0.01$)..... 112

Figure 5-1 Schematic representation of construction of trifunctional dendrimer combining "onion peel" approach and Passerini reaction 119

LIST OF SCHEMES

Scheme 1-1 Synthesis of cascade molecules by Vögle.	1
Scheme 1-2 Synthesis of Poly-Lysine dendrimer by Denkewalter and co-workers in 1981.....	2
Scheme 1-3 Divergent synthesis of PAMAM dendrimers with ammonia as a core. .	14
Scheme 1-4 Synthesis of poly benzyl ether dendrimers by convergent method.	16
Scheme 1-5 Schematic representation of synthesis of G7 layer block dendrimer using double stage convergent method.....	18
Scheme 1-6 Schematic representation of synthesis of poly benzyl ether dendrimer by hypermonomer method.....	19
Scheme 1-7 Construction of G4 polyphenylacetylene dendrimer by double exponential method.	20
Scheme 1-8 Construction of dendrimers by double-exponential method.....	21
Scheme 1-9 Synthesis of G4 dendrimer using double-exponential method.	22
Scheme 1-10 Synthesis of G4 dendrimer using orthogonal accelerated approach.....	23
Scheme 1-11 Orthogonal accelerated synthesis of generation 4 dendron using Mitsunobu and Sonogoshira reactions.	24
Scheme 1-12 Convergent synthesis of triazole dendrimers by copper(I) catalyzed alkyne-azide click reaction.	27
Scheme 1-13 Synthesis of generation 6 dendrimer <i>via</i> thiol-ene and CuAAC click reactions.....	28
Scheme 1-14 Synthesis of dendrimers using SPAAC strategy.	29
Scheme 1-15 Microwave assisted synthesis of polyphenol dendrimers using copper granules.....	30
Scheme 1-16 Synthesis of generation 4 dendrimer <i>via</i> thiol-ene click and esterification reaction.	33
Scheme 1-17 Synthesis of G2 glycodendrimer with 24 galactose units at the periphery.....	34

Scheme 1-18 Synthesis of fifth generation dendrimer via thiol-Michael addition click reaction.	36
Scheme 1-19 Synthesis of G3- Hydroxyl dendrimer with 192 end groups.	38
Scheme 1-20 Synthesis of G5 dendrimer using thiol-yne and aza Michael addition reaction.	39
Scheme 1-21 Synthesis of G1 to G9 dendrimers.	41
Scheme 1-22 Synthesis and functionalization of G1-G3 thermosensitive dendrimers.	43
Scheme 1-23 Synthesis of monomers by Passerini 3CR and Ugi 4CR.	44
Scheme 1-24 Convergent synthesis of surface block dendrimer using Passerini reaction.	45
Scheme 1-25 Divergent synthesis of 2nd generation dendrimer by the combination of thiol-yne and Passerini reaction.	46
Scheme 1-26 Synthesis of A ³ -Click G2 dendrimer.	47
Scheme 2-1 Sequential construction of sugar decorated “onion peel” dendritic structures via an accelerated divergent strategy.	59
Scheme 2-2 Synthesis of glycocluster 1 through TEC-Amidation-CuAAc (4×1×3) sequence.	62
Scheme 2-3 a) Accelerated divergent strategies for the syntheses of glycoclusters 2-5 harboring surface LacNAc residues; b) Structures of monomer used as references for SPR studies (see SI for the synthesis of 30).	64
Scheme 3-1 Divergent and convergent synthesis of octadecavalent galactodendrimer 8	85
Scheme 3-2 a) Syntheses of monomeric azido precursors 16-17 , b) reference compounds 18-19 and c) lactoside derivative immobilized on the chip for SPR studies.	87
Scheme 3-3 Synthesis of glycodendrimers 23 and 25	88

Scheme 4-1 A. Synthesis of aliphatic AB ₃ (13) and AB ₅ building blocks (16). B. Synthesis of AB ₅ aromatic building block 26 . C. Synthesis of AB ₇ sugar-based building block 31	101
Scheme 4-2 Synthesis of hyperbranched dendrimers through a highly divergent accelerated approach.	104

LIST OF TABLES

Table 2-1 Structural elements used to build polypropargylated scaffolds via an accelerated and orthogonal divergent strategy.....	63
Table 2-2 Mass Spectrometry results obtained from MALDI-TOF, ESI, and APCI Techniques for hyperbranched derivatives.....	68
Table 2-3 Kinetic parameters obtained for the interactions of glycodendrimers with the bound ECA. Data were fitted by using a 1:1 Langmuir model available in BIAevaluation software.....	71
Table 2-4 IC ₅₀ values of the glycodendrimers 1-5 and monomers 18 and 30 derived from competitive inhibition SPR studies.....	73
Table 3-1 IC ₅₀ values of glycodendrimers and their monomeric analogs derived from competitive inhibition SPR studies.....	89
Table 4-1 Summary of characterization of dendrimers.....	110

ABSTRACT

Dendrimers are well-defined, hyperbranched, monodisperse, three dimensional macromolecules which have attracted the focus of the scientific community for more than three decades now. Due to their unique architectural design and morphological properties, dendrimers have been extensively used in areas such as nanomedicine, catalysis, tissue engineering, diagnostics and electronics. In spite of the large number of reports on dendrimer synthesis, only a few have reached commercial availability. This limitation is due to the challenges associated with their complex multistep syntheses and the high cost involved. There is a need to expand the way dendrimers have been synthesized using classical strategies involving the same repeating units, which do not permit full control of their potential biophysical properties. To meet the increasing demands for dendrimers due to their numerous applications, there is a requirement for accelerated and modular synthetic strategies which can provide rapid and accurate access to these macromolecular entities. This thesis is an attempt to develop highly efficient and versatile synthetic strategies which can provide quick, easy, and economical routes to highly diversified dendrimers. We have developed a novel "onion peel strategy" for the construction of glycodendrimers using different families of building blocks at each layer of the dendritic growth. Dendrimers with chemically heterogeneous layers were constructed *via* a combination of successive highly efficient, versatile, and robust chemical reactions, namely thiol-ene or thiol-yne, esterification, and azide-alkyne click chemistry. Dendrimers constructed using this methodology are fundamentally different to conventional dendritic systems that are usually built from repetitive building blocks (nanosynthons). The dendrimer's surface was decorated with *N*-acetyllactosamine azide using click chemistry which led to new glycodendrimers having high affinities as compared to the corresponding monovalent analogs towards *Erythrina cristagalli*, a leguminous lectin known to bind natural killer cells through its galactoside recognition ability. We further evaluated

the versatility of this strategy by applying both convergent and divergent routes to produce dendrimers with rationally programmed branching units. Both the synthetic routes were efficient to synthesize structurally perfect dendrimers employing our "onion peel approach". One of the glycodendrimer constructed using this methodology resulted in one of the best multivalent ligands known against the virulent factor from a bacterial lectin isolated from *Pseudomonas aeruginosa*. In order to further explore the potential of our strategy, we developed a facile and accelerated microwave assisted "onion peel approach" for dendrimer synthesis to introduce a large number of functional groups at lower generations. In general, large numbers of end groups are achieved at higher generations after multistep synthesis using trivial synthetic protocols. Due to the increasing application of dendrimers having several end groups in gene delivery and electronics, new accelerated approaches are required which can generate monodisperse dendrimers at industrial scale. We prepared generation three dendrimers involving hypermonomers and hypercores to afford 108, 180 or 252 hydroxyl end groups. The synthetic sequence employed the combination of orthogonal building blocks and highly efficient chemical transformations hence did not require any protection/deprotection steps. This is one of the rarest reports where such highly dense dendritic structures have been acquired at lower generations. These dendrimers showed very low cytotoxicity which makes them potential candidates for biomedical applications. The onion peel strategy presented herein is an additional contribution to the wide arsenal of existing methodologies towards synthetic dendrimers and it should open new horizons in dendrimer research for the synthesis of much richer family of functionalized complex dendritic architectures in a rapid and efficient manner.

RÉSUMÉ

Les dendrimères sont des macromolécules tridimensionnelles bien définies, hyperbranchées, monodisperses, qui attirent l'attention de la communauté scientifique depuis maintenant plus de trois décennies. De par leur conception architecturale et leurs propriétés morphologiques uniques, les dendrimères ont été employés dans de nombreux domaines tels que la nanomédecine, la catalyse, l'ingénierie tissulaire, le diagnostic et l'électronique. Malgré le grand nombre d'études portant sur la synthèse de dendrimères, un nombre restreint a atteint l'étape de commercialisation. Cette limite est due à deux défis : la synthèse multi étapes complexes et les hauts coûts impliqués. Il est donc nécessaire de développer de nouvelles stratégies de synthèse de dendrimères, les classiques, impliquant la même unité de répétition, ne permettant pas un plein contrôle des propriétés biophysiques potentielles. Afin de répondre à la demande croissante en dendrimères dans de nombreux domaines, des stratégies de synthèse accélérées et modulaires, permettant d'accéder rapidement et précisément à ces entités macromoléculaires, doivent être envisagées. Ce projet de thèse porte sur le développement de stratégies de synthèses hautement efficaces et versatiles permettant d'obtenir rapidement, facilement et de manière économique des dendrimères hautement diversifiés. Nous avons développé une nouvelle stratégie de type "pelure d'oignon" pour la construction de glycodendrimères utilisant différentes familles de fragments à chaque couche de la croissance dendritique. Les dendrimères avec des couches chimiquement hétérogènes ont été construits via une combinaison de réactions successives, hautement efficaces, versatiles et robustes, à savoir thiol-ène ou thiol-yne, estérification, et chimie "click" ou cycloaddition azoture-alcyne. Les dendrimères construits à partir de cette méthodologie sont fondamentalement différents des systèmes dendritiques conventionnels, qui sont généralement construits à partir de fragments répétitifs (nanosynthons). La surface des dendrimères a été décorée d'azoture de *N*-acetylactosamine menant, après chimie "click", à de

nouveaux glycodendrimères ayant une haute affinité comparés aux analogues monovalents correspondants, vis à vis de la lectine légumineuse, *Erythrina Cristagalli*, connue pour lier des cellules NK grâce à sa capacité à reconnaître les galactosides. Par la suite, nous avons évalué la versatilité de cette stratégie en utilisant à la fois les voies divergente et convergente afin d'obtenir des dendrimères avec les unités de branchement désirées. Chacune des voies de synthèse a été efficace afin de synthétiser des dendrimères parfaitement structurés via notre approche "pelure d'oignon". Un des glycodendrimères construit via cette méthodologie s'avère être un des meilleurs ligands multivalents connu contre le facteur de virulence d'une lectine bactérienne isolée de *Pseudomonas aeruginosa*. Afin d'approfondir le potentiel de notre stratégie, nous avons développé une approche "pelure d'oignon" facile et accélérée, à l'aide d'énergie microonde, pour la synthèse de dendrimères en introduisant un grand nombre de groupements fonctionnels aux plus basses générations. Généralement, un grand nombre de groupements terminaux est atteint aux plus hautes générations, après des synthèses multi étapes utilisant des protocoles usuels. Due à l'application croissante des dendrimères ayant plusieurs groupements terminaux, dans la libération de gènes et l'électronique, de nouvelles approches accélérées, pouvant générer des dendrimères monodisperses à l'échelle industrielle, sont nécessaires. Nous avons préparé des dendrimères de troisième génération impliquant des hypermonomères et des hypercoeurs afin d'obtenir 108, 180 et 252 groupements terminaux hydroxylés. La séquence synthétique a combiné l'introduction de fragments orthogonaux et des transformations chimiques hautement efficaces, ne nécessitant aucune étape de protection/déprotection. Il s'agit d'un des plus rare cas où des structures dendritiques aussi denses ont été obtenues à des plus basses générations. Nos nouveaux dendrimères ont montré de très faibles cytotoxicités, ce qui en fait de très bons candidats potentiels pour des applications biomédicales. La stratégie "pelure d'oignon" présentée ici est une contribution additionnelle au large arsenal des méthodologies existantes dans la synthèse de dendrimères et permettra d'ouvrir de nouveaux horizons dans la recherche en

dendrimères portant sur la synthèse rapide et efficace d'architectures dendritiques complexes fonctionnalisées.

LIST OF ABBREVIATIONS

ACN	Acetonitrile
bis-MPA	Dimethylolpropionic acid
COSY	Correlation spectroscopy
CuAAC	Cu(I) catalyzed alkyne-azide click chemistry
DCC	<i>N,N'</i> -dicyclohexylcarbodiimide
DCM	Dichloromethane
DLS	Differential light scattering
DMAP	4(dimethylamino)pyridine
DMF	<i>N,N'</i> -dimethylformamide
DMPA	2,2-Dimethoxy-2-phenylacetophenone
DMSO	Dimethylsulfoxide
ECA	<i>Erythrina cristagalli</i>
EDC	1-Ethyl-3-(3-dimethylaminopropyl)carbodiimide
EDTA	Ethylenediaminetetraacetic acid
EPR	Enhanced permeability and retention
EtOAc	Ethyl acetate
GPC	Gel permeation chromatography
IC ₅₀	Half maximal inhibitory concentration
MALDI-TOF	Matrix assisted laser desorption ionization-time of flight
MeOH	Methanol
MeONa	Sodium methoxide
MRI	Magnetic resonance imaging
MTT	3-(4,5-dimethylthiazol-2-yl)-2,5-diphenyltetrazolium bromide
NaAsc	Sodium ascorbate
NaH	Sodium hydride
NaOH	Sodium hydroxide

NMR	Nuclear magnetic resonance
O/N	Overnight
PAMAM	Poly(amidoamine)
PDI	Polydispersity index
PEG	Poly(ethylene glycol)
PEI	Poly (ethylene imine)
POSS	Polyhedral oligomeric silsequioxanes
PPI	Poly(propylene imine)
siRNA	Small interfering ribonucleic acid
SPAAC	Strain-promoted alkyne-azide cycloaddition
SPR	Surface plasmon resonance
TBAF	Tetra- <i>n</i> -butylammonium fluoride
TBDPS	tert-Butyldiphenylsilylether
TEA	Triethylamine
TEC	Thiol-ene click
TEM	Transmission electron microscopy
TFA	Trifluoroacetic acid
THF	Tetrahydrofuran
TLC	Thin layer chromatography
TPP	Triphenylphosphonium
TYC	Thiol-yne click

CONTRIBUTION OF AUTHORS

CONTRIBUTION DE L'AUTEUR(E) PRINCIPAL(E) ET DES COAUTEURS
(Formulaire FSC-R3-S.7c)

Règle : Seul l'auteur(e) principal(e) peut utiliser l'article mentionné ci-dessous pour son mémoire ou sa thèse. Aucune autre personne, incluant les autres copremiers auteurs le cas échéant, ne pourra utiliser l'article dans un mémoire ou une thèse, sauf cas exceptionnel défini dans le Règlement no 6 de l'UQAM (Annexe 1, A1.1).

Description du rôle de chacun des auteurs en commençant par l'auteur(e) principal(e). Décrire la responsabilité spécifique relative de la contribution à l'article (idéation, expérimentation, figures, recherche bibliographique, etc.).

Rishi Sharma: All the experiments, characterization, and most of the preparation of the manuscript was done by the author. The co-authors have contributed in the following manner:

Kottari Nareesh: Surface plasmon resonance studies were done by Dr. Nareesh Kottari.

Younis M. Chabre: Dr. Chabre provided compound 19 and 27, and helped in the preparation of manuscript.

Rabindra Rej: Compound 22 and 24 was provided by Dr. Rabindra Rej.

Nadim K. Seadeh: Mr. Nadim carried out mass spectrometry analyses at McGill University.

René Roy: Dr. Roy provided guidance throughout the research and in writing of manuscript.

ATTESTATION DE L'AUTEUR(E) PRINCIPAL(E) ET DE SA DIRECTION DE RECHERCHE

L'auteur(e) principal(e) de l'article certifie :

"Orion peel" dendrimers: a straightforward synthetic approach towards highly diversified architectures.

Compte pour publication : ☐ accepté pour publication : ☒ ou publié dans :

Polymers Chemistry, 2019, 5, 4321-4331

ou :

Auteur(e) principal(e) RISHI SHARMA
Nom

Rishi Sharma
Signature

27-11-2019
Date

Dir. de recherche Rene Roy
Nom

Rene Roy
Signature

27.11.2019
Date

CONTRIBUTION DE L'AUTEUR(E) PRINCIPAL(E) ET DES COAUTEURS
(Formulaire FSC-R3-6.3c)

Note : Seul l'auteur(e) principal(e) peut utiliser l'article mentionné ci-dessous pour son mémoire ou sa thèse. Aucune autre personne, incluant les autres copremiers auteurs le cas échéant, ne pourra utiliser l'article dans un mémoire ou une thèse, sauf cas exceptionnel défini dans le Règlement no 8 de l'UQAM (Annexe 1, A1.1).

Décrivez brièvement de façon des auteurs se concernant par l'auteur(e) principal(e), tâches et responsabilités spécifiques, nature de la contribution à l'article (conception, expérimentation, figures, recherche bibliographique, etc.).

Mohi Shamsi: All the experiments, characterization, and most of the preparation of the manuscript was done by the author. The co-authors have contributed in the following manner:

Kottari Naresh: Surface plasmon resonance studies were done by Dr. Naresh Kottari.

Younis M. Chabre: Dr. Chabre provided helped in the preparation of manuscript.

Laila Abbassi: Compound 20 was provided by Laila.

Tze Chieh Shiao: Compound 21 was provided by Mr. Shiao.

René Roy: Dr. Roy provided guidance throughout the research project and in writing of manuscript.

ATTESTATION DE L'AUTEUR(E) PRINCIPAL(E) ET DE SA DIRECTION DE RECHERCHE

L'auteur principal de l'article déclare :

A highly versatile convergent/divergent "onion peel" synthetic strategy toward potent multivalent

glycomimetics

pour sa publication, soumission publication, ou autre Journal of Chemical Communications, 2014, 50.

13540-13302

Auteur principal R. Roy
Nom

[Signature]
Signature

21.11.2014
Date

Direction de recherche R. Roy
Nom

[Signature]
Signature

27.11.2014
Date

CONTRIBUTION DE L'AUTÉUR(ES) PRINCIPAL(ES) ET DE S. COLLABORATEURS
(Remplir le FSC-83-A (iv))

Note : Seul l'adhésif principal peut utiliser l'article mentionné ci-dessus pour son membre et le faire adhérer aux personnes indiquées les autres supposent ailleurs à cet égard, se pointer vers l'article dans ce membre de son point, sauf cas exceptionnel défini dans la Règlement n° 8 de l'UEM Processus 7.81.0.

Declarația de încredere în produsele și serviciile oferite de furnizorul principal este o declarație de încredere în produsele și serviciile oferite de furnizorul principal.

Rishi Sharma: All the chemistry experiments, characterization, and most of the preparation of the manuscript was done by the author. The co-authors have contributed in the following manner:

Isaac Zhang: All the biological experiments were performed and written by Isaac.

Lefko Aboussi: Compound 20 was provided by Lefko

Robindra Raj: Compound 28 was provided by Dr. Raj

Dusica Mayinger: Dr. Mayinger gave suggestions and guidance during the project.

Band Roy: Dr. Roy provided guidance throughout the research project and in writing of manuscript.

ATTESTATION DE L'AUTHEUR PRINCIPAL ET DE SA DIRECTION DE RECHERCHE

Abstract—The purpose of this study was to determine the effect of a 10-week training program on the heart rate (HR) and energy expenditure (EE) of sedentary, middle-aged women. The subjects were 12 women, 40 to 50 years of age, who were sedentary and had no cardiovascular or pulmonary disease. They were randomly assigned to either a control group or a training group. The control group continued with their sedentary lifestyle, while the training group participated in a 10-week program of aerobic exercise. The HR and EE were measured at rest and during a 30-minute period of moderate exercise. The results showed that the training group had a significantly lower HR and EE at rest and during exercise compared to the control group. These findings suggest that a 10-week training program can improve the cardiovascular and metabolic health of sedentary, middle-aged women.

A fast track strategy toward highly functionalized dendrimers with different structural layers:
"Onion peel approach"

THE UNIVERSITY OF CHICAGO PRESS

Polymer Chem, Accepted, Jan 2015

Reza Shadnia



27-11-2014

Rene Roy

[Signature]

82-112-18

100

RIGHTS AND PERMISSIONS

RSC | Advancing the
Chemical Sciences

Royal Society of Chemistry
Thomas Graham House
Science Park
Milton Road
Cambridge
CB4 0WF

Tel: +44 (0)1223 420 066
Fax: +44 (0)1223 423 623
Email: contracts-copyright@rsc.org

www.rsc.org

Acknowledgements to be used by RSC authors

Authors of RSC books and journal articles can reproduce material (for example a figure) from the RSC publication in a non-RSC publication, including theses, without formally requesting permission providing that the correct acknowledgement is given to the RSC publication. This permission extends to reproduction of large portions of text or the whole article or book chapter when being reproduced in a thesis.

The acknowledgement to be used depends on the RSC publication in which the material was published and the form of the acknowledgements is as follows:

- For material being reproduced from an article in *New Journal of Chemistry* the acknowledgement should be in the form:
 - [Original citation] - Reproduced by permission of The Royal Society of Chemistry (RSC) on behalf of the Centre National de la Recherche Scientifique (CNRS) and the RSC
- For material being reproduced from an article *Photochemical & Photobiological Sciences* the acknowledgement should be in the form:
 - [Original citation] - Reproduced by permission of The Royal Society of Chemistry (RSC) on behalf of the European Society for Photobiology, the European Photochemistry Association, and RSC
- For material being reproduced from an article in *Physical Chemistry Chemical Physics* the acknowledgement should be in the form:
 - [Original citation] - Reproduced by permission of the PCCP Owner Societies
- For material reproduced from books and any other journal the acknowledgement should be in the form:
 - [Original citation] - Reproduced by permission of The Royal Society of Chemistry

The acknowledgement should also include a hyperlink to the article on the RSC website.

The form of the acknowledgement is also specified in the RSC agreement/licence signed by the corresponding author.

Except in cases of republication in a thesis, this express permission does not cover the reproduction of large portions of text from the RSC publication or reproduction of the whole article or book chapter.

A publisher of a non-RSC publication can use this document as proof that permission is granted to use the material in the non-RSC publication.

12/1/2014

Rightsent Printable License

JOHN WILEY AND SONS LICENSE TERMS AND CONDITIONS

Dec 02, 2014

This is a License Agreement between Rishi Sharma ("You") and John Wiley and Sons ("John Wiley and Sons") provided by Copyright Clearance Center ("CCC"). The license consists of your order details, the terms and conditions provided by John Wiley and Sons, and the payment terms and conditions.

All payments must be made in full to CCC. For payment instructions, please see information listed at the bottom of this form.

License Number	3520570971845
License date	Dec 02, 2014
Licensed content publisher	John Wiley and Sons
Licensed content publication	Angewandte Chemie International Edition
Licensed content title	Molecularly Precise Dendrimer-Drug Conjugates with Tunable Drug Release for Cancer Therapy
Licensed copyright line	© 2014 WILEY-VCH Verlag GmbH & Co. KGaA, Weinheim
Licensed content author	Zhuxian Zhou,Xinpeng Ma,Caitlin J. Murphy,Eriei Jin,Qihang Sun,Youqing Shen,Edward A. Van Kirk,William J. Murdoch
Licensed content date	Aug 25, 2014
Start page	10949
End page	10955
Type of use	Dissertation/Thesis
Requestor type	University/Academic
Format	Print and electronic
Portion	Figure/table
Number of figures/tables	1
Original Wiley figure/table number(s)	1b
Will you be translating?	No
Title of your thesis / dissertation	"Onion Peel Approach": A Novel Strategy for Dendrimers Synthesis
Expected completion date	Jan 2015
Expected size (number of pages)	350
Total	0.00 USD
Terms and Conditions	

12/1/2014

Rightslink Printable License

**JOHN WILEY AND SONS LICENSE
TERMS AND CONDITIONS**

Dec 02, 2014

This is a License Agreement between Rishi Sharma ("You") and John Wiley and Sons ("John Wiley and Sons") provided by Copyright Clearance Center ("CCC"). The license consists of your order details, the terms and conditions provided by John Wiley and Sons, and the payment terms and conditions.

All payments must be made in full to CCC. For payment instructions, please see information listed at the bottom of this form.

License Number	3520571471137
License date	Dec 02, 2014
Licensed content publisher	John Wiley and Sons
Licensed content publication	Angewandte Chemie International Edition
Licensed content title	Adaptive Amphiphilic Dendrimer-Based Nanoassemblies as Robust and Versatile siRNA Delivery Systems
Licensed copyright line	© 2014 WILEY-VCH Verlag GmbH & Co. KGaA, Weinheim
Licensed content author	Xiaoxuan Liu, Jiehua Zhou, Tianzhu Yu, Chao Chen, Qiang Cheng, Kheya Sengupta, Yuanyu Huang, Haitang Li, Cheng Liu, Yang Wang, Paola Posocco, Menghua Wang, Qi Cui, Suzanne Giorgio, Maurizio Fermeleglia, Fangqi Qu, Sabrina Prid, Yanhong Shi, Zicai Liang, Palma Rocchi, John J. Rossi, Ling Peng
Licensed content date	Sep 12, 2014
Start page	11822
End page	11827
Type of use	Dissertation/Thesis
Requestor type	University/Academic
Format	Print and electronic
Port on	Figure/table
Number of figures/tables	1
Original Wiley figure/table number(s)	scheme 1
Will you be translating?	No
Title of your thesis / dissertation	"Onion Peel Approach": A Novel Strategy for Dendrimers Synthesis
Expected completion date	Jan 2015
Expected size (number of pages)	350
Total	0.00 USD

12/1/2014

Rightslink Printable License

ELSEVIER LICENSE TERMS AND CONDITIONS

Dec 02, 2014

This is a License Agreement between Rishi Sharma ("You") and Elsevier ("Elsevier") provided by Copyright Clearance Center ("CCC"). The license consists of your order details, the terms and conditions provided by Elsevier, and the payment terms and conditions.

All payments must be made in full to CCC. For payment instructions, please see information listed at the bottom of this form.

Supplier	Elsevier Limited The Boulevard, Langford Lane Kidlington, Oxford, OX5 1GB, UK
Registered Company Number	1982084
Customer name	Rishi Sharma
Customer address	Department of Chemistry Montreal, QC H3C3P8
License number	3520580649046
License date	Dec 02, 2014
Licensed content publisher	Elsevier
Licensed content publication	Biomaterials
Licensed content title	Multifunctional dendrimer-entrapped gold nanoparticles for dual mode CT/MR imaging applications
Licensed content author	Shihui Wen, Kangan Li, Hongdong Cai, Qian Chen, Mingwu Shen, Yunpeng Huang, Chen Peng, Wenxiu Hou, Meifang Zhu, Guixiang Zhang, Xiangyang Shi
Licensed content date	February 2013
Licensed content volume number	34
Licensed content issue number	5
Number of pages	11
Start Page	1570
End Page	1580
Type of Use	reuse in a thesis/dissertation
Intended publisher of new work	other
Portion	figures/tables/illustrations
Number of figures/tables/illustrations	1
Format	both print and electronic

5/14/2015

Rightslink Printable License

**THE AMERICAN ASSOCIATION FOR THE ADVANCEMENT OF SCIENCE LICENSE
TERMS AND CONDITIONS**

May 14, 2015

This is a License Agreement between Rishi Sharma ("You") and The American Association for the Advancement of Science ("The American Association for the Advancement of Science") provided by Copyright Clearance Center ("CCC"). The license consists of your order details, the terms and conditions provided by The American Association for the Advancement of Science, and the payment terms and conditions.

All payments must be made in full to CCC. For payment instructions, please see information listed at the bottom of this form.

License Number	3627910042369
License date	May 14, 2015
Licensed content publisher	The American Association for the Advancement of Science
Licensed content publication	Science
Licensed content title	Direct Evidence of a Dinuclear Copper Intermediate in Cu(I)-Catalyzed Azide-Alkyne Cycloadditions
Licensed content author	B. T. Worrell, J. A. Malik, V. V. Fokin
Licensed content date	Apr 26, 2013
Volume number	340
Issue number	6131
Type of Use	Thesis / Dissertation
Requestor type	Scientist/individual at a research institution
Format	Print and electronic
Portion	Figure
Number of figures/tables	1
Order reference number	None
Title of your thesis / dissertation	"Onion Peel Approach": A Novel Strategy for Dendrimer Synthesis
Expected completion date	May 2015
Estimated size(pages)	302
Total	0.00 USD

Terms and Conditions

American Association for the Advancement of Science TERMS AND CONDITIONS



RightsLink

Home

Account
Info

Help

ACS Publications
Most Trusted. Most Cited. Most Read.

Title: Recyclable Catalytic Dendrimer
Nanoreactor for Part-Per-Million
CuI Catalysis of "Click" Chemistry
in Water

Logged in as
Rishi Sharma

LOGOUT

Author: Christophe Deraedt, Noel Pinaud,
Didier Astruc

Publication: Journal of the American Chemical
Society

Publisher: American Chemical Society

Date: Aug 1, 2014

Copyright © 2014, American Chemical Society

PERMISSION/LICENSE IS GRANTED FOR YOUR ORDER AT NO CHARGE

This type of permission/license, instead of the standard Terms & Conditions, is sent to you because no fee is being charged for your order. Please note the following:

- Permission is granted for your request in both print and electronic formats, and translations.
- If figures and/or tables were requested, they may be adapted or used in part.
- Please print this page for your records and send a copy of it to your publisher/graduate school.
- Appropriate credit for the requested material should be given as follows: "Reprinted (adapted) with permission from (COMPLETE REFERENCE CITATION). Copyright (YEAR) American Chemical Society." Insert appropriate information in place of the capitalized words.
- One-time permission is granted only for the use specified in your request. No additional uses are granted (such as derivative works or other editions). For any other uses, please submit a new request.

If credit is given to another source for the material you requested, permission must be obtained from that source.



RightsLink

[Home](#)
[Account Info](#)
[Help](#)


ACS Publications Title:
Most Trusted. Most Cited. Most Read.

Facile and Efficient Synthesis of Dendrimers and One-Pot Preparation of Dendritic-Linear Polymer Conjugates via a Single Chemistry: Utilization of Kinetically Selective Thiol-Michael Addition Reactions

Logged in as
Rishi Sharma

[LOGOUT](#)

Author: Shunsuke Chatani, Maciej Podgórski, Chen Wang, et al

Publication: Macromolecules

Publisher: American Chemical Society

Date: Aug 1, 2014

Copyright © 2014, American Chemical Society

PERMISSION/LICENSE IS GRANTED FOR YOUR ORDER AT NO CHARGE

This type of permission/license, instead of the standard Terms & Conditions, is sent to you because no fee is being charged for your order. Please note the following:

- Permission is granted for your request in both print and electronic formats, and translations.
- If figures and/or tables were requested, they may be adapted or used in part.
- Please print this page for your records and send a copy of it to your publisher/graduate school.
- Appropriate credit for the requested material should be given as follows: "Reprinted (adapted) with permission from (COMPLETE REFERENCE CITATION). Copyright (YEAR) American Chemical Society." Insert appropriate information in place of the capitalized words.
- One-time permission is granted only for the use specified in your request. No additional uses are granted (such as derivative works or other editions). For any other uses, please submit a new request.

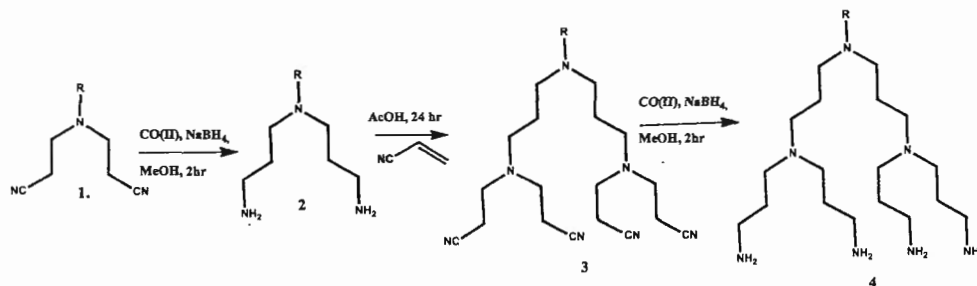
If credit is given to another source for the material you requested, permission must be obtained from that source.

CHAPTER 1

INTRODUCTION AND SCOPE OF THE THESIS

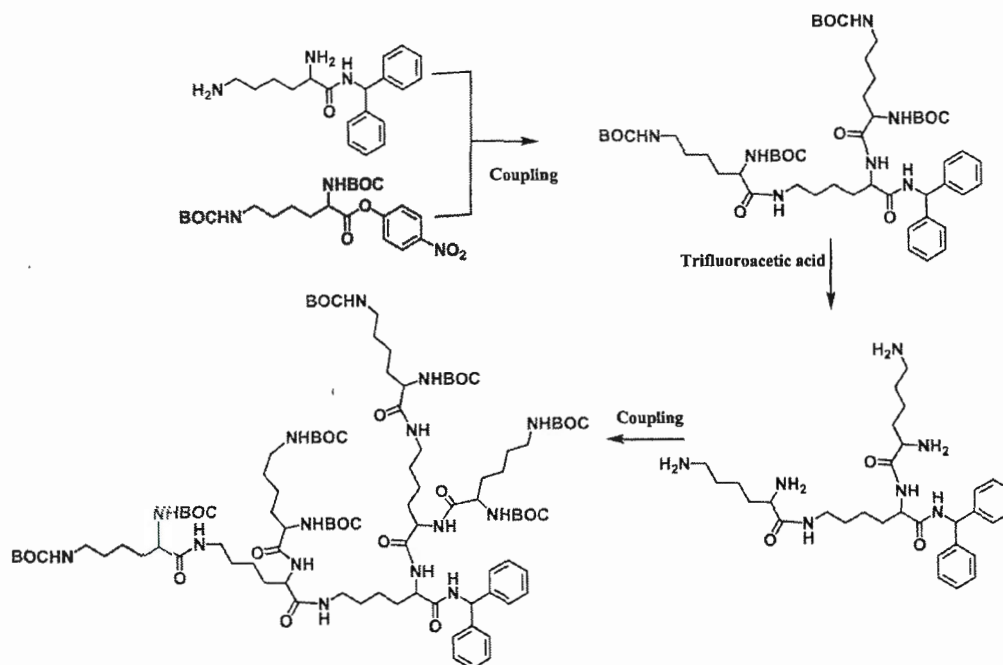
1.1 Introduction to dendrimers:

Dendrimers are hyperbranched, monodisperse three dimensional tree like macromolecules which have been extensively studied during the last twenty years.¹⁻⁵ Historically, the concept was the brainchild of Flory, who proposed the theoretical evidence for three dimensional hyperbranched polymeric architectures in 1940s.⁶⁻⁹ The scientific community took almost 40 years to interpret this riddle and finally a German scientist Fritz Vögtle successfully synthesized these molecules in 1978 at University of Bonn.¹⁰ He referred the cascade like synthesis of polyamines as cascade molecules. The synthesis involved the Michael reaction of acrylonitrile with mono or diamine derivatives to yield cyano terminated molecules which were further reduced to amines in the next step to yield polyamine compounds (Scheme 1-1).

Scheme 1-1 Synthesis of cascade molecules by Vögtle.¹⁰

Three years later, in 1981 R. G. Denkewalter patented lysine based highly branched macromolecules up to 10th generation (Scheme 1-2).³ In 1985 Donald Tomalia coined the term 'dendrimer' for these macro-entities and got acceptance from whole scientific community.¹¹ In the same year, Newkome assigned his

branched structures the term 'arborols' which consisted of saturated hydrocarbon skeleton.¹²



Scheme 1-2 Synthesis of Poly-Lysine dendrimer by Denkewalter and co-workers in 1981.³

The word 'dendrimer' has been derived from Greek language and consists of two words 'dendron' means "tree like" and 'meros' means "part of". Dendrimers are constructed in a sequential manner around a central core in a layer by layer fashion, where each layer provides new generation. The size (hydrodynamic radius) of the dendrimers tends to increase linearly with increase in generation numbers. In general, lower generation dendrimers are more planer and asymmetrical, while higher generation dendrimers tends to become spherical which results in internal cavities. There is an exponential increase in the number of surface groups with an increase in generation number. As the dendrimers grow bigger and bigger, the surface becomes more crowded and finally it cannot grow any further due to the steric factors involved. This phenomenon is called as "starburst limit effect" and occurs at different generations for different dendrimers. Figure 1-1 shows the anatomy of a dendrimer. A

typical dendrimer is made up of following structural components: 1) a central core; 2) repetitive branching units which form the generations, 3) peripheral end groups, and 4) internal cavities. Different components of dendrimers contribute to different properties. The core determines the overall shape and directionality of the dendrimers. The central core also affects the number of surface groups since the multiplicity of branches depends upon the type of core around which the dendrimer is built. The internal cavities of the dendrimers provide opportunities to physically entrap the guest species *e.g.* drug molecules in case of applications for drug delivery. All the structural elements listed above decide the physical and chemical properties of dendrimers but the solubility of these macromolecules mostly depends upon the nature of end groups.

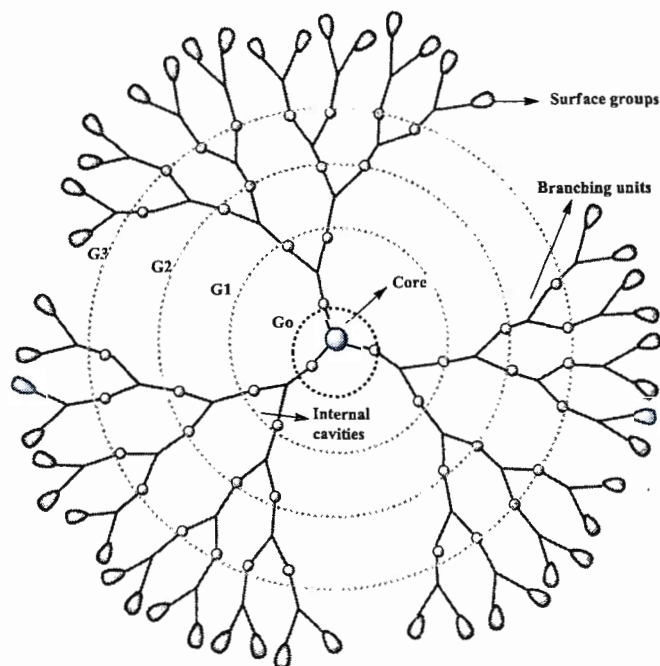


Figure 1-1 Anatomy of dendrimer.

1.2 Myths and facts about dendrimers:

Ever since their discovery, dendrimers have constantly found new applications in a variety of disciplines ranging from catalysis, sensing, electronics and drug and gene delivery. However, during the early years of their invention, many myths existed about these macromolecular entities. Scientists assumed that the cost of constructing dendrimers was too high to be useful for any kind of commercialization, and they were far away from real world applications. These myths have been knocked down by Starpharma, an Australian based pharmaceutical company, who has developed world's first dendrimer based drug VivaGel® which prevents the transmission of infection against HIV virus, HSV-2 and other sexually transmitted diseases (Figure 1-2).¹³ In addition, it also has spermicidal properties, thus can serve as a potential contraceptive. The drug has already been approved to be launched in the markets in Japan and Australia. The active component of the drug, SPL7013, is a fourth-generation polylysine dendrimer harbouring thirty-two sodium 1-(carboxymethoxy)naphthalene-3,6-disulfonate moieties on the surface attached *via* amide linkages. It is believed to work by attaching gp120 glycoproteins present on the surface of HIV loop and blocking their attachment with CD4 receptors present on the host cell.

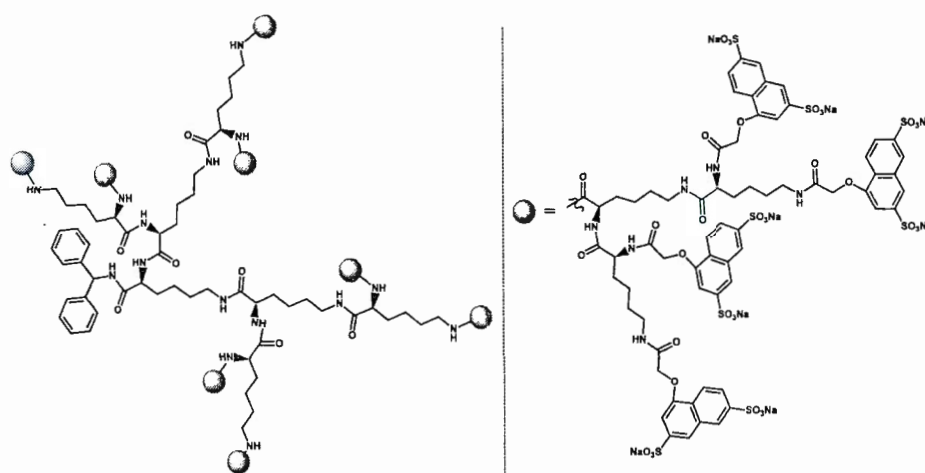


Figure 1-2 Structural representation of SPL 7013, the active component of VivaGel.¹³

The Stratus[®] CS (Dade Behring, Inc.) is another dendrimer based commercial product which is used as a fast detection tool for myocardial ischemia.¹⁴ This specific cardiac biomarker rapidly detects the presence of cardiac troponins in the serum which strongly indicates myocardial damage. In these systems, antibodies are first attached to the surface of 5th generation PAMAM dendrimers which are positively charged, and then these antibodies are glued with a glass fibre with the help of electrostatic interactions. The US army research laboratory has developed dendrimer-based diagnostic agent for anthrax detection, which is also referred as "Alert Ticket". SuperFect of Qiagen is a very famous gene transfection product which consists of spherical polycationic dendrimers consisting primary amines on periphery and tertiary amine on the branching units. The cationic polyamines can interact with negatively charged phosphates present on nucleic acids and the dendriplex formed can be taken up into the cell by the process of endocytosis. Gadomer-17 also known as Gd-DTPA-17, SH L 643 A, is an investigational magnetic resonance contrast agent based on dendrimers currently in phase II clinical trials.¹⁵ It is a poly-lysine dendrimer which consists of 24 terminal amino groups which are covalently linked to 24 gadolinium chelate groups capping the periphery of the dendrimer. Dendrimers also have applications in beauty industry and L'Oreal possesses highest number of patents on dendrimers. Moreover, a wide variety of dendrimers are commercially available these days (Figure 1-3).

1.3 Applications:

Dendrimers have been explored for applications in a wide range of fields such as catalysis,¹⁶⁻¹⁸ drug and gene delivery,¹⁹⁻²² sensing,^{23,24} electronics,^{25,26} diagnostics^{27, 28} and nanoengineering²⁹ (Figure 1-4). The dendrimers' unparalleled molecular uniformity, monodispersity, presence of internal cavities, and multifunctional surface make them potential candidates for various applications. The surface, interior as well as the core of the dendrimers can be used to attach different functional moieties.

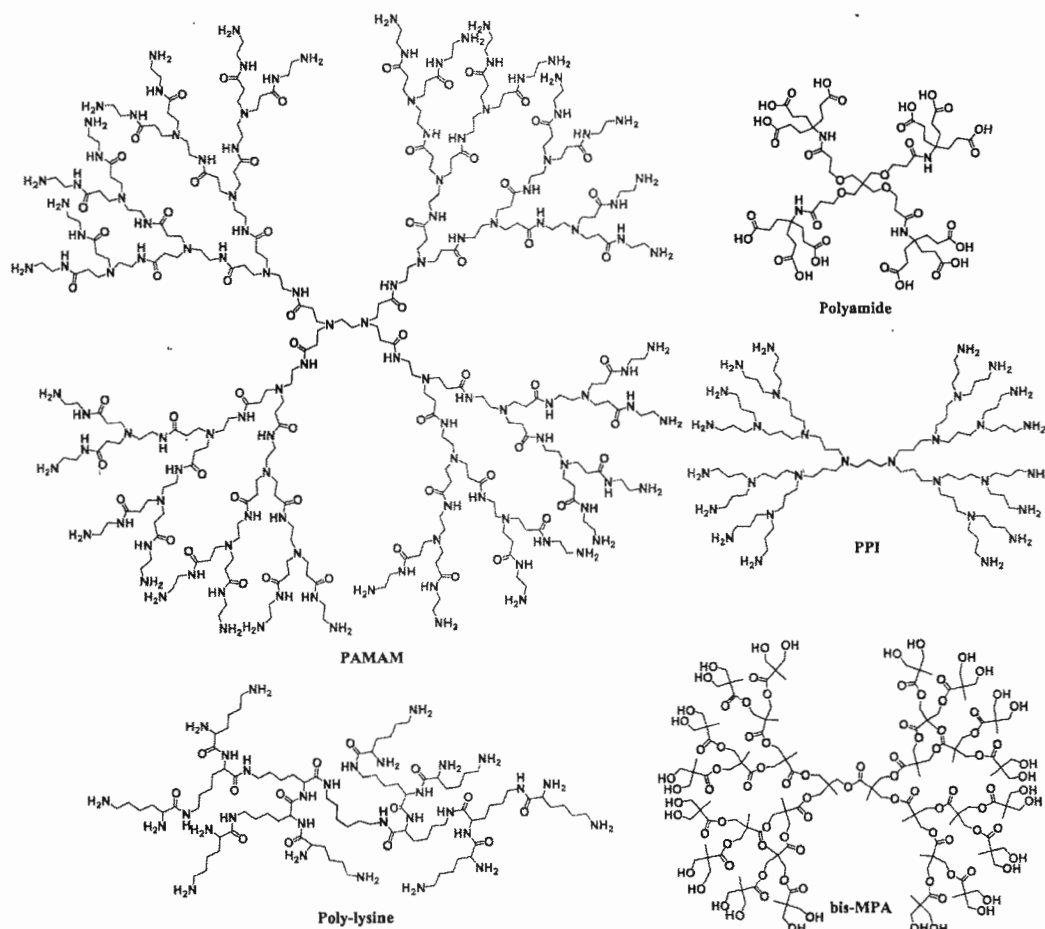


Figure 1-3 Chemical structures of the most common commercially available dendrimers.

Dendrimers have been well explored for applications in drug delivery due to their monodisperse architecture and nanometer size range. A variety of dendrimers have been evaluated thoroughly for drug delivery, for example, PAMAM,^{30, 31} PPI,³² poly-L-lysine³³ and triazine dendrimers³⁴. The drug molecules and targeting agents can be covalently attached to the multivalent surface of the dendrimers or can also be physically incorporated into the internal voids of higher generation dendrimers.³⁵ The dendrimers can provide site specific drug delivery and controlled release of the drugs, and can in turn significantly improve the bioavailability as well as reduce the

cytotoxicity of the drugs by decreasing their undesired localization. In addition to this, dendrimers can also facilitate the passive targeting of drugs to solid tumors due

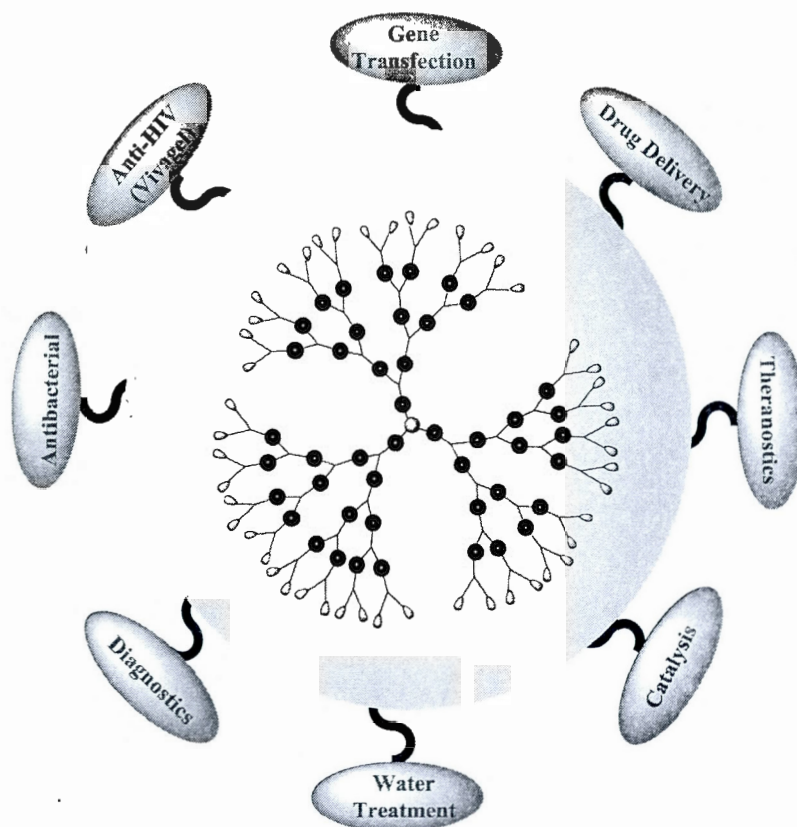


Figure 1-4 Representation of applications of dendrimers.

to leaky vasculature at tumor sites and the phenomenon is known as enhanced permeation and retention (EPR) effect. Recently, an interesting piece of work has been reported by Murdoch and coworkers.³⁶ They have developed molecularly precise dendrimer-camptothecin (CPT) conjugates as macromolecular prodrugs for cancer treatment with a tunable release of drug (Figure 1-5). They buried the anti-cancer drug CPT inside poly-L-lysine dendrimers as their core and the dendrimer-drug conjugates had fixed drug content. In addition to this, as the drug was not present at the surface and thus could not interact with blood components keeping its pharmacokinetics intact. The drug release rates were tunable depending upon the generation of dendrimer, surface chemistry and pH.

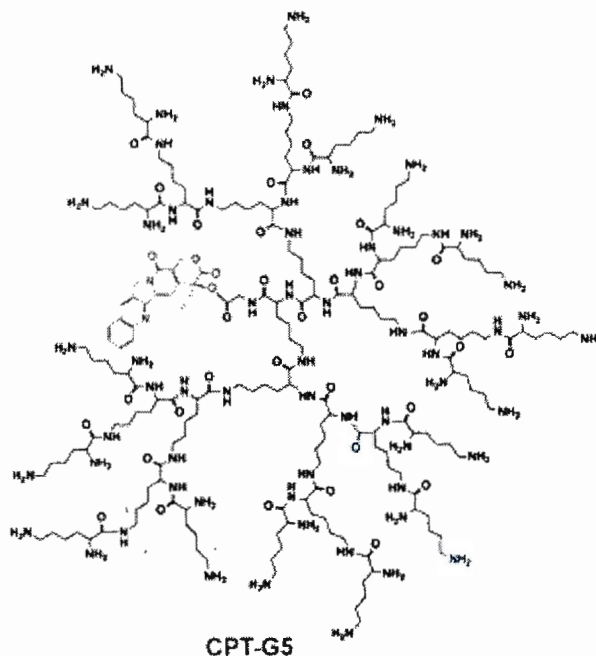


Figure 1-5 Structure of dendrimer-Camptothecin conjugate.³⁶

Well defined architecture of dendrimers and high ratio of multivalent surface moieties to molecular volume also make these materials potential candidates to be used to develop non-viral vectors for the delivery of nucleic acids. The interaction between cationic dendrimer and nucleic acid is based on electrostatic interactions and the resulting complex is called dendriplex. A wide variety of polycationic dendrimers have been explored for gene delivery including, PAMAM, poly(propylene imine) (PPI), poly(L-lysine), carbosilane, and triazine dendrimers etc.³⁷ Among these, PAMAM dendrimers have been most widely reported as siRNA delivery vectors due to their ease in synthesis and commercial availability. Although dendrimer-based gene delivery vehicles have shown considerable potential as tools for the development of gene therapy, still most of them have not been explored for *in vivo* administration. In a recent example, Peng and coworkers have reported a novel amphiphilic dendrimer-based nanoassembly as a versatile carrier for functional siRNA delivery (Figure 1-6).³⁸ This amphiphilic dendrimer could self assemble into

vesicle like dendrimersome and upon its interaction with siRNA could rearrange itself to smaller spherical micelles in order to maximise its interaction with siRNA. This dendrimer had the combined advantages of both polymer and lipid vectors and could successfully deliver siRNA into various cell types including human primary cells and stem cells which are quite challenging. This amphiphilic dendrimer based supramolecular nanoassembly vector for effective and safe delivery of siRNA represents a novel design in the field of siRNA based gene therapy.

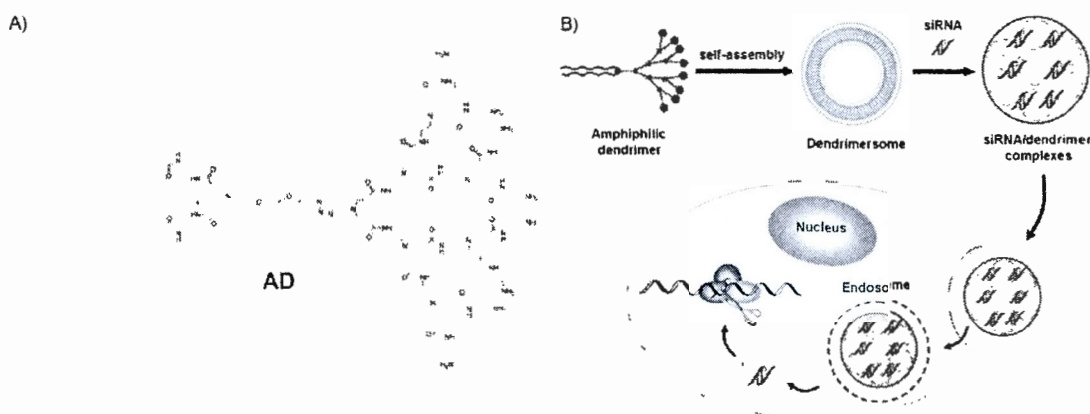


Figure 1-6 A) The structure of amphiphilic dendrimer and B) schematic illustration of self-assembly of dendrimer upon interaction with siRNA.³⁸

Dendrimers have also gathered a great deal of attention to be used for imaging contrast agents.³⁹ The highly branched interior and polyvalent peripheral structure offers unique advantages for dendrimers to be useful for the applications of contrast agents for various biomedical applications. Multiple imaging agents can be directly attached to the periphery of the dendrimers in order to have dual or multi modal imaging capabilities. There are different ways by which the dendrimers can be modified to be used as contrast agents. For example, dendrimers can be conjugated to the fluorescent molecules or can be used as templates to form dendrimer trapped or stabilized metal nanoparticles. Dendrimers based multimodal contrast agents can highly improve the diagnosis accuracy. In a recent study by Shi *et al.*, multifunctional gadolinium-loaded dendrimer entrapped gold nanoparticles (GdeAu

DENPs) were developed for dual imaging applications involving computed tomography (CT) and magnetic resonance (MR) (Figure 1-7).⁴⁰

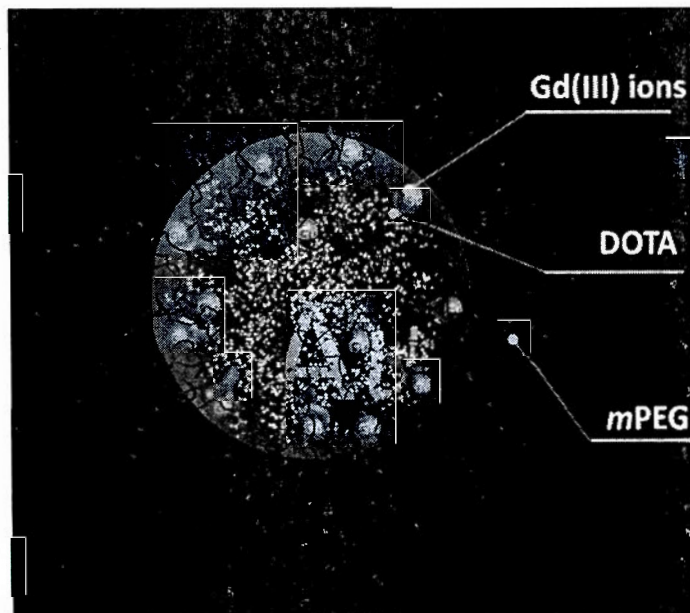


Figure 1-7 Schematic illustration of gadolinium-loaded dendrimer entrapped gold nanoparticles.⁴⁰

They used 5th generation amine terminated PAMAM dendrimers modified with Gd(III) chelator and polyethylene glycol (PEG) monomethyl ether to act as templates to construct gold nanoparticles in the interior of dendrimer. Due to the presence of double radiosense imaging materials gold nanoparticles and Gd(III) within one system, the formed GdeAuDENPs could show both r_1 relaxivity for MR imaging mode and X-ray attenuation for CT imaging mode, thus enabling CT/MR dual mode imaging of the heart, liver, kidney, and bladder of rat or mouse within a time frame of 45 min. These types of advanced imaging tools can be highly beneficial for the detection of early stage cancer with great accuracy.

Catalysis is another promising area where dendrimers have shown their potential.⁴¹ Since their first reports by the groups of van Leeuwen,⁴² Brunner,⁴³ van Koten,⁴⁴ and DuBois,⁴⁵ the field has advanced rapidly and several examples are now available in literature showing the role of dendrimers as catalysts.⁴⁶ The advantages

of using dendrimers to anchor catalytic sites are due to their well defined structures and molecular features, which can be highly useful for detailed analysis of catalytic events. High generation dendrimers consist of nanoscopic internal cavities and these cavities can serve as nanoscale reactor sites for catalysis. Dendrimers provide a unique platform where the advantages of both homogeneous and heterogeneous catalysis can be combined together. The dendrimer based catalysts can be designed in two ways: 1) The multivalent periphery of the dendrimers can be used to introduce multiple catalytic sites at the surface of dendrimers, 2) The catalytic site can be introduced at the central core of the dendrimer due to a well defined nano-environment and presence of voids in their interior which are isolated from the outside environment. The presence of large number of catalysts on the surface of dendrimers can provide additive or multivalent dendritic effect in terms of catalyst activity, which in turn will require less catalytic loading. Catalysts located at the periphery of the dendrimers can become easily accessible for various molecular interactions. On the other hand, large size of dendritic catalysts makes it easier to remove them from reaction mixture by simple precipitation or nano-filtration method. Moreover, the properties of dendritic catalysts can be easily fine-tuned by altering the dendrimer structure, size, shape, solubility and number of end groups. A large number of articles are available in the literature dealing with the applications of dendrimers in the field of catalysis.⁴⁶ An interesting example of application of dendrimers in catalysis has been recently reported by Astruc *et. al.*⁴⁷ They have developed a dendrimer based recyclable catalytic nanoreactor for the catalysis of extremely useful Cu(I) catalyzed alkyne-azide Click (CuAAC) reaction in water using as low as parts per million concentration of Cu(I). The amphiphilic dendrimer having 27 triethylene glycol termini and 9 intradendritic triazole rings works as a molecular micelle nanoreactor and considerably accelerates the CuAAC reaction using Cu(hexabenzyl triaminoethylamine)Br as a catalyst (Figure 1-8). In addition, this dendrimer nanoreactor is fully recyclable and can be used multiple times without decomposition. Moreover, as a synergistic effect, this dendrimer with intradendritic

triazole rings also activates commercial $\text{CuSO}_4 \cdot 5\text{H}_2\text{O}$ and sodium ascorbate in water under ambient conditions decreasing their amounts upto 4 ppm for quantitative yields and 1 ppm for 50% yields. The development of this fully recyclable dendrimer nanoreactor for click reaction with a considerable decrease in the use of copper catalyst is a remarkable achievement for click reaction, and can be highly beneficial for the use of this reaction for biomedical applications.

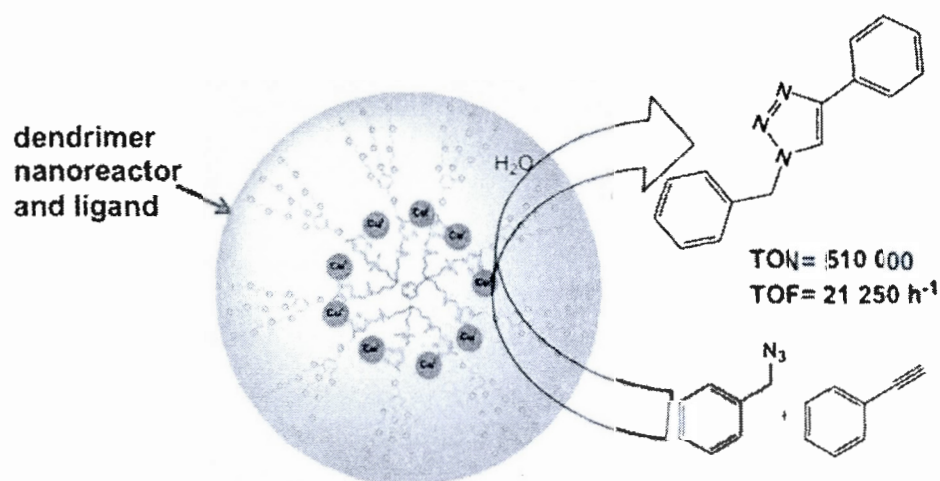


Figure 1-8 Dendrimer nanoreactor for catalysis of Cu(I) catalyzed click reaction.⁴⁷

Dendrimers have also shown promising results for application in waste water treatment.^{48, 49} They have unique physicochemical properties and excellent abilities to coordinate metal ions which make them potential candidates to be used as separation and reaction media for water purification. Dendrimers can encapsulate a wide range of cations, anions and organic compounds present in water. The presence of toxic metals *e.g.* lead in water is a serious threat to human health. Even minute concentrations of these heavy metals are toxic. Adsorption is a very useful and economic technique in recent time to remove heavy metals from aqueous solutions, and most widely the activated carbon has been used for this purpose. But being expensive, constant efforts were made to find alternatives and dendrimers seem to have potential for this application. The recent example of use of dendrimers for Pb^{2+} ions adsorption from aqueous solutions is reported by Woodcock and colleagues.⁴⁸

They used generation 4 polyamidoamine dendrimer immobilized over titanium(iv) oxide as adsorbent to remove lead ions from aqueous solutions and the maximum capacity of PAMAM dendrimers to adsorb Pb^{2+} ions came out to be around 400 mg/g.

In addition to these, dendrimers have applications as demulsifiers,⁵⁰ bacterial biofilm inhibitors,⁵¹ in detection of explosives,⁵² and as therapeutic agents⁵³. Despite this long list of applications, dendrimers technology still has a long road ahead.

1.4 Strategies for dendrimer synthesis:

1.4.1 Classical methods: There are many existing synthetic routes and protocols for dendrimer construction but dendrimer synthesis is generally followed by two most widely used classical synthetic approaches: divergent¹¹ and convergent^{54, 55} (Figure 1-9). Each approach has its own advantages and disadvantages.

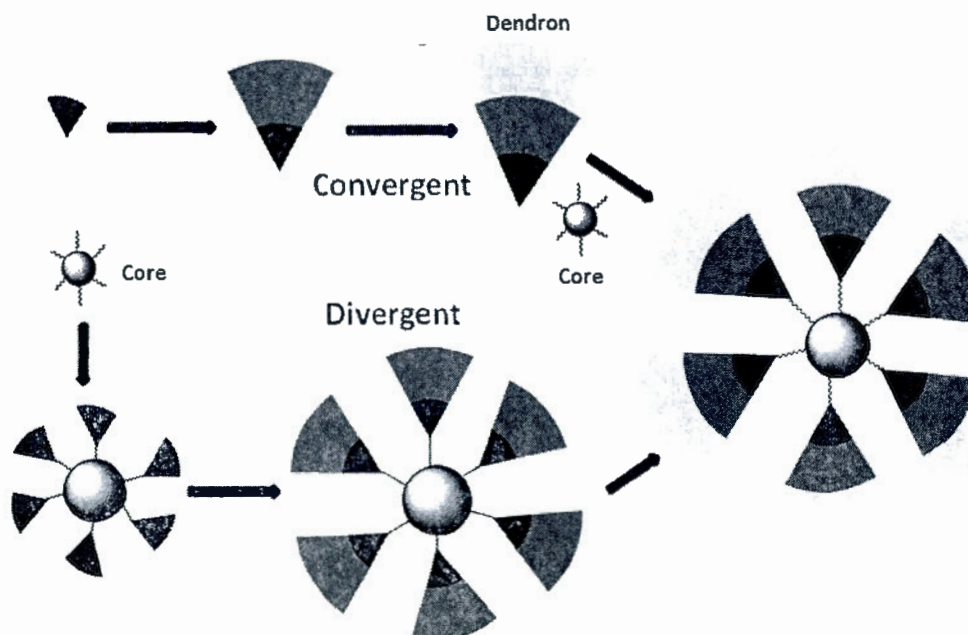
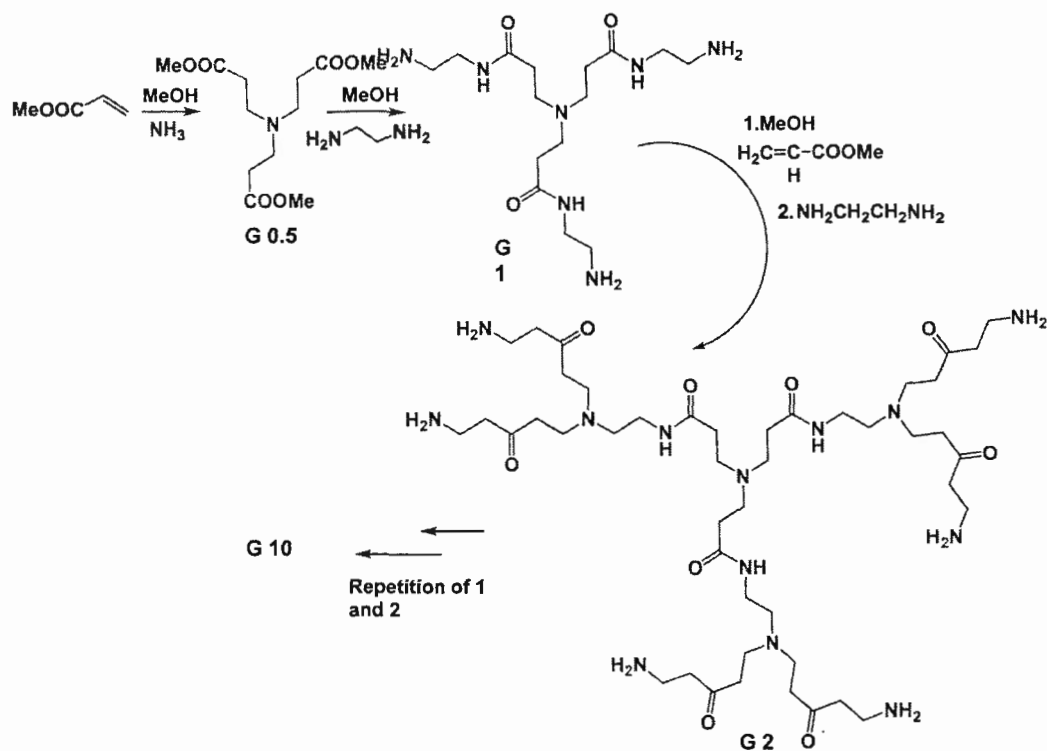


Figure 1-9 Divergent and convergent methods for dendrimer synthesis.

1.4.1.1 Divergent Method: All the pioneers in the field like Tomalia,¹¹ Vögle¹⁰ and Newkome¹² used divergent approach for the construction of dendrimers. In fact for

the first decade after their discovery, every single dendrimer was constructed using divergent method. The divergent method is an inside-outward approach, where the synthesis starts at the core and progresses towards the periphery generation after generation in a repetitive manner. The classical divergent method involves protection and deprotection, and the activation is required at each generation which dramatically increases the number of reaction steps. The divergent approach allows to construct higher generation dendrimers as reported by, Tomalia *et al* who have synthesized dendrimers up to seventh generation using divergent approach around ethylenediamine core *via* iterative sequence of Michael addition and aminolysis (Scheme 1-3).¹¹



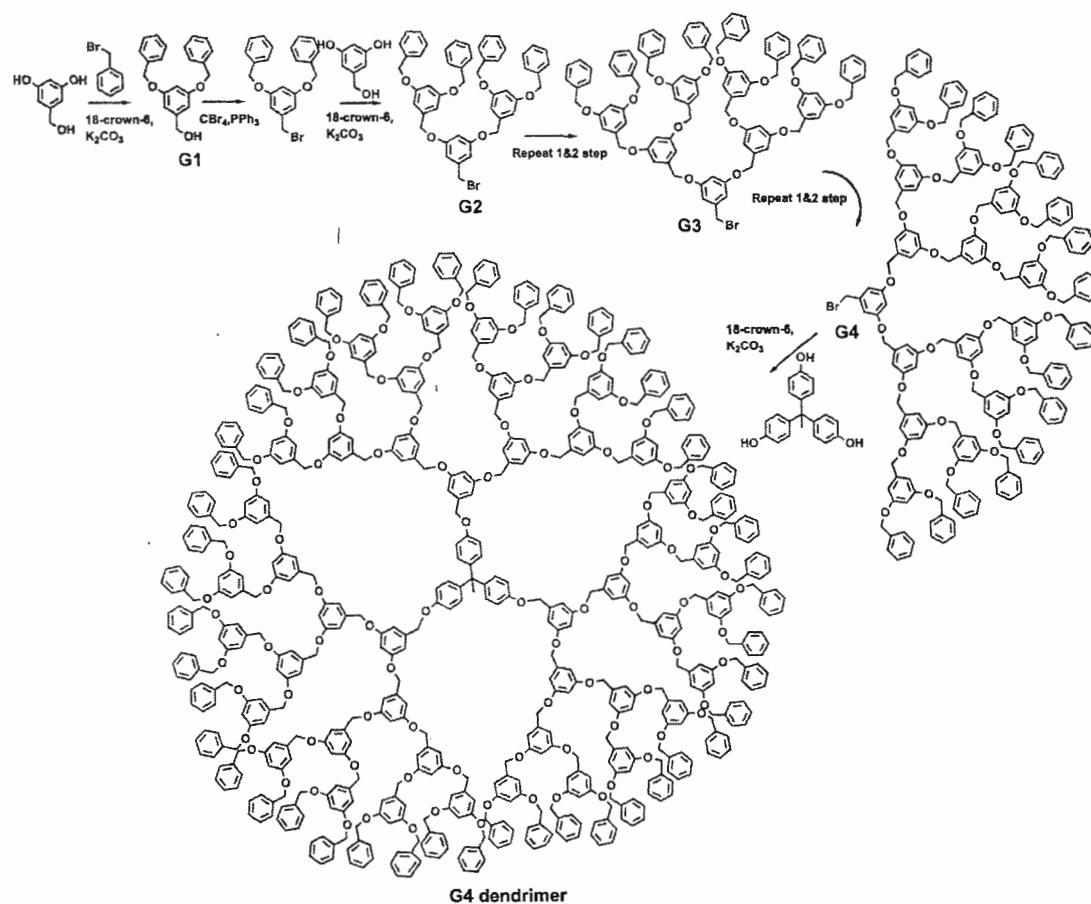
Scheme 1-3 Divergent synthesis of PAMAM dendrimers with ammonia as a core.¹¹

Another advantage of using divergent methodology is that the synthesis can be stopped at any generation and surface can be functionalized with various end groups which is not possible during the convergent growth. Divergent synthesis is the

only successful approach which provides high generation dendrimers in kilogram scale and most of the commercially available dendrimers are synthesized using divergent approach. The main drawback of divergent strategy is that as we proceed towards higher generations, the chances of getting defect-free dendrimers decrease. This is because the number of end groups increases exponentially with each generation. Due to the dense packing of surface groups at higher generations, the steric factors start to play their role and prevent the full conversion even with the addition of large excess of reagents and monomers. The physical and chemical properties of dendrimers with slight imperfections are so close to the structurally perfect dendrimers that it is almost impossible to purify those using standard techniques. These reasons make the dendrimers synthesis troublesome and time consuming. In addition, the divergent approach does not provide us the freedom to introduce multiple functions at the periphery due to identical nature and reactivity of surface groups.

1.4.1.2 Convergent Method: In order to deal with the problems of divergent synthesis, Fréchet and Hawker in 1990 introduced a convergent approach for dendrimer synthesis.⁵⁵ The methodology was used to construct dendrimers with poly aryl ether units (Scheme 1-4). This is an outside inward approach which starts with the synthesis of dendron wedges followed by their attachment onto the core. The convergent synthesis concept is very similar to the retro synthesis where a target chemical entity is achieved by backward synthesis. The convergent method produces dendrimers with much higher purity as the number of sites per reaction are far less than in the case of divergent, thus reducing the number of structural defects. The dendron wedges are much smaller in size than their dendrimer analogs and are thus easier to purify at each step. Overall, there is a greater control and reduced consumption of reagents throughout the synthesis. The convergent approach can also be used to develop multifunctional dendrimers by attaching different dendrons to polyfunctional cores. The drawback of convergent methodology is that only low generation dendrimers can be successfully achieved with this methodology as the

linking of higher generation dendron wedges on to the core is tedious due to the involvement of steric hinderance.



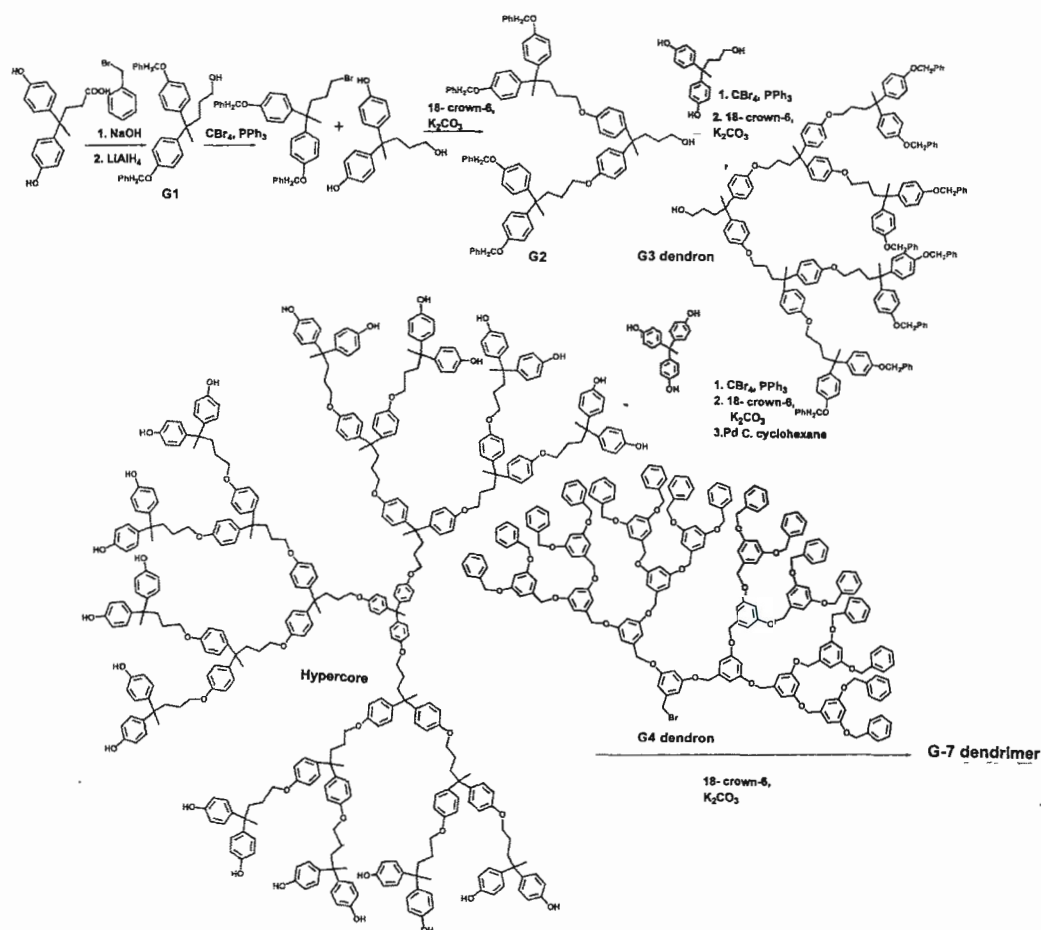
Scheme 1-4 Synthesis of poly benzyl ether dendrimers by convergent method.

1.4.2 Accelerated approaches for dendrimer synthesis: With the increasing popularity of dendrimers and their great potential in many vibrant fields, the scientific community sensed the urgency of highly efficient alternative synthetic protocols for their development. The last few years have seen exponential increase in the number of publications and patents in the field of dendrimer chemistry but not many dendrimers have successfully fulfilled the commercial requirements. The classical approaches used for dendrimer synthesis are very long, tedious and time consuming.

In addition, huge excess of reagents make the purification troublesome. On an average, two synthetic steps are required for each generation growth, for example, at least ten reaction steps are needed to construct a 5th generation PAMAM dendrimer. The situation becomes even more demanding in the case of high generation dendrimers. Therefore, innovative synthetic protocols are desired which can provide the shortest possible route by decreasing the number of reaction steps.

1.4.2.1 Double stage convergent method: To improve the existing strategies and for rapid synthesis of high generation dendrimers, first attempt was done by Fréchet and coworkers in 1990 who developed double-stage convergent method.⁵⁶ To build high generation dendrimers using divergent methodology can lead to imperfect dendrimers due to the presence of huge number of end groups involved in chemical conjugation and, on the other hand, with convergent approach steric factors are involved due to the use of bulkier dendrons. This double stage convergent approach was the combination of convergent and divergent strategies where generation 3 flexible dendrons were prepared with protected peripheral groups (Scheme 1-5). During the next step these dendrons were clicked on the multifunctional core through the focal points. Subsequent deprotection of terminal groups yielded generation 3 flexible dendrimer with large number of reactive termini on the surface, which was further reacted with chemically different more rigid 4th generation dendron in a divergent manner to provide a perfect generation 7 dendrimer in 61% yield. The constructed dendrimer consists of two different layers, a flexible inner layer and a rigid outer layer; and due to heterogeneous layers was known as layer block dendrimer. The success of this approach lies in the deliberate selection of flexible hypercore made up of longer spacers which reduces the impact of steric hindrance. The other advantage provided by this approach was the less number of reactive end groups at the periphery of hypercore as compared to numerous groups in divergent approach which insures the formation of perfect dendrimer. The drawback of this strategy is that it was not able to minimize the number of reaction steps as a lot of reaction steps were still

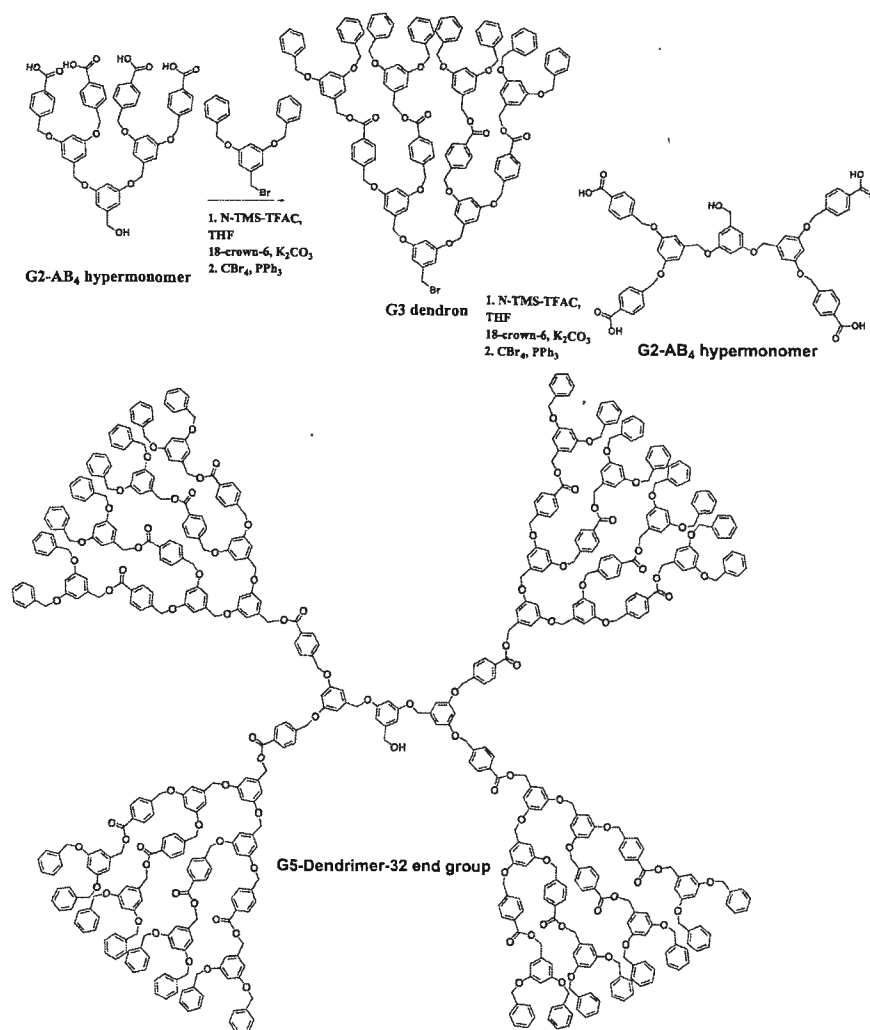
required for the synthesis of dendrons and hypercore which were constructed using classical methods. Due to this reason it is not an extensively used method for dendrimer synthesis.



Scheme 1-5 Schematic representation of synthesis of G7 layer block dendrimer using double stage convergent method.⁵⁶

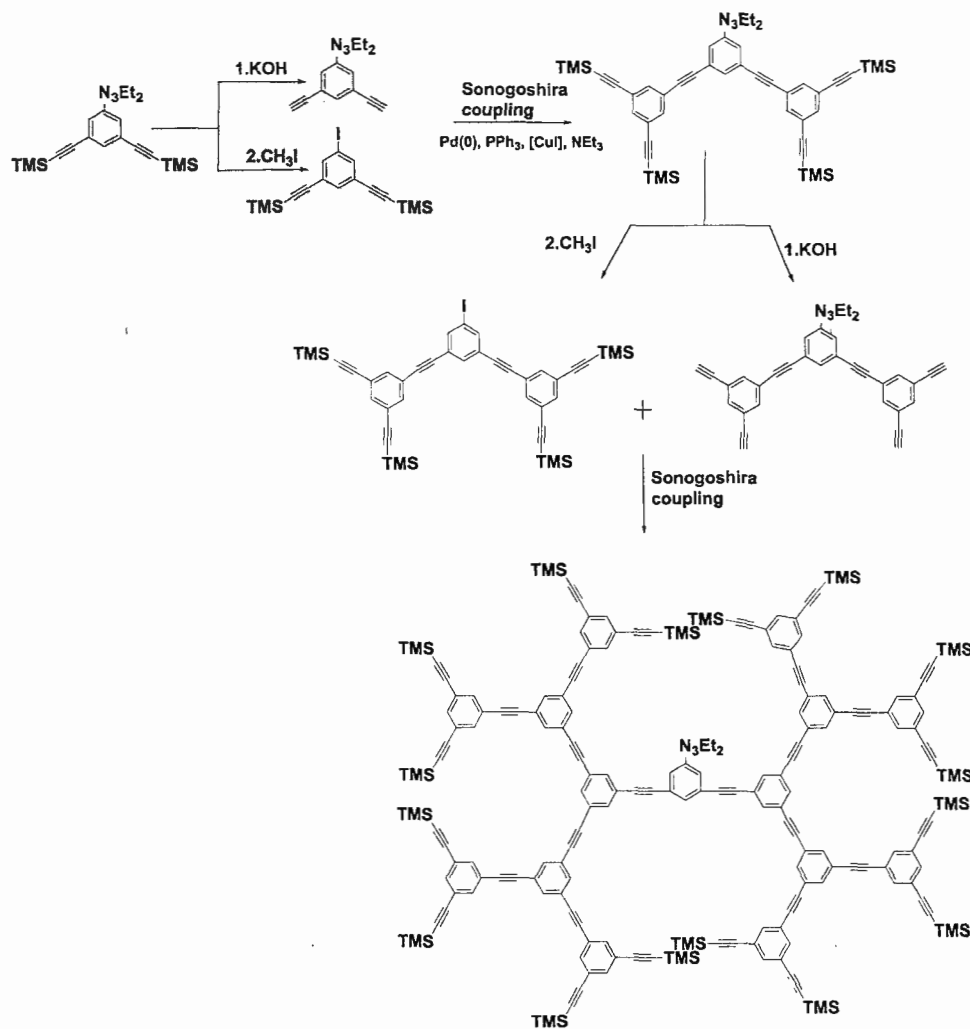
1.4.2.2. Hypermonomer strategy: In contrast to classical methods where generally AB₂ and AB₃ monomers are explored, hypermonomer strategy employs the use of denser monomers like AB₄, AB₅ and AB₈ which result in dendrimers with huge number of end groups in fewer steps. Most commonly the lower generation dendrons are used as hyper monomers. This strategy was first reported by Fréchet and co-

workers where they successfully constructed fifth generation poly-aryl dendrimer reacting generation 2 AB₄ hypermonomer and generation 3 dendron having 8 benzene rings on the periphery (Scheme 1-6).⁵⁷ Although this strategy exponentially increased the number of end groups and resulted in high molecular weight dendrimers but it couldn't remove protection/deprotection steps. In addition, it requires additional steps for the syntheses of hypermonomers. Hence, this is not a frequently employed strategy for dendrimer synthesis.



Scheme 1-6 Schematic representation of synthesis of poly benzyl ether dendrimer by hypermonomer method.⁵⁷

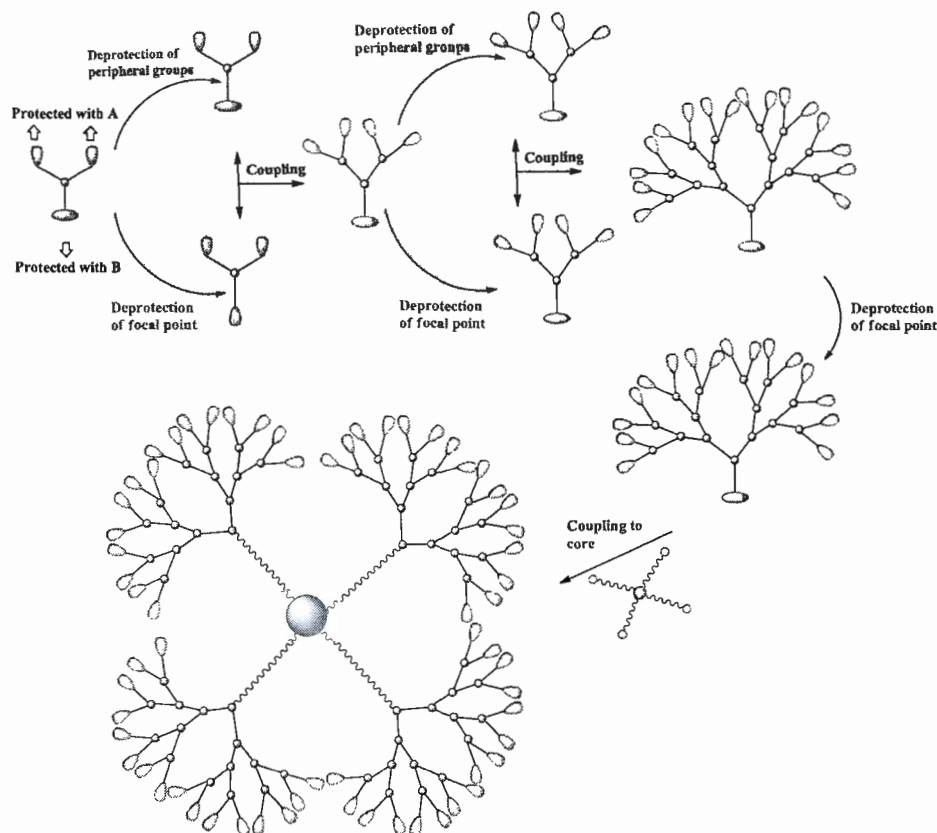
1.4.2.3. Double exponential method: This elegant accelerated approach was designed by Moore and co-workers in 1995 where they obtained generation 4 poly-phenyl acetylene dendrimer in a rapid manner (Scheme 1-7).⁵⁸



Scheme 1-7 Construction of G4 polyphenylacetylene dendrimer by double exponential method.⁵⁸

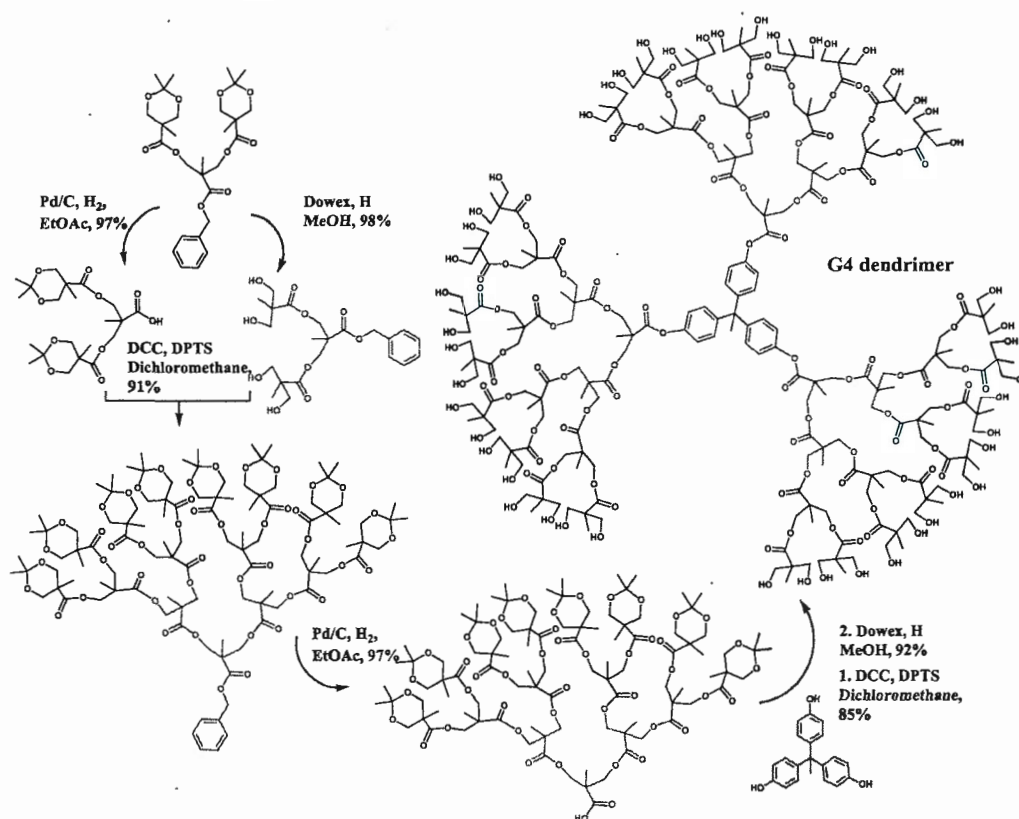
This method requires an AB₂ monomer in which peripheral groups and the focal point is protected with different protecting groups (Scheme 1-8). These protecting groups can be cleaved selectively under different chemical conditions, which results in two different sets of periphery activated and focal point activated monomers. These

two monomers are coupled together to obtain a higher generation protected dendron which is finally stitched to the active multifunctional core. A coupling reaction between a second generation focal point activated dendron and second generation periphery activated hypermonomers can provide 4th generation dendron. Notably, there is a generation jump after every iterative sequence of activation and coupling. This strategy is excellent for the construction of higher generation dendrimers as number of steps are reduced considerably due to a generation jump. As this strategy was the combination of divergent and convergent approaches, the drawbacks of both the strategies were present. Steric hindrance is the limiting factor for the synthesis of high generation dendrimers and the protection/deprotection of different protecting groups requires highly selective reactions.



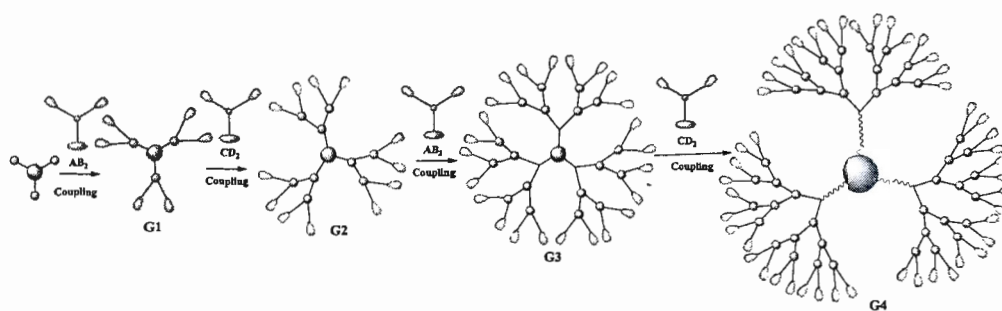
Scheme 1-8 Construction of dendrimers by double-exponential method.

Hult and co-workers used double exponential strategy for the formation of 4th generation 2,2-bis(methylol)-propionic acid (bis-MPA) based polyester dendrimers (Scheme 1-9).⁵⁹ A second generation dendron was first constructed by convergent method which consisted of two acetonide protected peripheral groups and a focal point protected with benzyl group. Chemoselective deprotection of the dendron yielded two different monomers, one having free peripheral hydroxyl groups with protected focal point, and the other having free acid group with protected periphery. These two monomers participated in an esterification reaction to yield high generation dendron. Using sequential deprotection and esterification, a 4th generation acetonide protected bis-MPA monodendron was produced which was further conjugated to a triphenolic core in a divergent fashion. Final deprotection step yielded a 4th generation bis-MPA dendrimer having 48 hydroxyl groups on the periphery.



Scheme 1-9 Synthesis of G4 dendrimer using double-exponential method.⁵⁹

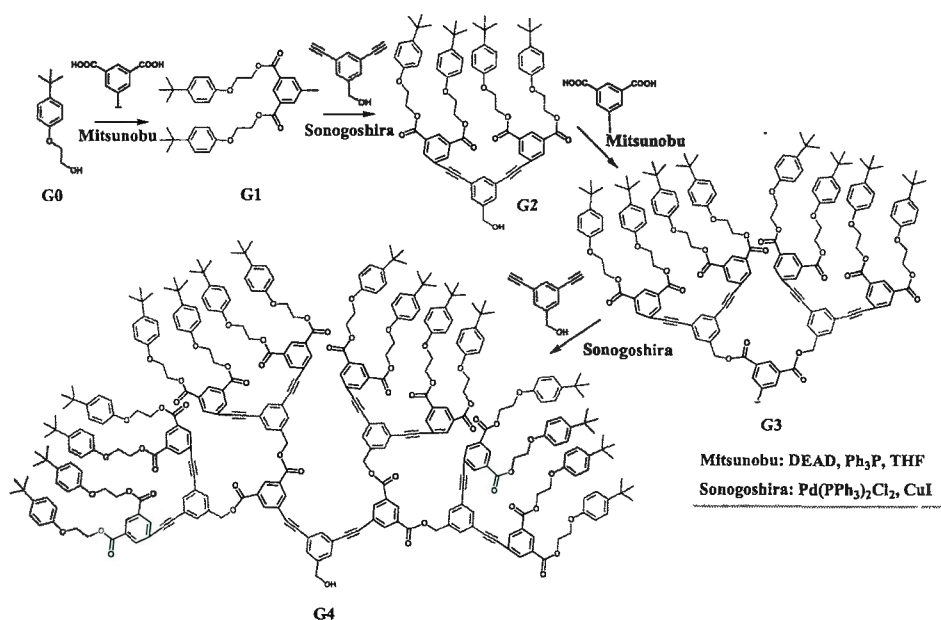
1.4.2.4. Orthogonal accelerated synthesis: The concept of orthogonality was given by Barany and Merrifield in 1977.⁶⁰ According to this concept a particular protecting group can be selectively removed from a group of protecting groups by different chemical mechanism. Orthogonal accelerated synthesis involves convergent or divergent growth by employing two types of different AB_n (AB_2 , CD_4) monomers which are harbouring chemoselective functional groups (Scheme 1-10). These functional groups should be selected in such a manner that the peripheral groups of one monomer will react only with the focal point of other monomer. For example, it has been depicted in the scheme below where A group from AB_2 can only react with the D group in CD_2 and B can only react with C, by involving two different chemoselective chemical reactions. This kind of orthogonal approach removes the need of protection and deprotection steps, and provides much shorter synthetic routes which makes dendrimer synthesis less tedious and more economical. This type of strategy is very efficient for the construction of high generation dendrimers as every reaction step provides a new generation having exact double number of functional groups than the previous generation. The use of monomers with high branching like AB_4 , AB_5 , AB_6 and AB_7 , can generate high density dendrimers at lower generations which can be useful for various applications.



Scheme 1-10 Synthesis of G4 dendrimer using orthogonal accelerated approach.

The orthogonal strategy was proposed by Spindler and Fréchet back in 1993, who synthesized poly(ether urethane) dendron using 3,5-diisocyanatobenzyl chloride and 3,5-dihydroxybenzyl alcohol as orthogonal monomers.⁶¹ A combination

of Williamson etherification and urethane formation reaction (between isocyanate and alcohol) was selected for this one pot transformation. Unfortunately, because of low chemoselectivity and potency, these reactions couldn't succeed to deliver high generation dendrimers. The first successful attempt for orthogonal strategy was provided by Zimmerman and Zeng in the year 1996 where 6th generation dendrimer was synthesized with this methodology by the combination of two orthogonal coupling reactions *i.e.* Mitsunobu and Sonogoshira coupling (Scheme 1-11).⁶² Using two orthogonally different monomer, 4th generation dendrimer was synthesized in just four steps. This path breaking work of Zimmerman and co-workers was followed by many reports where numerous new combinations of different highly chemoselective, robust and high yielding reactions were explored. Malkoch and co-workers⁶³ developed accelerated approach where they used the cocktail of chemoselectivity with highly efficient chemical transformations. A combination of CuAAC and etherification reactions was used to for the successful formation of generation 4 bis-MPA and Fréchet type dendrimer.



Scheme 1-11 Orthogonal accelerated synthesis of generation 4 dendron using Mitsunobu and Sonogoshira reactions.⁶²

1.4.3. The 'Click' chemistry concept: Dendrimer synthesis has been a very tedious task and usually requires an excess of reagents. The situation becomes more difficult when the building blocks require multistep syntheses. Moreover, the reactions which show high efficiency and great yields for the synthesis of lower generation dendrimers, can become inefficient for multiple sites in case of higher generation dendrimers, and lead to imperfect structures. Recently, the introduction of "click chemistry" to dendrimer synthesis has benefitted the field in various ways.⁶⁴⁻⁶⁸ The "click chemistry" involves the group of reactions which have high yields, high atom economy, can be performed in a variety of solvents, have tolerance to a wide range of functional groups and have minimum side products.⁶⁹ The emergence of "click chemistry" has brought a revolution in the synthesis of dendrimers.

1.4.3.1. Cu (I) catalyzed alkyne-azide click (CuAAC): Although a number of reactions fall in the category of click chemistry, CuAAC is the most famous click reaction which fuses together an azide and alkyne stereospecifically to yield 1,4 triazoles. During the last decade it has become a cornerstone for the scientific community. It was first reported by Meldal⁷⁰ in 2001 and published by Kolb⁶⁹ at the same time. Historically 1,3 dipolar cycloaddition to form 1,2,3 triazoles was first introduced by Huisgen in 1963 but it was not explored due to requirement of high reaction temperature and pressure, and formation of mixture of 1,4 and 1,5 regioisomers as the products. The addition of Cu(I) not only accelerated the rate of reaction by 10^7 but also made it regiospecific. CuAAC is a very powerful reaction which is having inherent potential to generate rapid libraries of molecules in medicinal chemistry and due to this feature it has become a very desirable reaction in pharmaceutical industry.

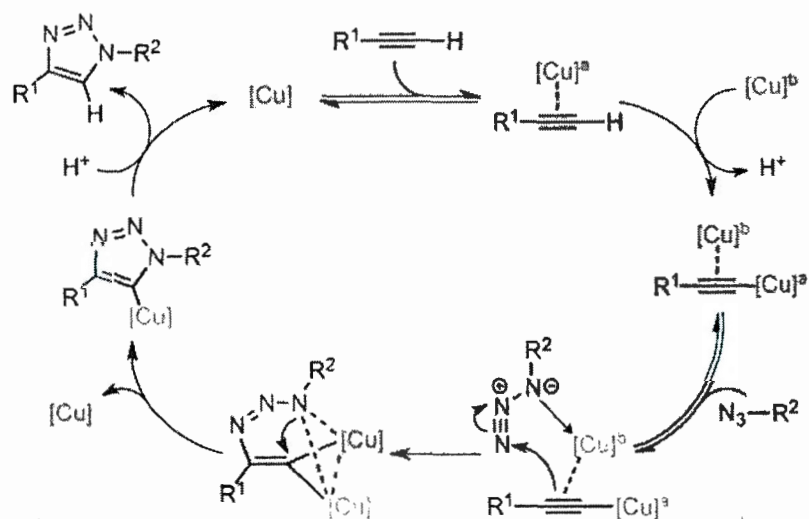
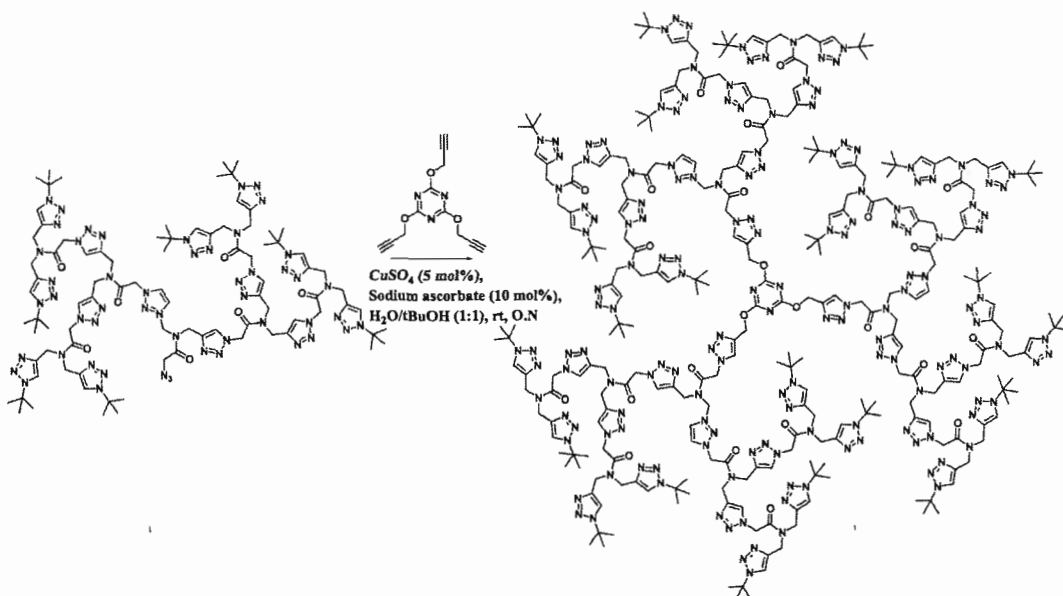


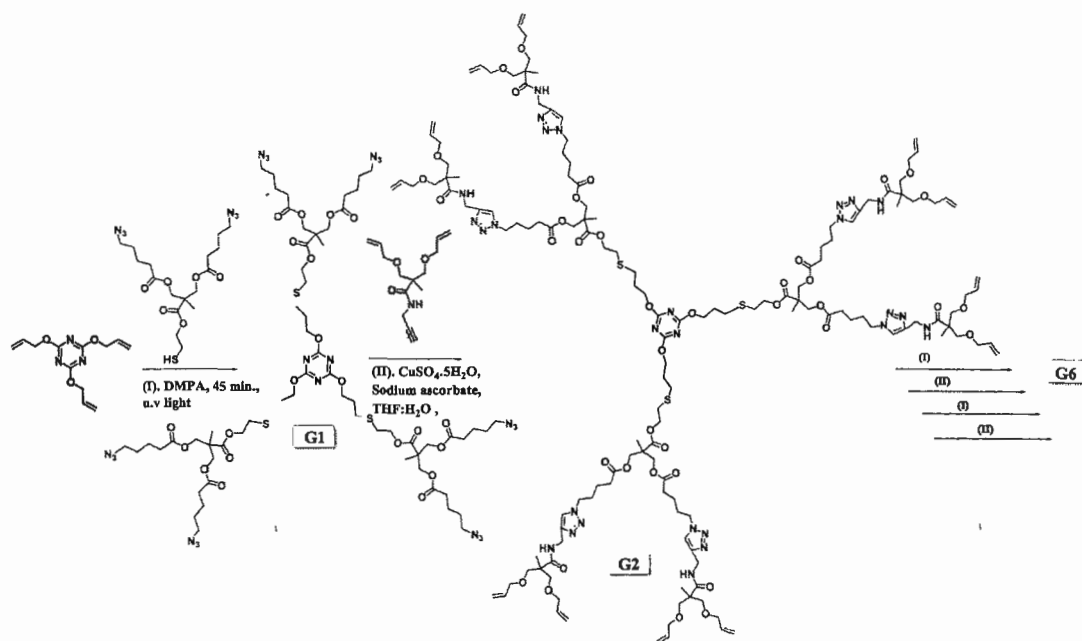
Figure 1-10 Proposed mechanism for CuAAC click reaction.⁷¹

The click chemistry was introduced to dendrimers synthesis by the groups of Hawker, Sharpless, and Fokin.⁷² They constructed generation 4 dendrimer in a convergent way using CuAAC reaction in high purity and excellent yield (Scheme 1-12). The synthesis involved the construction of generation three dendron with chloride functional group which was subsequently converted to an azide to participate in click reaction. The dendron was further clicked on to a polyacetylene core to obtain generation 4 triazole dendrimer in a convergent way. Since then the click reaction has been extensively utilized both in the convergent and divergent synthesis of dendrimers as well as for their peripheral functionalization.⁶⁴



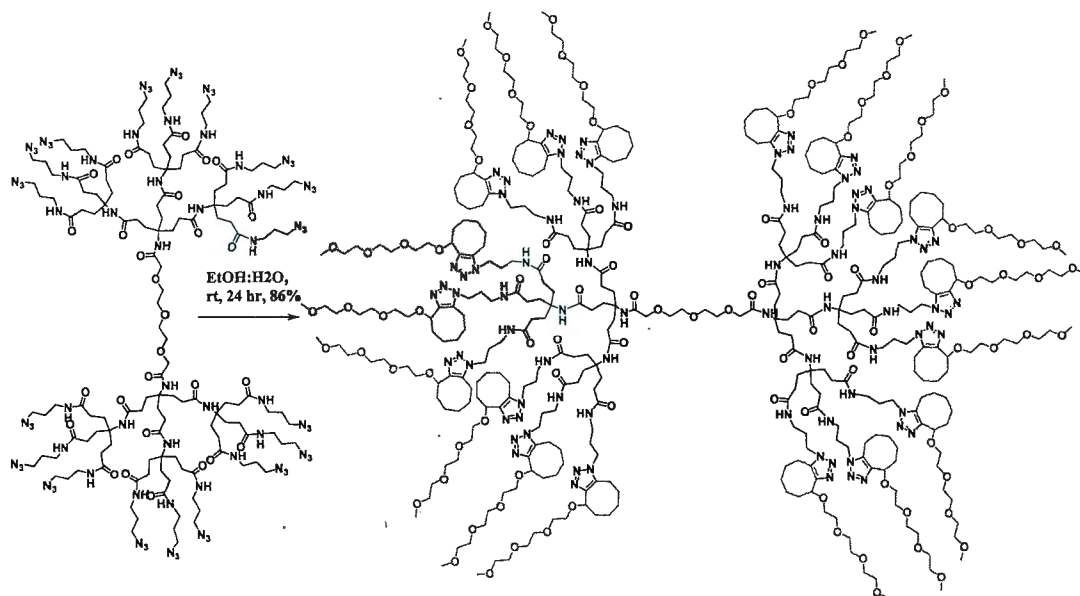
Scheme 1-12 Convergent synthesis of triazole dendrimers by copper(I) catalyzed alkyne-azide click reaction.⁷²

Hawker and co-workers further exploited the potential of CuAAC and claimed to synthesize 6th generation dendrimer within a day.⁷³ For the construction of dendrimers, two different orthogonal building blocks AB₂ and CD₄ were synthesized. Thiol-ene reaction was first performed reacting AB₂ monomer with tri-allyl core which resulted in G1 dendrimer consisting of six azido peripheral functionalities. The reaction was catalyzed photochemically by employing uv light and 2,2-dimethoxy-2-phenylacetophenone as initiator. During the next step, CuAAC was performed using CD₂ monomer in which the propargyl group was reacted with 6 azido moieties on G1 dendrimer providing G2 dendrimer with 12 allylated groups. Repetition of thiol-ene and click chemistry in sequence yielded 6th generation dendrimer with high yield and high purity (Scheme 1-13). The combination of both click reactions and orthogonal building blocks provided high generation dendrimers within a day and proved that high generation dendrimers can be acquired with ease by opting highly efficient chemical transformation and orthogonal monomers.



Scheme 1-13 Synthesis of generation 6 dendrimer *via* thiol-ene and CuAAC click reactions.⁷³

Although click chemistry contributes as a potential synthetic tool towards dendrimer synthesis, however the cytotoxicity of copper is a major drawback of this reaction for biological applications. To overcome this issue, significant modifications have been done, for example, the addition of copper sequestering agents and the use of copper wire, but none of these methods could result in completely copper free products, which resulted in limited use of this reaction for biomedical purposes.^{74, 75} To address this issue, Bertozzi and coworkers have developed an interesting strain promoted copper free click reaction for covalent modification of biomolecules.⁷⁶ This reaction works by the release of ring strain in a cycloalkyne precursor and ultimately lowers the activation energy for the cycloaddition process. Weck and coworkers first reported the use of strain promoted azide-alkyne click (SPAAC) reaction for dendrimer synthesis.⁷⁷ Employing SPAAC strategy they were able to synthesize cyclooctyne functionalised Poly (amide) based dendrimers with high yields, under mild reaction conditions.

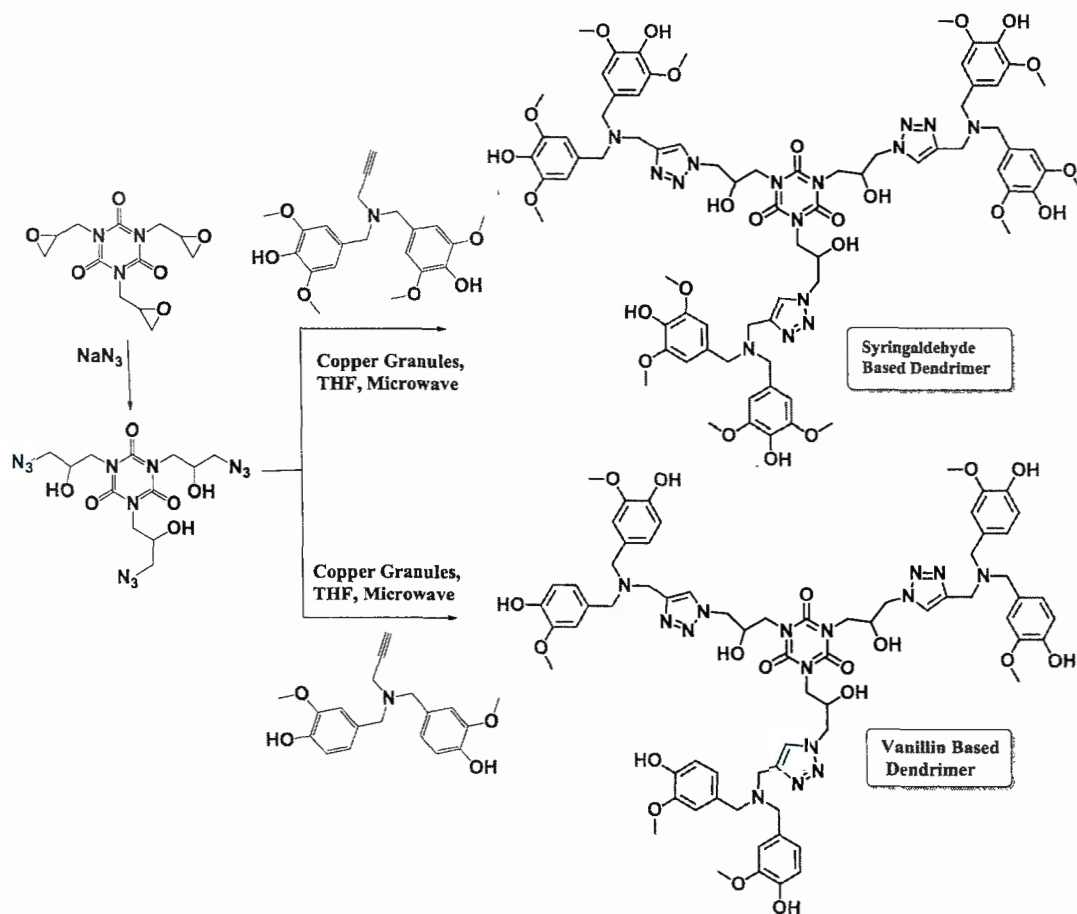


Scheme 1-14 Synthesis of dendrimers using SPAAC strategy.⁷⁷

The absence of residual copper makes this mild and metal free reaction a highly useful tool to construct biomaterials. They used functionalized cyclooctynes as strained alkynes to facilitate the reaction without the addition of Cu(I) catalyst to construct poly(amide) based dendrons and dendrimers. (Scheme 1-14). Although SPAAC is becoming more and more popular in the recent time, still it has some disadvantages. 1) It is not as quick as copper catalyzed reaction. 2) The reaction provides mixture of regioisomers *i.e.* 1,4 and 1,5 triazoles. 3) It involves the multistep synthesis to construct cyclooctyne based building blocks and moreover, multiple cyclooctyne rings are introduced in the molecule. There is no doubt that copper catalyzed click is a better chemical transformation and clearly stands out of these existing non metal based methods.

Recently, Syringaldehyde- and vanillin-based dendrimers have been reported by Du and co-workers where copper granules were employed for azide-alkyne click (Scheme 1-15).⁷⁸ The reactions were performed using microwave energy as there was no reaction observed at room temperature and upon refluxing. Microwave energy accelerated the rate of reactions and yielded generation one dendrimers with more

than 90% yield after 8 hrs. ICP-MS analysis showed negligible amounts of copper. The reaction provided products without the use of any reducing agents. The reaction was sluggish and took almost 8 hrs for only 3 click conjugations under microwave. The situation would become more difficult when multiple click reactions have to be performed or higher generation dendrimers are pursued. This methodology is also not suitable for microwave sensitive substrates.



Scheme 1-15 Microwave assisted synthesis of polyphenol dendrimers using copper granules.⁷⁸

1.4.3.2. Thiol-ene click (TEC): The click reaction which is emerging very rapidly in the field of dendrimer synthesis as an alternative of CuAAC is metal free thiol-ene click reaction.⁷⁹⁻⁸² It is indeed a very efficient reaction having comparable qualities to the CuAAC. Thiol-ene reaction was discovered almost 100 years ago and has been

used in making crosslinked networks. This reaction proceeds by the addition of thiol radicals to non-activated double bonds either thermally or photochemically in an anti-Markovnikov's fashion to yield thioethers (Figure 1-11). Although radical initiation can be achieved by employing u.v light of 254 nm by homolysis of sulphur and hydrogen bond, but for faster radical generation a variety of photoinitiators are used and most commonly used ones are benzophenone and DMPA. This reaction like CuAAC click is highly efficient, modular, orthogonal to wide range of functional groups, easy to execute, does not need inert environment, and sometimes can even be performed without solvent. Moreover, this reaction does not require the use of toxic transition metal catalysts.

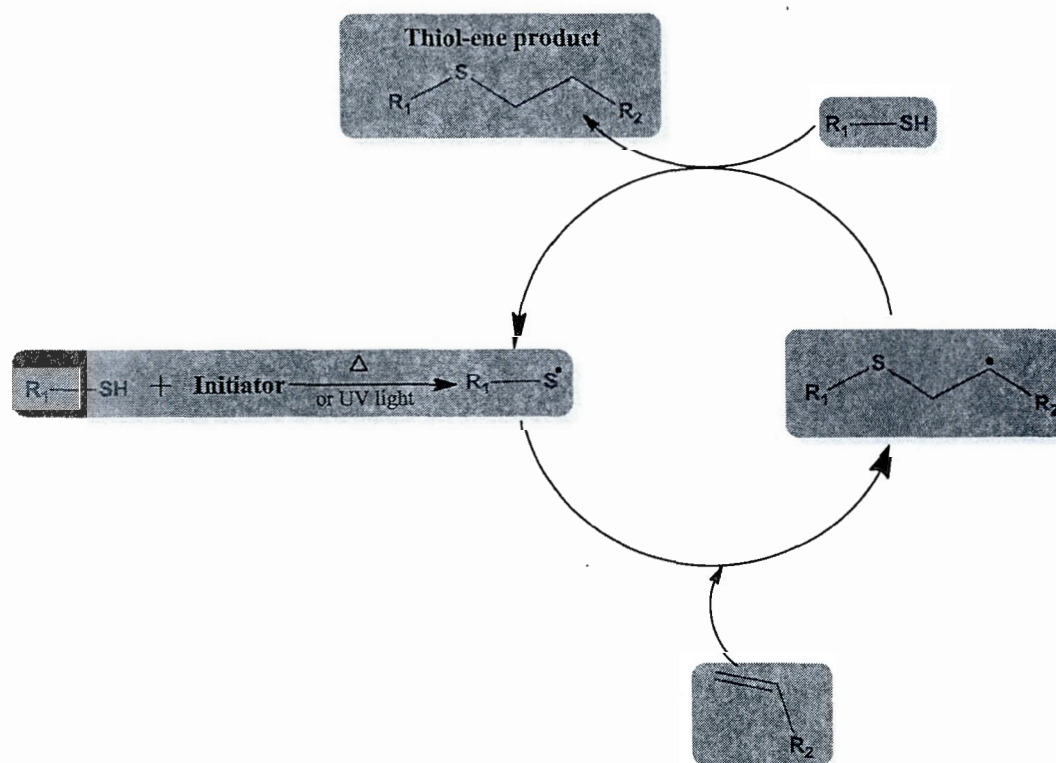
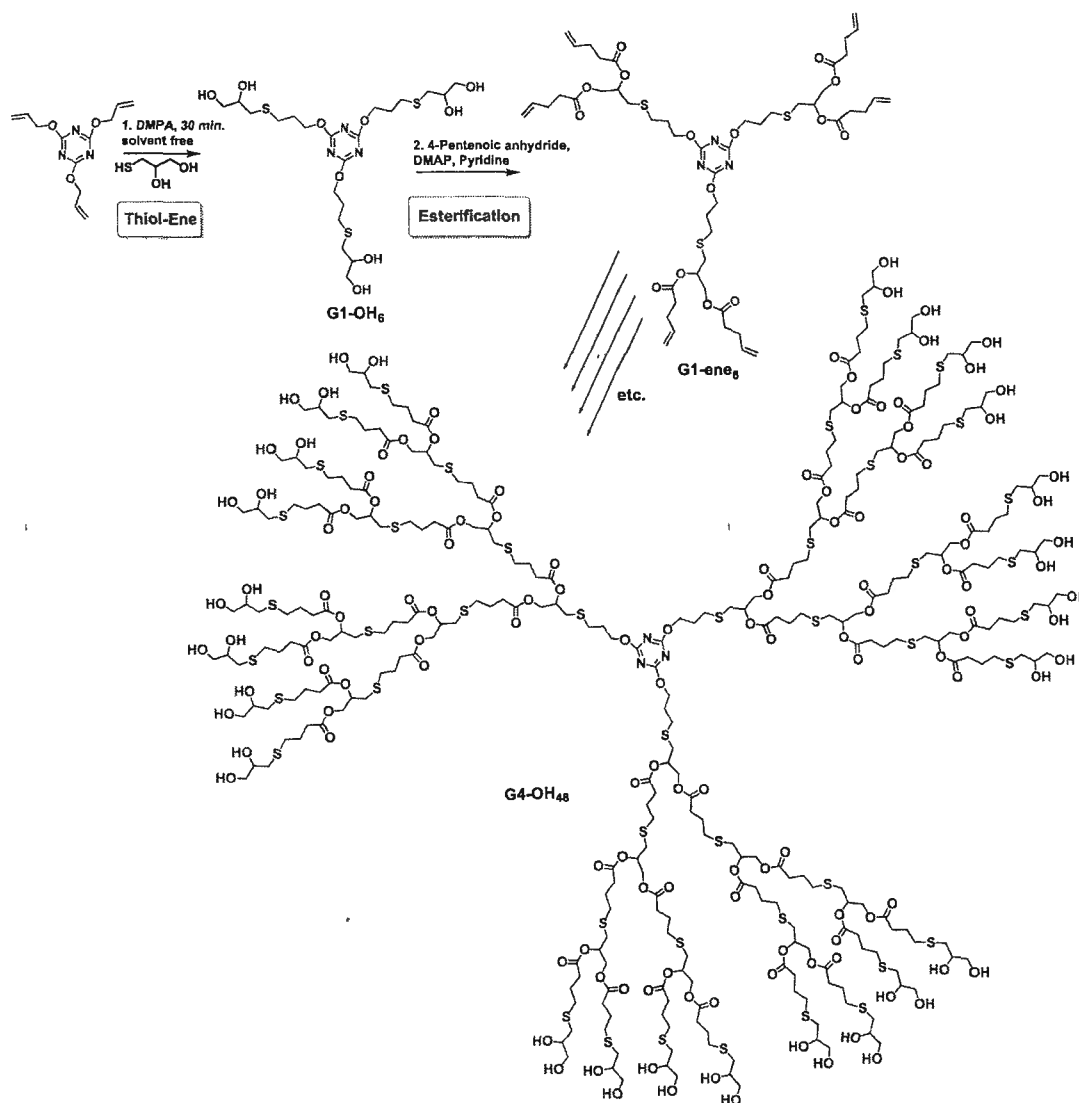


Figure 1-11 Mechanism of radical mediated thiol-ene click reaction.

Thiol-ene reaction was used recently by Hawker and coworkers for dendrimer synthesis and they reported the successful synthesis of 4th generation poly(thioether) dendrimers in 8 steps using commercially available monomers.⁸² Synthesis of

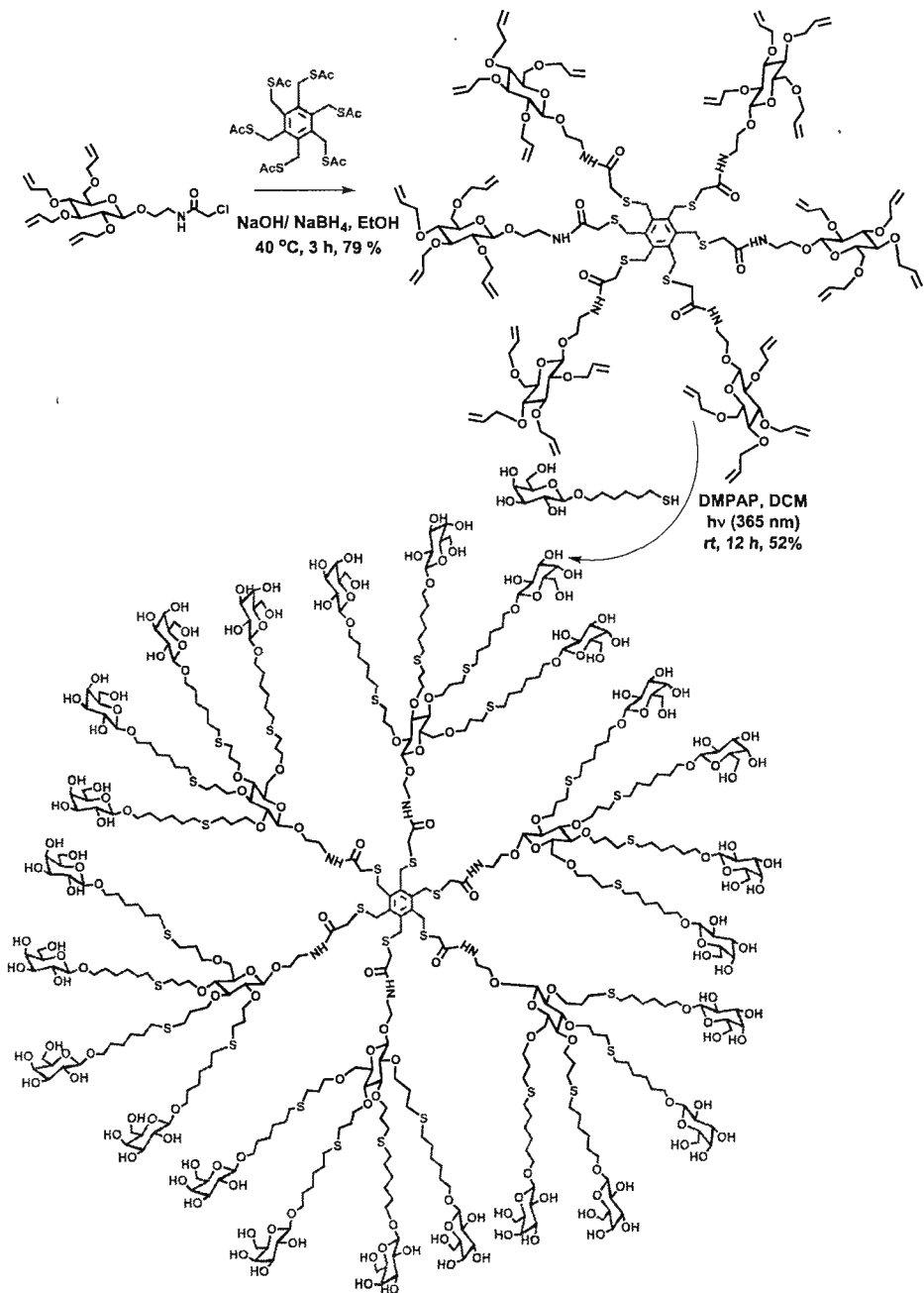
dendrimer was started with 2,4,6-triallyloxy-1,3,5-triazine selected as a core molecule on which photoinitiated thiol-ene was performed using thioglycerol as AB₂ monomer in the presence of trace amount of 2,2-dimethoxy-2-phenylacetophenone as photoinitiator. The reaction was carried out neat under u.v light of 365 nm for 30 minutes which provided G1 dendrimer harbouring 6 peripheral hydroxyl groups in quantitative yield. In the next step, 6 hydroxyl end groups of G1 dendrimer were utilized in esterification reaction with 2,4-pentenoic anhydride to yield G1 dendrimer having 6 alkene peripheral groups. The repeated sequence of thiol-ene and esterification was performed to synthesize 4th generation poly(thioether) based dendrimer (Scheme 1-16).

Roy and coworkers developed an accelerated orthogonal approach by combining thiol-ene chemistry and SN₂ reaction to construct multifunctional glycodendrimers.⁶⁸ They constructed two different orthogonal AB₄ monomers (Scheme 1-17). First monomer consisted of a chloroacetyl group as a focal point with 4 allyl groups on the periphery while the other was a thiogalactoside consisting of -SH focal point and 4 hydroxyl groups on the surface. The synthesis began around A₆ hexaacetylated core by performing SN₂ reaction using tetraallylated AB₄ precursor



Scheme 1-16 Synthesis of generation 4 dendrimer *via* thiol-ene click and esterification reaction.⁸²

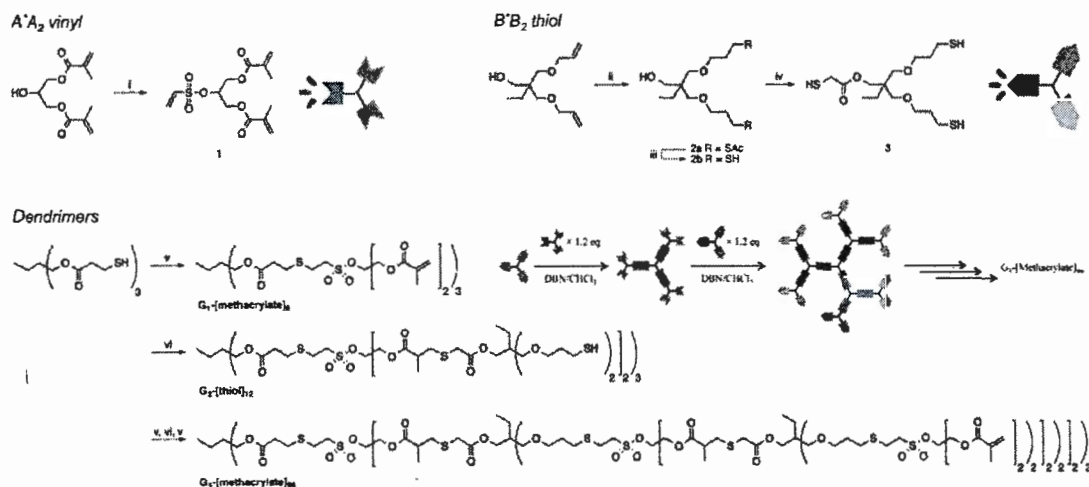
yielding 24 alkene groups at G1 stage. In the next step, thiol-ene reaction between thiogalactoside monomer and G1 dendrimer yielded 2nd generation glycodendrimer harbouring 24 galactose on the periphery. No protection/deprotection steps were required throughout the process and monodisperse dendrimers were achieved with great ease in decent yields.



Scheme 1-17 Synthesis of G2 glycodendrimer with 24 galactose units at the periphery.⁶⁸

During last 5 years, there has been a tremendous growth in the number of publications where thiol-ene click is involved in generating wide variety of dendrimers and polymers. The scientific community has declared it as a powerful alternative of copper catalyzed click reaction because it doesn't require any metal catalysts. This reaction has its own limitations and drawbacks. The excess of thiols used in the reaction cause problem by making disulfide and other impurities. The reaction produces certain percentage of Markonikov's addition product which is usually not highlighted by the researchers.⁶⁵

1.4.3.3. Thiol-Michael addition click: The thiol-Michael addition reaction is another highly efficient and modular thiol mediated click reaction that has been extensively implemented for polymer synthesis and functionalization.^{80, 83, 84} It is a reaction between a thiol and an electron-deficient vinyl group that can be carried out under benign and solventfree conditions using mild catalysts. Bowman and coworkers have recently reported the use of kinetically selective thiol-Michael addition reaction for the synthesis of dendrimers and dendritic linear polymer conjugates.⁸⁵ This was the first example where dendrimers were synthesized using single chemistry without carrying out any protection/deprotection steps. They designed A^*A_2 vinyl and B^*B_2 thiol based monomers with three functional groups, with one functional moiety selectively having much higher reactivity than the other two, and were successfully able to construct fifth generation dendrimer with 96 end groups in less than half a day using solely single chemistry (Scheme 1-18).



Scheme 1-18 Synthesis of fifth generation dendrimer *via* thiol-Michael addition click reaction.⁸⁵

1.4.3.4. Thiol-yne click: Thiol-yne reaction is another efficient reaction which possesses the features of click chemistry.^{65, 66, 86-88} Thiol-yne is more than a 100 years old reaction and can also be considered as a sister reaction of thiol-ene click; the only difference is the double hydrothiolation addition around the alkyne (Figure 1-12).

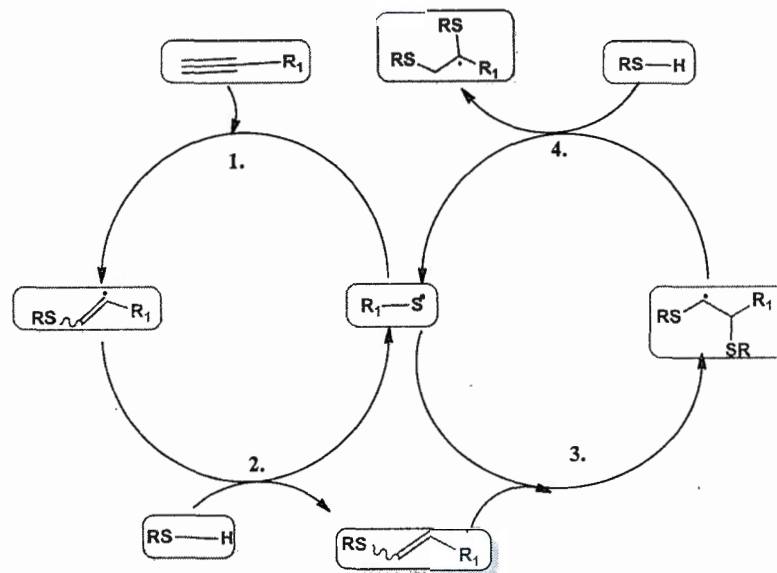
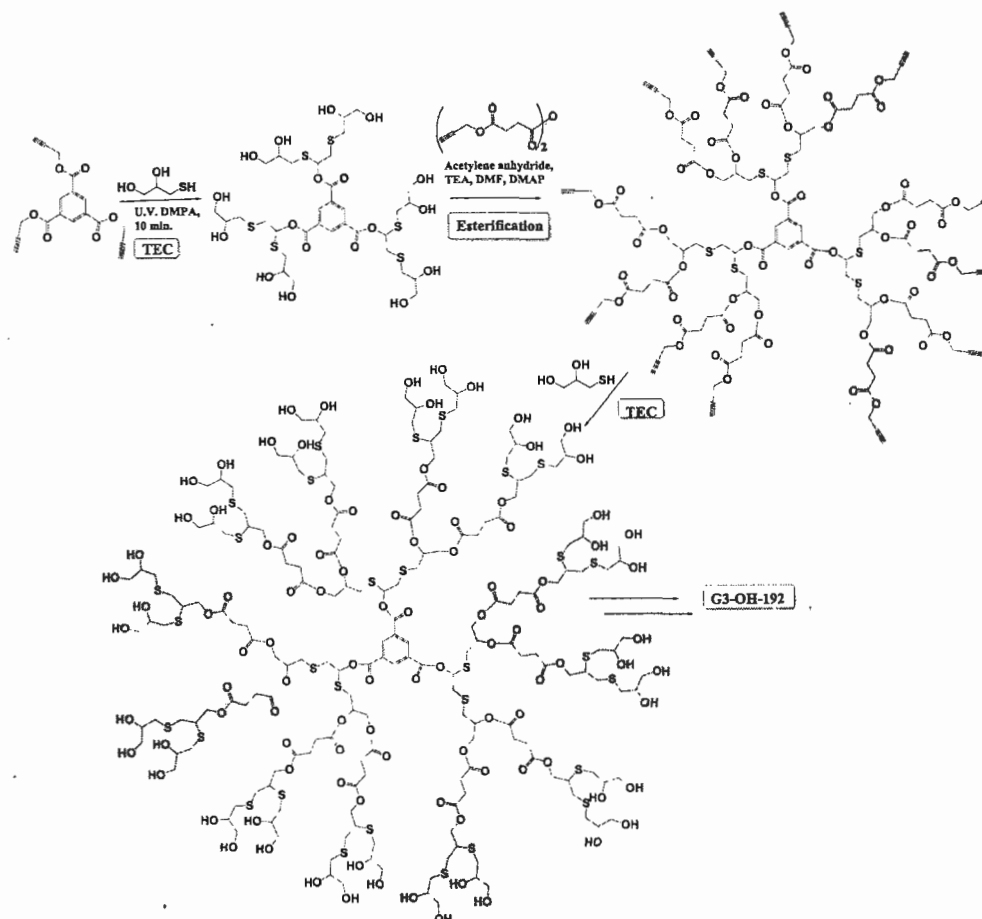


Figure 1-12 Mechanism of radical mediated thiol-yne click reaction.

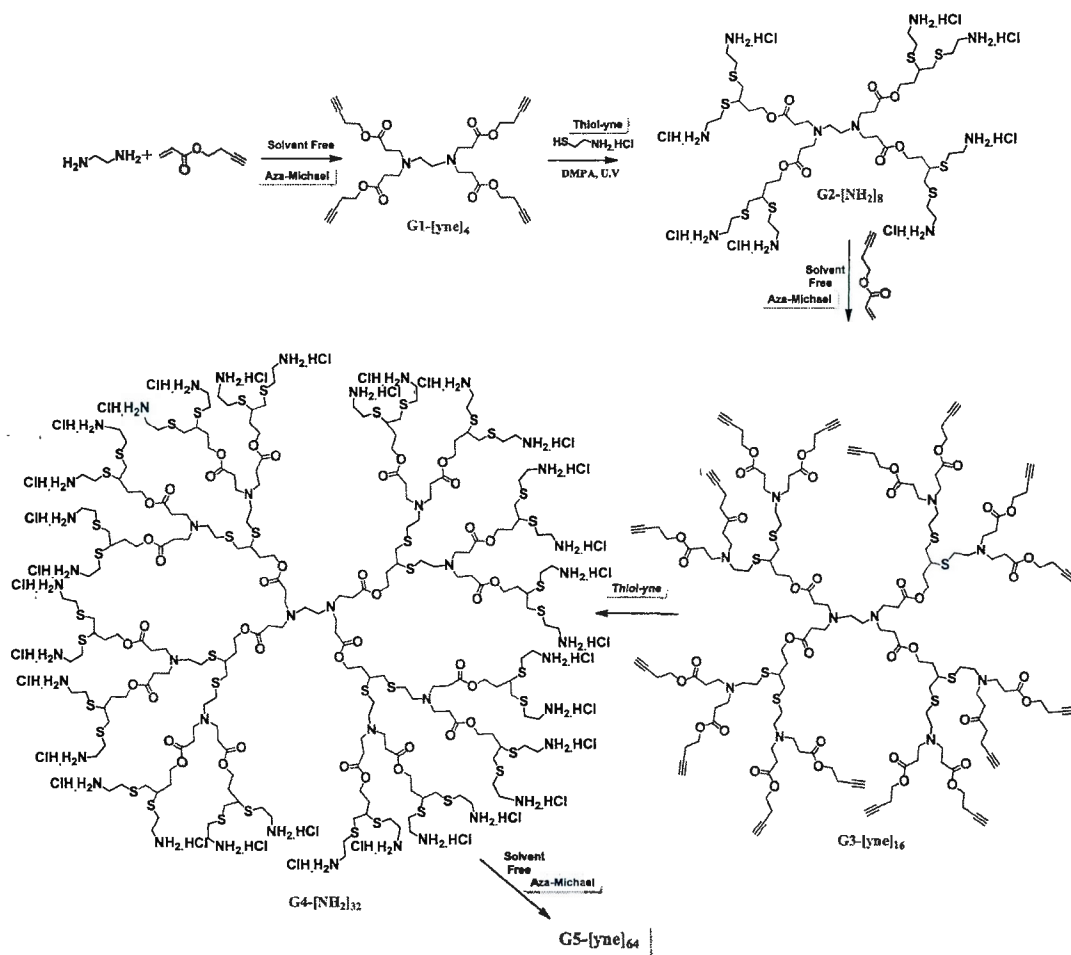
Thiol-yne reaction is the new entry in the family of click reactions because it possesses many traits of the click reactions and it can be a very handy tool for generating novel multifunctional dendritic structures. Radical initiation can be introduced *via* photochemical and thermal sources. Radical mediated thiol-yne polymerisation is already a popular method to make hyperbranched polymers that has potential applications in drug delivery, gene therapy and catalysis. Recently, this reaction was explored for the first time for the construction of dendrimers by Stanzel and coworkers.⁸⁶ Third generation (G3) dendrimers were synthesised in a divergent manner using the combination of photochemical addition of thiol to alkyne (thiol-yne) and base catalyzed esterification reaction in five synthetic steps (Scheme 1-19). The first reaction was carried out around benzene core having three acetylenes on the periphery using commercially available 1-thioglycerol in the presence of DMPA as photoinitiator under u.v light (365 nm). The reaction was very quick and delivered G1 dendrimer having 12 peripheral hydroxyl groups. Thiol-yne reaction was followed by esterification with acetylene anhydride which helped in anchoring the same number of alkynes as the peripheral functional groups. Repeating both reactions in sequence provided final G3 dendrimer with 192 hydroxyl end groups with decent yield. Unlike other click reactions, thiol-yne introduces two functionalities around one acetylene and because of this particular advantage thiol-yne is the perfect choice for accelerated synthesis of dendrimers.



Scheme 1-19 Synthesis of G3- Hydroxyl dendrimer with 192 end groups.⁸⁶

In one recent report, 5th generation dendrimer has been synthesized only in five steps using a combination of highly efficient thiol-yne and aza-Michael addition reaction.⁸⁷ Aza-Michael addition reaction is also very efficient and an orthogonal reaction which possesses the characters of a click reaction. The reaction is easy to execute as well as having high tolerance for a variety of functional groups. The use of two orthogonal reactions resulted in high generation dendrimers in facile and highly efficient manner. The purifications were very easy requiring only precipitation and extraction. The synthetic protocol was followed under benign reaction conditions without the use of any transition metal catalyst. Moreover, thiol-yne was performed in a solvent free

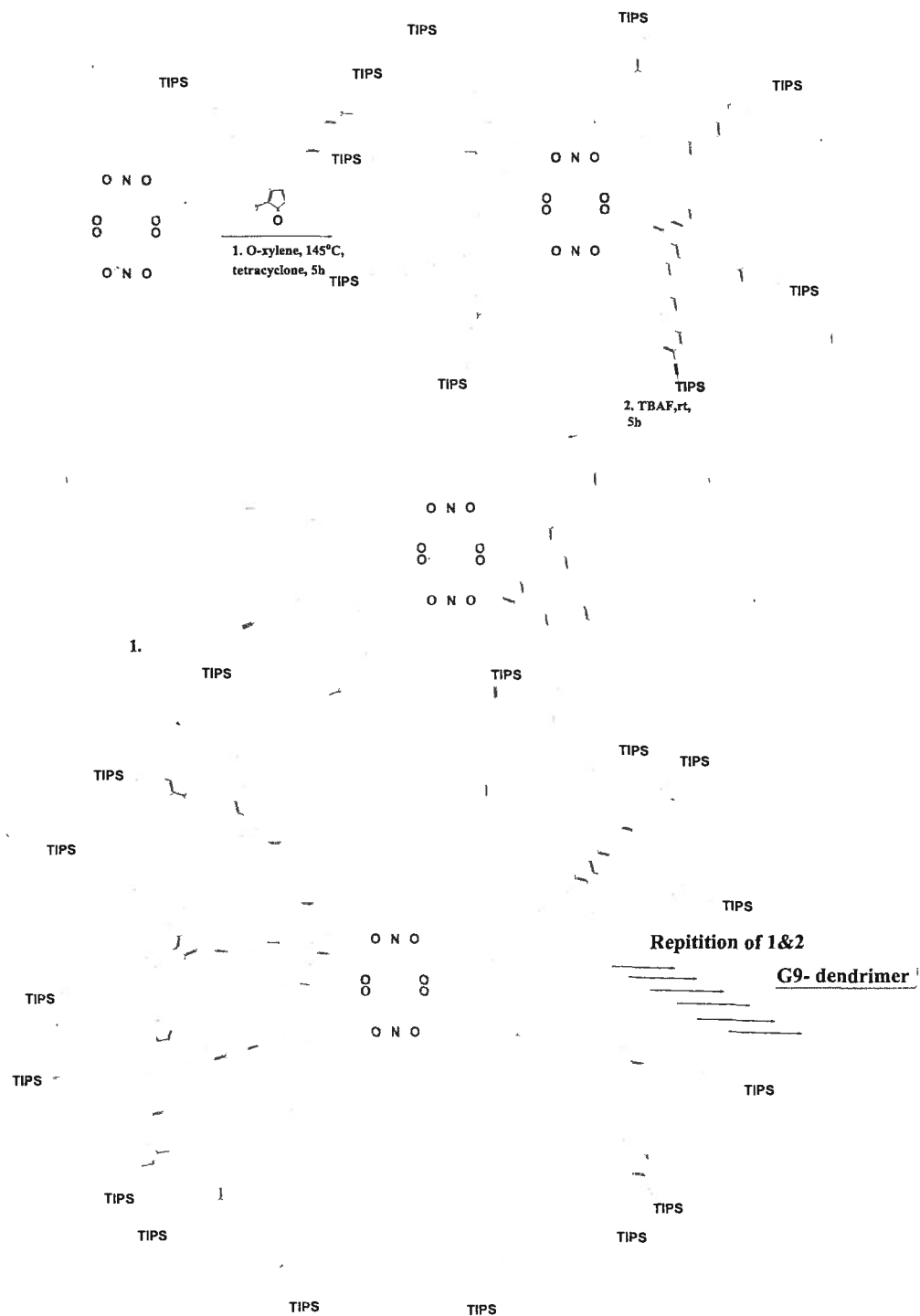
environment providing a greener approach for dendrimer chemistry (Scheme 1-20).



Scheme 1-20 Synthesis of G5 dendrimer using thiol-yne and aza Michael addition reaction.⁸⁷

There are a few drawbacks for thiol-yne reaction also. Thiol-yne addition is generally slower than the thiol-ene reaction because of double hydrothiolation and thus requires high excess of thiols to ensure the completion of reaction. The excess of thiols results in the formation of disulfide and other side products. Another disadvantage is that the dithiolation addition around triple bond creates a chiral centre in the molecule, and in case of dendrimers where multiple TYC reactions are performed at numerous end groups, it results in a soup of diastereomers which is indeed a limiting factor for the construction of biomaterials.

1.4.3.5. Diels-Alder click: Diels-Alder click is a thermosensitive and metal free addition reaction between an electron-rich diene and electron-deficient dienophile to give rise to a cyclic adduct. Like other click reactions mentioned above, Diels-Alder click reaction is another greener approach towards dendrimer synthesis.^{64, 89} The reaction can be carried out even in water, produces minimum by-products, and requires simple purification techniques. The reaction has been first demonstrated for dendrimer construction by Müllen and coworkers in 1990's to synthesize polyphenylene dendrimers.⁹⁰ Since then many reports have been published by various groups for the use of Diels-Alder reaction in macromolecules synthesis and functionalizations.^{89, 90, 91} Recently, Müllen and coworkers have demonstrated the divergent synthesis of up to generation 9 polyphenylene dendrimers using catalyst free Diels-alder click reaction.⁹² They claimed the dendrimer structures to be highly perfect and monodisperse as revealed by MALDI-TOF mass spectrometry. The synthesis was carried out around a large perylenediimide (PDI) core using repetitive Diels-Alder cycloaddition reaction to produce G1-G9 dendrimers in high yields (Scheme 1-21). The syntheses of such high generations were successfully achieved as the reactive end groups were easily accessible due to lack of backfolding in these rigid dendrimers. The ninth generation dendrimer reported by Müllen's group had an expected molecular mass of up to 1.9 MDa and the longest-extension diameter of up to 33 nm, as confirmed by TEM imaging technique. These scales make this polyphenylene G9 dendrimer as the biggest aromatic dendrimer reported so far.

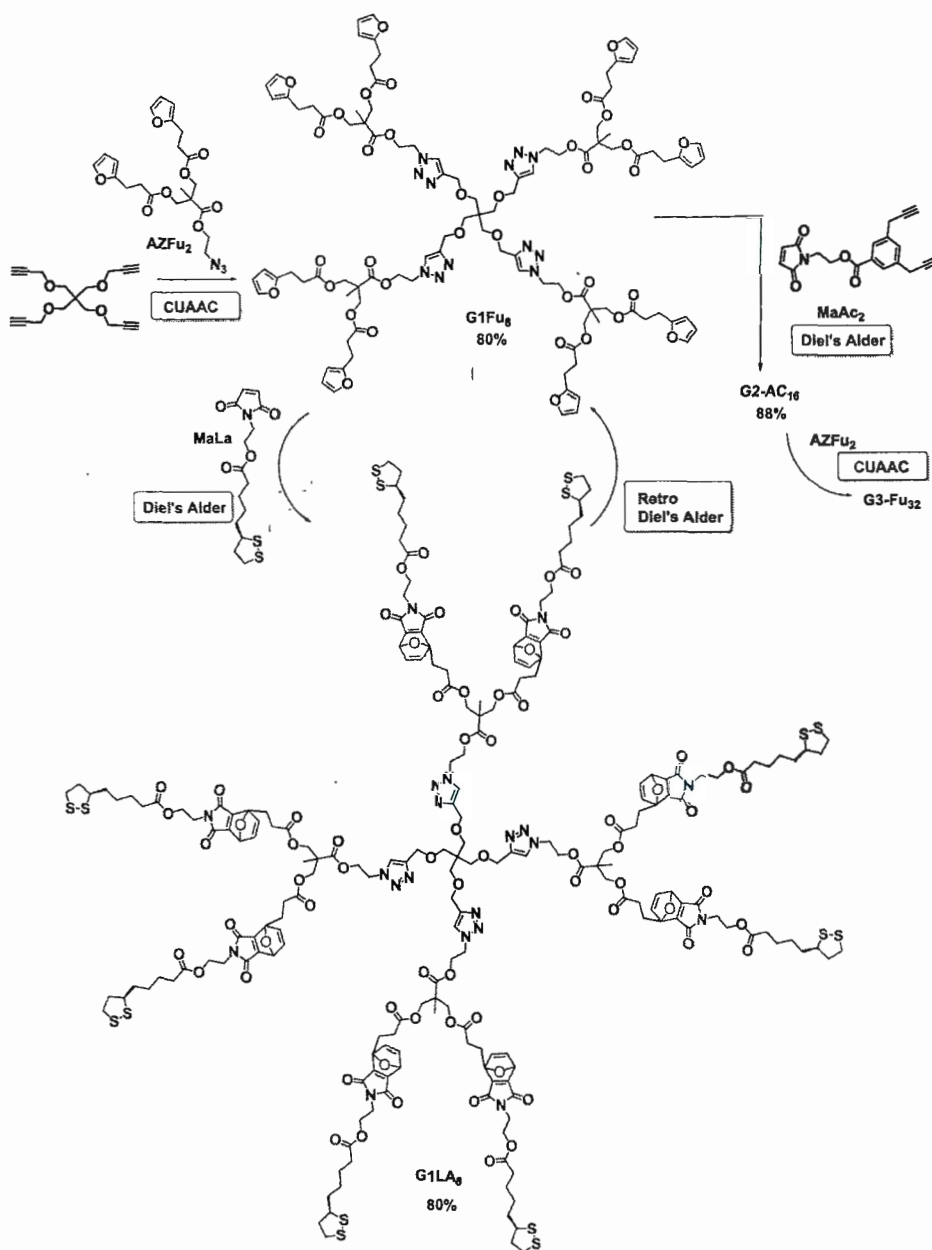


Scheme 1-21 Synthesis of G1 to G9 dendrimers.⁹²

Another interesting feature of Diels-Alder cycloaddition reaction is its reversible nature due to heat sensitivity and this attribute of the reaction has been utilized by Kakkar and coworkers to construct thermosensitive dendrimers for drug delivery applications.⁹³ They have developed a dendrimer based formulation to deliver the therapeutic agent at physiologically relevant temperature. The dendrimer synthesis was carried out divergently around a four-arm flexible core using a combination of CuAAC and Diels-Alder “click” reactions in sequence (Scheme 1-22). The periphery of the dendrimer was functionalized with multiple units of antioxidant lipoic acid as a model therapeutic agent *via* orthogonal Diels-Alder cycloaddition reaction. These drug molecules could be released under physiological (37 °C) or pathological (42 °C) temperatures by retro Diels-Alder reaction. This strategy clearly demonstrates that the release of active drug molecules *via* retro Diels-Alder at physiological temperature range can be highly advantageous to design drug delivery systems.

1.4.4. Multi component reactions based approach for dendrimer synthesis:

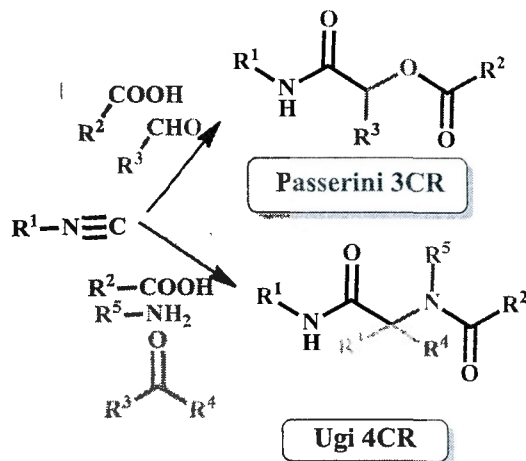
In the recent times multicomponent reactions (MCR) based approach has gained a lot of attention for the construction of polymers and dendrimers.⁹⁴ The first multicomponent reaction was introduced back in 1850 by Strecker which consists of three components amine, aldehyde and hydrogen cyanide, and known as the Strecker reaction. MCR involves multiple components which are allowed to react in one pot and give rise to core structural motif without producing lot of side products under benign reaction conditions. Here are a few MCRs which are very famous in the field of organic synthesis like Passerini, Ugi, Mannich and Gewald reaction.^{95, 96, 97} These reactions possess the inherited potential for rapid development of structurally diverse multifunctional dendrimers and polymers. From the synthetic point of view, it is a challenging job to design bi-functional or tri-functional dendritic structures which can offer many advantages in terms of biological applications and can be achieved



Scheme 1-22 Synthesis and functionalization of G1-G3 thermosensitive dendrimers.⁹³

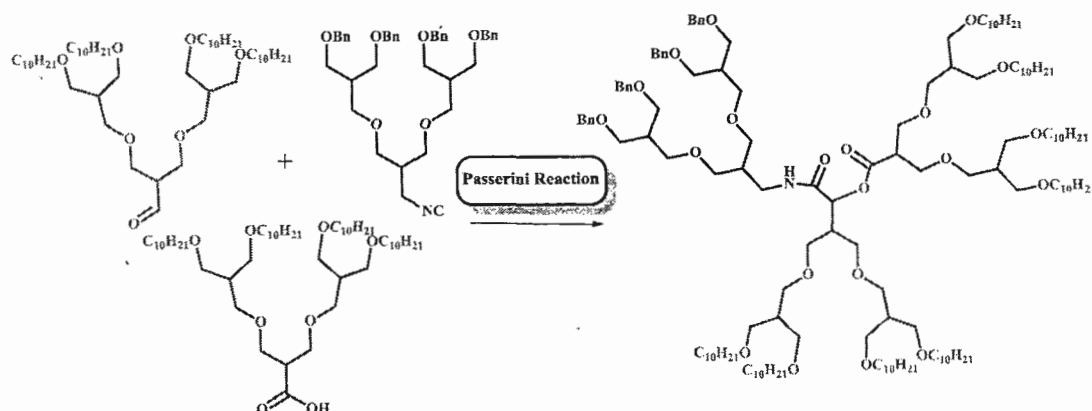
conveniently by employing multicomponent reactions. The first report for polymer synthesis using MCR was given by Meier and coworkers where three component Passerini reaction was employed for the synthesis of novel polyesters having amide side chains.⁹⁸ In case of dendrimers, first report came in 2011 by Rivera and

coworkers, who employed Passerini three component and Ugi four component reactions for the synthesis of 4th generation peptide-peptoidic dendrimers in a divergent manner (Scheme 1-23).⁹⁸ These two reactions which involve coupling of isocyanides with aldehydes and carboxylic acids are the most widely explored MCR reactions for the synthesis of dendrimers.



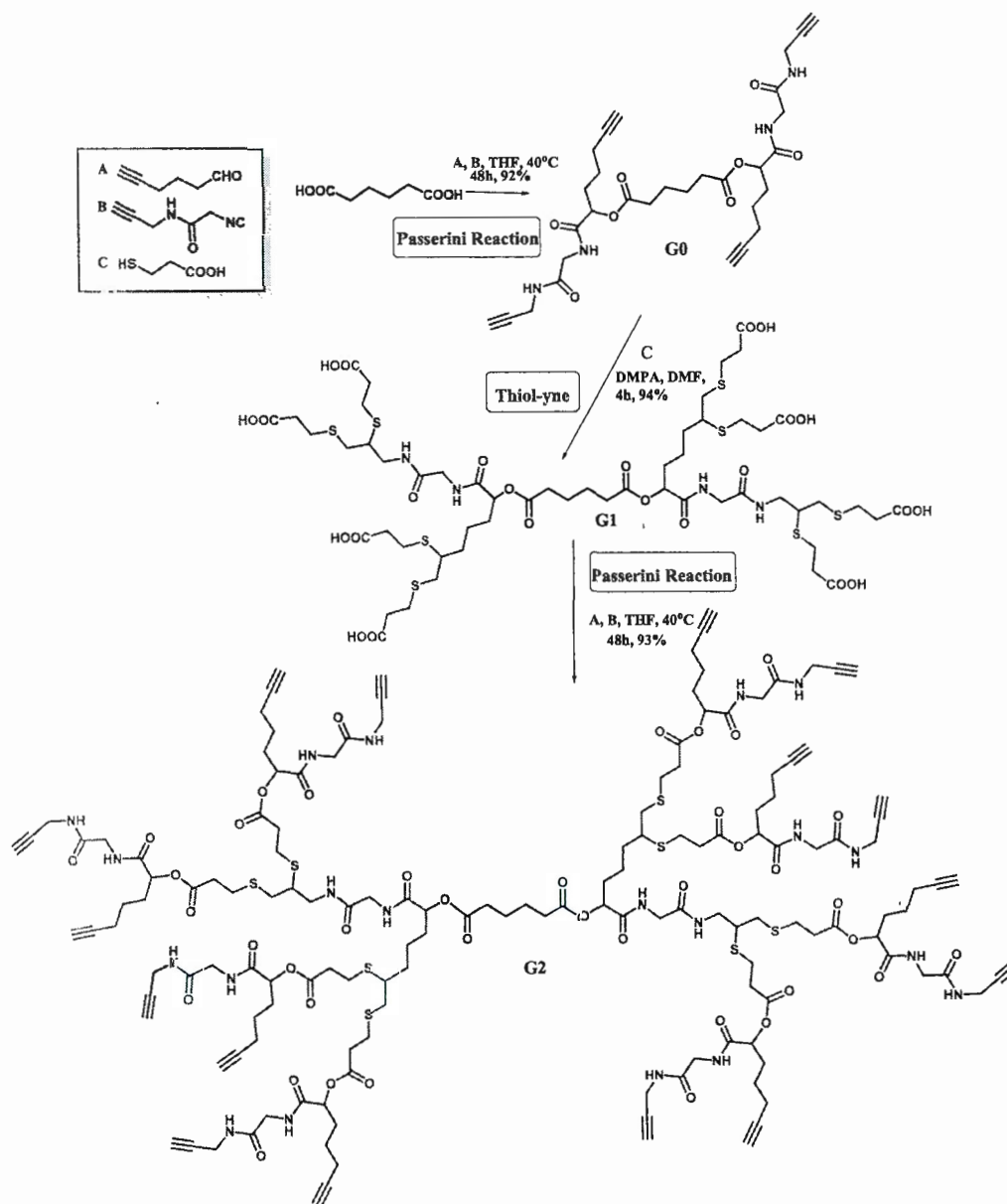
Scheme 1-23 Synthesis of monomers by Passerini 3CR and Ugi 4CR.⁹⁸

Rudick and coworkers reported an efficient method to construct surface tri-block dendrimer in convergent manner using 3CR Passerini reaction.⁹⁹ Three integral components of Passerini reaction *i.e.* isocyanide, aldehyde and carboxylic acid bearing dendrons of second generation were synthesized separately and then fused together using simple reaction conditions (Scheme 1-24). This reaction has provided a one step strategy to access triblock dendrimers which was considered a highly challenging task in the dendrimer synthesis.



Scheme 1-24 Convergent synthesis of surface block dendrimer using Passerini reaction.⁹⁹

Li and coworkers have recently published the divergent synthesis of structurally diverse dendrimers using a combination of two efficient and orthogonal multicomponent reactions (ABC Passerini and ABB thiol-yne) (Scheme 1-25).¹⁰⁰ Using this strategy, they synthesized two different kinds of dendrimers; 1) G2 dendrimers in three steps and 2) G2 functional dendrimers in five steps having three different kinds of functional moieties-type one in the interior of dendrimer and two other types on the surface. During the first synthetic step, Passerini reaction was employed to react 1,6-hexanedioic acid, 5-hexyn-1-al, and propargyl isocyanacetamide in THF to provide tetrapropargylated G0 core molecule. It was then followed by photocatalysed thiol-yne click reaction on G0 with the commercially available 3-mercaptopropionic acid and resulted in G1 dendrimer having 8 carboxylic acids on the periphery. During the final step Passerini reaction was again performed to yield G2 dendrimer harbouring 16 alkyne end groups. The whole synthetic protocol was easy to execute and products were purified with minimum efforts.

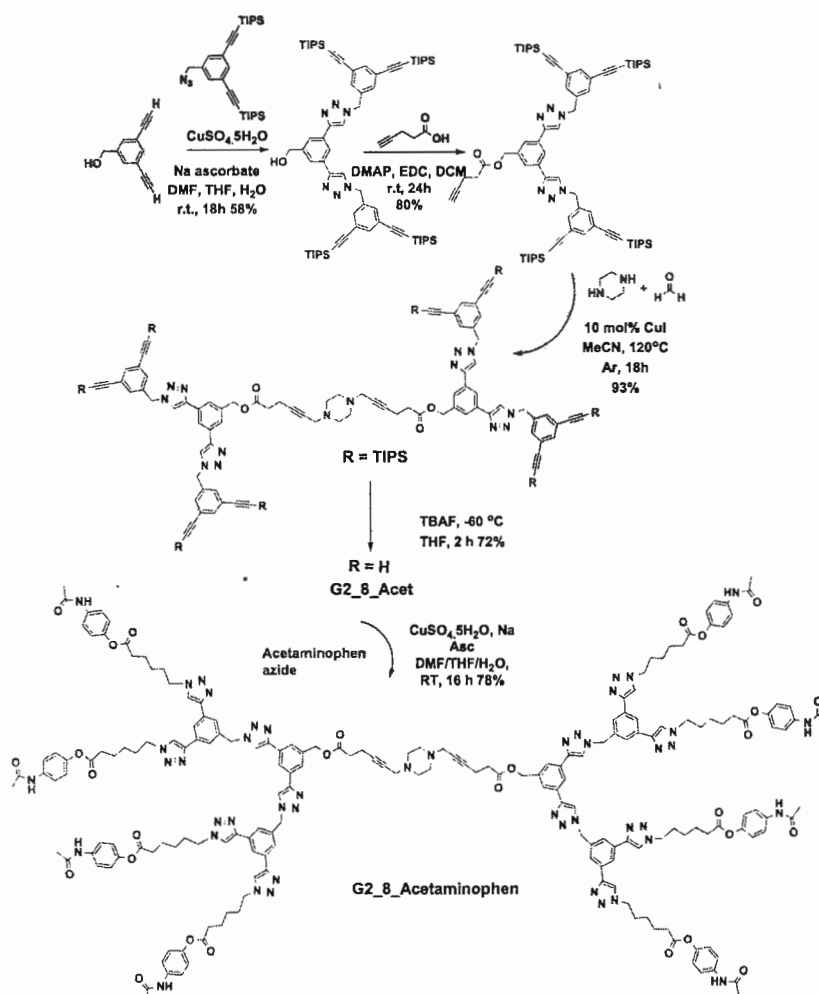


Scheme 1-25 Divergent synthesis of 2nd generation dendrimer by the combination of thiol-yne and Passerini reaction.¹⁰⁰

Kakkar, Li and coworkers have recently reported a versatile synthetic strategy for the construction of dendrimers for biomedical applications using a combination of highly efficient CuAAC click and multicomponent A^3 coupling reactions.¹⁰¹ The dendrimers up to generation 3 were synthesized using convergent approach. The dendrons were first assembled together utilizing copper (I) catalyzed alkyne-azide

click reaction and then dendrimers were stitched on to piperazine based core *via* multicomponent A³ click reaction (Scheme 1-26). The surface of the dendrimers was utilized to covalently append a variety of functional groups including imaging agents, therapeutic molecules and solubilizing polymers. The A³-click dendrimers were non-cytotoxic up to 1 μ M concentration and thus have potential to be used as biological tools to develop dendrimer based imaging and drug delivery systems.

Multicomponent reactions are not very successful to construct high generation dendrimers due to steric hindrance involved.



Scheme 1-26 Synthesis of A³-Click G2 dendrimer.¹⁰¹

1.5 Conclusions:

Since their first reports in 1978, the construction of dendrimers has gone through remarkable development. A wide range of methodologies now exist for the synthesis of these unique macromolecular entities. The introduction of highly efficient click reactions have brought a revolution to the field and generated various dendritic scaffolds. However, despite the development of various versatile and facile strategies for the synthesis of dendrimers, the field still suffers from tedious synthetic protocols especially for the construction of high generation dendrimers with huge number of surface groups. The increasing potential of dendrimers towards various applications requires the development of novel strategies which can allow the easy and accelerated synthesis of structurally diverse dendrimers.

1.6 Scope of the thesis

Dendrimers are highly branched mono-disperse macromolecules with precise constitutions that have been explored in a wide variety of chemical, biological, and material studies. A large number of synthetic strategies have been developed for their construction such as the most popular convergent, divergent and accelerated approaches. However, despite these major achievements, their syntheses can still be problematic due to the multistep protocols, and trivial purifications. This dissertation is an attempt towards the development of novel highly efficient synthetic strategies which can deliver dendrimers in an improved and rapid manner. Following is the summary of the results presented in the thesis:

Chapter 1: Chapter 1 provides us an overview about the origin of dendrimers, their applications in modern world and the famous synthetic strategies used for the construction of dendrimers.

Chapter 2: Chapter 2 presents the development of a novel “onion peel strategy” for the divergent construction of glycodendrimers using different families of building blocks at each layer of the dendritic growth. A combination of successive highly efficient, orthogonal, atom economical, and robust chemical reactions generated

dendrimers having chemically heterogeneous layers. The dendrimers constructed using this strategy are fundamentally different to conventional dendrimers which are usually built from repetitive building nanosynthons.

Chapter 3: In this chapter, we further evaluated the versatility of onion peel approach by developing an inverted strategy with multivalent presentation of different types of ligands around a fixed “onion peel” dendritic scaffold. We assembled chemically heterogeneous layers at each generation by both convergent and divergent strategies using a combination of orthogonal building blocks and highly efficient chemical reactions. We demonstrated that the structural diversity in the construction of “onion peel” dendrimers, accessible *via* both convergent and divergent routes, represents an additional strategy for the build-up of dense surface groups at low dendrimer generations. The glycodendrimer resulted in one of the most potent multivalent ligands known against the virulent factor from a bacterial lectin isolated from *Pseudomonas aeruginosa*.

Chapter 4: High generation dendrimers with numerous end groups have great importance with applications in the fields of gene transfection and photonics. It is really a challenging task to construct low generation dendrimers with huge number of terminal functions due to time and cost involved in the synthetic procedures. In this chapter, we tried to address this problem by utilizing accelerated onion peel approach for constructing low generation dendrimers with high number of peripheral groups. We involved hypercore and hypermonomers and successfully demonstrated the formation of highly dense (252 end groups at G3) low generation dendrimers in just 4 steps. The onion peel strategy presented herein may lead to new directions in dendrimer research for the synthesis of much richer family of functionalized dendritic structures.

Chapter 5: This chapter describes the summary of our results as well as the future perspectives of the research in the field of dendrimer construction.

1.7 References:

- 1 A.-M. Caminade and C.-O. Turrin, *J. Mater. Chem. B*, 2014, **2**, 4055-4066.
- 2 L. L'Haridon and J.-M. Mallet, in *Carbohydrate Chem: Volume 40*, The Royal Society of Chemistry, 2014, vol. **40**, pp. 257-269.
- 3 M. Sowinska and Z. Urbanczyk-Lipkowska, *New J. Chem.*, 2014, **38**, 2168-2203.
- 4 M. A. Mintzer and M. W. Grinstaff, *Chem. Soc. Rev.*, 2011, **40**, 173-190.
- 5 Y. Cheng, L. Zhao, Y. Li and T. Xu, *Chem. Soc. Rev.*, 2011, **40**, 2673-2703.
- 6 P. J. Flory, *J. Am. Chem. Soc.*, 1941, **63**, 3083-3090.
- 7 P. J. Flory, *J. Am. Chem. Soc.*, 1941, **63**, 3091-3096.
- 8 P. J. Flory, *J. Am. Chem. Soc.*, 1941, **63**, 3096-3100.
- 9 P. J. Flory, *J. Am. Chem. Soc.*, 1947, **69**, 30-35.
- 10 E. Buhleier, W. Wehner and F. Vögtle, *Synthesis*, 1978, **1978**, 155-158.
- 11 D. A. Tomalia, H. Baker, J. Dewald, M. Hall, G. Kallos, S. Martin, J. Roeck, J. Ryder and P. Smith, *Polym. J.*, 1985, **17**, 117-132.
- 12 G. R. Newkome, Z. Yao, G. R. Baker and V. K. Gupta, *J. Org. Chem.*, 1985, **50**, 2003-2004.
- 13 T. D. McCarthy, P. Karellas, S. A. Henderson, M. Giannis, D. F. O'Keefe, G. Heery, J. R. A. Paull, B. R. Matthews and G. Holan, *Mol. Pharm.*, 2005, **2**, 312-318.
- 14 S. Altinier, M. Mion, A. Cappelletti, M. Zaninotto and M. Plebani, *Clin. Chem.*, 2000, **46**, 991-993.
- 15 B. Misselwitz, H. Schmitt-Willich, W. Ebert, T. Frenzel and H.-J. Weinmann, *MAGMA*, 2001, **12**, 128-134.
- 16 D. Wang and D. Astruc, *Coord. Chem. Rev.*, 2013, **257**, 2317-2334.
- 17 N. Li, P. Zhao, M. E. Igartua, A. Rapakousiou, L. Salmon, S. Moya, J. Ruiz and D. Astruc, *Inorg. Chem.*, 2014, **53**, 11802-11808.
- 18 D. Astruc, C. Ornelas and J. Ruiz, *Acc. Chem. Res.*, 2008, **41**, 841-856.
- 19 E. R. Gillies and J. M. J. Fréchet, *Drug Discovery Today*, 2005, **10**, 35-43.
- 20 C. C. Lee, J. A. MacKay, J. M. J. Frechet and F. C. Szoka, *Nat. Biotech.*, 2005, **23**, 1517-1526.
- 21 D. Shcharbin, A. Shakhbazau and M. Bryszewska, *Exp. Opin. Drug Deliv.*, 2013, **10**, 1687-1698.
- 22 M. J. Cloninger, *Curr. Opin. Chem. Biol.*, 2002, **6**, 742-748.
- 23 B. B. Prasad and D. Jauhari, *Sens. Actuators, B*, 2015, **207**, 542-551.
- 24 E. Sorsak, J. Volmajer Valh, S. Korent Urek and A. Lobnik, *Analyst*, 2014, DOI: 10.1039/C4AN00825A.
- 25 P. Bhattacharya, E. N. Nasybulin, M. H. Engelhard, L. Kovarik, M. E. Bowden, X. S. Li, D. J. Gaspar, W. Xu and J.-G. Zhang, *Adv. Funct. Mater.*, 2014, **24**, 7510-7519.

- 26 M. Shellaiah, M. V. Ramakrishnam Raju, A. Singh, H.-C. Lin, K.-H. Wei and H.-C. Lin, *J. Mater. Chem. A*, 2014, **2**, 17463-17476.
- 27 C. t. Ornelas, R. Pennell, L. F. Liebes and M. Weck, *Org. Lett.*, 2011, **13**, 976-979.
- 28 Z. Qiao and X. Shi, *Prog. Polym. Sci.*, DOI: <http://dx.doi.org/10.1016/j.progpolymsci.2014.08.002>.
- 29 L. R. Dalton, S. J. Benight, L. E. Johnson, D. B. Knorr, I. Kosilkin, B. E. Eichinger, B. H. Robinson, A. K. Y. Jen and R. M. Overney, *Chem. Mater.*, 2010, **23**, 430-445.
- 30 S. N. Goonewardena, J. D. Kratz, H. Zong, A. M. Desai, S. Tang, S. Emery, J. R. Baker Jr and B. Huang, *Bioorg. Med. Chem. Lett.*, 2013, **23**, 2872-2875.
- 31 U. H. Sk, S. P. Kambhampati, M. K. Mishra, W. G. Lesniak, F. Zhang and R. M. Kannan, *Biomacromolecules*, 2013, **14**, 801-810.
- 32 S. Somani, D. R. Blatchford, O. Millington, M. L. Stevenson and C. Dufès, *J. Control. Release*, 2014, **188**, 78-86.
- 33 K. T. Al-Jamal, W. T. Al-Jamal, J. T. W. Wang, N. Rubio, J. Buddle, D. Gathercole, M. Zloh and K. Kostarelos, *ACS Nano*, 2013, **7**, 1905-1917.
- 34 J. Lim and E. E. Simanek, *Adv. Drug Deliv. Rev.*, 2012, **64**, 826-835.
- 35 G. M. Soliman, A. Sharma, D. Maysinger and A. Kakkar, *Chem. Commun.*, 2011, **47**, 9572-9587.
- 36 Z. Zhou, X. Ma, C. J. Murphy, E. Jin, Q. Sun, Y. Shen, E. A. Van Kirk and W. J. Murdoch, *Angew. Chem. Int. Ed.*, 2014, **53**, 10949-10955.
- 37 G. M. Pavan, *Chem. Med. Chem.*, 2014, **9**, 2623-2631.
- 38 X. Liu, J. Zhou, T. Yu, C. Chen, Q. Cheng, K. Sengupta, Y. Huang, H. Li, C. Liu, Y. Wang, P. Posocco, M. Wang, Q. Cui, S. Giorgio, M. Fermeglia, F. Qu, S. Pricl, Y. Shi, Z. Liang, P. Rocchi, J. J. Rossi and L. Peng, *Angew. Chem. Int. Ed.*, 2014, **53**, 11822-11827.
- 39 J. B. Wolinsky and M. W. Grinstaff, *Adv. Drug Deliv. Rev.*, 2008, **60**, 1037-1055.
- 40 S. Wen, K. Li, H. Cai, Q. Chen, M. Shen, Y. Huang, C. Peng, W. Hou, M. Zhu, G. Zhang and X. Shi, *Biomaterials*, 2013, **34**, 1570-1580.
- 41 M. Shema-Mizrachi, G. M. Pavan, E. Levin, A. Danani and N. G. Lemcoff, *J. Am. Chem. Soc.*, 2011, **133**, 14359-14367.
- 42 J. W. J. Knapen, A. W. van der Made, J. C. de Wilde, P. W. N. M. van Leeuwen, P. Wijkens, D. M. Grove and G. van Koten, *Nature*, 1994, **372**, 659-663.
- 43 H. Brunner, *J. Organomet. Chem.*, 1995, **500**, 39-46.
- 44 N. J. Hovestad, J. L. Hoare, J. T. B. H. Jastrzebski, A. J. Canty, W. J. J. Smeets, A. L. Spek and G. van Koten, *Organometallics*, 1999, **18**, 2970-2980.
- 45 A. Miedaner, C. J. Curtis, R. M. Barkley and D. L. DuBois, *Inorg. Chem.*, 1994, **33**, 5482-5490.
- 46 J. N. H. Reek, D. de Groot, G. Eric Oosterom, P. C. J. Kamer and P. W. N. M. van Leeuwen, *C. R. Chim.*, 2003, **6**, 1061-1077.

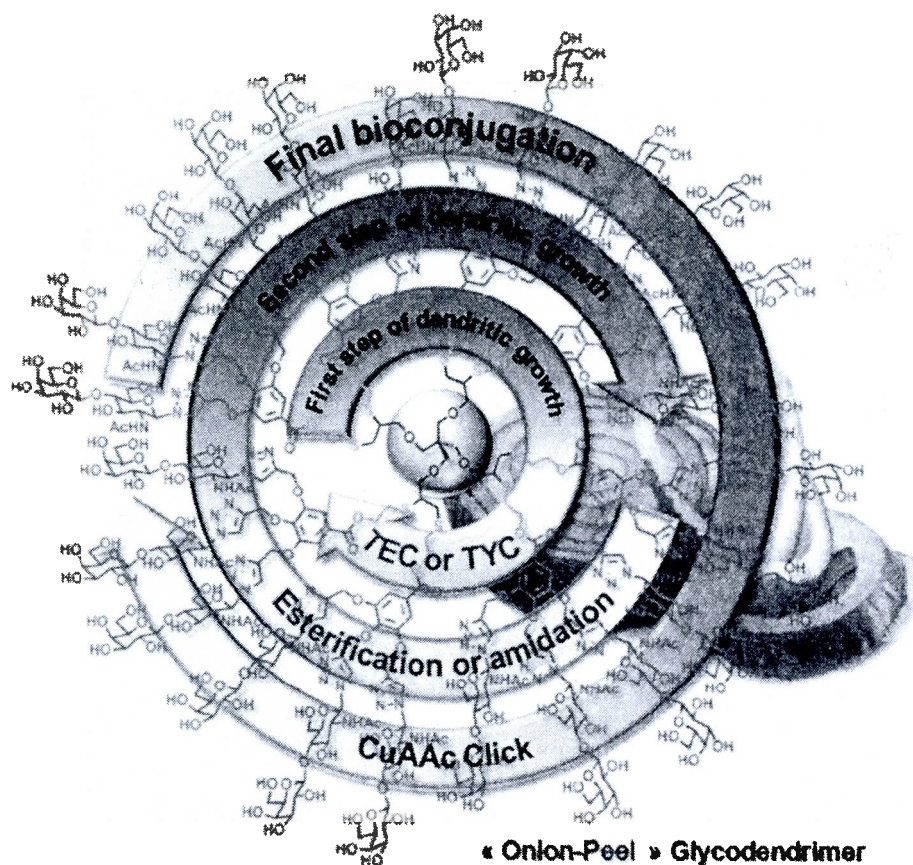
- 47 C. Deraedt, N. Pinaud and D. Astruc, *J. Am. Chem. Soc.*, 2014, **136**, 12092-12098.
- 48 M. A. Barakat, M. H. Ramadan, J. N. Kuhn and H. L. Woodcock, *Desalin. Water Treat.*, 2013, **52**, 5869-5875.
- 49 S. Zhang, G. Qiu, Y. P. Ting and T.-S. Chung, *Colloids Surf A Physicochem. Eng. Asp.*, 2013, **436**, 207-214.
- 50 X. Yao, B. Jiang, L. Zhang, Y. Sun, X. Xiao, Z. Zhang and Z. Zhao, *Energy & Fuels*, 2014, **28**, 5998-6005.
- 51 R. U. Kadam, M. Bergmann, M. Hurley, D. Garg, M. Cacciarini, M. A. Swiderska, C. Nativi, M. Sattler, A. R. Smyth, P. Williams, M. Cámara, A. Stocker, T. Darbre and J.-L. Reymond, *Angew. Chem. Int. Ed.*, 2011, **50**, 10631-10635.
- 52 P. E. Shaw, S. S. Y. Chen, X. Wang, P. L. Burn and P. Meredith, *J. Phys. Chem. C*, 2013, **117**, 5328-5337.
- 53 K. Neibert, V. Gosein, A. Sharma, M. Khan, M. A. Whitehead, D. Maysinger and A. Kakkar, *Mol. Pharm.*, 2013, **10**, 2502-2508.
- 54 C. J. Hawker and J. M. J. Frechet, *Macromolecules*, 1990, **23**, 4726-4729.
- 55 C. J. Hawker and J. M. J. Frechet, *J. Am. Chem. Soc.*, 1990, **112**, 7638-7647.
- 56 K. L. Wooley, C. J. Hawker and J. M. J. Frechet, *J. Am. Chem. Soc.*, 1991, **113**, 4252-4261.
- 57 K. L. Wooley, C. J. Hawker and J. M. J. Fréchet, *Angew. Chem. Int. Ed.*, 1994, **33**, 82-85.
- 58 T. Kawaguchi, K. L. Walker, C. L. Wilkins and J. S. Moore, *J. Am. Chem. Soc.*, 1995, **117**, 2159-2165.
- 59 H. Ihre, A. Hult, J. M. J. Fréchet and I. Gitsov, *Macromolecules*, 1998, **31**, 4061-4068.
- 60 G. Barany and R. B. Merrifield, *J. Am. Chem. Soc.*, 1977, **99**, 7363-7365.
- 61 R. Spindler and J. M. J. Frechet, *J. Chem. Soc., Perkin Trans. 1*, 1993, DOI: 10.1039/P19930000913, 913-918.
- 62 F. Zeng and S. C. Zimmerman, *J. Am. Chem. Soc.*, 1996, **118**, 5326-5327.
- 63 P. Antoni, D. Nystrom, C. J. Hawker, A. Hult and M. Malkoch, *Chem. Commun.*, 2007, 2249-2251.
- 64 G. Franc and A. K. Kakkar, *Chem. Soc. Rev.*, 2010, **39**, 1536-1544.
- 65 R. Sharma, K. Naresh, Y. M. Chabre, R. Rej, N. K. Saadeh and R. Roy, *Polym. Chem.*, 2014, **5**, 4321-4331.
- 66 R. Sharma, N. Kottari, Y. M. Chabre, L. Abbassi, T. C. Shiao and R. Roy, *Chem. Commun.*, 2014, **50**, 13300-13303.
- 67 D. Kushwaha and V. K. Tiwari, *J. Org. Chem.*, 2013, **78**, 8184-8190.
- 68 N. Kottari, Y. M. Chabre, T. C. Shiao, R. Rej and R. Roy, *Chem. Commun.*, 2014, **50**, 1983-1985.
- 69 H. C. Kolb, M. G. Finn and K. B. Sharpless, *Angew. Chem. Int. Ed.*, 2001, **40**, 2004-2021.

- 70 C. W. Tornøe, C. Christensen and M. Meldal, *J. Org. Chem.*, 2002, **67**, 3057-3064.
- 71 B. T. Worrell, J. A. Malik, and V. V. Fokin *Science*, 2013, **340**, 457-460.
- 72 P. Wu, A. K. Feldman, A. K. Nugent, C. J. Hawker, A. Scheel, B. Voit, J. Pyun, J. M. J. Fréchet, K. B. Sharpless and V. V. Fokin, *Angew. Chem. Int. Ed.*, 2004, **43**, 3928-3932.
- 73 P. Antoni, M. J. Robb, L. Campos, M. Montanez, A. Hult, E. Malmström, M. Malkoch and C. J. Hawker, *Macromolecules*, 2010, **43**, 6625-6631.
- 74 C. Hein, X.-M. Liu and D. Wang, *Pharm Res*, 2008, **25**, 2216-2230.
- 75 C. N. Urbani, C. A. Bell, M. R. Whittaker and M. J. Monteiro, *Macromolecules*, 2008, **41**, 1057-1060.
- 76 N. J. Agard, J. A. Prescher and C. R. Bertozzi, *J. Am. Chem. Soc.*, 2004, **126**, 15046-15047.
- 77 C. Ornelas, J. Broichhagen and M. Weck, *J. Am. Chem. Soc.*, 2010, **132**, 3923-3931.
- 78 C. Y. Lee, R. Held, A. Sharma, R. Baral, C. Nanah, D. Dumas, S. Jenkins, S. Upadhaya and W. Du, *J. Org. Chem.*, 2013, **78**, 11221-11228.
- 79 C. E. Hoyle and C. N. Bowman, *Angew. Chem. Int. Ed.*, 2010, **49**, 1540-1573.
- 80 A. B. Lowe, *Polym. Chem.*, 2014, **5**, 4820-4870.
- 81 E. Fuentes-Paniagua, J. M. Hernandez-Ros, M. Sanchez-Milla, M. A. Camero, M. Maly, J. Perez-Serrano, J. L. Copa-Patino, J. Sanchez-Nieves, J. Soliveri, R. Gomez and F. Javier de la Mata, *RSC Adv.*, 2014, **4**, 1256-1265.
- 82 K. L. Killops, L. M. Campos and C. J. Hawker, *J. Am. Chem. Soc.*, 2008, **130**, 5062-5064.
- 83 D. P. Nair, M. Podgórski, S. Chatani, T. Gong, W. Xi, C. R. Fenoli and C. N. Bowman, *Chem. Mater.*, 2013, **26**, 724-744.
- 84 S. E. R. Auty, O. C. J. Andren, F. Y. Hern, M. Malkoch and S. P. Rannard, *Polym. Chem.*, 2015, **6**, 573-582.
- 85 S. Chatani, M. Podgórski, C. Wang and C. N. Bowman, *Macromolecules*, 2014, **47**, 4894-4900.
- 86 G. Chen, J. Kumar, A. Gregory and M. H. Stenzel, *Chem. Commun.*, 2009, DOI: 10.1039/B910340F, 6291-6293.
- 87 Y. Shen, Y. Ma and Z. Li, *J. Polym. Sci. A Polym. Chem.*, 2013, **51**, 708-715.
- 88 A. Massi and D. Nanni, *Org. Biomol. Chem.*, 2012, **10**, 3791-3807.
- 89 A. Vieyres, T. Lam, R. Gillet, G. Franc, A. Castonguay and A. Kakkar, *Chem. Commun.*, 2010, **46**, 1875-1877.
- 90 F. Morgenroth, C. Kubel and K. Mullen, *J. Mater. Chem.*, 1997, **7**, 1207-1211.
- 91 M. M. Kose, G. Yesilbag and A. Sanyal, *Org. Lett.*, 2008, **10**, 2353-2356.
- 92 T.-T.-T. Nguyen, M. Baumgarten, A. Rouharipour, H. J. Räder, I. Lieberwirth and K. Müllen, *J. Am. Chem. Soc.*, 2013, **135**, 4183-4186.

- 93 A. Castonguay, E. Wilson, N. Al-Hajaj, L. Petitjean, J. Paoletti, D. Maysinger and A. Kakkar, *Chem. Commun.*, 2011, **47**, 12146-12148.
- 94 R. Kakuchi, *Angew. Chem. Int. Ed.*, 2014, **53**, 46-48.
- 95 J. G. Rudick, *J. Polym. Sci. A Polym. Chem.*, 2013, **51**, 3985-3991.
- 96 O. Kreye, D. Kugele, L. Faust and M. A. R. Meier, *Macromol. Rapid Commun.*, 2014, **35**, 317-322.
- 97 O. Kreye, T. Tóth and M. A. R. Meier, *J. Am. Chem. Soc.*, 2011, **133**, 1790-1792.
- 98 L. A. Wessjohann, M. Henze, , O. Kreye, D. G. Rivera, 2013, USP 20130203960
- 99 J.-A. Jee, L. A. Spagnuolo and J. G. Rudick, *Org. Lett.*, 2012, **14**, 3292-3295.
- 100 X.-X. Deng, F.-S. Du and Z.-C. Li, *ACS Macro Lett.*, 2014, **3**, 667-670.
- 101 A. Sharma, D. Mejía, A. Regnaud, N. Uhlig, C.-J. Li, D. Maysinger and A. Kakkar, *ACS Macro Lett.*, 2014, **3**, 1079-1083.

CHAPTER 2

“ONION PEEL” DENDRIMERS: A STRAIGHTFORWARD SYNTHETIC
APPROACH TOWARDS HIGHLY DIVERSIFIED ARCHITECTURES



In this chapter, we have developed a novel “onion peel strategy” for the divergent construction of glycodendrimers using different building blocks at each layer of the dendritic growth. A combination of successive highly efficient, versatile, and robust chemical reactions, namely thiol-ene or thiol-yne, esterification, and azide-alkyne click chemistry, generated dendrimers having chemically heterogeneous layers, some of which with UV-visible functions. The strategy is fundamentally different to

conventional dendritic systems usually built from repetitive building nanosynthons of limited surface groups. The validity of this novel approach towards the construction of biologically active glycodendrimers having dense surface sugar residues within low dendrimer generations was fully demonstrated using *Erythrina cristagalli*, a leguminous lectin known to bind natural killer cells through its galactoside recognition ability. The dendrimer's surface was decorated with an azido derivative of *N*-acetyllactosamine using click chemistry which led to new glycodendrimers having high affinities as compared to the corresponding monovalent analog. The ongoing quest for a better parameterization of critical carbohydrate-protein recognition factors urgently requires structures with tailored biophysical properties, sizes, and shapes together with optimized tri-dimensional architectures. The proposed methodology, for which entirely orthogonal building blocks can be applied, represents an additional contribution to the wide arsenal of existing strategies which can create higher structural diversity among dendritic structures of biological interests.

Reproduced in part with permission from:

Rishi Sharma, Kottari Naresh, Yoann M. Chabre, Rabindra Rej, Nadim K. Saadeh and René Roy *Polymer Chemistry*, **2014**, 5, 4321-4331.

Copyright, 2014, Royal Society of Chemistry

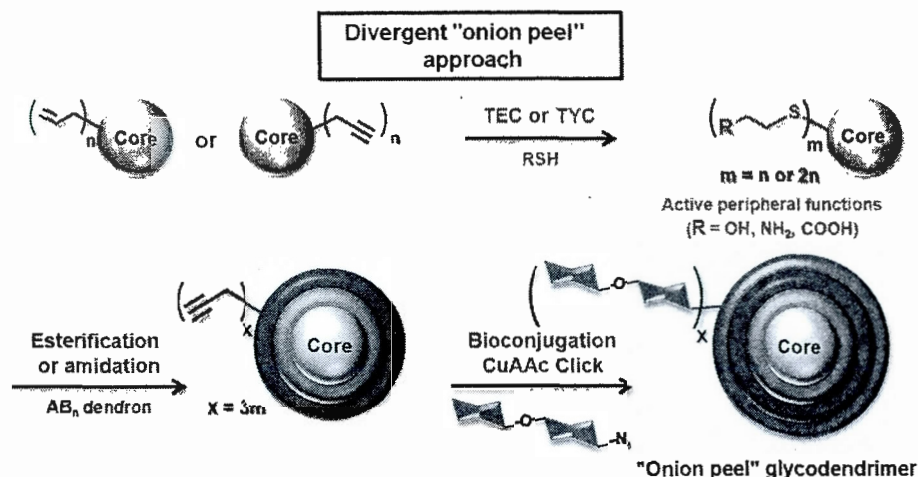
2.1 Introduction:

Dendrimers are highly branched mono-disperse macromolecules with precise constitutions that have been explored in a wide variety of chemical, biological, and material studies.¹ A large number of synthetic strategies have been developed for their construction such as the most popular convergent, divergent and accelerated approaches.¹ However, despite these major achievements, their syntheses can still be tedious due to the inherent complexities associated with each repetitive methodology, most of which using narrow AB₂ monomer building blocks. Based on this observation, new strategies allowing easier preparation of homogenous and constitutionally diversified macromolecular structures are deemed necessary. Interestingly, besides classical strategies involving “hypercores”² and “hypermonomers”,³ one of the first breakthroughs towards accelerated dendritic syntheses has been carried out in the mid-90s⁴ with the application of orthogonal coupling strategies⁵ allowing the building of complex biomolecules.⁶ The orthogonality concept dramatically reduced the number of required synthetic steps by using complementary bifunctional precursors that were coupled together by obviating deprotection or activation steps. Moreover, most common dendrimers are based on identical repeating units at each generation, thus greatly limiting the tailoring of biophysical properties that prevent structural diversity.

More particularly and despite their roles as well-defined artificial glycoconjugates, most glycodendrimers⁷ do not depart from these constraints. Since the first report,⁸ the ongoing quest toward more active hypervalent carbohydrate-loaded dendrimers exhibiting a range of activities has systematically grown.⁹ The emergence of these mono-disperse glycomacromolecules has significantly contributed to our understanding of multivalent carbohydrate-protein interactions through the “cluster glycoside effect”, according to which the binding affinities of multivalent carbohydrates are significantly higher than the sum of individual ligands.¹⁰ In addition, glycodendrimers have received considerable attention for their use in

biomedical applications, such as anti-adhesins, drug delivery, biosensors, gene transfections, and vaccines.¹¹ As the design of multivalent glycodendrimers strongly depends on the unique structural features of the protein receptors, the conception of tailored systems is highly desirable. It can thus be considered that the art of synthetic design of multivalent scaffolds remains open to alternative and improved strategies that will allow better controlled structural diversity.

To address these issues, we propose a new type of “onion peel strategy” for the divergent construction of original dendritic architectures, involving the incorporation of different families of building blocks containing orthogonal functional groups at each layer (or generation) some of which having UV-visible moieties. The flexibility of the strategy will be demonstrated by choosing intentionally different but adapted building blocks that could differ in terms of constitution, valency, and peripheral functionalities. The layout diversity of each final biomolecule is thus programmed. Hence, the proposed approach leading to a controlled assembly of structural elements does not only rely on a “branching pattern” requirement but can extend the concept to smart multifunctional tools with tailored structures and properties. For example, once optimized, this approach may generate the desired hydrophobic/hydrophilic and rigidity/flexibility balances at each step of the dendritic growth. The general methodology for the sequential construction of our set of glycosylated architectures is proposed in Scheme 2-1. The application of a distinct mode of coupling at each layer generated an original heterogeneity in the internal functionalities and branched moieties, as opposed to conventional dendritic systems built from repetitive, or at least alternate, synthetic patterns. Thus, the proposed “onion peel” methodology, for which an entire orthogonality can be applied, could represent an alternative contribution to the wide arsenal of methodologies towards the rapid and sequential construction of dendritic architectures.



Scheme 2-1 Sequential construction of sugar decorated "onion peel" dendritic structures via an accelerated divergent strategy.

By successfully adapting the proposed onion peel strategy, we present herein the synthesis of a new family of model glycoclusters and glycodendrimers **1-5** decorated with *N*-acetyllactosamine (LacNAc) termini (Figure 2-1). The key-reactions involved in the elaboration of our set of glycosylated structures concerned the application of three different atom economical-"click" reactions that can provide high yields from simplified set-up and purification protocols, together with a highly desired tolerance toward a broad range of solvents and functional groups.¹² High chemo- and regioselectivities popularized some of these fast-growing orthogonal methodologies to ease the construction of sophisticated but well-defined (glyco)dendritic architectures.¹³ Among the most efficient and orthogonal, the photolytic thiol-ene coupling (TEC)¹⁴ will be advantageously applied to initiate the uniform growth of our dendritic scaffolds through the formation of internal robust thioether linkages. Higher degree of branching will be insured with the utilization of less-developed thiol-yne coupling (TYC)¹⁵ involving a double hydrothiolation of terminal alkynes *via* a similar free-radical chain mechanism. EDC-mediated esterifications (or amidations)¹⁶ will represent the last step of the dendritic growth with the introduction of polypropargylated dendrons equipped with the complementary focal function. The regioselective Cu(I)-catalyzed azide-alkyne [1,3]-dipolar Huisgen cycloaddition

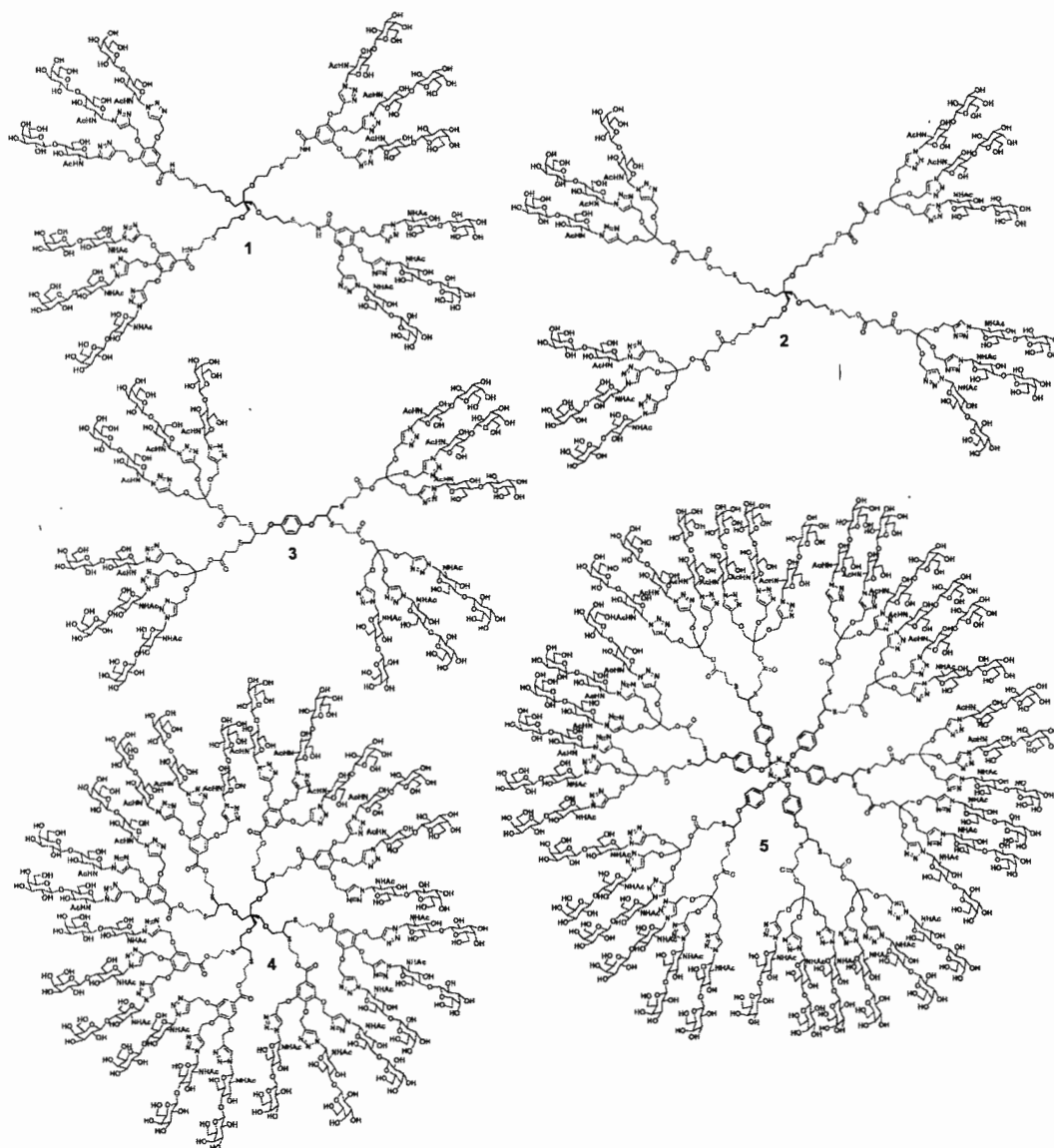


Figure 2-1 Molecular structures of targeted glycodendrimers 1-5.

(CuAAC)¹⁷ will be performed as an efficient ligation methodology for the peripheral glycoconjugation. In this context, LacNAc was chosen as a decorative sugar head group. It notably represents part of biologically active tumor associated carbohydrate antigens found in several natural glycoproteins and glycolipids presented by the blood groups, Lewis^X, and Lewis^Y.¹⁸ Similarly important, LacNAc possess strong binding affinities toward a cancer associated family of proteins known

as galectins.¹⁹ In spite of its biological significance, the multivalent display of LacNAc residues onto dendritic scaffolds has been only reported in scarce occasions.²⁰ Consequently, the protein binding studies involving derivatives **1-5** have been assessed by using surface plasmon resonance (SPR) with a model leguminous lectin from *Erythrina cristagalli* agglutinin (ECA).²¹ The main goal of this experiment is to establish the validity of the “onion peel” approach for the construction of biologically functional glycodendrimers. In addition, the influence of subtle structural parameters on the relative binding properties will be evaluated to extract fundamental trends towards optimized parameters.

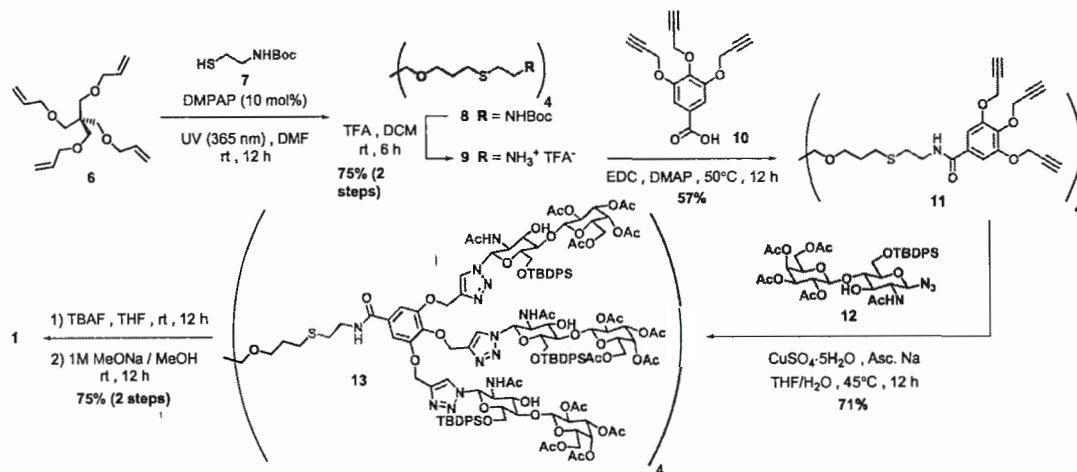
2.2 Results and discussion:

2.2.1 Synthesis

The first step of our synthetic investigation dealt with the photolytic addition of *N*-Boc-cysteamine **7** on *tetrakis*-allylpentaerythritol **6** under standard *TEC* conditions (Scheme 2-2) to afford **8**. Similarly to well-documented quasi-exclusive *anti*-Markovnikov addition observed for this type of hydrothiolation,^{14,22,23} we also noticed an analogous trend for some α -addition. (See Appendix A, SI for all tested conditions).

Subsequent removal of Boc-protecting groups in **8** using TFA in DCM furnished intermediate **9** after solvent evaporation in 75% yield over two steps. Amide coupling of **9** with bifunctional AB₃ derivative **10**²⁴ under basic conditions resulted in the formation of dodecapropargylated **11** in 57% yield (87% yield per amidation). The complete attachment of the protected β -azido LacNAc derivative **12**²⁵ under classical CuAAC conditions led to the multivalent derivative **13**. MALDI-TOF experiment furnished a unique signal in the expected region (11457.6 for a theoretical M.W. = 11448.9) while GPC indicated the uniformity of the structure (PDI (M_w/M_n) = 1.031) (Appendix A, SI). Finally, TBAF removal of TBDPS-protecting groups in the sugar

residues, followed by de-*O*-acetylation under Zemplén conditions (NaOMe, MeOH) efficiently provided glycocluster **1** having twelve LacNAc moieties.



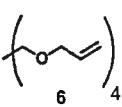
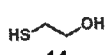
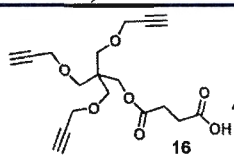
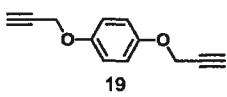
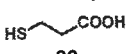
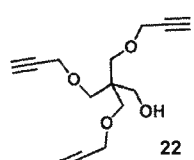
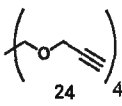
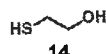
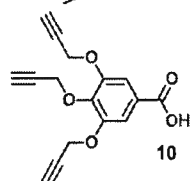
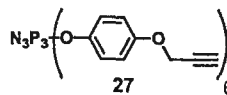
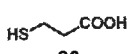
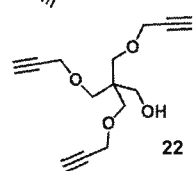
Scheme 2-2 Synthesis of glycocluster **1** through TEC-Amidation-CuAAc (4×1×3) sequence.

An alternative synthetic pathway was next explored to circumvent the above activation/deprotection steps in order to obtain congeners with equal or higher surface groups. As illustrated in Scheme 2-1, the optimized sequence was based on the integration of an orthogonal three steps-sequence consisting in hydrothiolation/esterification/click cycloaddition. Table 2-1 summarizes the structural elements that were assembled. Scheme 2-3 illustrates the critical steps towards the accelerated syntheses of glycoclusters **2-5** through an orthogonal and divergent dendritic growth.

The photoaddition of mercaptoethanol **14** on pentaerythritol derivative **6** afforded tetrahydroxylated core **15** in 85% yield which initiated the sequence towards the synthesis of glycocluster **2** (Scheme 2-3, sequence 1). Interestingly, the proportions of α -addition remained negligible in this case ($\leq 5\%$), in agreement with previous works using hydroxylated thiol precursors.^{14d,23} The ^1H NMR spectra clearly illustrated completion of the multiple hydrothiolation process by the entire disappearance of signals belonging to the alkene function at δ 5.90 and 5.25 ppm

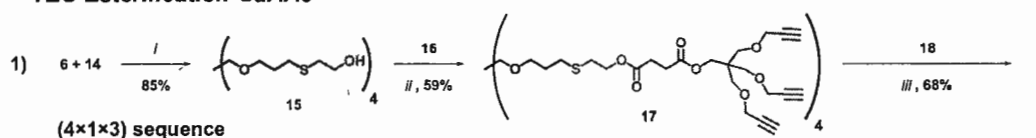
together with the presence of the characteristic quintuplet signal at δ 1.80 ppm corresponding to the newly formed aliphatic $-\text{OCH}_2\text{CH}_2\text{CH}_2\text{S}-$ motif (Figure 2-2). In addition, all the relative integrations of each proton presented in the external section of the core were in perfect agreement with those of the internal $\text{C}_6\text{CH}_2\text{O}$ region. Esterification of tetraol **15** in the presence of TRIS-based AB_3 dendron **16**²⁶ further insured the efficient incorporation of surface active propargylic functionalities to provide **17**. Figure 2-2 illustrates completion of esterifications by the addition of characteristic signals of the succinate (δ 2.70 ppm), TRIS (δ 4.15 and 3.55 ppm), and propargylic signals (doublet at δ 4.10 and triplet at δ 2.45 ppm) showing the expected relative integrations.

Table 2-1 Structural elements used to build polypropargylated scaffolds *via* an accelerated and orthogonal divergent strategy.

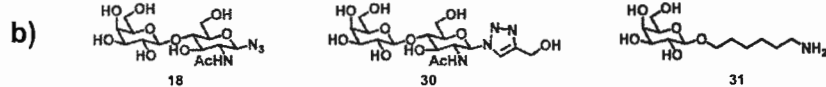
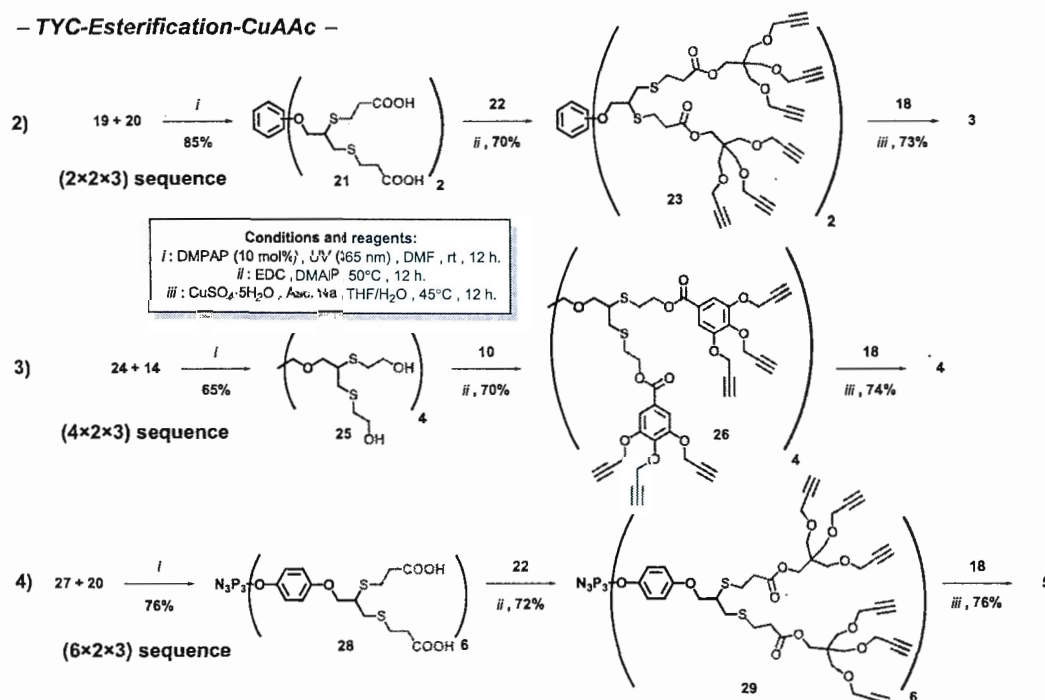
Entry	Core	Thiol Reaction type	Polypropargylated scaffolds (Esterification)	Dendritic growth	Vale ncy	Polypropargylated scaffolds
1		 14 TEC		$4 \times 1 \times 3$	12	17
2		 20 TYC		$2 \times 2 \times 3$	12	23
3		 14 TYC		$4 \times 2 \times 3$	24	26
4		 20 TYC		$6 \times 2 \times 3$	36	29

Twelve deprotected LacNAc termini were subsequently grafted *via* standard CuAAC conditions. The presence of internal ester functions implicated the use of deprotected β -azido LacNAc **18**²⁵ which was successfully integrated to the polypropargylated scaffold to lead to dodecavalent cluster **2** in 68% yield. The direct coupling of hydroxylated ligands advantageously avoided classical de-*O*-acetylation step and purifications by column chromatography when protected sugars are used.

a) – TEC-Esterification-CuAAC –



– TYC-Esterification-CuAAC –



Scheme 2-3 a) Accelerated divergent strategies for the syntheses of glycoclusters **2-5** harbouring surface LacNAc residues; b) Structures of monomer used as references for SPR studies (see Appendix A, SI for the synthesis of **30**).

In order to explore the flexibility of our global synthetic approach and to enhance the density of termini using a limited number of steps, poly-propargylated cores were used to perform TYC chemistry that enabled to double the number of attachments at each individual reactive terminal alkyne. Accordingly, a third dodecavalent homolog was synthesized, differing from the previous ones by the nature of the core from which emanated the clusters of epitopes, together with the mode of dendritic growth. To this end, a double hydrothiolation was first performed

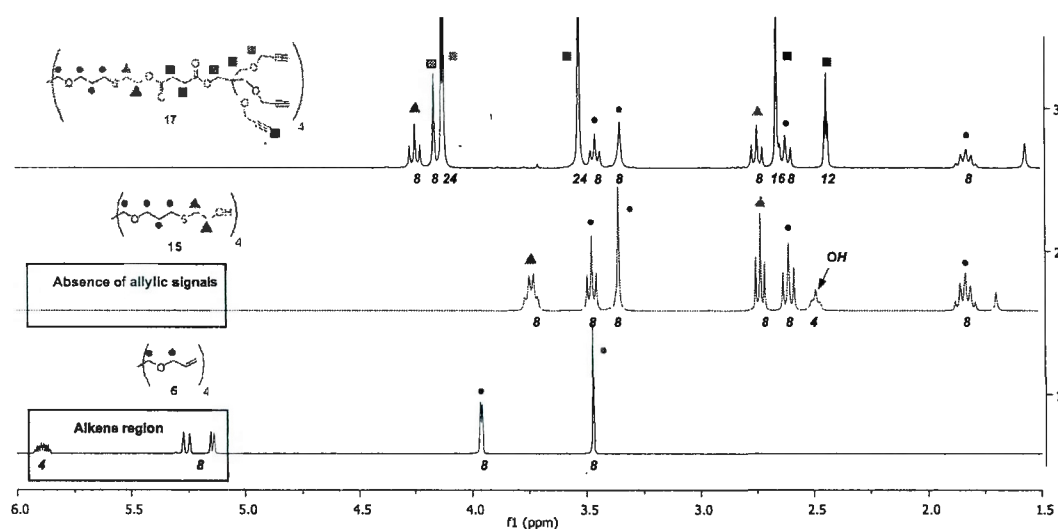


Figure 2-2 Comparison of ^1H NMR spectra (CDCl₃, 300 MHz) of **6**, **15** and **17** with the appearance/disappearance of characteristic signals towards the construction of dodecapropargylated scaffold **17** (observed proton integrations are indicated in italic below each signal).

on dipropargylated hydroquinone **19**²⁷ by means of mercaptopropionic acid **20** to provide pure derivative **21** in 85% (Scheme 2-3, sequence 2). This scaffold, having four carboxylic acids, was subsequently treated with hydroxylated AB₃ dendron **22**²⁶ through the efficient formation of ester bonds *via* EDC/DMAP coupling. As described above, complete capping with LacNAc residues **18** was accomplished on the newly formed dodecavalent derivative **23** using the above CuAAc conditions to

afford **3** in good yield. Thus, three linear orthogonal synthetic steps with an overall 43% yield allowed the straightforward formation of a dodecavalent LacNAc dendrimer. Interestingly, the application of similar three steps-sequences consisting in successive TEC/TYC-esterification-CuAAc allowed the addition of two dodecavalent “onion peel” glycoclusters to **1**, creating structural diversity in 1) the dendritic growth with $4 \times 1 \times 3$ - (for **1** and **2**) or $2 \times 2 \times 3$ - (for **3**) patterns together with the possibility to integrate efficient orthogonality; 2) the inner functionalities responsible for the stability of the constructs by the presence of thioether, ester and amide linkages; 3) the compaction of the scaffolds; 4) the aromatic/aliphatic character of the inner sections using gallic acid or pentaerythritol derivatives as secondary cores; 5) the presentation of the peripheral sugar termini emanating from the main and secondary cores.

The generation of higher analogs containing more sugar residues has also been explored *via* the proposed orthogonal three steps sequence. Thus, the first hyperbranched glycosylated structure (**4**) emanated from the known **24**,²⁸ (*See Appendix A, SI for improved synthesis of 24*) obtained in high yields according to optimized conditions on which was performed the TYC chemistry in the presence of mercaptoethanol **14** (Scheme 2-3, sequence 3). The resulting octa-hydroxylated scaffold **25** was further decorated with eight aromatic carboxylic acid precursor **10** to afford tetracosapropargylated core **26** harbouring 24 reactive propargyl functions in a 70% yield (96% yield per individual esterification sequence). Once again, complete derivatization was confirmed by mass spectrometry together with IR and NMR spectroscopy. In particular, the ¹H NMR spectra clearly indicated the disappearance of propargylic signals for **25** (δ 4.20 and 2.40 ppm in precursor **24**) and the predicted relative integration of newly formed moiety in comparison to protons located in the core (Figure 2-3, middle section). In addition, esterification also led to distinctive addition of signals such as those corresponding to aromatic (δ 7.45 ppm) and terminal propargylic protons (δ 4.75 and δ 2.50 ppm) having the calculated integrations. As observed for previous analogs with exposed LacNAc residues, final bioconjugation

proceeded efficiently using azido sugar **18** to afford the densely packed macromolecule **4** having 24 termini after dialysis.

A similar methodology was adapted with the same efficiency for the synthesis of higher analogue **5** containing 36 LacNAc appendages and an aliphatic backbone. The construction started from hexapropargylated cyclotriphosphazene **27**²⁹ known to afford 3-up/3-down wedges in both solid state and solution.^{30,30b} Twelve-fold addition of mercaptopropionic acid **20** on **27** led to **28** in good yield (76%) after purification by silica gel chromatography (Scheme 2-3, sequence 4). Once again, high resolution mass spectrometry (ESI- technique) confirmed the formation of $[M-2H]^{2-}$ adducts, thus perfectly matching the expected theoretical pattern (Figure 2-4, see Appendix A, SI for full spectrum).

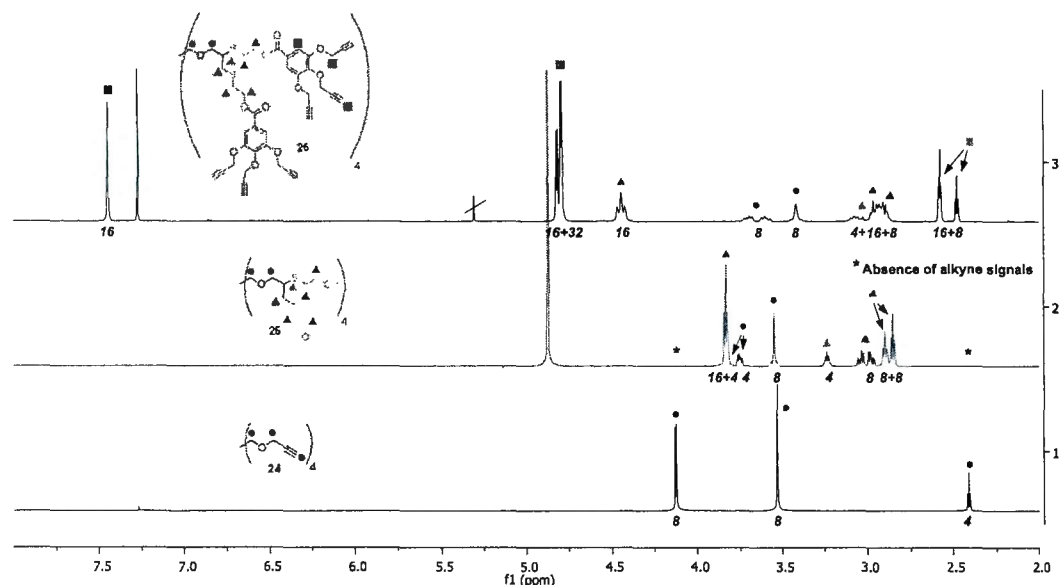


Figure 2-3 Direct comparison of ^1H NMR spectra (in CDCl_3 for top and bottom spectra and in D_2O for middle spectrum, 300 MHz) of **24**, **25** and **26** with the appearance/disappearance of characteristic signals towards the construction of tetracosavalent scaffold **26** (observed proton integrations are indicated in italic below each signal and stars in middle spectrum indicates the absence of propargylic signals).

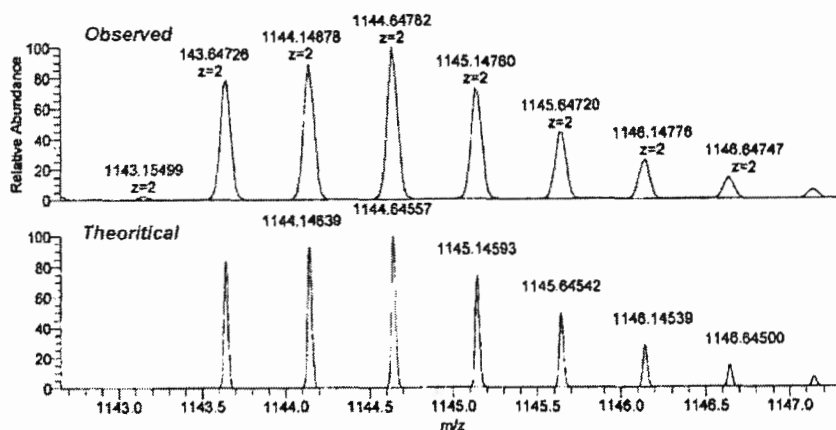


Figure 2-4 Specific region of negative HR-ESI observed (top) and theoretical (bottom) isotopic distributions for **28** exhibiting 12 carboxylic acid functions ($[M-2H]^{2-}$ signal).

Tripropargylated AB_3 wedges **22** were subsequently anchored *via* carbodiimide-mediated esterification to achieve the construction of hypercore **29** in an excellent yield. The exhibited thirty-six propargylated peripheral functions of **29** were finally transformed into triazoles during the multiple CuAAC process. Complete bioconjugation of **29** in the presence of **18** provided glycodendrimer **5**, as seen from its 1H NMR spectra showing the absence of propargylic signals using the above conditions.

Interestingly, low and high resolution Mass Spectrometry analyses furnished consistent results for the hyperbranched macromolecules together with polypropargylated precursors as indicated in Table 2-2.

Table 2-2 Mass Spectrometry results obtained from MALDI-TOF, ESI, and APCI Techniques for hyperbranched derivatives.

Entry	Compound	M.W. ^a	Exp. Mass [adduct] (Technique)
<i>Polypropargylated scaffolds</i>			
1	11	1668.5501	1691.5360 $[M+Na]^+$ HR-ESI ⁺
2	17	1936.7585	1937.7621 $[M+H]^+$ HR-APCI ⁺

3	23	<i>1538.5433</i>	1539.5506 [M+H] ⁺ HR-ESI ⁺
4	26	3043.4	3049.0 [M+Li] ⁺ LR-MALDI-TOF
5	29	5078.9	5077.5 LR-MALDI-TOF
<i>LacNAc-terminated dendrimers^b</i>			
6	13	11448.9	11457.9
7	1	6570.3	6597.9
8	2	6838.6	6862.3
9	3	6440.2	6464.0
10	4	12844.1	12735.6
11	5	19779.9	19774.8

^a Exact mass values are indicated in italic when high resolution analyses were performed. ^b Low-resolution mass values were obtained by MALDI-TOF technique ([M+Na]⁺ adducts).

2.2.2 Surface plasmon resonance studies

Subsequent to synthesis, surface plasmon resonance (SPR) studies have been conducted to assess the relative protein binding abilities of glycodendrimers **1-5** with the LacNAc-specific leguminous lectin (ECA) from *Erythrina Cristagalli*. In these studies, the lectin was immobilized onto CM5 sensor surface (Biacore) to a level of ~1200 RU, by using the manufacturer's amide coupling methodology. As a blank reference, ethanolamine was immobilized onto one of the flow cell of the sensor chip. Solutions with various concentrations of LacNAc-functionalized dendrimers have been flowed over surface-bound lectin and significant interactions were determined for each glycodendrimers and compared to monovalent standard **30**. A representative sensorgram was obtained for each ligand (see Figure 2-5 for glycodendrimer **4** and Appendix A, SI for the remaining compounds). Determination of the kinetic parameters relative to the glycodendrimer-lectin interactions were fitted by using a

1:1 Langmuir model available in BIAevaluation software.³¹ The corresponding data (k_{on} , k_{off} , K_D and relative binding affinities) are given in Table 2-3.

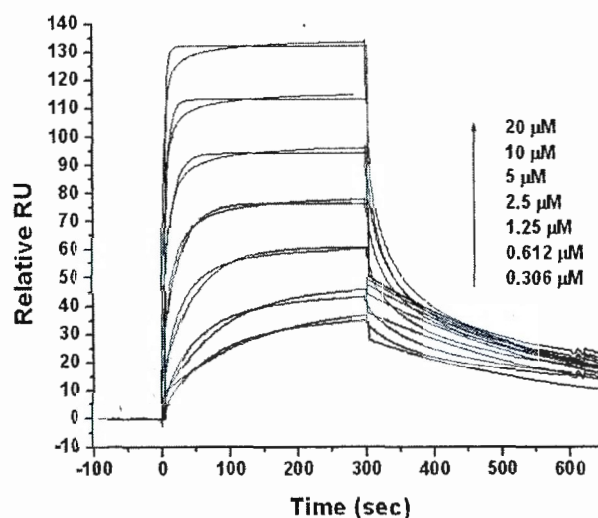


Figure 2-5 SPR sensorgrams for the interactions of glycodendrimer **4** (0.306 μM to 20 μM) with the surface bound ECA lectin. The binding data are overlaid with the fit (in red) of a 1:1 Langmuir interaction model.

In each case, simple-exponential binding profiles were obtained with association phase free of mass transport phenomenon. Overall and as expected, the glycodendrimers exhibited higher k_{on} and lower k_{off} values than those of monovalent **30**. As a result, multivalent compounds exhibited high nanomolar affinities with the dimeric ECA. Although no K_D values were previously determined by SPR for monovalent LacNAc derivatives with ECA, the experimental value for **30** consistently stands in micromolar values as compared to similar references.^{20d,32} The glycodendrimers exhibited interesting high relative potencies, with an up to 216-fold enhancement in global affinity for the best candidate **4**, while corresponding to a modest improvement for each peripheral LacNAc moieties of **4** compared to **30**. In fact, the meek glycocluster effects observed throughout the series is typical of divalent lectin interactions which usually reflect a predominance of kinetic (82-fold faster k_{on}) rather than thermodynamic improvement. In fact, the best recorded value was obtained with dodecavalent **2** for which each termini was only 14-fold more

active than the reference monomer. With a noticeable exception,³³ this observation remains consistent with earlier investigations that ascertained the fact that ECA had a small multivalency enhancement ability, as determined with LacNac-glycopolymers.³⁴

Table 2-3 Kinetic parameters obtained for the interactions of glycodendrimers with the bound ECA. Data were fitted by using a 1:1 Langmuir model available in BIAevaluation software.

Cpd	k_{on} ($M^{-1}s^{-1}$)	k_{off} (s^{-1})	K_D (nM)	r.p. ^a	r.p./sugar
30	375	7.26×10^{-3}	19400 ± 560	1	1
1	6.13×10^3	3.33×10^{-3}	543 ± 28	35	2.9
2	3.25×10^4	3.57×10^{-3}	109 ± 7	176	14.6
3	1.79×10^4	4.71×10^{-3}	263 ± 14	75	6.2
4	3.08×10^4	2.82×10^{-3}	92 ± 4	216	9
5	3.05×10^3	1.00×10^{-3}	329 ± 20	58	4.8

^a Relative potency

Although no impressive thermodynamic trends can be extracted from the above data, the relative kinetic values can lead to interesting observations that pinpoint the influence of structural parameters toward relative affinity with ECA. First, glycodendrimer **5** harbouring the largest number of peripheral sugars do not necessarily represent the best candidate, since its K_D value is worst than two of the three dodecavalent congeners **2** and **3**. Interestingly, although exhibiting similar lowest valencies, these clusters were built around distinct building blocks and displayed different kinetic values. Predominantly, distinct k_{on} values indicate that the rates of association were strongly dependent to the nature of the structural elements that dictate the tri-dimensional organization of the sugars. In this series, aromatic branching units as in **1** seemed to hamper the optimal display of the LacNAc residues while aliphatic homologs, and especially elongated **2** allowed a better recognition. On the other hand, a noticeable enhancement in affinity was obtained for **4** having UV-

visible gallic acid moieties incorporated in the scaffold, in comparison to **1** (Figure 2-6).

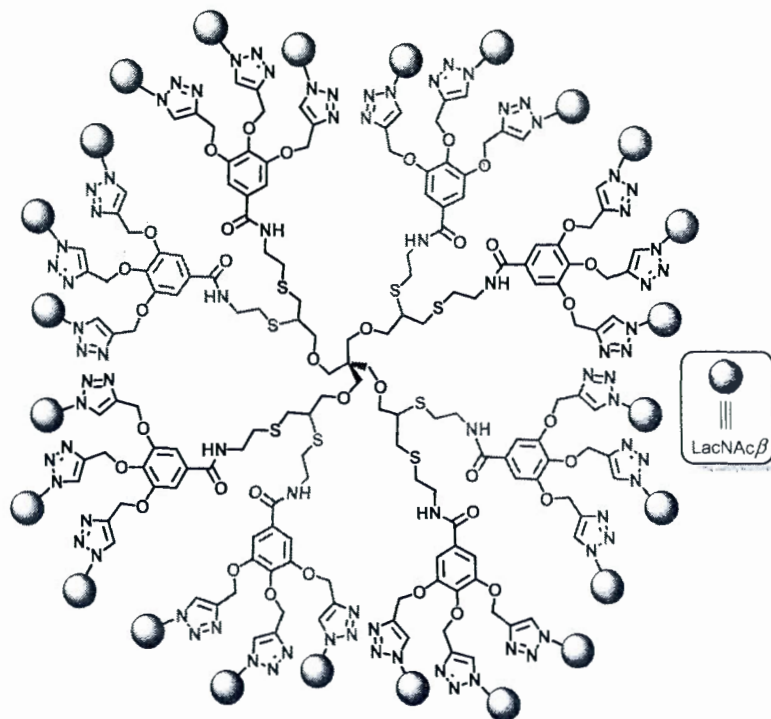


Figure 2-6 Superimposition of glycoclusters **1** (black, 12 sugars) and **4** (black + green + red, 24 sugars) to illustrate their similar composition but different epitopes' density.

This result further highlights the role of multivalency and more precisely the epitopes' density which led to an enhancement in activity from binding events. Noteworthy is the fact that this trend is not obvious when comparison between **3** and **5** is made. Although similar cluster of six epitopes emanating from the same dithiolated moieties are present at the periphery, their spatial presentation is insured from various cores and is responsible for the different binding behaviours against ECA. Thus, in this experiment, the focal branching emanating from the templates that direct the repeating units is also likely playing a critical role in the ligand-lectin recognition phenomenon. In addition, the stereoisomers created by the TYC reaction could not be accounted for the binding differences as the chiral centers are 14-15

atoms away from the anomeric carbon of the Glc residues bound to the external outer limit of the galactoside binding site (see *Appendix A, Fig. S101*).

In order to get more insight into the relative “multivalent effect” of the glycodendrimers, we have also performed another SPR-based assay involving a competitive inhibition studies. In this context, 6-amino hexyl β -D-galactopyranoside **31**³⁵ was immobilized onto the sensor surface to provide a more realistic mimetic system of the eukaryotic cell surface that can recognize the lectin. For the determination of IC₅₀ values, equilibrium mixtures of ECA (5 μ M) in contact with increasing concentrations of glycodendrimers **1-5** and monomers **18** and **30** have been used as analytes over the surface of galactoside **31**. Thus, the affinity of ECA towards the bound galactoside in the presence of different concentrations of glycodendrimers was measured (Table 2-4).

Table 2-4 IC₅₀ values of the glycodendrimers **1-5** and monomers **18** and **30** derived from competitive inhibition SPR studies.

Cpd	IC ₅₀ (μ M)	r.p. ^a	r.p./sugar
18	563 \pm 34	-	-
30	362 \pm 20	1	1
1	3.82 \pm 0.23	95	8
2	3.07 \pm 0.09	118	10
3	6.19 \pm 0.52	58	5
4	0.61 \pm 0.02	593	25
5	0.31 \pm 0.01	1168	32

^a Relative potency

A typical sensorgram profile and the corresponding inhibition curve derived from the sensorgrams are shown in Figure 1-7 for glycodendrimer **5**, the best ligand in this experiment (see *Appendix A, SI* for the remaining glycodendrimers **2-5** and for monomers **18** and **30**). Once again, consistent high micromolar IC₅₀ values were obtained for monomers **18** and **30**, with a slightly better activity for the latter having a

triazole group at the anomeric position which could be attributed to known “aglycon-assisted” binding events.³⁶

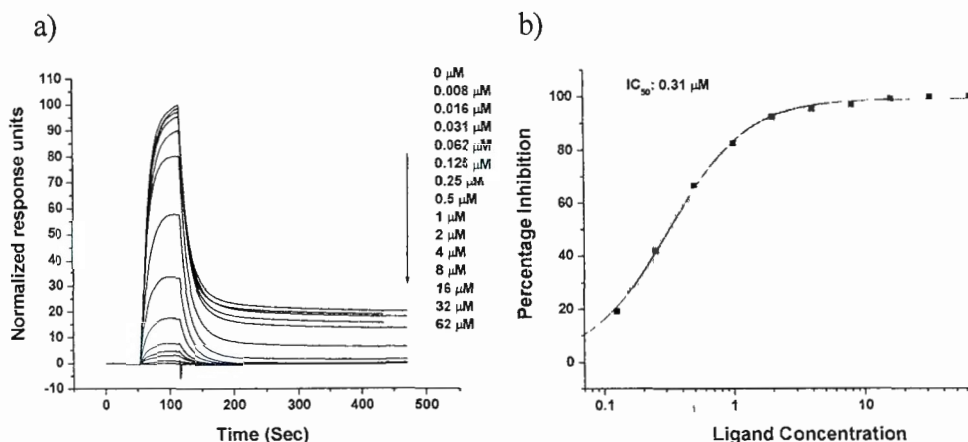


Figure 2-7 (a) Sensorgrams obtained by injection of ECA (5 μM) incubated with different concentrations of glycodendrimer **5** varying from 0.008 μM (top curve) to 62 μM (bottom curve) on the surface of immobilized galactoside **31**. (b) The inhibitory curve for the glycodendrimer **5**. IC_{50} value was extracted from the sigmoidal fit of the inhibition curve.

Overall, similar tendencies obtained during the previous assays were observed, however with enhanced effects. Indeed, the improved affinity corresponded to an increased number of ligands with relative potencies exceeding 1000 for the best candidate **5**, resulting in a 32- fold better affinity for each sugar in comparison to monomer **30**. Also, similar discrepancies were obtained throughout the dodecavalent glycoclusters **1-3**, reinforcing the importance of structural parameters' arrangement and the induced organization of dendronized moieties. In this series, elongated ligand **2** exhibited the best results with an interesting 3.1 μM value. As observed earlier, the addition of four trivalent dendrons (comparing between **1** and **4**, Figure 2-6) allowed favorable effects since the increase in density was responsible for an important drop in IC_{50} values. Notably, this corresponds to a relative potency enhancement of 2.5-fold for each epitope on tetra-cosavalent **4** compared to dodecavalent glycocluster **1**. Contrary to studies for K_D determination, this tendency is also effective with the

multivalent contribution afforded by aliphatic scaffolds. While **3** constitutes the worst ligand overall, the multiplication of the hexavalent motif from dithiolation strategy afforded stunning enhancement in affinity with best results for **5**.

Though the relative affinities differ from both SPR studies, the proposed family of multivalent LacNAc- dendrimers **1-5** contains some of the best ECA ligands known to date, with high nanomolar affinities. The observed discrepancies throughout the assays may be explained from the fact that the kinetic data (Table 2-3) was obtained by assuming the simple 1:1 Langmuir model binding between the surface-bound dimeric ECA and the multivalent ligands, although attempts to avoid this situation were made by low density ligand immobilization. It is interesting to note that the relative potencies were found to be higher in competitive inhibition studies than in the surface-bound ECA. It may be partly attributable to the fact that in solution phase competitive studies, upon equilibration for 1 h, glycodendrimers may have enough time to bind almost irreversibly with ECA through multivalent cross-linking lattice interactions when compared to instantaneous binding in solid phase interactions.

2.3 Conclusions:

In conclusion, a novel type of onion peel strategy was designed for the synthesis of glycodendrimers by using different families of building blocks containing orthogonal functional groups at each layer or generation of the dendritic growth. The synthesis was achieved by using highly efficient reactions, such as, thiol-ene or thiol-yne, esterification, and azide-alkyne click chemistry. The robustness and flexibility of this approach were translated by the efficiency of each coupling step, regardless of the nature of terminal reactive functionalities, as exemplified with the elaboration and use of polyamine, polyol, polyacid, polyalkene, and polyalkyne multivalent templates. The onion peel strategy presented herein may lead to new directions in dendrimer research for the synthesis of much richer family of functionalized dendritic structures and for creating higher structural diversity. To exemplify the influence of such structural diversity, two distinct SPR studies with the leguminous lectin *Erythrina*

crisagalli (ECA) as a model were conducted and led to interesting results towards the design of optimized lectin ligands. Most importantly, the proposed synthetic approach validates the concept according to which each structural element influences the recognition processes. Thus, this work brings a valuable complement to a recent study³⁷ that investigated the influence of different “click” ligation modes on glycodendrimers-induced lectin recognition. The present synthetic strategy allows a better rationally programmed arrangement of branching units towards biologically active multivalent constructs. This investigation is directed to the development and the application of this approach towards the construction of potent ligands against human lectins. The conception of functionalized templates as promising candidates in vaccine immunotherapy³⁸ is also under the scope and will be reported in due course.

2.4 References:

- 1 (a) G. R. Newkome, C. N. Moorefield and F. Vögtle, *Dendrimers and Dendrons: Concepts, Synthesis, Applications*. Wiley-VCH, New York, 2001. (b) J. M. J. Fréchet and D. Tomalia, *Dendrimers and Other Dendritic Polymers*, John Wiley & Sons, New York, 2001. (c) A.-M. Caminade, C.-O. Turrin and J.-P. Majoral, *New J. Chem.*, 2010, **34**, 1512-1524.
- 2 K. L. Wooley, C. J. Hawker and J. M. J. Fréchet, *J. Am. Chem. Soc.*, 1991, **113**, 4252-4261.
- 3 K. L. Wooley, C. J. Hawker and J. M. J. Fréchet, *Angew. Chem., Int. Ed. Engl.*, 1994, **33**, 82-85.
- 4 F. Zeng and S. C. Zimmerman, *J. Am. Chem. Soc.*, 1996, **118**, 5326-5327.
- 5 C.-H. Wong and S. C. Zimmerman, *Chem. Commun.*, 2013, **49**, 1679-1695.
- 6 (a) A. Carlmark, C. Hawker, A. Hult and M. Malkoch, *Chem. Soc. Rev.*, 2009, **38**, 352-362; (b) N. Kottari, Y. M. Chabre, T. C. Shiao, R. Rej and R. Roy, *Chem. Commun.*, 2014, **50**, 1983-1985; (c) P. Antoni, D. Nyström, C. J. Hawker, A. Hult and M. Malkoch, *Chem. Commun.*, 2007, 2249-2251; (d) T. Kang, R. J. Amir, A. Khan, K. Ohshimizu, J. N. Hunt, K. Sivanandan, M. I. Montañez, M. Malkoch, M.

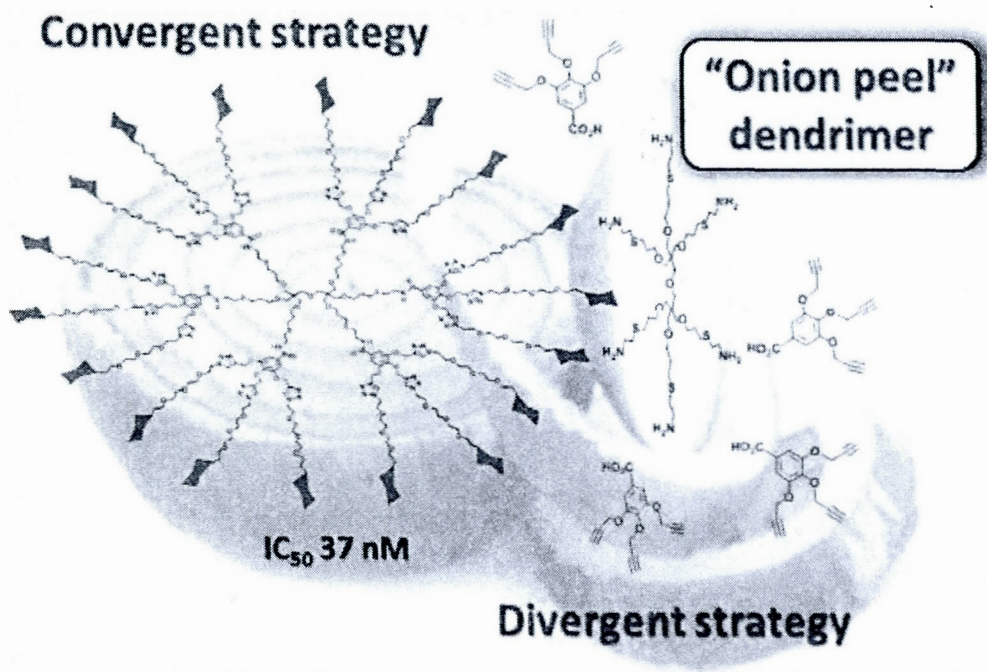
- Ueda and C. J. Hawker, *Chem. Commun.*, 2010, **46**, 1556–1558; (e) P. Antoni, M. J. Robb, L. Campos, M. Montanez, A. Hult, E. Malmström, M. Malkoch and C. J. Hawker, *Macromolecules*, 2010, **43**, 6625–6631; (f) J. W. Chan, C. E. Hoyle and A. B. Lowe, *J. Am. Chem. Soc.*, 2009, **131**, 5751–5753; (g) A. Carlmark, E. Malmström and M. Malkoch, *Chem. Soc. Rev.*, 2013, **42**, 5858–5879; (h) M. V. Walter and M. Malkoch, *Chem. Soc. Rev.*, 2012, **41**, 4593–4609.
- 7 (a) Y. M. Chabre and R. Roy, *Chem. Soc. Rev.*, 2013, **42**, 4657–4708; (b) Y. M. Chabre and R. Roy, *Adv. Carbohydr. Chem. Biochem.*, 2010, **63**, 165–393; (c) Y. Li, Y. Cheng and T. Xu, *Curr. Drug Discovery Technol.*, 2007, **4**, 246–254; (d) R. Roy, *Trends. Glycosci. Glycotechnol.*, 2003, **15**, 291–310; (e) M. Touaibia and R. Roy, *Mini-Rev. Med. Chem.*, 2007, **7**, 1270–1283; (f) S. A. Nepogodiev and J. F. Stoddart, *Adv. Macromol. Carbohydr. Res.*, 2003, **2**, 191–239; (g) N. Röckendorf and T. K. Lindhorst, *Top. Curr. Chem.* 2001, **217**, 201–238; (h) M. J. Cloninger, *Curr. Opin. Chem. Biol.*, 2002, **6**, 742–748.
- 8 R. Roy, D. Zanini, S. J. Meunier and A. Romanowska, *J. Chem. Soc. Chem. Commun.*, 1993, 1869–1872.
- 9 For recent reviews: O. Renaudet and R. Roy, *Chem. Soc. Rev.*, 2013, **425**, 4515–4517 (Themed Issues “Multivalent Scaffolds in Glycoscience: An Overview”).
- 10 (a) Y. C. Lee and R. T. Lee, *Acc. Chem. Res.*, 1995, **28**, 321–327; (b) R. Roy, *Curr. Opin. Struct. Biol.*, 1996, **6**, 692–702; (c) M. Mammen, S. K. Choi and G. M. Whitesides, *Angew. Chem. Int. Ed.*, 1998, **37**, 2754–2794; (d) J. J. Lundquist and E. J. Toone, *Chem. Rev.* 2002, **102**, 555–578; (e) N. Jayaraman, *Chem. Soc. Rev.*, **2009**, **38**, 346–3483.
- 11 Y. M. Chabre and R. Roy, *Curr. Top. Med. Chem.*, 2008, **8**, 1237–1285.
- 12 H. C. Kolb and K. B. Sharpless, *Drug Discovery Today*, 2003, **8**, 1128–1137.
- 13 (a) M. J. Robb and C. J. Hawker, In *Synthesis of Polymers*, Eds. D. A. Schlueter, C. J. Hawker, J. Sakamoto, Wiley-VCH Verlag, Weinheim, 2012; (b) G. Franc and A. K. Kakkar, *Chem. Soc. Rev.*, 2010, **39**, 1536–1544; (c) R. K. Iha, K. L. Wooley,

- A. M. Nyström, D. J. Burke, M. J. Kade and C. J. Hawker *Chem. Rev.*, 2009, **109**, 5620–5686.
- 14 (a) A. Dondoni and A. Marra, *Chem. Soc. Rev.*, 2012, **41**, 573–586; (b) M. J. Kade, D. J. Burke and C. J. Hawker, *J. Polym. Sci., Part A: Polym. Chem.*, 2010, **48**, 743–750; (c) M. A. Cole and C. A. Bowman, *J. Polym. Sci., Part A: Polym. Chem.*, 2012, **50**, 4325–4333; (d) K. L. Killops, L. M. Campos and C. J. Hawker, *J. Am. Chem. Soc.*, 2008, **130**, 5062–5064; (e) J. W. Chan, B. Yu, C. E. Hoyle and A. B. Lowe, *Chem. Commun.*, 2008, 4959–4961.
- 15 (a) R. Hoogenboom, *Angew. Chem. Int. Ed.*, 2010, **49**, 3415–3417; (b) A. B. Lowe, C. E. Hoyle, C. N. J. Bowman, *Mater. Chem.*, 2010, **20**, 4745–4750; (c) B. D. Fairbanks, T. F. Scott, C. J. Kloxin, K. S. Anseth and C. N. Bowman, *Macromolecules*, 2009, **42**, 211–217; (d) G. Chen, J. Kumar, A. Gregory and M. H. Stenzel, *Chem. Commun.*, 2009, 6291–6293; (e) J. W. Chan, C. E. Hoyle and A. B. Lowe, *J. Am. Chem. Soc.*, 2009, **131**, 5751–5753.
- 16 (a) B. Neises and W. Steglich, *Angew. Chem. Int. Ed.*, 1978, **17**, 522–524.
- 17 (a) M. Meldal and C. W. Tornøe, *Chem. Rev.*, 2008, **108**, 2952–3015; (b) P. Wu, M. Malkoch, J. N. Hunt, R. Vestberg, E. Kaltgrad, M. G. Finn, V. V. Fokin, K. B. Sharpless and C. J. Hawker, *Chem. Commun.*, 2005, 5775–5777; (c) F. Himo, T. Lovell, R. Hilgraf, V. V. Rostovtsev, L. Noodleman, K. B. Sharpless and V. V. Fokin, *J. Am. Chem. Soc.*, 2005, **127**, 210–216; (d) S. Dedola, S. A. Nepogodiev and R. A. Field, *Org. Biomol. Chem.*, 2007, **5**, 1006–1017; (d) V. Aragão-Leoneti, V. L. Campo, A. S. Gomes, R. A. Field and I. Carvalho, *Tetrahedron*, 2010, **66**, 9475–9492.
- 18 (a) G. A. Rabinovich and M. A. Toscano, *Nat. Rev. Immunol.*, 2009, **9**, 338–352; (b) D. P. Zhou, *Curr. Protein Pept. Sci.*, 2003, **4**, 1–9.
- 19 (a) F.-T. Liu and G. A. Rabinovich, *Nat. Rev. Cancer*, 2005, **5**, 29–41; (b) M. Salatino, D. O. Croci, G. A. Bianco, J. M. Ilarregui, M. A. Toscano and G. A. Rabinovich, *Expert Rev. Biol. Ther.*, 2008, **8**, 45–57.

- 20 (a) D. Zanini and R. Roy, *Bioconjugate Chem.*, 1997, **8**, 187-192; (b) Y. Gao, A. Eguchi, K. Kakehi and Y. C. Lee, *Bioorg. Med. Chem.*, 2005, **13**, 6151-6157; (c) R. Masaka, M. Ogata, Y. Misawa, M. Yano, C. Hashimoto, T. Murata, H. Kawagishi and T. Usui, *Bioorg. Med. Chem.*, 2010, **18**, 621-629; (d) C. Scheibe, A. Bujotzek, J. Dervede, M. Weber and O. Seitz, *Chem. Sci.*, 2011, **2**, 770-775.
- 21 (a) C. Svensson, S. Teneberg, C. L. Nilsson, A. Kjellberg, F. P. Schwarz, N. Sharon and U. J. Krenkel, *Mol. Biol.*, 2002, **321**, 69-83.
- 22 (a) T. Kang, R. J. Amir, A. Khan, K. Ohshimizu, J. N. Hunt, K. Sivanandan, M. I. Montañez, M. Malkoch, M. Ueda and C. J. Hawker, *Chem. Commun.*, 2010, **46**, 4556-1558; (b) C. D. Heideke and T. K. Lindhorst, *Chem. Eur. J.*, 2007, **13**, 9056-9067; (c) M. Lo Conte, S. Staderini, A. Chambery, N. Berthet, P. Dumy, O. Renaudet, A. Marra and A. Dondoni, *Org. Biomol. Chem.*, 2012, **10**, 3269-3277.
- 23 (a) C. Rissing and D. Y. Son, *Organometallics*, 2008, **27**, 5394-5397; (b) G. Povie, A.-T. Tran, D. Bonnaffé, J. Habegger, Z. Hu, C. Le Narvor, and P. Renaud, *Angew. Chem. Int. Ed. Eng.*, 2014, **53**, DOI: 10.1002/anie.201309984.
- 24 S. Zhang and Y. Zhao, *Bioconjugate Chem.*, 2011, **22**, 523-528.
- 25 Z. Gan, S. Cao, Q. Wu and R. Roy, *J. Carbohydr. Chem.*, 1999, **18**, 755-773.
- 26 A. Mollard and I. Zharov, *Inorg. Chem.*, 2006, **45**, 10172-10179.
- 27 M. Srinivasan, S. Sankaraman, H. Hopf, I. Dix and P. G. Jones, *J. Org. Chem.*, 2001, **66**, 4299-4303.
- 28 F. Yao, L. Xu, G.-D. Fu and B. Lin, *Macromolecules*, 2010, **43**, 9761-9770.
- 29 E. Cavero, M. Zablocka, A.-M. Caminade and J. P. Majoral, *Eur. J. Org. Chem.*, 2010, 2759-2767.
- 30 (a) N. Lejeune, I. Dez, P.-A. Jaffrès, J.-F. Lohier, P.-J. Madec and J. Sopkova-de Oliveira Santos, *Eur. J. Inorg. Chem.*, 2008, 138-143; (b) E. Badetti, V. Lloveras, K. Wurst, R. M. Sebastián, A.-M. Caminade, J.-P. Majoral, J. Veciana and J. Vidal-Gancedo, *Org. Lett.*, 2013, **15**, 3490-3493.
- 31 BIAevaluation version 4.1, BIAcore, Uppsala, Sweden, 2003.

- 32 (a) J. L. Iglesias, H. Lis and N. Sharon, *Eur. J. Biochem.*, 1982, **123**, 247–252; (b) For K_D determination by frontal affinity chromatography: Y. Itakura, S. Nakamura-Tsuruta, J. Kominami, N. Sharon, K. Kasai and J. Hirabayashi, *J. Biochem.*, 2007, **142**, 459–469; (c) C. Jiménez-Castells, B. G. de la Torre, D. Andreu and R. Gutiérrez-Gallego, *Glycoconj. J.*, 2008, **25**, 879–887.
- 33 C. Scheibe, A. Bujotzek, J. Dervede, M. Weber and O. Seitz, *Chem. Sci.*, 2011, **2**, 770–775.
- 34 X. Zheng, T. Murata, H. Kawagishi, T. Usui and K. Kobayashi, *Carbohydr. Res.*, 1998, **312**, 209–217.
- 35 H. Tamiaki, A. Shinkai and Y. Kataoka, *J. Photochem. Photobiol. A*, 2009, **207**, 115–125.
- 36 (a) N. Sharon, *FEBS Lett.*, 1987, **217**, 145–157; (b) P. Arya, K. M. K. Kutterer, H. Qin, R. Huiping, J. Roby, M. L. Barnes, J. M. Kim and R. Roy, *Bioorg. Med. Chem. Lett.*, 1998, **8**, 1127–1132.
- 37 M. Fiore, N. Berthet, A. Marra, E. Gillon, P. Dumy, A. Dondoni, A. Imberty and O. Renaudet, *Org. Biomol. Chem.*, 2013, **11**, 7113–7122.
- 38 (a) T. C. Shiao and R. Roy, *New J. Chem.*, 2012, **36**, 324–339; (b) R. Roy and T. C. Shiao, *Chimia*, 2011, **65**, 24–29; (c) R. Roy, T. C. Shiao and K. Rittenhouse-Olson, *Braz. J. Pharm. Sci.*, 2013, **49**, 85–109.

CHAPTER 3

HIGHLY VERSATILE CONVERGENT/DIVERGENT "ONION PEEL"
STRATEGY TOWARD POTENT MULTIVALENT GLYCODENDRIMERS

In this chapter, we have further explored the versatility of "onion peel approach" reported in previous chapter. We used both convergent and divergent routes to construct "onion peel" glycodendrimers and demonstrated that this strategy is highly efficient in both ways and represents an additional strategy for the construction of highly diversified dendrimers. We assembled chemically heterogeneous layers at each generation by using a combination of orthogonal building blocks and highly efficient chemical reactions. Glycodendrimers constructed using this methodology resulted in one of the best multivalent ligand known against the virulent factor from bacterial lectin isolated from *Pseudomonas aeruginosa*.

Reproduced in part with permission from:

Rishi Sharma, Naresh Kottari, Yoann M. Chabre, Leïla Abbassi, Tze Chieh Shiao,
and René Roy *Chemical Communication*, **2014**, 50, 13300-13303.

Copyright, 2014, Royal Society of Chemistry

3.1 Introduction:

Dendrimers are well-defined, hyperbranched tree like macromolecules which have shown great potential for applications in diverse areas ranging from nanoengineering to medicine.¹ Their striking architecture leads to excellent properties, but unfortunately brings in many synthetic challenges as well. Traditionally, their iterative construction emanates from a central core in a layer by layer fashion using repetitive moieties *via* most popular divergent² and convergent³ methods. Both strategies have their own drawbacks and often require tedious repetitive synthetic steps, with classically only a slow enhancement in the number of peripheral functionalities at each generation. To meet the increasing demand of dendrimers for advanced applications, the scientific focus has been shifted towards their efficient and rapid construction involving a minimum number of reactions and with access to a large number of surface active functionalities. Notably, the introduction of orthogonal building blocks, the use of hyperfunctionalized synthons combined to robust and highly efficient chemical reactions has recently fulfilled these specifications.⁴⁻⁶

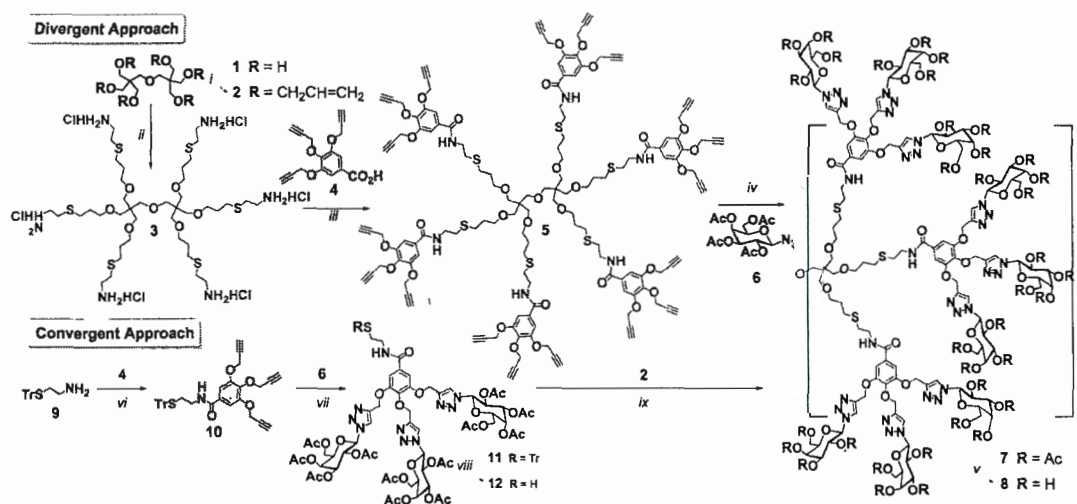
Glycodendrimers in particular, with their widespread applications⁷ as microbial antiadhesins, biosensors, vaccines, drug delivery, and gene transfection do not depart from this efficacy pursuit. In this context, we recently reported a novel divergent “onion peel” approach to construct glycodendrimers using distinct and orthogonal building blocks at each generation growth.⁸ With this strategy, we demonstrated that structural diversities could be efficiently and rapidly harnessed at low generation. Notably, distinct hydrophobic/hydrophilic and rigidity/flexibility balances together with different epitopes’ presentations clearly influenced their potencies as protein ligands. In complement to this rationally programmed arrangement of branching units, we wish to report herein the inverted strategy with the multivalent presentation of different types of ligands around a fixed “onion peel” dendritic scaffold. Chemically heterogeneous layers were assembled at each generation in both convergent and divergent strategies using a combination of orthogonal building

blocks and highly efficient chemical reactions such as radical initiated photochemical thiol-ene reaction (TEC),^{5,9} amidation,¹⁰ and copper-catalyzed azide-alkyne cycloadditions (CuAAC) reactions.¹¹

3.2 Results and discussion:

The divergent construction of these novel dendrimers was initiated with inexpensive commercially available dipentaerythritol **1** serving as a dense A₆ core. Per-*O*-allylation with allyl bromide in the presence of NaH in DMF provided *hexakis*allylated G(0) derivative **2** in 80% yield (Scheme 3-1). Complete allylation was clearly confirmed by ¹H NMR, which showed the characteristic allylic signals at δ 5.90 and 5.34-5.08 ppm and the disappearance of OH signals together with its predicted HRMS. Core structure **2** was next subjected to radical TEC reaction with excess of cysteamine hydrochloride in the presence of photoinitiator 2,2 dimethoxy-2-phenylacetophenone (DMPAP, 10 mol%) under UV irradiation at 365 nm in DMF. Water soluble hydrochloride **3** was uneventfully isolated in 75% yield after dialysis and fully characterized by ¹H- and ¹³C-NMR spectroscopy that showed the absence of olefinic signals, and by HRMS. Polyamine **3** was then treated with tripropargylated gallic acid derivative **4**¹² by amidation under classical carbodiimide coupling (72%). Notably, the use of AB₃ monomer **4**, when combined to our A₆ core **2**, readily provided G(1) hypercore **5** already possessing eighteen surface functional groups. For comparison purposes, PAMAM dendrimers and the like, built around AB₂ monomers, only reach these values at the G(2) level. Dendrimer **5** was next treated with peracetylated β-D-galactopyranosyl azide **6**¹³ under classical click reaction conditions (CuSO₄·5H₂O, Na-ascorbate in THF/H₂O) to afford octadecavalent galactodendrimer **7**. ¹H-NMR spectrum showed the complete disappearance of the propargylic C≡CH signals at δ 2.50 ppm and the expected appearance of two distinct triazole signals integrating in a 2:1 ratio at δ 8.09 and 8.16 ppm. Another evidence for the monodispersity of the dendritic structure was further confirmed by gel permeation chromatography (GPC) which showed a narrow and symmetrical Gaussian pattern

with a PDI of 1.03. Subsequently, de-*O*-acetylation of **7** under Zemplén conditions (NaOMe, MeOH) provided the final glycodendrimer **8** having 18 deprotected galactopyranoside moieties in quantitative yield (a molecule having 72-OH groups)!



Scheme 3-1 Divergent and convergent synthesis of octadecavalent galactodendrimer **8**.

Reagents and conditions: (i) NaH, Allyl bromide, DMF, 0°C to rt, 5h, 80%; (ii) Cysteamine·HCl, DMPAP, DMF, 365 nm, 3h, 75%; (iii) EDC, DMAP, DIPEA, DMF, 60°C, o.n., 72%; (iv) CuSO₄·5H₂O, Na ascorbate, THF/H₂O (1:1), 40°C, 12h, 81%; (v) MeONa/MeOH, rt, o.n., 88%; (vi) EDC, DMAP, DMF, rt, o.n., 78%; (vii) CuSO₄·5H₂O, Na ascorbate, THF/H₂O (1:1), 40°C, 5h, 84%; (viii) Et₃SiH, TFA, 0°C, 3h, DCM, 85%; (ix) AIBN, Dioxane, 75°C, 5h, 53%.

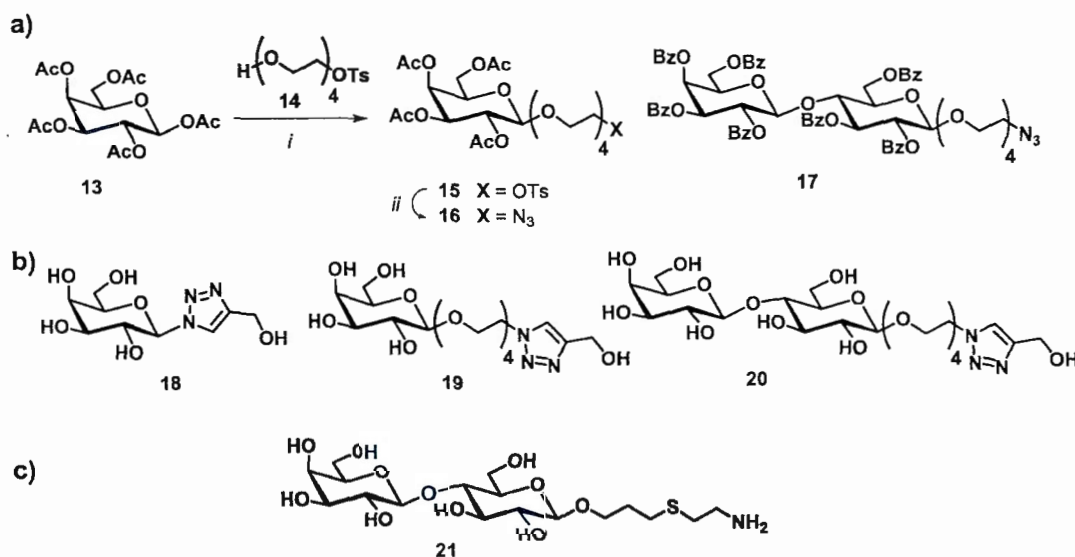
In order to illustrate the full versatility of this “onion peel” strategy for the rapid access to structurally diversified dendrimers, we also envisaged the construction of dendrimer **7** by a convergent approach. This alternative was initiated with *S*-trityl cysteamine **9** prepared by a slight modification (Appendix B, SI, Scheme 1) of literature procedure.¹⁴ Classical amidation conditions with **4** (EDC, DMAP, DMF) provided intermediate **10** in 78% yield. Cu-catalyzed click reaction was then performed in the presence of galactosyl azide **6** to afford wedged glycodendron **11** in 84% yield. Once again, the apparition of two discrete triazole singlets in ¹H NMR

with suitable integration (δ 8.04 and 8.15 ppm; 2:1 ratio), coupled with the disappearance of propargylic signals confirmed the triple grafting of the sugar ligand. Chemoselective deprotection of the thiol group using 5% TFA in the presence of Et_3SiH as a cation scavenger afforded dendron **12** in excellent yield (85%), without any trace of disulfide side-products. The aromatic protons corresponding to the trityl group at δ 7.46-7.17 ppm completely disappeared. Notably, the triplet corresponding to the CH_2 in the α -position of tritylated thiol **11** at δ 2.50 ppm shifted down-field at δ 2.75 ppm. Final ligation of thiol **12** with *hexakis*allylated core **2** was achieved using thiol-ene coupling reaction (AIBN, Dioxane, 75°C , 5h.) to provide pure glycodendrimer **7** in a 53% yield (not optimized). Hence, we clearly demonstrated that the convergent sequence could be applied toward the construction of functionalized "onion peel" glycodendrimers without substantial loss of efficiency (5 steps and 24% overall yield from **1** vs 4 steps and 35% for the divergent method).

It is well established that key factors for improving the overall avidity of glycodendritic architectures against bacterial and leguminous lectins through multivalent binding processes originate from: 1) the relative accessibility of the sugar ligands at the dendritic surfaces⁸ and 2) the inner scaffold structures/valency themselves.^{7c,15,16} In order to further our understanding and the rationalization of these features using the above unique flexible "onion peel" template from which emanated galactopyranoside ligands with different aglycones, glycodendrimers with longer penultimate spacers were next constructed. Hence, for lectin's better accessibility toward the sugar ligands, longer branching residues and the choice of the peripheral sugars should constitute improved design. Toward this goal, we synthesised both galactopyranoside and lactoside dendrimers with tetraethylene glycol (TEG) spacers (Scheme 3-2).

Treatment of galactopyranose pentaacetate **13** with monotosylated tetraethylene glycol **14**¹⁷ under Lewis acid-catalyzed conditions ($\text{BF}_3 \cdot \text{Et}_2\text{O}$ in DCM) afforded compound **15** in 55% yield. Substitution of the tosylate in **15** by a terminal azide function was readily accomplished using NaN_3 in DMF to give **16** in 82%

yield. Analogously, coupling tosylated TEG derivative **14** onto its peracetylated lactose homolog, followed by substitution with azide were performed as previously described,¹⁷ but better results were ultimately obtained through the *per*-benzoylated derivative **17**, which allowed easier purification and increased yields (see *Appendix B, SI* for protocol). Both azido-terminated sugar ligands **16** and **17** were coupled onto scaffold **5** via CuAAC to afford glycodendrimers **22** and **24** in 76-77% yields, which correspond to nearly quantitative individual coupling (Scheme 3-3).

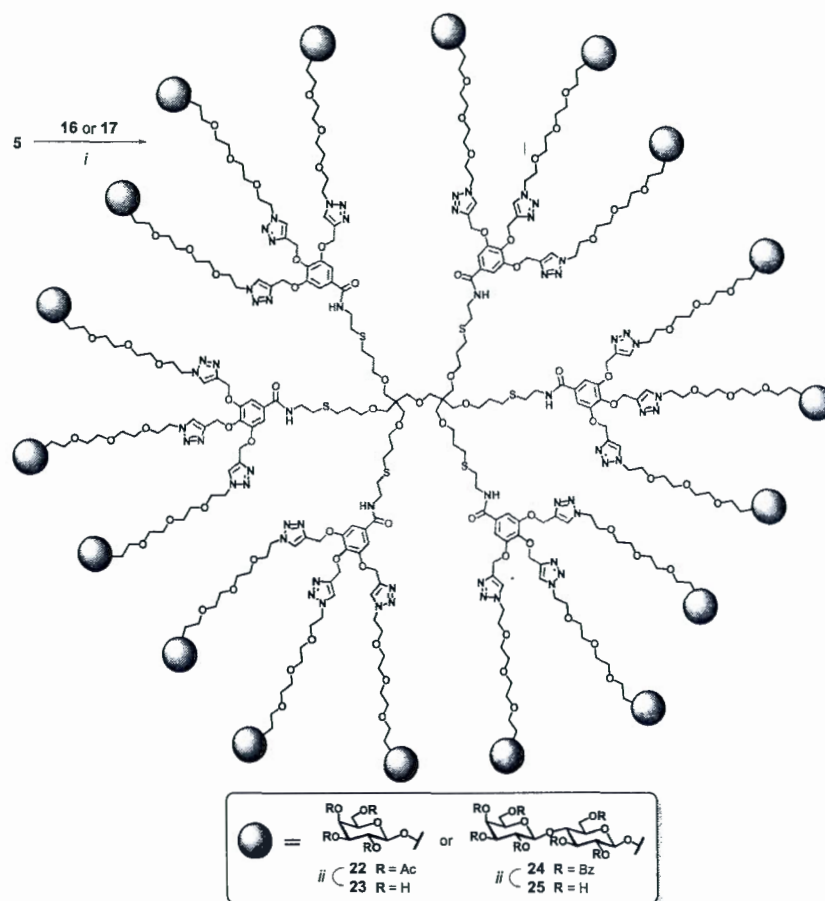


Scheme 3-2 a) Syntheses of monomeric azido precursors **16-17**, b) reference compounds **18-19** and c) lactoside derivative immobilized on the chip for SPR studies.

Reagents and conditions: i) BF₃·Et₂O, DCM, 0°C to rt, 4h, 55%; ii) NaN₃, DMF, 90°C, o.n., 82%.

Unequivocally, both ¹H and ¹³C NMR spectra indicated complete disappearance of propargylic signals and sugar incorporation with calculated relative integration. HRMS together with the presence of molecular ions and fragmentations corresponding to regular losses of carbohydrate moieties gave convincing proofs of structural integrity. Zemplén transesterification (NaOMe, MeOH) furnished two additional water soluble glycodendritic candidates **23** (90%) and **25** (86%) for

comparative inhibition experiments with a bacterial lectin from *Pseudomonas aeruginosa*. Note that dendrimer **25** possesses 126 peripheral OH groups and thus, can serve on its own as an interesting precursor for further functionalization and applications.



Scheme 3-3 Synthesis of glycodendrimers **23** and **25**.

Reagents and conditions: i) $\text{CuSO}_4 \cdot 5\text{H}_2\text{O}$, Na ascorbate, THF/ H_2O , 40°C , 12h, 76%-**22**, 77%-**24**; ii) NaOMe, DCM, MeOH, pH 9-10, rt, o.n., 90%-**23**, 86%-**25**.

In this context, the relative binding affinities of three novel glycodendrimers **8**, **23**, and **25** were evaluated by competitive surface plasmon resonance (SPR) using the galactoside specific bacterial lectin from the gram-negative bacteria *P. aeruginosa*.^{6,18} This protein constitutes a virulence factor and is involved in the pathogenesis of the bacteria in cystic fibrosis patients. To suitably evaluate the beneficial presentation of

the multivalent sugar ligands, monomeric standards **18**¹⁹, **19** and **20** corresponding to mimetics of the peripheral saccharidic belt of each conjugate were synthesized. To this end, CuAAc conditions were applied on glycosyl azides **6**, **16**, and peracetylated derivative of **17**, respectively, in the presence of propargylic alcohol, followed by classical de-*O*-acetylation under the Zemplén conditions (see *Appendix B, SI* for protocols).

Table 3-1 IC₅₀ values of glycodendrimers and their monomeric analogs derived from competitive inhibition SPR studies.

Entry	Cpd	IC ₅₀ (μM)	R.p. ^a	R.p./sugar ^b	β ^b
Galactoside					
1	18	43 ± 1.5	1	1	11
2	8	0.22 ± 0.02	195	11	
TEG-Galactoside					
3	19	21 ± 1.5 ^c	2	2	32
4	23	0.037 ± 0.005	1162	65	
TEG-Lactoside					
5	20	958 ± 34	0.05	0.05	11
6	25	4.2 ± 0.4	10	0.6	

^a Relative potency. ^b Potency enhancement of individual sugar throughout the same family. ^c This value is consistent with the one previously described for the tri(ethylene)glycol congener.²¹

For the competitive inhibition studies, the lactoside derivative **21**²⁰ was immobilized onto the commercial SPR sensor chip (CM5) following the manufacturer's procedure. IC₅₀ values (Table 3-1) were determined from the pre-incubated mixtures of PA-IL lectin (1.5 μM) with increasing concentrations of monomers or glycodendrimers used as analytes over the surface of CM5-bound **21**. The SPR experiments clearly demonstrated that glycodendrimers **8**, **23**, and **25** exhibited much higher binding affinity compared to their corresponding monovalent

derivatives **18**, **19**, and **20** due to “multivalent or glycoside cluster effect”.²² As expected, monomeric lactoside **20** represented a weaker ligand for PA-IL¹⁸ while the addition of a TEG linker to the galactoside moiety (**19** vs **18**) allowed a 2-fold enhancement of the affinity for the lectin. Thus, the additional glucoside residue in lactosides is playing a detrimental effect which therefore cannot just be simply accounted for a longer linker. Interestingly, galactosylated dendrimer **8** exhibited low micromolar IC₅₀ values (0.22 μ M), while most notably, the multivalent presentation of TEGylated galactodendrimer **23** afforded one of the best ligand known to date with an IC₅₀ value of 37 nM that compared well with the results obtained with multivalent conjugates built around flexible or rigid scaffolds.²³ These results unambiguously highlight the key-role of linkers in the interactions with lectin, with a counter-balanced entropic cost due to their flexibility. Additionally, tri-dimensional distribution of terminal and optimized galactosides crucially contributed to high potencies since a substantial improvement (32-fold) was observed for each ligand in **23**, when compared to monomeric reference **19**, while weaker individual enhancements were obtained with congested (**8** vs **18**) or unoptimized (**20** vs **25**) conjugates (11-fold).

3.3 Conclusions:

In summary, we demonstrated that the structural diversity in the construction of “onion peel” dendrimers, accessible *via* both convergent and divergent routes, represents an additional strategy for the build-up of dense surface groups within low dendrimer generation. It also represents clear advantages over existing approaches by providing versatile hypercore building blocks. Moreover, by not restricting layer by layer syntheses with identical subunits, one can programme the physical/biophysical properties of the dendrimers, as exemplified here with TEG residues. Of particular interest in this instance, is the use of underexploited dipentaerythritol as an A₆ core molecule. In fact, work is now in progress for further application on this useful building block as an AB₅ moiety. The work presented herein will undoubtedly be

useful to generate efficient and programmable multivalent antiadhesive agents against bacterial infections.^{7a,24} Rationalization of the preferential binding mode(s) together with determination of the precise role of each structural parameter leading to high avidity ligands such as in compound **23** are under investigation. Multivalent “onion peel” inhibitors harbouring optimized sugar epitopes, notably containing aromatic residue, are also presently under the scope. Further applications as antiadhesins towards galectins,¹⁷ or as vectors for vaccines or drug targeting nanomaterials²⁵ are also under investigation.

3.4 References:

1. (a) E. Buhleier, W. Wehner and F. Vögtle, *Synthesis*, 1978, 155–158; (b) A.-M. Caminade, C.-O. Turrin and J.-P. Majoral, *New J. Chem.*, 2010, **34**, 1512–1524; (c) S. Svenson and D. A. Tomalia, *Adv. Drug Deliver. Rev.*, 2005, **57**, 2106–2129; (d) M. A. Mintzer and M. W. Grinstaff, *Chem. Soc. Rev.*, 2011, **40**, 173–190; (e) M. Sowinska and Z. Urbanczyk-Lipkowska, *New J. Chem.*, 2014, **38**, 2168–2203.
2. (a) D. A. Tomalia, H. Baker, J. Dewald, M. Hall, G. Kallos, S. Martin, J. Roeck, J. Ryder and P. Smith, *Polym. J.*, 1985, **17**, 117–132; (b) N. Launay, A.-M. Caminade and J.-P. Majoral, *J. Am. Chem. Soc.*, 1995, **117**, 3282–3283.
3. C. J. Hawker and J. M. J. Fréchet, *J. Am. Chem. Soc.*, 1990, **112**, 7638–7647.
4. F. Zeng and S. C. Zimmerman, *J. Am. Chem. Soc.*, 1996, **118**, 5326–5327.
5. K. L. Killops, L. M. Campos and C. J. Hawker, *J. Am. Chem. Soc.*, 2008, **130**, 5062–5064.
6. (a) N. Kottari, Y. M. Chabre, T. C. Shiao, R. Rej and R. Roy, *Chem. Commun.*, 2014, **50**, 1983–1985; (b) S. Chatani, M. Podgórski, C. Wang and C. N. Bowman, *Macromolecules*, 2014, dx.doi.org/10.1021/ma501418r.
7. (a) Y. M. Chabre and R. Roy, *Adv. Carbohydr. Chem. Biochem.*, 2010, **63**, 165–393; (b) Y. M. Chabre and R. Roy, *Curr. Top. Med. Chem.*, 2008, **8**, 1237–1285; (c) Y. M. Chabre and R. Roy, *Chem. Soc. Rev.*, 2013, **42**, 4657–4708; (d) O.

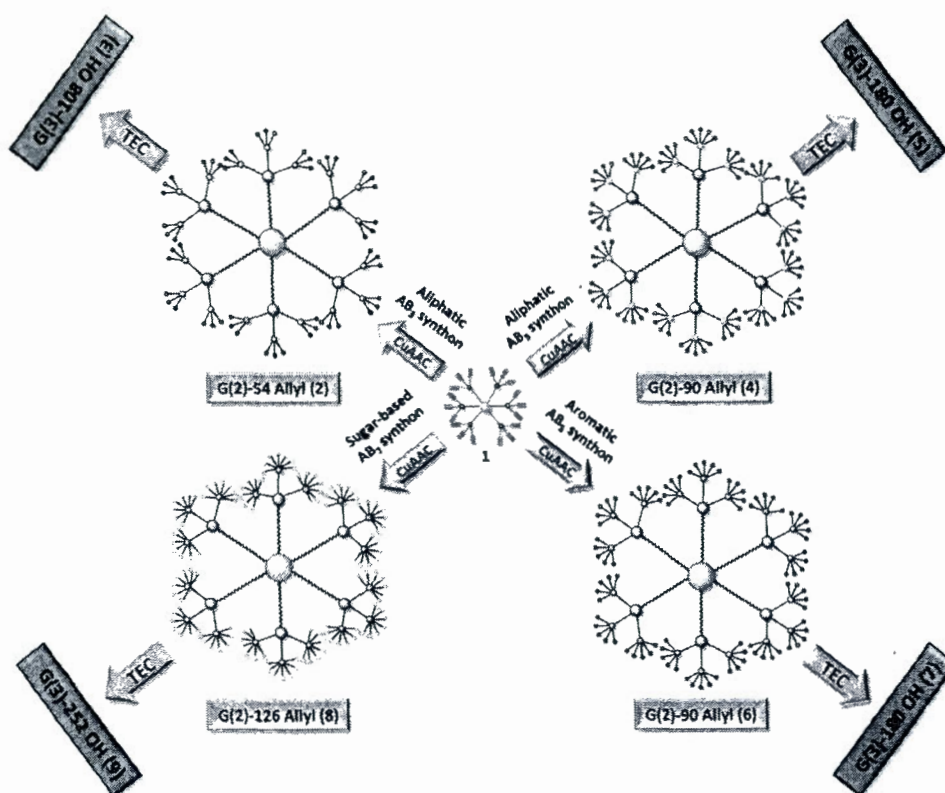
- Renaudet and R. Roy, *Chem. Soc. Rev.*, 2013, **42**, 4515–4517; (e) M. Gingras, Y. M. Chabre, M. Roy and R. Roy, *Chem. Soc. Rev.*, 2013, **42**, 4823–4841.
8. R. Sharma, K. Naresh, Y. M. Chabre, R. Rej, N. K. Saadeh and R. Roy, *Polym. Chem.*, 2014, **5**, 4321–4331.
 9. A. Dondoni and A. Marra, *Chem. Soc. Rev.*, 2012, **41**, 573–586; J. W. Chan, B. Yu, C. E. Hoyle and A. B. Lowe, *Chem. Commun.*, 2008, 4959–4961.
 10. B. Neises and W. Steglich, *Angew. Chem. Int. Ed.*, 1978, **17**, 522–524.
 11. H. C. Kolb, M. G. Finn and K. B. Sharpless, *Angew. Chem. Int. Ed.*, 2001, **40**, 2004–2021; P. Wu, A. K. Feldman, A. K. Nugent, C. J. Hawker, A. Scheel, B. Voit, J. Pyun, J. M. J. Fréchet, K. B. Sharpless and V. V. Fokin, *Angew. Chem. Int. Ed.*, 2004, **43**, 3928–3932.
 12. S. Zhang and Y. Zhao, *Bioconjugate Chem.*, 2011, **22**, 523–528.
 13. F. Li, S. Yamada, Basappa, A. Shetty, M. Sugiura and K. Sugahara, *Glycoconjugate J.*, 2008, **25**, 603–610.
 14. K. M. Halkes, A. Carvalho de Souza, C. E. P. Maljaars, G. J. Gerwig and J. P. Kamerling, *Eur. J. Org. Chem.*, 2005, **2005**, 3650–3659.
 15. Y. M. Chabre, A. Papadopoulos, A. Arnold and R. Roy, *Beilstein J. Org. Chem.*, 2014, **10**, 1524–1535.
 16. M. L. Talaga, N. Fan, A. L. Fueri, R. K. Brown, Y. M. Chabre, P. Bandyopadhyay, R. Roy and T. K. Dam, *Biochemistry*, 2014, **53**, 4445–4454.
 17. (a) V. Percec, P. Leowanawat, H.-J. Sun, O. Kulikov, C. D. Nusbaum, T. M. Tran, A. Bertin, D. A. Wilson, M. Peterca, S. Zhang, N. P. Kamat, K. Vargo, D. Moock, E. D. Johnston, D. A. Hammer, D. J. Pochan, Y. Chen, Y. M. Chabre, T. C. Shiao, M. Bergeron-Brlek, S. André, R. Roy, H.-J. Gabius and P. A. Heiney, *J. Am. Chem. Soc.*, 2013, **135**, 9055–9077; (b) S. Zhang, R.-O. Moussodia, H.-J. Sun, P. Leowanawat, A. Muncan, C. D. Nusbaum, K. M. Chelling, P. A. Heiney, M. L. Klein, S. André, R. Roy, H.-J. Gabius and V. Percec, *Angew. Chem. Int. Ed.*, 2014, doi: 10.1002/anie.201403186.

18. (a) J. Rodrigue, G. Ganne, B. Blanchard, C. Saucier, D. Giguère, T. C. Shiao, A. Varrot, A. Imberty and R. Roy, *Org. Biomol. Chem.*, 2013, **11**, 6906–6918; (b) A. Imberty, Y. M. Chabre and R. Roy, *Chem-Eur. J.* 2008, **14**, 7490–7499; (c) J.-L. Reymond, M. Bergmann and T. Darbre, *Chem. Soc. Rev.*, 2013, **42**, 4814–4822.
19. L. Harmand, S. Cadet, B. Kauffmann, L. Scarpantonio, P. Batat, G. Jonusauskas, N. D. McClenaghan, D. Lastécouères and J.-M. Vincent, *Angew. Chem. Int. Ed.*, 2012, **51**, 7137–7141.
20. H. Tamiaki, A. Shinkai and Y. Kataoka, *J. Photochem. Photobiol., A*, 2009, **207**, 115–125.
21. S. Cecioni, J.-P. Praly, S. E. Matthews, M. Wimmerová, A. Imberty and S. Vidal, *Chem. Eur. J.*, 2012, **18**, 6250–6263.
22. (a) Y. C. Lee and R. T. Lee, *Acc. Chem. Res.*, 1995, **28**, 321–327; (b) R. Roy, *Curr. Opin. Struct. Biol.* 1996, **6**, 692–702; (c) J. J. Lundquist and E. J. Toone, *Chem. Rev.*, 2002, **102**, 555–578.
23. (a) S. Cecioni, V. Oerthel, J. Iehl, M. Holler, D. Goyard, J.-P. Praly, A. Imberty, J.-F. Nierengarten and S. Vidal, *Chem. Eur. J.*, 2011, **17**, 3252–3261; (b) S. Cecioni, S. Faure, U. Darbost, I. Bonnamour, H. Parrot-Lopez, O. Roy, C. Taillefumier, M. Wimmerová, J.-P. Praly, A. Imberty and S. Vidal, *Chem. Eur. J.*, 2011, **17**, 2146–2159.
24. (a) A. Bernardi, J. Jimenez-Barbero, A. Casnati, C. De Castro, T. Darbre, F. Fieschi, J. Finne, H. Funken, K.-E. Jaeger, M. Lahmann, T. K. Lindhorst, M. Marradi, P. Messner, A. Molinaro, P. V. Murphy, C. Nativi, S. Oscarson, S. Penades, F. Peri, R. J. Pieters, O. Renaudet, J.-L. Reymond, B. Richichi, J. Rojo, F. Sansone, C. Schaffer, W. B. Turnbull, T. Velasco-Torrijos, S. Vidal, S. Vincent, T. Wennekes, H. Zuilhof and A. Imberty, *Chem. Soc. Rev.*, 2013, **42**, 4709–4727; (b) N. Berthet, B. Thomas, I. Bossu, E. Dufour, E. Gillon, J. Garcia, N. Spinelli, A. Imberty, P. Dumy and O. Renaudet, *Bioconjugate Chem.*, 2013, **24**, 1598–1611.
25. (a) S. André, P. J. C. Ortega, M. A. Perez, R. Roy and H.-J. Gabius, *Glycobiology* 1999, **9**, 1253–1261; (b) D. Giguère, S. André, M. A. Bonin, M. A.

Bellefleur, A. Provencal, P. Cloutier, B. Pucci, R. Roy and H. J. Gabius, *Bioorg. Med. Chem.*, 2011, **19**, 3280–3287; (c) S. André, B. Liu, H.-J. Gabius and R. Roy, *Org. Biomol. Chem.*, 2003, **1**, 3909–3916; (d) N. Ahmad, H.-J. Gabius, S. André, H. Kaltner, S. Sabesan, R. Roy, B. Liu, F. Macaluso and C. F. J. Brewer, *Biol. Chem.*, 2004, **279**, 10841–10847.

CHAPTER 4

A FAST TRACK STRATEGY TOWARD HIGHLY FUNCTIONALIZED
DENDRIMERS WITH DIFFERENT STRUCTURAL LAYERS: "ONION PEEL
APPROACH"



In this chapter, we report an accelerated onion peel strategy to construct a library of third generation dendrimers with 108, 180 and 252 hydroxyl end groups using a combination of microwave assisted highly efficient *CUAAC* and thiol-ene click reactions. These dendrimers were conveniently acquired with high purity and good yields in divergent manner using a variety of orthogonal building blocks having 1→3, 1→5 and 1→7 branching motifs. Multihydroxylated dendrimers tested in several

human cell types did not impair mitochondrial metabolic function or cell viability suggesting that they are good candidates for applications in biological investigations.

Reproduced in part with permission from:

Rishi Sharma, Issan Zhang, Leïla Abbassi, Rabindra Rej, Dusica Maysinger, and René Roy *Polymer Chemistry*, 2015 (**Accepted**).

Copyright, 2015, Royal Society of Chemistry

4.1 Introduction:

The last three decades have marked the emergence of dendrimers with their manifold uses in diverse areas ranging from nanomedicine, drug delivery, pharmaceuticals, material sciences, catalysis, and gene therapy.¹⁻⁸ Due to the staggering growth and high demands for the rapid and efficient access to dendrimers, researchers were motivated to introduce new innovative strategies to produce these macromolecular entities in higher yields, fewer steps, and in more economical ways. Recent advances in synthetic methodologies have boosted the development of dendrimers in an efficient and rapid manner, but access to low generation dendrimers with large number of surface groups is still a challenge.

Since the first attempts toward accelerated construction of high generation dendrimers using double stage convergent method were described,⁹ one of the major breakthrough was introduced wherein protection/deprotection steps were eliminated using orthogonal building blocks.^{9,10} The concept of orthogonality was next exploited whereby successful sixth generation dendrimer could be achieved rapidly.¹¹ Higher generation dendrimers with large number of surface groups have gained great interest in recent years due to their potential use in electronics and nanomedicine.¹²⁻¹⁸ However, only a handful approaches exist to synthesize dendrimers with large number of surface groups in few steps. One such example is a three-step synthesis of a POSS dendrimer having 392 end groups.¹⁹ Hence, an additional clue for the rapid growth lies in the choice of highly functionalized cores.

In order to improve the art in the synthetic design of these well-defined macromolecular architectures, an "onion peel" approach was recently introduced by employing a combination of a variety of orthogonal building blocks and robust chemical reactions at each generation giving rise to structurally controlled smart dendrimers.²⁰ The versatility of this strategy was further demonstrated using both convergent and divergent routes to produce dendrimers with rationally programmed branching units.²¹ Herein, a facile and accelerated "onion peel" dendrimer synthesis

approach to provide large numbers of surface groups at low generations is reported. Thus, G3 dendrimers using AB₃, AB₅ and AB₇ orthogonal hypermonomers were generated to afford 108, 180, and 252 surface groups respectively in only 2 steps starting from a common G1 dendrimer (Figure 4-1). These hypermonomers were systematically scaffolded employing highly efficient atom economical chemical reactions such as Cu(I)-catalyzed alkyne-azide (CuAAC)²² and thiol-ene reactions^{23,24} using microwave radiations.²⁵ Microwave-assisted reactions have been used in several instances in polymer synthesis to provide remarkable accessibility of reactive functionalities leading to higher yields.^{26, 27} The present strategy also takes advantage of microwave radiations to enhance the rate of reaction and decrease the reaction time as we were attempting to conjugate bulky building blocks on large number of reactive surface functionalities. The syntheses were fast, convenient, and resulted in defect free monodisperse dendrimers in high yields.

Generally, the binding interactions between synthetic ligands and their cognate biological targets increase with increasing number of peripheral groups.²⁸⁻³⁰ It is necessary to compare different generations of multivalent dendrimers to observe the effect of multivalency. The most attractive advantage of this accelerated approach is that by using orthogonal building blocks with different number of surface groups, it is possible to generate a library of dendrimers with different numbers of functional groups at the same generation.

To assess the dendrimers safety in biological systems, the cytotoxicity of the synthetic dendrimers with 108, 180 and 252-OH terminal groups in human liver carcinoma (HepG2), glioblastoma (U251), and breast adenocarcinoma (MCF-7) cells were evaluated.

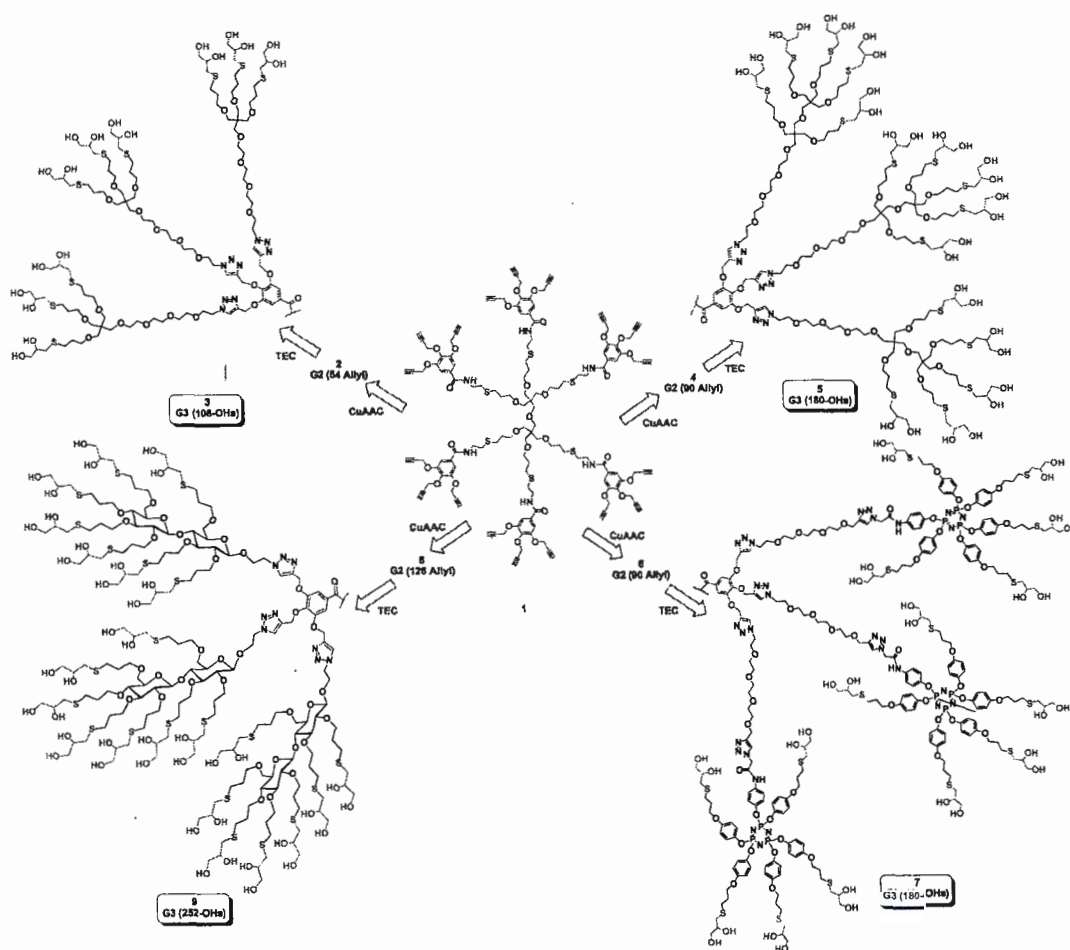


Figure 4-1 Schematic illustration of accelerated divergent dendrimer synthesis from octadecavalent hypercore **1** via onion peel approach using CuAAC and thiol-ene click reactions with AB₃, AB₅, and AB₇ monomers giving rise to G(3)-dendrimers containing 108, 180, and 252 end groups respectively.

4.2 Results and Discussion:

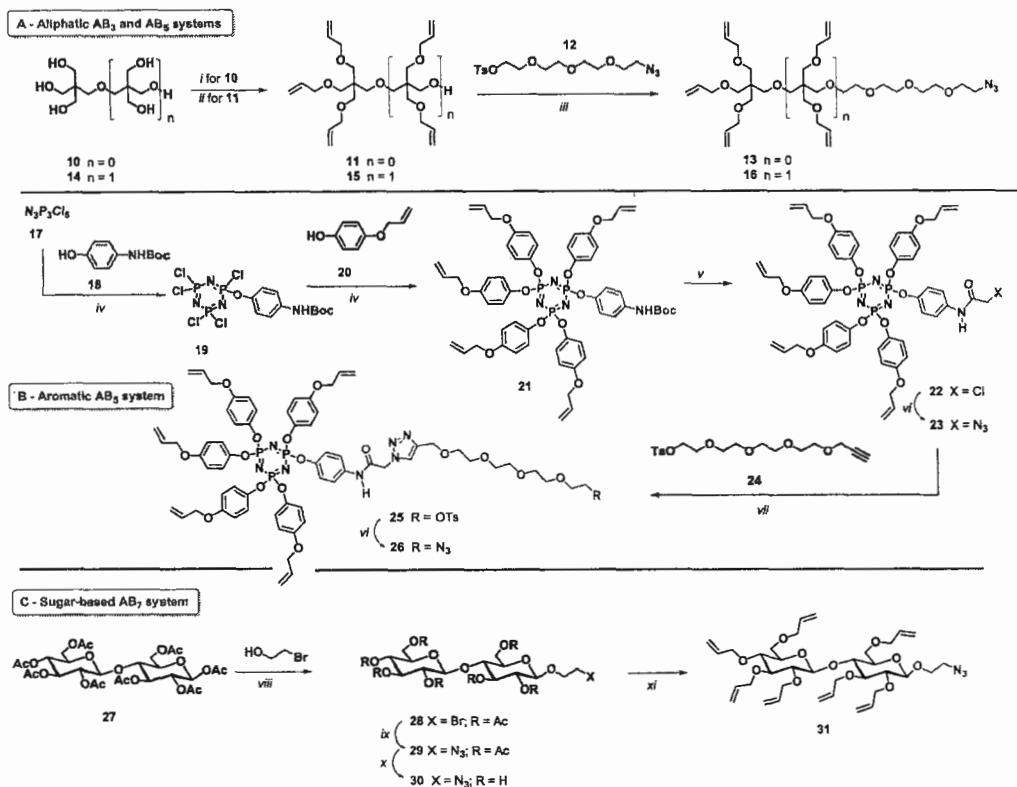
The new polyhydroxylated dendrimer series (**3**, **5**, **7**, and **9**) were constructed by a divergent manner around an octadecavalent hypercore **1**²¹ equipped with propargyl groups and hypermonomers to generate large number of surface groups at very low generations (Fig. 4-1). Scaffold **1**, incorporating a dipentaerythritol and gallic acid moieties, was synthesized by employing a previously reported procedure to provide 18 terminal acetylene groups at the G1 stage.²¹ Novel orthogonal AB₃, AB₅, and AB₇ dendrons having different branching subunits with a focal azide group and terminal

alkenes functionalities were created to first participate into powerful Cu(I) catalyzed alkyne-azide cycloadditions (CuAAC) followed at the next layer by multiple thiol-ene reactions (Scheme 4-1). The synthesis of the initial AB₃ building block **13** was initiated by treating pentaerythritol **10** with allyl bromide and sodium hydroxide that provided pentaerythritol triallyl ether **11** in 75% yield.³¹ Compound **11** was next reacted with monotosylated tetraethylene glycol azide **12**³² (NaH and DMF) to afford first intermediate **13** in 80% yield (Scheme 4-1A) clearly showing its characteristic stretching azide band at 2102 cm⁻¹ by IR spectroscopy.

Analogous aliphatic AB₅ monomer **16** was similarly prepared using commercially available and inexpensive dipentaerythritol **14**, which upon treatment with allyl bromide (10 equivalents) in 40% solution of sodium hydroxide in DMSO gave pentakis allyl derivative **15** in 40% yield along with its partially tetrakis allylated intermediate in 49% yield. It is worth mentioning here that the use of NaH instead of NaOH resulted in the formation of fully allylated derivative as the major product with minor amount (15%) of the pentakis allyl derivative **15**. Compound **15** was transformed as above with **12** into azide **16** in 68% yield (NaH, DMF, 4 h, 0°C) after column chromatography (Scheme 4-1A).

Alternatively, subsequent aromatic AB₅ dendron **26**, possessing the analogous azido-alkene functionalities, was prepared starting from hexachlorocyclotriphosphazene **17** (N₃P₃Cl₆) (Scheme 4-1B). To this end, monofunctionalization of **17** was first carried out by treatment with 0.5 equivalent of *N*-Boc-protected 4-aminophenol (**18**) in the presence of dry cesium carbonate (THF, reflux, 18 h) to afford the expected compound **19** in a moderate yield (50%). The ³¹P-NMR spectrum of **19** showed the characteristic triplet signal of the P-O-linked phosphorous at δ 12.8 ppm and a doublet signal at δ 22.4 ppm (P-Cl) due to the unsymmetrical environment of the molecule.³³ Using similar conditions, pentachloride **19** was treated with excess of *p*-allyloxyphenol **20** to provide pentakis-allylated dendron **21** in 88% yield, which showed identical phosphorous chemical shift at δ 9.89 ppm (triplet). *N*-Boc-deprotection of **21** (TFA, DCM, 0°C-rt) and

subsequent *N*-chloroacetylation with chloroacetyl chloride and Hunig's base provided **22** in 76% yield. The chloride group in **22** was further substituted by an azide group using NaN_3 and NaI in DMF to give **23** in 81% yield. An upfield shift of the α -methylene protons from δ 4.18 to 4.12 ppm in its ^1H -NMR spectrum unequivocally confirmed the product formation.

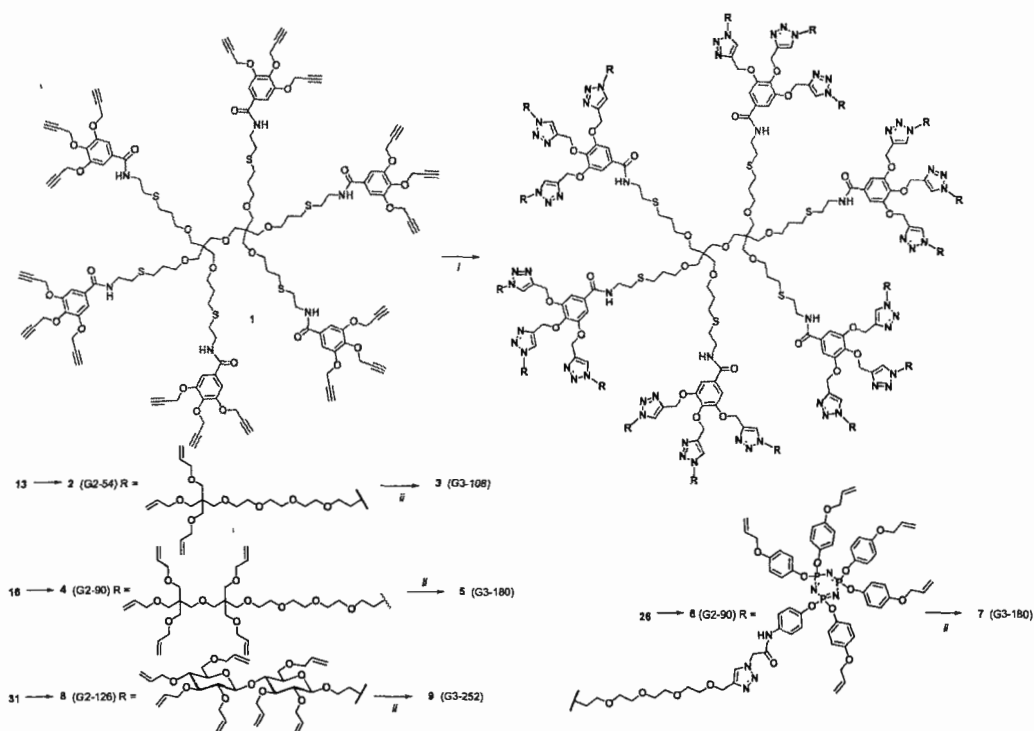


Scheme 4-1 A. Synthesis of aliphatic AB₃ (**13**) and AB₅ building blocks (**16**). *Reagents and conditions:* (i) AllylBr, NaOH, H₂O, rt, 75%; (ii) AllylBr, 40% NaOH, DMSO, 16h., 0°C–rt, 40%; (iii) NaH, DMF, 4h., 0 °C, 80% for **13** and 68% for **16**. B. Synthesis of AB₅ aromatic building block **26**. *Reagents and conditions:* (iv) Cs₂CO₃/anhy., dry THF, reflux, 18h., 75% (with 0.5 eq. of **18**) and 88% (with 10.0 eq. of **20**); (v) TFA, DCM, 0 °C–rt, 4h. then DIPEA, chloroacetyl chloride, DCM, rt, 4h., 76% (2 steps); (vi) NaN₃, NaI, DMF, 60°C 12h., 81% for **23** and 86% for **26**; (vii) CuSO₄·5H₂O, Na Asc., THF/water (1:1), 55°C, overnight, 64%. C. Synthesis of AB₇ sugar-based building block **31**. *Reagents and conditions:* (viii) BF₃ etherate, DCM, 0°C, 4h., 50% ; (ix) NaN₃, DMF, 70°C, 4h., 92%; (x) NaOMe/MeOH, rt, 3h., 90%; (xi) AllylBr, NaH, DMF, 0°C–rt, 2h., 85%.

To avoid the possibility of partial reactions due to the steric hindrance of this bulky AB₅ system with the dense G1 core, an extended linker was incorporated. Thus, azido alkene **23** was treated with monopropargylated tosyltetraethylene glycol (TEG **24**)³⁴ under classical click reaction conditions (CuSO₄·5H₂O, Na ascorbate in THF/H₂O) to afford dendron **25** in 64% yield. ¹H-NMR spectroscopy confirmed the completion of reaction as the sharp singlet for triazole proton appearing at δ 7.81 ppm integrated nicely with the NH (δ 8.73 ppm) and one of the allyl signal (δ 6.08-5.93 ppm). In the next step, the tosyl group of dendron **25** was substituted with an azide group using NaN₃ in DMF to afford **26** in 86% yield (Scheme 4-1B). In the ¹H NMR spectrum of the final pentaallylated azidodendron, the diagnostic signals related to tosyl group at δ 7.37, 7.26 and 2.38 ppm completely disappeared, thus confirming complete conversion. For the synthesis of the sugar-based AB₇ hypermonomer **31**, boron trifluoride etherate (BF₃·Et₂O) promoted glycosylation was performed between cellobiose octaacetate **27** and 2-bromoethanol which lead to the formation of **28** in 50% yield based on the isolated β-anomer. Bromide substitution in **28** using sodium azide in DMF gave azido derivative **29** in 92% yield. Again, the characteristic frequency of the azide stretching was observed in the IR spectrum at 2105 cm⁻¹. Treatment of peracetate **29** under typical Zemplén conditions (NaOMe/MeOH) provided completely de-*O*-acetylated dendron **30** in 90% yield. Per-*O*-allylation with allyl bromide under usual conditions (NaH, DMF) provided cellobiose-based AB₇ derivative **31** in 85% yield (Scheme 4-1C). Complete allylation was confirmed by ¹H-NMR as distinct allyl signals appeared at δ 6.07-5.79 and 5.35-5.04 ppm.

All the orthogonal building blocks were thus successfully achieved in high purity with excellent to moderate yields. They were fully characterized by ¹H-, ¹³C-, ³¹P-NMR, COSY experiments, HRMS, and IR spectroscopy (see Appendix C). These modular bifunctional building blocks were designed and synthesized to satisfy the ongoing quest to create complex dendritic scaffolds with high functionalities at low generation and using efficient ligation chemistry.

After building the hypermonomer subfragments **13**, **16**, **26**, and **31**, representing perallylated azides, key steps to construct the final dendrimers were followed. In order to construct the final dendrimers, a divergent "onion peel" route using CuAAC and thiol-ene reactions as synthetic tools were followed. Both these reactions have been successfully established for the synthesis of dendrimers and polymeric materials due to their desired features including simple execution, high reaction yields, few undesired side products, and easy purifications. The most attractive feature of these reactions is the introduction of orthogonality, which improves the synthetic route by dramatically decreasing the number of reaction steps. The synthesis of the next G2 dendrimer **2**, having 54 peripheral allyl groups, was achieved by ligating the AB₃ building block **13** with hypercore **1** employing standard CuAAC click reaction under microwave at 50°C (Scheme 4-2). The complete conversion was obtained within 5 hours to yield the G2 dendrimer **2** easily purified using silica gel column chromatography in 78% yield.



Scheme 4-2 Synthesis of hyperbranched 0dendrimers through a highly divergent accelerated approach. *Reagents and conditions:* (i) $\text{CuSO}_4 \cdot 5\text{H}_2\text{O}$, Na Asc., 50°C , 5h., microwave, G(2)-54 Allyl(**2**, from **13**): 78%, G(2)-90 Allyl(**4**, from **16**): 71%, G(2)-90 Allyl(**6**, from **26**): 50%, G(2)-126 Allyl(**8**, from **31**): 75%; (ii) 1-Thioglycerol, AIBN, methanol, 90°C , 6h., microwave, G(3)-108 OH (**3**): 86%, G(3)-180 OH (**5**): 82%, G(3)-180 OH (**7**): 63%, G(3)-252 OH (**9**): 85%.

Completion of the reaction was clearly established by ^1H NMR spectroscopy which showed the complete disappearance of the propargylic $\text{C}\equiv\text{CH}$ signals at δ 2.50 ppm and the expected appearance of two distinct triazole signals integrating in a 2:1 ratio at δ 7.92 and 7.84 ppm, respectively. In addition, characteristic signals for the allylic proton were also observed at δ 5.93-5.80 ppm.

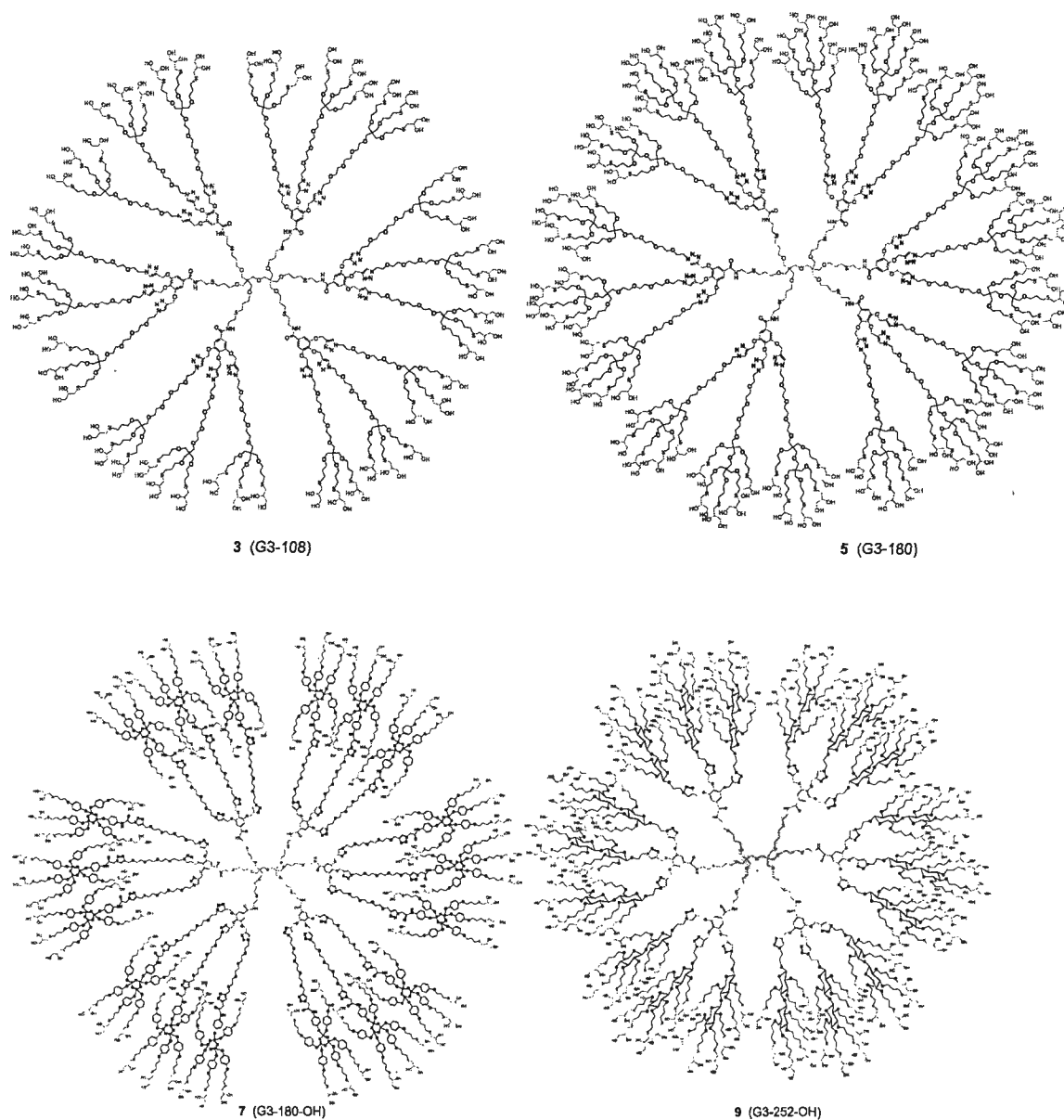


Figure 4-2 Molecular structures of dendrimers with 108, 180, and 252 end groups at third generation.

The monodisperse nature of dendrimer was also confirmed by MALDI-TOF data and GPC. MALDI-TOF spectrum showed the molecular ion peak corresponding to Na^+ adduct at 10814 ($10791 \text{ M}^+ + 23$). The same (click) reaction was also carried out using an oil bath under similar conditions, but multiple spots were observed on

TLC indicating partial conversions. Dendrimer **2** was further subjected to thermal thiol-ene reaction using 1-thioglycerol as an AB₂ monomer to afford G3 dendrimer **3** having 108-OHs surface groups. The purification was carried out by simply washing the reaction mixture with diethylether, followed by dialysing against distilled water using 1000-MW cut-off dialysis membrane. Complete disappearance of allylic signals and appearance of signals for protons corresponding to thioglycerol confirmed the product formation. HRMS (ESI⁺) spectrum showed the expected molecular ion peak at 16631 (see Table 4-1 and SI (Appendix C)).

After the successful execution of the above synthetic strategy with aliphatic AB₃ monomer **13**, the synthesis of the next higher order branching units was attempted. The synthesis of perallylated dendrimer **4** was carried out by treating hypercore **1** with penta-allylated AB₅ monomer **16** using the above CuAAC conditions under microwave to afford G2 dendrimer **4** harbouring 90 active alkene functions in 71% yield. The terminal alkenes of dendrimer **4** were next treated with 1-thioglycerol as above to provide G3 dendrimer **5** accommodating 180 terminal hydroxyl groups. The dendrimer was purified by precipitation with diethyl ether followed by dialysis against water to give the pure product in 86% yield. Once again, our accelerated “onion peel” approach proved to be efficient enough to introduce 180 surface groups at G3 stage only.

The next goal was to try even bulkier building blocks to test the potential of the strategy for complex dendrimers construction. In general, bulky hypermonomers are responsible for creating structural defects in dendritic scaffolds due to steric hindrance. Perpropargylated hypercore **1** was further reacted with a bulkier AB₅-based hypermonomer **26** (N₃P₃ core) via CuAAC click reaction using microwave radiations to generate G2 dendrimer **6** in an acceptable 50% yield after purification as above. The GPC chromatogram showed a narrow and symmetrical Gaussian pattern with a polydispersity index of 1.03, confirming the monodisperse nature of the dendrimer. Its ³¹P-NMR spectrum showed a singlet for phosphorous indicating the symmetrical structure. In the next step, dendrimer **6** was subjected to the above thiol-

ene conditions with 1-thioglycerol to afford dendrimer **7** with 180-OHs surface groups in 63% yield. The ^1H -NMR spectrum indicated the complete disappearance of all the allylic signals, again confirming the product formation.

Finally, the synthesis of perallylated dendrimer **8** using the novel glyconanosynthon,⁸ constituting an AB_7 branching motif, was carried out. It has to be noted that the use of such an hyper functionalized synthons has been rarely described in the literature and reported only once for dendrimer synthesis.¹⁹ The synthesis was achieved by treating hepta-allylated AB_7 monomer **31** with **1** using CuAAC click reaction under microwave to furnish G2 dendrimer **8** possessing 126 allyl groups at the periphery in 75% yield. Final coupling of excess 1-thioglycerol onto dendrimer **8** was achieved through thiol-ene coupling as mentioned in the general protocol described above. To test the reliability and sensitivity of NMR for complete conversion, the reaction conditions described above was used. As shown by ^1H -NMR spectroscopy (Figure 4-3), incomplete conversion (80%) was observed after 5 hours. The reaction was resubmitted for another 2 hours with the addition of more 1-thioglycerol (2 eq/alkene), which led to complete conversion as shown by the ^1H -NMR spectrum which indicated complete disappearance of all allyl signals. MALDI-TOF spectrometry also confirmed product formation by showing mass peaks corresponding to sodium adducts perfectly matching with the calculated value (SI, Appendix C). It is worth mentioning here that the resulting dendrimer **9** possesses 252 hydroxyl surface groups at the G3 stage only and can still be used as a precursor for further functionalization. There is still the possibility to generate an even greater number of peripheral groups at the G3 stage by using higher order AB_3 or AB_4 building blocks such as the AB_2 monomer (1-thioglycerol) used above. As a comparison, PAMAM dendrimer with ethylenediamine core (A_2 and AB_2 building blocks) bearing 256 surface groups requires generation 6 (G6) and approximately twelve steps, while the accelerated "onion peel" strategy allows us to acquire 252 surface groups at exactly half the number of generations and one third of the number of necessary reaction steps.

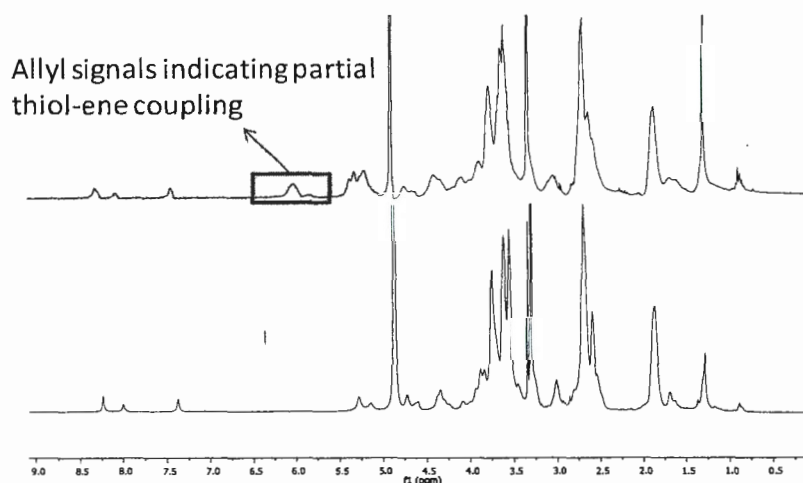


Figure 4-3 ^1H NMR spectrum of **9 (G3-252)** (Top) After 5 hours in microwave 50°C indicating 80% conversion, (Bottom) After 7 hours in microwave at 50°C indicating 100% conversion.

All dendrimers described herein were fully characterized using NMR (^1H , ^{13}C , ^{31}P , COSY), IR, mass spectrometry and were shown to be in full agreement with the structures presented. Gel permeation chromatography (GPC) were performed at the penultimate steps and all the chromatograms showed narrow peaks with low polydispersity indexes (PDI) indicating the monodisperse nature of the products (Figure 4-4 and Table 4-1). The M_n values obtained from GPC exhibited very good correlation with theoretical molecular weights as well as molecular weights acquired from mass spectrometric data. The dendrimer diameters in solution were calculated with the help of dynamic light scattering (DLS) and diffusion NMR spectroscopy experiments (Table 4-1). Diffusion NMR experiments were carried out in methanol at 25°C to measure diffusion coefficients D .³⁵ The corresponding solvodynamic diameters ($D_s = 2 \times R_s$) were calculated using the Stokes–Einstein equation and the viscosity of pure CD_3OD (Table 4-1). The sizes of the dendrimers were also obtained using DLS technique in methanol. Hydrodynamic diameters calculated from both methods were remarkably close and were in the range of approximately 2–8 nm for the G3 dendrimers. Interestingly, dendrimer **7**, having a dense N_3P_3 scaffold, appears

as an unusually packed structure by both DLS and DOSY-NMR, Table 4-1). This could be rationalized on the basis of its 3D structure having 3-up/3-down substituent orientations.^{3,33}

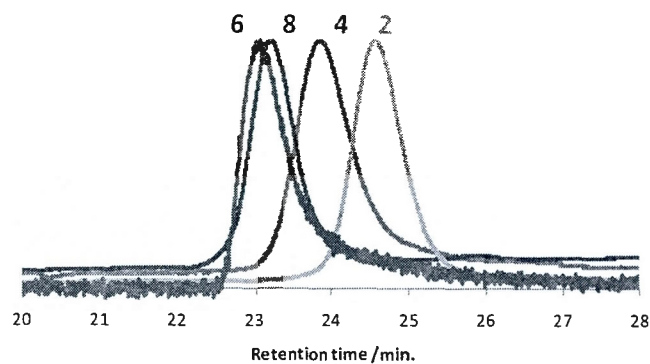


Figure 4-4 GPC traces of the dendrimers: (2)G2-54, (4)G2-90, (6)G2-90, and (8)G2-126

Table 4-1 Summary of characterization of dendrimers.

Entry	Dendrimer	Theoretical MW	Exp. Mass [MALDI/MS]	M_n^a (g/mol)	PDI	D^b (m^2s^{-1})	D_s^c (nm)	D_H^d (nm)
1	2 (G2-54)	10791.1392	10814.3920 [M+Na] ⁺	10770	1.08	-	-	-
2	3 (G3-108)	16631.7479	16631.7480	-	-	1.15×10^{-10}	6.30	5.70
3	4 (G2-90)	14359.7980	14385.1000 [M+Na] ⁺	14490	1.2	-	-	-
4	5 (G3-180)	24110.1882	24124.9040	-	-	1.05×10^{-10}	6.90	8.22
5	6 (G2-90)	26481.1320	26249.7870	26350	1.03	-	-	-
6	7 (G3-180)	36215.4798	37226.6720	-	-	2.54×10^{-10}	2.85	1.95
7	8 (G2-126)	15007.6007	15011.0180	15140	1.07	-	-	-
8	9 (G3-252)	28667.7725	28690.0370 [M+Na] ⁺	-	-	1.23×10^{-10}	5.90	6.41

^aDetermined from GPC.^bDiffusion coefficient measured in CD₃OD at 25 °C.^cSolvodynamic diameter from diffusion NMR experiment calculated using the Stokes-Einstein equation.^dHydrodynamic diameter determined from DLS experiment in methanol.

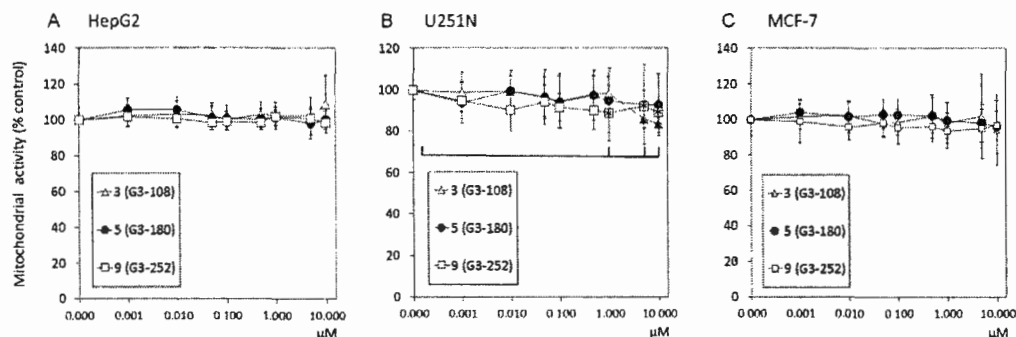


Figure 4-5 Low cytotoxicity of dendrimers in human cells. Dendrimers **3** (G3-108), **5** (G3-180) and **9** (G3-252) were tested in: (A) HepG2 liver carcinoma, (B) U251N glioblastoma and (C) MCF-7 breast adenocarcinoma cells. Increasing concentrations of dendrimers (1 nM – 10 μM) were incubated with the cells for 24h. Mitochondrial metabolic activity was assessed using the MTT assay. Values are presented as mean percentages \pm S.D relative to untreated controls (set as 100%). The data is reported for six measurements for each concentration. Three independent experiments performed $^{*}(p < 0.01)$

The cytotoxicity of the polyhydroxylated dendrimers **3**, **5** and **9** was evaluated *in vitro* using three different human cell lines. Human liver, glioblastoma and breast cancer cells were selected as models commonly used for the screening of polymeric biomaterials. Mitochondrial metabolic activity was determined using the MTT assay (*i.e.* formazan production by mitochondrial dehydrogenases).³⁷ Cell viability upon dendrimer treatment was also determined by nuclear labelling with Hoechst 33342 (10 μM, 10 mins), and cells were imaged with a fluorescence microscope. The concentration range used in both assays (1 nM to 10 μM) was delimited based on previous dendrimer cytotoxicity studies.³⁸ Concentration-dependant effects of dendrimers on mitochondrial activity in human cells exposed for 24h is shown (Figure 4-5).

No significant decrease in metabolic activity was observed in HepG2 and MCF-7 cells at any treatment concentration. In turn, dendrimers **3** and **9** were mildly cytotoxic in the highly proliferative U251N cells at 5-10 μM and 1-10 μM concentrations, respectively. Similar results were obtained in the viability assay based on nuclear labelling with Hoechst 33342 and subsequent cell counting (Figure 4-6).

The suitability of dendrimers for drug delivery or other biomedical applications is dependent on the number and the nature of their end groups.⁷ Here, the hydroxyl groups found on the surface of dendrimers **3**, **5**, and **9** provide a neutral outer shell that reduces toxicity.^{39, 40} In contrast, cationic end groups, such as the primary amines in poly(amidoamine) dendrimers, tend to induce concentration-dependent and generation-dependent toxicity both *in vitro* and *in vivo*.⁴¹⁻⁴³ Overall, dendrimers **3**, **5**, and **9** displayed very low toxicity in the human cell lines and concentration range tested, rendering them suitable for biomedical applications.

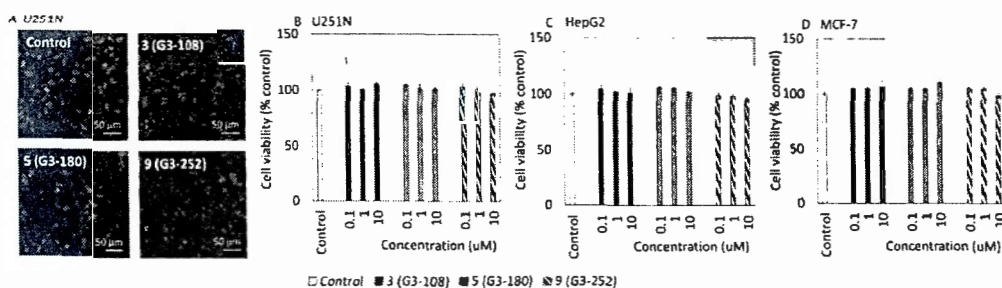


Figure 4-6 Concentration-dependent effect of dendrimers on human cell viability. Fluorescence micrograph (A) U251N glioblastoma treated with dendrimers **3**, **5**, and **9** (10 μ M, 24h) and labelled with Hoechst 33342 (10 μ M, 10 mins) (scale = 50 μ m). The cytotoxicity of dendrimers **3** (G3-108), **5** (G3-180) and **9** (G3-252) was tested in (B) U251N glioblastoma, (C) HepG2 liver carcinoma, and (D) MCF-7 breast adenocarcinoma cells. Dendrimers in increasing concentrations (up to 10 μ M) were incubated with the cells for 24h. Cell viability was assessed by high-throughput imaging (Operetta, Perkin Elmer)

4.3 Conclusions:

The syntheses of G3 dendrimers bearing 108, 180, and 252 hydroxyl surface groups using AB₃, AB₅, and AB₇ hypermonomers were successfully achieved. The dendrimers were constructed using highly efficient and facile accelerated “onion peel” approach without requiring any protection/deprotection steps. The use of hypercore and hypermonomers along with the combination of highly efficient chemical reactions (CuAAC and thiol-ene) provided rapid access to introduce high number of precise surface groups at low generations. Click reactions turned out to be highly efficient in ligating large number of functional groups and producing

monodisperse dendrimers. The outer hydroxyl terminal groups provide a reactive platform for further growth and attachment of several other types of functionalities.⁴⁴⁻

⁵¹ Hydroxylated dendrimers presented here and their derivatives could be easily synthesized and used for diverse range of applications. A particular attraction of these dendrimers for applications in biology is their low toxicity. Future studies should include the investigations of dendrimer pharmacokinetics and pharmacodynamics as well as their cellular uptakes. Relative ease of tailoring dendrimer chemistry to best fit physical and chemical properties of selected biologically active agents makes these dendrimers attractive candidates for further biological investigations in primary human cell cultures and experimental animal models mimicking different pathologies. In addition, the strategy described herein nicely complements the one using self-assembling Janus dendrimersomes.⁵²⁻⁵³

4.4 References:

1. D. A. Tomalia, *Aldrichimica Acta*, 2004, **37**, 39-57.
2. G. R. Newkome and C. Shreiner, *Chem. Rev.* 2010, **110**, 6338–6442.
3. A.-M. Caminade, C.-O. Turrin and J.-P. Majoral, *New J. Chem.*, 2010, **34**, 1512–1524;
4. A. W. Bosman, H. M. Janssen and E. W. Meijer, *Chem. Rev.*, 1999, **99**, 1665–1688.
5. M. V. Walter and M. Malkoch, *Chem. Soc. Rev.*, 2012, **41**, 4593–4609;
6. A. Carlmark, E. Malmström and M. Malkoch, *Chem. Soc. Rev.*, 2013, **42**, 5858–5879;
7. M. Sowinska and Z. Urbanczyk-Lipkowska, *New J. Chem.*, 2014, **38**, 2168–2203.
8. R. Roy and T. C. Shiao, *Chem. Soc. Rev.*, accepted, CS-REV-10-2014-000359.R1
9. K. L. Wooley, C. J. Hawker and J. M. J. Frechet, *J. Am. Chem. Soc.*, 1991, **113**, 4252-4261.
10. F. Zeng and S. C. Zimmerman, *J. Am. Chem. Soc.*, 1996, **118**, 5326-5327.
11. P. Antoni, M. J. Robb, L. Campos, M. Montanez, A. Hult, E. Malmström, M. Malkoch and C. J. Hawker, *Macromolecules*, 2010, **43**, 6625-6631.
12. W. Wu, C. Wang, Q. Li, C. Ye, J. Qin and Z. Li, *Sci. Rep.*, 2014, **4**.

- 13 P. E. Shaw, S. S. Y. Chen, X. Wang, P. L. Burn and P. Meredith, *J. Phys. Chem. C*, 2013, **117**, 5328-5337.
- 14 Z.-Y. Zhang and B. D. Smith, *Bioconjugate Chem.*, 2000, **11**, 805-814.
- 15 L. B. Jensen, K. Mortensen, G. M. Pavan, M. R. Kasimova, D. K. Jensen, V. Gadzhieva, H. M. Nielsen and C. Foged, *Biomacromolecules*, 2010, **11**, 3571-3577.
- 16 C. A. S. Regino, S. Walbridge, M. Bernardo, K. J. Wong, D. Johnson, R. Lonser, E. H. Oldfield, P. L. Choyke and M. W. Brechbiel, *Contrast Media Mol. Imaging*, 2008, **3**, 2-8.
- 17 N. Shao, T. Dai, Y. Liu, L. Li and Y. Cheng, *Soft Matter*, 2014, **10**, 9153-9158.
- 18 J. Lim, M. Kostianen, J. Maly, V. C. P. da Costa, O. Annunziata, G. M. Pavan and E. E. Simanek, *J. Am. Chem. Soc.*, 2013, **135**, 4660-4663.
- 19 X. Wang, Y. Yang, P. Gao, D. Li, F. Yang, H. Shen, H. Guo, F. Xu and D. Wu, *Chem. Commun.*, 2014, **50**, 6126-6129.
- 20 R. Sharma, K. Naresh, Y. M. Chabre, R. Rej, N. K. Saadeh and R. Roy, *Polym. Chem.*, 2014, **5**, 4321-4331.
- 21 R. Sharma, N. Kottari, Y. M. Chabre, L. Abbassi, T. C. Shiao and R. Roy, *Chem. Commun.*, 2014, 13300-13303.
- 22 H. C. Kolb and K. B. Sharpless, *Drug Discovery Today*, 2003, **8**, 1128-1137.
- 23 K. L. Killops, L. M. Campos and C. J. Hawker, *J. Am. Chem. Soc.*, 2008, **130**, 5062-5064.
- 24 A. Dondoni and A. Marra, *Chem. Soc. Rev.*, 2012, **41**, 573-586.
- 25 R. Gedye, F. Smith, K. Westaway, H. Ali, L. Baldisera, L. Laberge and J. Rousell, *Tetrahedron Lett.*, 1986, **27**, 279-282.
- 26 A. E. Enciso, Z. M. Abid and E. E. Simanek, *Polym. Chem.*, 2014, **5**, 4635-4640.
- 27 F. Wiesbrock, R. Hoogenboom and U. S. Schubert, *Macromol. Rapid Commun.*, 2004, **25**, 1739-1764.
- 28 R. Roy, *Curr. Opin. Struct. Biol.* 1996, **6**, 692-702.
- 29 Y. C. Lee and R. T. Lee, *Acc. Chem. Res.*, 1995, **28**, 321-327.
- 30 O. Renaudet and R. Roy, *Chem. Soc. Rev.*, 2013, **42**, 4515-4517.
- 31 R. Turgis, I. Billault, S. Acherar, J. Auge and M.-C. Scherrmann, *Green Chem.*, 2013, **15**, 1016-1029.
- 32 Z. Luo, X. Ding, Y. Hu, S. Wu, Y. Xiang, Y. Zeng, B. Zhang, H. Yan, H. Zhang, L. Zhu, J. Liu, J. Li, K. Cai and Y. Zhao, *ACS Nano*, 2013, **7**, 10271-10284.
- 33 A. Hameau, S. Fuchs, R. Laurent, J.-P. Majoral and A.-M. Caminade, *Beilstein J. Org. Chem.*, 2011, **7**, 1577-1583.

- 34 K.-L. Dao, R. R. Sawant, J. A. Hendricks, V. Ronga, V. P. Torchilin and R. N. Hanson, *Bioconjugate Chem.*, 2012, **23**, 785-795.
- 35 Y. M. Chabre, A. Papadopoulos, A. A. Arnold and R. Roy, *Beilstein J. Org. Chem*, 2014, **10**, 1524-1535.
- 36 M. A. van Dongen, B. G. Orr and M. M. Banaszak Holl, *J. Phys. Chem. B*, 2014, **118**, 7195-7202.
- 37 T. Mosmann, *J. Immunol. Methods*, 1983, **65**, 55-63.
- 38 R. Duncan and L. Izzo, *Adv. Drug Deliv. Rev.*, 2005, **57**, 2215-2237.
- 39 S. Fuchs, T. Kapp, H. Otto, T. Schöneberg, P. Franke, R. Gust and A. D. Schlüter, *Chem. Eur. J*, 2004, **10**, 1167-1192.
- 40 J. B. Wolinsky and M. W. Grinstaff, *Adv. Drug Deliv. Rev.*, 2008, **60**, 1037-1055.
- 41 M. A. Dobrovolskaia and S. E. McNeil, *Nat Nano*, 2007, **2**, 469-478.
- 42 N. Malik, R. Wiwattanapatapee, R. Klopsch, K. Lorenz, H. Frey, J. W. Weener, E. W. Meijer, W. Paulus and R. Duncan, *J. Control. Release*, 2000, **65**, 133-148.
- 43 H.-T. Chen, M. F. Neerman, A. R. Parrish and E. E. Simanek, *J. Am. Chem. Soc.*, 2004, **126**, 10044-10048.
- 44 Y. M. Chabre and R. Roy, *Chem. Soc. Rev.*, 2013, **42**, 4657-4708.
- 45 Y. M. Chabre and R. Roy, *Adv. Carbohydr. Chem. Biochem.*, 2010, **63**, 165-393.
- 46 R. Roy, *Trends. Glycosci. Glycotechnol.*, 2003, **15**, 291-310.
- 47 Y. M. Chabre and R. Roy, *Curr. Top. Med. Chem.*, 2008, **8**, 1237-1285.
- 48 S. M. Grayson, M. Jayaraman and J. M. J. Frechet, *Chem. Commun.*, 1999, 1329-1330.
- 49 J. Khandare, M. Calderon, N. M. Dagia and R. Haag, *Chem. Soc. Rev.*, 2012, **41**, 2824-2848.
- 50 A. Sharma, A. Khatchadourian, K. Khanna, R. Sharma, A. Kakkar and D. Maysinger, *Biomaterials*, 2011, **32**, 1419-1429.
- 51 N. Kottari, Y. M. Chabre, T. C. Shiao, R. Rej and R. Roy, *Chem. Commun.*, 2014, **50**, 1983-1985.
- 52 V. Percec, P. Leowanawat, H.-J. Sun, O. Kulikov, C. D. Nusbaum, T. M. Tran, A. Bertin, D. A. Wilson, M. Peterca, S. Zhang, N. P. Kamat, K. Vargo, D. Moock, E. D. Johnston, D. A. Hammer, D. J. Pochan, Y. Chen, Y. M. Chabre, T. C. Shiao, M. Bergeron-Brelek, S. André, R. Roy, H.-J. Gabius and P. A. Heiney, *J. Am. Chem. Soc.*, 2013, **135**, 9055-9077.
- 53 S. Zhang, R.-O. Moussodia, H.-J. Sun, P. Leowanawat, A. Muncan, C. D. Nusbaum, K. M. Chelling, P. A. Heiney, M. L. Klein, S. André, R. Roy, H.-J. Gabius and V. Percec, *Angew. Chem Int. Ed.*, 2014, **53**, 10899-10903.

CHAPTER 5

CONCLUSIONS AND SUGGESTIONS FOR FUTURE WORK

5.1 Conclusions

In recent years, dendrimers have gained enormous success in diverse areas ranging from biomedicine to nanoengineering. In general, dendrimers synthesis is very lengthy, tedious and time consuming especially in the case of high generation dendrimers. Due to their increased demand for various applications, new highly efficient and shorter synthetic protocols are required for the construction of dendrimers which can deliver these macromolecules with perfect structure in a rapid manner.

In this thesis, we have presented a novel "onion peel strategy" for the construction of dendrimers. This highly versatile synthetic approach is different from conventional methods of dendrimers synthesis in terms of using different families of building blocks containing orthogonal functional groups at each layer of the dendritic growth. The dendrimers were synthesized using a combination of highly efficient and robust chemical reactions, namely, thiol-ene, thiol-yne, esterification, and azide-alkyne click chemistry. Using this strategy, we demonstrated that structural diversities could be efficiently and rapidly harnessed at low generations. By carefully optimizing the choice of monomers, we generated a library of dendrimers with desired hydrophobic/hydrophilic and rigidity/flexibility balances at each generation of dendrimers growth. The dendrimer's surface was decorated with an azido derivative of *N*-acetyllactosamine which led to new glycodendrimers having high affinities as compared to the corresponding monovalent analog towards *Erythrina*

crisagalli, a leguminous lectin known to bind natural killer cells through its galactoside recognition ability.

In order to evaluate the versatility of "onion peel strategy" we employed this approach to construct dendrimers in both convergent and divergent manner. The approach turned out to be extremely facile to construct lactoside and galactoside based dendrimers in both ways. The dendrimers constructed using this strategy resulted in one of the most potent multivalent ligands known against the virulent factor from a bacterial lectin isolated from *Pseudomonas aeruginosa*.

In our next attempt, we evaluated the potential of "onion peel approach" and developed microwave assisted accelerated strategy to construct dendrimers with large number of exact end groups at lower generations. The use of hypercore and hypermonomers along with the combination of highly efficient chemical reactions (CuAAC and thiol-ene click) provided rapid access to dense dendrimer scaffolds. The hydroxyl terminated dendrimers displayed very low toxicity in the human cell lines, making them suitable for various biomedical applications.

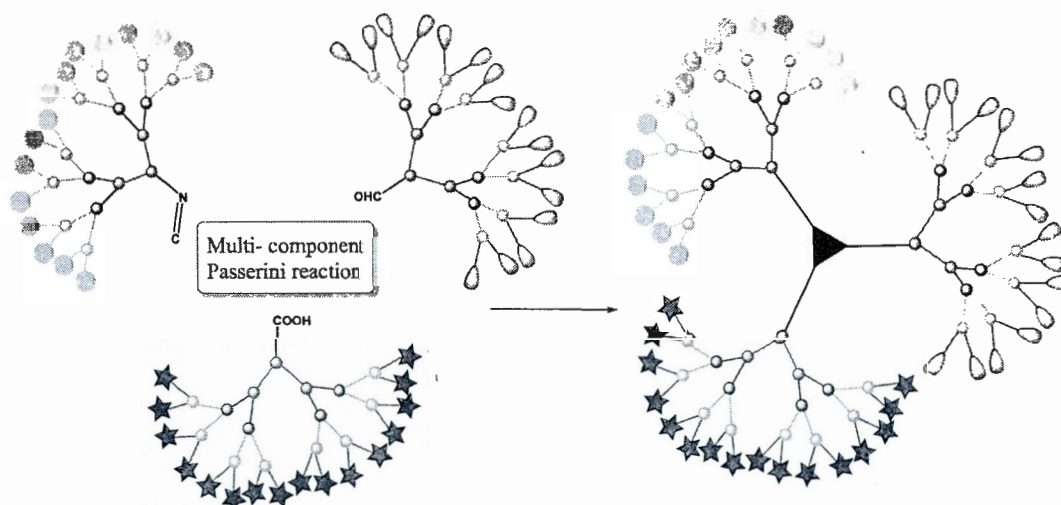
The novel onion peel approach presented in this thesis has numerous advantages over the existing strategies for the construction of complex macromolecular structures. In fact, this is highly efficient method where a dendrimer can be constructed with precise sequence in a tailor made fashion to address many biological issues. Freedom of using different building blocks provides excellent control at each growth stage and helps to regulate the rigidity and flexibility required in the backbone. It also allows us to create vital hydrophobic and hydrophilic balance in the molecule with the help of smart orthogonal building blocks; and even molecularly precise modifications can be introduced. This approach opens up new avenues where we can generate dendrimers with a wide variety of functional end groups which can be further employed in different chemical transformations of our choice. This strategy is quite convenient in conjugating different molecules on the periphery as well as can enable us to include exact number of the required ligands. Due to flexibility of the approach, entire synthetic protocol up to the final molecule

can be achieved maintaining orthogonality and leads to rapid construction of dendrimers involving fewer synthetic steps which makes overall process greener. Even the selection of the orthogonal building blocks at each generation can be performed in such a manner that available surface groups remain active all the time for further functionalization. It is observed in many cases that a particular reaction which is used to construct dendrimers is very effective at lower generations where very few end groups are involved in chemical transformation, but becomes very sluggish when higher generation dendrimers are pursued and ends up forming imperfect dendrimers. Onion peel approach allows us to introduce similar building block to synthesize higher generation dendrimer by employing a variety of highly efficient chemical transformation which can work better with large number of end-groups. The most important and attractive feature of this approach is that by using chemically similar orthogonal building block with different valency, it is possible to generate a library of dendrimers with different number of end groups at same generation. Hence, this type of strategy eliminates the need of comparing different generations to observe the effect of multivalency, rather it can be achieved at same generation.

5.2 Suggestions for future work

Multifunctional dendrimers have recently shown remarkable potential for applications in biology. The multifunctionalization of most widely studied and commercially available PAMAM dendrimers is usually carried out in a random statistical manner, which leads to the formation of a complex mixture of products without any control on the attachment of individual functional moiety. The construction of well-defined multifunctional dendrimers with exact number of different functional moieties is a challenging task, and is highly required for applications in drug delivery. The developments of synthetic strategies which can build dendrimers with different functional moieties in a controlled manner are highly desirable.

5.2.1 Design and development of trifunctional dendrimers using a combination of "onion peel" approach and "multicomponent Passerini reaction"



Onion peel dendrons with different peripheral functionalization

Figure 5-1 Schematic representation of construction of trifunctional dendrimer combining "onion peel" approach and Passerini reaction

In this thesis, we have developed a novel "onion peel" approach to synthesize monofunctional dendrimers. We have demonstrated that this approach provides us full freedom about the choice of building blocks, which results in diverse range of dendrimers with different properties, sizes, and number of end groups at same generations. This "onion peel" approach has a lot of potential which can be exploited to build multifunctional dendrimers. It will be interesting in future to combine the advantages of "onion peel" approach together with "multicomponent Passerini reaction" to develop trifunctional dendrimer in a convergent way (Figure 5.1). Three different dendrons can first be synthesized *via* "onion peel" strategy using atom economical reactions and orthogonal building blocks. All three dendrons will be consisting of three different focal points (*i.e.* isocyanide, aldehyde and carboxylic acid) to participate in the Passerini reaction to yield the trifunctional dendrimer in one step in a convergent way. The periphery of dendritic wedges can be decorated with

desired functionalities *e.g.* drug molecules, targeting ligands, and imaging dyes etc. This approach can be highly advantageous to construct multifunctional dendrimers in a tailor made fashion.

APPENDIX A

SUPPORTING INFORMATION-CHAPTER 2: "ONION-PEEL" DENDRIMERS: A
STRAIGHTFORWARD SYNTHETIC APPROACH TOWARDS HIGHLY
DIVERSIFIED ARCHITECTURES

1. Materials and methods:

All reactions in organic medium were performed in standard oven dried glassware under an inert atmosphere of nitrogen using freshly distilled solvents. CH_2Cl_2 was distilled from CaH_2 and DMF from ninhydrin, and kept over molecular sieves. Solvents and reagents were deoxygenated when necessary by purging with nitrogen. Water used for lyophilisation of final dendrimers was nanopure grade, purified through Barnstead NANOPure II Filter with Barnstead MegOhm-CM Sybron meter. All reagents were used as supplied without prior purification unless otherwise stated, and obtained from Sigma-Aldrich Chemical Co. Ltd. Reactions were monitored by analytical thin-layer chromatography using silica gel 60 F254 precoated plates (E. Merck) and compounds were visualized by 254 nm light, a mixture of Iodine/silica gel and/or mixture of Ceric Ammonium Molybdate solution (100 ml H_2SO_4 , 900 ml H_2O , 25g $(\text{NH}_4)_6\text{Mo}_7\text{O}_{24}\cdot\text{H}_2\text{O}$, 10g $\text{Ce}(\text{SO}_4)_2$) and subsequent development by gentle warming with a heat-gun. Purifications were performed by flash column chromatography using silica gel from Silicycle (60 Å, 40-63 μm) with the indicated eluent.

^1H NMR and ^{13}C NMR spectra were recorded at 300 or 600 MHz and 75 or 150 MHz, respectively, on a Bruker spectrometer (300 MHz) and Varian spectrometer (600 MHz). All NMR spectra were measured at 25°C in indicated deuterated solvents. Proton and carbon chemical shifts (δ) are reported in ppm and coupling constants (J) are reported in Hertz (Hz). The resonance multiplicity in the ^1H NMR spectra are described as "s" (singlet), "d" (doublet), "t" (triplet), "quint" (quintuplet) and "m" (multiplet) and broad resonances are indicated by "br". Residual protic solvent of CDCl_3 (^1H , δ 7.27 ppm; ^{13}C , δ 77.0 ppm (central resonance of the triplet)), D_2O (^1H , δ 4.79 ppm and 30.9 ppm for CH_3 of Acetone for ^{13}C spectra of de-*O*-acetylated compounds), MeOD (^1H , δ 3.31 ppm and ^{13}C , δ 49.0 ppm). 2D Homonuclear correlation 1H-1H COSY experiments were used to confirm NMR peak assignments. Gel Permeation Chromatography (GPC) was performed using THF as the eluent, at 40°C with a 1 mL/min flow rate on a Viscotek VE 2001 GPCmax (SEC System) with Wyatt DSP/Dawn EOS and refractive index RI/LS system as detectors. 2 PLGel mixed B LS (10 μm , 300×7.5 mm) and LS-MALLS detection with

performances verified with polystyrene 100 kDa and 2000 kDa were used to determine the number-average molecular weight (M_n) and polydispersity index (M_w/M_n). Calculations were performed with Zimm Plot (model). Fourier transform infrared (FTIR) spectra were obtained with Thermo-scientific, Nicolet model 6700 equipped with ATR. The absorptions are given in wavenumbers (cm^{-1}). The intensity of the bands is described as s (strong), m (medium) or w (weak). Melting points were measured on a Electrothermal MEL-TEMP apparatus and are uncorrected.

Accurate mass measurements (HRMS) were performed on a LC-MSD-ToF instrument from Agilent Technologies in positive electrospray mode. Low-resolution mass spectra were performed on the same apparatus or on a LCQ Advantage ion trap instrument from Thermo Fisher Scientific in positive electrospray mode (Mass Spectrometry Laboratory (Université de Montréal), or Plateforme analytique pour molécules organiques (Université du Québec à Montréal), Québec, Canada). Either protonated molecular ions $[M+nH]^{n+}$ or adducts $[M+nX]^{n+}$ ($X = \text{Na}, \text{K}, \text{NH}_4$) were used for empirical formula confirmation. MALDI-TOF experiments were performed on an Autoflex III from Brucker Smarteam in linear positive mode (Mass Spectrometry Laboratory (McGill University)) to afford adducts $[M+nX]^{n+}$ ($X = \text{Na}, \text{K}$ or Li). Samples were solubilized in H_2O for a final concentration of 6 mg/mL. Dihydroxybenzoic acid (DHB) was used as the matrix. Cationization was eased by the use of the corresponding sodium salt (2 mg/mL).

Particle size distribution (DLS) was measured in water with the help of Zetasizer Nano S90 from Malvern.

2. Synthetic protocols and characterization:

General procedure for thiol-ene click reaction (Procedure A):

To a stirring solution of alkene derivative (1.0 eq.), 2,2'-dimethoxy-2-phenylacetophenone (DMPA) (10 mol %) in dry DMF (0.2 ml/mmol) was added thiol derivative (excess per alkene) under nitrogen. The vial was then purged with N_2 for 10 min and irradiated for 12 hrs using UV lamp at room temperature (*classical glassware, UV lamp (365 nm, Model UVGL-58 MINERALIGHT® LAMP) in a cardboard box*). Upon completion of reaction, the solvent was removed under vacuum and residue was subsequently washed three times with diethyl ether to remove excess of thiol, affording a clear viscous liquid. The crude product was further purified by column chromatography.

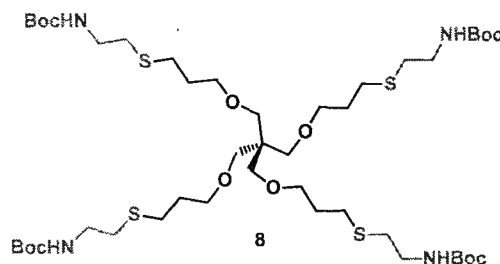
Optimized conditions for the synthesis of derivative 8 will be summarized in the corresponding section.

General procedure for thiol-yne click reaction (Procedure B):

To a stirring solution of alkyne derivative (1.0 eq.), 2,2'-dimethoxy-2-phenylacetophenone (DMPA) (10 mol %) in dry DMF (0.2 ml/mmol) was added thiol derivative (excess per alkyne) under nitrogen. The vial was then purged with N₂ for 10 min and irradiated for 12 hrs using UV lamp at room temperature (*classical glassware, UV lamp (365 nm, Model UVGL-58 MINERALIGHT® LAMP) in a cardboard box*). Upon completion of reaction, the solvent was removed under vacuum and residue was subsequently washed three times with diethyl ether to get rid of excess of thiol, affording a clear viscous liquid. The crude product was further purified by column chromatography.

General procedure for CuAAC click reaction (Procedure C):

To a solution of acetylene terminated dendrimer (1.0 eq.) in THF (5 ml/mmol) was added azido derivative (1.2 eq. per acetylene) dissolved in H₂O, followed by the addition of sodium ascorbate (0.5 eq. per acetylene) and CuSO₄·5H₂O (0.5 eq. per acetylene) dissolved in minimum amount of water. The final ratio of H₂O to THF was kept 1:1. The reaction mixture was stirred at 40°C for 12 hrs. The solvent was evaporated and residue was dissolved in minimum amount of water. The solution was then dialyzed using 2kDa cut off membrane bag against 5% aqueous EDTA solution followed by millipore water. The dialysis was continued until light green colour disappeared in aqueous solution in the bag. The sample was lyophilised to afford white amorphous solid.



Synthesis of compound 8: Compound 6 (0.150 g, 1.027 mmol, 1.0 eq.), and compound 7 (1.456 g, 8.216 mmol, 8.0 eq) were reacted together according to **procedure A** to give 8 which was further purified by column chromatography. The

pure product (0.597 g, 0.791 mmol) was isolated using 60% Et₂O in Toluene as eluent. **Yield: 77%.**

¹H NMR (300 MHz, CDCl₃) δ (ppm) 5.00 (s, 4H), 3.45 (t, J = 6.0 Hz, 8H), 3.38–3.26 (m, 16H), 2.70–2.52 (m, 16H), 1.96–1.71 (m, 8H), 1.45 (s, 36H).

¹³C{¹H} NMR (75 MHz, CDCl₃) δ (ppm) 155.8, 79.3, 69.6, 45.4, 39.7, 32.2, 29.8, 28.4.

HRMS (ESI⁺-TOF) m/z : calculated for C₄₅H₈₈N₄O₁₂S₄ [M+Na]⁺: 1027.5174, found: 1027.5194.

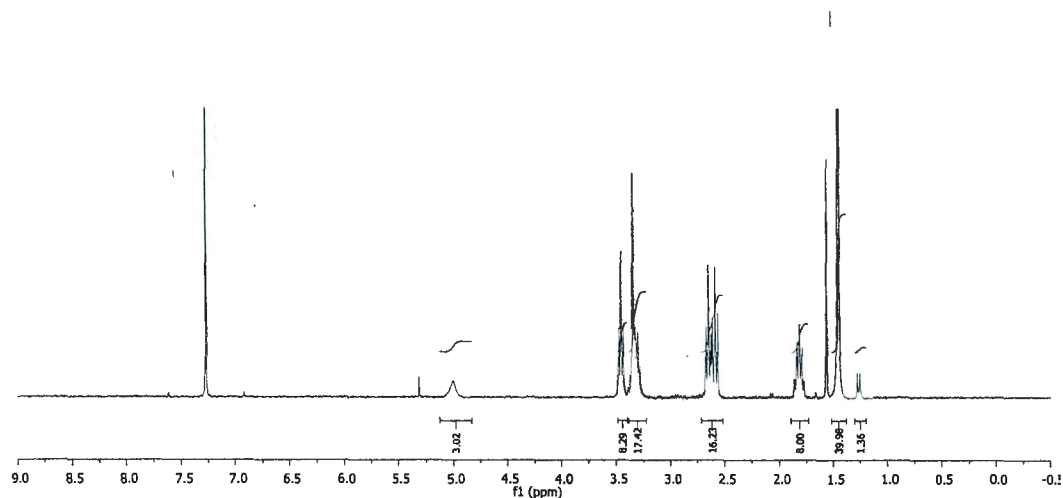


Figure S1 ¹H NMR spectrum of compound **8** (CDCl₃, 300 MHz).

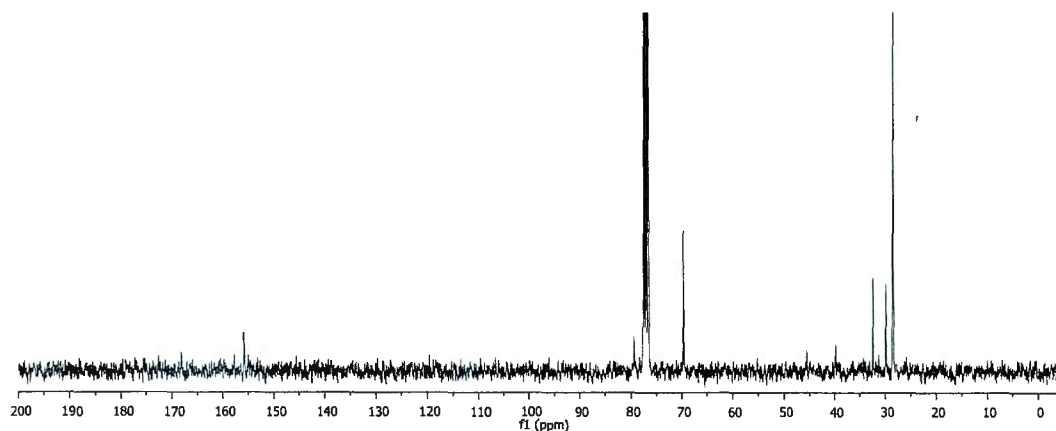


Figure S2 ¹³C NMR spectrum of compound **8** (CDCl₃, 75 MHz).

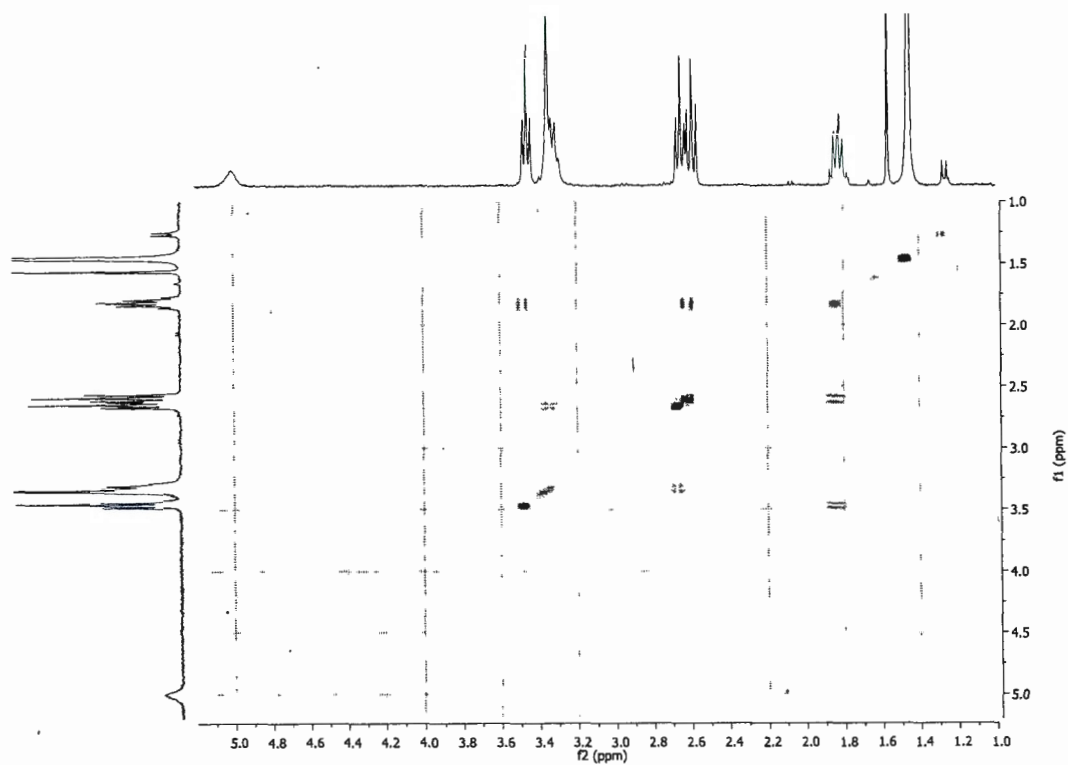


Figure S3 COSY spectrum of compound 8.

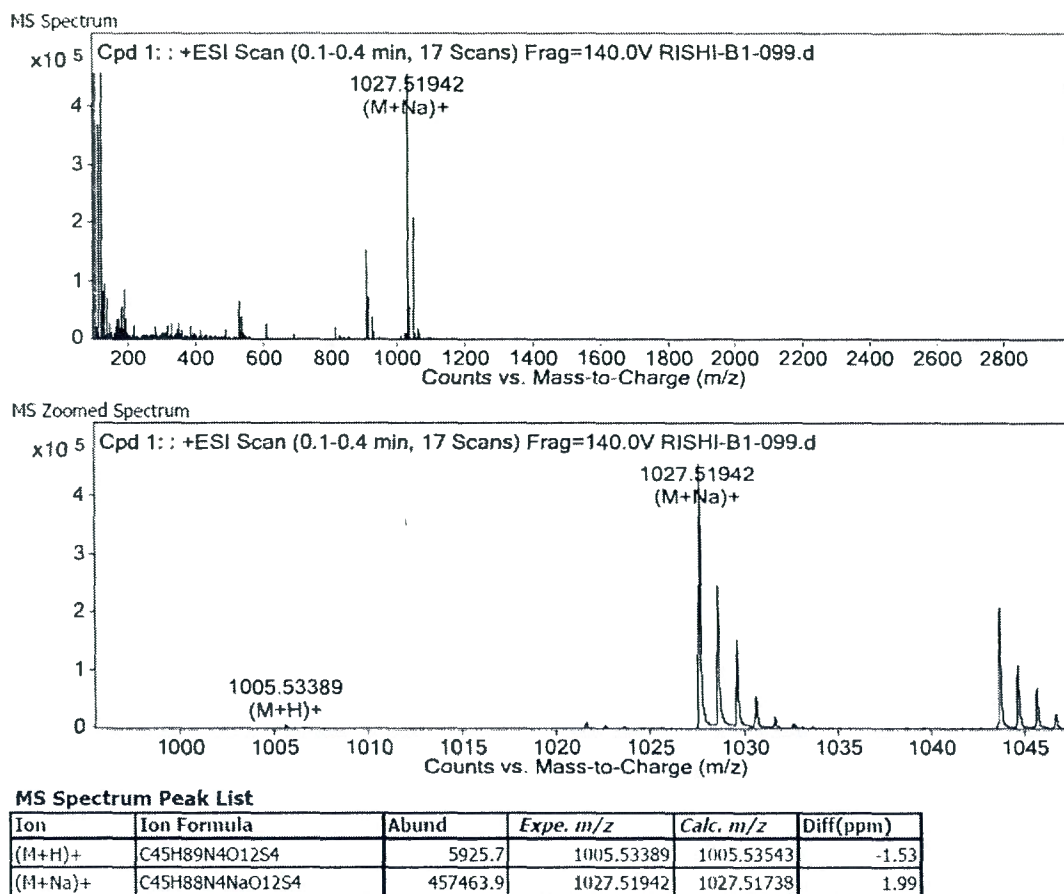


Figure S4. HRMS analysis (ESI⁺) for compound 8.

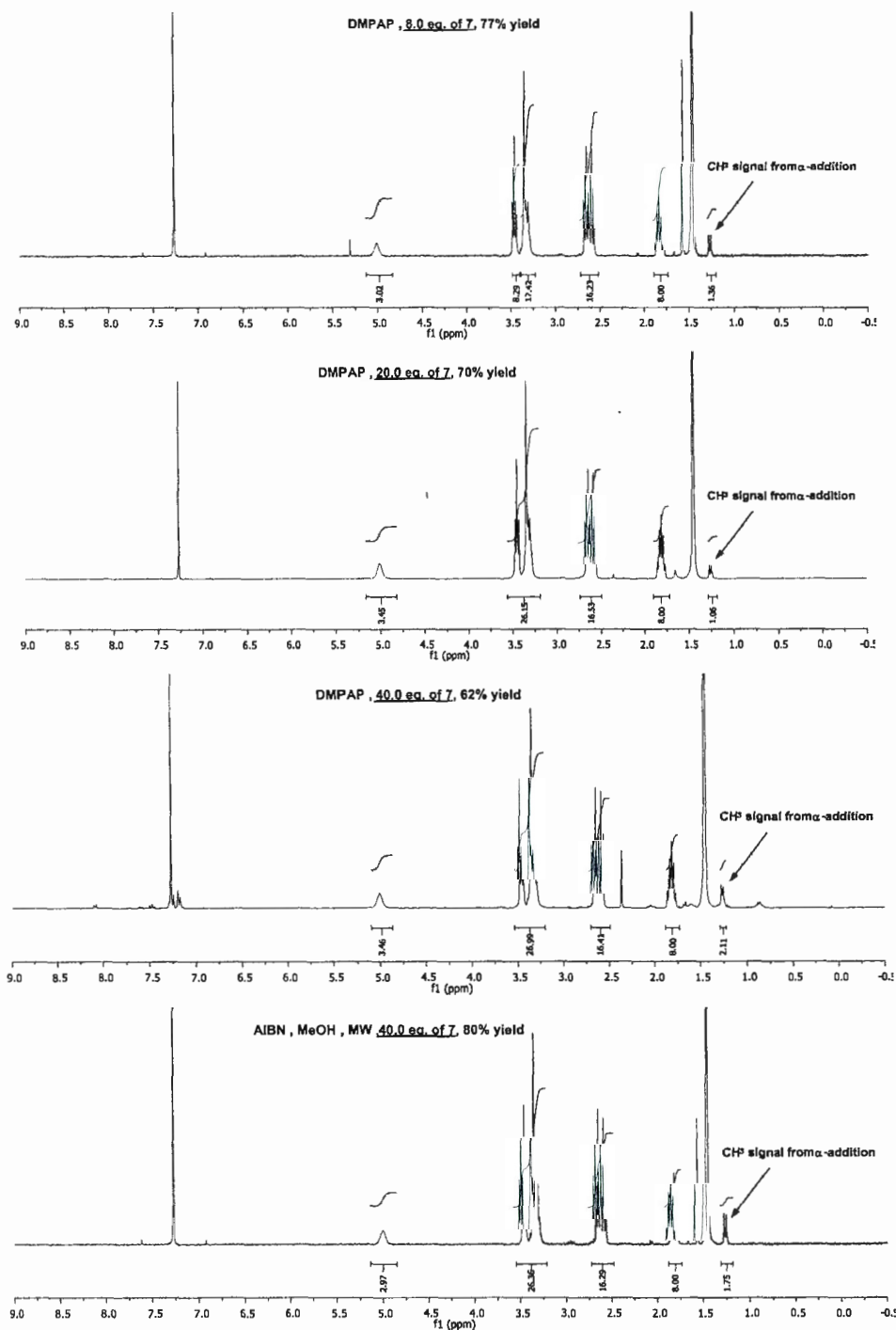
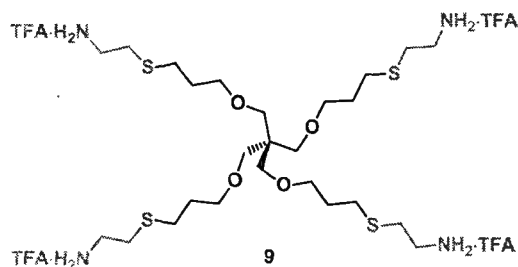


Figure S5. Comparison of proportion of undesired α -addition during thiol-ene process between compounds 6 and 7, depending on experimental conditions.



Synthesis of compound 9: To a stirring solution of compound 8 (430 mg, 0.42 mmol) in DCM (10 ml), was added 1.5 ml of trifluoroacetic acid (TFA) at 0°C and reaction mixture was left at room temperature for overnight. The completion of reaction was monitored by TLC. Upon completion, the solvent was evaporated. The residue was diluted with 10 ml methanol and co-evaporated with Toluene under reduced pressure. This step was repeated 5-6 times. **Yield: 97%** (as a TFA salt).

^1H NMR (300 MHz, MeOD) δ (ppm) 3.49 (t, $J = 6.0$ Hz, 8H), 3.38 (s, 8H), 3.14 (t, $J = 6.9$ Hz, 8H), 2.80 (t, $J = 6.9$ Hz, 8H), 2.66 (t, $J = 7.2$ Hz, 8H), 1.93–1.77 (m, 8H).
 $^{13}\text{C}\{^1\text{H}\}$ NMR (75 MHz, MeOD), (TFA salt not indicated) δ (ppm) 70.6, 49.9, 46.7, 39.9, 30.6, 29.7, 29.2.

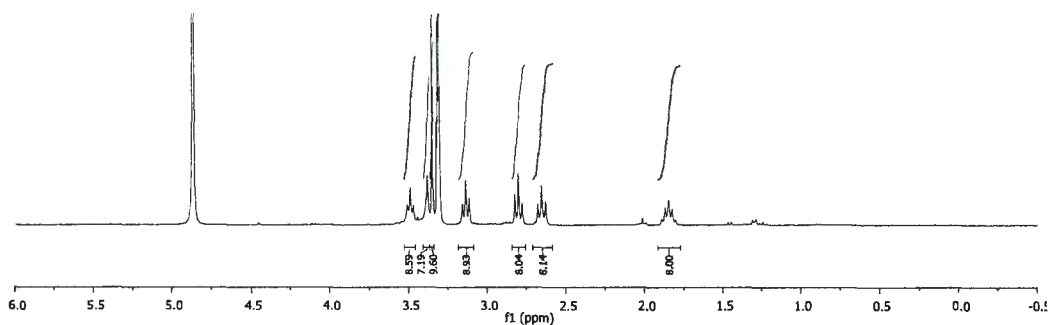


Figure S6. ^1H NMR spectrum of compound 9 (MeOD, 300 MHz).

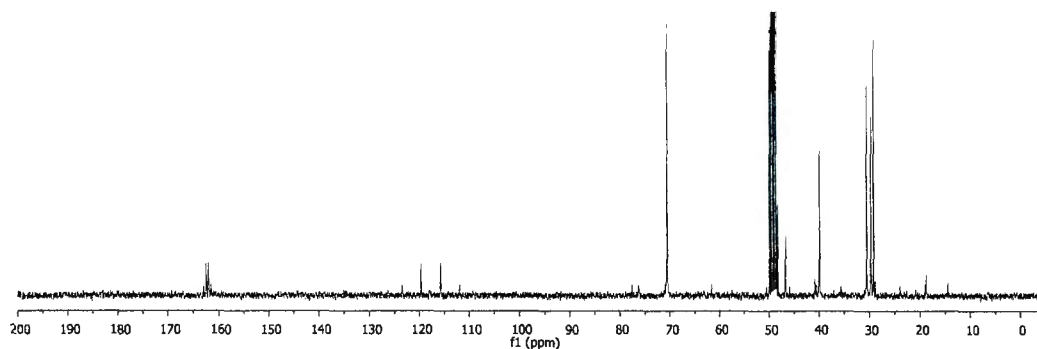


Figure S7. ^{13}C NMR spectrum of compound 9 (MeOD, 75 MHz).

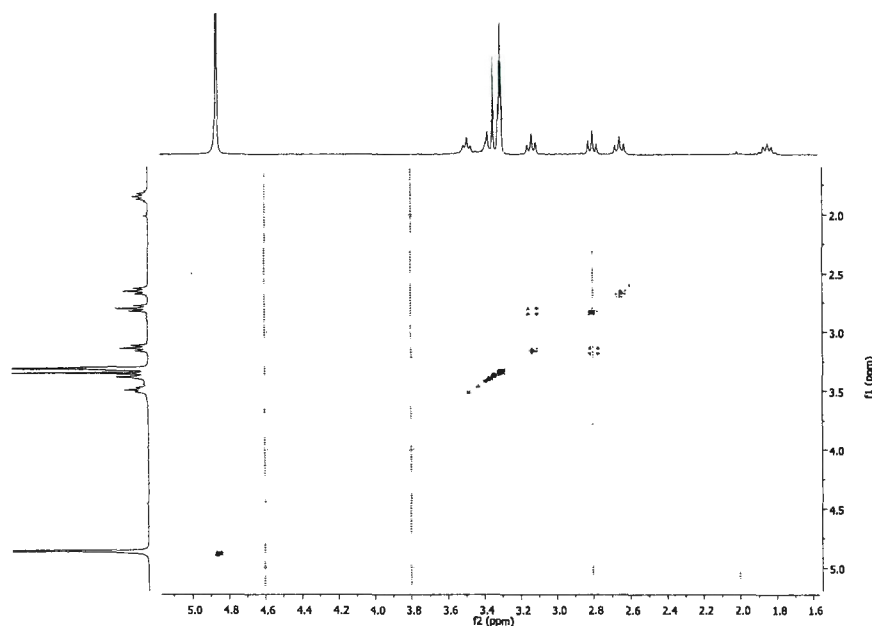
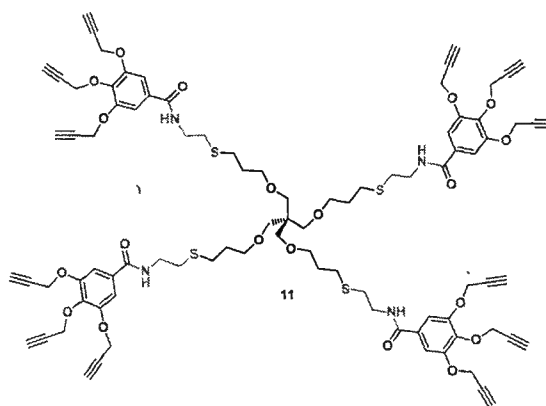


Figure S8. COSY spectrum of compound **9**.



Synthesis of compound 11: To a solution of compound **9** (50 mg, 0.047 mmol, 1.0 eq.) in DMF (1 ml), was added diisopropylethylamine (0.04 ml, 0.24 mmol, 5.0 eq.) and stirred for 30 min., followed by the addition of tripropargylated gallic acid **10** (80 mg, 0.28 mmol, 6.0 eq.), EDC·HCl (54 mg, 0.28 mmol, 6.0 eq.), DMAP (46 mg, 0.38 mmol, 8.0 eq.). The reaction mixture was heated at 50°C overnight. The completion of reaction was monitored by TLC. Upon completion, the reaction mixture was diluted with water (2 ml) and extracted with ethyl acetate (3x10 ml). The combined

organic extracts were washed with 0.1N HCl (3x5 ml), followed by saturated NaHCO₃ solution and brine. The organic layer was dried over anhydrous sodium sulfate, filtered and then evaporated under reduced pressure. The crude mixture was then purified with the help of column chromatography on silica using 70% ethyl acetate in hexanes as eluent to afford the desired compound **11** as colorless viscous oil (0.027 mmol, 45 mg). **Yield: 57%**.

¹H NMR (300 MHz, CDCl₃) δ (ppm) 7.24 (s, 8H), 6.91 (br s, 4H), 4.78 (2xd, J = 2.4 Hz, 24H), 3.61 (d, J = 5.9 Hz, 8H), 3.44 (t, J = 5.9 Hz, 8H), 3.32 (s, 8H), 2.75 (t, J = 6Hz, 8H), 2.60 (t, J = 6Hz, 8H), 2.55 (d, J = 2.2 Hz, 8H), 2.47 (d, J = 2.4 Hz, 4H), 1.81 (s, 8H).

¹³C{¹H} NMR (75 MHz, CD₃Cl) δ (ppm) 166.6, 151.5, 140.0, 130.2, 107.9, 69.5, 60.3, 57.2, 39.0, 31.6, 29.7, 28.3.

IR (cm⁻¹) 3284, 2924, 2867, 2121, 1639, 1582, 1493, 1323, 1208, 1107, 1033, 991.

HRMS (ESI⁺-TOF) m/z : calculated for C₈₉H₉₆N₄O₂₀S₄ [M+Na]⁺: 1691.5393, found: 1691.5360.

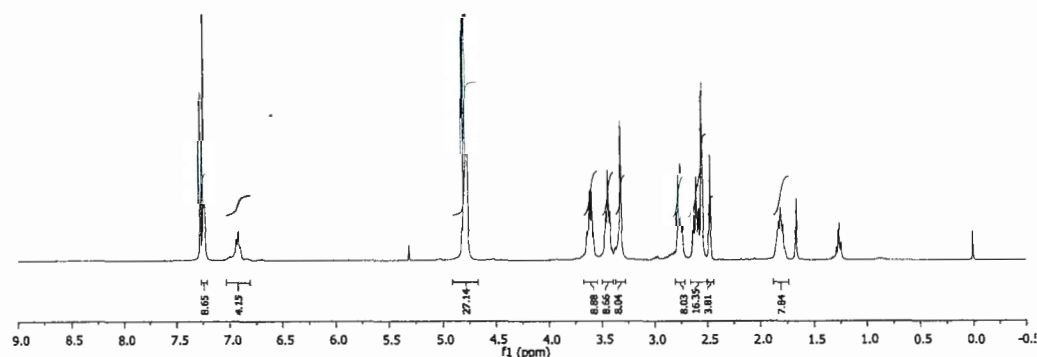


Figure S9. ¹H NMR spectrum of compound **11** (CDCl₃, 300 MHz).

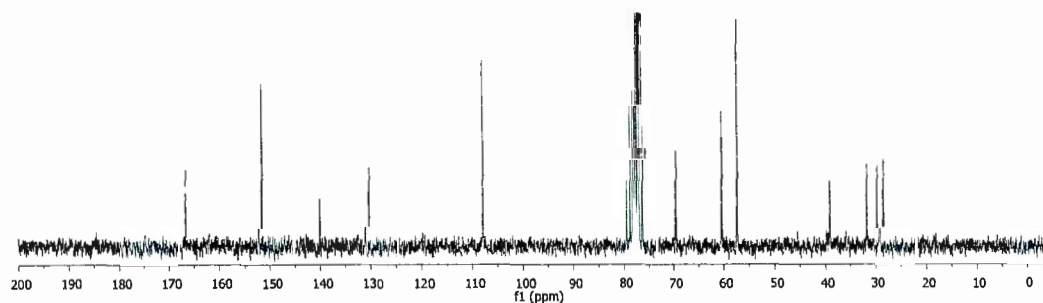


Figure S10. ¹³C NMR spectrum of compound **11** (CDCl₃, 75 MHz).

Figure S12. COSY spectrum of compound **11**.

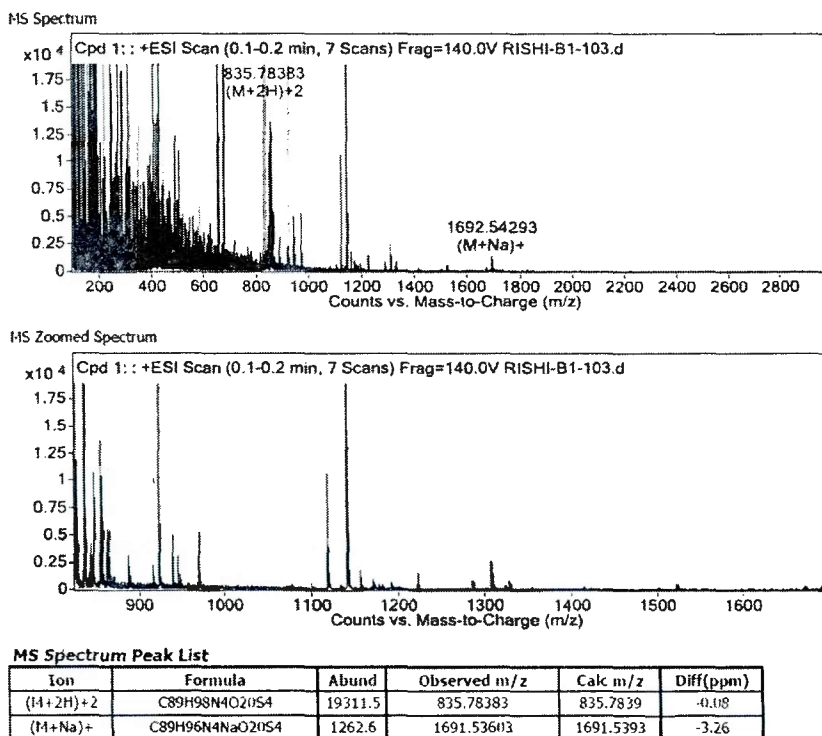
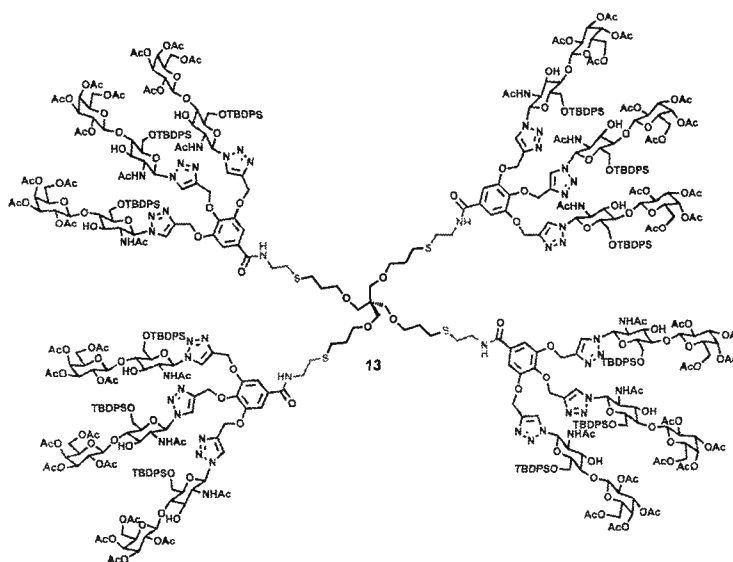


Figure S13. HRMS analysis (ESI⁺) for compound 11.



Synthesis of compound 13: To a stirring solution of compound 11 (12 mg, 0.007 mmol, 1.0 eq.) and compound 12 (81 mg, 0.10 mmol, 14.4 eq.) in THF/H₂O mixture (1:1) was added sodium ascorbate (11 mg, 0.051 mmol, 7.2 eq.) and stirred for 5

minutes. It was followed by dropwise addition of $\text{CuSO}_4 \cdot 5\text{H}_2\text{O}$ (9.0 mg, 0.051 mmol, 7.2 eq.) dissolved in water (1 ml). The reaction mixture was then stirred for 12 hrs at 40°C . A 30 ml of EtOAc/aqueous solution of saturated NH_4Cl (20:10) was added to the mixture. Extraction, followed by subsequent washing of organic phase (2×10 ml of H_2O), drying over anhydrous Na_2SO_4 , filtration and evaporation in vacuo furnished a crude oil. Silica gel column chromatography was performed and pure compound was obtained as a colorless oil using 80% EtOAc in hexanes as eluent (57 mg, 5.0 μmol). **Yield: 71%.**

^1H NMR (600 MHz, CDCl_3) δ (ppm) 7.94 (s, 8H), 7.72–7.46 (m, 52H), 7.43–7.28 (m, 44H), 7.27–7.12 (m, 36H), 6.03 (m, 12H), 5.39 (s, 12H), 5.34–5.09 (m, 32H), 4.99 (d, $J = 8.6$ Hz, 12H), 4.83–4.67 (m, 12H), 4.33–3.58 (m, 134H), 3.45 (br s, 12H), 3.34 (br s, 8H), 2.75 (br s, 8H), 2.63 (br s, 8H), 2.24–1.92 (m, 112), 1.85–1.63 (m, 76H), 1.10–0.94 (m, 108).

$^{13}\text{C}\{^1\text{H}\}$ NMR (151 MHz, CDCl_3) δ (ppm) 171.0, 170.3, 170.1, 169.8, 169.1, 152.1, 143.7, 135.6, 135.4, 133.1, 132.3, 129.9, 128.1, 126.9, 122.3, 108.7, 101.14, 85.6, 79.7, 72.6, 71.8, 71.2, 70.7, 69.4, 68.7, 66.7, 63.3, 61.6, 61.1, 55.4, 39.6, 31.2, 29.6, 28.5, 26.8, 22.9, 20.5, 19.2.

IR (cm^{-1}): 2955, 2927, 2856, 1752, 1667, 1428, 1369, 1428, 1369, 1218, 1104, 1069.

(MALDI-TOF) m/z : calculated for $\text{C}_{545}\text{H}_{696}\text{N}_{52}\text{O}_{188}\text{S}_4\text{Si}_{12}$: 11448.879, found: 11457.922. (DHB matrix)

GPC: $M_n = 11220$ g/mol, $M_w/M_n = 1.031$.

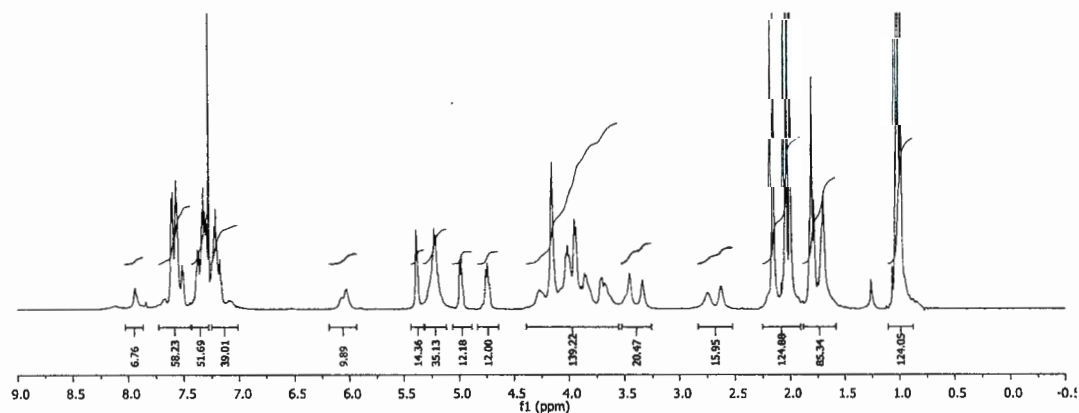


Figure S14. ^1H NMR spectrum of compound **13** (CDCl_3 , 600 MHz).

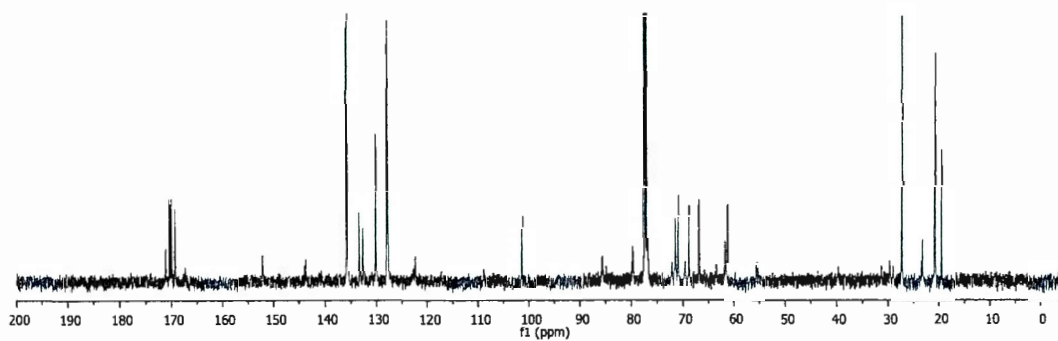


Figure S15. ^{13}C NMR spectrum of compound **13** (CDCl_3 , 150 MHz).

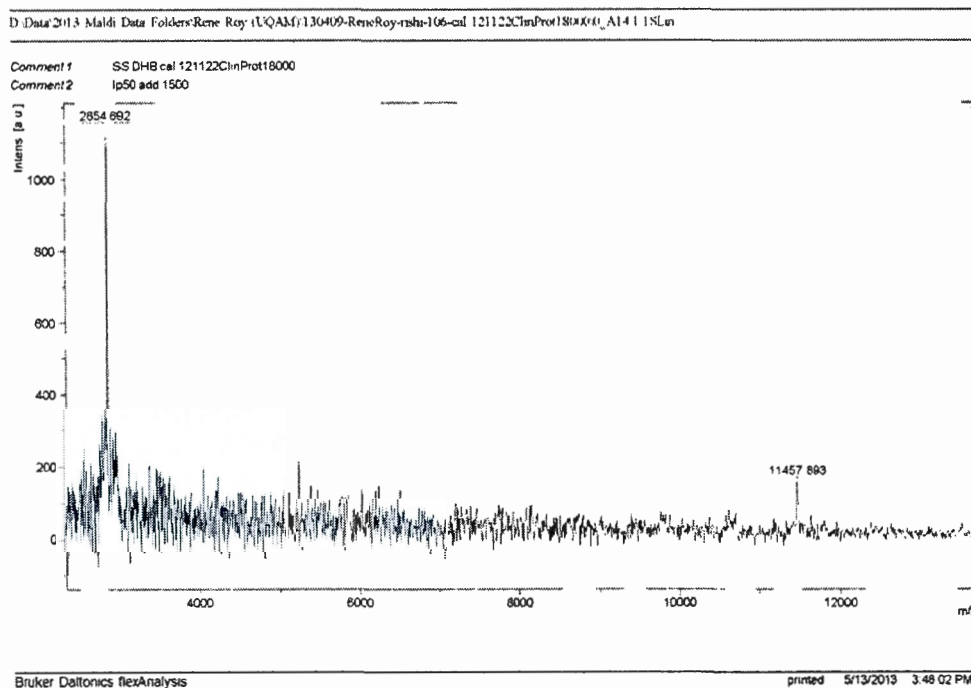


Figure S16. MALDI-TOF trace for compound **13** (DHB matrix).

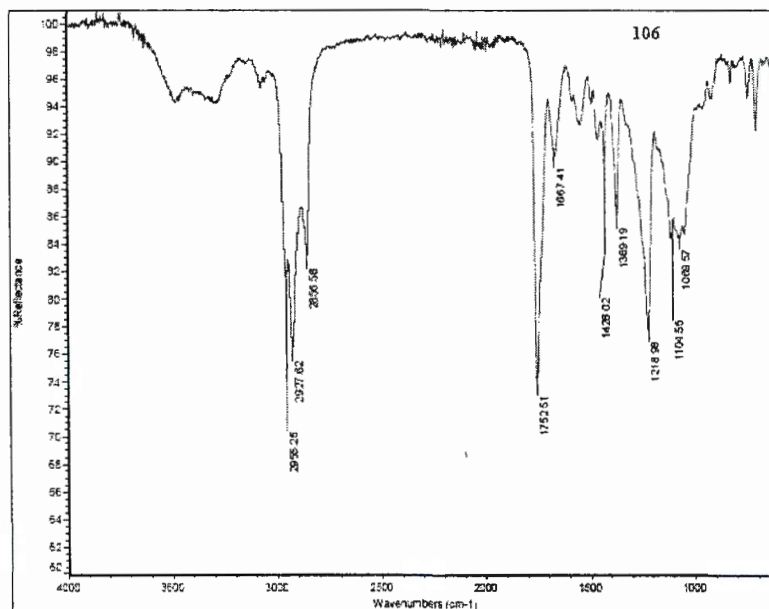
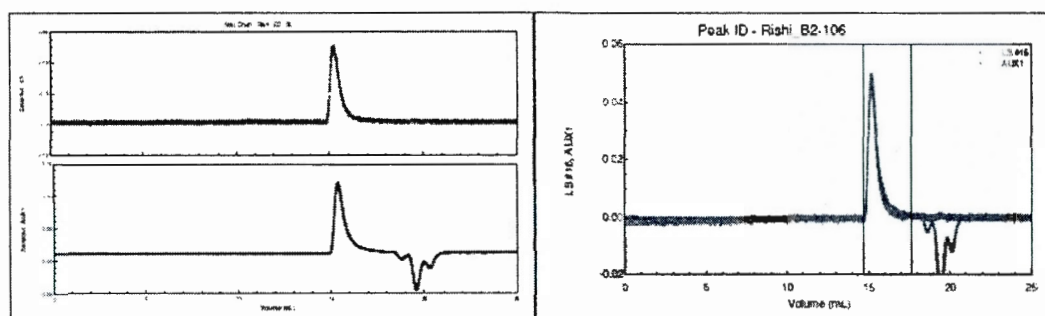


Figure S17. IR spectrum of compound 13.



Polydispersity(M_w/M_n) : 1.031 ± 0.145 (14%)

Polydispersity(M_z/M_n) : 1.062 ± 0.264 (25%)

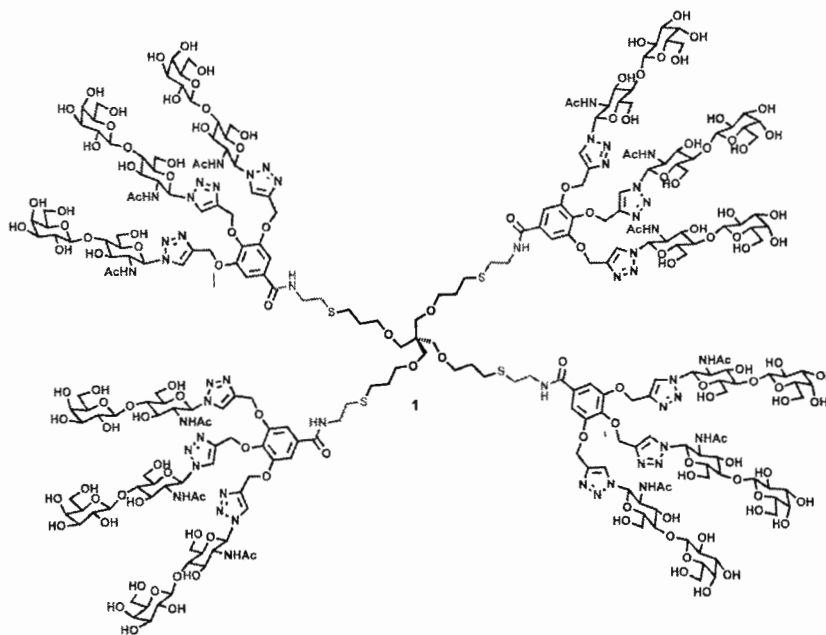
Molar Mass Moments (g/mol)

M_n : 1.122×10^4 (10%)

M_w : 1.157×10^4 (9%)

M_z : 1.192×10^4 (22%)

Figure S18. GPC trace of compound 13.



Synthesis of compound 1: To a stirring solution of compound **13** (55 mg, 5.0 μmol , 1.0 eq.) in THF, TBAF (0.078 ml, 0.078 mmol, 15.6 eq.) was added at 0°C. The reaction mixture was stirred at room temperature for 6 hrs. The solvent was then evaporated and solid was washed with diethylether. The residue was dissolved in 3ml of methanol followed by the addition of 1M solution of MeONa in MeOH to adjust the pH 9-10 and reaction mixture was left for stirring overnight. The reaction pH was then adjusted with H^+ resin to reach 6. After filtration, solvent was evaporated and residue was dissolved in 3ml of water and extracted with diethyl ether (3x15 ml). The aqueous layer was lyophilized to yield a white solid (25 mg, 3.8 μmol). **Yield: 75%.**

^1H NMR (300 MHz, D_2O) δ (ppm) 8.27 (2xbr s, 12H), 7.19 (br s, 8H), 5.79 (m, 12H), 5.39–4.82 (m, 24H), 4.54 (m, 12H), 4.26 (m, 12H), 4.13–3.00 (m, 156H), 2.60 (2xbr s, 16H), 1.70 (m, 44H).

$^{13}\text{C}\{^1\text{H}\}$ NMR (151 MHz, D_2O) δ (ppm) 174.2, 169.0, 152.1, 143.7, 139.1, 130.6, 124.7, 107.5, 103.6, 86.8, 86.6, 85.7, 78.5, 78.2, 76.0, 73.0, 72.8, 71.6, 70.3, 69.2, 65.5, 62.5, 61.7, 60.4, 58.7, 55.5, 55.3, 40.1, 31.3, 29.0, 28.7, 28.6, 23.7, 22.3, 19.8, 13.4.

IR (cm^{-1}): 3289, 2868, 1650, 1543, 1426, 1374, 1321, 1236, 1040, 896, 727.

(MALDI-TOF) m/z : calculated for $\text{C}_{257}\text{H}_{384}\text{N}_{52}\text{O}_{140}\text{S}_4$ $[\text{M}+\text{Na}]^+$: 6593.3, found: 6597.9.

Melting point: $\geq 214^\circ\text{C}$ (dec.).

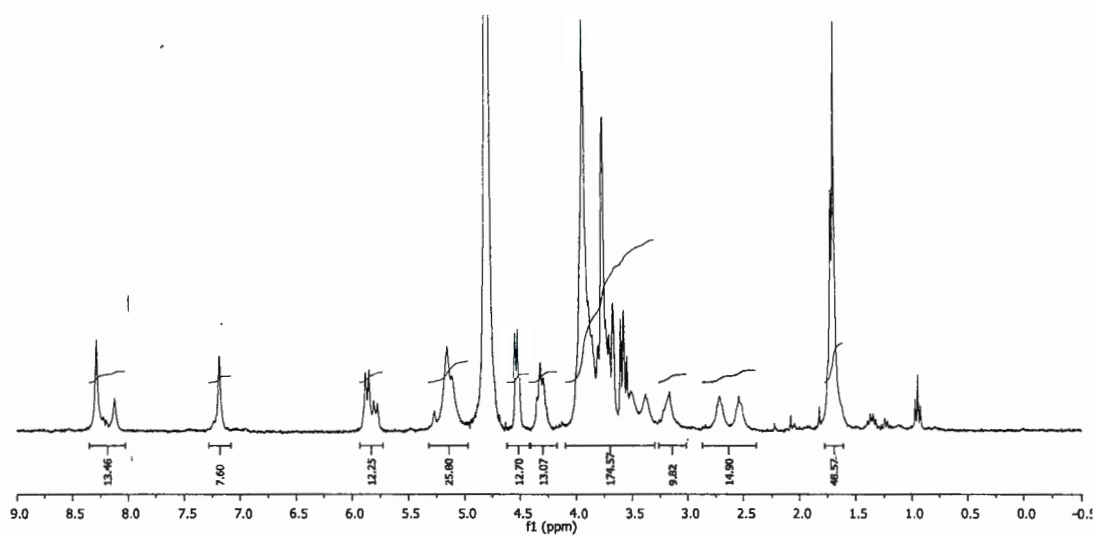


Figure S19. ^1H NMR spectrum of compound **1** (D_2O , 300 MHz).

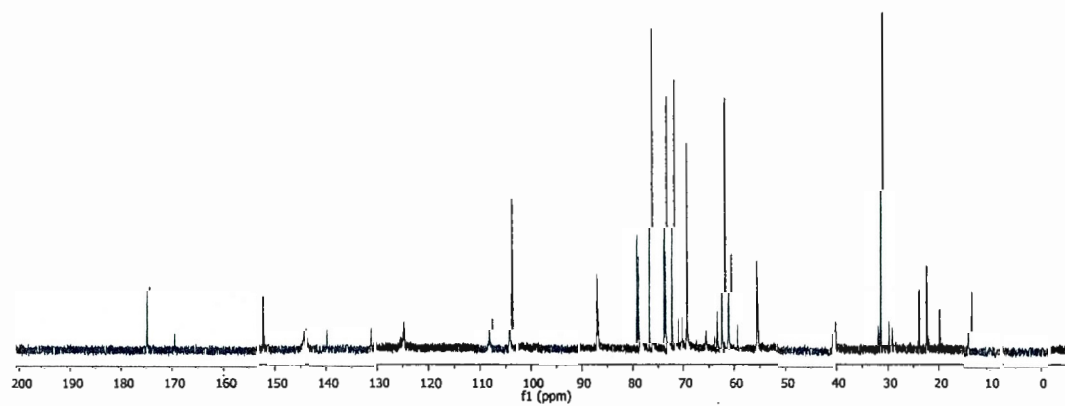


Figure S20. ^{13}C NMR spectrum of compound **1** (D_2O , 150 MHz).

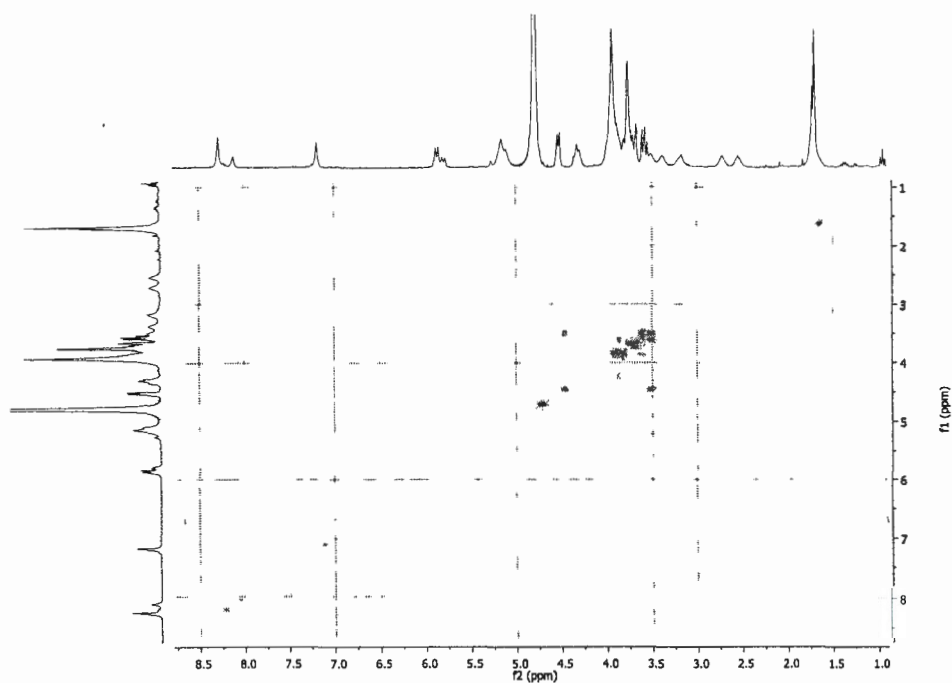


Figure S21. COSY spectrum of compound 1.

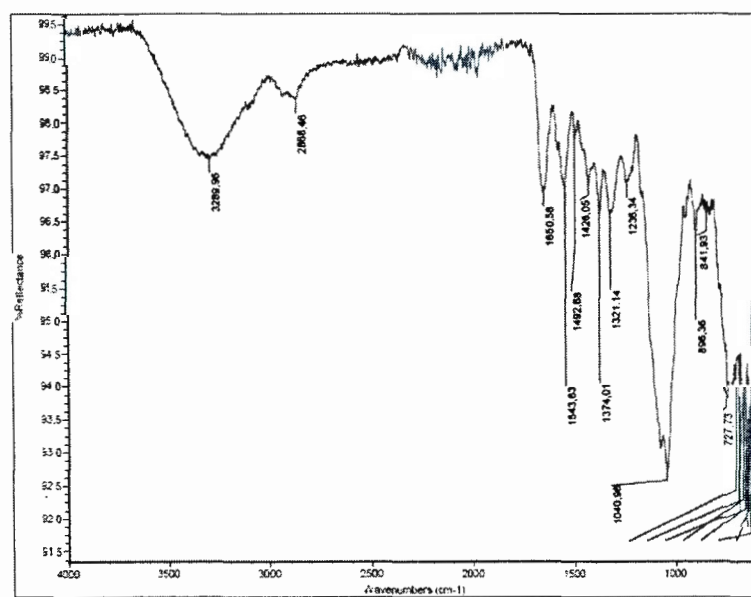


Figure S22. IR spectrum of compound 1.

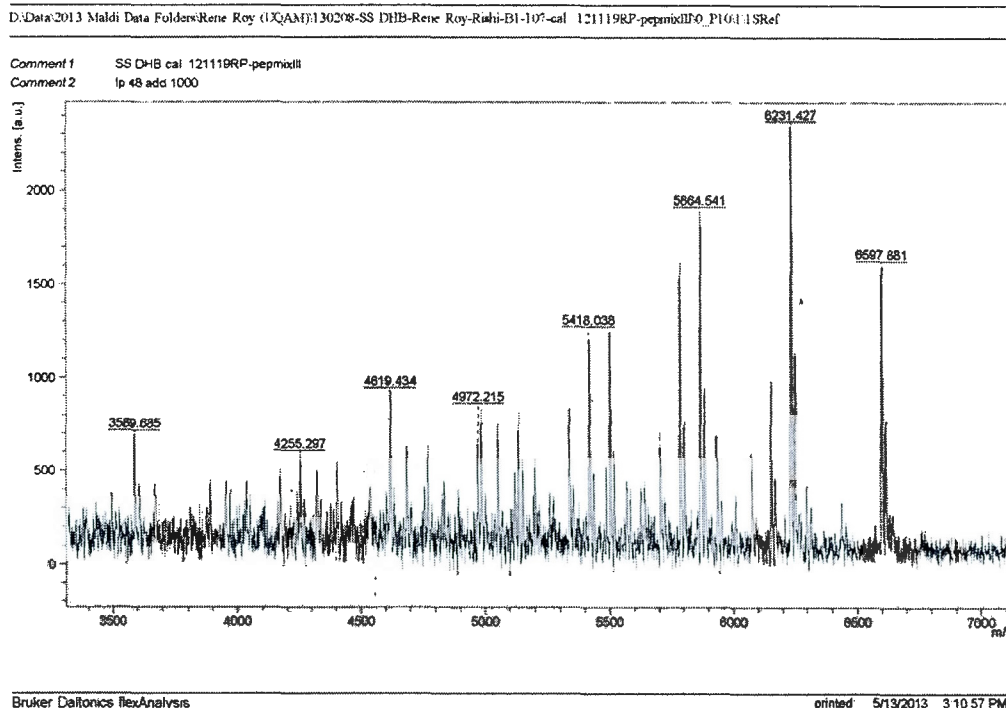
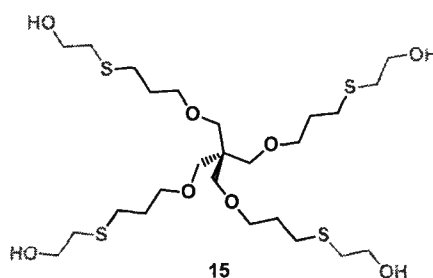


Figure S23. MALDI-TOF trace for compound 1 (DHB matrix).



Synthesis of compound 15: Compound **6** (200 mg, 0.680 mmol, 1.0 eq.) and **14** (1.91 ml, 27.2 mmol, 40.0 eq.) were reacted together following the procedure **A** and was further purified by column chromatography (5% MeOH in DCM as eluent) to yield compound **15** as a viscous oil (310 mg, 0.507 mmol). **Yield: 75%.**

^1H NMR (300 MHz, CDCl_3) δ (ppm) 3.72 (q, $J = 6.0$ Hz, 8H), 3.46 (t, $J = 6.0$ Hz, 8H), 3.34 (s, 8H), 2.72 (t, $J = 6.0$ Hz, 8H), 2.59 (t, $J = 7.5$ Hz, 8H), 2.48 (t, $J = 4.5$ Hz, 4H), 1.90–1.74 (m, 8H). $^{13}\text{C}\{^1\text{H}\}$ NMR (151 MHz, CDCl_3) δ (ppm) 69.6, 60.6, 60.3, 35.3, 29.8, 28.4.

IR (cm^{-1}): 3385, 2916, 2868, 1461, 1420, 1371, 1266, 1170, 1069, 1043, 1009, 933, 903, 667.

HRMS (ESI⁺-TOF) m/z: calculated for C₂₅H₅₂O₈S₄ [M+H]⁺: 609.2618; found: 609.2604.

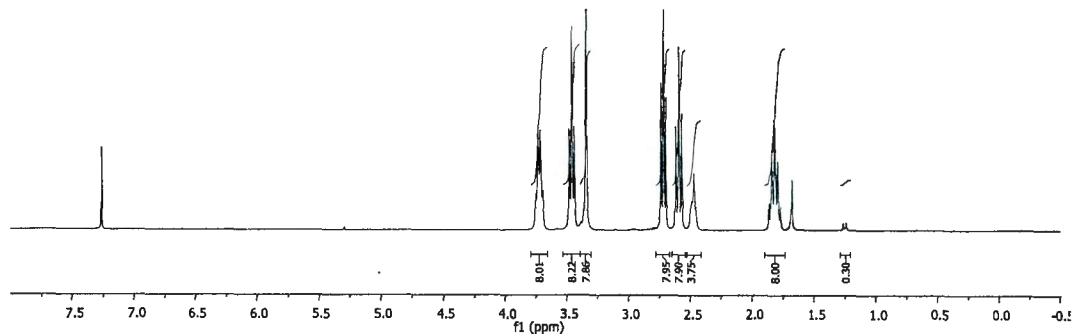


Figure S24. ¹H NMR spectrum of compound **15** (CDCl₃, 300 MHz).

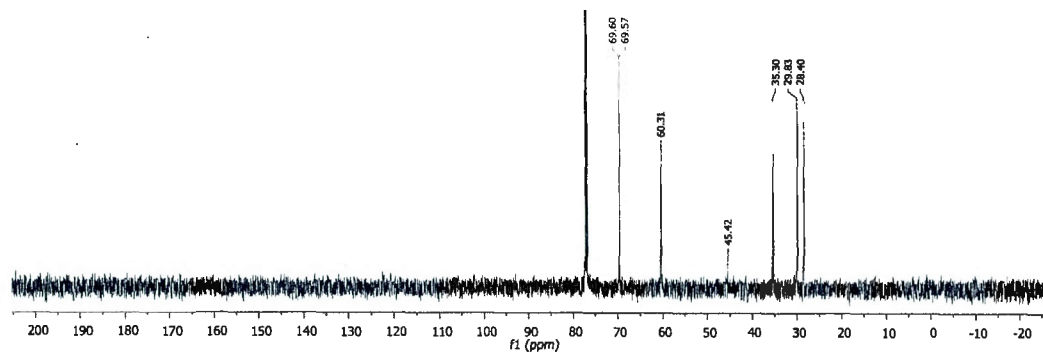


Figure S25. ¹³C NMR spectrum of compound **15** (CDCl₃, 75 MHz).

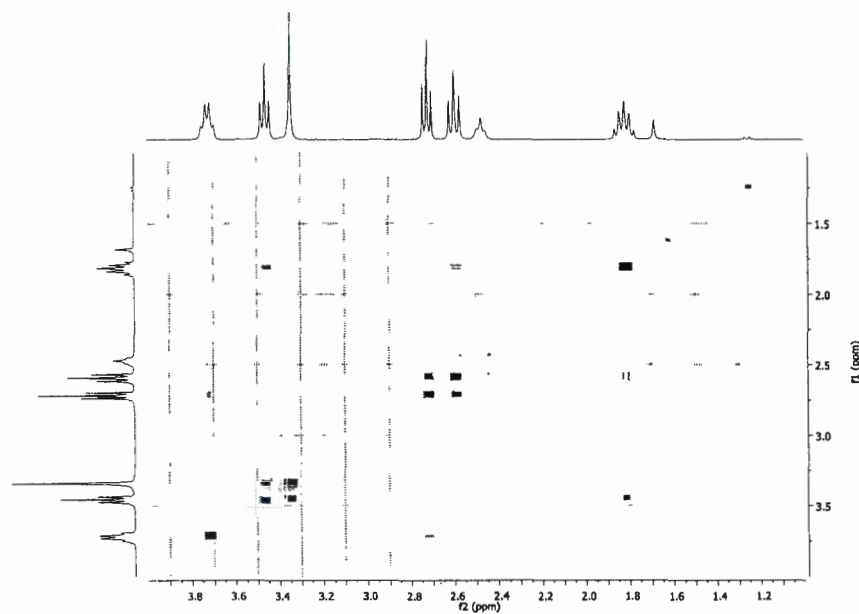
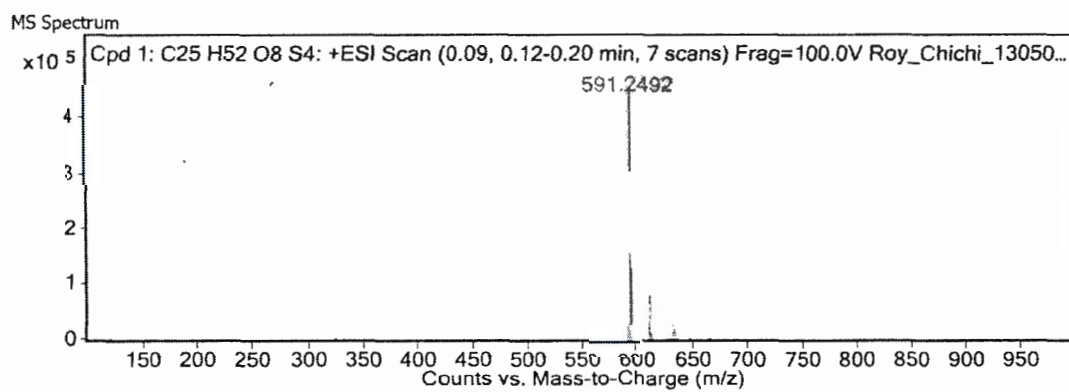
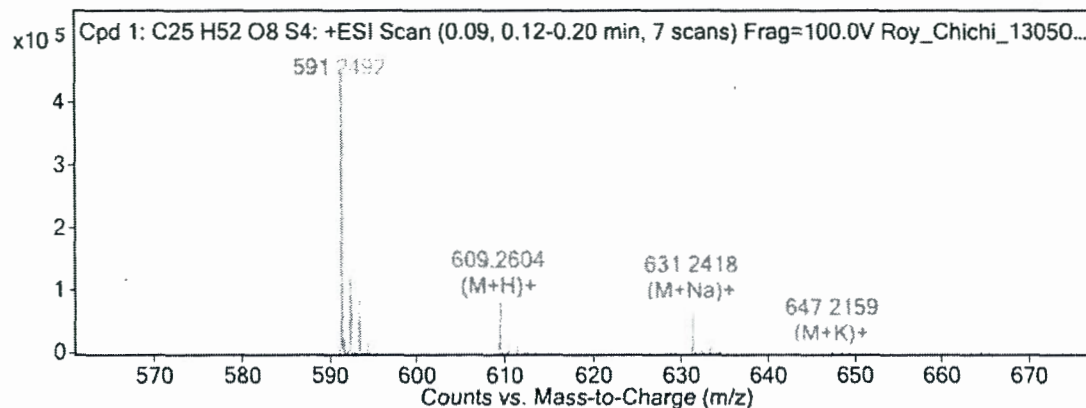


Figure S26. COSY spectrum of compound 15.

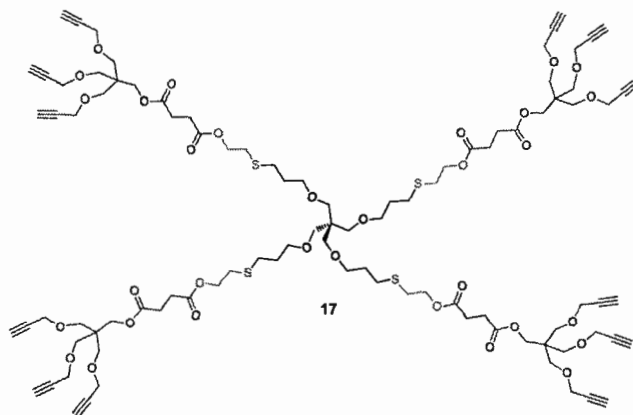




MS Spectrum Peak List

m/z	Calc m/z	Diff(ppm)	z	Abund	Formula	Ion
591.2492				468071		
591.2492	591.2512	-3.36	1	468071	C25 H51 O7 S4	(M+H)+[-H2O]
591.5557				26900		
591.855				3896		
592.2527	592.2542	-2.55		135373	C25 H51 O7 S4	(M+H)+[-H2O]
592.5604				6257		
593.248	593.2495	-2.47		97508	C25 H51 O7 S4	(M+H)+[-H2O]
593.5528				3929		
594.2503	594.2514	-1.92		21101	C25 H51 O7 S4	(M+H)+[-H2O]
595.2471				6962		
609.2604	609.2618	-2.2	1	86750	C25 H53 O8 S4	(M+H)+
610.2642	610.2648	-0.92	1	22764	C25 H53 O8 S4	(M+H)+
611.2591	611.2601	-1.7	1	15941	C25 H53 O8 S4	(M+H)+
612.2606	612.2621	-2.49	1	3860	C25 H53 O8 S4	(M+H)+
626.287	626.2883	-2.08	1	3386	C25 H56 N O8 S4	(M+NH4)+
631.2418	631.2437	-3.06	1	79852	C25 H52 Na O8 S4	(M+Na)+
632.2453	632.2467	-2.36	1	20401	C25 H52 Na O8 S4	(M+Na)+
633.2368	633.2421	-8.3	1	17552	C25 H52 Na O8 S4	(M+Na)+
634.2377	634.244	-10.02	1	4397	C25 H52 Na O8 S4	(M+Na)+
647.2159	647.2177	-2.67	1	7061	C25 H52 K O8 S4	(M+K)+

Figure S27. HRMS spectra and report for compound 15.



Synthesis of compound 17: To a solution of compound **15** (200 mg, 0.328 mmol, 1.0 eq.), EDC·HCl (307 mg, 1.59 mmol, 4.8 eq.), and DMAP (240 mg, 1.97 mmol, 6.0 eq.) in DMF (5ml) was added derivative **16** (4-oxo-4-((3-(prop-2-yn-1-yloxy)-2,2-bis((prop-2-yn-1-yloxy) methyl)-propoxy)methoxy)butanoic acid) (633 mg, 1.80 mmol, 5.5 eq.). The reaction mixture was heated overnight at 50°C. The completion of reaction was monitored by TLC. Upon completion, the reaction mixture was diluted with water (2ml) and extracted with ethyl acetate (3x10ml). The combined organic extracts were washed with 0.1 N HCl (3x5ml), followed by saturated NaHCO₃ solution (3x10ml) and brine. The organic layer was dried over anhydrous sodium sulfate, filtered and evaporated under reduced pressure. The crude mixture was then purified with the help of column chromatography using 5% acetone in hexanes as eluent. A yellowish oil was obtained (375 mg, 0.194 mmol). **Yield: 59%.**

¹H NMR (600 MHz, CDCl₃) δ (ppm) 4.24 (t, *J* = 7.1 Hz, 8H), 4.16 (s, 8H), 4.12 (d, *J* = 2.4 Hz, 24H), 3.52 (s, 24H), 3.45 (t, *J* = 6.1 Hz, 8H), 3.34 (s, 8H), 2.74 (t, *J* = 7.1 Hz, 8H), 2.69–2.56 (m, 24H), 2.43 (t, *J* = 2.3 Hz, 12H), 1.90–1.73 (m, 8H).

¹³C{¹H} NMR (151 MHz, CDCl₃) δ (ppm) 172.2, 171.9, 79.9, 74.5, 69.7, 68.7, 63.8, 58.8, 45.5, 44.1, 30.4, 29.9, 29.2.

IR (cm⁻¹): 3282, 2980, 2881, 2116, 1732, 1474, 1384, 1358, 1264, 1156, 1020, 958, 907, 658.

HRMS (APCI⁺) *m/z*: calculated for C₉₇H₁₃₂O₃₂S₄ [M+H]⁺: 1937.7657, found: 1937.7621.

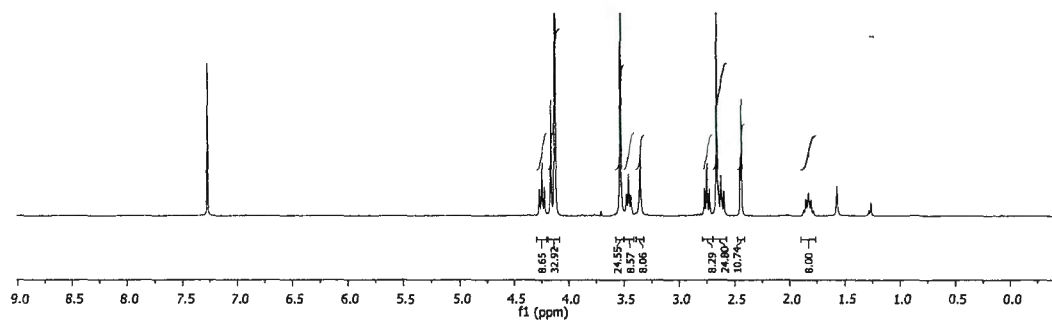


Figure S28. ^1H NMR spectrum of compound 17 (CDCl_3 , 600 MHz).

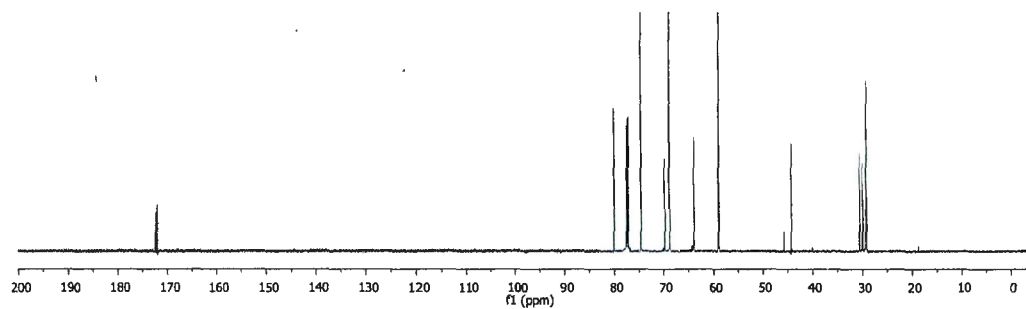


Figure S29. ^{13}C NMR spectrum of compound 17 (CDCl_3 , 150 MHz).

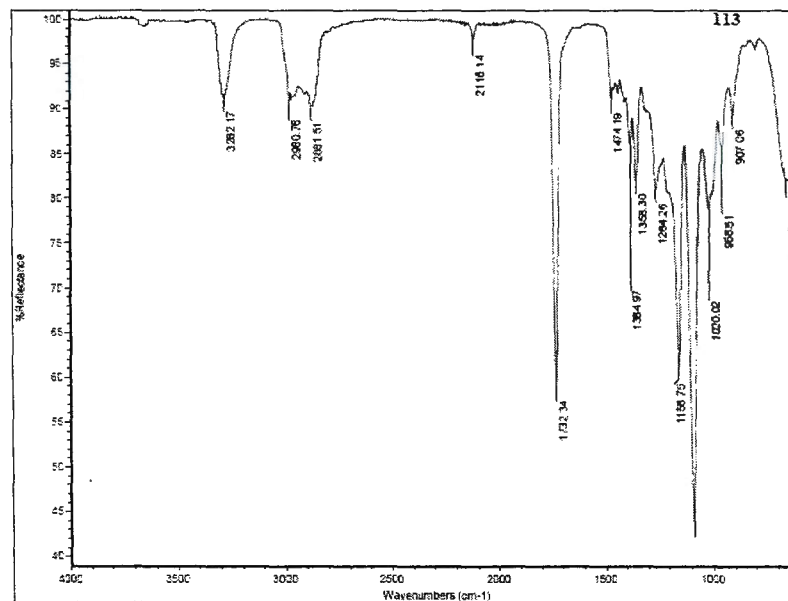
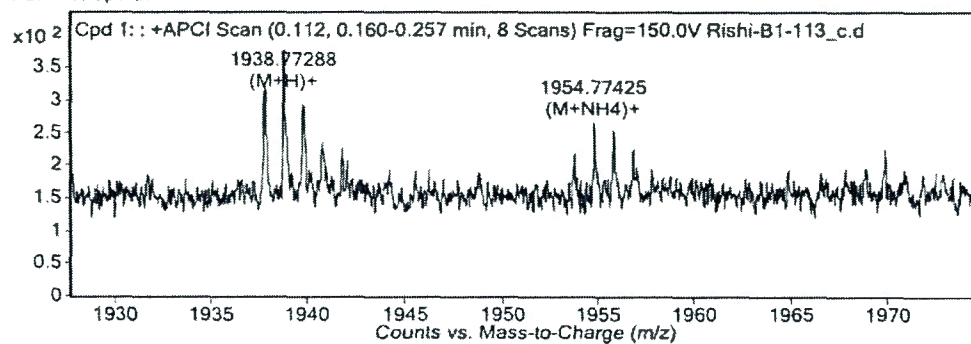


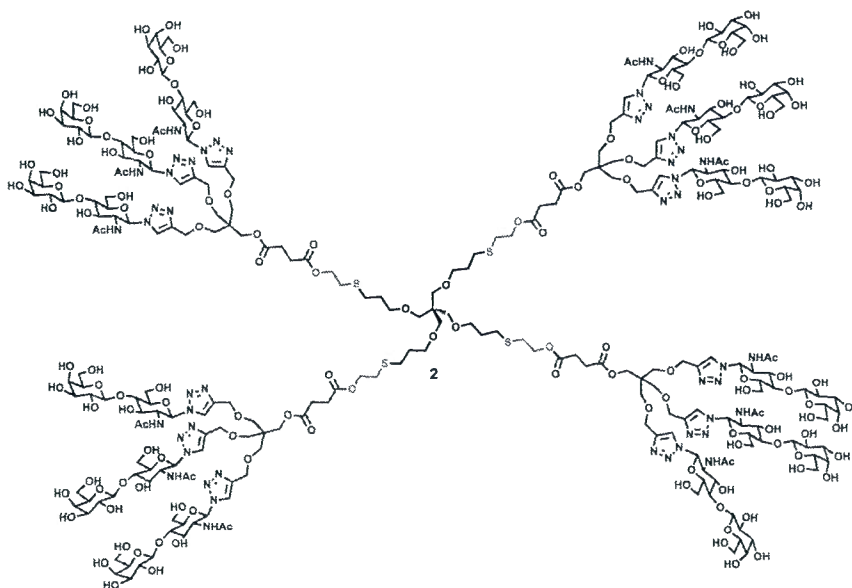
Figure S30. IR spectrum of compound 17.

MS Zoomed Spectrum



MS Spectrum Peak List

Ion	Ion Formula	Abund	Expe. m/z	Calc. m/z	Diff(ppm)
(M+H) ⁺	C ₉₇ H ₁₃₃ O ₃₂ S ₄	219.9	1937.76209	1937.76573	-1.88

Figure S31. HRMS (APCI⁺) for compound 17.

Synthesis of glycodendrimer 2: Compound 17 (13.0 mg, 6.71 μ mol, 1.0 eq.) and compound 18 (46.6 mg, 0.114 mmol, 17.0 eq.) were reacted together using **procedure C** to give dendrimer 2 as a colorless solid (31.2 mg, 4.56 μ mol). **Yield:** 68%.

^1H NMR (300 MHz, D_2O) δ (ppm) 8.21 (s, 12H), 5.87 (d, $J = 9.5$ Hz, 12H), 4.55 (br s, 36H), 4.29 (m, 24H), 4.14–3.14 (m, 172H), 2.85–2.47 (m, 36H), 1.78 (s, 44H).

$^{13}\text{C}\{^1\text{H}\}$ NMR (75 MHz, D_2O) δ (ppm) 180.7, 175.7, 175.1, 174.6, 145.0, 124.3, 103.6, 86.9, 78.3, 76.1, 73.2, 72.9, 71.7, 70.0, 69.6, 68.7, 64.8, 64.2, 61.7, 60.5, 55.6, 44.6, 30.6, 29.5, 28.9, 22.4.

IR (cm^{-1}): 3840, 3364, 2927, 1731, 1657, 1593, 1375, 1315, 1046.

(MALDI-TOF) m/z : calculated for $\text{C}_{265}\text{H}_{420}\text{N}_{48}\text{O}_{152}\text{S}_4$ $[\text{M}+\text{Na}]^+$: 6861.6, found: 6862.3.

Melting point: $\geq 218^\circ\text{C}$ (dec.).

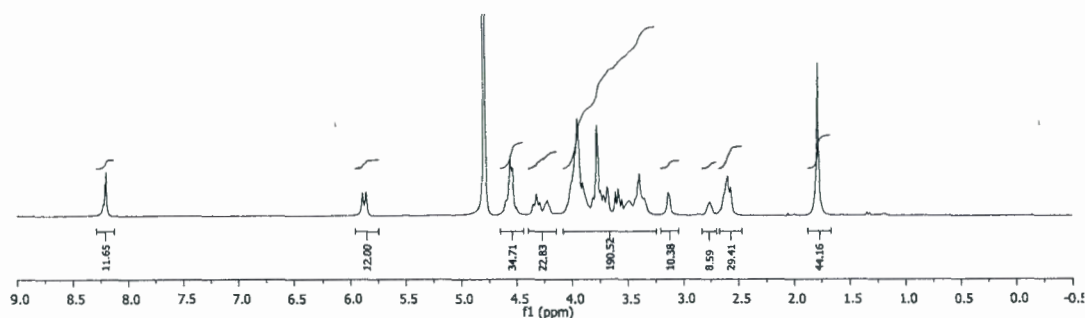


Figure S32. ^1H NMR spectrum of glycodendrimer **2** (D_2O , 300 MHz).

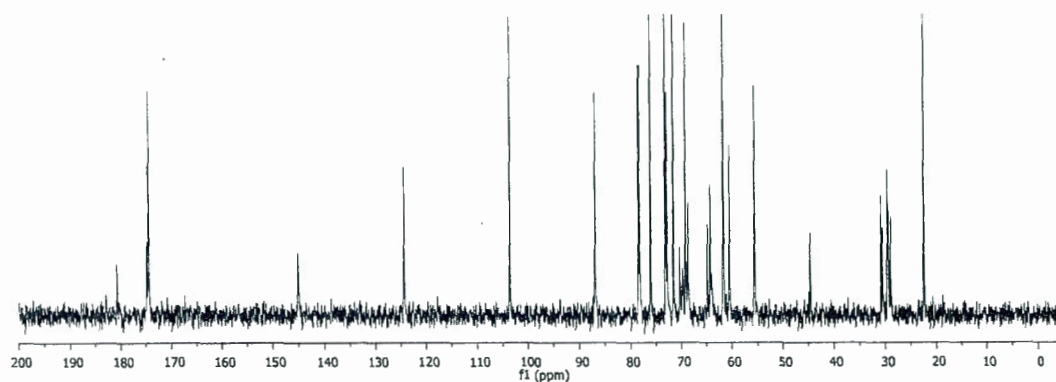


Figure S33. ^{13}C NMR spectrum of glycodendrimer **2** (D_2O , 75 MHz).

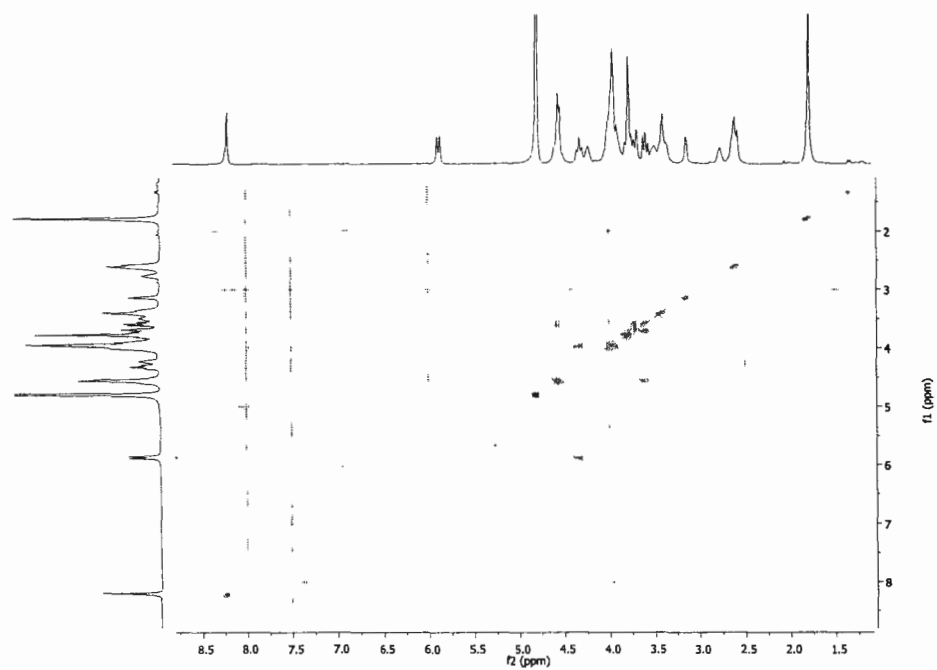


Figure S34. COSY spectrum of glycodendrimer 2.

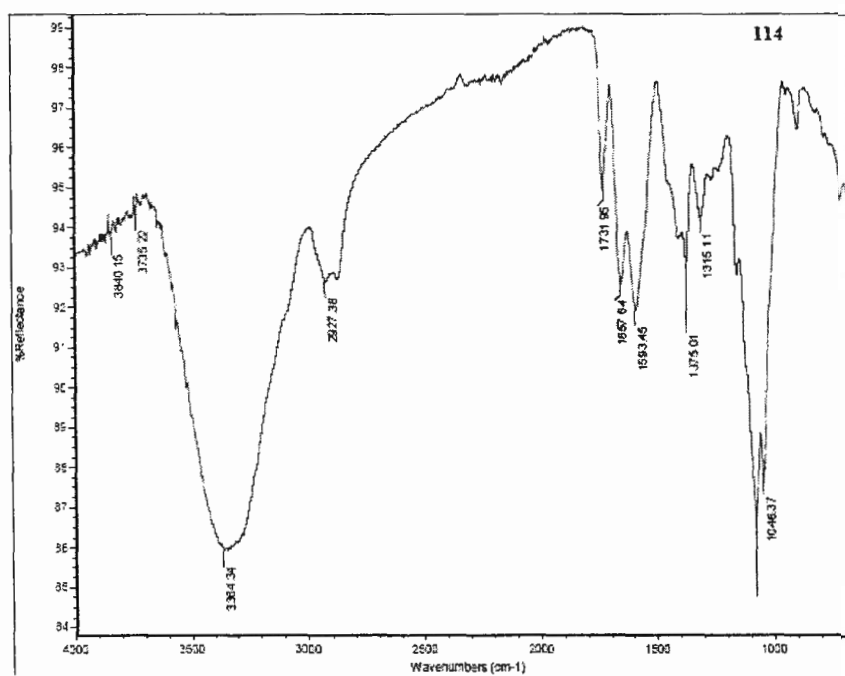
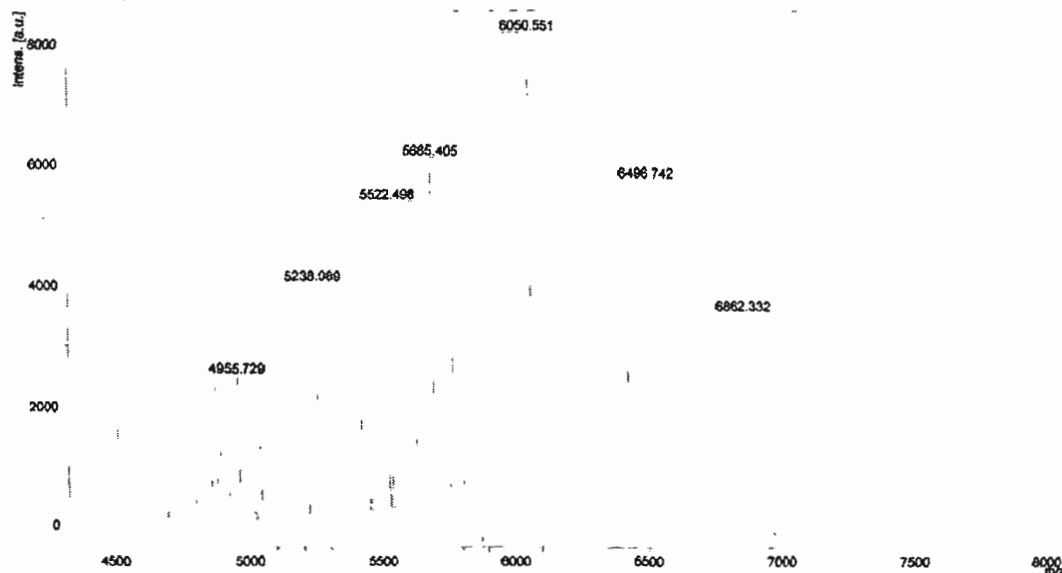


Figure S35. IR spectrum of glycodendrimer 2.

D:\Data\2013 Maldi Data Folders\René Roy (UQAM)\130212-SSDHB-Roy UQAM-Rishi-114-cal-121122LPClinProt0_K24\1\SLin

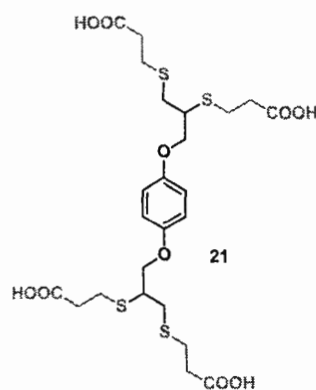
Comment 1 SSDHB cal 121122LPClinProt
Comment 2 lp32 add 3000



Bruker Daltonics flexAnalysis

printed: 2/12/2013 6:13:02 PM

Figure S36. MALDI-TOF trace for glycodendrimer 2 (DHB matrix).



Synthesis of compound 21: Compound 19 (50 mg, 0.27 mmol, 1.0 eq.) and compound 20 (227 mg, 2.15 mmol, 8.0 eq.) were reacted together according to general **procedure B** and then purified by column chromatography using 5% MeOH

in DCM as eluent to give compound **21** as a colorless oil (140 mg, 0.227 mmol).

Yield: 85%.

^1H NMR (300 MHz, CD_3OD) δ (ppm) 6.91 (s, 4H), 4.22–4.13 (m, 4H), 3.21 (m, 2H), 3.04–2.86 (m, 8H), 2.82 (m, 4H), 2.63 (m, 8H).

$^{13}\text{C}\{^1\text{H}\}$ NMR (75 MHz, CD_3OD) δ (ppm) 176.0, 154.3, 116.9, 71.4, 46.7, 36.0, 35.7, 35.5, 28.8, 27.6.

IR (cm^{-1}): 3334, 2944, 2832, 1449, 1022, 639.

HRMS (ESI-TOF) m/z : calculated for $\text{C}_{24}\text{H}_{34}\text{O}_{10}\text{S}_4$ $[\text{M}-\text{H}]^-$: 609.0964; found: 609.0962.

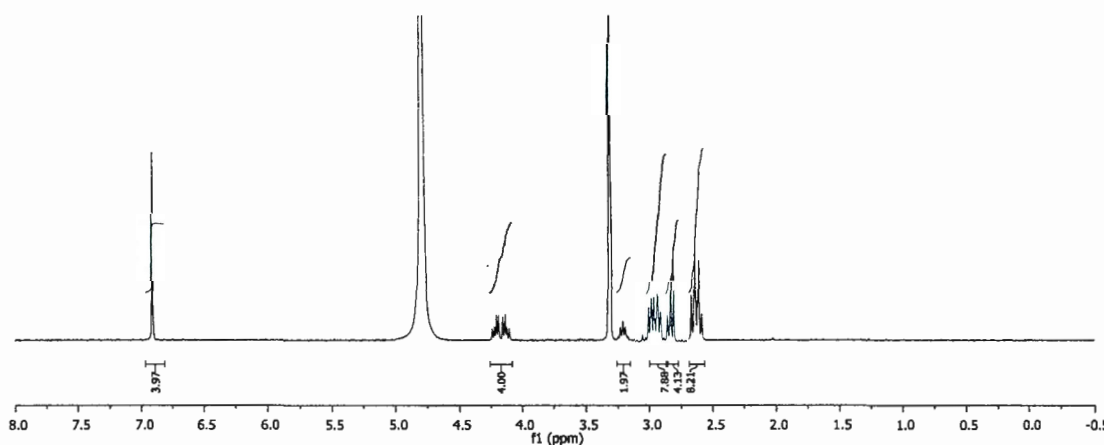


Figure S37. ^1H NMR spectrum of compound **21** (CD_3OD , 300 MHz).

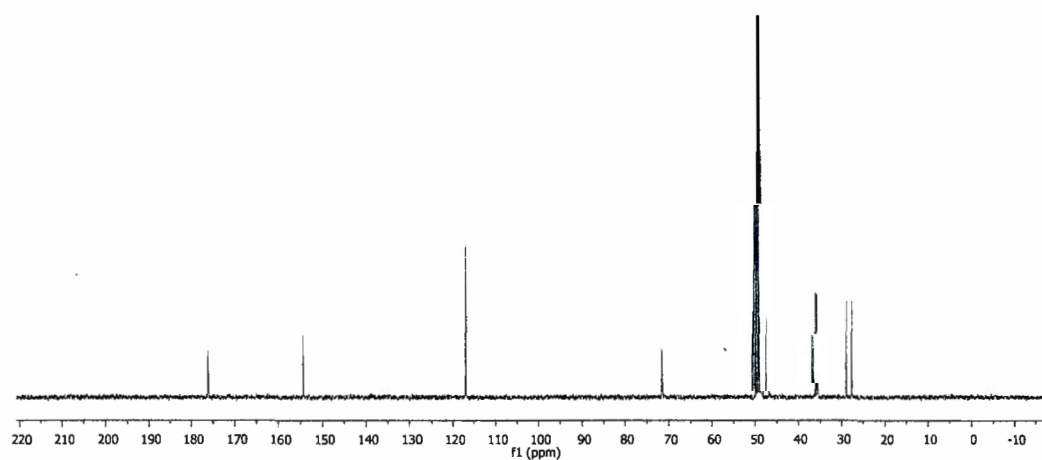


Figure S38. ^{13}C NMR spectrum of compound **21** (CD_3OD , 75 MHz).

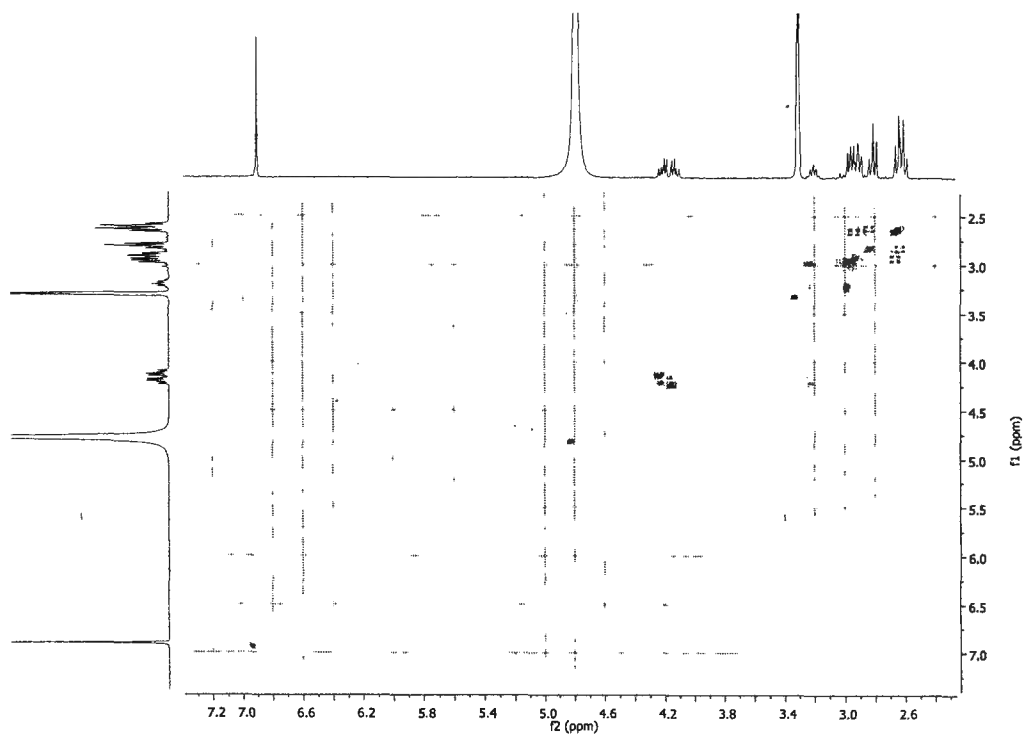


Figure S39. COSY spectrum of compound 21.

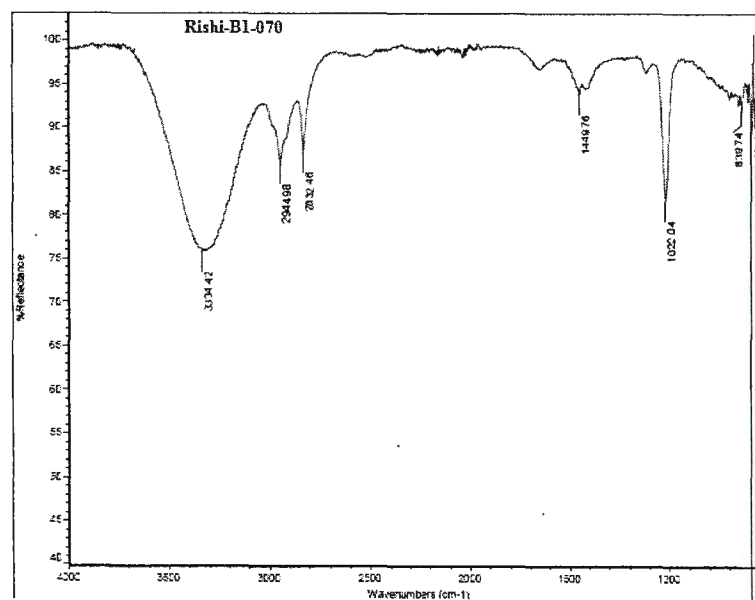


Figure S40. IR spectrum of compound 21.

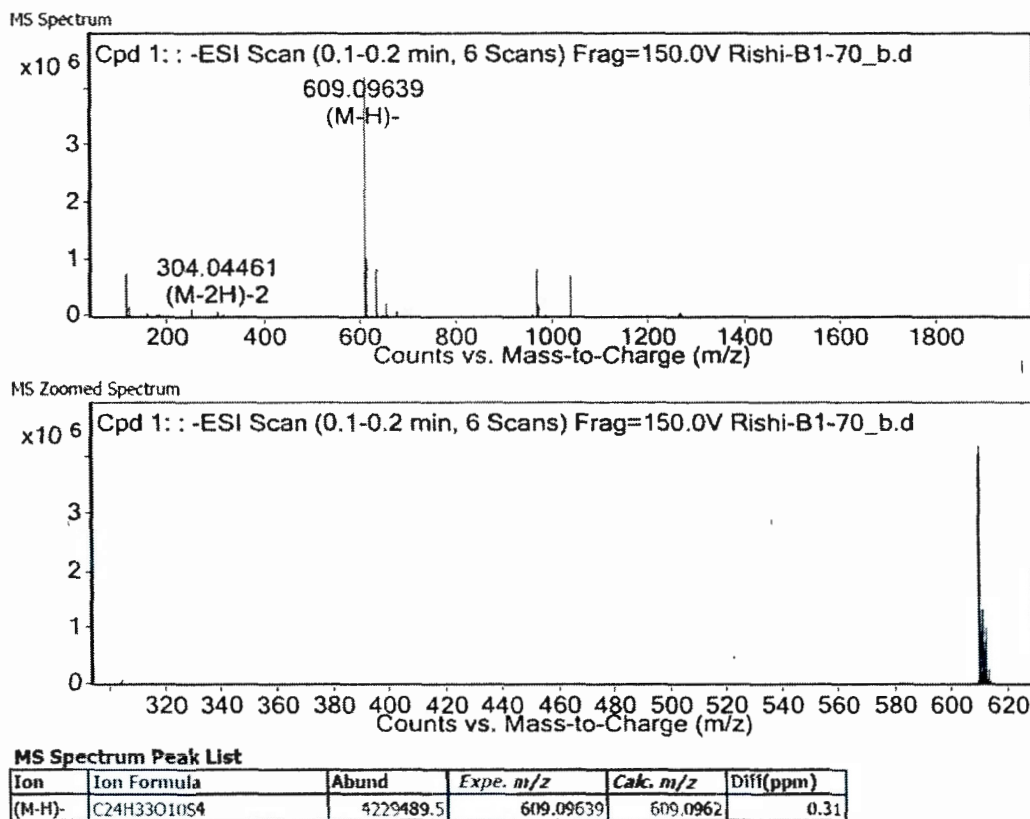
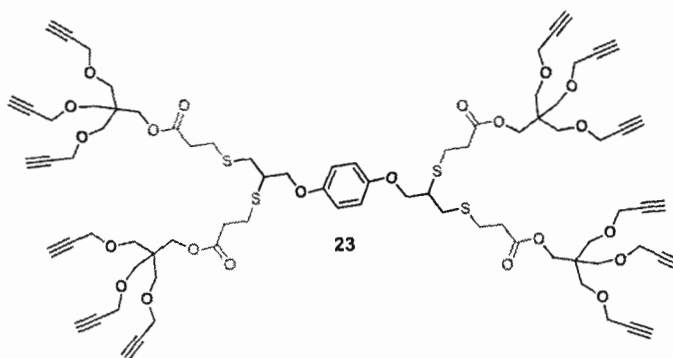


Figure S41. ESI⁻ spectrum of compound 21.



Synthesis of compound 23: To a stirring solution of compound **21** (41 mg, 0.067mmol, 1.0 eq.) in DMF (1 ml), were added compound **22** (85 mg, 0.35 mmol, 5.2 eq.), EDC·HCl (77 mg, 0.40 mmol, 6.0 eq.), DMAP (66 mg, 0.54 mmol, 8.0 eq.) and the reaction mixture was heated overnight at 50°C. The completion of reaction was monitored by TLC. Upon completion; the reaction mixture was diluted with

water (2 ml) and extracted with ethyl acetate (3x10ml). The combined organic extracts were washed with 0.1N HCl (3x5ml), followed by saturated NaHCO₃ solution (3x5ml), and brine. The organic layer was dried over anhydrous sodium sulfate, filtered and evaporated under reduced pressure. The crude mixture was then purified by column chromatography using 5% Acetone in DCM as eluent to afford **23** as a yellowish foam (72 mg, 0.047 mmol). **Yield: 70%.**

¹H NMR (300 MHz, CDCl₃) δ (ppm) 6.85 (s, 4H), 4.18–4.08 (2xs, 36H), 3.52 (s, 24H) 3.16 (m, 2H), 3.07–2.79 (m, 12H), 2.65 (m, 8H), 2.42 (t_{app}, 12H).

¹³C{¹H} NMR (75 MHz, CDCl₃) δ (ppm) 171.4, 171.4, 153.0, 115.8, 79.9, 74.5, 70.4, 68.7, 63.8, 63.8, 58.7, 45.7, 44.1, 35.1, 34.9, 34.9, 28.2, 26.8.

IR (cm⁻¹): 3285, 2875, 2115, 1731, 1506, 1440, 1358, 1223, 1019, 958, 905, 805, 638.

HRMS (ESI⁺-TOF) m/z: calculated for C₈₀H₉₈O₂₂S₄ [M+H]⁺:1539.5505; found; 1539.5506.

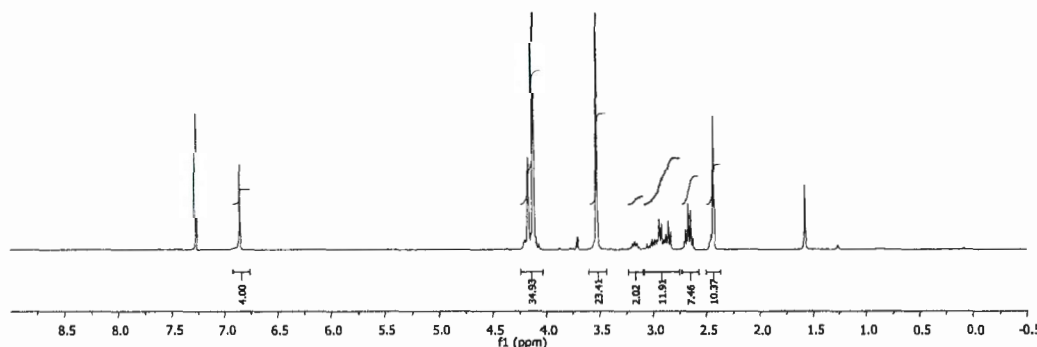


Figure S42. ¹H NMR spectrum of compound **23** (CDCl₃, 300 MHz).

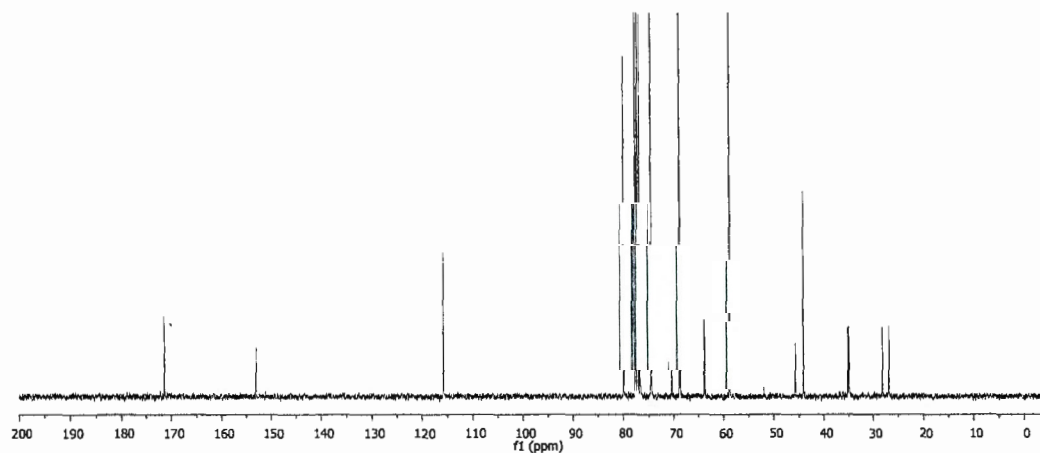


Figure S43. ¹³C NMR spectrum of compound **23** (CDCl₃, 75 MHz).

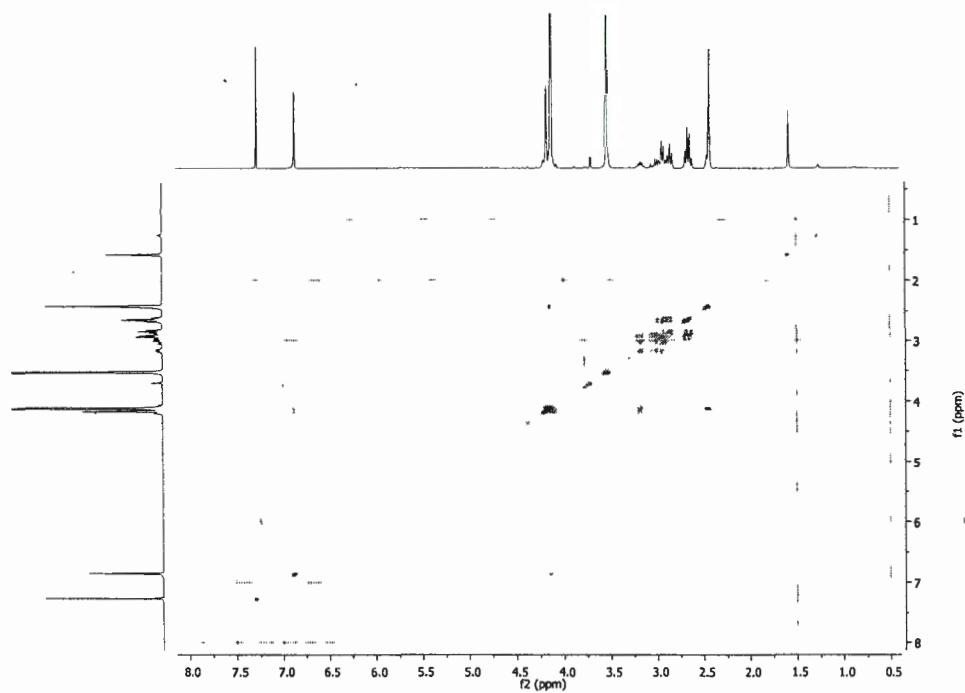


Figure S44. COSY spectrum of compound 23.

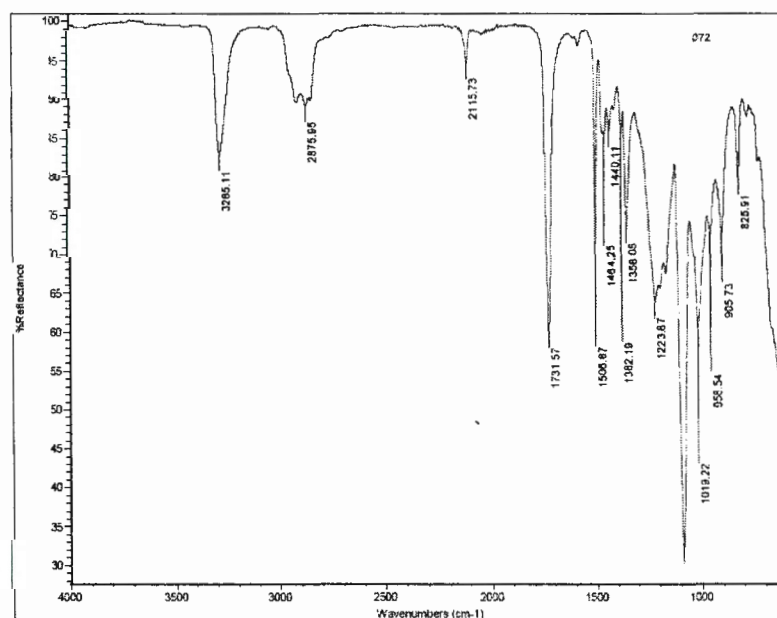
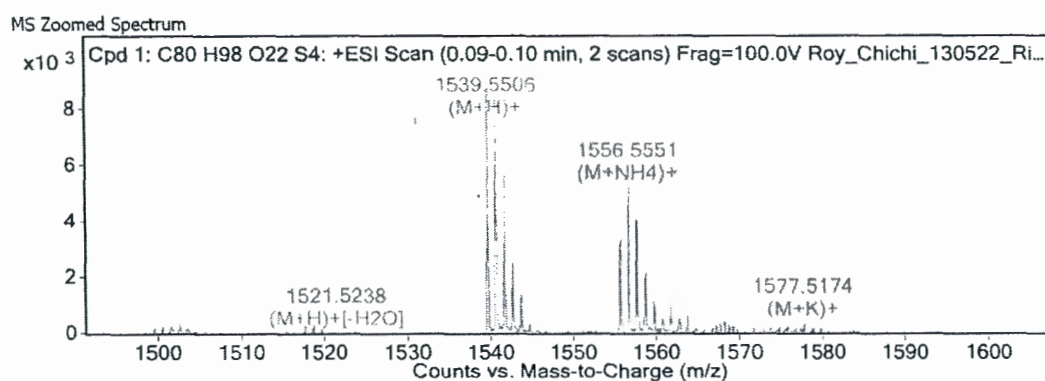
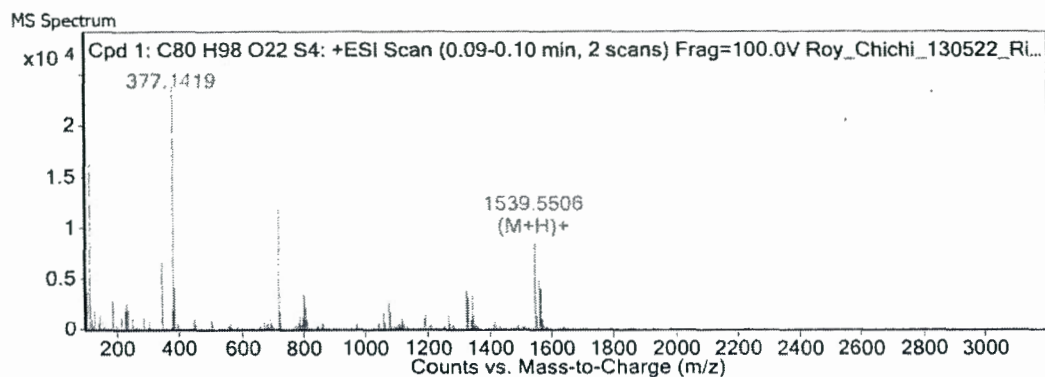


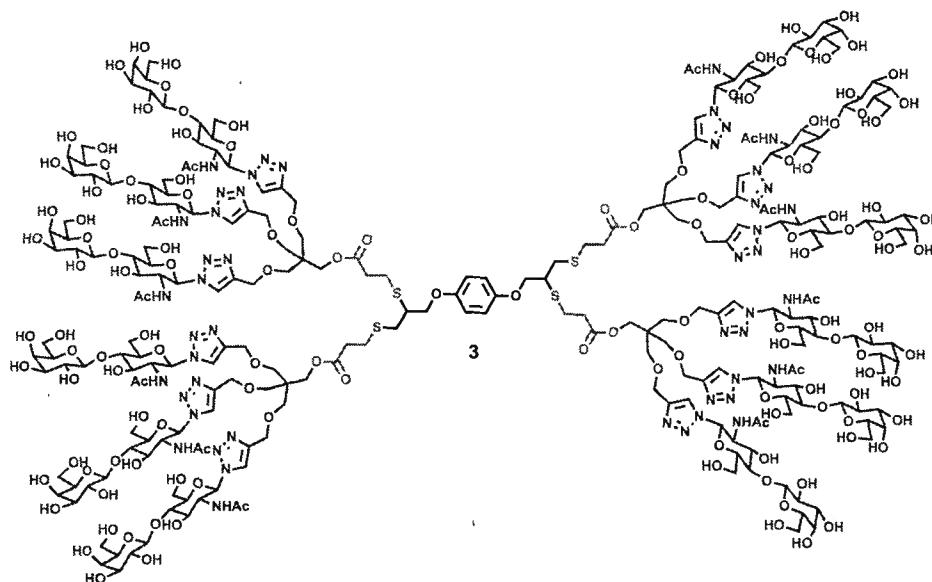
Figure S45. IR spectrum of compound 23.



MS Spectrum Peak List

m/z	Calc m/z	Diff(ppm)	z	Abund	Formula	Ion
373.0964				506		
377.1419				24324		
378.1444				4306		
379.1404				1481		
1521.5238	1521.54	-10.66	1	64	C80 H97 O21 S4	(M+H)+[-H2O]
1538.5392	1538.5665	-17.77	1	115	C80 H100 N O21 S4	(M+NH4)+[-H2O]
1539.5506	1539.5505	0.05	1	9269	C80 H99 O22 S4	(M+H)+
1540.5511	1540.5538	-1.76	1	8605	C80 H99 O22 S4	(M+H)+
1541.5523	1541.5539	-1.04	1	5735	C80 H99 O22 S4	(M+H)+
1542.5569	1542.5547	1.42	1	2614	C80 H99 O22 S4	(M+H)+
1543.5573	1543.5219	22.91	1	1420	C80 H96 Na O21 S4	(M+Na)+[-H2O]
1556.5551	1556.5771	-14.11	1	5248	C80 H102 N O22 S4	(M+NH4)+
1557.5618	1557.5803	-11.87	1	4304	C80 H102 N O22 S4	(M+NH4)+
1558.5631	1558.5804	-11.11	1	2247	C80 H102 N O22 S4	(M+NH4)+
1559.5562	1559.4959	38.68	1	1219	C80 H96 K O21 S4	(M+K)+[-H2O]
1560.5394	1560.4991	25.83	1	558	C80 H96 K O21 S4	(M+K)+[-H2O]
1561.5297	1561.5325	-1.81	1	1219	C80 H98 Na O22 S4	(M+Na)+
1562.5253	1562.5357	-6.7	1	987	C80 H98 Na O22 S4	(M+Na)+
1563.5351	1563.5358	-0.48	1	674	C80 H98 Na O22 S4	(M+Na)+
1577.5174	1577.5064	6.94	1	369	C80 H98 K O22 S4	(M+K)+

Figure S46. ESI⁺ trace (+ report) of compound 23.



Synthesis of compound 3: Compound **23** (20 mg, 0.013 mmol, 1.0 eq.) and compound **18** (85 mg, 0.21 mmol, 15.8 eq.) were reacted together according to **procedure C** to give glycodendrimer **3** as a white solid (61 mg, 9.5 μ mol). **Yield:** 73%.

^1H NMR (300 MHz, D_2O) δ (ppm) 8.17 (br s, 12H), 6.88 (br s, 4H), 5.85 (d, $J = 9.3$ Hz, 12H), 4.69–4.24 (m, 44H), 4.07–3.37 (m, 174H), 3.08–2.38 (m, 20H), 1.77 (s, 36H).

$^{13}\text{C}\{^1\text{H}\}$ NMR (75 MHz, D_2O) δ (ppm) 174.4, 172.1, 153.3, 145.0, 124.4, 117.0, 103.6, 87.0, 78.4, 78.2, 76.1, 73.2, 72.9, 71.7, 69.2, 68.5, 64.2, 61.7, 60.5, 58.9, 55.6, 52.5, 44.6, 34.8, 34.7, 34.6, 28.1, 26.7, 22.4.

IR (cm^{-1}): 3320, 2884, 1723, 1608, 1507, 1404, 1317, 1234, 1046, 898.

(MALDI-TOF) m/z : calculated for $\text{C}_{248}\text{H}_{386}\text{N}_{48}\text{O}_{142}\text{S}_4$ $[\text{M}+\text{Na}]^+$: 6463.2, found: 6463.7.

Melting point: $\geq 210^\circ\text{C}$ (dec.).

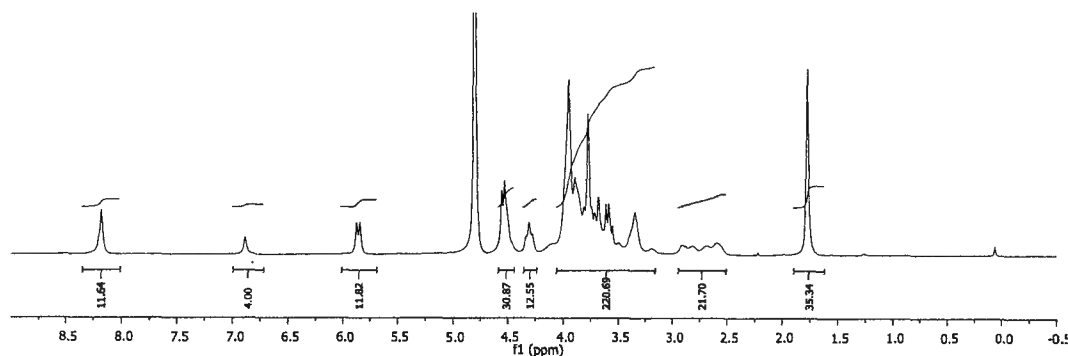


Figure S47. ^1H NMR spectrum of glycodendrimer **3** (D_2O , 300 MHz).

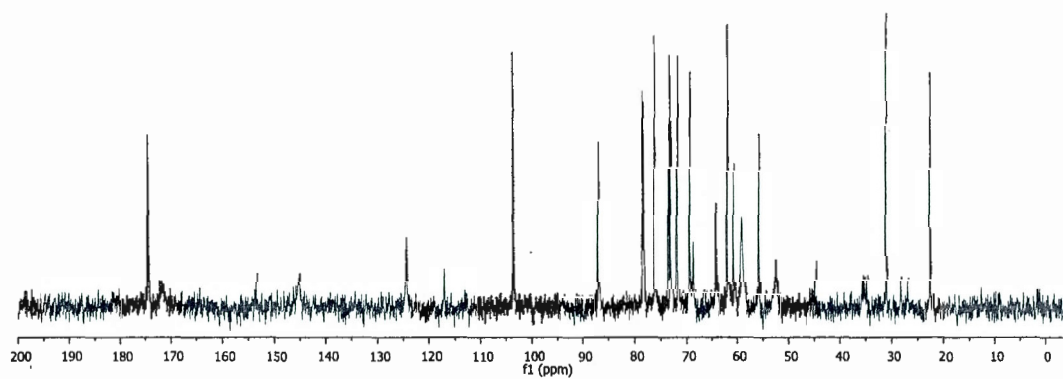


Figure S48. ^{13}C NMR spectrum of glycodendrimer 3 (D_2O , 75 MHz).

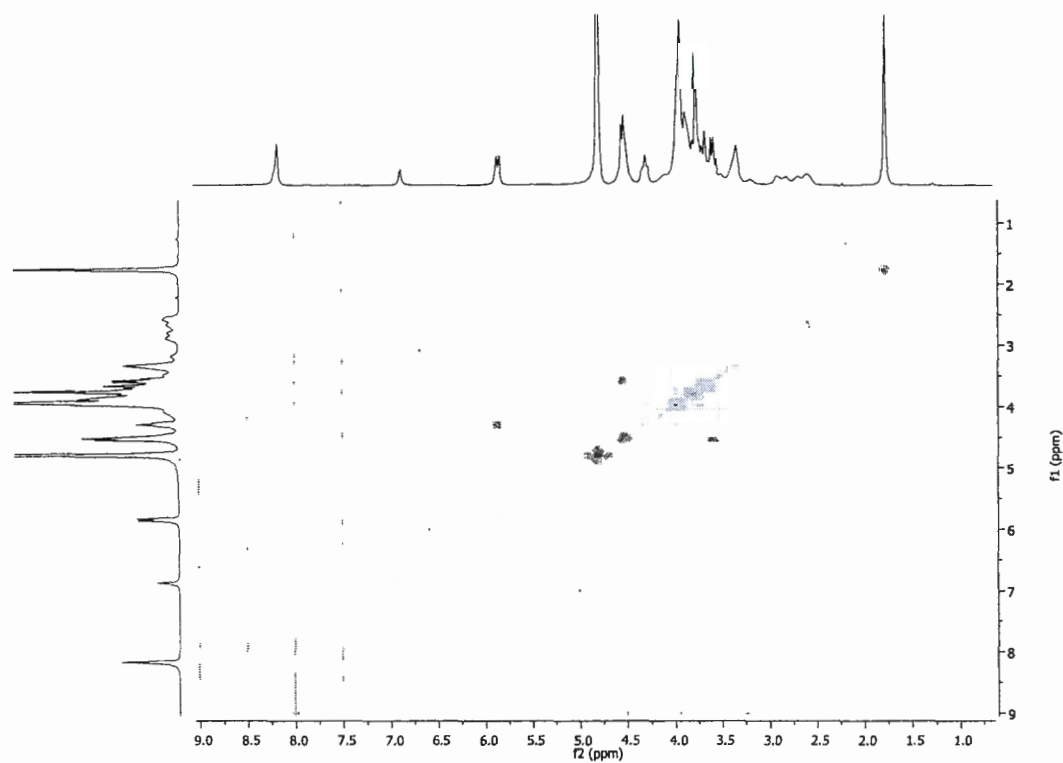


Figure S49. COSY spectrum of glycodendrimer 3.

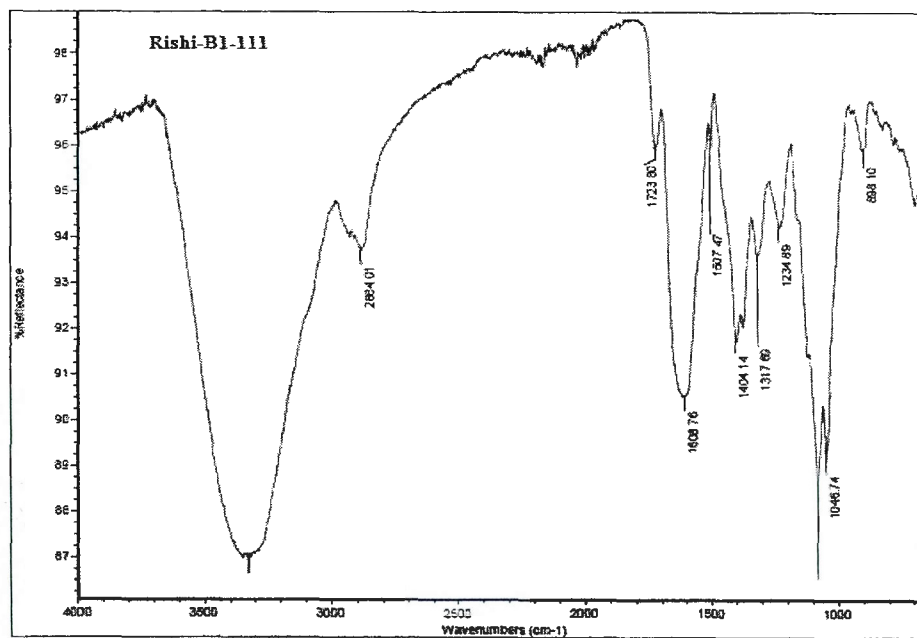
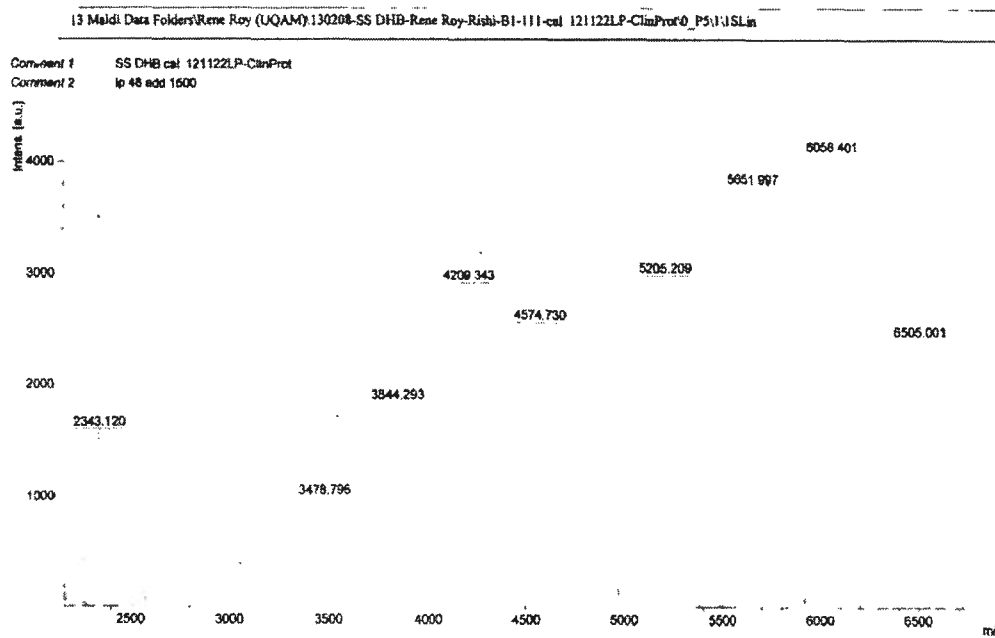


Figure S50. IR spectrum of glycodendrimer 3.



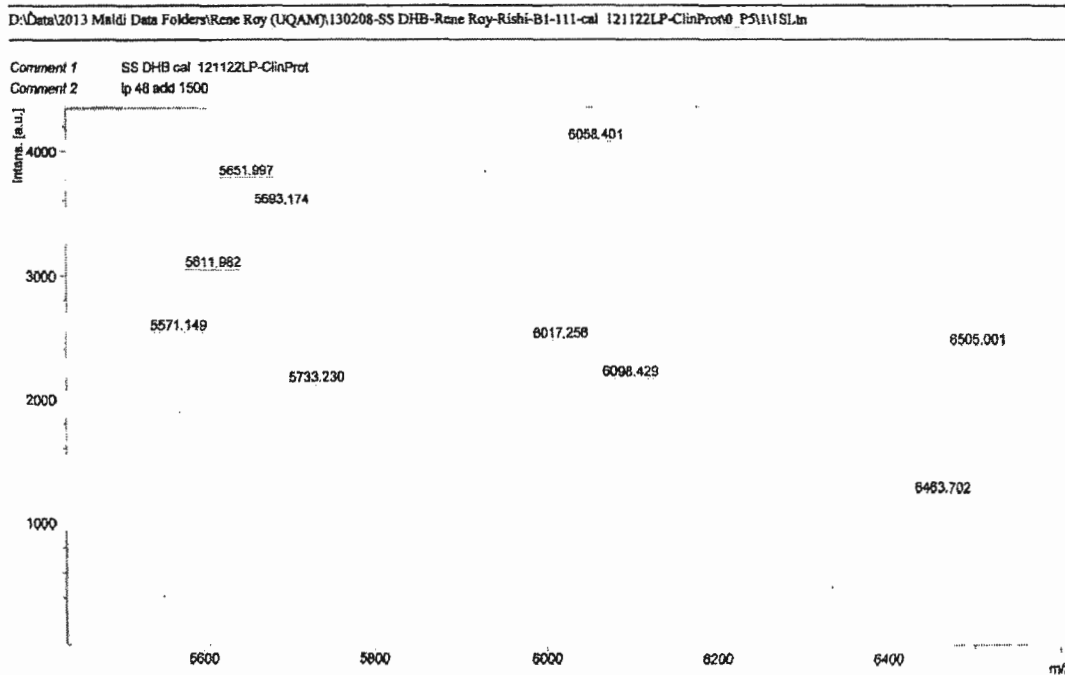
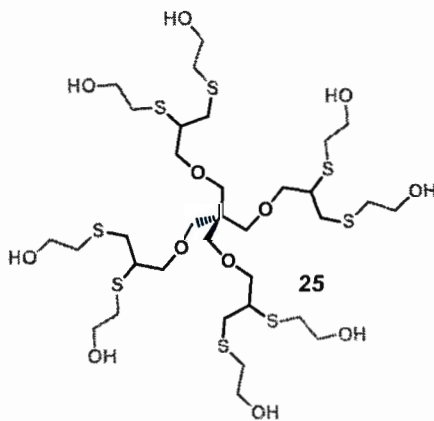


Figure S51. MALDI-TOF spectrum (full + zoom) of glycodendrimer **3** (DHB matrix).



Synthesis of compound 25: Compound **24*** (400 mg, 1.39 mmol, 1.0 eq.) and compound **14** (4.0 ml, 57 mmol, 40 eq.) were reacted together according to **procedure B** and subsequent purification by column chromatography (10% MeOH in DCM as eluent) afforded compound **25** as a viscous transparent oil (825 mg, 0.904 mmol). **Yield: 65%.**

¹H NMR (600 MHz, D₂O) δ (ppm) 3.75 (m, 16H + 4H), 3.67 (dd, $J = 10.4, 5.9$ Hz, 4H), 3.50–3.43 (br s, 8H), 3.15 (m, 4H), 2.96 (dd, $J = 13.5, 7.0$ Hz, 4H), 2.90 (dd, $J = 13.5, 6.2$ Hz, 4H), 2.84–2.75 (m, 16H).

¹³C{¹H} NMR (151 MHz, D₂O) δ (ppm) 73.4, 69.9, 61.5, 61.2, 46.3, 45.8, 35.1, 34.8, 34.6, 28.9.

IR (cm⁻¹): 3359, 2915, 2871, 1458, 1418, 1366, 1288, 1172, 1108, 1010, 755.

HRMS (ESI⁺-TOF) m/z : calculated for C₃₃H₆₈O₁₂S₈ [M+H]⁺: 913.2549; found, 913.2521.

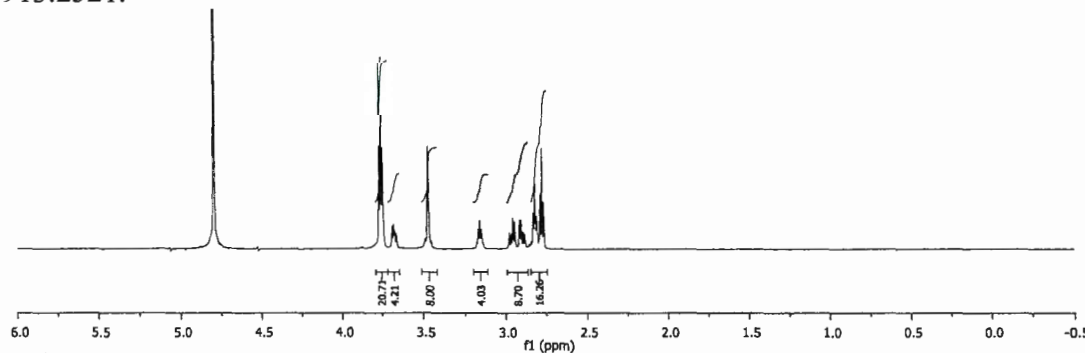


Figure S52. ¹H NMR spectrum of compound **25** (D₂O, 600 MHz).

* Protocol for the synthesis of tetrapropargylated pentaerythritol **24** was optimized, based on the one previous described by Gervay-Hague *et al.* (*Chem. Commun.*, 2007, 7, 695-697). Modifications mainly concerned temperature (0°C) and reaction time (2 hours) that allow a very clean work-up by only quenching with an aqueous saturated solution of NH₄Cl, extraction and a column chromatography (in contrast with reactions involving higher temperature or KOH as a base for which extraction steps are more tedious). Yield is 75%.

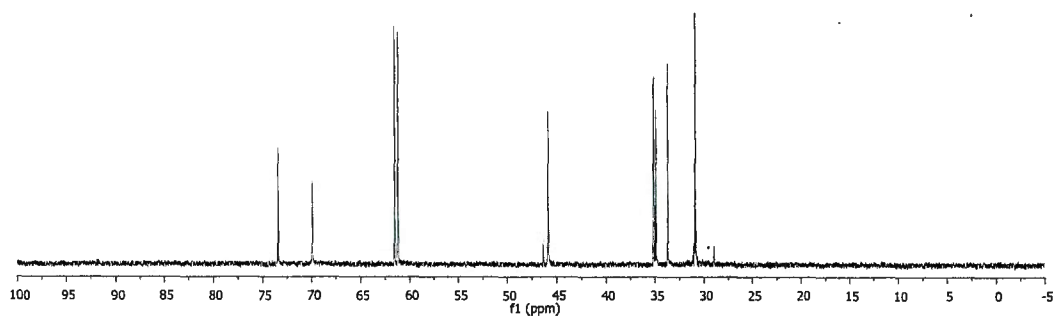


Figure S53. ^{13}C NMR spectrum of compound **25** (D_2O , 150 MHz).

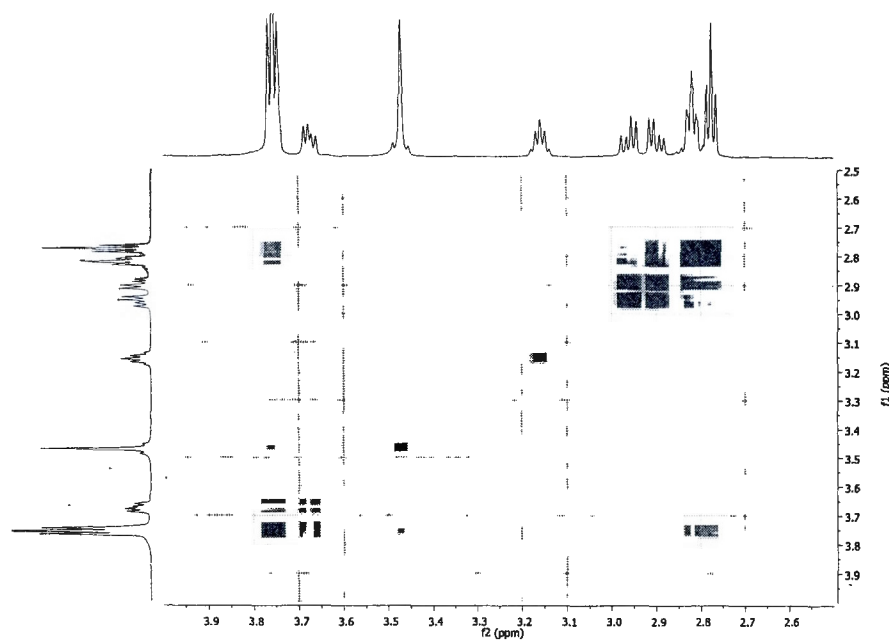


Figure S54. COSY spectrum (zoom) of compound **25**.

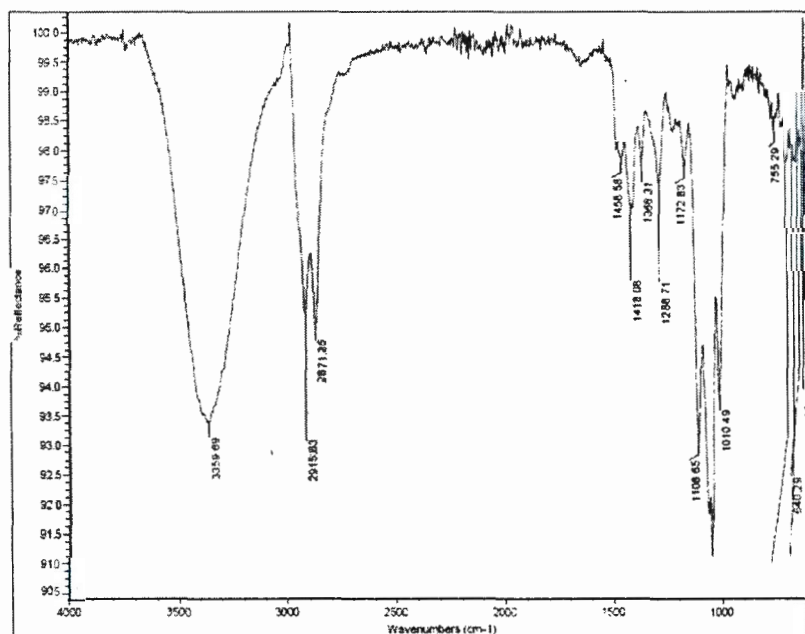
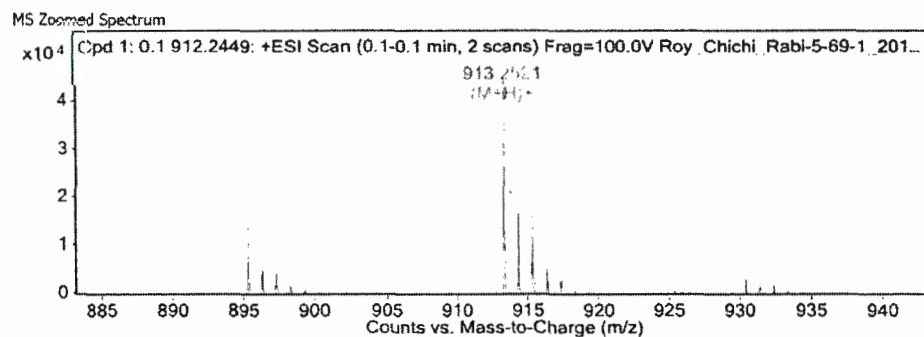


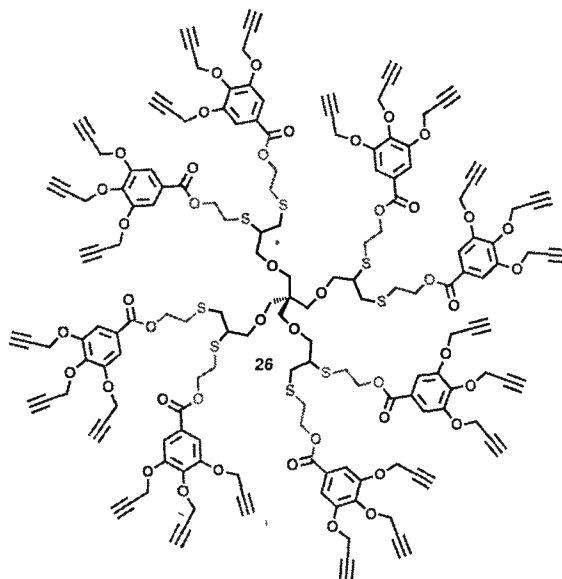
Figure S55. IR spectrum of compound 25.



MS Spectrum Peak List

m/z	Calc m/z	Diff (ppm)	z	Abund	Formula	Ion
195.0567				112016		
195.2211				4844		
196.0536				8403		
197.0469				8120		
913.2521	913.2549	-3.04	1	45779	C33 H69 O12 S8	(M+H)+
914.2549	914.2578	-3.09	1	17008	C33 H69 O12 S8	(M+H)+
915.2502	915.2531	-3.1	1	17381	C33 H69 O12 S8	(M+H)+
916.252	916.2548	-3.06	1	5582	C33 H69 O12 S8	(M+H)+
917.2491	917.2511	-2.18	1	3067	C33 H69 O12 S8	(M+H)+
918.2436	918.2521	-9.3	1	1025	C33 H69 O12 S8	(M+H)+

Figure S56. ESI+ spectrum of compound 25.



Synthesis of compound 26: To a stirring solution of compound **25** (33 mg, 0.036 mmol, 1.0 eq.) in DMF (1 ml), were added tripropargylated gallic acid **10** (106 mg, 0.375 mmol, 10.0 eq.), EDC·HCl (71 mg, 0.38 mmol, 10.0 eq.), DMAP (70 mg, 0.577 mmol, 16.0 eq.) and the reaction mixture was heated overnight at 50°C. The completion of reaction was monitored by TLC. Upon completion, the reaction mixture was diluted with water (2 ml) and extracted with ethyl acetate (3x10 ml). The combined organic extracts were washed with 0.1N HCl (3x5 ml), followed by saturated NaHCO₃ solution (3x5 ml) and finally with brine. The organic layer was dried over anhydrous sodium sulfate, filtered and then evaporated under reduced pressure. The crude mixture was then purified by column chromatography using 4% Acetone in DCM as eluent to afford desired compound as colorless viscous oil (76 mg, 0.025 mmol). **Yield: 70%.**

¹H NMR (300 MHz, CDCl₃) δ (ppm) 7.43 (d, *J* = 0.9 Hz, 16H), 4.81 (d, *J* = 2.4 Hz, 16H), 4.78 (d, *J* = 2.4 Hz, 32H), 4.43 (t, *J* = 6.9 Hz, 16H), 3.69 (dd, *J* = 9.9, 4.7 Hz, 4H), 3.59 (dd, *J* = 9.8, 5.7 Hz, 4H), 3.41 (s, 8H), 3.12–3.00 (m, 4H), 3.01–2.78 (m, 24H), 2.63–2.52 (m, 16H), 2.47 (t, *J* = 2.4 Hz, 8H).

¹³C{¹H} NMR (75 MHz, CDCl₃) δ (ppm) 165.4, 151.3, 141.4, 125.4, 125.4, 110.1, 78.7, 78.0, 73.0, 69.7, 64.3, 64.1, 60.3, 57.2, 46.4, 45.8, 35.2, 31.6, 30.1.

IR (cm⁻¹): 3725, 3608, 2924, 2850, 2181, 2148, 1729, 1436, 1264, 730.

(MALDI-TOF) *m/z*: calculated for C₁₆₁H₁₄₈O₄₄S₈ [M+Li]⁺: 3050.3, Found: 3049.0.

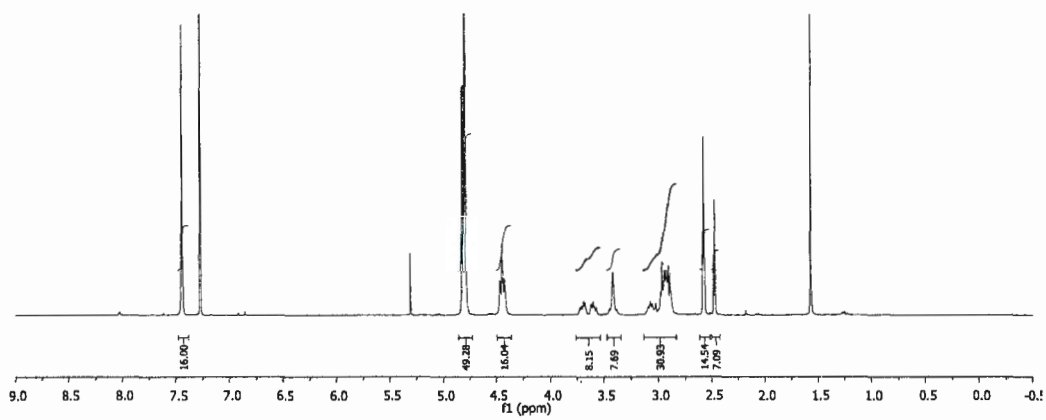


Figure S57. ^1H NMR spectrum of compound 26 (CDCl_3 , 300 MHz).

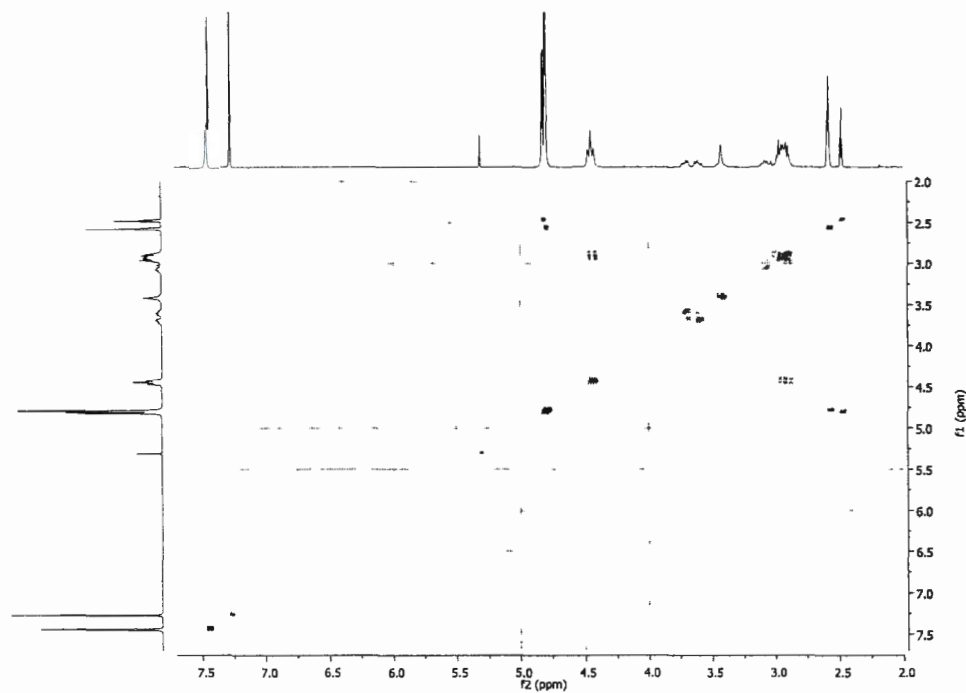


Figure S58. COSY spectrum of compound 26.

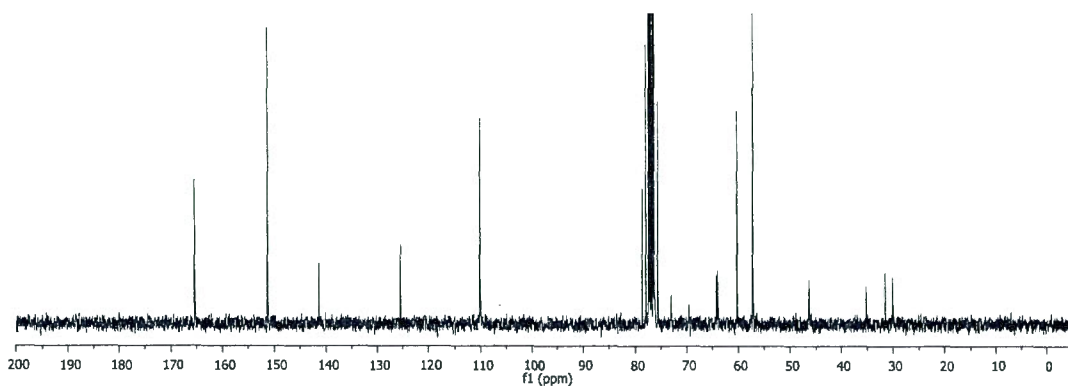


Figure S59. ^{13}C NMR spectrum of compound **26** (CDCl_3 , 75 MHz).

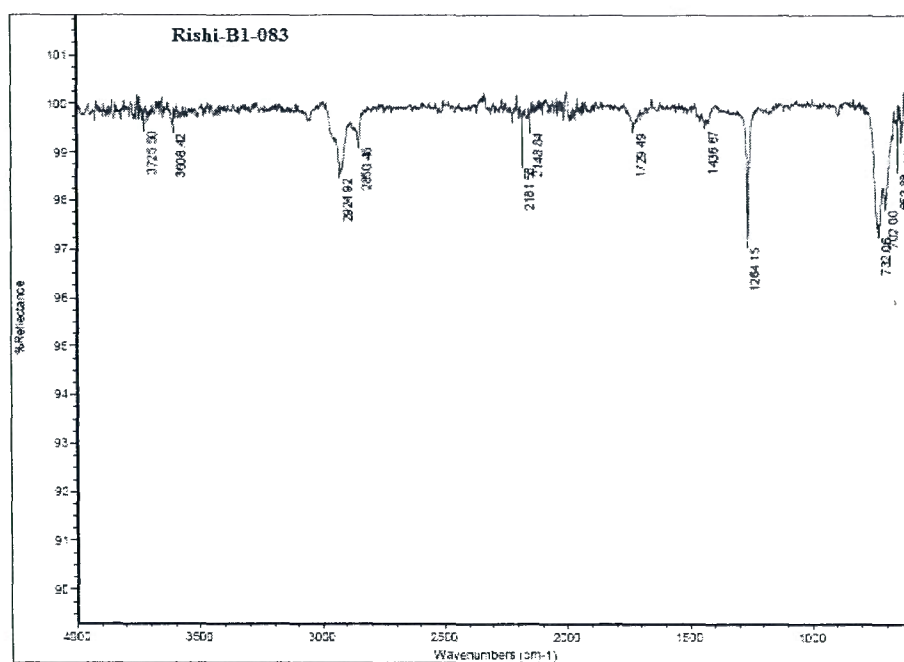


Figure S60. IR spectrum of compound **26**.

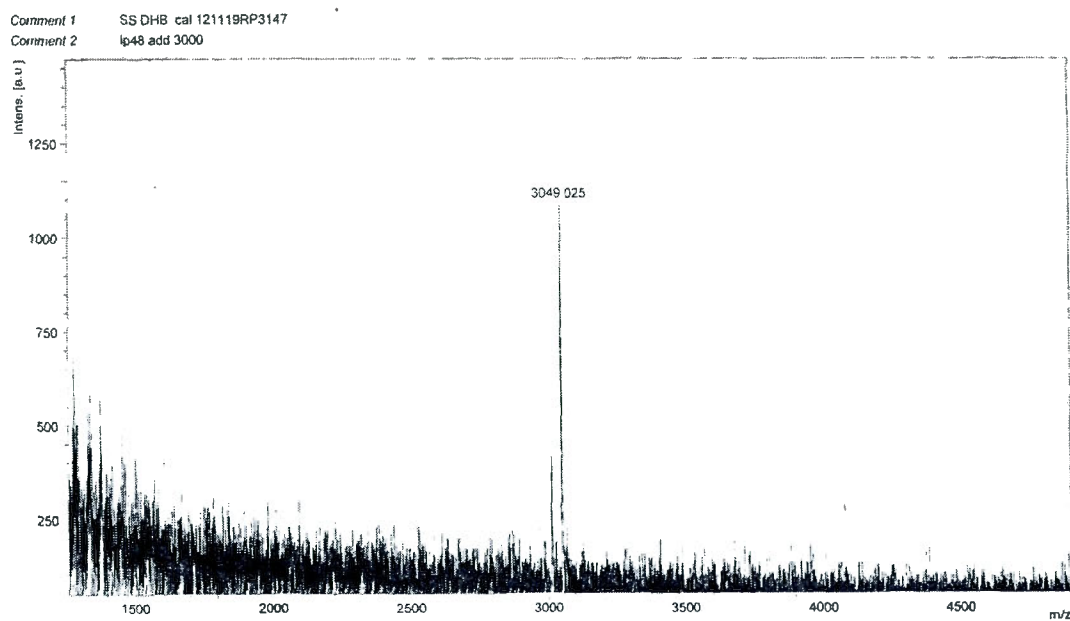
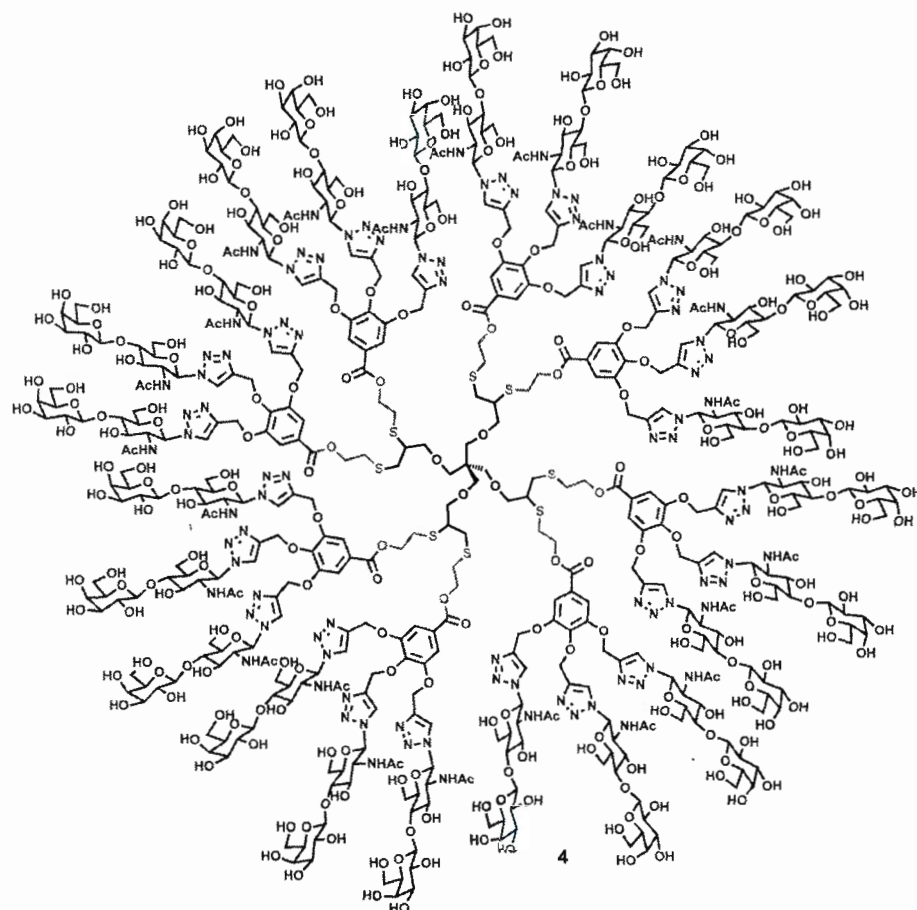


Figure S61. MALDI-TOF spectrum of compound **26** (DHB matrix).



Synthesis of compound 4: Compounds **26** (10 mg, 3.3 μmol , 1.0 eq.) and **18** (41 mg, 100 μmol , 30 eq.) were reacted together according to **procedure C** to give dendrimer **4** (31 mg, 2.4 μmol). **Yield: 74%.**

^1H NMR (300 MHz, D_2O) δ (ppm) 8.40–8.05 (m, 24H), 7.40–6.95 (m, 16H), 6.05–5.70 (m, 24H), 5.22–4.97 (br s, 48H), 4.55–4.22 (m, 64H), 4.15–2.68 (m, 308H), 1.68 (m, 72H).

$^{13}\text{C}\{^1\text{H}\}$ NMR (150 MHz, D_2O) δ (ppm) 175.5, 174.0, 171.6, 152.0, 143.9, 143.6, 140.8, 125.9, 125.2, 124.8, 109.3, 103.6, 89.2, 86.7, 78.5, 78.3, 77.4, 76.0, 73.2, 73.0, 72.9, 72.0, 71.6, 69.2, 65.6, 62.6, 61.6, 60.5, 58.0, 55.5, 55.2, 52.0, 46.3, 45.8, 35.3, 31.8, 30.2, 22.7, 22.4.

IR (cm^{-1}): 3705, 3680, 3667, 2900, 2864, 2843, 2826, 1346, 1054, 1032, 1015.

(MALDI-TOF) m/z : calculated for $\text{C}_{497}\text{H}_{724}\text{N}_{96}\text{O}_{284}\text{S}_8$: 12844.1, Found: 12735.6.

Melting point: $\geq 222^\circ\text{C}$ (dec.).

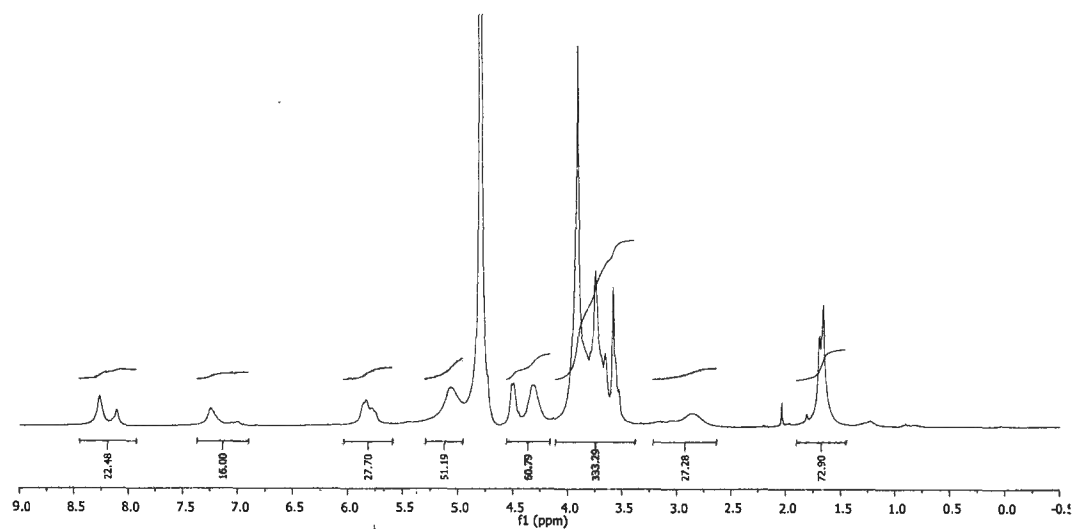


Figure S62. ^1H NMR spectrum of glycodendrimer **4** (D_2O , 300 MHz).

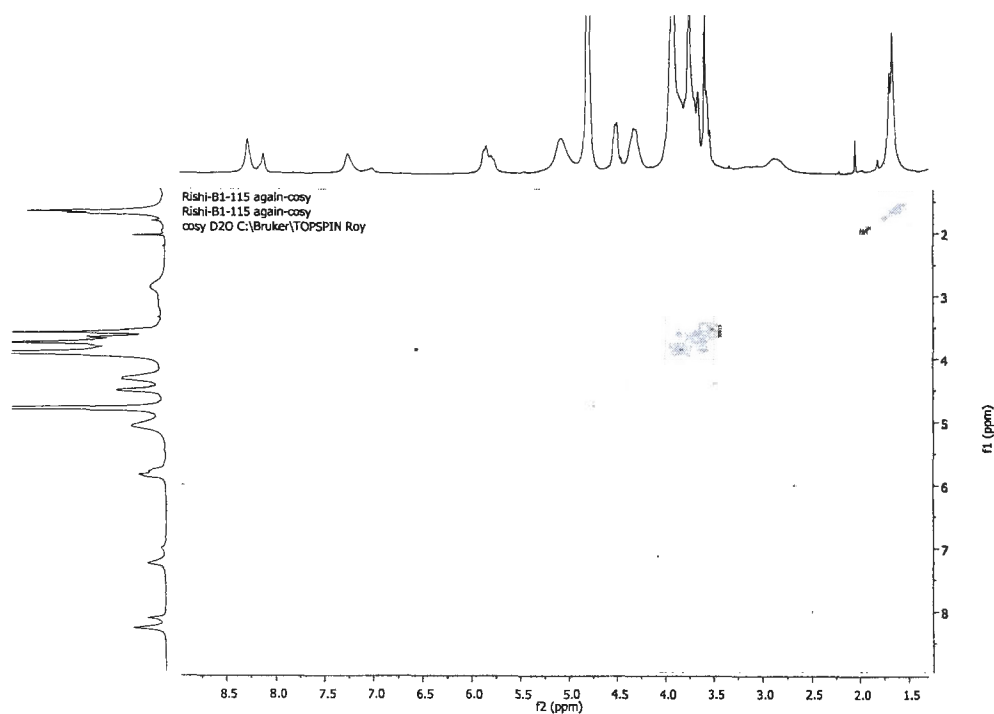


Figure S63. COSY spectrum of glycodendrimer **4**.

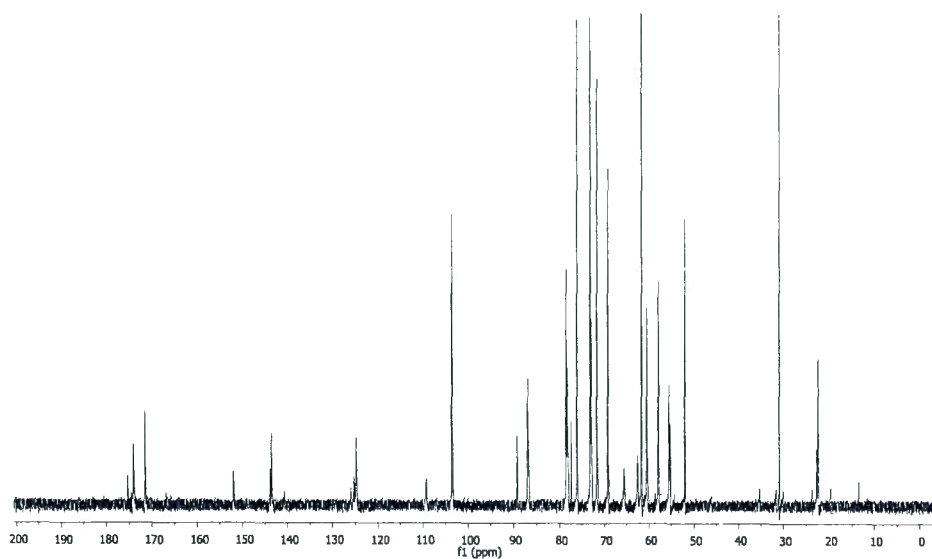


Figure S64. ^{13}C NMR spectrum of glycodendrimer 4 (D_2O , 150 MHz).

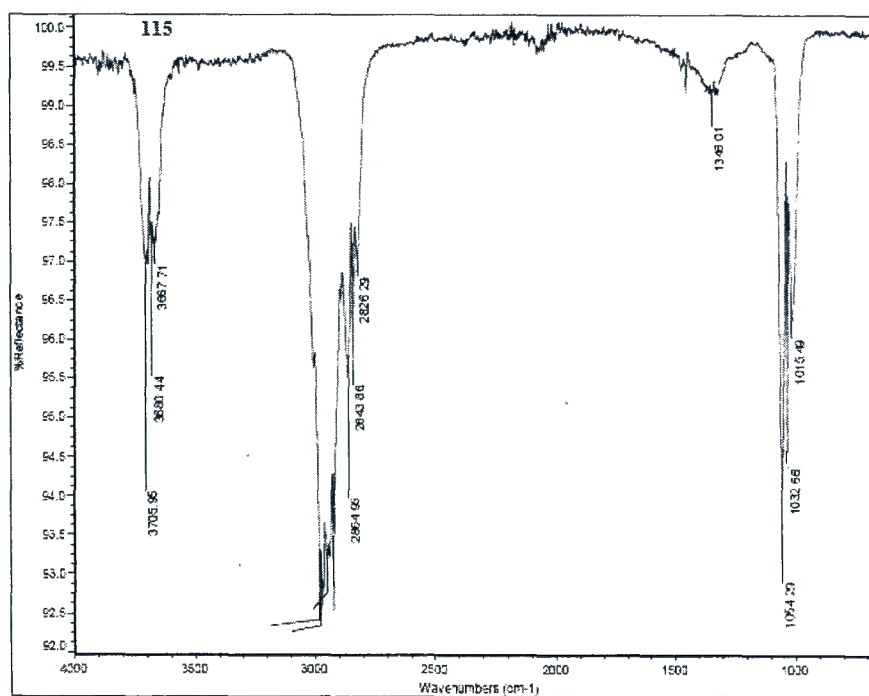


Figure S65. IR spectrum of glycodendrimer 4.

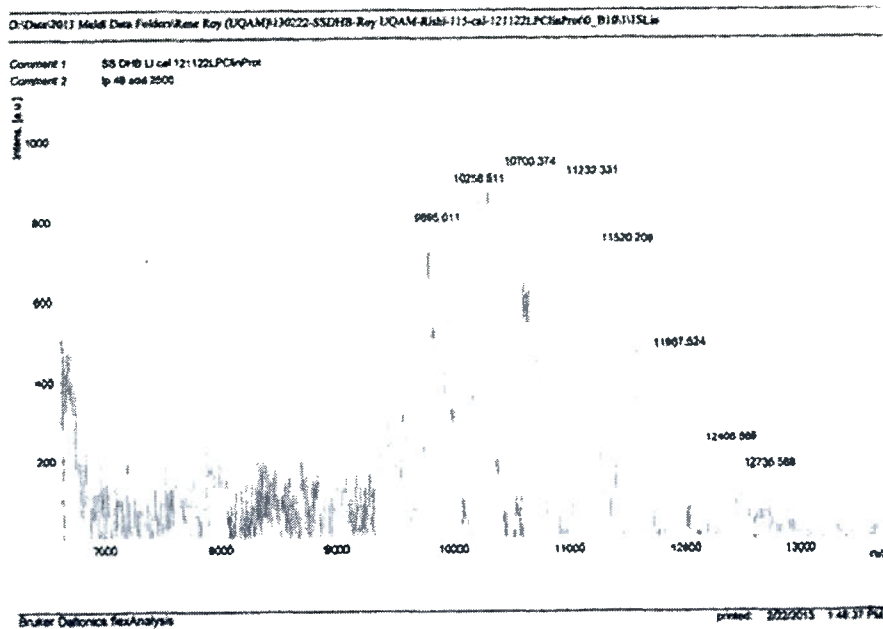


Figure S66. MALDI-TOF spectra of glycodendrimer 4 (DHB matrix, zoom).

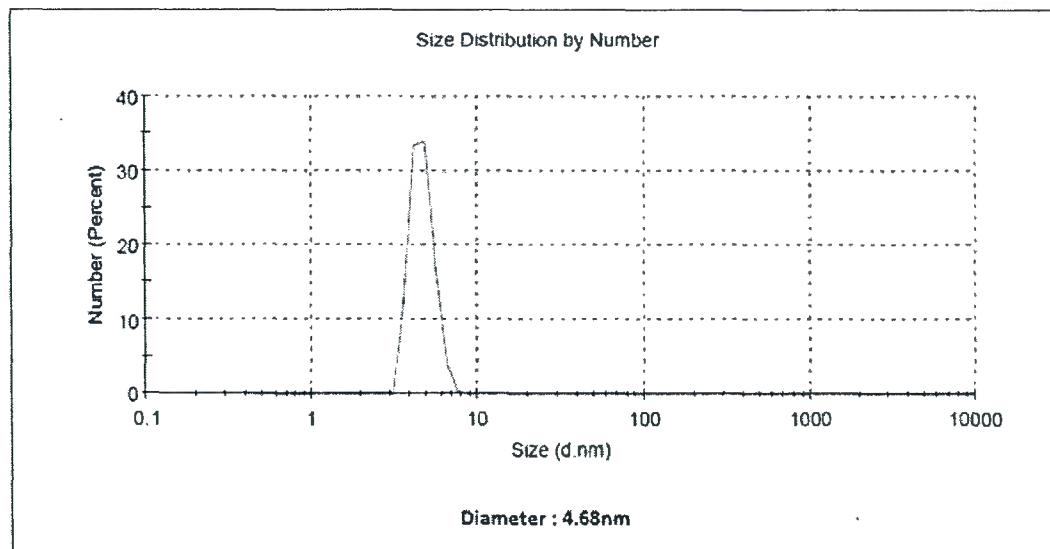
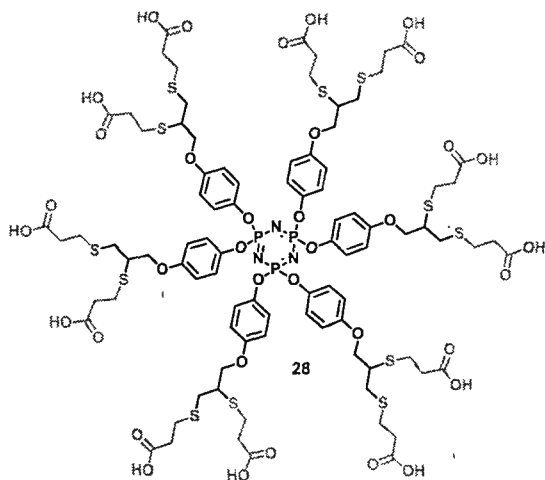


Figure S67. Size distribution of glycodendrimer 4 by DLS (in water).



Synthesis of compound 28: Compounds **27** (25 mg, 0.026 mmol, 1.0 eq.) and **20** (66 mg, 0.62 mmol, 24.0 eq.) reacted together according to **procedure B** and purification by column chromatography (10% MeOH in DCM then 10% H₂O in ACN as eluents) furnished desired compound **28** (41 mg, 0.018 mmol). **Yield: 68%.**

¹H NMR (300 MHz, CD₃OD) δ (ppm) 6.73 (m, 24H), 4.17 (m, 12H), 3.21 (m, 6H), 3.06–2.84 (m, 24H), 2.79 (t, $J = 7.1$ Hz, 12H), 2.58 (m, 24H).

¹³C{¹H} (75 MHz, CD₃OD) δ (ppm) 176.0, 157.2, 145.6, 123.1, 116.6, 71.4, 46.8, 36.5, 36.1, 35.7, 29.1, 28.0.

³¹P NMR (122 MHz, CD₃OD) δ 10.4 (s, N₃P₃).

HRMS (ESI⁺-TOF) m/z : calculated for C₉₀H₁₁₄N₃O₃₆P₃S₁₂ [M-2H]²⁺: 1143.6449, Found: 1143.6473.

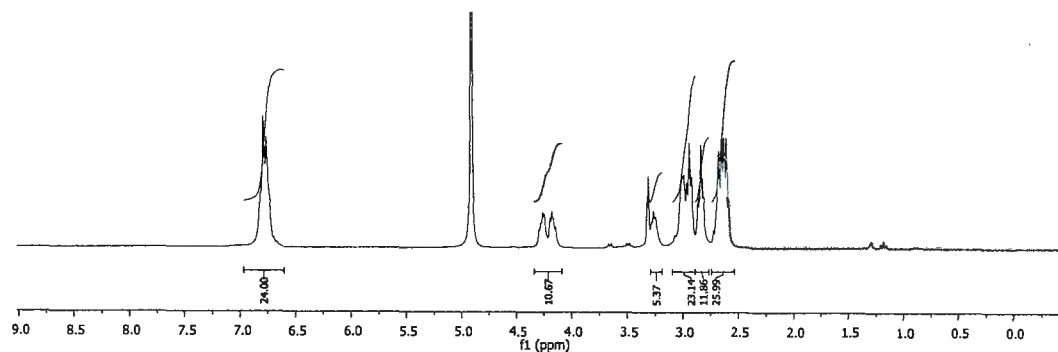


Figure S68. ¹H NMR spectrum of compound **28** (CD₃OD, 300 MHz).

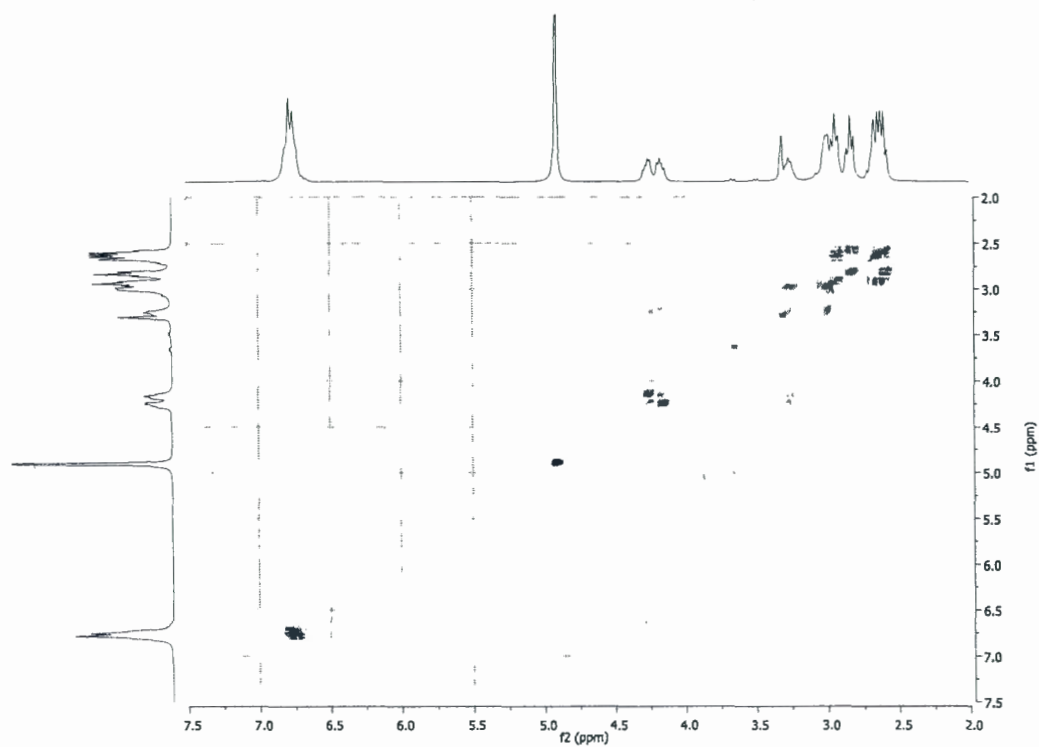


Figure S69. COSY spectrum of compound 28.

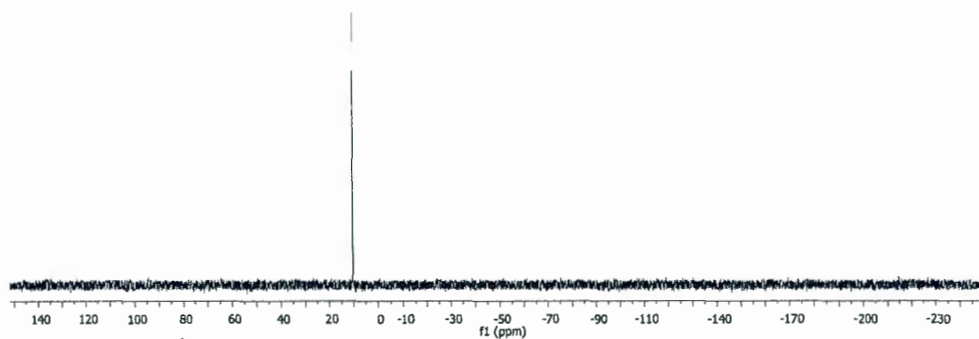


Figure S70. ^{31}P NMR spectrum of compound 28 (122 MHz, CD_3OD).

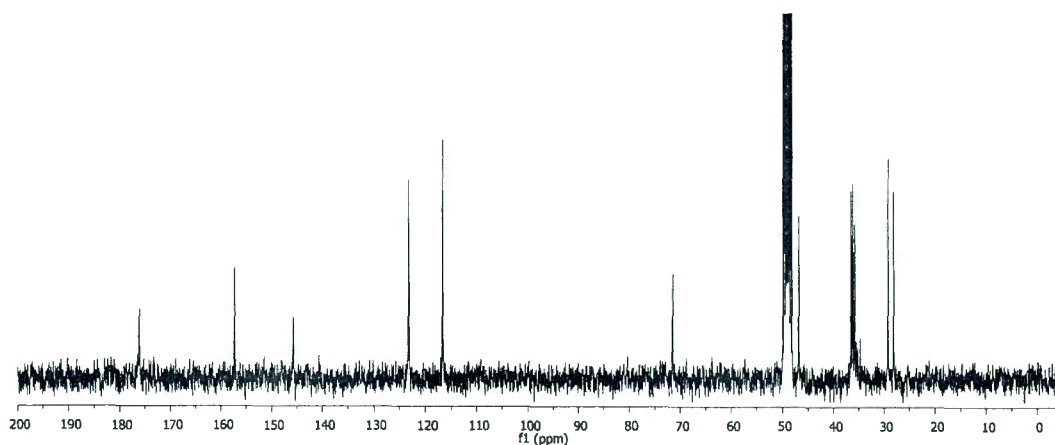


Figure S71. ^{13}C NMR spectrum of compound **28** (CD_3OD , 75 MHz).

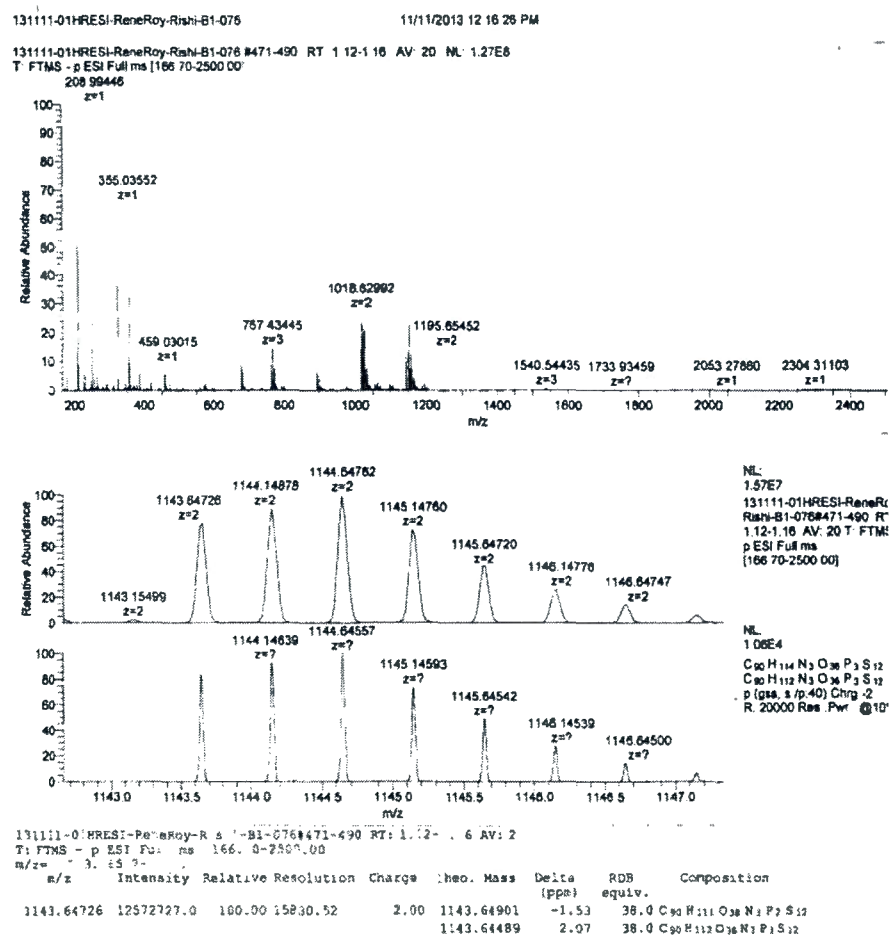
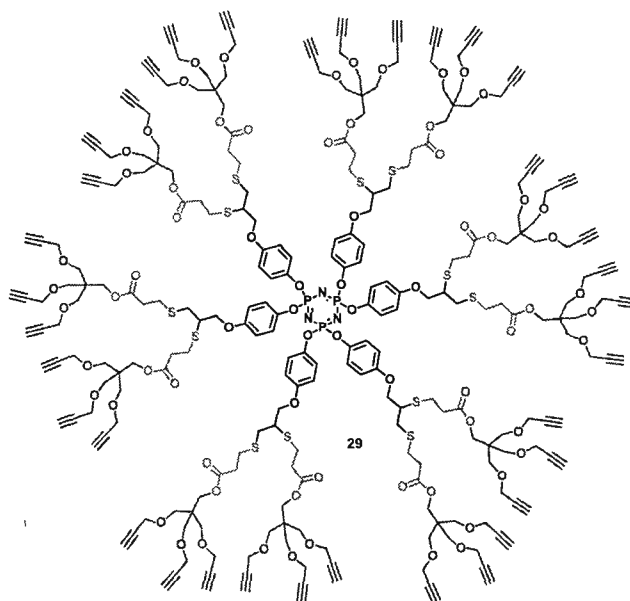


Figure S72. HR ESI spectrum of compound **28** with comparison of specific theoretical and experimental sections.



Synthesis of compound 29: To a stirring solution of compound **28** (25 mg, 11 μ mol, 1.0 eq.) in DMF (1 ml), were added EDC·HCl (32 mg, 0.16 mmol, 16.0 eq.) and DMAP (32 mg, 0.26 mmol, 26.0 eq.). After 10 minutes under nitrogen atmosphere, compound **22** (41 mg, 0.16 mmol, 16 eq.). The reaction mixture was heated overnight at 50°C. The completion of reaction was monitored by TLC. Upon completion, the reaction mixture was diluted with water (2 ml) and extracted with ethyl acetate (3x10 ml). The combined organic extracts were washed with 0.1N HCl (3x5 ml), followed by saturated NaHCO₃ solution and brine. The organic layer was dried over anhydrous sodium sulfate, filtered and evaporated under reduced pressure. The crude mixture was purified by column chromatography using 2% MeOH in CHCl₃ as eluent to afford **28** (36 mg, 7.2 μ mol) as a pale yellow oil. **Yield: 72%.**

¹H NMR (600 MHz, CDCl₃) δ (ppm) 6.98–6.70 (m, 24H), 4.22–4.08 (m, 108H), 3.52 (m, 72H), 3.25–3.15 (br s, 6H), 3.09–2.77 (m, 36H), 2.66 (m, 24H), 2.54–2.42 (m, 36H).

¹³C{¹H} (150 MHz, CDCl₃) δ (ppm) 171.3, 155.4, 144.7, 121.9, 115.2, 79.8, 74.5, 70.1, 68.6, 64.2, 63.7, 63.6, 58.7, 47.4, 45.5, 43.9, 35.0, 34.8, 34.8, 29.7, 28.1, 26.8.

³¹P NMR (122 MHz, CDCl₃) δ 9.01 (s, N₃P₃).

IR (cm⁻¹): 3291, 2921, 2115, 1731, 1640, 1500, 1358, 1464, 1358, 1242, 1168, 1010, 884, 833, 733.

(MALDI-TOF) m/z : calculated for C₂₅₈H₃₀₆N₃O₇₂P₃S₁₂: 5078.9, found: 5077.5 (*With regular losses of peripheral moieties*).

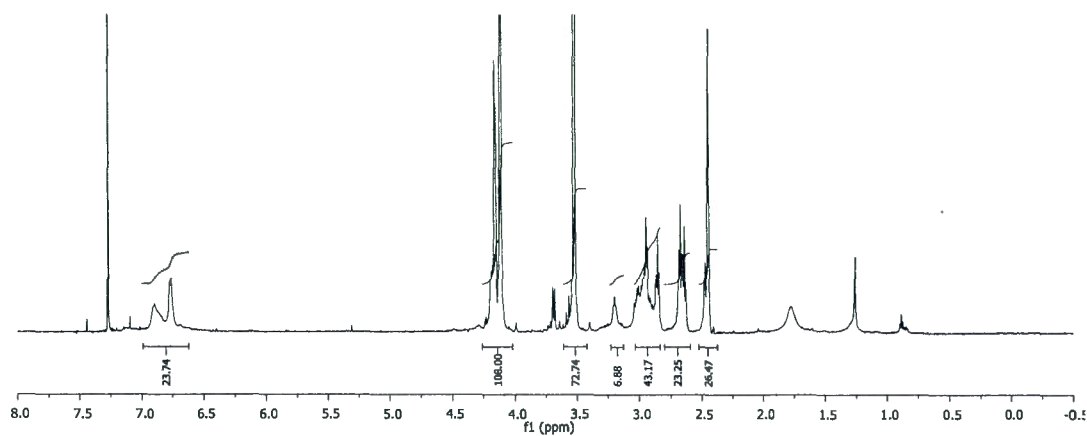


Figure S73. ^1H NMR spectrum of compound **29** (CDCl_3 , 600 MHz).

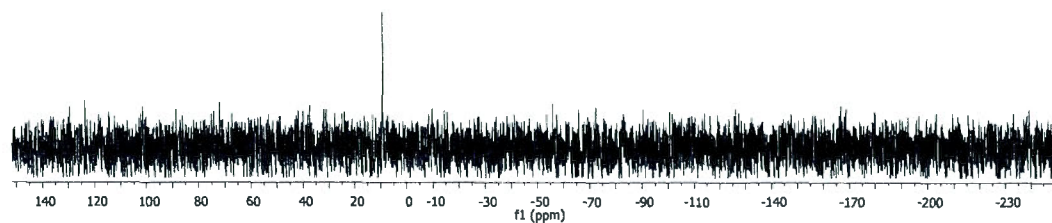


Figure S74. ^{31}P NMR spectrum of compound **29** (CDCl_3 , 122 MHz).

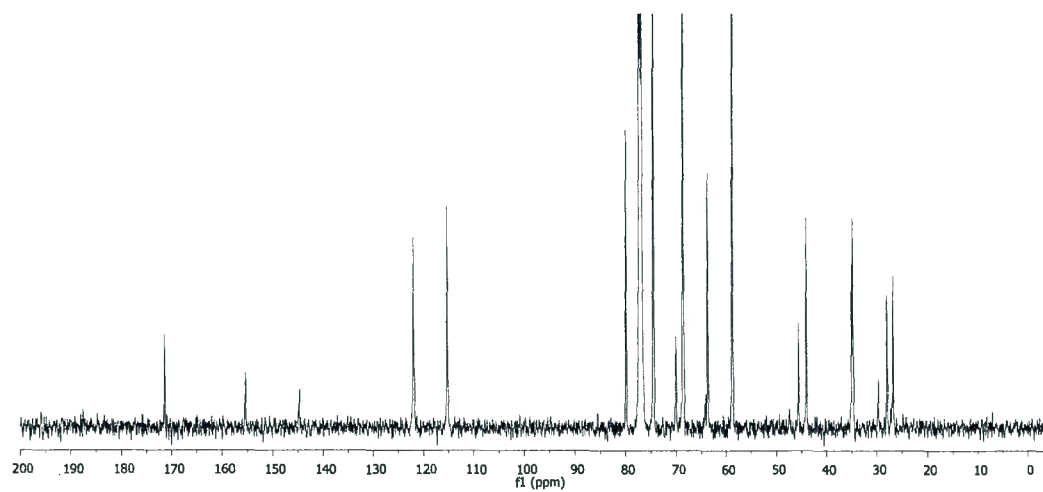


Figure S75. ^{13}C NMR spectrum of compound **29** (CDCl_3 , 150 MHz).

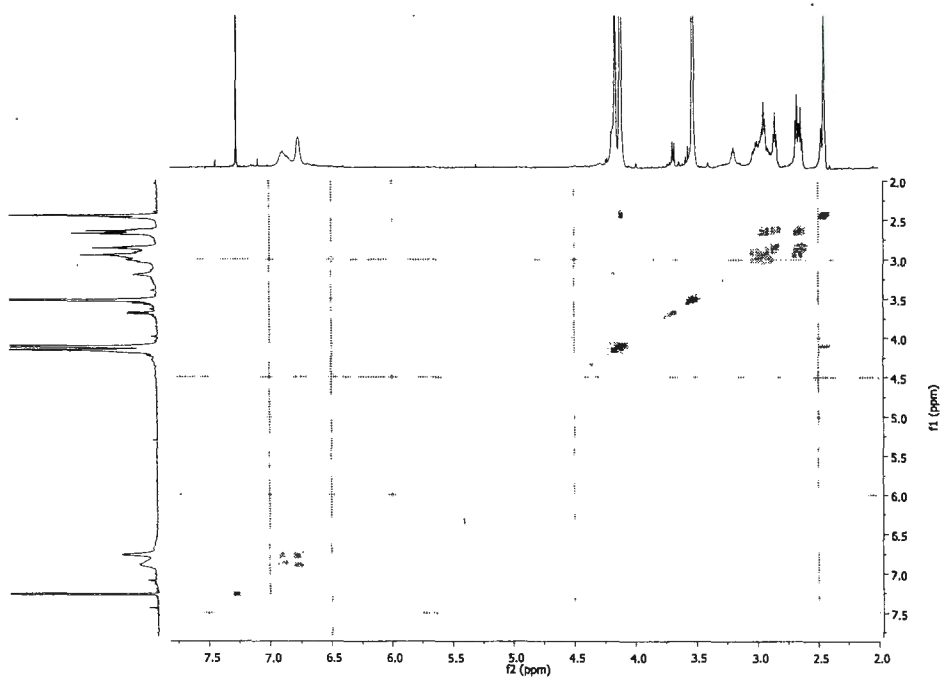


Figure S76. COSY spectrum of compound 29.

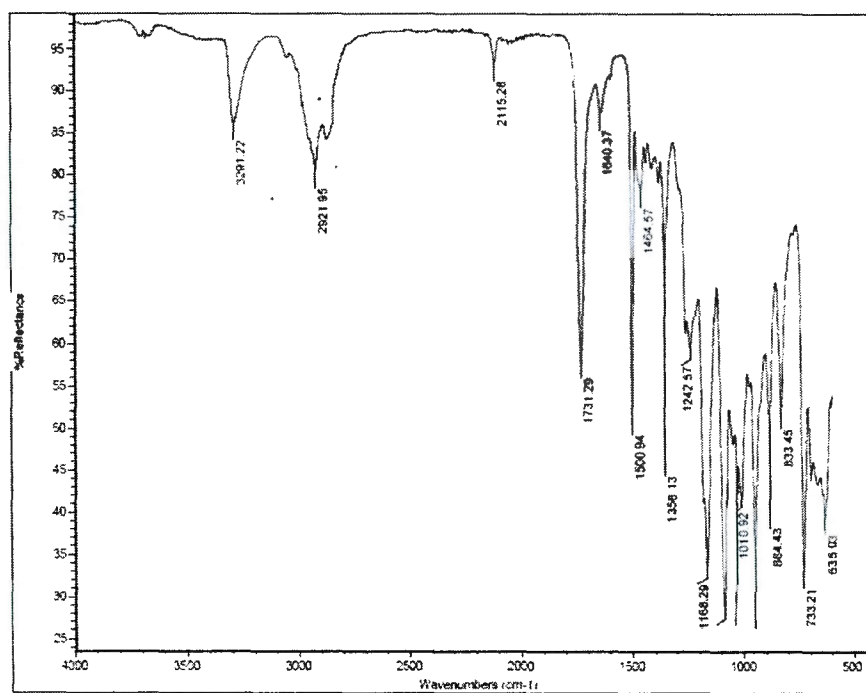


Figure S77. IR spectrum of compound 29.

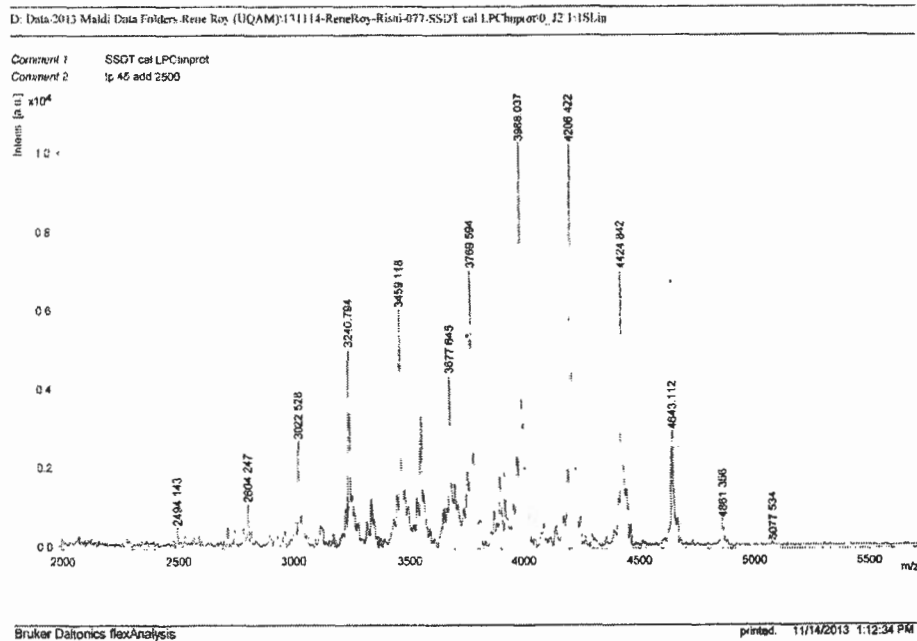
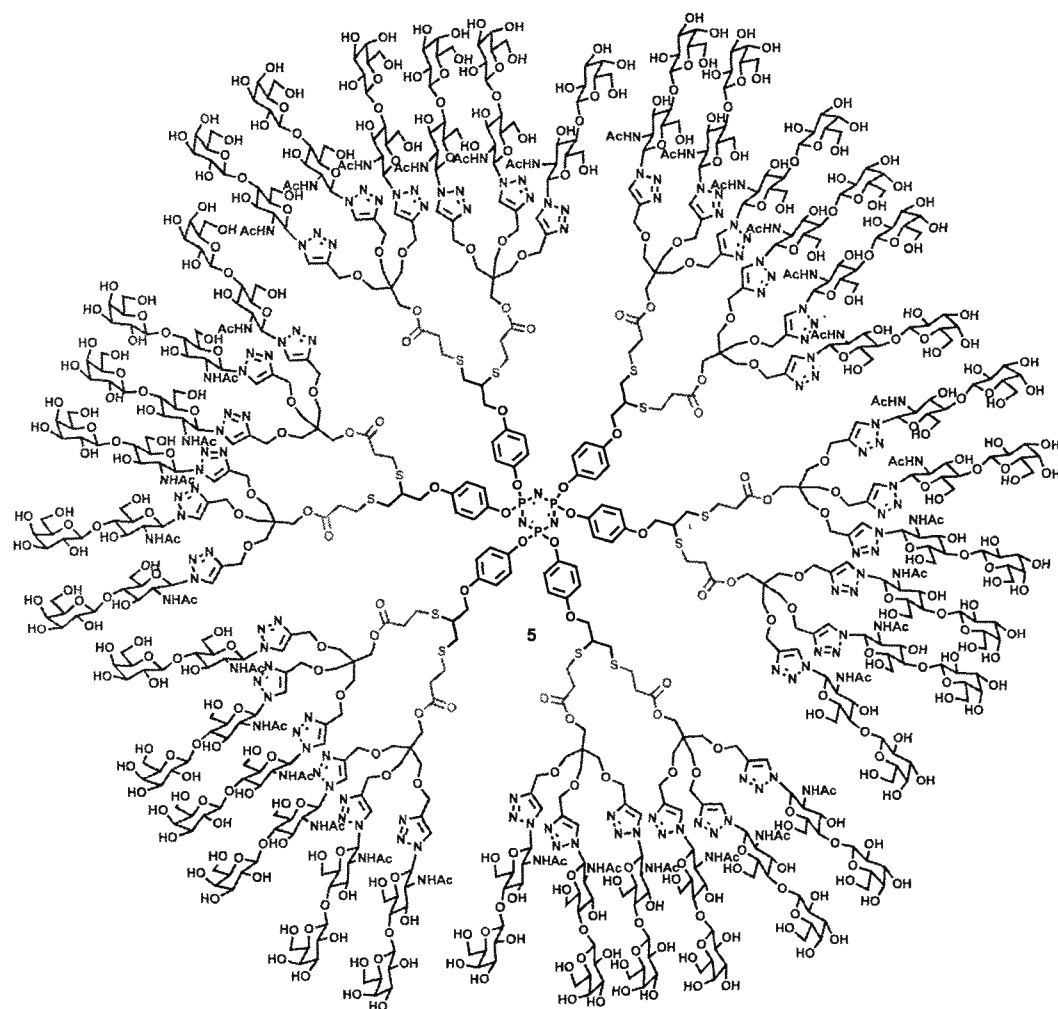


Figure S78. MALDI-TOF spectra of compound 29.



Synthesis of compound 5: Compounds **29** (15 mg, 2.9 μmol , 1.0 eq.) and **18** (60 mg, 0.15 mmol, 50 eq.) were reacted together according to **procedure C** to obtain glycodendrimer **5** (48 mg, 2.2 μmol) as a white amorphous solid. **Yield:** 76%.

^1H NMR (300 MHz, D_2O) δ (ppm) 8.22 (s, 36H), 7.01–6.58 (m, 24H), 5.92 (m, 36H), 4.75–2.62 (m, 714H), 1.82 (br s, 108H).

$^{13}\text{C}\{^1\text{H}\}$ NMR (151 MHz, D_2O) δ (ppm) 174.3, 173.0, 156.3, 145.0, 124.3, 122.6, 116.3, 103.6, 86.9, 78.4, 78.2, 76.0, 73.2, 72.9, 71.6, 69.2, 68.7, 64.2, 61.8, 61.2, 60.5, 57.2, 55.6, 45.0, 44.7, 35.2, 30.5, 25.1, 27.8, 26.9, 22.5.

^{31}P NMR (122 MHz, D_2O) δ 10.8 (s, N_3P_3).

(MALDI-TOF) m/z calculated for $\text{C}_{762}\text{H}_{1170}\text{N}_{147}\text{O}_{432}\text{P}_3\text{S}_{12}$: 19779.8, Found: 19774.7 (DHB matrix).

Melting Point: $\geq 219^\circ\text{C}$ (dec.).

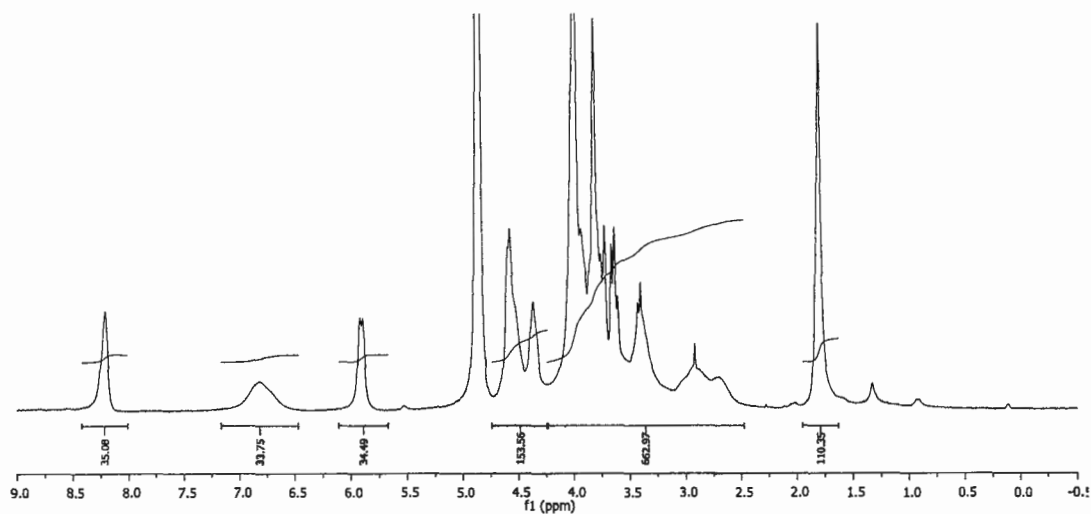


Figure S79. ^1H NMR spectrum of glycodendrimer **5** (D_2O , 300 MHz).

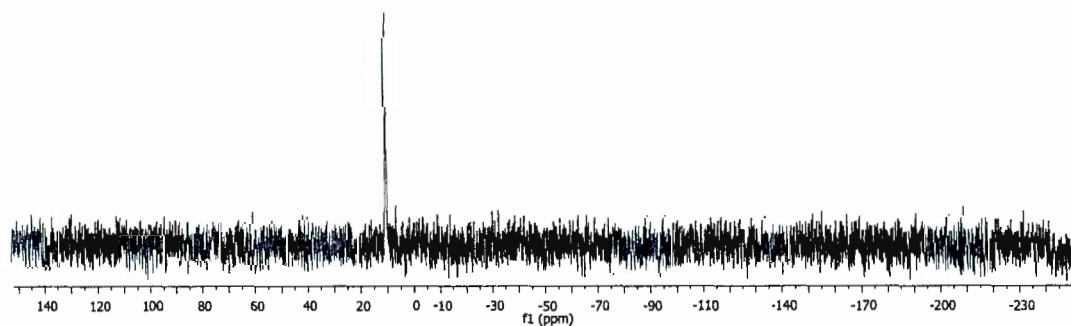


Figure S80. ^{31}P NMR spectrum of glycodendrimer **5** (D_2O , 122 MHz).

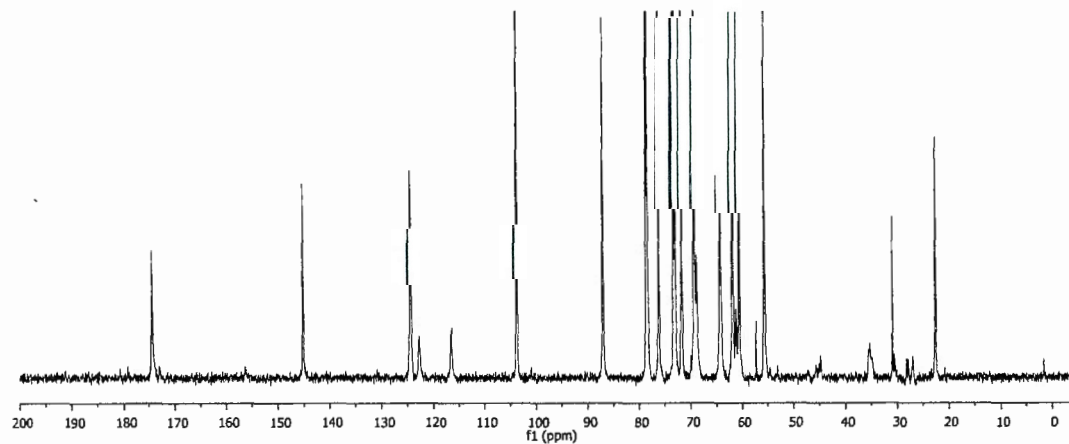
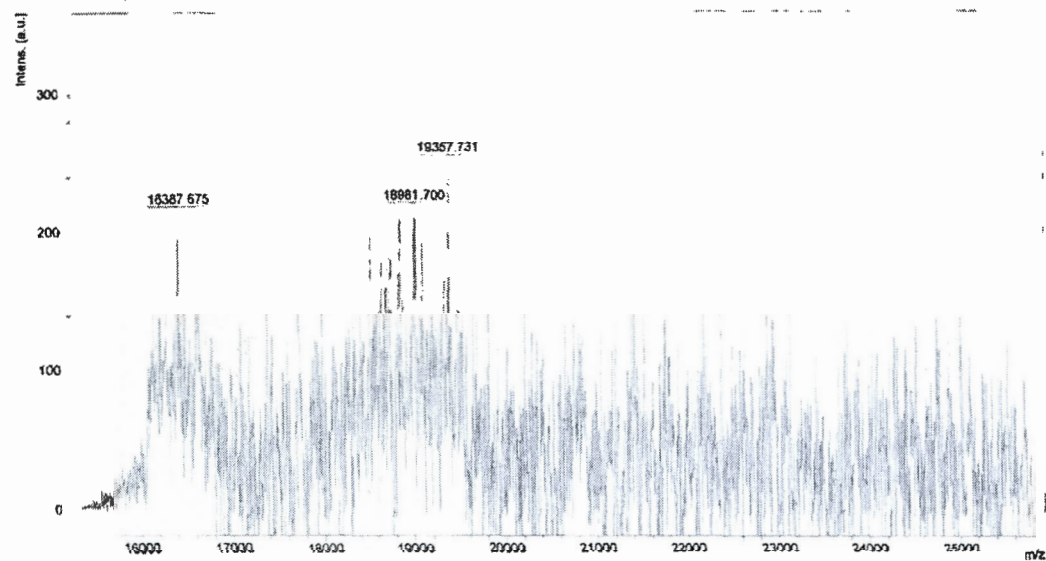


Figure S81. ^{13}C NMR spectrum of glycodendrimer **5** (D_2O , 150 MHz).

D:\Data\2013 Maldi Data Folders\René Roy (UQAM)\130222-SSDHB-Roy UQAM-Rishi-116-15000 20000-cal-121122LPCinProt0_B17A1\1SLin

Comment 1 SS DHB cal 121122LPCinProt

Comment 2 Ip 46 add 2000



Comment 1 SS DHB cal 121122LPCinProt

Comment 2 Ip 46 add 2000

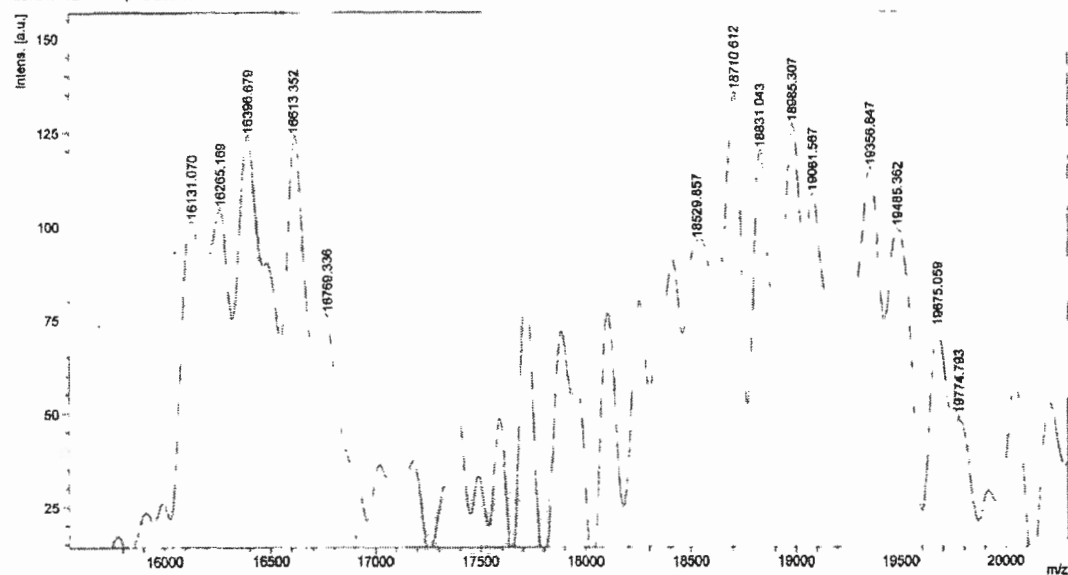
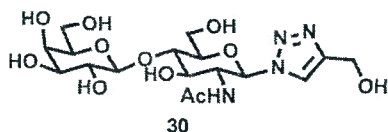


Figure S82. MALDI-TOF spectrum of glycodendrimer 5 (DHB matrix)



Synthesis of compound 30: To a solution of compound **18** (40 mg, 0.098 mmol, 1.0 eq.) in THF (1 ml) was added propargyl alcohol (17.5 μ l, 0.30 mmol, 3.0 eq.) under stirring. Water (1.0 ml) was then added, followed by sodium ascorbate (19 mg, 0.098 mmol, 1.0 eq.) and $\text{CuSO}_4 \cdot 5\text{H}_2\text{O}$ (24 mg, 0.098 mmol, 1.0 eq.). The final ratio of H_2O to THF was kept 1:1. The reaction mixture was stirred at 40°C for 12 hours. After completion of reaction, the solvent was evaporated and crude mixture was directly loaded on column for purification. The impurities were removed using 5% MeOH in CHCl_3 as eluent. The pure compound was obtained, using a gradient of eluents varying from 5% MeOH in CHCl_3 to 15% MeOH in CHCl_3 , as a white amorphous solid (29 mg, 0.063 mmol). **Yield: 64%.**

^1H NMR (300 MHz, CD_3OD) δ (ppm) 8.22 (s, 1H), 5.88 (d, $J = 9.6$ Hz, 1H), 4.73 (s, 2H), 4.54 (d, $J = 7.7$ Hz, 1H), 4.32 (t, $J = 9.7$ Hz, 1H), 4.12–3.85 (m, 6H), 3.84–3.73 (m, 3H), 3.69 (dd, $J = 9.9, 3.3$ Hz, 1H), 3.58 (dd, $J = 9.9, 7.7$ Hz, 1H), 1.82 (s, 3H).

$^{13}\text{C}\{^1\text{H}\}$ NMR (75 MHz, CD_3OD) δ (ppm) 173.4, 149.3, 123.0, 105.1, 88.1, 79.9, 79.6, 77.2, 74.8, 74.0, 72.6, 70.3, 62.5, 61.4, 56.5, 56.2, 22.5.

IR (cm^{-1}) 3340, 2943, 2167, 1973, 1654, 1561, 1374, 1314, 1057, 1033.

HRMS (ESI^+ -TOF) m/z calculated for $\text{C}_{17}\text{H}_{28}\text{N}_4\text{O}_{11}$ $[\text{M}+\text{Na}]^+$: 487.1647, found: 487.1668.

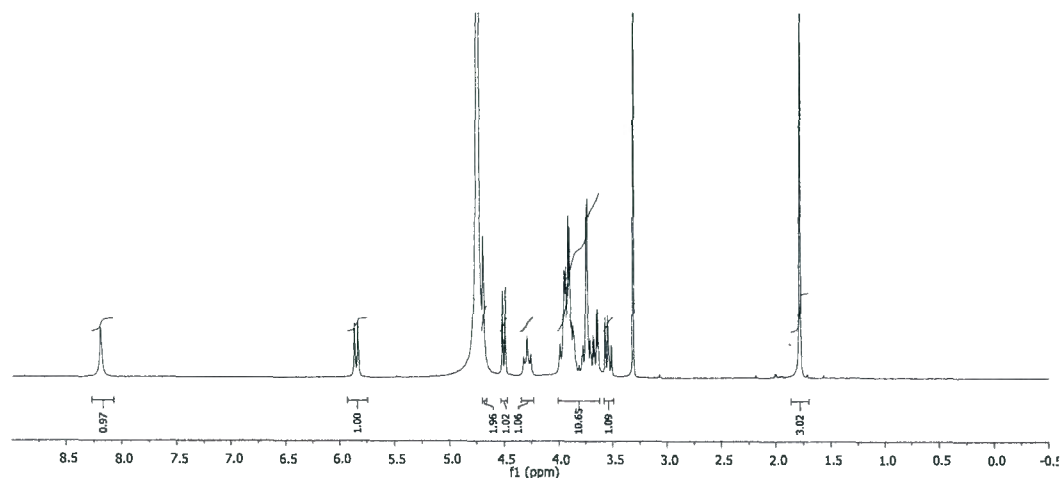


Figure S83. ^1H NMR spectrum of compound **30** (CD_3OD , 300 MHz).

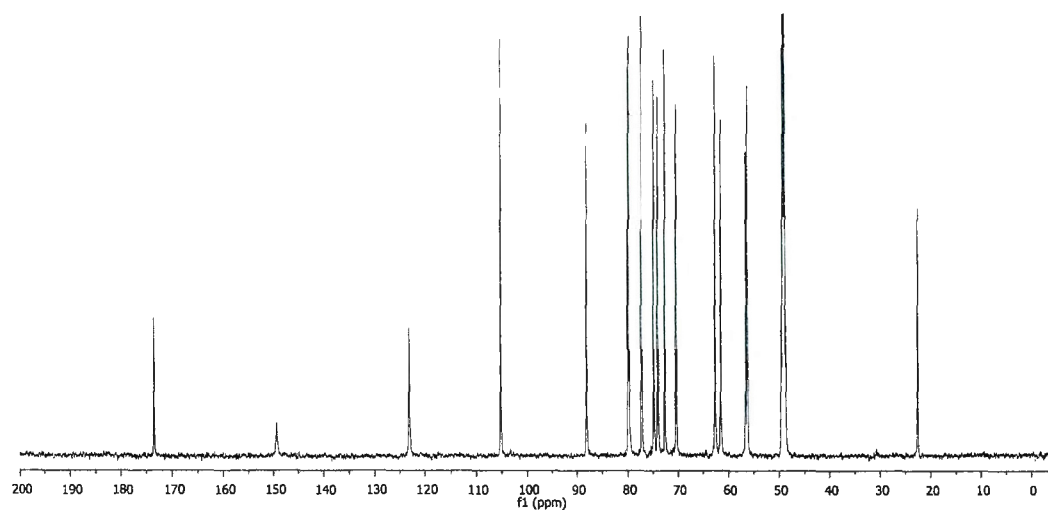


Figure S84. ^{13}C NMR spectrum of compound 30 (CD_3OD , 150 MHz).

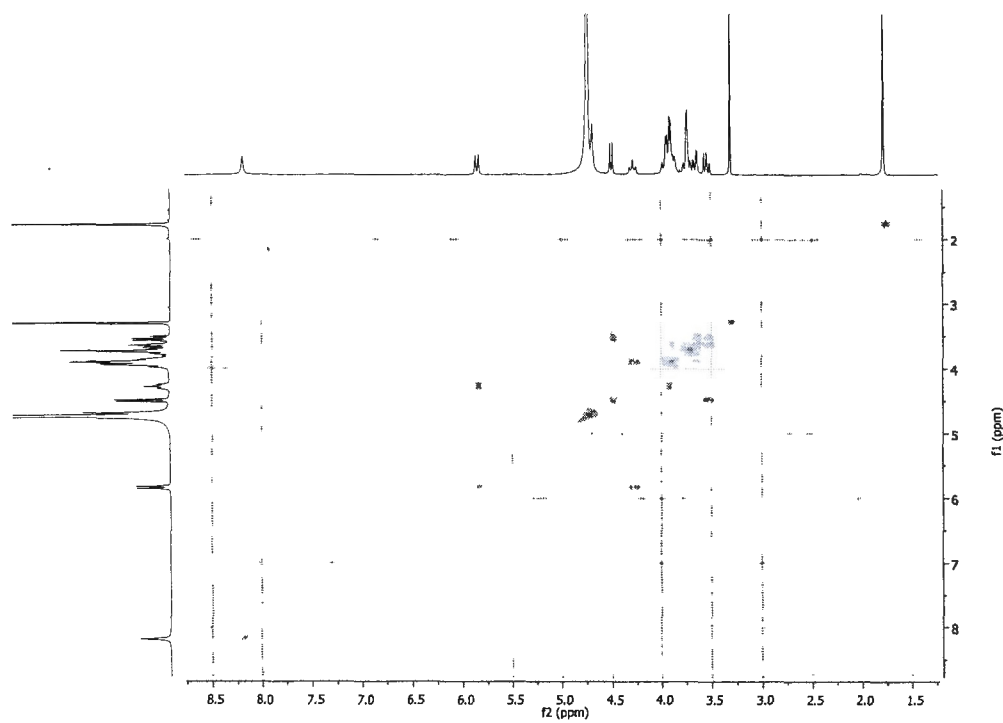


Figure S85. COSY spectrum of compound 30.

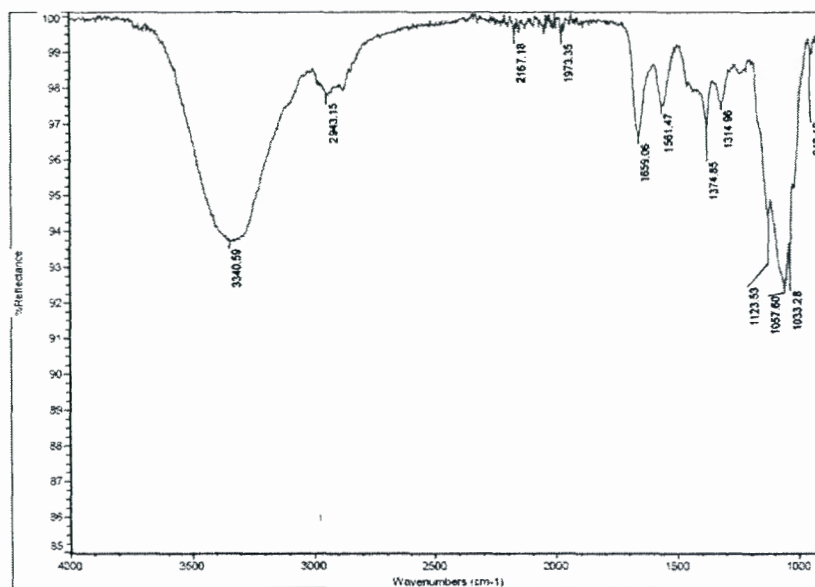
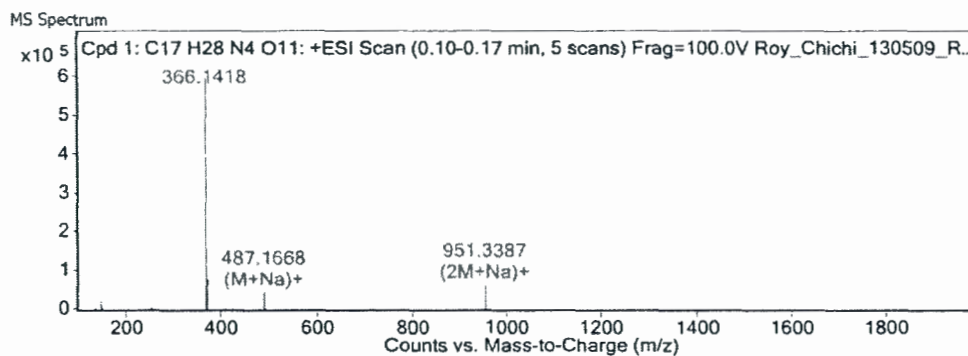


Figure S86. IR spectrum of compound 30.



MS Spectrum Peak List

<i>m/z</i>	<i>Calc m/z</i>	Diff(ppm)	<i>z</i>	Abund	Formula	Ion
487.1668	487.1647	4.32	1	46966	C17 H28 N4 Na O11	(M+Na) ⁺
488.1698	488.1676	4.33	1	8417	C17 H28 N4 Na O11	(M+Na) ⁺
489.1693	489.1697	-0.94	1	1844	C17 H28 N4 Na O11	(M+Na) ⁺
503.1402	503.1386	3.12	1	1467	C17 H28 K N4 O11	(M+K) ⁺
951.3387	951.3401	-1.47	1	65247	C34 H56 N8 Na O22	(2M+Na) ⁺
952.3416	952.3431	-1.54	1	23274	C34 H56 N8 Na O22	(2M+Na) ⁺
953.3455	953.3455	0	1	6818	C34 H56 N8 Na O22	(2M+Na) ⁺
954.3466	954.348	-1.42	1	1523	C34 H56 N8 Na O22	(2M+Na) ⁺
967.313	967.3141	-1.14	1	1124	C34 H56 K N8 O22	(2M+K) ⁺

Figure S87. ESI⁺-TOF spectra (+ report) for compound 30.

3. Surface Plasmon Resonance Studies

Surface plasmon resonance studies (K_D): The studies were conducted using a Biacore T200 SPR instrument with a CM5 sensor chip. A continuous flow of HEPES buffer (10 mM HEPES and 10 mM NaCl, 2 mM CaCl_2 , 2 mM MnCl_2 , pH 7.4) was maintained over the sensor surface at a flow rate of 10 $\mu\text{L}/\text{min}$. The CM5 sensor chip was activated with an injection of a solution containing *N*-ethyl-*N'*-(3-diethylaminopropyl) carbodiimide (EDC) (0.2 M) and *N*-hydroxysuccinimide (NHS) (0.05 M) for 7 minutes. ECA lectin (Pure *Erythrina cristagalli* (Coral Tree) from EY Laboratories, Inc., 50 $\mu\text{g}/\text{mL}$) in NaOAc buffer (pH 4.5) was injected over the activated flow cell at flow rate of 10 $\mu\text{L}/\text{min}$ for 1 minute to achieve a ~ 1200 RU immobilization. The immobilization procedure was completed by an injection of ethanolamine hydrochloride (1 M) (70 μL), followed by a flow of the buffer (100 $\mu\text{L}/\text{min}$), in order to eliminate physically adsorbed compounds. Ethanol amine alone was used in one of the flow-cell as a reference. Glycodendrimers **1-5** and monomer **30** were dissolved in running HEPES buffer and passed over flow cells of the ECL lectin and ethanol amine (Association: 5 min and dissociation: 5 min). The sensor chip was regenerated with D-Galactose (0.25 M, 5 min), 10 mM Glycine.HCl (pH 2.0, 90 sec) followed by an injection of running buffer for 3 minutes. Response units from the surface of ECL lectin were subtracted from the surface of ethanol amine to eliminate non-specific interactions, as well as, bulk change in RU due to variation in refractive index of the medium. The primary subtracted sensorgrams were analyzed by 1:1 Langmuir model fitting, using the BIAevaluation software.

For IC_{50} determination: The studies were conducted using a Biacore T200 SPR instrument with a CM5 sensor chip. A continuous flow of HEPES buffer (10 mM HEPES and 10 mM NaCl, 2 mM CaCl_2 , 2 mM MnCl_2 , pH 7.4) was maintained over the sensor surface at a flow rate of 10 $\mu\text{L}/\text{min}$. The CM5 sensor chip was activated with an injection of a solution containing *N*-ethyl-*N'*-(3-diethylaminopropyl) carbodiimide (EDC) (0.2 M) and *N*-hydroxysuccinimide (NHS) (0.05 M) for 7 minutes. Galactoside **31** (200 $\mu\text{g}/\text{mL}$) in NaOAc buffer (pH 4.5) was injected over the activated flow cell at flow rate of 10 $\mu\text{L}/\text{min}$ for 3 minute to achieve a ~ 170 RU immobilization. The immobilization procedure was completed by an injection of ethanolamine hydrochloride (1 M) (70 μL), followed by a flow of the buffer (100 $\mu\text{L}/\text{min}$), in order to eliminate physically adsorbed compounds. Ethanol amine alone was used in one of the flow-cell as a reference. The solutions of pre incubated (1 h) mixtures of glycodendrimers or monomer (with the various concentrations) and ECL lectin (5 μM) in running HEPES buffer are passed over flow cells of the galactoside and ethanol amine (Association: 2 min and dissociation: 2 min). The sensor chip was regenerated with D-Galactose (0.25 M, 5 min), 10 mM Glycine.HCl (pH 2.0, 90 sec) followed by an injection of running buffer for 3 minutes. For each inhibition assay, ECL lectin (5 μM) without inhibitor was injected

to observe the full adhesion of the lectin onto the sugar-coated surface (0% inhibition). Response units from the surface of galactoside were subtracted from the surface of ethanol amine to eliminate non-specific interactions, as well as, bulk change in RU due to variation in refractive index of the medium. The primary subtracted sensorgrams were analyzed by 1:1 Langmuir model fitting, using the BIAevaluation software. For IC₅₀ evaluation, the response units at the equilibrium was considered as the amount of lectin bound to the sugar surface in the presence of a defined concentration of inhibitor. Inhibition curves were obtained by plotting the percentage of inhibition against the inhibitor concentration (on a logarithmic scale) by using Origin 7.0 software (OriginLab Corp.) and IC₅₀ values were extracted from a sigmoidal fit of the inhibition curve.

4. Sensorgrams obtained from SPR studies:

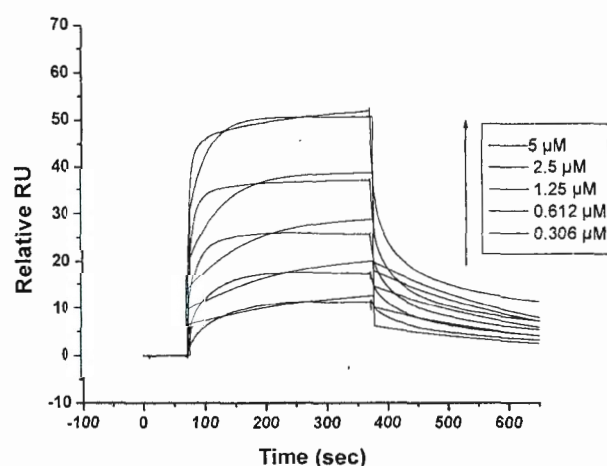


Figure S88. SPR sensorgrams for the interactions of glycodendrimer **1** (12-mer) (0.306 μM to 5 μM) with the surface bound ECA lectin.

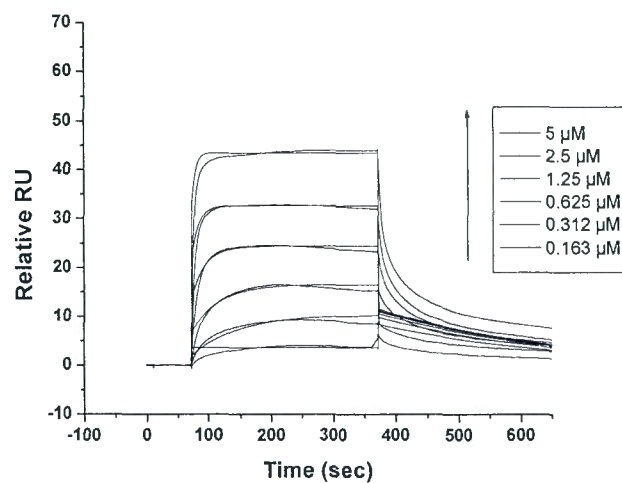


Figure S89. SPR sensorgrams for the interactions of glycodendrimer 2 (12-mer) (0.163 μM to 5 μM) with the surface bound ECA lectin.

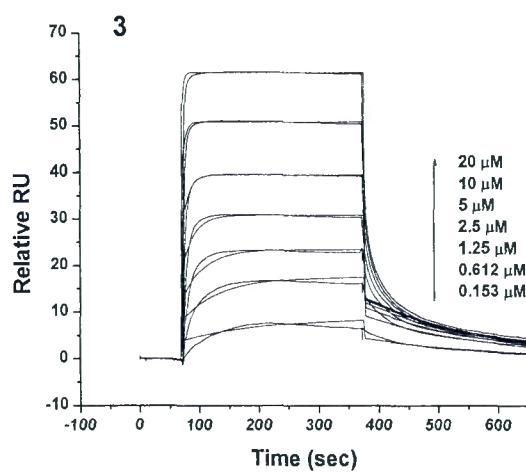


Figure S90. SPR sensorgrams for the interactions of glycodendrimer 3 (12-mer) (0.163 μM to 20 μM) with the surface bound ECA lectin.

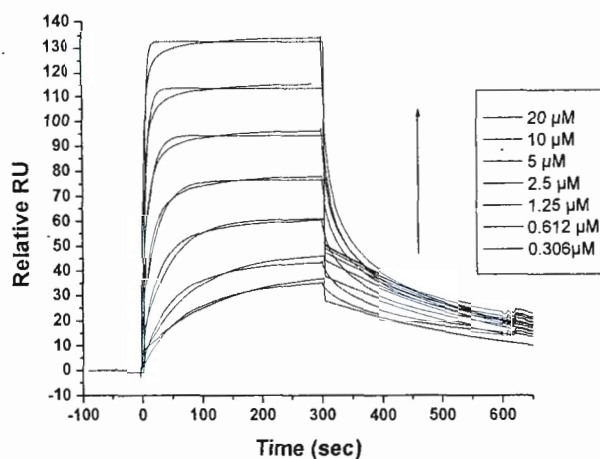


Figure S91. SPR sensorgrams for the interactions of glycodendrimer 4 (0.306 μM to 20 μM) with the surface bound ECA lectin (24-mer).

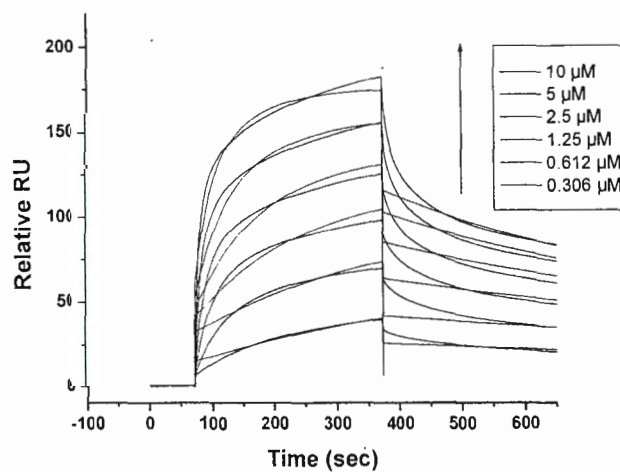


Figure S92. SPR sensorgrams for the interactions of glycodendrimer 5 (0.306 μM to 10 μM) with the surface bound ECA lectin (36-mer).

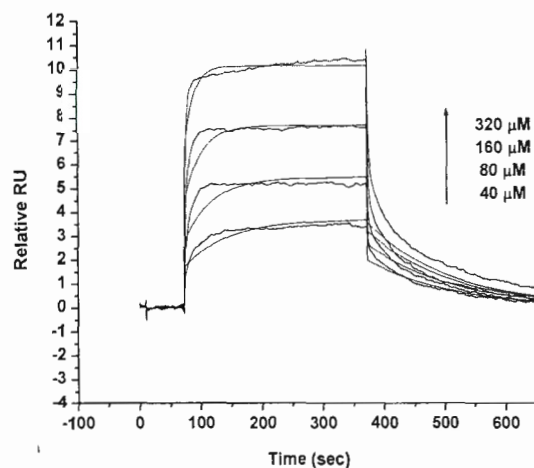


Figure S93. SPR sensorgrams for the interactions of monomer **30** (40 μ M to 320 μ M) with the surface bound ECA lectin.

Competitive studies with sugar on chip (IC_{50} values)

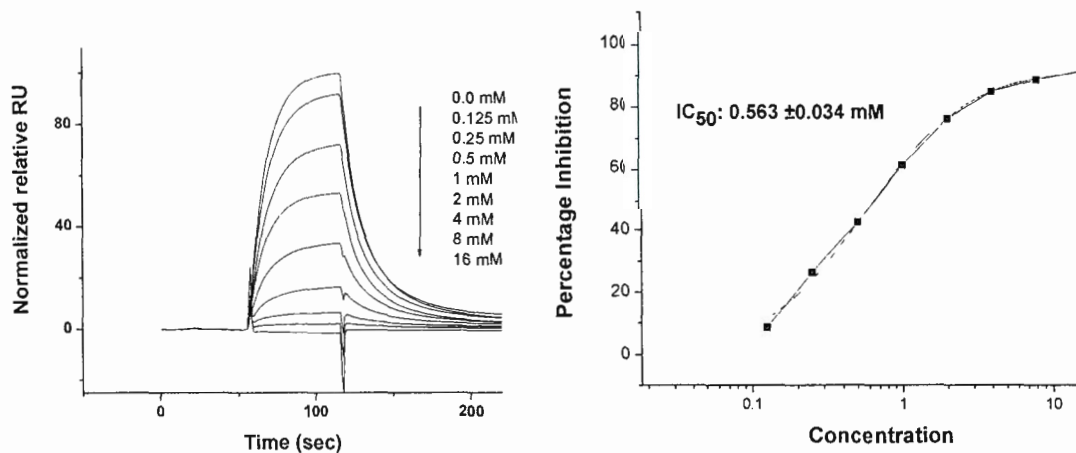


Figure S94. (left) Sensorgrams obtained by injection of ECA (5 μ M) lectin incubated with different concentrations of **18** varying from 0.125 mM (top curve) to 16 mM (bottom curve) on the surface of immobilized galactoside **31**. (right) The inhibitory curve for the compound **18**.

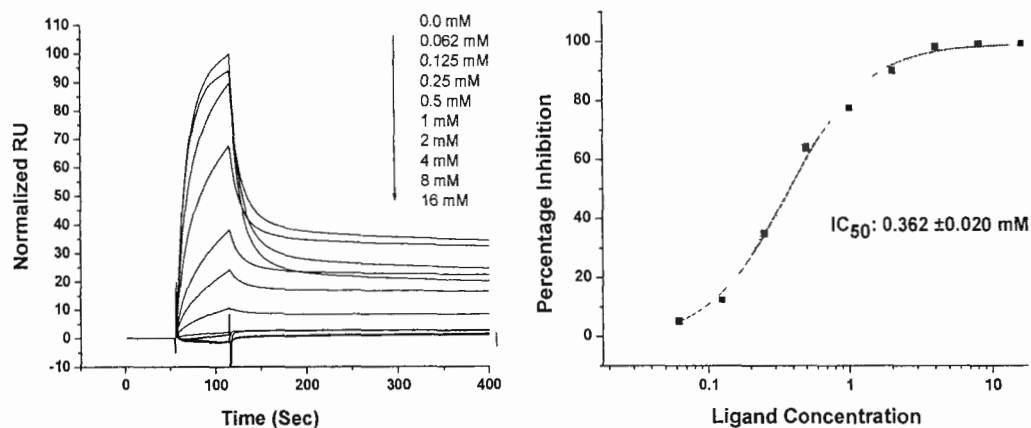


Figure S95. (left) Sensorgrams obtained by injection of ECA (5 μ M) lectin incubated with different concentrations of **30** varying from 0.062 mM (top curve) to 16 mM (bottom curve) on the surface of immobilized galactoside **31**. (right) The inhibitory curve for the compound **30**.

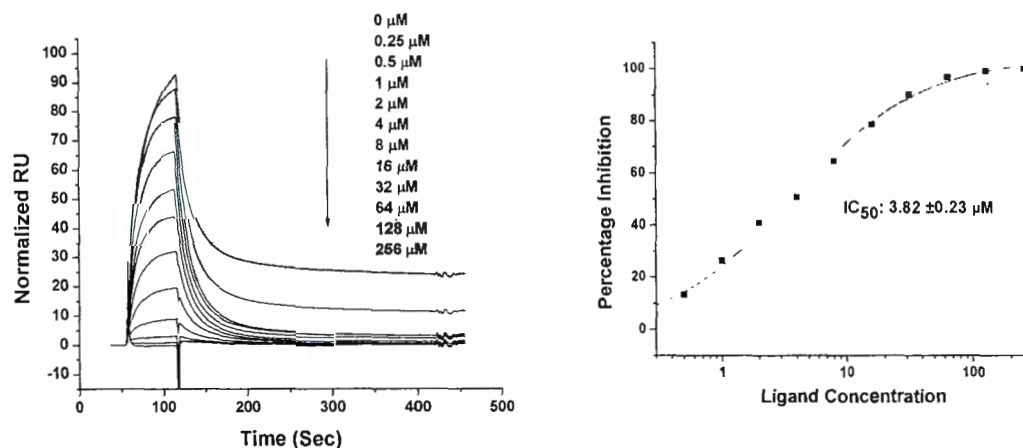


Figure S96. (left) Sensorgrams obtained by injection of ECL (5 μ M) lectin incubated with different concentrations of **1** varying from 0.25 μ M (top curve) to 256 μ M (bottom curve) on the surface of immobilized galactoside **31**. (right) The inhibitory curve for the glycodendrimer **1**.

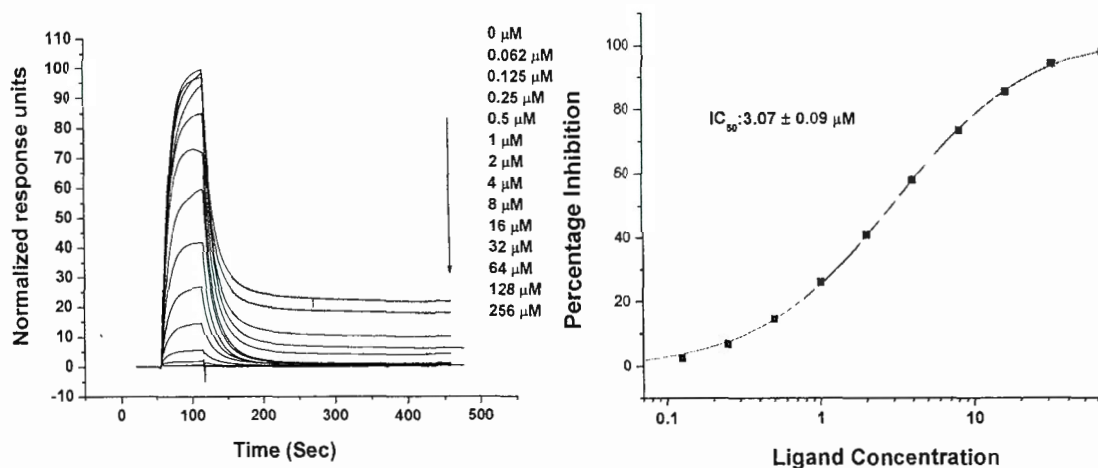


Figure S97. (left) Sensorgrams obtained by injection of ECA (5 μM) lectin incubated with different concentrations of **2** varying from 0.062 μM (top curve) to 256 μM (bottom curve) on the surface of immobilized galactoside **31**. (right) The inhibitory curve for the glycodendrimer **2**.

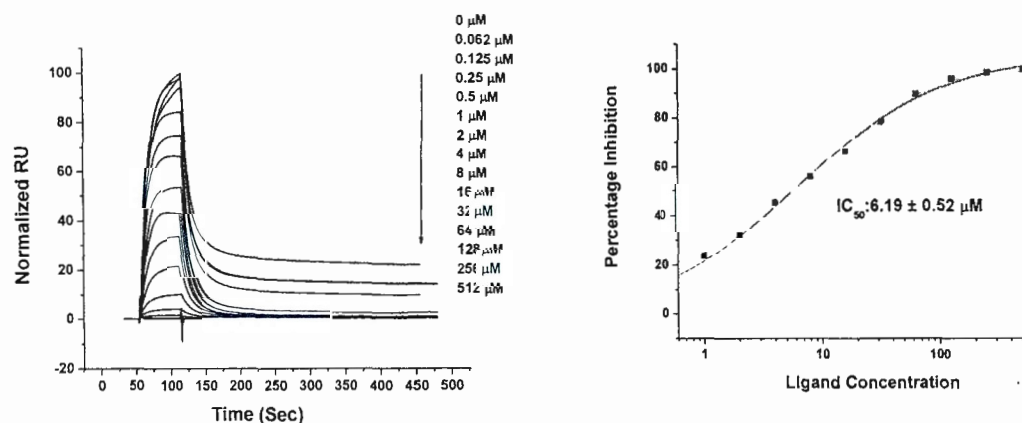


Figure S98. (left) Sensorgrams obtained by injection of ECL (5 μM) lectin incubated with different concentrations of **3** varying from 0.062 μM (top curve) to 512 μM (bottom curve) on the surface of immobilized galactoside **31**. (right) The inhibitory curve for the glycodendrimer **3**.

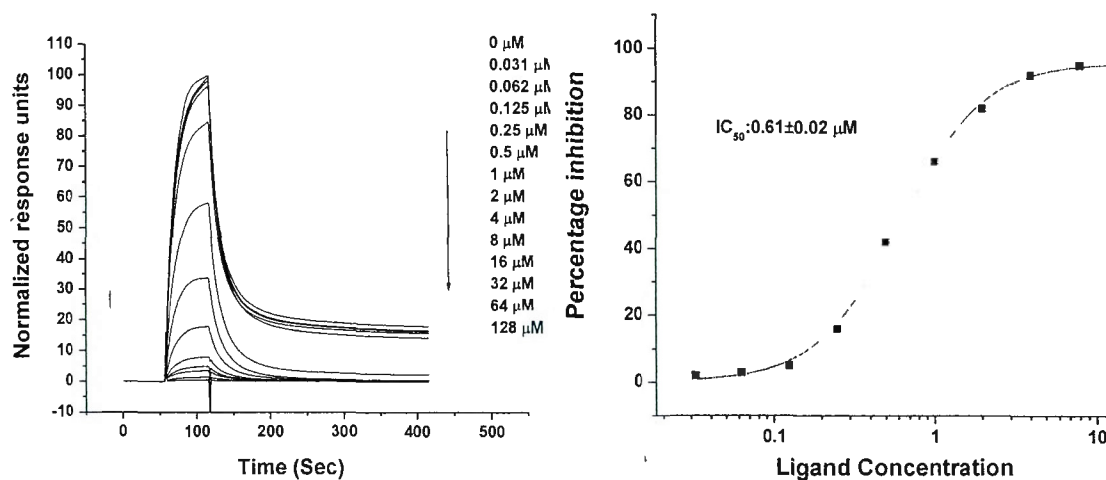


Figure S99. (left) Sensorgrams obtained by injection of ECL (5 μM) lectin incubated with different concentrations of **4** varying from 0.031 μM (top curve) to 128 μM (bottom curve) on the surface of immobilized galactoside **31**. (right) The inhibitory curve for the glycodendrimer **4**.

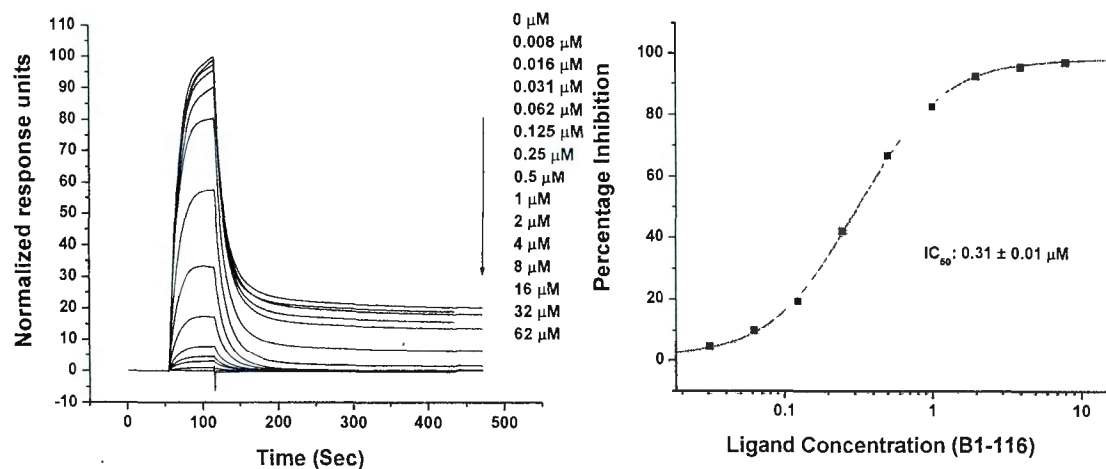


Figure S100. (left) Sensorgrams obtained by injection of ECL (5 μM) lectin incubated with different concentrations of **5** varying from 0.008 μM (top curve) to 64 μM (bottom curve) on the surface of immobilized galactoside **31**. (right) Inhibitory curve for the glycodendrimer **5**.

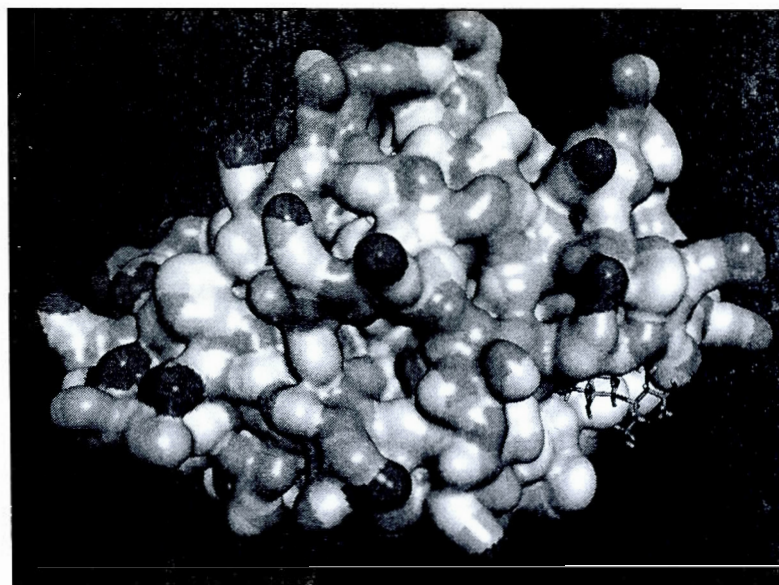


Figure S101. X-Ray structure of a monomer of the lectin ECA bound to Lactose clearly shows the anomeric carbon of the Glucose residue pointing out of the shallow binding pocket wherein the Galactoside moiety resides. The stereocenters formed during the TYC reaction are found 14-15 atoms away from the anomeric Glc carbon.

Figure obtained from Protein Data Bank (PDB) access No.1v00

APPENDIX B

SUPPORTING INFORMATION-CHAPTER 3: HIGHLY VERSATILE
CONVERGENT/DIVERGENT "ONION PEEL" STRATEGY TOWARD POTENT
MULTIVALENT GLYCODENDRIMERS**1. Materials and methods:**

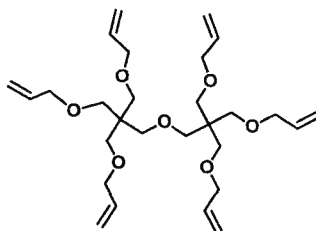
All reactions in organic medium were performed in standard oven dried glassware under an inert atmosphere of nitrogen using freshly distilled solvents. CH_2Cl_2 and DMF were distilled from CaH_2 and ninhydrin respectively, and kept over molecular sieves. Solvents and reagents were deoxygenated when necessary by purging with nitrogen. Water used for lyophilization of final dendrimers was nanopure grade, purified through Barnstead NANOPure II Filter with Barnstead MegOhm-CM Sybron meter. All reagents were used as supplied without prior purification unless otherwise stated, and obtained from Sigma-Aldrich Chemical Co. Ltd. Reactions were monitored by analytical thin-layer chromatography (TLC) using silica gel 60 F254 precoated plates (E. Merck) and compounds were visualized by 254 nm light, a mixture of iodine/silica gel and/or mixture of ceric ammonium molybdate solution (100 ml H_2SO_4 , 900 ml H_2O , 25g $(\text{NH}_4)_6\text{Mo}_7\text{O}_{24}\cdot\text{H}_2\text{O}$, 10g $\text{Ce}(\text{SO}_4)_2$) and subsequent development by gentle warming with a heat-gun. Purifications were performed by flash column chromatography using silica gel from Silicycle (60 Å, 40-63 μm) with the indicated eluent.

^1H NMR and $^{13}\text{C}\{^1\text{H}\}$ NMR spectra were recorded at 300 or 600 MHz and 75 or 150 MHz, respectively, on a Bruker spectrometer (300 MHz) and Varian spectrometer (600 MHz). All NMR spectra were measured at 25°C in indicated deuterated solvents. Proton and carbon chemical shifts (δ) are reported in ppm and coupling constants (J) are reported in Hertz (Hz). The resonance multiplicity in the ^1H NMR spectra are described as "s" (singlet), "d" (doublet), "t" (triplet), "quint" (quintuplet) and "m" (multiplet) and broad resonances are indicated by "br". Residual protic solvent of CDCl_3 (^1H , δ 7.27 ppm; ^{13}C , δ 77.0 ppm (central resonance of the triplet)), D_2O (^1H , δ 4.79 ppm and 30.9 ppm for CH_3 of Acetone for ^{13}C spectra of de-*O*-acetylated compounds), MeOD (^1H , δ 3.31 ppm and ^{13}C , δ 49.0 ppm. 2D Homonuclear correlation ^1H - ^1H COSY experiments were used to confirm NMR peak assignments. Gel Permeation Chromatography (GPC) was performed using THF as the eluent, at 40°C with a 1 mL/min flow rate on a Viscotek VE 2001 GPCmax (SEC System) with Wyatt DSP/Dawn EOS and refractive index RI/LS system as detectors. 2 PLGel mixed B LS (10 μm , 300×7.5 mm) and LS-MALLS detection with

performances verified with polystyrene 100 kDa and 2000 kDa were used to determine the number-average molecular weight (M_n) and polydispersity index (M_w/M_n). Calculations were performed with Zimm Plot (model). Fourier transform infrared (FTIR) spectra were obtained with Thermo-scientific, Nicolet model 6700 equipped with ATR. The absorptions are given in wavenumbers (cm^{-1}).

Accurate mass measurements (HRMS) were performed on a LC-MSD-ToF instrument from Agilent Technologies in positive electrospray mode. Low-resolution mass spectra were performed on the same apparatus or on a LCQ Advantage ion trap instrument from Thermo Fisher Scientific in positive electrospray mode (Mass Spectrometry Laboratory (Université de Montréal), or Plateforme analytique pour molécules organiques (Université du Québec à Montréal), Québec, Canada). Either protonated molecular ions $[M+nH]^{n+}$ or adducts $[M+nX]^{n+}$ ($X = \text{Na}, \text{K}, \text{NH}_4$) were used for empirical formula confirmation. MALDI-TOF experiments were performed on an Autoflex III from Brucker Smarteam in linear positive mode (Mass Spectrometry Laboratory (McGill University)) to afford adducts $[M+nX]^{n+}$ ($X = \text{Na}, \text{K}$ or Li). Samples were solubilized in H_2O for a final concentration of 6 mg/mL. Dihydroxybenzoic acid was used as the matrix. Cationization was eased by the use of the corresponding sodium salt (2 mg/mL).

2. Synthetic protocols and characterization:



Synthesis of compound 2: A flame dried two-neck round bottom flask (250mL) was charged with dipentaerythritol **1** (4.00g, 15.7mmol) and sodium hydride (3.77g, 157.4mmol). To this, DMF (60ml) was added slowly at 0°C under nitrogen atmosphere. The reaction mixture was stirred for 20 minutes at 0°C. It was followed by the addition of allyl bromide (16.3mL, 188.8mmol) and stirred for 5 hrs at room temp. The completion of reaction was monitored by TLC. The reaction mixture was then quenched with methanol at 0°C. Solvent was evaporated and the residue was dissolved in ethyl acetate (100mL) and washed with water. Organic layer was separated, dried with Na_2SO_4 , filtered and concentrated under reduced pressure. The crude compound was purified by column chromatography using 7% ethyl acetate in hexanes as eluent to afford desired compound **2** (6.22g, 12.6mmol) in 80% yield as light yellow oil.

^1H NMR (300 MHz, CDCl_3) δ 5.88 (ddt, $J = 17.1, 10.5, 5.3$ Hz, 6H), 5.34–5.08 (m, 12H), 3.94 (dt, $J = 5.2, 1.4$ Hz, 12H), 3.46 (d, $J = 7.9$ Hz, 12H), 3.40 (s, 4H).

$^{13}\text{C}\{^1\text{H}\}$ NMR (75 MHz, CDCl_3) δ 135.3, 116.0, 72.3, 70.1, 69.4, 45.6.

IR (cm^{-1}) 3079, 2980, 2903, 2867, 1646, 1478, 1420, 1349, 1269, 1173, 989, 920.

HRMS (ESI^+) for $\text{C}_{28}\text{H}_{46}\text{O}_7$ m/z calc for $\text{C}_{28}\text{H}_{46}\text{O}_7$, 495.3316 $[\text{M}+\text{H}]^+$; found: 495.3299.

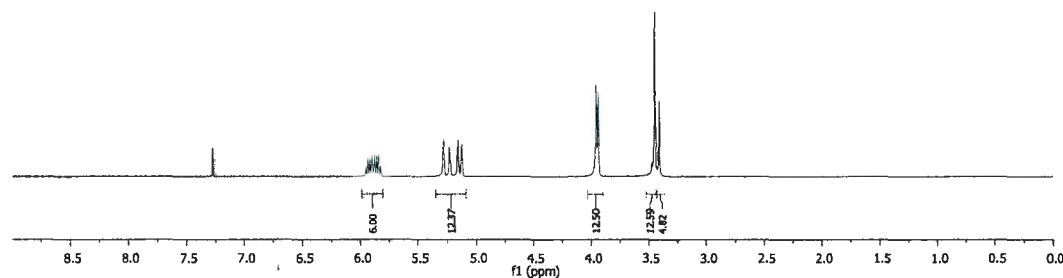


Figure S1. ^1H NMR spectrum of compound 2 (CDCl_3 , 300 MHz).

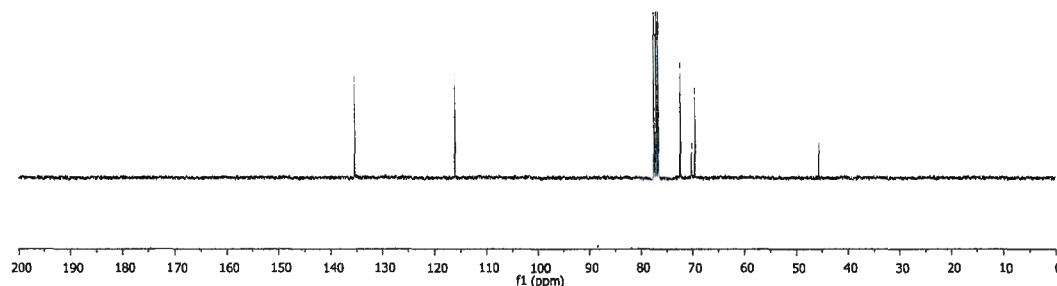


Figure S2. $^{13}\text{C}\{^1\text{H}\}$ NMR spectrum of compound 2 (CDCl_3 , 75 MHz).

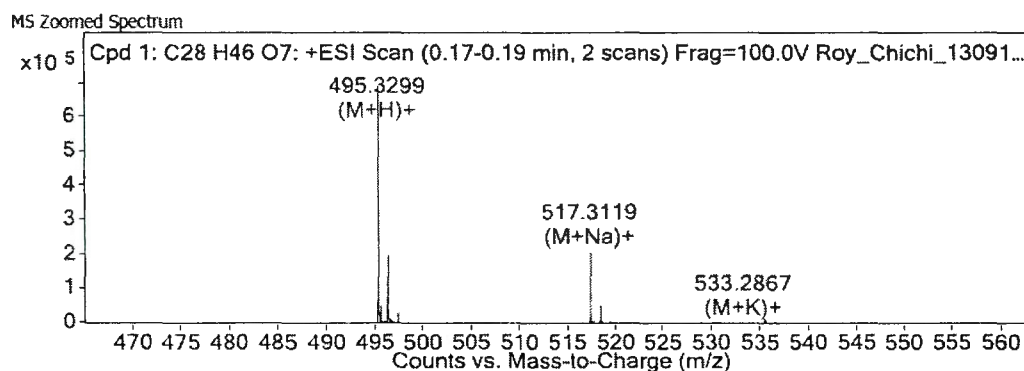


Figure S3. HRMS (ESI^+) spectrum of compound 2.

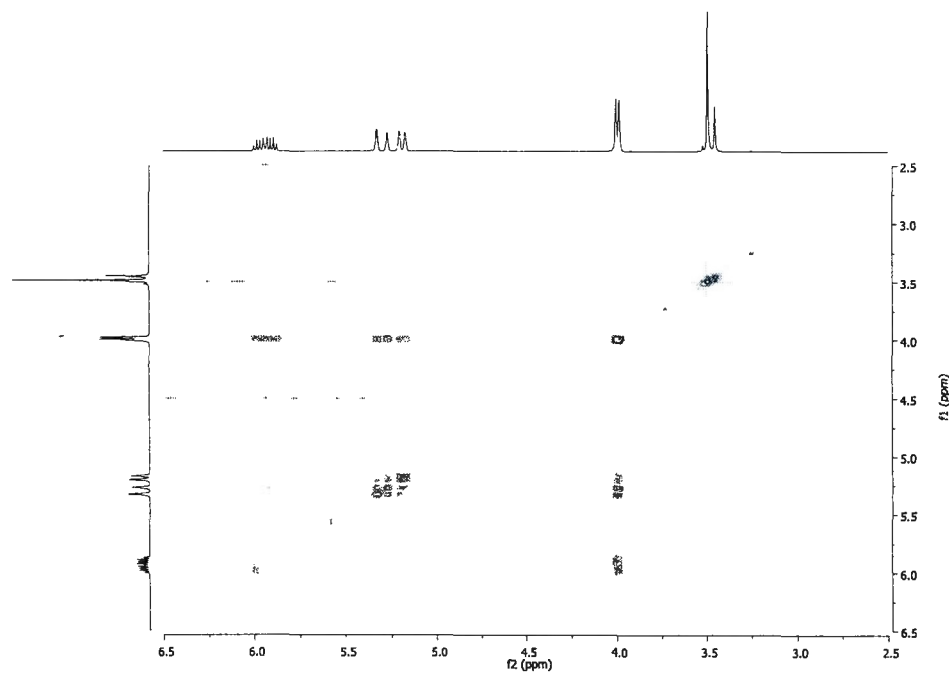


Figure S4. COSY spectrum of compound 2.

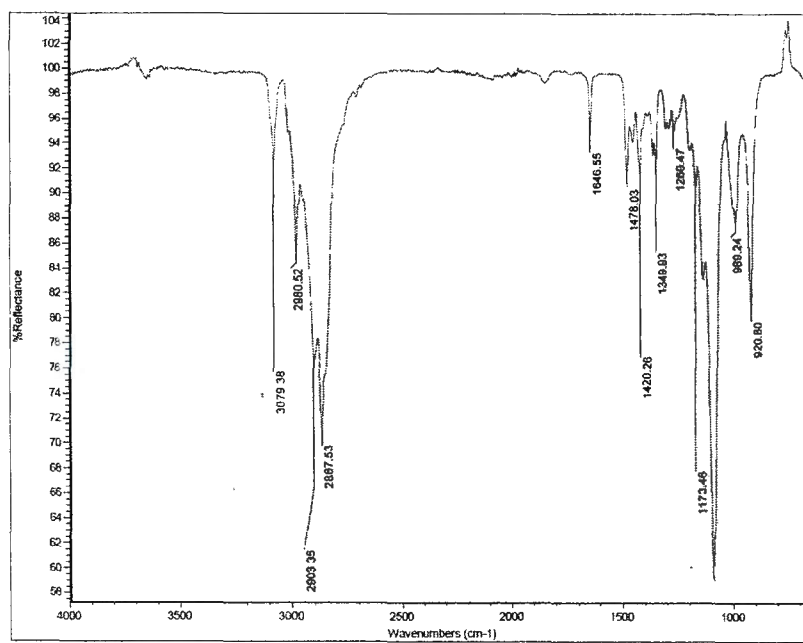
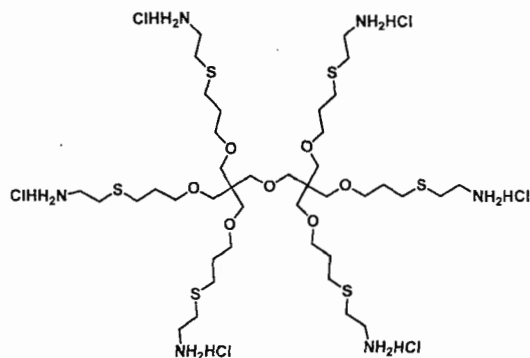


Figure S5. IR spectrum of compound 2.



Synthesis of compound 3: To a stirring solution of hexa-allyl derivative **2** (300mg, 0.606mmol), 2,2'-dimethoxy-2-phenylacetophenone (DMPAP) (155mg, 0.606mmol) in dry DMF (3ml) was added cysteamine hydrochloride (1.03g, 9.07mmol) under nitrogen. The vial was then purged with N₂ for 10 min and irradiated for 4-6 hrs with UV lamp (365nm) at room temperature. Upon completion of the reaction, the contents of the vial were washed three times with diethyl ether to remove excess of thiol, affording a clear viscous liquid. It was further purified using dialysis bag (cut-off 1000 Da, spectrum). Dialysis bath water was changed 4-5 times in the span of 6 hrs to remove all the impurities. The compound was lyophilized to yield white hygroscopic solid **3** (534mg, 0.455mmol) in 75% yield.

¹H NMR (300 MHz, D₂O) δ 3.62 (t, *J* = 6.2 Hz, 12H), 3.48 (s, 12H), 3.39 (s, 4H), 3.26 (t, *J* = 6.7 Hz, 12H), 2.90 (t, *J* = 6.8 Hz, 12H), 2.70 (t, *J* = 7.2 Hz, 12H), 1.98–1.83 (m, 12H).

¹³C{¹H} NMR (75 MHz, D₂O) δ 70.5, 69.9, 45.8, 38.9, 28.8, 28.0.

IR (cm⁻¹) 3637, 2980, 2971, 2883, 1382, 1150, 1070, 954.

HRMS (ESI+) *m/z* calc. for C₄₀H₈₈N₆O₇S₆, 957.5112 [*M*+H]⁺; found, 957.5134.

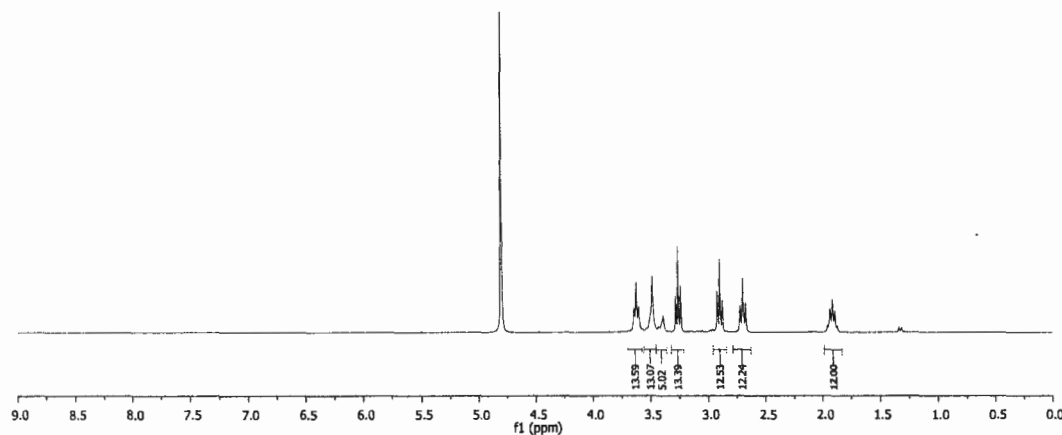


Figure S6. ¹H NMR spectrum of compound **3** (300 MHz, D₂O).

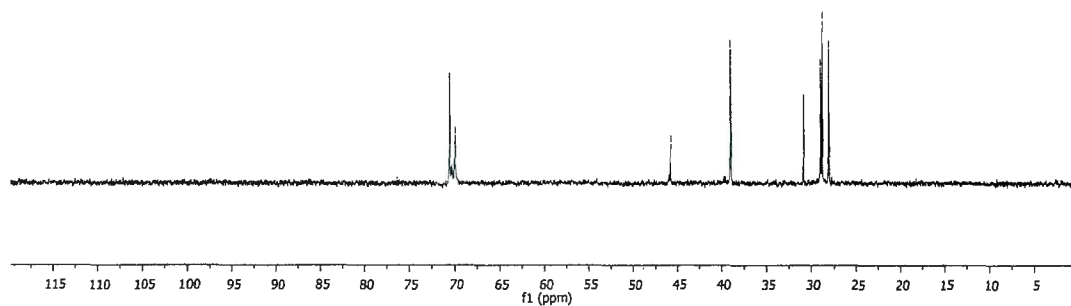


Figure S7. $^{13}\text{C}\{^1\text{H}\}$ NMR spectrum of compound **3** (75 MHz, D_2O).

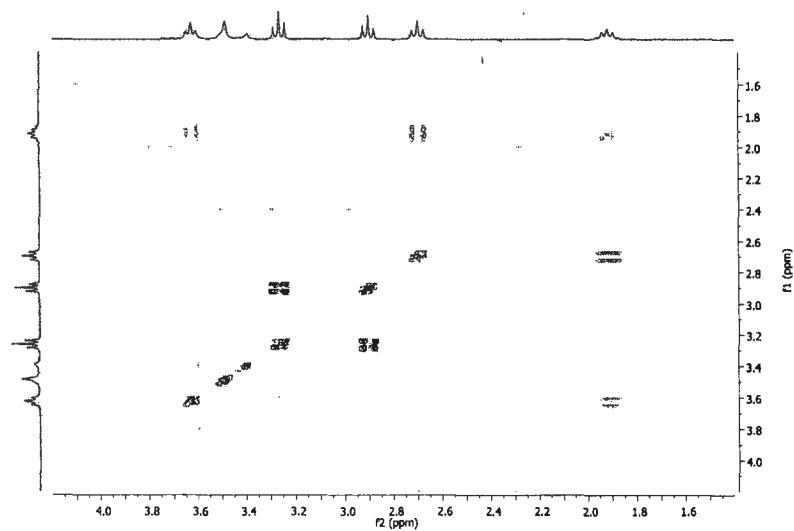


Figure S8. COSY spectrum of compound **3**.

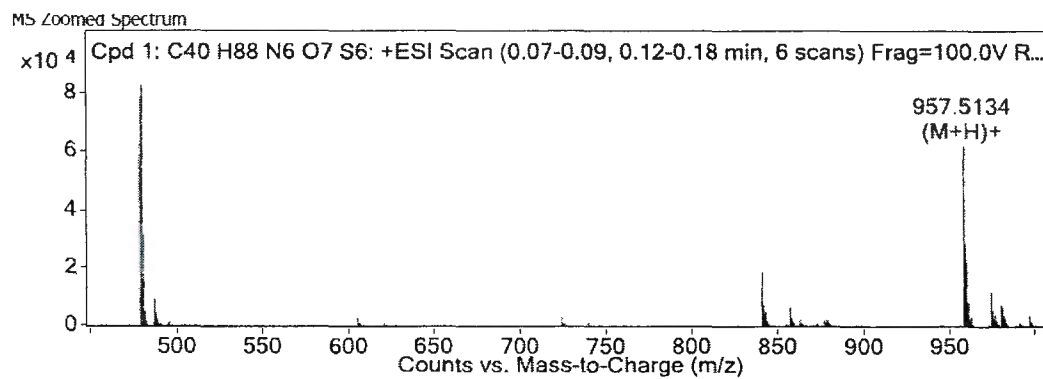


Figure S9. HRMS (ESI⁺) spectrum of compound **3**.

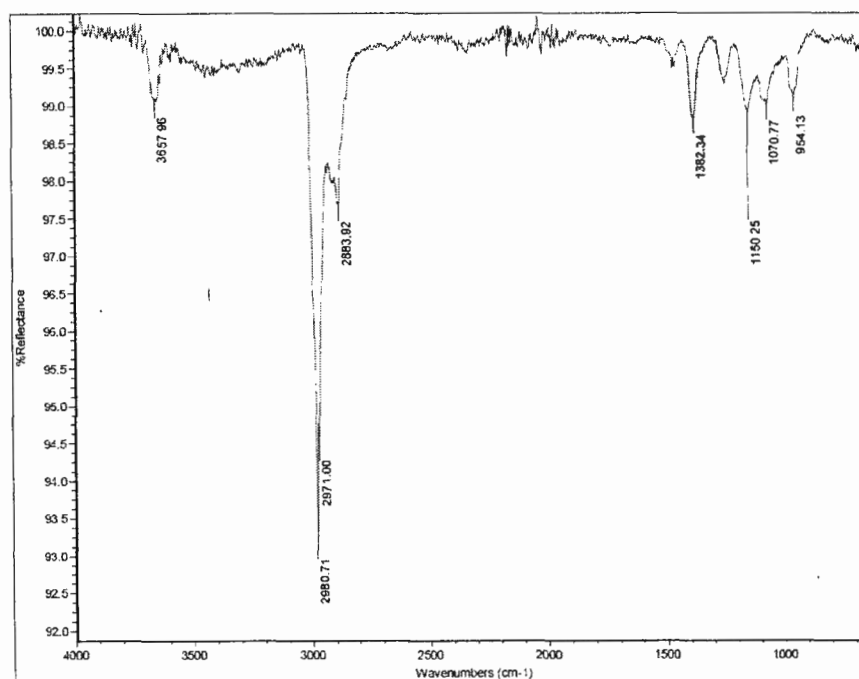
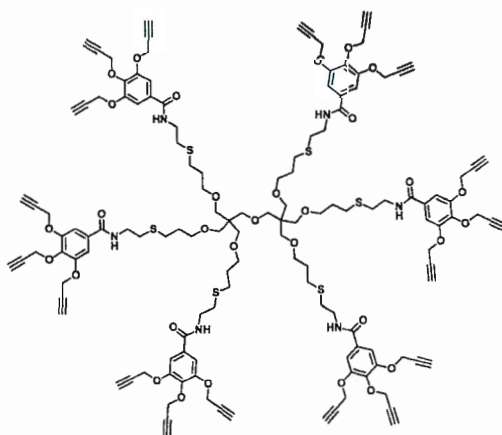


Figure S10. IR spectrum of compound 3.



Synthesis of compound 5: A solution of hexa-amine hydrochloride **3** (150mg, 0.127mmol) and *N,N*-diisopropylethylamine (0.26ml, 1.48mmol) in DMF (2ml) was stirred for 30 minutes. In another two neck flask, 1-ethyl-3-(3-dimethylaminopropyl) carbodiimide hydrochloride (EDC.HCl) (243mg, 1.27mmol), and 4-(dimethylamino)pyridine (DMAP) (155mg, 1.27mmol) were added in DMF (4mL) and stirred for 10 minutes followed by the addition of tripropargylated gallic acid **4** (434mg, 1.53mmol). The free amine solution from first flask was then transferred to

the reaction mixture of the second flask with the help of canula syringe and was heated at 50°C for overnight. The completion of reaction was monitored by TLC. Upon completion, the reaction mixture was diluted with water (40mL) and extracted with ethyl acetate (3×40mL). The combined organic extracts were washed with 0.1 N HCl (3×15mL), followed by saturated NaHCO₃ solution and brine. The organic layer was dried over anhydrous sodium sulfate, filtered and evaporated under reduced pressure. The crude mixture was then purified with the help of flash column chromatography using 80% EtOAc in hexanes as eluent. The desired compound **5** (232.5mg, 0.0910mmol) was achieved in 72% yield as light yellow oil.

¹H NMR (300 MHz, CDCl₃) δ 7.27–7.23 (m, 12H), 7.07 (br s, 6H), 4.78 (dd, *J* = 2.3, 2.3 Hz, 36H), 3.60 (d, *J* = 6.0 Hz, 12H), 3.43 (t, *J* = 5.9 Hz, 12H), 3.31 (d, *J* = 8.1 Hz, 16H), 2.74 (t, *J* = 6.6 Hz, 12H), 2.59 (t, *J* = 7.2 Hz, 12H), 2.55 (t, *J* = 2.3 Hz, 12H), 2.48 (t, *J* = 2.4 Hz, 6H), 1.92–1.70 (m, 12H).

¹³C{¹H} NMR (75 MHz, CDCl₃) δ 166.7, 151.5, 140.0, 130.2, 107.9, 78.7, 78.1, 76.4, 75.7, 69.6, 60.3, 57.3, 45.6, 39.2, 31.6, 29.8, 28.4.

IR (cm⁻¹) 3290, 3005, 2922, 2867, 2122, 1637, 1581, 1541, 1492, 1428, 1365, 1323, 1275, 1261, 1207, 1106, 1032, 992, 764, 750, 671.

HRMS (ESI⁺) *m/z* for C₁₃₆H₁₄₈N₆O₃₁S₆, 1277.4329 [*M*+2H]²⁺; found, 1277.4359, 2576.8406 [*M*+Na]⁺; found 2575.8346.

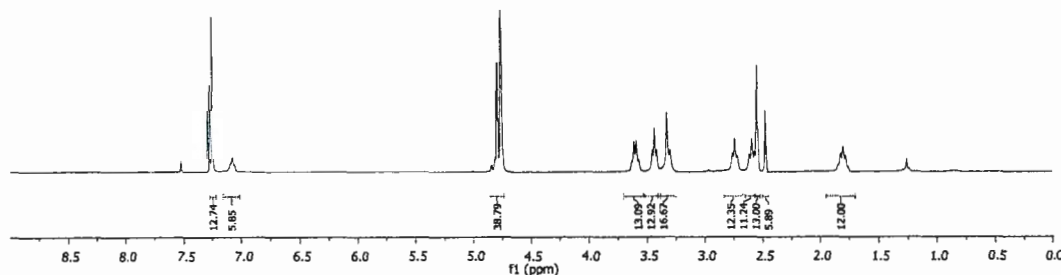


Figure S11. ¹H NMR spectrum of compound **5** (300 MHz, CDCl₃).

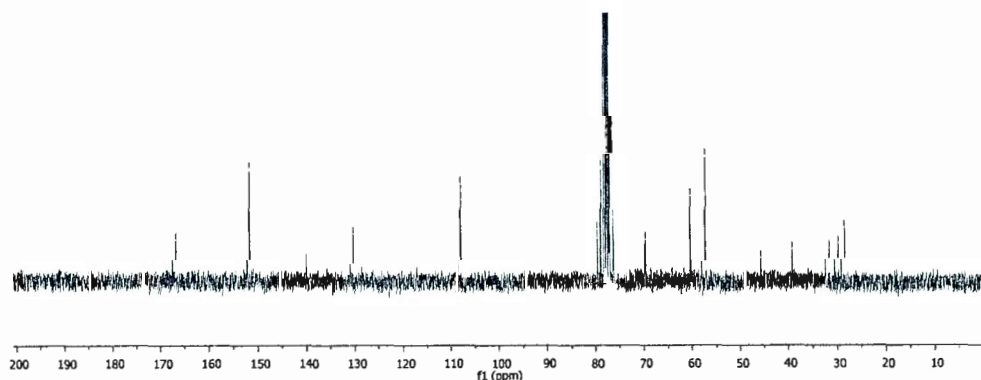


Figure S12. ¹³C{¹H} NMR spectrum of compound **5** (75 MHz, CDCl₃).

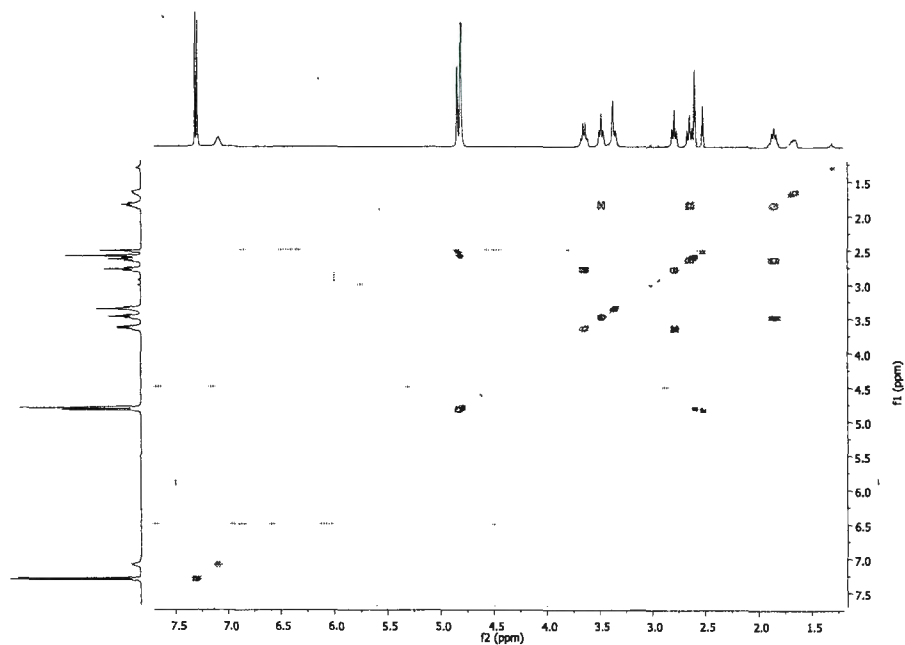


Figure S13. COSY spectrum of compound 5.

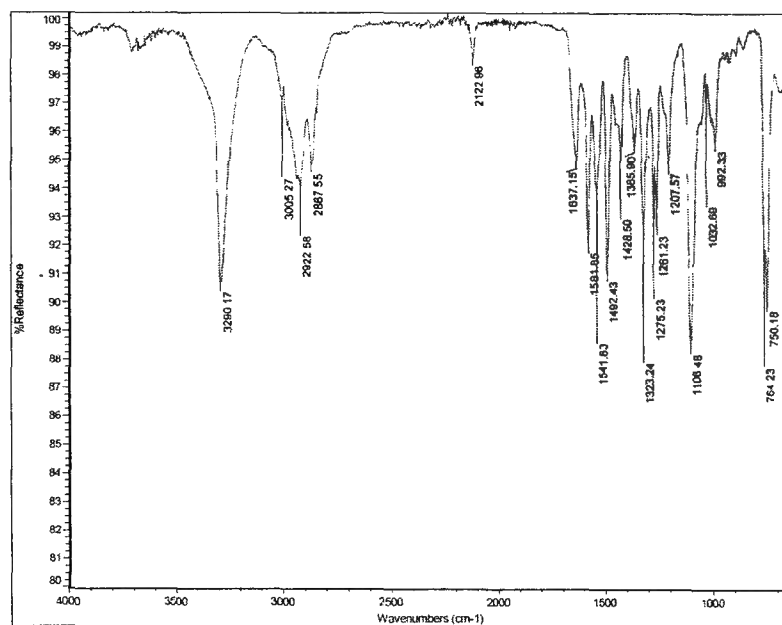


Figure S14. IR spectrum of compound 5.

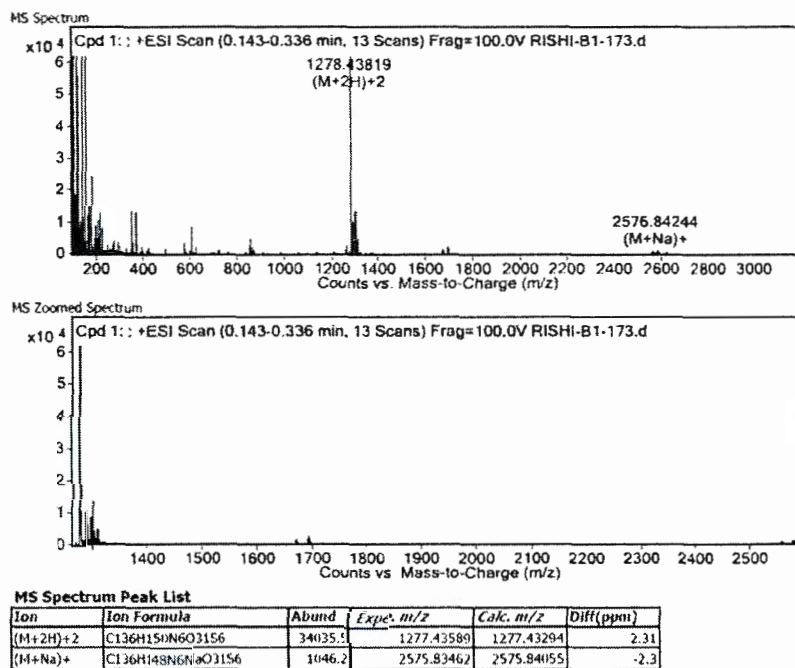
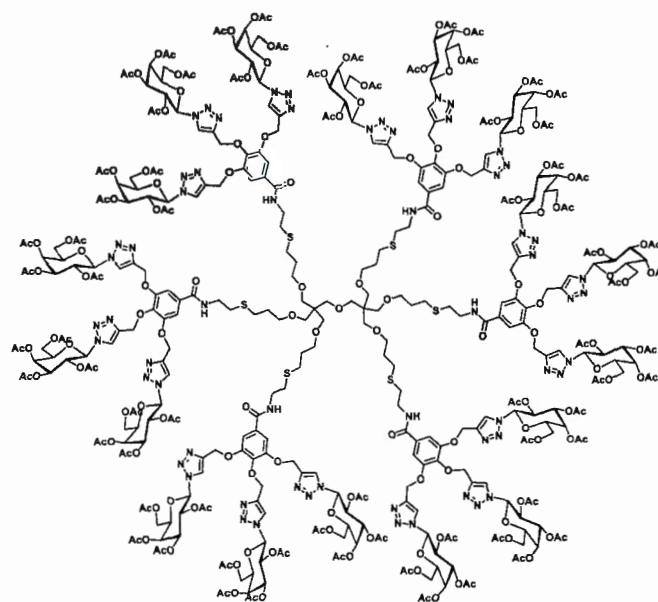


Figure S15. HRMS (ESI⁺) spectrum of compound 5.



Synthesis of compound 7: Divergent approach: To a solution of compound 5 (50.0mg, 0.0195mmol) in THF (3mL) was added azido derivative 6 (261mg,

0.702mmol) dissolved in THF (2mL), followed by the addition of sodium ascorbate (70.0mg, 0.351mmol). An aqueous solution of $\text{CuSO}_4 \cdot 5\text{H}_2\text{O}$ (88.0 mg, 0.351mmol) was then added to the reaction mixture. The final ratio of H_2O to THF was kept 1:1. The reaction mixture was stirred at 40°C for 12 hrs. The progress of the reaction was monitored with the help of TLC. Upon completion, reaction mixture was diluted with EtOAc (25mL) and washed with a saturated solution of EDTA ($2 \times 15\text{mL}$). Organic layer was washed with brine, dried over anhydrous Na_2SO_4 , filtered and concentrated under reduced pressure. Purification of the crude compound was achieved *via* flash column chromatography on silica gel using 2-4% MeOH in DCM as eluent gradient to afford desired compound **7** (146.5mg, 0.0158mmol) in 81% yield as a white solid.

^1H NMR (300 MHz, CDCl_3) δ 8.16 (s, 6H), 8.09 (s, 12H), 7.19 (s, 12H), 5.94 (d, $J = 9.2$ Hz, 18H), 5.68 (t, $J = 9.8$ Hz, 6H), 5.56 (dd, $J = 10.9, 6.9$ Hz, 32H), 5.38–5.12 (m, 55H), 4.32 (t, $J = 6.4$ Hz, 18H), 4.27–4.06 (m, 38H), 3.58 (d, $J = 5.5$ Hz, 12H), 3.45 (s, 12H), 3.34 (s, 16H), 2.74 (t, $J = 6.5$ Hz, 12H), 2.63 (t, $J = 6.9$ Hz, 12H), 2.20 (s, 58H), 2.01 (d, $J = 8.4$ Hz, 118H), 1.77 (d, $J = 18.0$ Hz, 54H).

$^{13}\text{C}\{^1\text{H}\}$ NMR (75 MHz, CDCl_3) δ 170.3, 170.3, 170.1, 170.1, 169.9, 169.8, 169.6, 169.0, 168.7, 166.7, 151.9, 144.6, 144.0, 140.1, 130.3, 123.3, 122.3, 107.2, 86.1, 85.7, 73.7, 73.5, 73.2, 71.0, 70.7, 69.7, 67.9, 67.7–67.5, 66.8, 66.1, 62.8, 61.0, 31.3, 29.8, 28.5, 20.5, 20.1.

IR (cm^{-1}): 3628, 2994, 2947, 1751, 1651, 1583, 1491, 1428, 1370, 1218, 1093, 1064, 923, 732, 667.

MALDI-TOF: m/z calc. for $\text{C}_{388}\text{H}_{490}\text{N}_{60}\text{O}_{193}\text{S}_6$, 9297.7 $[M+\text{Na}]^+$; found, 9296.4.

GPC (THF): $M_n = 9600$ g/mol. $M_w/M_n = 1.03$

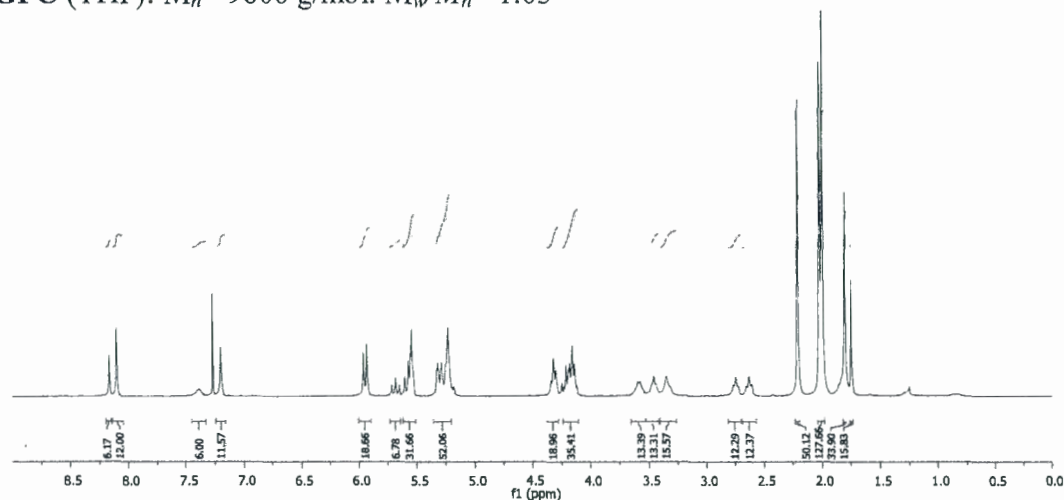


Figure S16. ^1H NMR spectrum of compound **7** (300 MHz, CDCl_3).

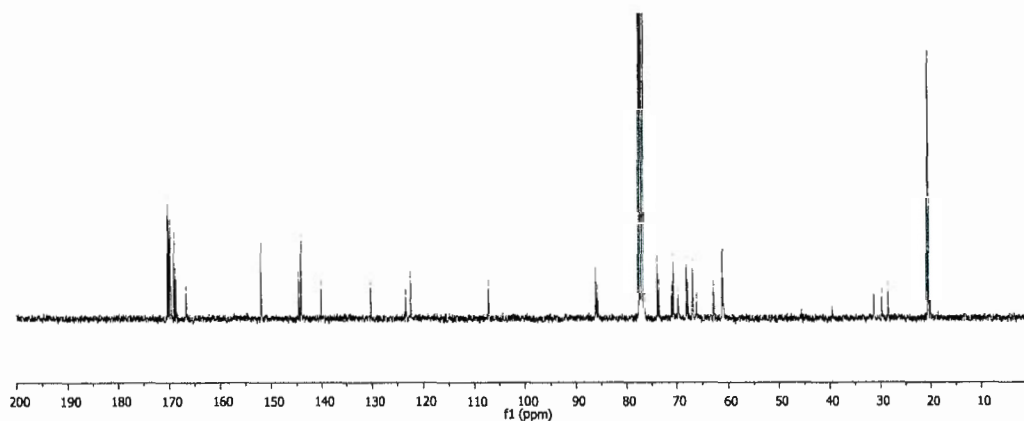


Figure S17. $^{13}\text{C}\{^1\text{H}\}$ NMR spectrum of compound 7 (75 MHz, CDCl_3).

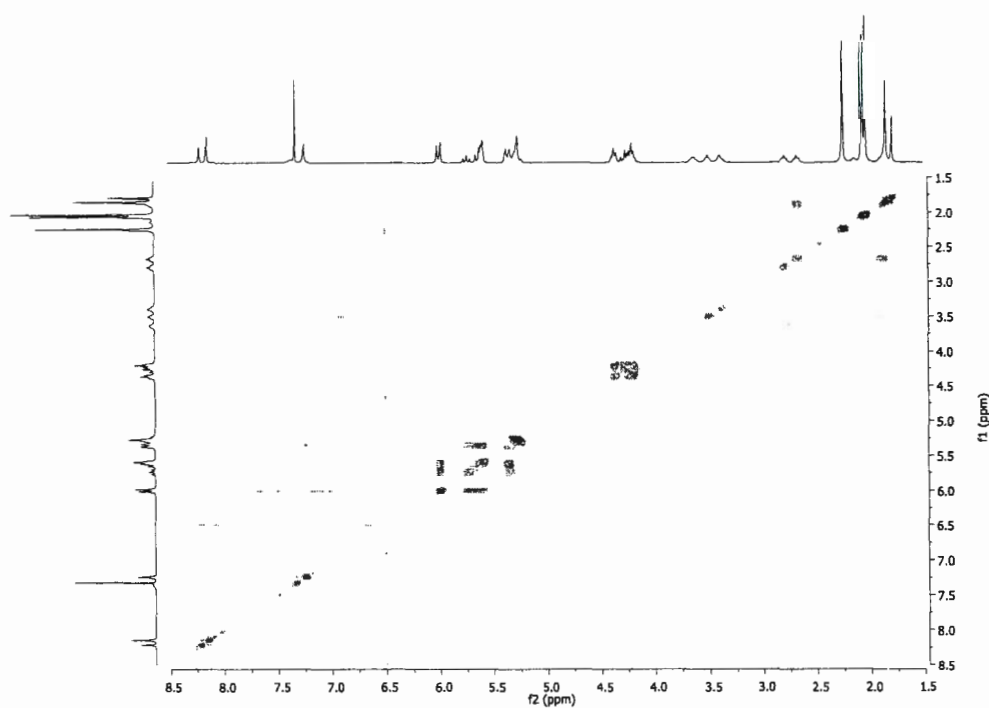


Figure S18. COSY spectrum of compound 7.

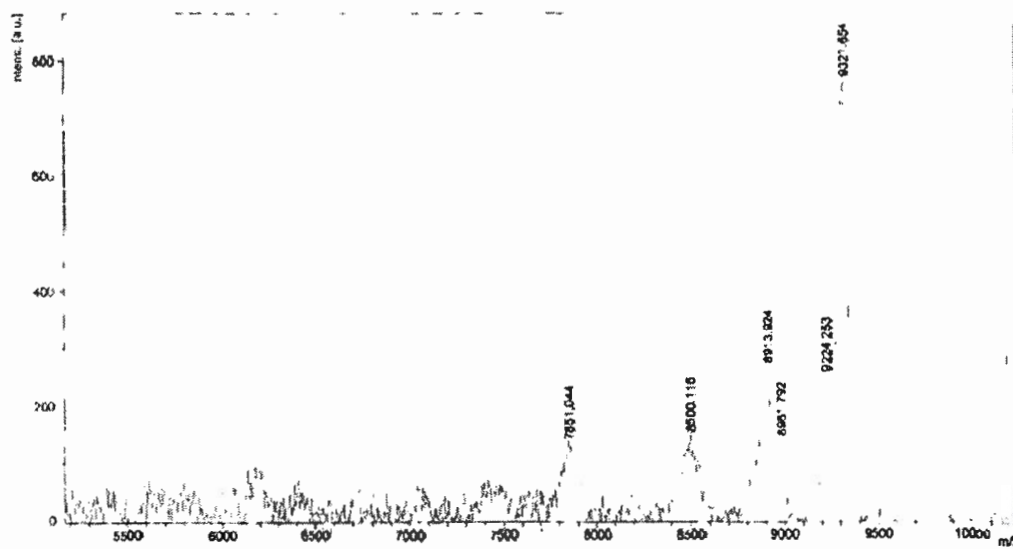


Figure S19. MALDI ToF spectrum of compound 7.

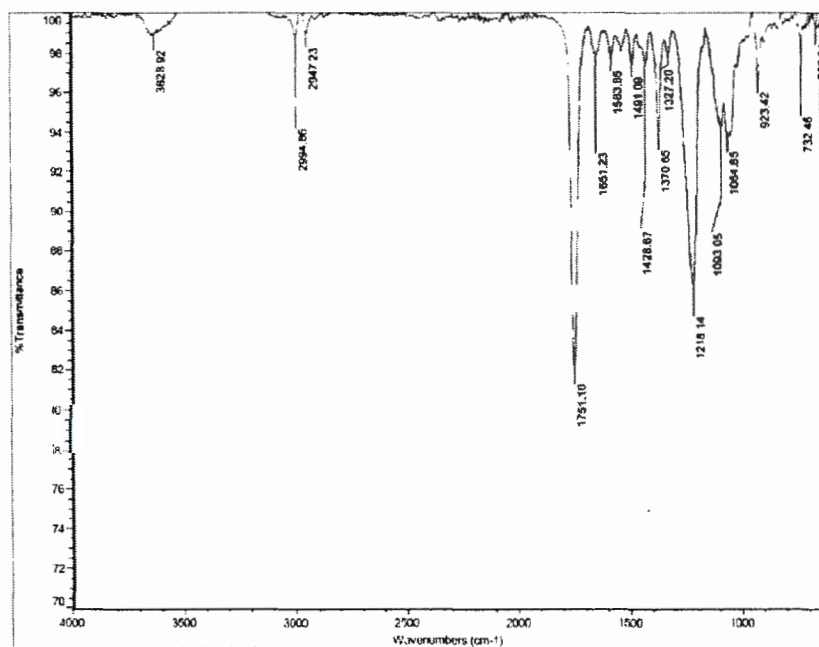


Figure S20. IR spectrum of compound 7.

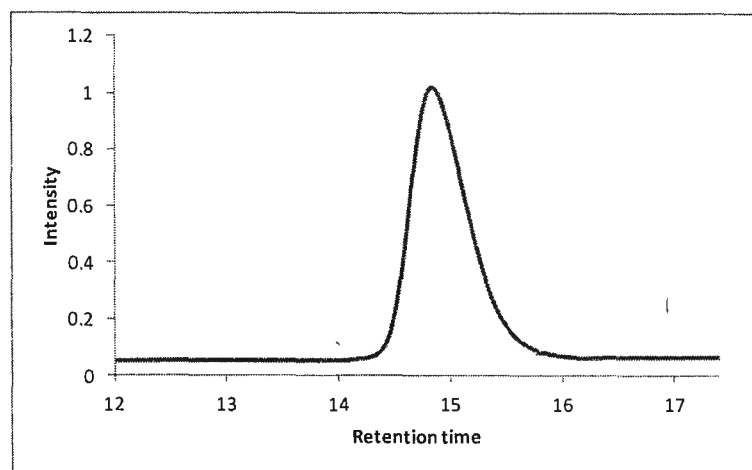
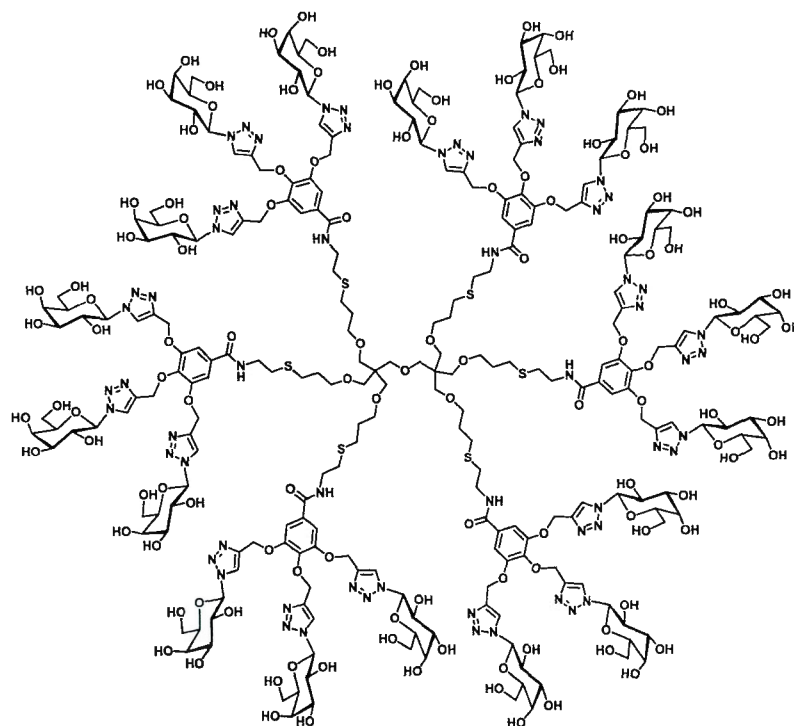


Figure S21. GPC traces of compound 7.



Synthesis of compound 8: To a stirring solution of compound 7 (100mg, 0.0107mmol) in MeOH (3mL) was slowly added 1M solution of MeONa in MeOH to adjust the pH 9–10. Reaction mixture was left for overnight stirring at room temperature. The reaction pH was then adjusted with H^+ resin to pH 6. Solvent was evaporated and the residue was dissolved in 3mL of water and washed with diethyl

ether (3×15mL) to remove impurities. Aqueous layer was finally lyophilized to yield **8** (58.8mg, 9.42μmol) as a white solid with a 88% yield.

¹H NMR (600 MHz, D₂O) δ 8.29 (s, 12H), 7.98 (s, 6H), 7.15 (s, 12H), 5.59 (d, *J* = 65.2 Hz, 18H), 5.04–4.79 (m, 112H), 4.29–3.22 (m, 150H), 2.68 (t, *J* = 56.2 Hz, 24H), 1.97–1.70 (m, 12H).

¹³C{¹H} NMR (151 MHz, D₂O) δ 168.6, 152.2, 144.0, 143.7, 139.3, 130.6, 125.2, 124.5, 107.3, 88.8, 88.6, 78.8, 73.7, 70.3, 69.8, 69.2, 65.8, 62.7, 61.4, 40.5, 30.1, 28.9.

IR (cm⁻¹) 3350, 2879, 1637, 1583, 1494, 1428, 1327, 1233, 1095, 1057, 891, 825, 760, 703.

HRMS (ESI⁺) *m/z* calc. for C₂₄₄H₃₄₆N₆₀O₁₂₁S₆, 1584.0165 ([*M*+4Na]⁴⁺); found, 1584.0122.

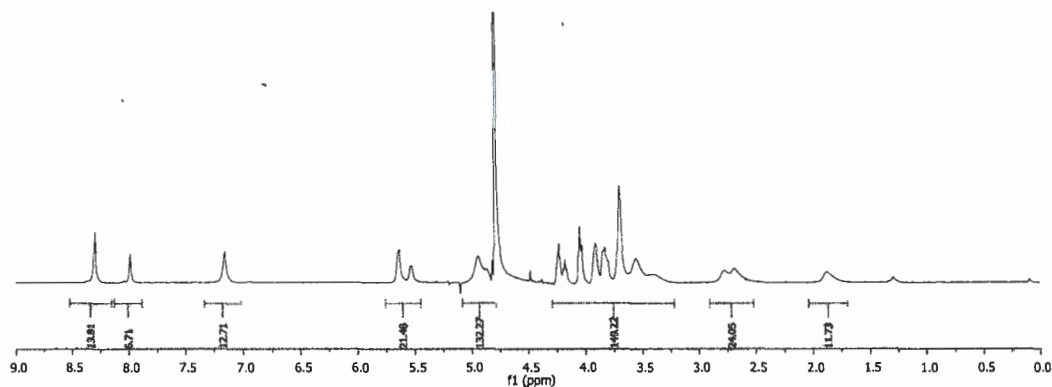


Figure S22. ¹H NMR spectrum of compound **8** (600 MHz, D₂O).

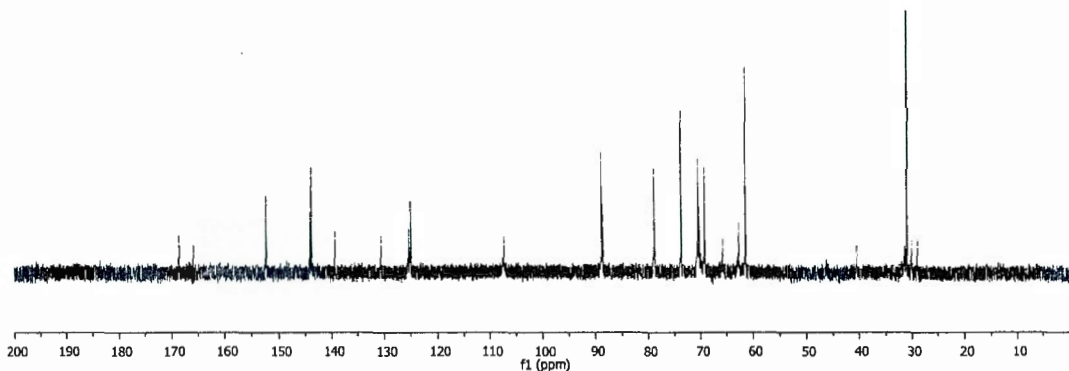


Figure S23. ¹³C{¹H} NMR spectrum of compound **8** (151 MHz, D₂O).

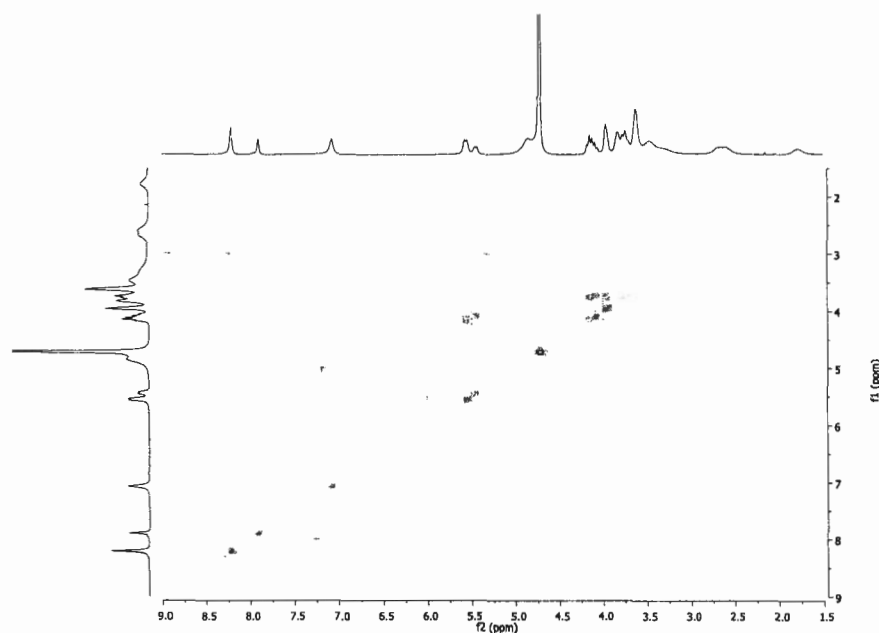


Figure S24. COSY spectrum of compound 8 (300 MHz, D₂O).

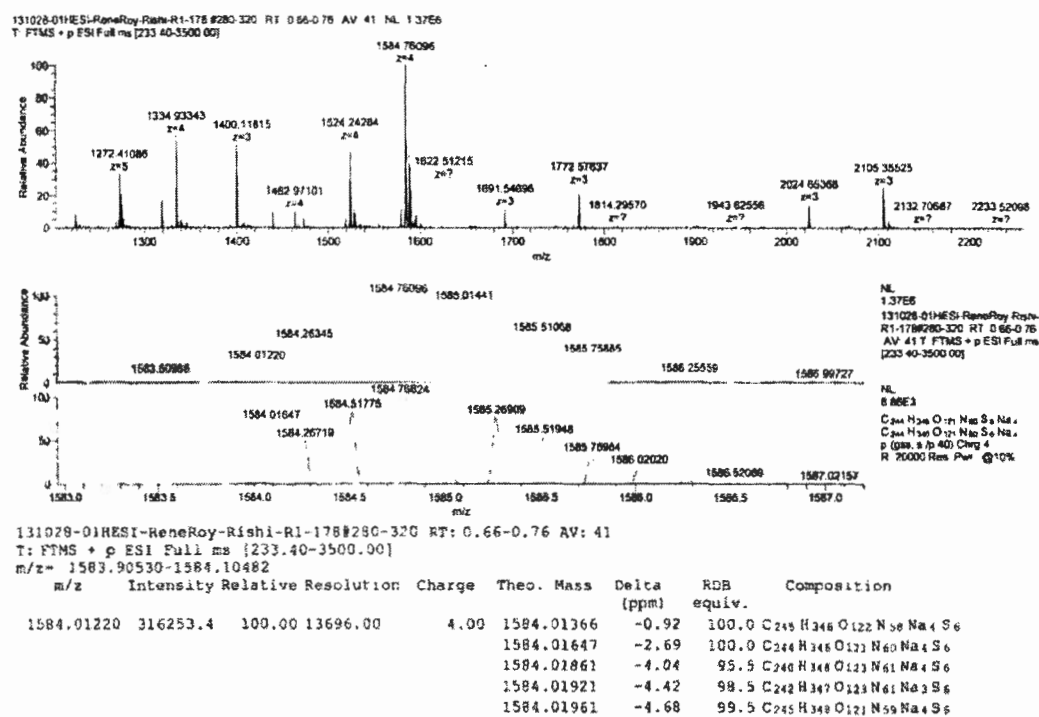


Figure S25. HRMS (ESI⁺) spectrum of compound 8.

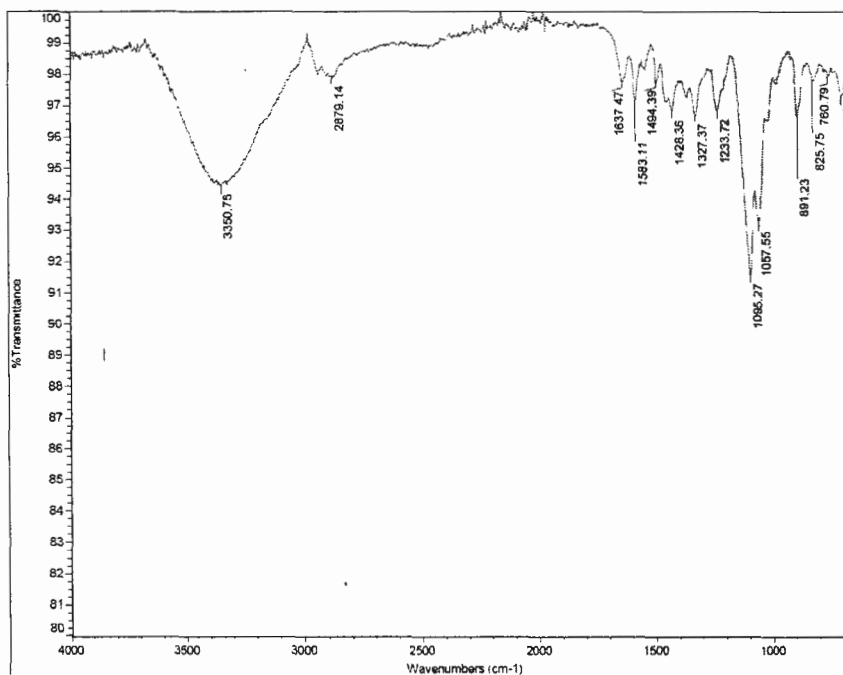
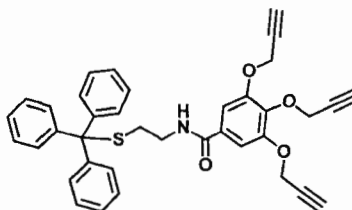


Figure S26. IR spectrum of compound **8**.



Synthesis of compound 10: To a stirring solution of tripropargyl gallic acid **4** (562mg, 1.98mmol) in DMF (3mL) were added EDC·HCl (529mg, 2.77mmol) and DMAP (290mg, 2.37mmol). The reaction mixture was stirred under nitrogen atmosphere for 15 minutes. Amine terminated compound **9** (600mg, 1.98mmol) was then added and the reaction mixture was stirred at 50°C for overnight. The completion of reaction was monitored by TLC. Upon completion, the reaction mixture was diluted with water (50mL) and extracted with ethyl acetate (3×30mL). The combined organic extracts were washed with 0.1N HCl (3×10mL), followed by saturated NaHCO₃ solution and brine. The organic layer was dried over anhydrous Na₂SO₄, filtered and evaporated under reduced pressure. The crude mixture was then purified by flash column chromatography using 2% MeOH in DCM as eluent to furnish **10** (905mg, 1.54mmol) in a 78% yield as an off-white solid.

^1H NMR (300 MHz, CDCl_3) δ 7.40–7.27 (m, 5H), 7.24–7.04 (m, 12H), 6.20 (s, 1H), 4.72 (dd, $J = 2.4, 2.4$ Hz, 6H), 3.20 (m, 2H), 2.46 (t, $J = 6.2$ Hz, 2H), 2.38 (t, $J = 2.4$ Hz, 1H), 2.32 (t, $J = 2.3$ Hz, 2H).

$^{13}\text{C}\{^1\text{H}\}$ NMR (75 MHz, CDCl_3) δ 166.1, 151.1, 144.3, 139.4, 130.0, 129.2, 127.7, 126.5, 107.5, 78.52, 77.8, 76.2, 75.5, 66.5, 60.0, 56.9, 38.4, 31.7.

IR (cm^{-1}): 3284, 3057, 2937, 2121, 1750, 1647, 1582, 1537, 1489, 1444, 1427, 1368, 1323, 1214, 1106, 1063, 952, 923, 734, 700.

HRMS (ESI^+) m/z calc for $\text{C}_{37}\text{H}_{31}\text{NO}_4\text{S}$, 608.1866 $[\text{M}+\text{Na}]^+$; found, 608.1863.

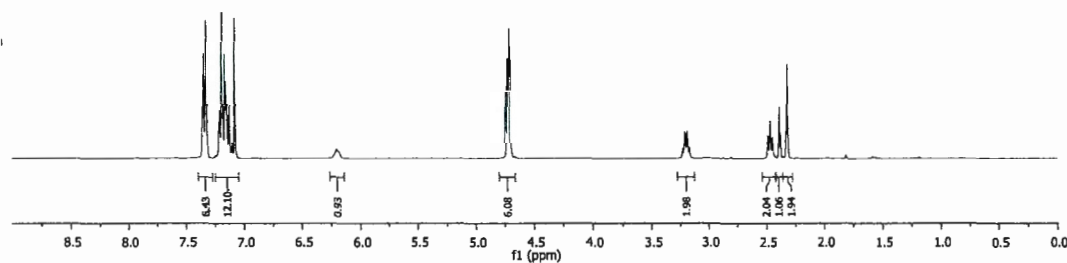


Figure S27. ^1H NMR spectrum of compound 10 (300 MHz, CDCl_3).

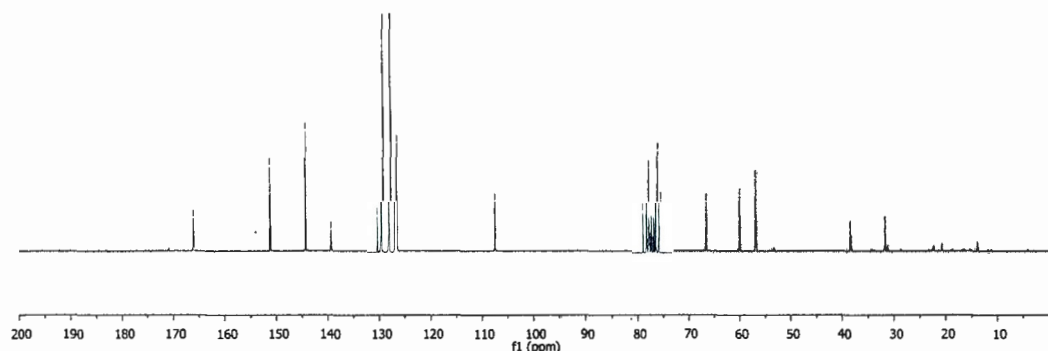


Figure S28. $^{13}\text{C}\{^1\text{H}\}$ NMR spectrum of compound 10 (75 MHz, CDCl_3).

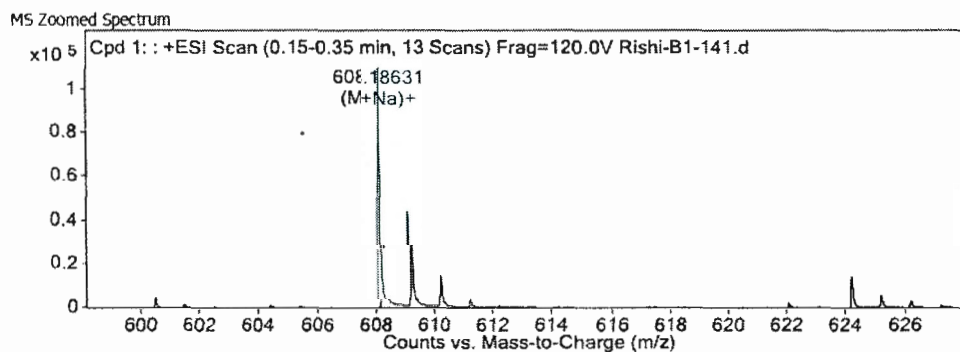


Figure S29. HRMS (ESI^+) spectrum of compound 10.

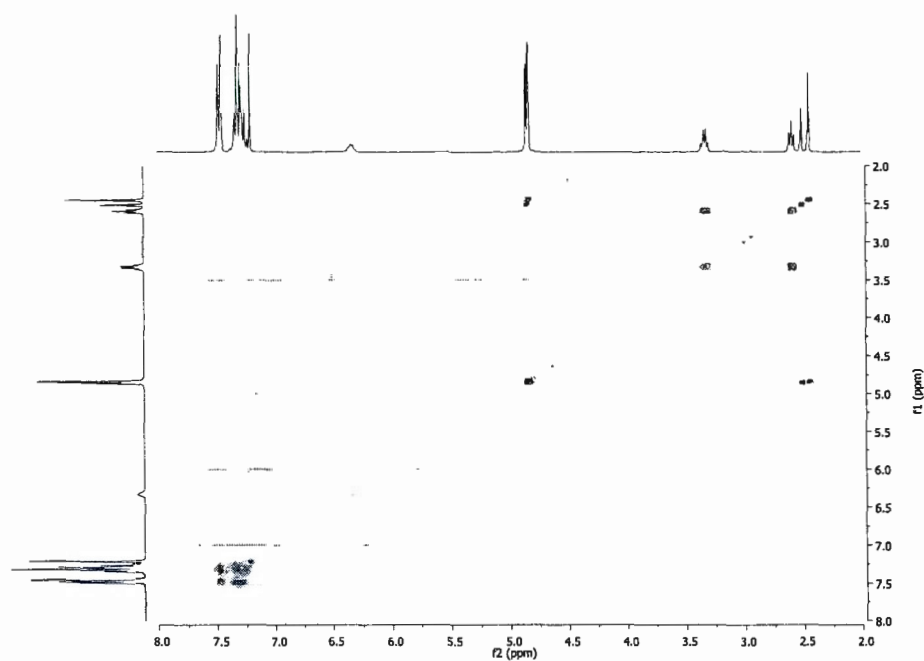


Figure S30. COSY spectrum of compound 10.

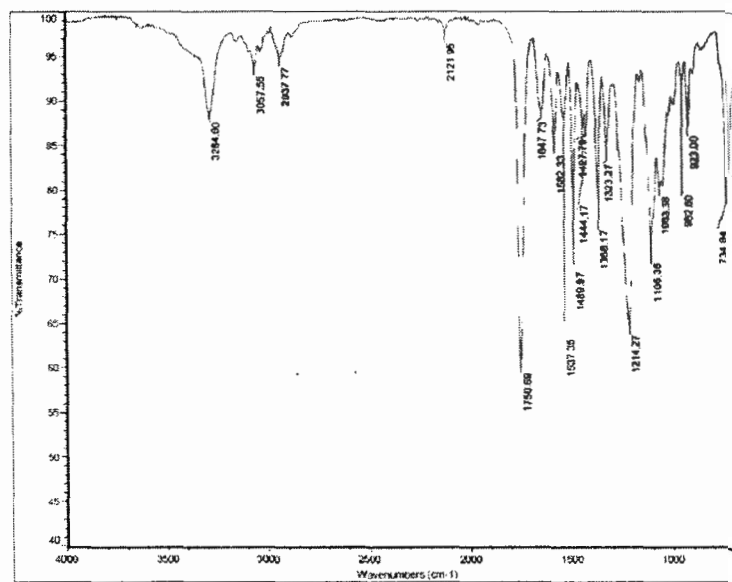
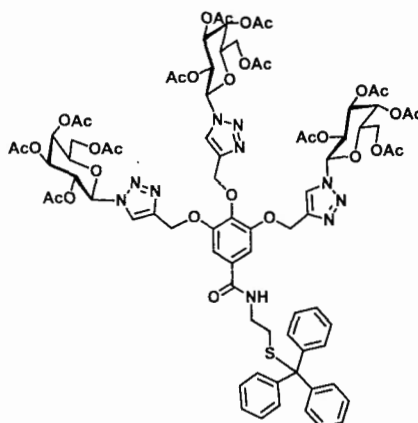


Figure S31. IR spectrum of compound 10.



Synthesis of compound 11: To a solution of compound **10** (200mg, 0.341mmol) in THF (2mL) was added galactosyl azide **6** (442mg, 1.196mmol) dissolved in THF (3mL), followed by the addition of sodium ascorbate (67mg, 0.34mmol). An aqueous solution of $\text{CuSO}_4 \cdot 5\text{H}_2\text{O}$ (85mg, 0.34mmol) was added and the final ratio of H_2O and THF was kept 1:1. The reaction mixture was stirred at 40°C for 12 hrs. The progress of the reaction was monitored with the help of TLC. Upon completion, reaction mixture was diluted with EtOAc (25mL) and washed with saturated solution of EDTA ($2 \times 15\text{mL}$). Organic layer was finally washed with brine solution, dried with anhydrous Na_2SO_4 , filtered and concentrated under reduced pressure. Purification of the residue was achieved *via* flash column chromatography on silica gel using 2% MeOH in DCM as eluent to afford the desired compound **11** (488mg, 0.286mmol) in a 84% yield as an off-white solid.

^1H NMR (300 MHz, CDCl_3) δ 8.16 (s, 1H), 8.04 (s, 2H), 7.49–7.38 (m, 6H), 7.30–7.17 (m, 15H), 7.09 (s, 2H), 6.47 (s, 1H), 5.90 (m, 3H), 5.69 (t, $J = 9.8$ Hz, 1H), 5.63–5.45 (m, 5H), 5.39–5.20 (m, 9H), 4.37–4.10 (m, 9H), 3.34–3.13 (m, 2H), 2.51 (t, $J = 6.5$ Hz, 2H), 2.22 (s, 9H), 2.08–1.98 (m, 18H), 1.82 (s, 6H), 1.77 (s, 3H).

$^{13}\text{C}\{^1\text{H}\}$ NMR (75 MHz, CDCl_3) δ 170.1, 170.0, 169.9, 169.8, 169.4, 168.8, 168.5, 166.2, 151.6, 144.4, 143.8, 140.0, 130.0, 129.2, 127.7, 126.5, 122.9, 121.9, 107.1, 85.9, 85.5, 73.5, 70.8, 70.4, 67.8, 67.6, 66.6, 65.9, 62.7, 60.9, 38.7, 31.7, 20.3, 19.9.

IR (cm^{-1}) 2980, 1750, 1654, 1584, 1535, 1490, 1428, 1369, 1324, 1216, 1100, 1047, 953, 923, 733, 702.

HRMS (ESI^+) m/z calc for $\text{C}_{79}\text{H}_{88}\text{N}_{10}\text{O}_{31}\text{S}$, 1727.5230 $[\text{M}+\text{Na}]^+$; found, 1727.5256, 1705.5410 $[\text{M}+\text{H}]^+$; found 1705.5452.

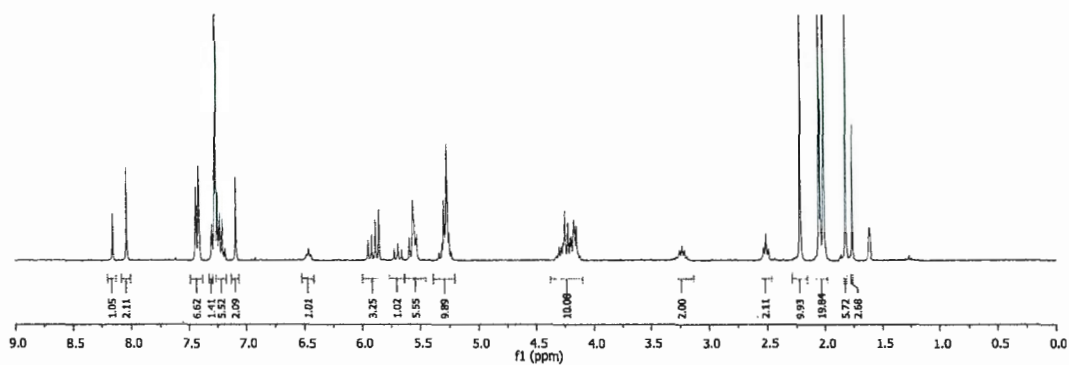


Figure S32. ^1H NMR spectrum of compound **11** (300 MHz, CDCl_3).

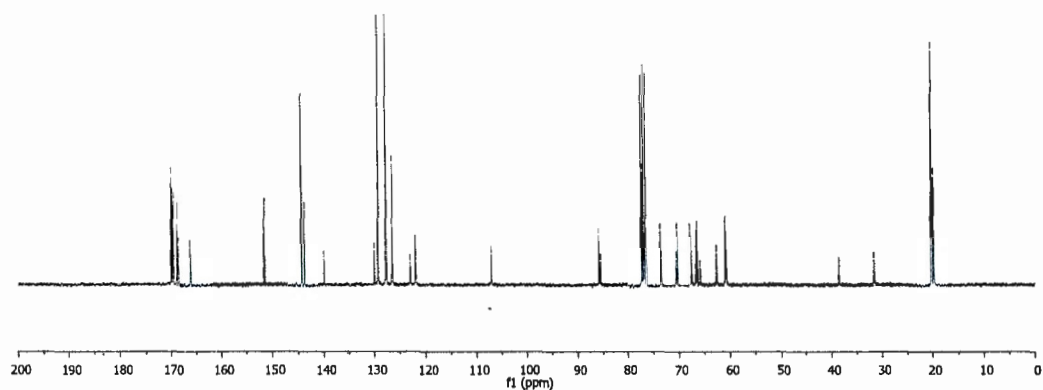


Figure S33. $^{13}\text{C}\{^1\text{H}\}$ NMR spectrum of compound **11** (75 MHz, CDCl_3).

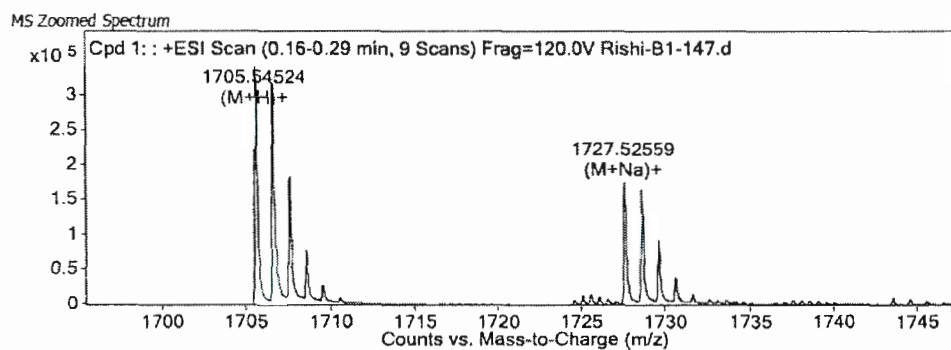


Figure S34. HRMS (ESI^+) spectrum of compound **11**.

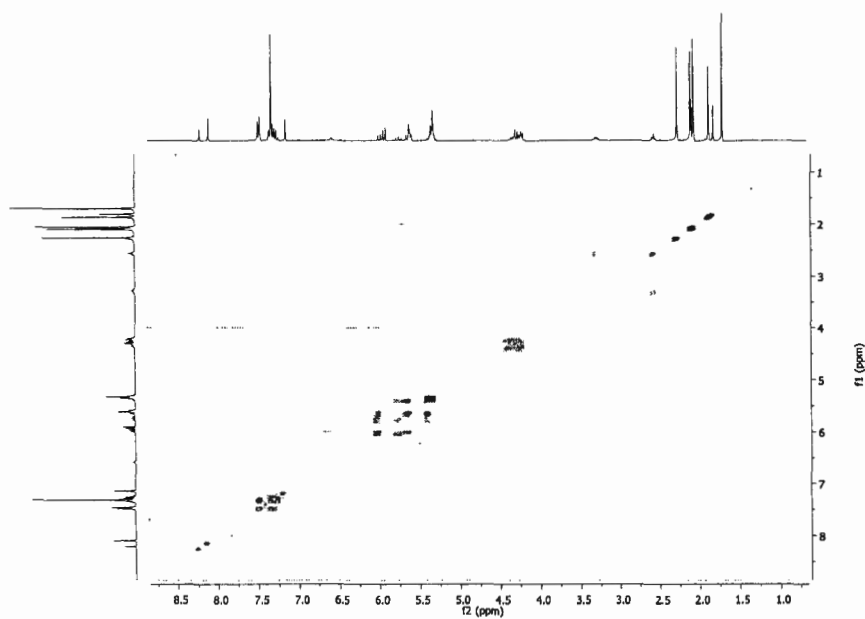


Figure S35. COSY spectrum of compound 11.

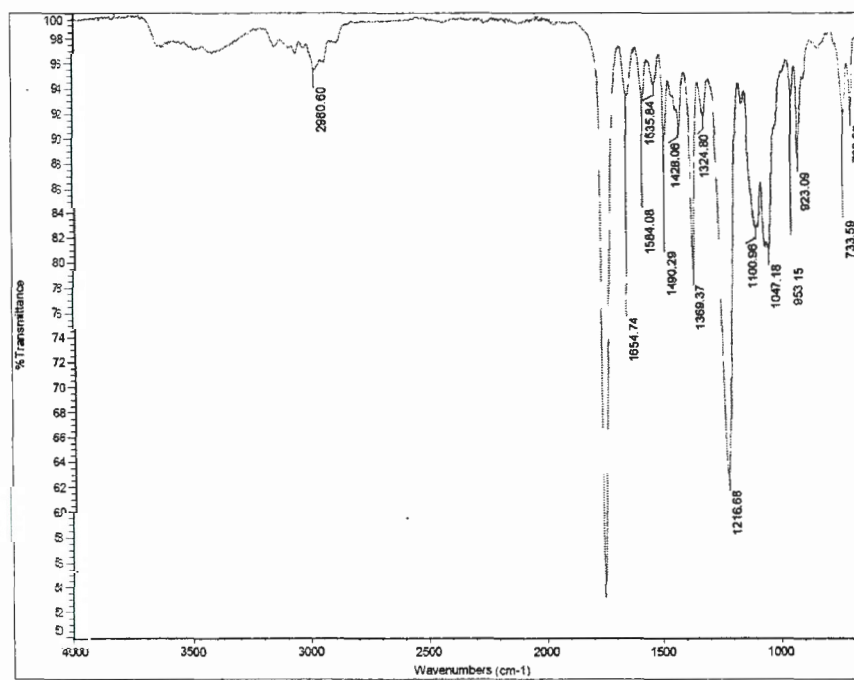
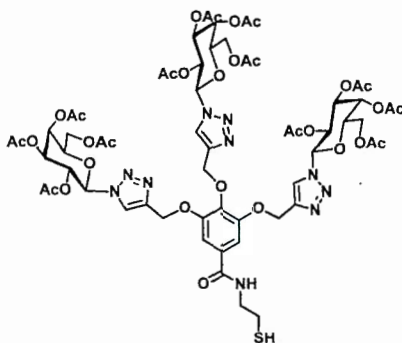


Figure S36. IR spectrum of compound 11.



Synthesis of compound 12: To a stirring solution of 3% trifluoroacetic acid in DCM (1.5mL), was added a solution of **11** (300mg, 0.176mmol) in dichloromethane (1.5mL). Et₃SiH (28μL, 0.18mmol) was added to the orange solution. After 3 hrs, toluene (4mL) was added and the solvents were evaporated under vacuum. The addition of toluene and evaporation was repeated twice. The product **12** was isolated by quick flash chromatography using 3% MeOH in DCM in a 86% yield (221mg, 0.151mmol).

¹H NMR (300 MHz, CDCl₃) δ 8.15 (s, 1H), 8.04 (s, 2H), 7.16 (s, 2H), 6.91 (s, 1H), 5.91 (m, 3H), 5.67 (t, *J* = 9.8 Hz, 1H), 5.64–5.48 (m, 5H), 5.39–5.17 (m, 9H), 4.39–4.06 (m, 9H), 3.73–3.46 (m, 2H), 2.76 (dd, *J* = 14.9, 6.5 Hz, 2H), 2.22 (d, *J* = 2.3 Hz, 9H), 2.14–1.96 (m, 18H), 1.81 (d, *J* = 18.4 Hz, 9H), 1.48 (t, *S_H*, *J* = 8.5 Hz, 1H).

¹³C{¹H} NMR (75 MHz, CDCl₃) δ 170.3, 169.9, 169.2, 168.8, 151.9, 144.2, 107.4, 86.3, 74.0, 70.7, 68.2, 66.8, 62.9, 61.1, 43.0, 24.5, 20.6, 20.2.

IR (cm⁻¹) 3649, 2980, 2888, 1754, 1382, 1249, 1153, 1079, 955.

HRMS (ESI⁺) *m/z* calc for C₆₀H₇₄N₁₀O₃₁S 1463.4315 [*M*+H]⁺; found, 1463.4317.

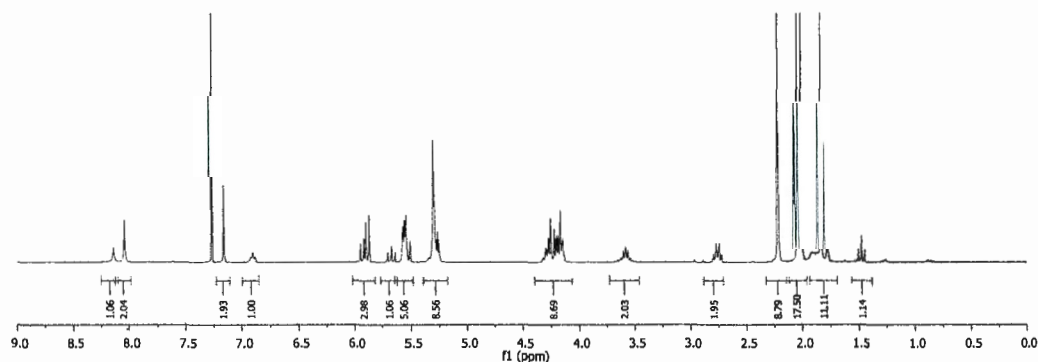


Figure S37. ¹H NMR spectrum of compound **12** (300 MHz, CDCl₃).

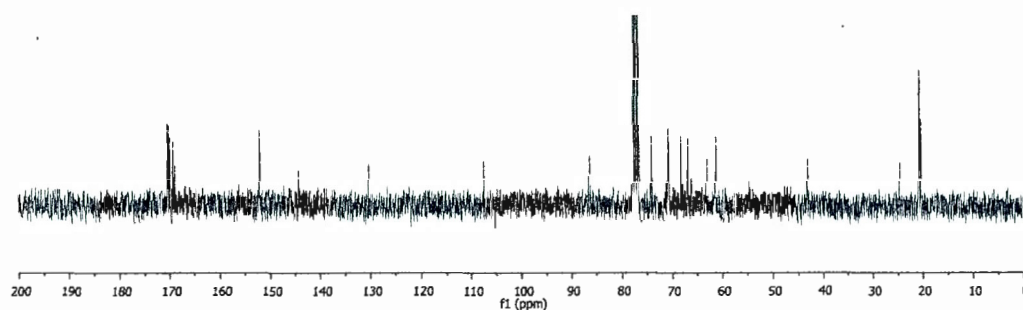


Figure S38. $^{13}\text{C}\{^1\text{H}\}$ NMR spectrum of compound **12** (75 MHz, CDCl_3).

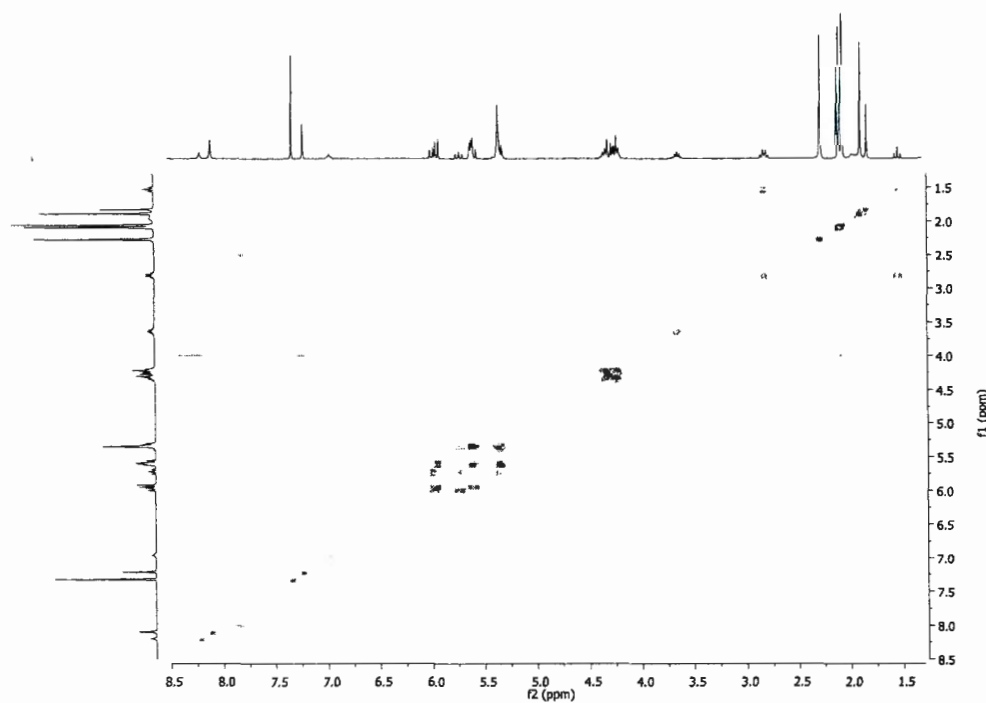


Figure S39. COSY spectrum of compound **12**.

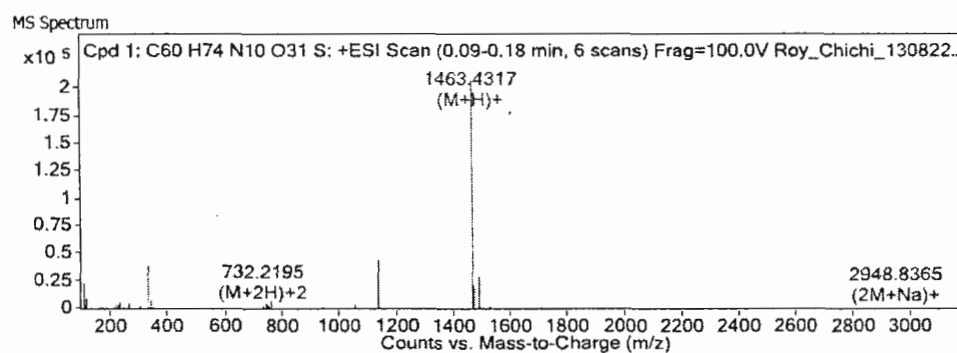


Figure S40. HRMS (ESI^+) spectrum of compound **12**.

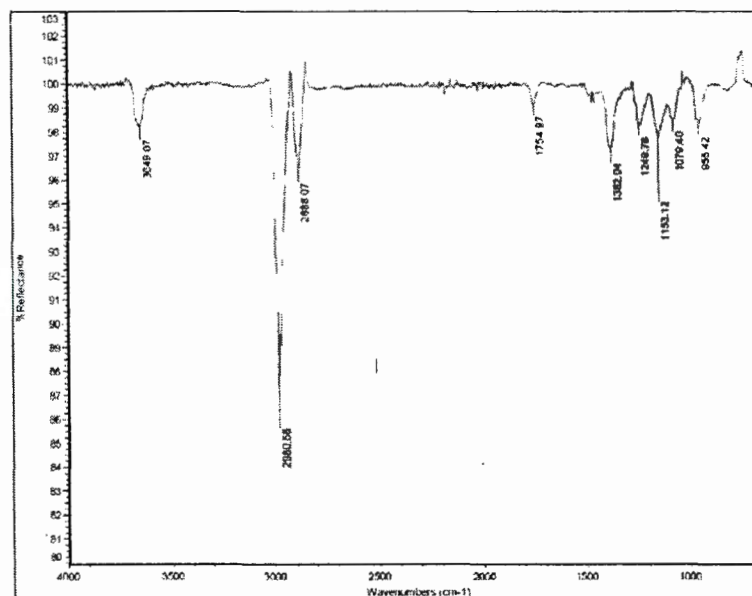
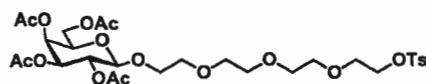


Figure S41. I.R spectrum of compound **12** (75 MHz, CDCl_3).

Synthesis of galactodendrimer 7 according to a convergent strategy

Compound **2** (3mg, $6\mu\text{mol}$) and compound **12** (263mg, 0.180mmol , 5eq/alkene) were suspended in dioxane (1mL) in a 5 mL glass vial equipped with a small magnetic stirring bar. To this was added AIBN (1mg, $0.5\mu\text{mol}$, 0.15eq/alkene), and the vial was tightly sealed with an aluminum/Teflon® crimp top. The mixture was then heated at 75°C for 5 hrs. After completion of the reaction, the vial was cooled to 25°C before it was opened. Dioxane was removed under vacuum. Purification of the crude compound was achieved *via* flash column chromatography on silica gel using 2-4% MeOH in DCM as eluent gradient to afford desired compound **7** (29.8mg, $3.22\mu\text{mol}$) in 53% yield as a white solid. *Spectroscopic data for compound 7 obtained via convergent strategy are in full agreement with those of one originated from divergent approach.*



Synthesis of compound 15: β -D-Galactopyranose pentaacetate **13** (300mg, 0.769mmol) and monotosylated tetra(ethylene)glycol **14** (669mg, 1.92mmol) were mixed in dry DCM (5mL) and stirred for 1 hr with 4\AA molecular sieves. The reaction mixture was then cooled to 0°C , followed by the addition of $\text{BF}_3 \cdot \text{Et}_2\text{O}$ ($660\mu\text{L}$, 5.38mmol). The reaction mixture was stirred for 4 hrs at room temperature. Upon

completion of reaction, the mixture was diluted with DCM (30mL), washed with water, saturated NaHCO₃ solution followed by brine. Drying over Na₂SO₄ and concentration under vacuum afforded crude compound that was purified by column chromatography (60% EtOAc in hexanes as eluent) to give **15** (287mg, 0.423mmol) colourless oil in 55% yield.

¹H NMR (300 MHz, CDCl₃) δ 7.81 (d, *J* = 8.2 Hz, 2H), 7.35 (d, *J* = 8.2 Hz, 2H), 5.39 (d, *J* = 3.3 Hz, 1H), 5.21 (dd, *J* = 10.4, 8.0 Hz, 1H), 5.02 (dd, *J* = 10.5, 3.4 Hz, 1H), 4.57 (d, *J* = 7.9 Hz, 1H), 4.15 (dt, *J* = 15.5, 7.8 Hz, 4H), 4.05 – 3.87 (m, 2H), 3.82–3.53 (m, 13H), 2.46 (s, 3H), 2.15 (s, 3H), 2.06 (d, *J* = 1.9 Hz, 6H), 1.99 (s, 3H).

¹³C{¹H} NMR (75 MHz, CDCl₃) δ 170.2, 170.1, 169.9, 169.3, 144.6, 132.8, 129.6, 127.7, 101.1, 77.2, 70.5, 70.4, 70.4, 70.3, 68.8, 66.9, 61.1, 21.4, 20.5, 20.5, 20.4.

IR (cm⁻¹) 2923, 1748, 1367, 1221, 1176, 1075.

HRMS (ESI⁺) *m/z* calc for C₂₉H₄₂O₁₆S, 701.2086 [*M*+Na]⁺; found, 701.2073.

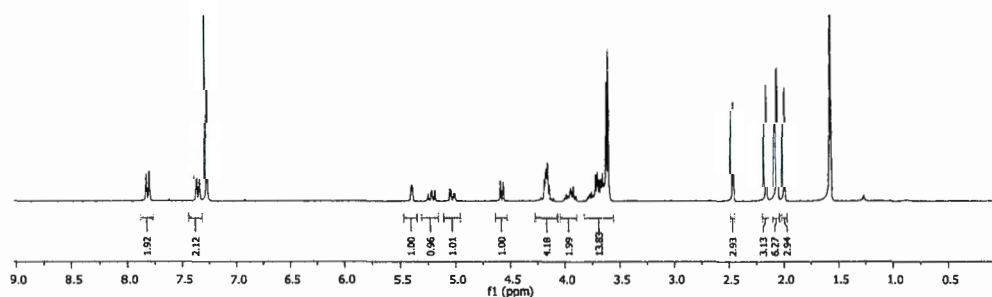


Figure S42. ¹H NMR spectrum of compound **15** (300 MHz, CDCl₃).

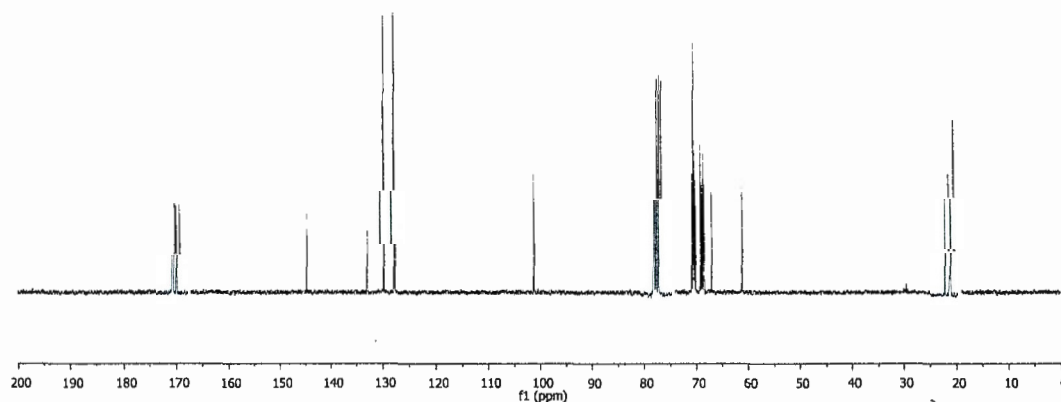


Figure S43. ¹³C{¹H} NMR spectrum of compound **15** (75 MHz, CDCl₃).

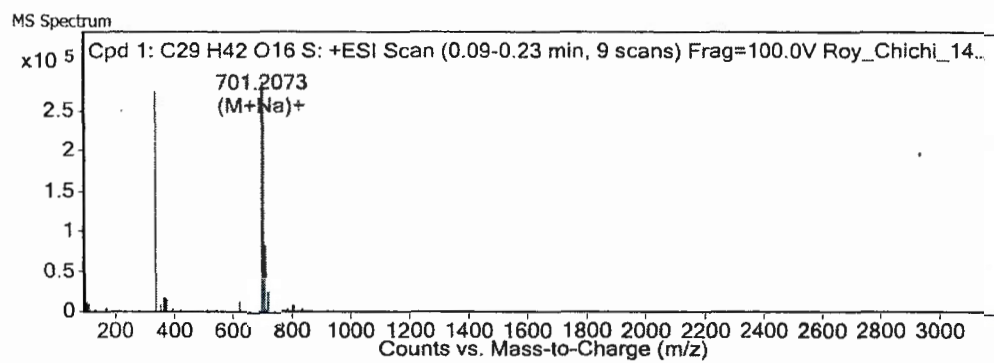


Figure S44. HRMS (ESI⁺) spectrum of compound **15**.

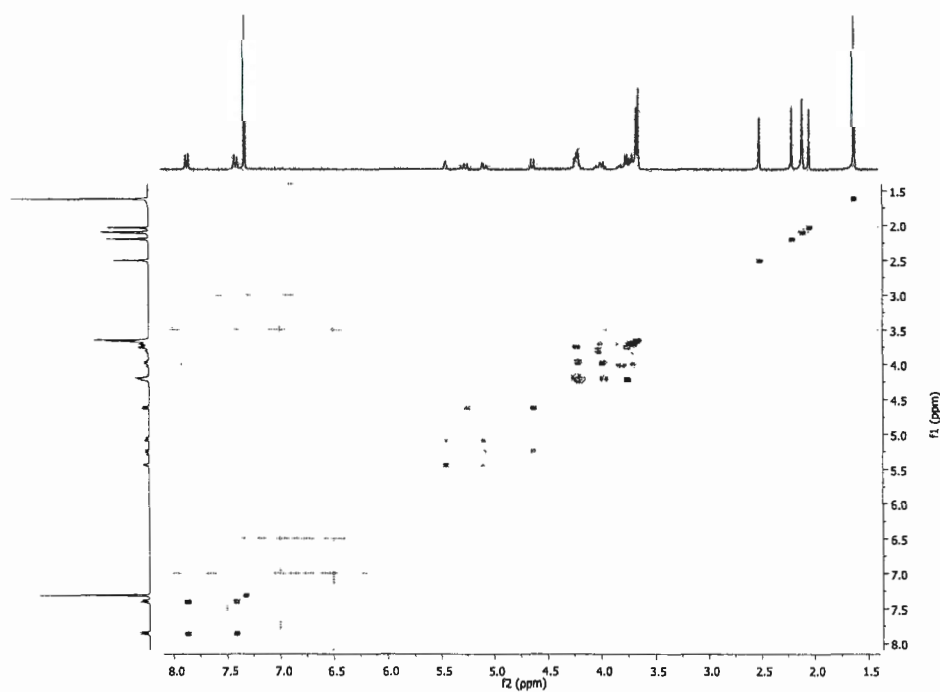


Figure S45. COSY spectrum of compound **15**.

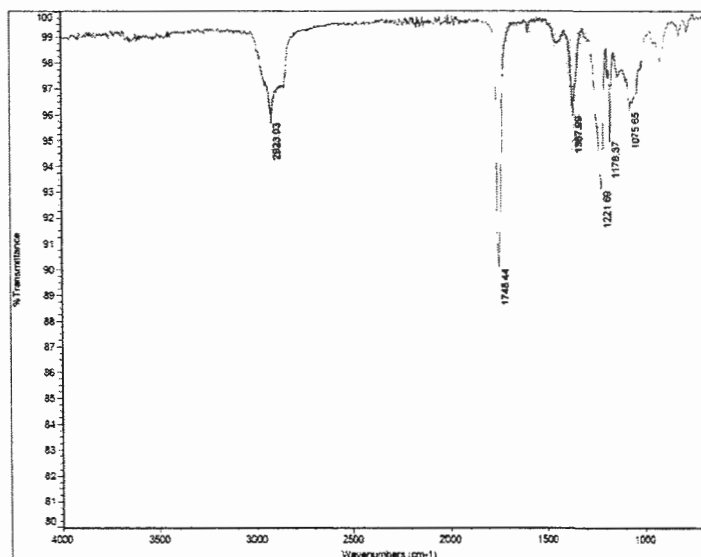
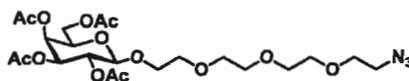


Figure S46. IR spectrum of compound **15**.



Synthesis of compound 16: Compound **15** (2.000g, 2.949mmol) and sodium azide (958mg, 15.0mmol) in dry DMF (20mL) were stirred at 80°C for 6 hrs. The solvent was evaporated under reduced pressure and crude was diluted with ethyl acetate (50mL), washed with water (2×30mL) and brine, dried over Na₂SO₄ and concentrated in *vacuo*. Column chromatography of the residual crude mixture was performed using 60% EtOAc in hexanes as eluent to give **16** (1.329g, 2.410mmol) as a yellowish oil in 82% yield.

¹H NMR (600 MHz, CDCl₃) δ 5.42–5.35 (m, 1H), 5.24–5.15 (m, 1H), 5.00 (ddd, *J* = 10.5, 3.4, 1.7 Hz, 1H), 4.56 (dd, *J* = 8.0, 1.6 Hz, 1H), 4.14 (dddd, *J* = 25.6, 11.3, 6.7, 1.5 Hz, 2H), 4.01–3.87 (m, 2H), 3.80–3.70 (m, 1H), 3.72–3.58 (m, 12H), 3.38 (t, *J* = 4.3 Hz, 2H), 2.13 (d, *J* = 1.7 Hz, 3H), 2.11–2.00 (m, 5H), 1.97 (d, *J* = 1.7 Hz, 3H).

¹³C{¹H} NMR (151 MHz, CDCl₃) δ 170.4, 170.2, 170.1, 169.5, 101.3, 70.9, 70.7, 70.6, 70.3, 70.0, 69.0, 68.8, 67.0, 61.3, 50.6, 20.7, 20.6, 20.6, 20.6.

IR (cm⁻¹) 2980, 2881, 2098, 1749, 1369, 1223, 1073.

HRMS (ESI⁺) *m/z* calc for C₂₂H₃₅N₃O₁₃, 567.2508 [*M*+NH₄]⁺; found, 567.2480, 588.1802 [*M*+K]⁺; 588.1789.

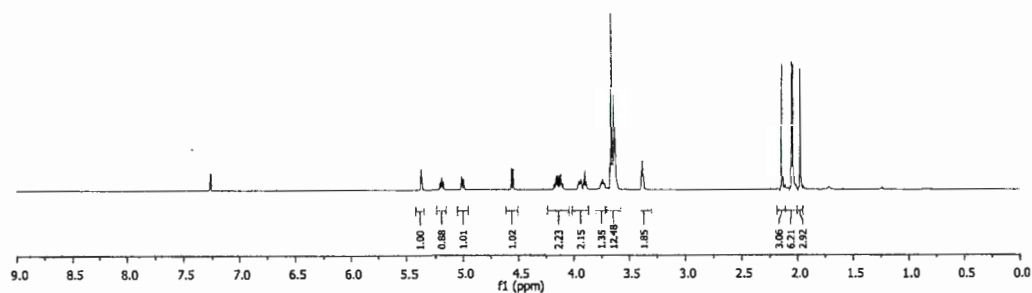


Figure S47. ¹H NMR spectrum of compound **16** (600 MHz, CDCl₃).

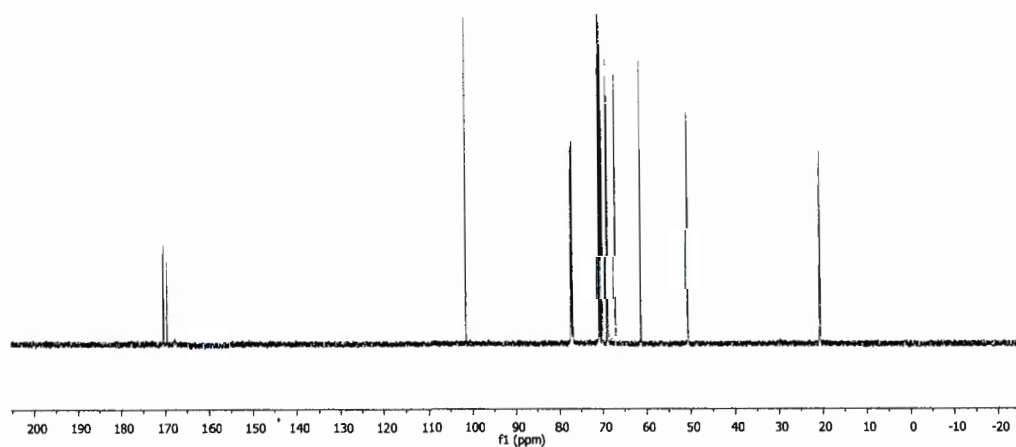


Figure S48. ¹³C{¹H} NMR spectrum of compound **16** (151 MHz, CDCl₃).

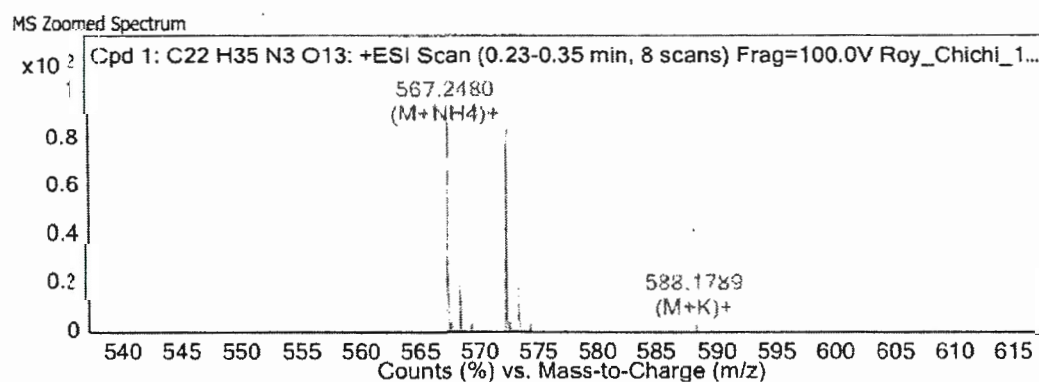


Figure S49. HRMS (ESI⁺) spectrum of compound **16**.

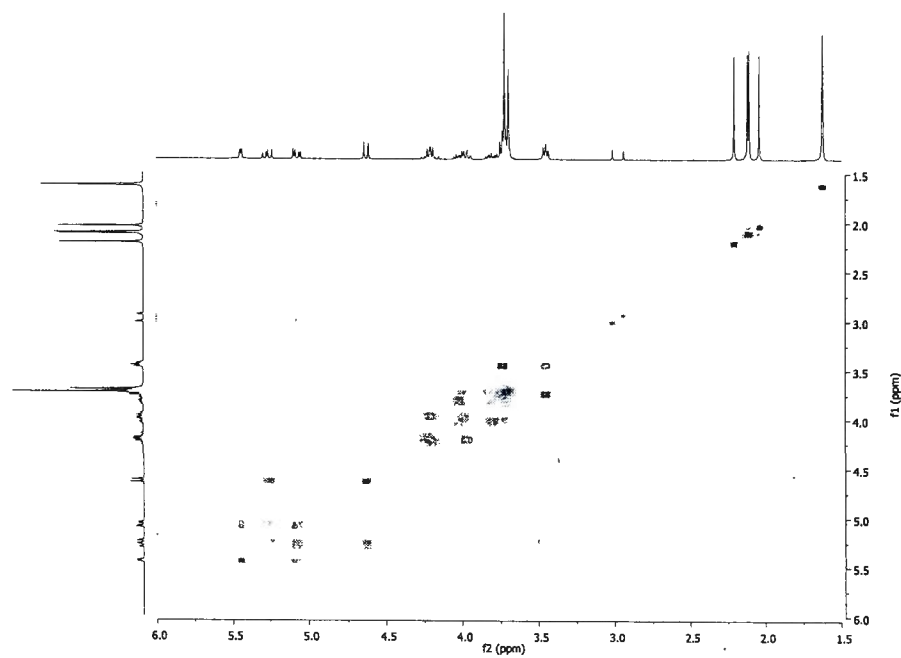


Figure S50. COSY NMR spectrum of compound 16.

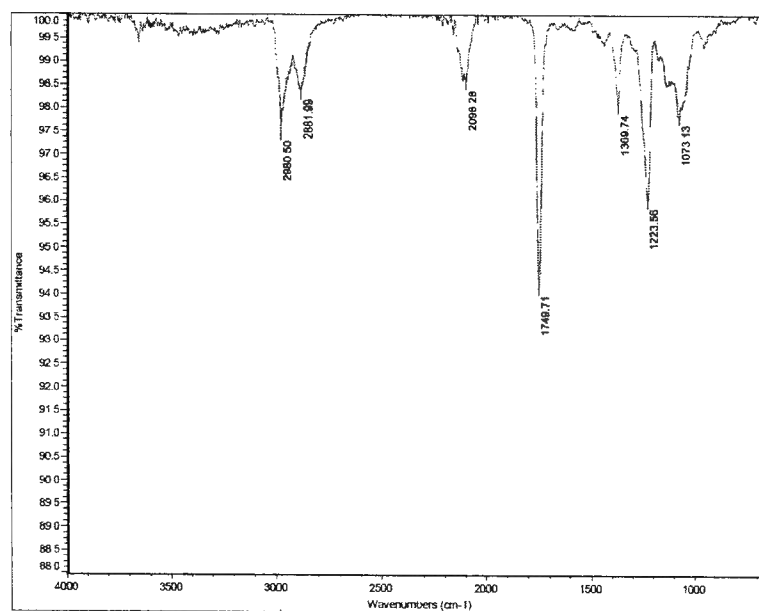
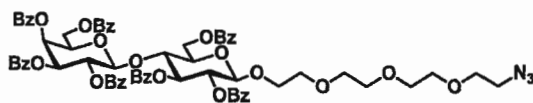


Figure S51. IR spectrum of compound 16.



Synthesis of compound 17: To a solution of per-*O*-acetylated lactose (β anomer,¹ 5.00g, 7.40mmol) and tetra(ethylene)glycol monotosylate (synthesized as previously described,² 8.10g, 22.1mmol) in dry DCM (60mL) under a nitrogen atmosphere and at 0°C was added dropwise $\text{BF}_3 \cdot \text{Et}_2\text{O}$ (2.7mL, 22.1mmol) over a 15 minutes period. After stirring overnight (12 hrs) at r.t., the solvent was removed and EtOAc was added, then the solution was washed successively with NaHCO_3 (40mL), water (40mL) and brine (40mL). The organic phase was then dried over MgSO_4 and concentrated under reduced pressure. The crude residue was directly re-dissolved in DMF (70mL) under a nitrogen atmosphere and sodium azide (962mg, 14.8mmol) together with sodium iodide (11.1mg, 0.11mmol) were added. After stirring overnight (16 h) at 70°C, the solvent was removed and EtOAc (100mL) was added, then the solution was washed successively with water (4×40mL) and brine (3×50mL). The organic phase was then dried over MgSO_4 and concentrated under reduced pressure. After a short flash column chromatography on silica (EtOAc/Hexanes 6:4 to 8:2), the crude was subjected to de-*O*-acetylation protocol and dissolved in MeOH (40mL). To this solution was slowly added 1M MeONa/MeOH to adjust the pH 9–10. Reaction mixture was left for stirring overnight. The reaction pH was then adjusted with H^+ resin to adjust pH to 6. Solvent was evaporated and the residue was benzoylated with benzoyl chloride (20.8g, 17.2mL, 148mmol) in pyridine (50mL) for overnight stirring at room temperature. Upon completion solvents were removed and reaction mixture was dissolved in DCM (100mL) and washed with 0.1N HCl (3×50 mL) followed by saturated solution of NaHCO_3 (3×75mL) and finally with brine. Organic layer was then dried with anhydrous sodium sulphate filtered and evaporated. Crude compound was then purified with the help of column chromatography using Hexane/Ethyl Acetate (1:1) as eluent. Desired compound 17 (5.93g, 4.66mmol) was isolated in a 63% overall yield as a yellow oil.

¹ Wolfrom, M. L., Thompson, A. *Methods. Carbohydr. Chem.* **1963**, 211-215.

² Zhang, L.; Sun, L.; Cui, Z.; Gottlieb, R. L.; Zhang, B. *Bioconjugate Chem.* **2001**, 12, 939-948.

^1H NMR (300 MHz, CDCl_3) δ 8.12–7.94 (m, 10H), 7.94–7.87 (m, 2H), 7.77–7.69 (m, 2H), 7.69–7.29 (m, 17H), 7.18 (m, 4H), 5.87–5.68 (m, 3H), 5.53–5.41 (m, 1H), 5.37 (dd, $J = 10.3, 3.4$ Hz, 1H), 4.86 (dd, $J = 10.8, 7.9$ Hz, 2H), 4.61 (d, $J = 11.1$ Hz, 1H), 4.49 (dd, $J = 12.1, 4.0$ Hz, 1H), 4.26 (t, $J = 9.5$ Hz, 1H), 3.87 (dd, $J = 13.3, 8.1$ Hz, 3H), 3.69 (ddd, $J = 14.0, 10.4, 5.0$ Hz, 5H), 3.62–3.48 (m, 6H), 3.47–3.33 (m, 6H).

^{13}C NMR (75 MHz, CDCl_3) δ 165.8, 165.5, 165.4, 165.2, 165.1, 164.8, 133.5, 133.4, 133.2, 133.7, 130.0, 129.8, 129.7, 129.6, 129.6, 129.5, 129.4, 128.8, 128.7, 128.6, 128.5, 128.5, 128.31, 128.20, 101.2, 101.0, 76.0, 72.9, 72.9, 71.8, 70.6, 70.5, 70.5, 70.3, 69.9, 69.9, 69.2, 67.5, 62.4, 61.0, 50.6.

IR (cm^{-1}) 2980, 2883, 2104, 1728, 1601, 1451, 1314, 1267, 1176, 1094, 1069, 1027, 709.

HRMS (ESI $^+$) m/z calc for $\text{C}_{69}\text{H}_{65}\text{N}_3\text{O}_{21}$, 1294.4003 [$M+\text{Na}$] $^+$; found, 1294.4031

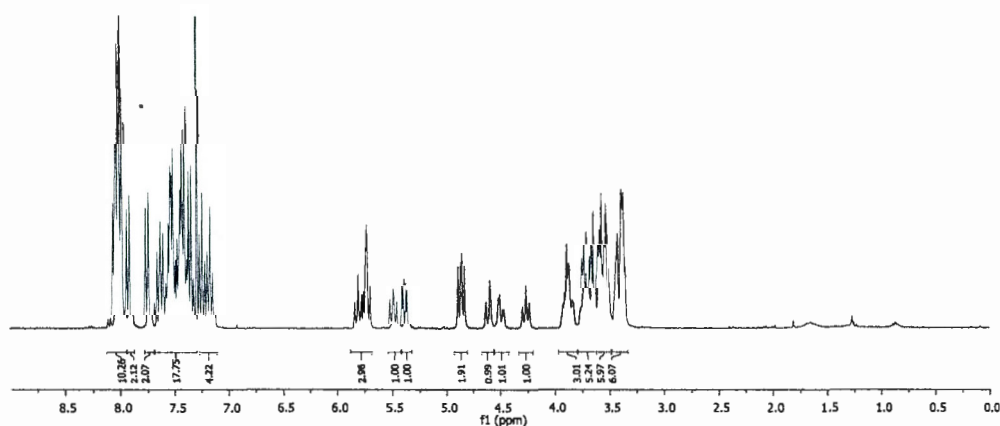


Figure S52. ^1H NMR spectrum of compound 17 (300 MHz, CDCl_3).

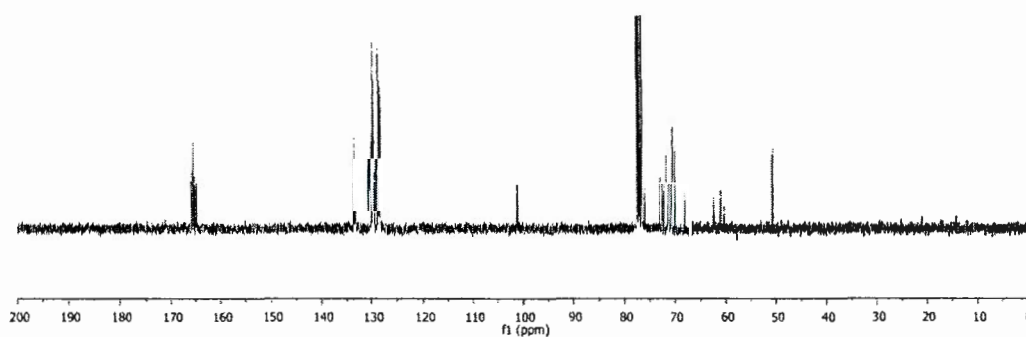


Figure S53. $^{13}\text{C}\{^1\text{H}\}$ NMR spectrum of compound 17 (300 MHz, CDCl_3)

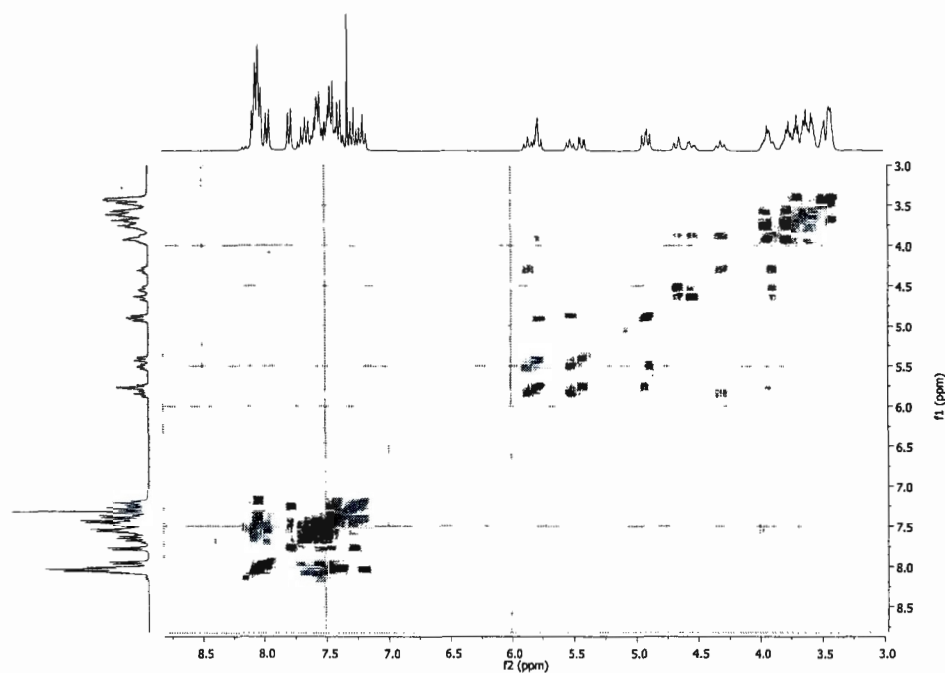


Figure S54. COSY spectrum of compound 17 (300 MHz, CDCl₃).

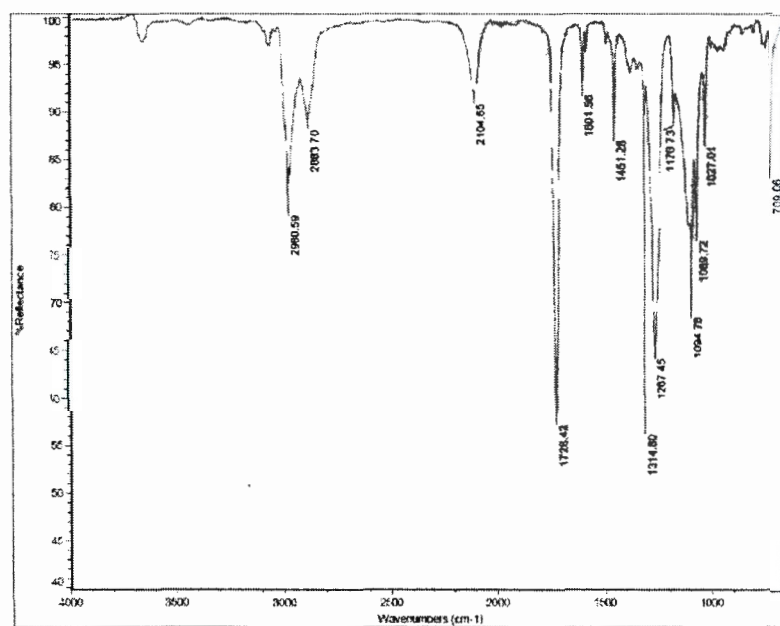


Figure S55. IR spectrum of compound 17.

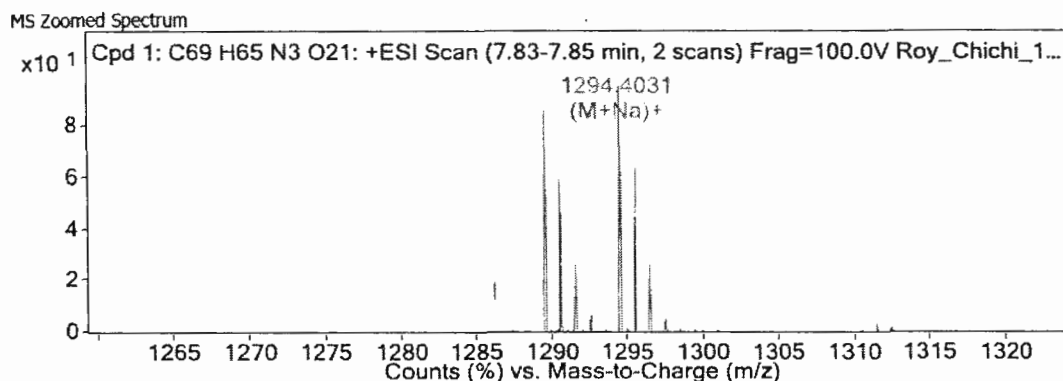
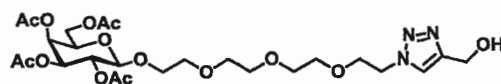


Figure S56. HRMS (ESI⁺) spectrum of compound 17.



Synthesis of compound 19a: To a solution of azide terminated compound **16** (100mg, 0.181mmol) in THF (4mL), was added propargyl alcohol (0.021ml, 0.363mmol), followed by sodium ascorbate (36mg, 0.181mmol). An aqueous solution of CuSO₄·5H₂O (45mg, 0.181mmol) was added and the final ratio of H₂O to THF was kept 1:1. The reaction mixture was stirred at 40°C for 12 hrs. Progress of the reaction was monitored with the help of TLC. Upon completion, reaction mixture was diluted with EtOAc (25mL) and washed with a saturated solution of EDTA (2×15mL). Organic layer was washed with brine solution, dried with anhydrous Na₂SO₄, filtered and concentrated under reduced pressure. Purification of the crude was achieved *via* flash column chromatography on silica gel using 2% MeOH in DCM as eluent to afford acetylated compound **19a** (93.2mg, 0.154mmol) in a 85% yield as a yellowish oil.

¹H NMR (300 MHz, CDCl₃) δ 7.79 (s, 1H), 5.38 (d, *J* = 3.2 Hz, 1H), 5.19 (dd, *J* = 10.4, 7.9 Hz, 1H), 5.02 (dd, *J* = 10.5, 3.4 Hz, 1H), 4.79 (d, *J* = 5.0 Hz, 2H), 4.55 (dd, *J* = 6.3, 4.9 Hz, 3H), 4.25–4.06 (m, 2H), 4.04–3.82 (m, 4H), 3.78–3.51 (m, 11H), 2.14 (s, 3H), 2.04 (s, 6H), 1.98 (s, 3H).

$^{13}\text{C}\{^1\text{H}\}$ NMR (75 MHz, CDCl_3) δ 170.4, 170.2, 170.2, 169.3, 70.8, 70.7, 70.6, 70.5, 70.5, 70.4, 70.2, 69.4, 69.1, 68.8, 67.0, 61.2, 56.6, 50.2, 20.7, 20.7, 20.6, 20.6.

IR (cm^{-1}): 3478, 2881, 1744, 1433, 1369, 1219, 1175, 1047, 954.

HRMS (ESI^+) m/z calc for $\text{C}_{25}\text{H}_{39}\text{N}_3\text{O}_{14}$ 606.2505 $[\text{M}+\text{H}]^+$; found, 606.2501.

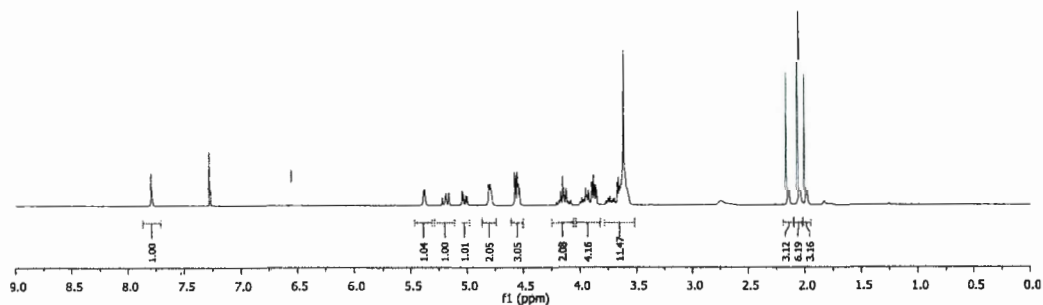


Figure S57. ^1H NMR. spectrum of compound **19a** (300 MHz, CDCl_3).

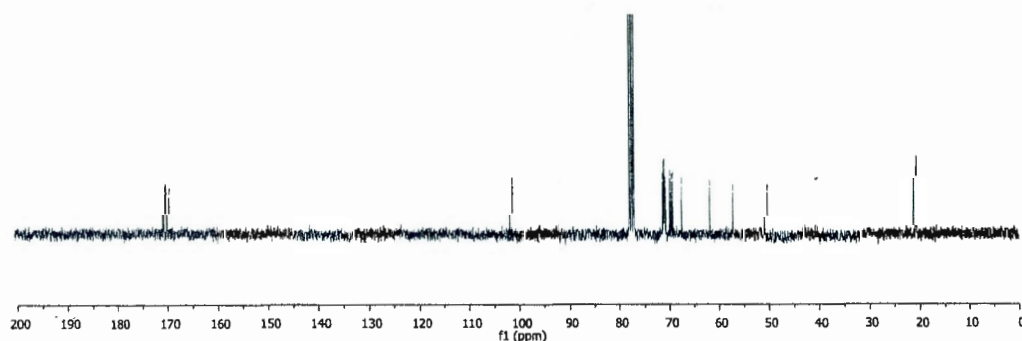


Figure S58. $^{13}\text{C}\{^1\text{H}\}$ NMR. spectrum of compound **19a** (75 MHz, CDCl_3).

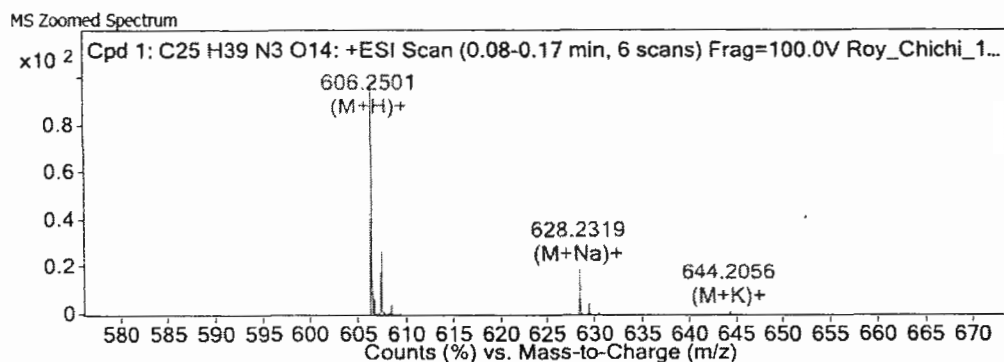


Figure S59. HRMS (ESI^+) of compound **19a**.

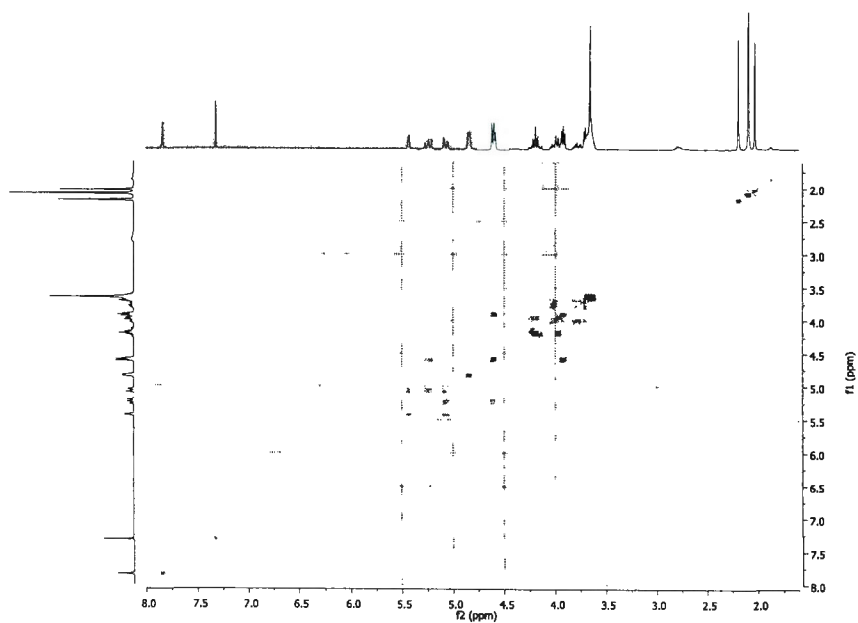


Figure S60. COSY spectrum of compound 19a.

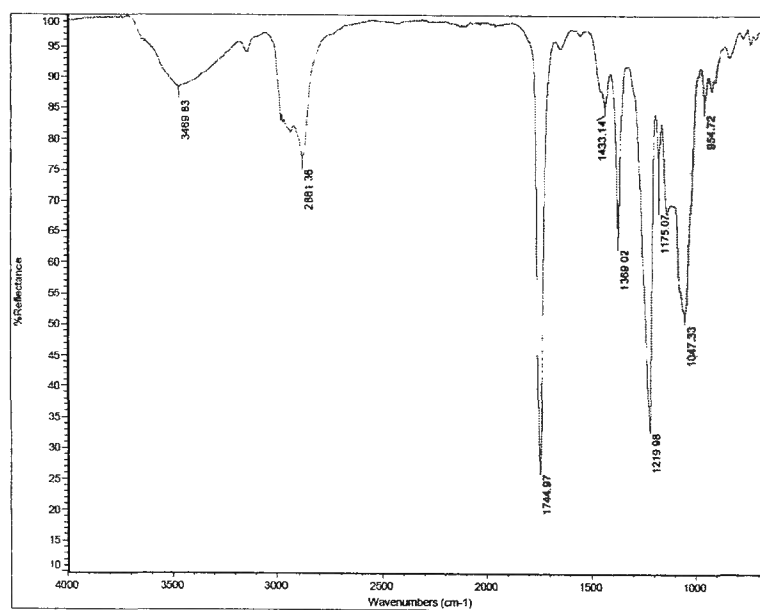
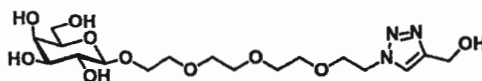


Figure S61. IR spectrum of compound 19a.



Synthesis of compound 19: To a stirring solution of compound **19a** (100mg, 0.165mmol) in MeOH (3mL) was slowly added 1M MeONa/MeOH solution to adjust the pH to 9-10. Reaction mixture was left to stir overnight. The reaction pH was then adjusted to 6 with H⁺ resin. The solvent was evaporated and the residue was dissolved in 3mL of water, and washed with diethyl ether (3×15mL) to remove impurities. Aqueous layer was lyophilized to provide **19** (65mg, 0.149mmol) as a white solid in a 90% yield.

¹H NMR (300 MHz, CD₃OD) δ 8.11 (br s, 1H), 4.74 (s, 2H), 4.63 (d, *J* = 4.7 Hz, 2H), 4.27 (d, *J* = 7.0 Hz, 1H), 4.09–3.97 (m, 1H), 3.93 (t, *J* = 5.0 Hz, 2H), 3.84 (d, *J* = 2.2 Hz, 1H), 3.79–3.57 (m, 13H), 3.57–3.44 (m, 3H).

¹³C{¹H} NMR (75 MHz, CD₃OD) δ 105.0, 76.7, 74.8, 72.5, 71.4, 70.3, 70.2, 69.6, 62.5, 51.8.

IR (cm⁻¹) 3358, 2924, 2502, 1643, 1455, 1073.

HRMS (ESI⁺) *m/z* calc for C₁₇H₃₁N₃O₁₀, 438.2082 [*M*+H]⁺; found, 438.2107.

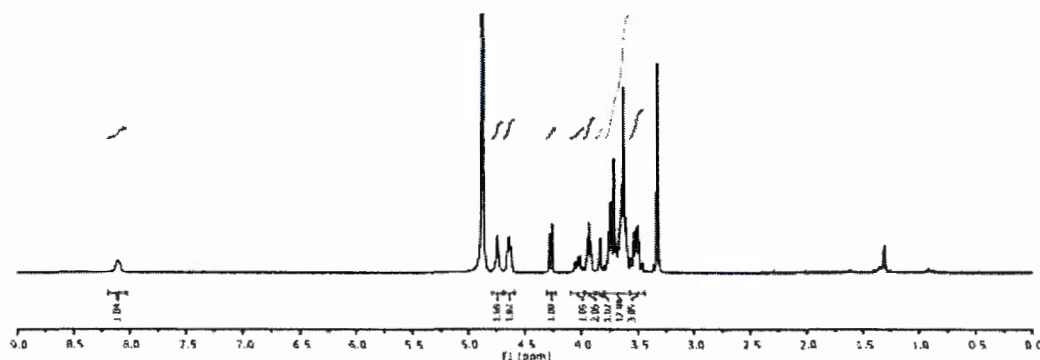


Figure S62. ¹H NMR spectrum of compound **19** (300 MHz, CD₃OD).

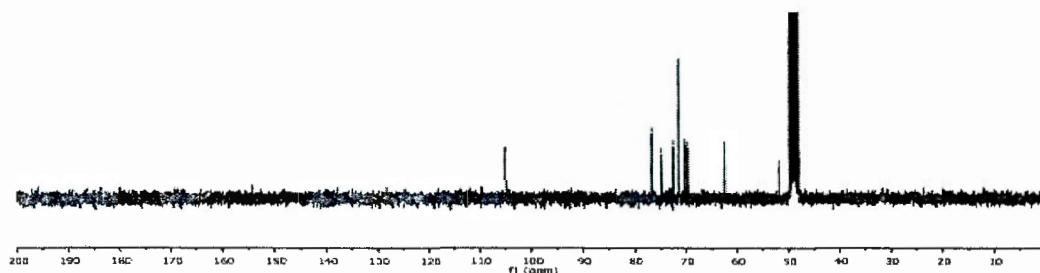


Figure S63. ¹³C{¹H} NMR spectrum of compound **19** (75 MHz, CD₃OD)

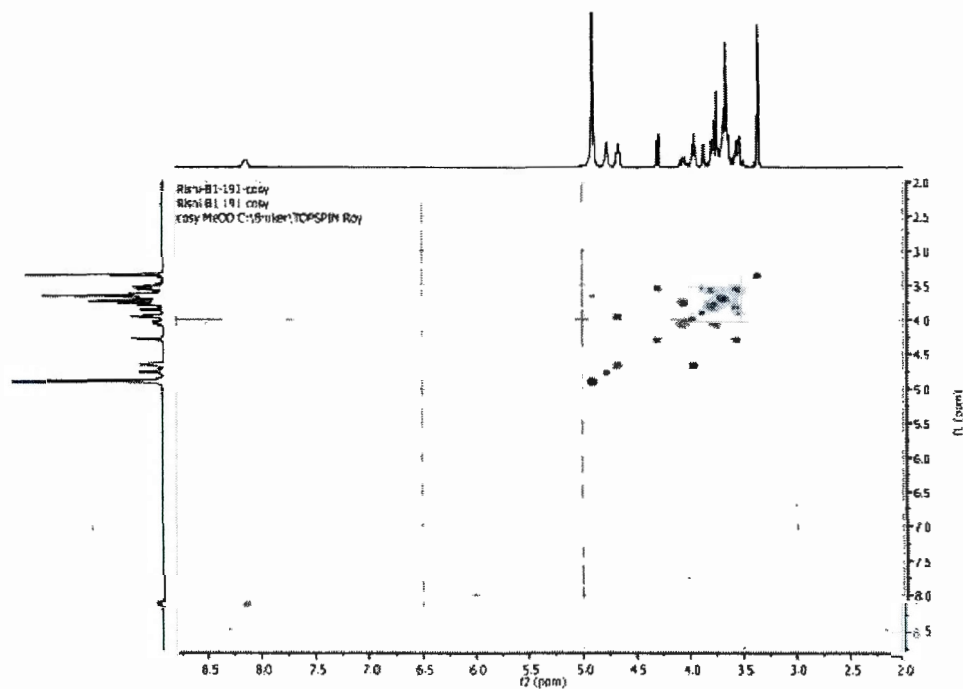


Figure S64. COSY spectrum of compound 19.

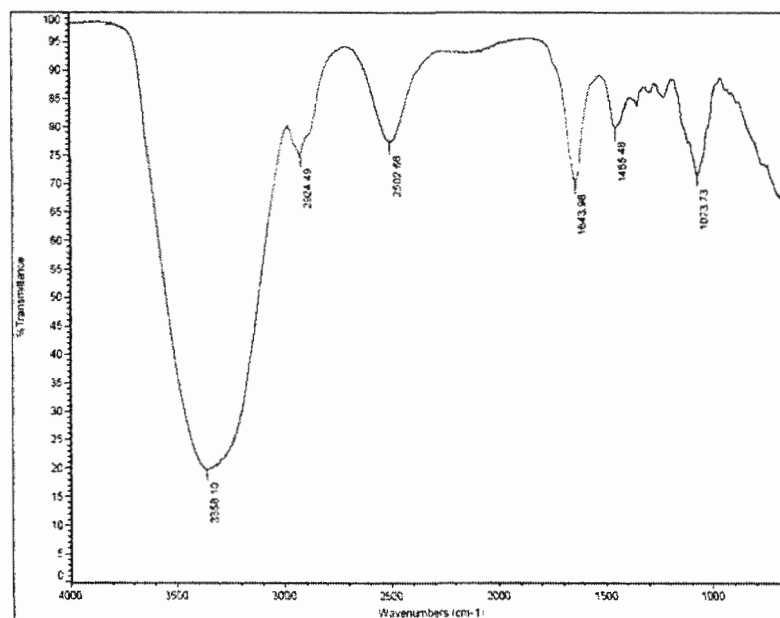


Figure S65. IR spectrum of compound 19.

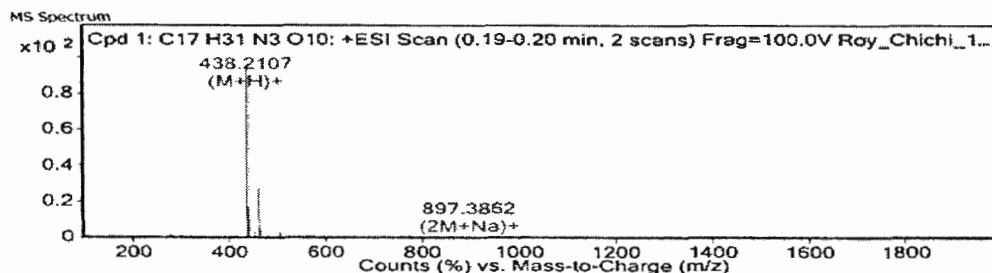
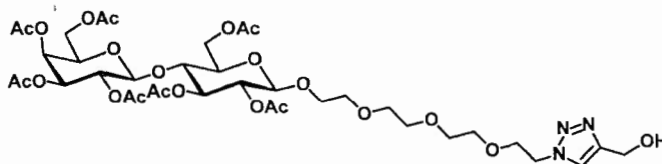


Figure S66. HRMS (ESI⁺) of compound 19.



Synthesis of compound 20a: To a solution of per-*O*-acetylated galactose (100mg, 119 μ mol) in a 1:1 mixture of H₂O/THF_{anh} (5 mL), were added propargyl alcohol (29.1 μ L, 501 μ mol), CuSO₄·5H₂O (14.9mg, 59.7 μ mol) and sodium ascorbate (11.8mg, 59.7 μ mol). While stirring, the mixture was first heated at 50°C for 3 hrs and at room temperature for additional 18 hours. Ethyl acetate (15mL) was added and the solution was poured into a separatory funnel containing ethyl acetate (10mL), washed with saturated aqueous NH₄Cl (2×10mL), water (10mL) and brine (5mL). Organics were collected, dried over Na₂SO₄ and concentrated to dryness *in vacuo* with rotary evaporator. Purification by flash chromatography (SiO₂, DCM/MeOH 100:0 to 92:8) afforded desired multivalent compound **20a** (86.0mg, 96.6 μ mol) as a white foam in a 91% yield.

¹H NMR (600 MHz, CDCl₃, δ ppm): 7.75 (s, 1H), 5.29 (d_{app}, 1H), 5.14 (dd, ³J_{4,3} = 9.4 Hz, ³J_{3,2} = 9.1 Hz, 1H), 5.05 (dd, ³J_{2,1} = 10.5 Hz, ³J_{3,2} = 8.0 Hz, 1H), 4.93 (dd, ³J_{2,3} = 10.5 Hz, ³J_{3,4} = 3.4 Hz, 1H), 4.83 (dd, ³J_{2,1} = 9.4 Hz, ³J_{3,2} = 8.0 Hz, 1H), 4.73 (br s, 2H), 4.53 (d, ³J_{1,2} = 9.4 Hz, 1H), 4.50 (t_{app}, 2H), 4.48 (dd, ²J_{6a,6b} = 12.0 Hz, ³J_{5,6a} = 2.1 Hz, 1H), 4.47 (d, ³J_{1,2} = 7.9 Hz, 1H), 4.12–4.00 (m, 3H), 3.90–3.52 (m, 17H), 3.30 (br s, 1H), 2.15 (s, 3H), 2.12 (s, 3H), 2.06 (s, 3H), 2.04 (3s, 9H), 1.96 (s, 3H).

^{13}C NMR (150 MHz, CDCl_3 , δ ppm): 170.3, 170.2, 170.0, 169.9, 169.7, 169.6, 169.0, 147., 122.9, 100.9, 100.4, 76.6, 72.6, 72.5, 71.5, 70.8, 70.5, 70.3, 70.3, 70.2, 70.2, 69.3, 69.0, 68.9, 66.5, 61.8, 60.7, 56.3, 50.0, 20.8, 20.8, 20.7, 20.6, 20.6, 20.6, 20.5.

HRMS (ESI^+) m/z for $\text{C}_{37}\text{H}_{55}\text{N}_3\text{O}_{22}$, 894.3350 $[\text{M}+\text{H}]^+$; found 894.3361, 916.3169 $[\text{M}+\text{Na}]^+$; found 916.3181.

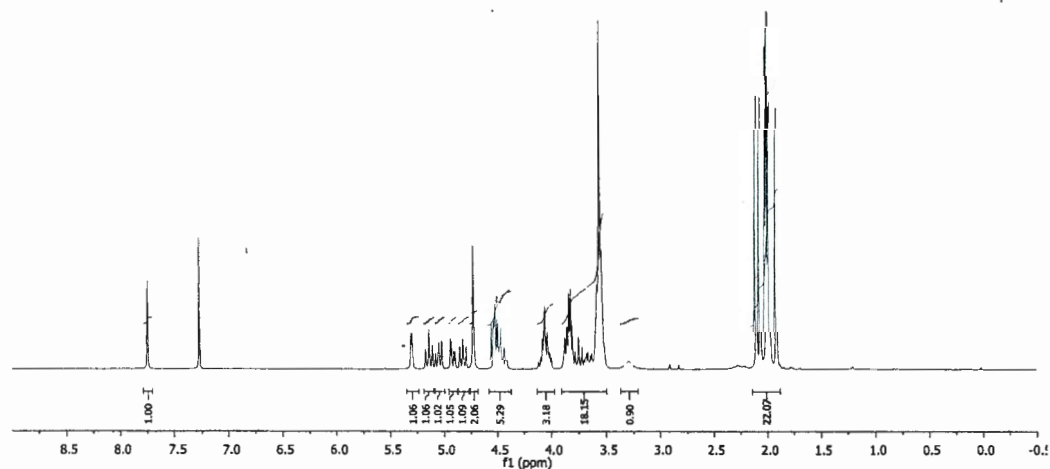


Figure S67. ^1H NMR spectrum of compound **20a** (600 MHz, CDCl_3).

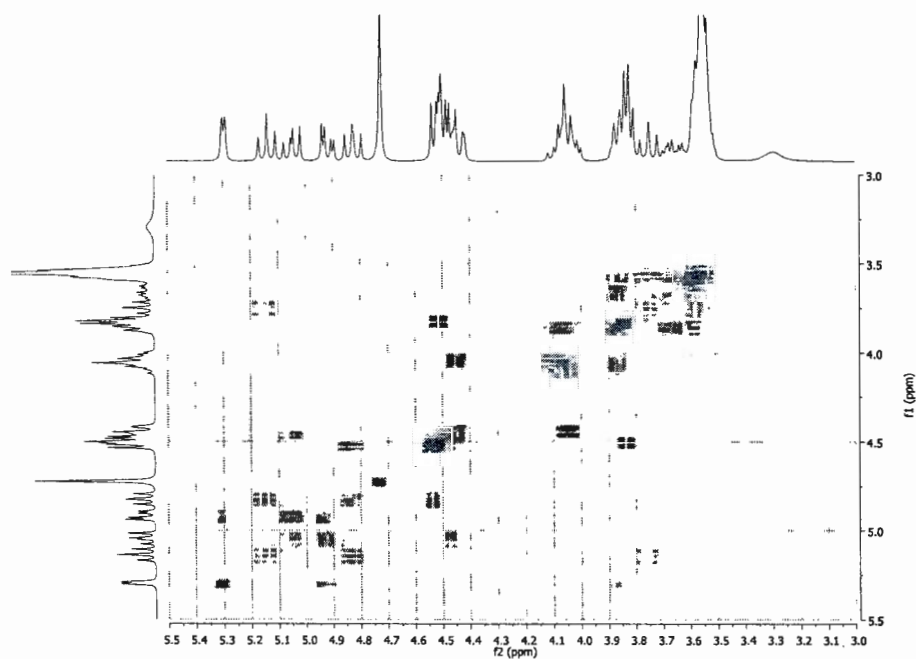


Figure S68. COSY spectrum of compound **20a**.

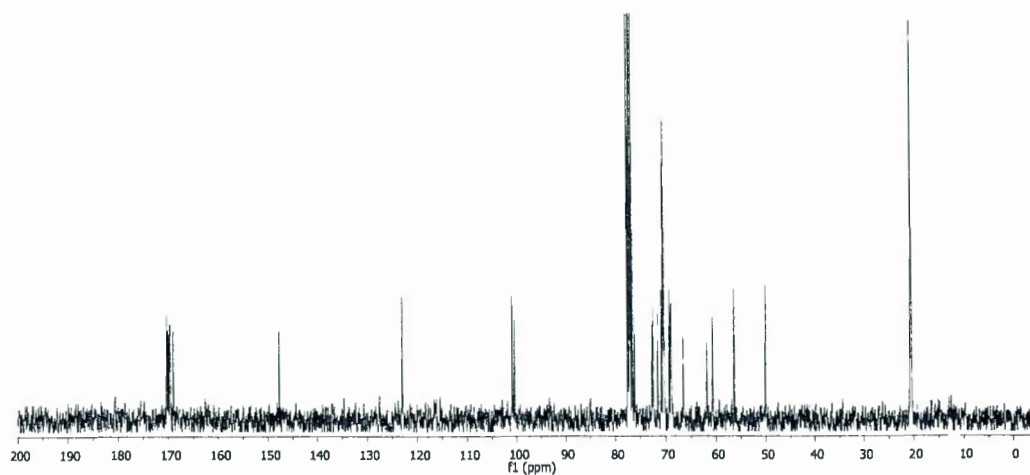
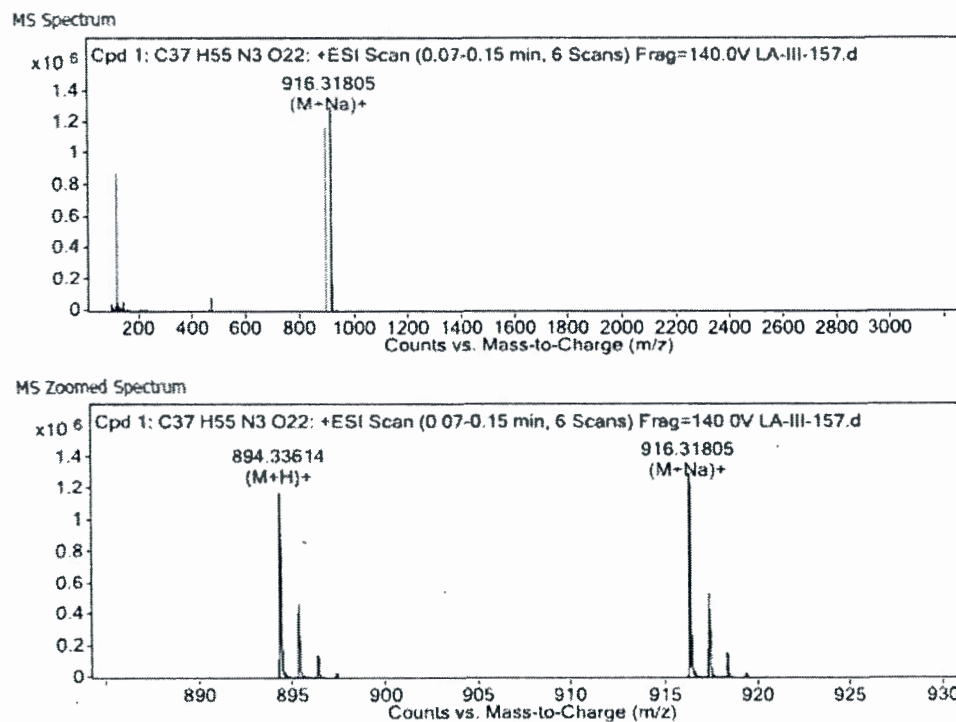


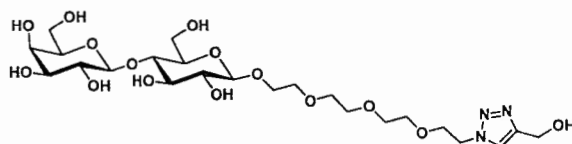
Figure S69. $^{13}\text{C}\{^1\text{H}\}$ NMR spectrum of compound **20a** (151 MHz, CDCl_3).



MS Spectrum Peak List

Ion	Formula	Abund	Observed m/z	Calc m/z	Diff (ppm)
(M+H)+	C ₃₇ H ₅₆ N ₃ O ₂₂	1193152.62	894.33614	894.335	1.27
(M+Na)+	C ₃₇ H ₅₅ N ₃ NaO ₂₂	1308225.57	916.31805	916.31694	1.21

Figure S70. HRMS (ESI^+) of compound **20a**.



Synthesis of compound 20: Acetylated compound **20a** (86.0mg, 96.6 μ mol) was dissolved in dry MeOH (4mL) and a solution of sodium methoxide (1M in MeOH, 150 μ L) was added until pH 9-10. The reaction mixture was stirred at room temperature for 24 hrs. The pH was adjusted to 6-7 with addition of ion-exchange resin (Amberlite IR 120 H⁺). After filtration, the solvent was removed under *vacuum* with rotary evaporator, lyophilized to yield the fully deprotected reference **20** as a white solid (52.5mg, 87.6 μ mol) in a 91% yield.

¹H NMR (300 MHz, D₂O, δ ppm): 8.03 (s, 1H), 4.73 (s, 2H), 4.64 (t, J = 5.0 Hz, 2H), 4.52 (d, J = 7.9 Hz, 1H), 4.46 (d, J = 7.7 Hz, 1H), 4.08-3.53 (m, 25H), 3.36 (m, 6H).

¹³C NMR (75 MHz, D₂O, δ ppm): 147.5, 125.1, 103.6, 102.7, 79.0, 76.0, 75.4, 75.0, 73.5, 73.2, 71.6, 70.3, 70.2, 70.1, 70.1, 69.4, 69.2, 61.7, 60.7, 55.3, 50.7.

HRMS (ESI⁺) m/z for C₂₃H₄₁N₃O₁₅, 600.2610 [M+H]⁺; found 600.2618, 622.2430 [M+Na]⁺; found 622.2438.

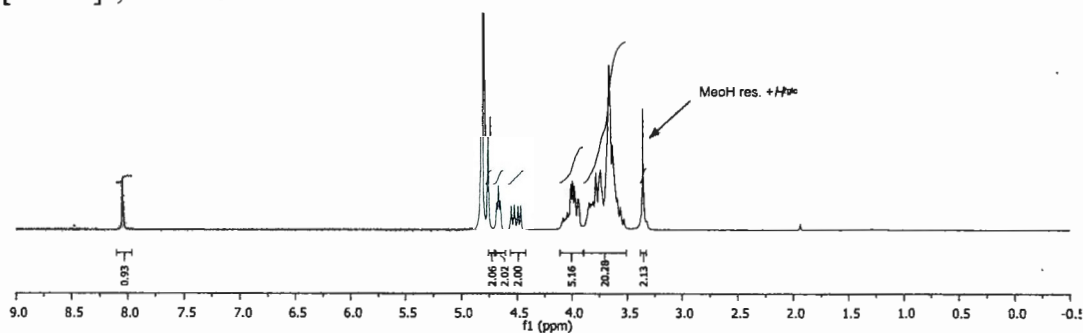


Figure S71. ¹H NMR spectrum of compound **20** (300 MHz, D₂O).

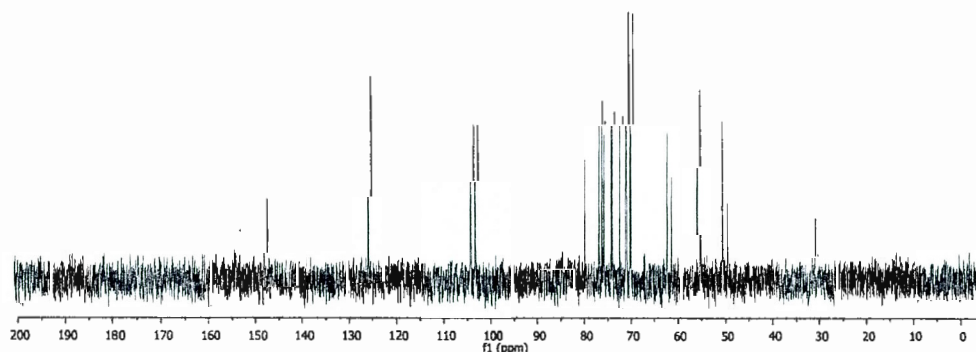


Figure S72. ¹³C{¹H} NMR spectrum of compound **20** (75 MHz, CDCl₃).

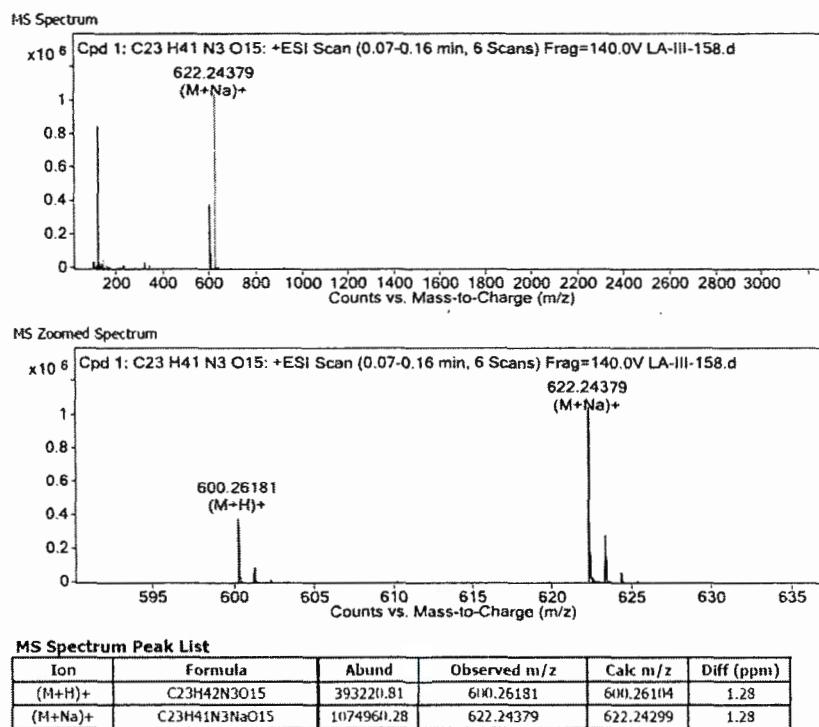


Figure S73. HRMS (ESI⁺) of compound 20.

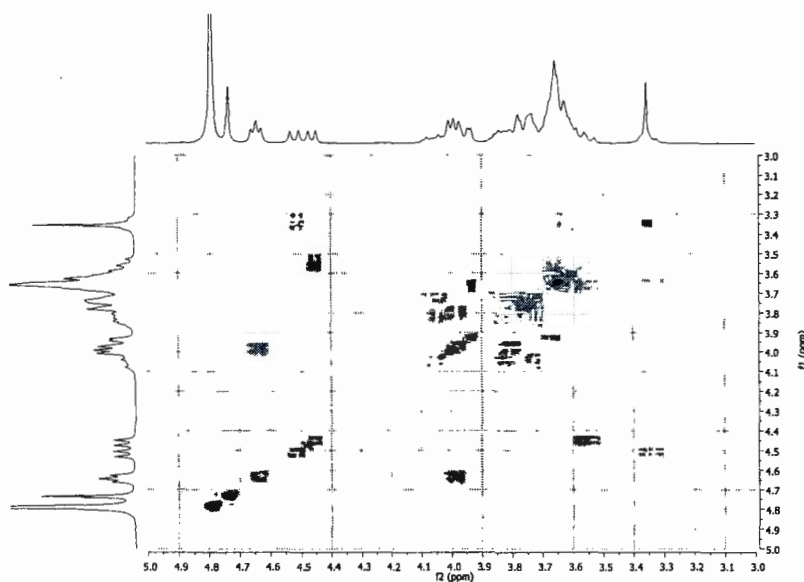
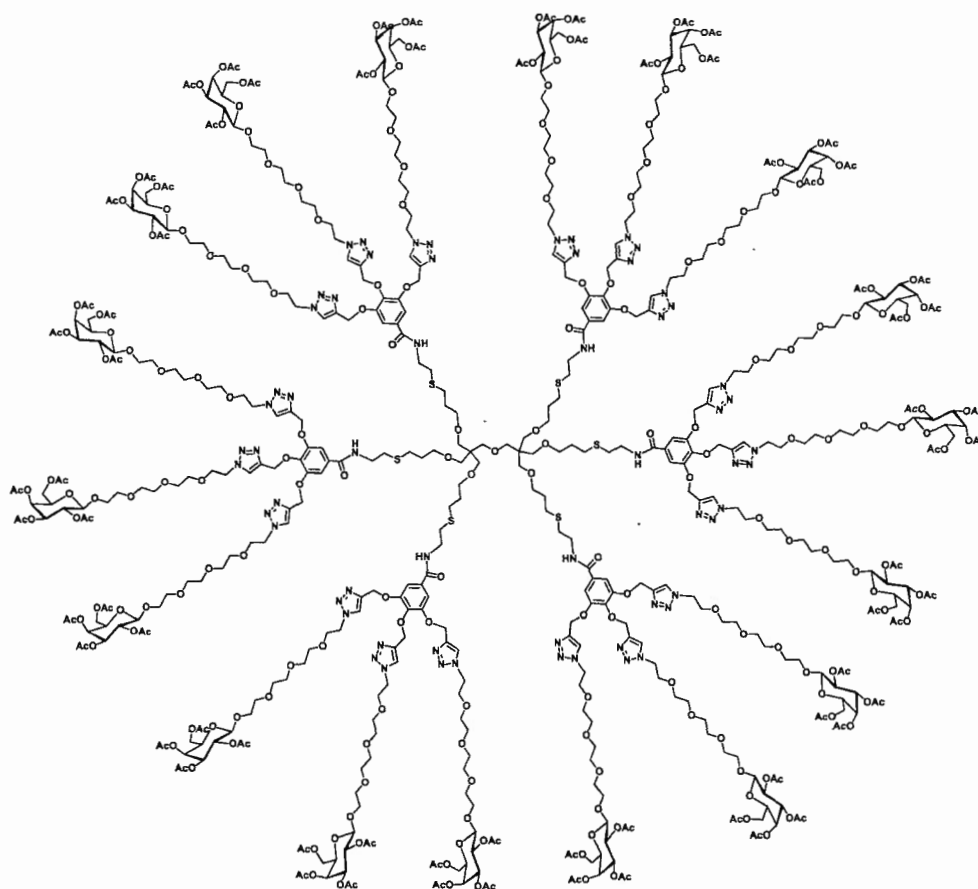


Figure S74. COSY spectrum of compound 20.



Synthesis of compound 22: To a solution of propargylated scaffold **5** (55mg, 0.022mmol) in THF (5mL) was added galactoside **16** (354mg, 0.645mmol), followed by sodium ascorbate (68mg, 0.39mmol). An aqueous solution of $\text{CuSO}_4 \cdot 5\text{H}_2\text{O}$ (96mg, 0.39mmol) was added and the final ratio of H_2O to THF was kept 1:1. The reaction mixture was stirred at 40°C for 24 hrs. The progress of the reaction was monitored with the help of TLC. Upon completion, the reaction mixture was diluted with EtOAc (25mL) and washed with saturated solution of EDTA ($2 \times 15\text{mL}$). Organic layer was washed with brine solution, dried with anhydrous Na_2SO_4 , filtered and concentrated under reduced pressure. Purification of the crude compound was achieved *via* flash column chromatography on silica gel using 5% MeOH in DCM as eluent to afford the desired compound **22** (208mg, 0.0167mmol) in 76% yield.

^1H NMR (600 MHz, CDCl_3) δ 7.92 (s, 12H), 7.84 (s, 6H), 7.25–7.230 (m, 12H), 5.40–5.31 (m, 18H), 5.30–5.27 (m, 7H), 5.19–5.07 (m, 53H), 4.99 (dd, $J = 10.5, 3.4$ Hz, 19H), 4.52 (dd, $J = 22.2, 19.3$ Hz, 57H), 4.18–4.04 (m, 36H), 3.97–3.77 (m, 75H), 3.70 (ddd, $J = 10.8, 6.9, 3.9$ Hz, 19H), 3.63–3.50 (m, 176H), 3.45 (br s, 18H), 3.34 (s,

18H), 2.75 (br s, 1 2H), 2.63 (br s, 12H), 2.12 (d, $J = 1.4$ Hz, 52H), 2.04–1.93 (m, 164H), 1.83 (s, 12H).

¹³C{¹H} NMR (151 MHz, CDCl₃) δ 170.2, 170.0, 170.0, 170.0, 169.3, 166.7, 152.0, 144.0, 143.2, 140.1, 130.1, 124.7, 124.4, 107.3, 101.2, 70.8, 70.6, 70.5, 70.5, 70.4, 70.4, 70.1, 69.7, 69.3, 69.2, 69.0, 68.8, 67.1, 66.3, 63.0, 61.2, 50.2, 39.6, 31.4, 29.7, 28.6.

IR (cm⁻¹) 2872, 1747, 1491, 1427, 1368, 1325, 1221, 1175, 1104, 1050, 732.

MALDI-TOF (DHB matrix) m/z calc. for $C_{532}H_{778}N_{60}O_{265}S_6$, 12446.5; found, 12446.0.

GPC M_n = 12500 g/mol. M_w/M_n = 1.06.

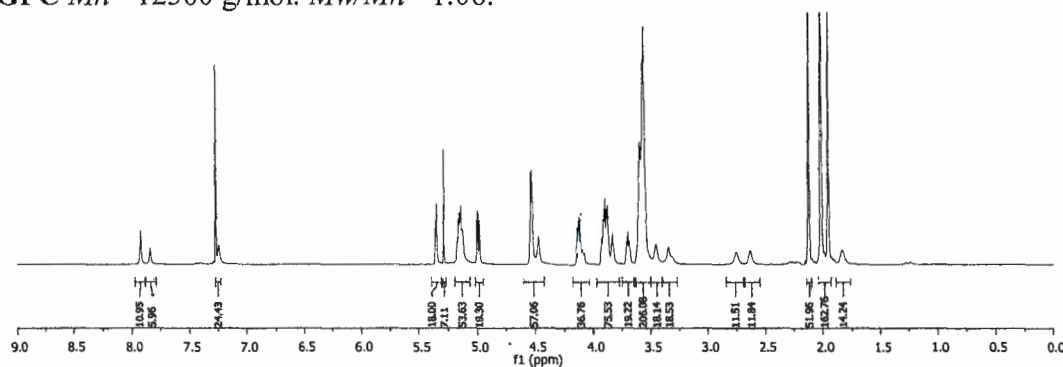


Figure S75. ^1H NMR spectrum of compound **22** (600 MHz, CDCl_3).

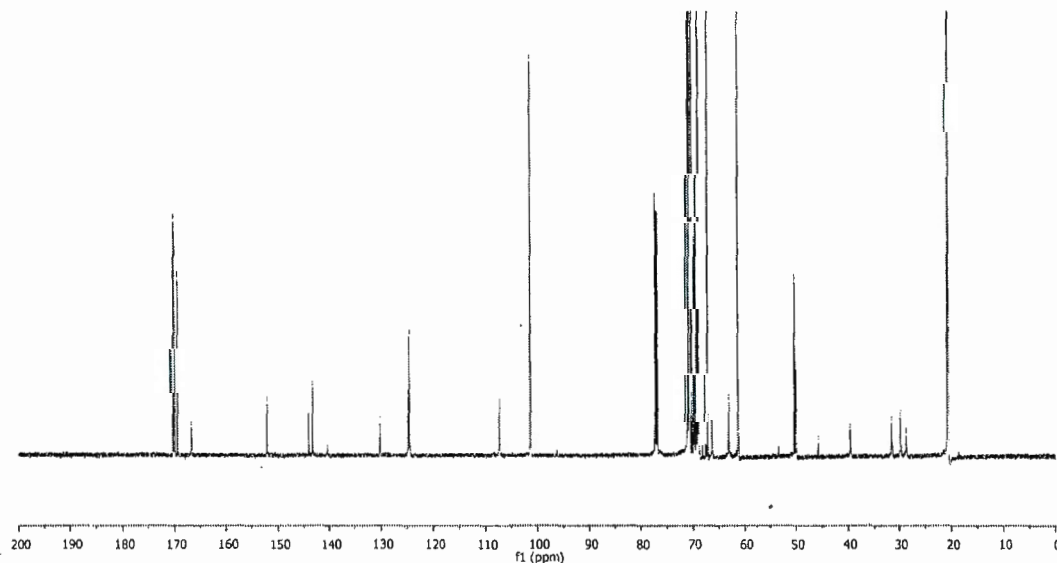


Figure S76. $^{13}\text{C}\{^1\text{H}\}$ NMR spectrum of compound **22** (151 MHz, CDCl_3).

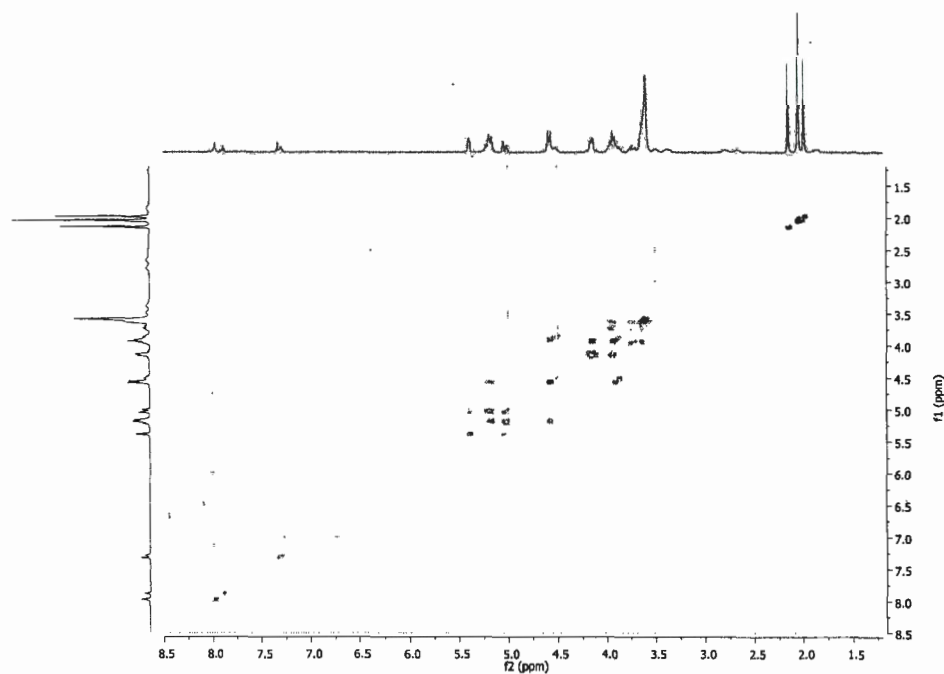
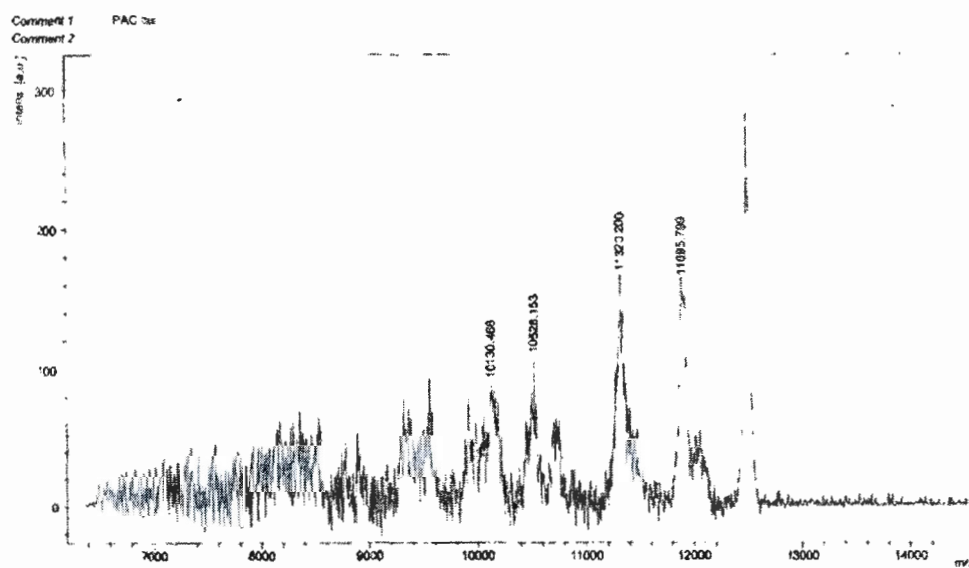


Figure S77. COSY spectrum of compound 22.



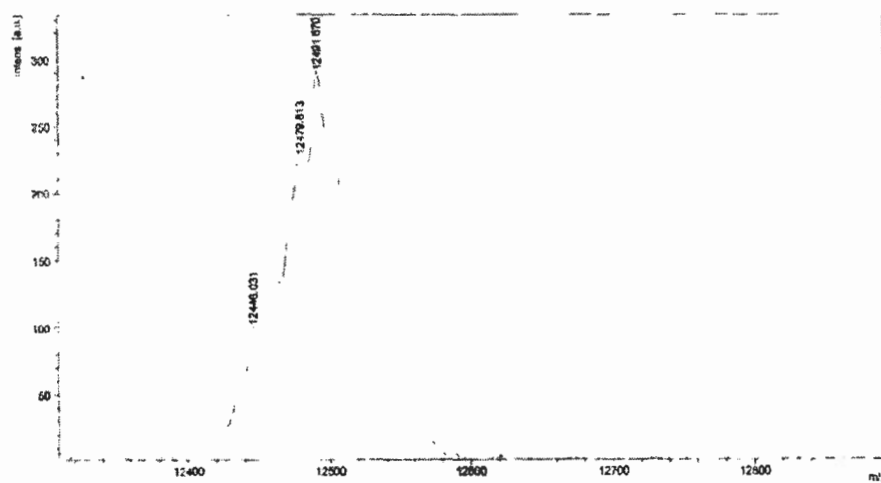


Figure S78. MALDI TOF spectrum of compound 22.

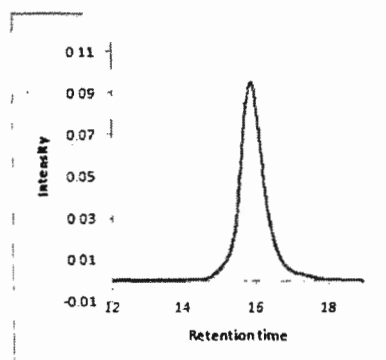


Figure S79. GPC traces of compound 22.

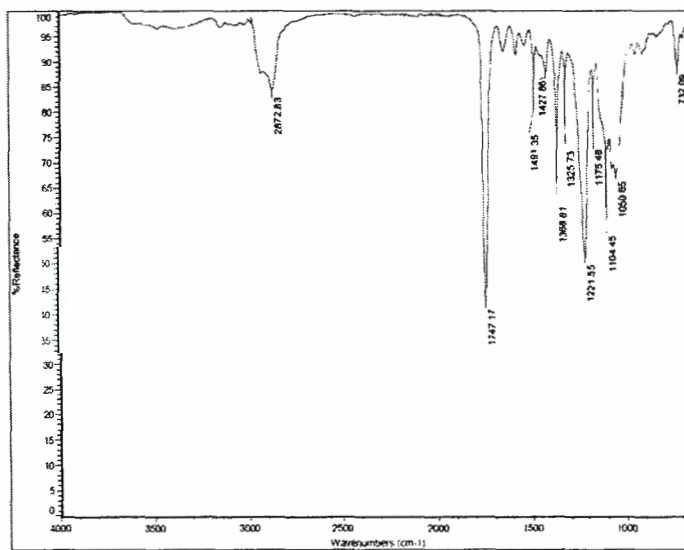
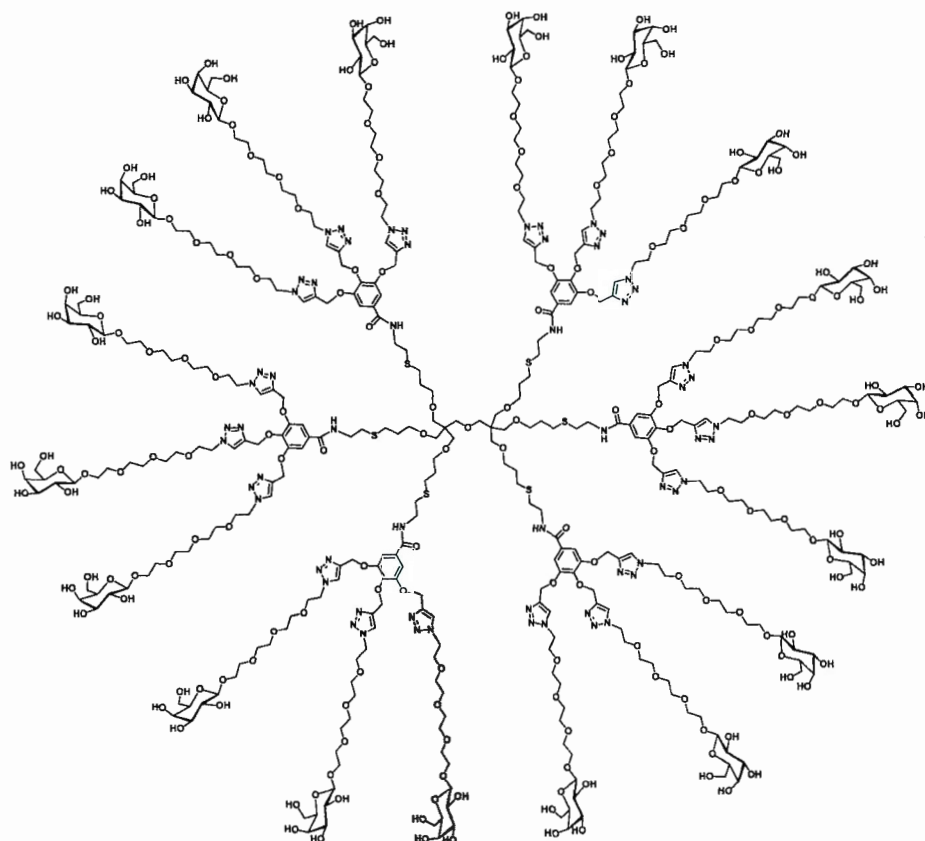


Figure S80. IR spectrum of compound 22.



Synthesis of compound 23: To a stirring solution of compound **22** (100mg, 0.080mmol) in MeOH (3mL), was slowly added a 1M solution of MeONa/MeOH to adjust the pH to 9-10. The reaction mixture was left stirring overnight. The reaction pH was then adjusted to 6 with H^+ resin. Solvent was evaporated and the residue was dissolved in 3 mL of water and washed with diethyl ether (3x15ml) to remove impurities. Aqueous layer was finally lyophilized to yield **23** (68mg, 0.072mmol) as a white solid in 90% yield.

1H NMR (600 MHz, D_2O) δ 8.40–7.80 (m, 18H), 7.28 (br s, 12H), 5.30–5.00 (m, 30H), 4.62–4.49 (m, 36H), 4.38 (d, $J = 8.0$ Hz, 15H), 4.02 (d, $J = 11.4$ Hz, 18H), 3.93 (d, $J = 13.8$ Hz, 39H), 3.88–3.82 (m, 12H), 3.80–3.71 (m, 54H), 3.69–3.61 (m, 75H), 3.62–3.49 (m, 165 H), 3.45–3.38 (m, 16H), 3.37–3.35 (m, 100H), 3.28–3.22 (m, 9H), 2.86–2.70 (m, 12H), 2.68–2.49 (m, 12H), 1.85–1.65 (m, 12H).

$^{13}C\{^1H\}$ NMR (151 MHz, D_2O) δ 168.8, 152.7, 140.1, 130.7, 107.8, 103.9, 76.1, 73.7, 73.0, 71.7, 70.7, 70.6, 70.5, 70.5, 69.7, 69.6, 69.5, 63.5, 61.9, 61.4, 51.2, 40.5, 31.7, 29.9, 29.1 (*C and CH of triazole rings not visible*).

IR (cm^{-1}) 3377, 2917, 1653, 1586, 1495, 1239, 1104.

MS (ESI $^+$) m/z calc for $C_{388}H_{634}N_{60}O_{193}S_6$, 9420.9 $[M+H]^+$; found (deconvoluted), 9414.0.

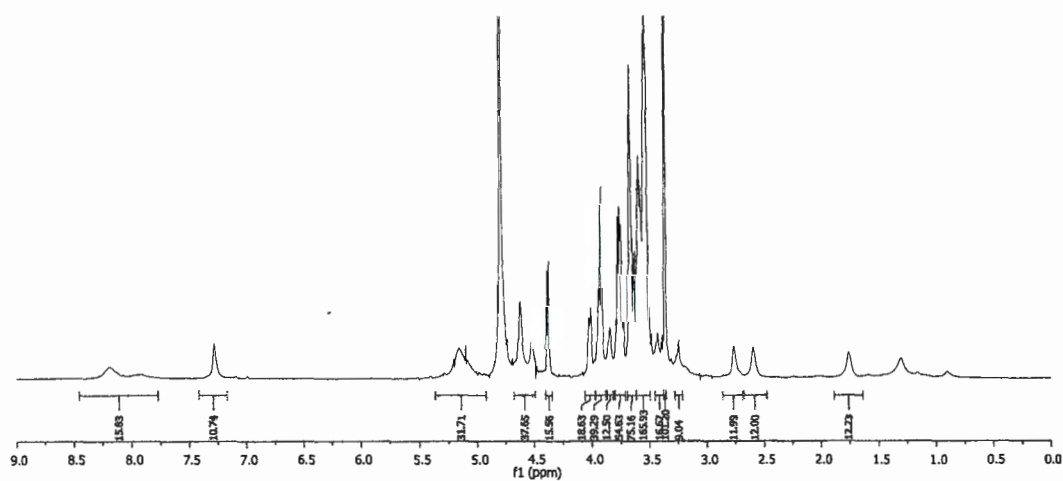


Figure S81. ^1H NMR spectrum of compound **23** (600 MHz, D_2O).

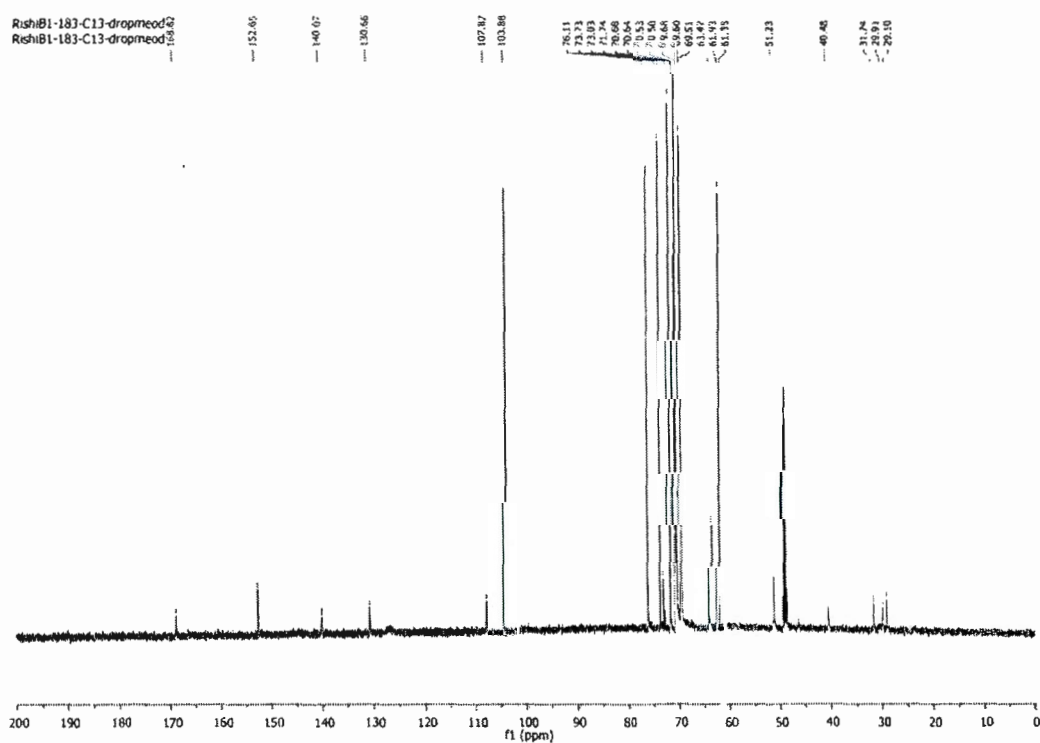


Figure S82. $^{13}\text{C}\{^1\text{H}\}$ NMR spectrum of compound **23** (151 MHz, D_2O).

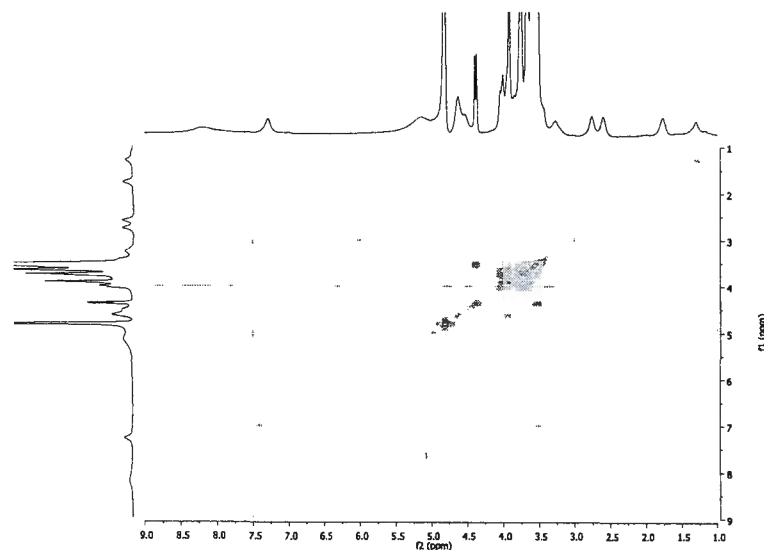


Figure S83. COSY spectrum of compound 23.

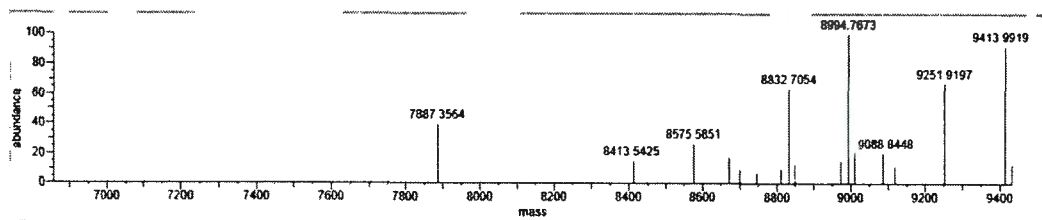


Figure S84. HRMS (ESI⁺) spectrum of compound 23.

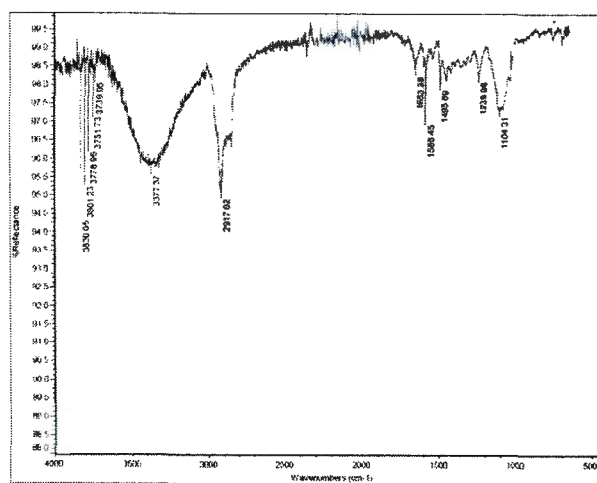
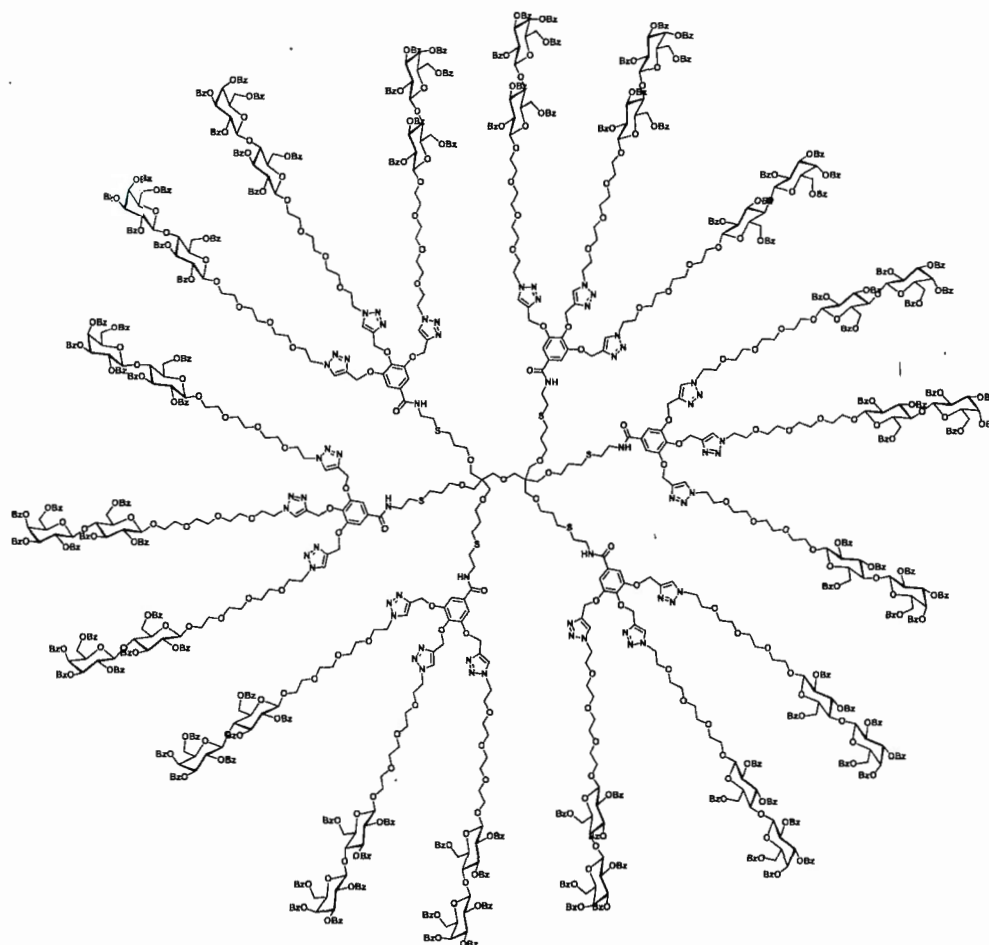


Figure S85. IR spectrum of compound 23.



Synthesis of compound 24: To a solution of propargylated scaffold **5** (20mg, 7.8 μ mol) in THF (5mL) was added PEGylated lactoside **17** (302mg, 0.234mmol), followed by sodium ascorbate (28mg, 0.14mmol). An aqueous solution of CuSO₄·5H₂O (35mg, 0.14mmol) was added and the final ratio of H₂O to THF was kept 1:1. The reaction mixture was stirred at 40°C for 24 hrs. The progress of the reaction was monitored by TLC. Upon completion, the reaction mixture was diluted with EtOAc (25mL) and washed with sat. solution of EDTA (2×15mL). Organic layer was washed with brine solution, dried with anhydrous Na₂SO₄, filtered and concentrated under reduced pressure. Purification of the residue was achieved *via* flash column chromatography on silica gel using 5% MeOH in DCM as eluent to afford desired compound **24** (153mg, 6.0 μ mol) as an off-white viscous solid in 77% yield.

¹H NMR (300 MHz, CDCl₃) δ 8.06–7.14 (m, 666H), 5.83–5.67 (m, 54H), 5.49–5.34 (m, 36H), 5.11 (s, 32H), 4.88 (d, J = 7.9 Hz, 18H), 4.80 (d, J = 7.8 Hz, 18H), 4.65–

4.55 (m, 18H), 4.53–4.38 (m, 54H), 4.26 (t, $J = 9.4$ Hz, 18H), 3.95–3.20 (m, 368H), 2.85–2.50 (m, 24H), 1.82 (br s, 12H).

$^{13}\text{C}\{^1\text{H}\}$ NMR (151 MHz, CDCl_3) δ 166.7, 165.8, 165.5, 165.4, 165.2, 165.1, 164.8, 152.0, 144.6, 140.0, 133.5, 130.2, 133.4, 133.3, 129.7, 129.6, 129.5, 129.3, 128.6, 128.6, 128.5, 128.4, 128.2, 107.9, 101.2, 101.0, 76.0, 75.7, 70.5, 69.9, 69.6, 67.5, 62.4, 61.0, 60.3, 57.3, 45.6, 39.2, 31.6, 29.8, 28.4 (Signals corresponding to CONH, $\text{C}_{\text{ar}}\text{H}$, CH_2 and C_{q} (*in italic*) located in inner positions are not visible in this case, even after 30000 scans).

IR (cm^{-1}): 2879, 1730, 1601, 1584, 1451, 1369, 1315, 1269, 1250, 1175, 1069, 1026, and 708.

MALDI-TOF m/z calc. for $\text{C}_{1378}\text{H}_{1318}\text{N}_{60}\text{O}_{409}\text{S}_6$, 25478.7 $[\text{M}+\text{Na}]^+$; found, 25602.3.

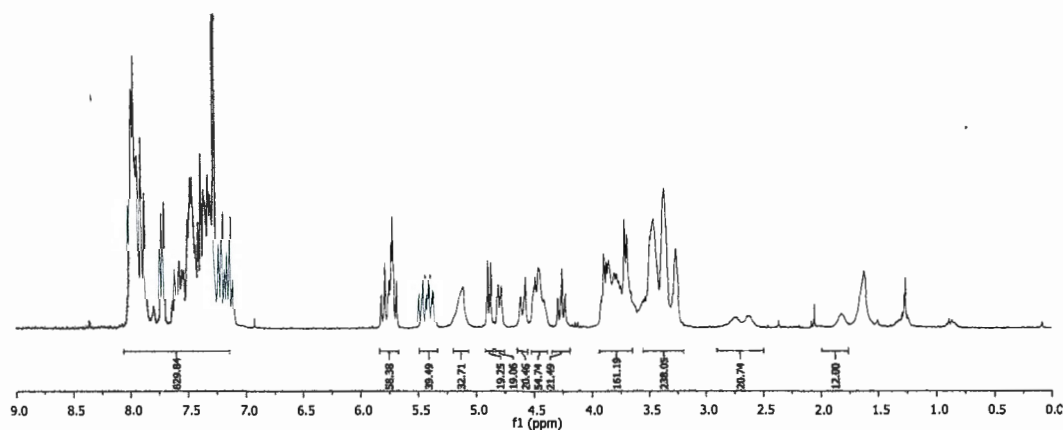


Figure S86. ^1H NMR spectrum of compound 24 (300 MHz, CDCl_3).

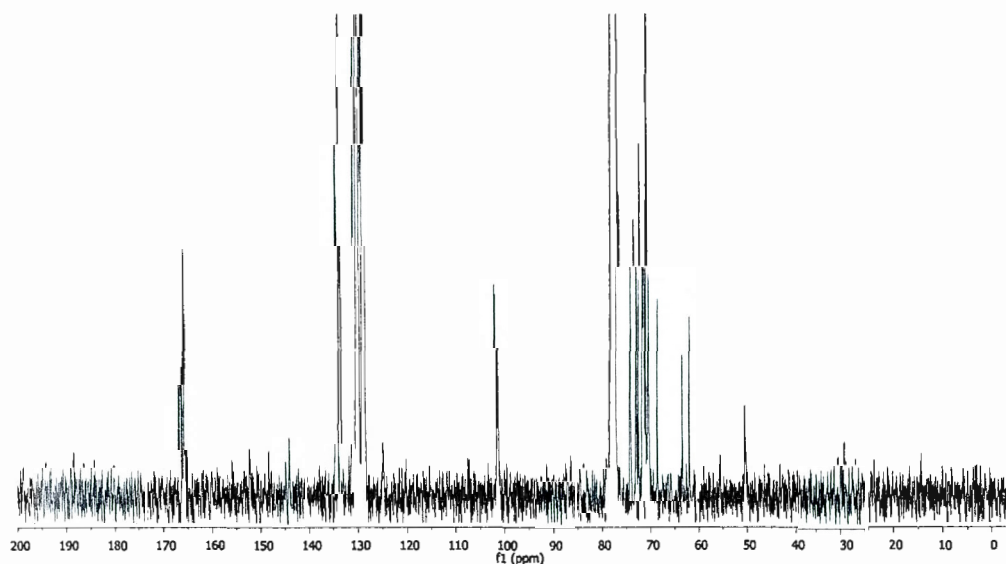


Figure S87. $^{13}\text{C}\{^1\text{H}\}$ NMR spectrum of compound 24 (151 MHz, CDCl_3).

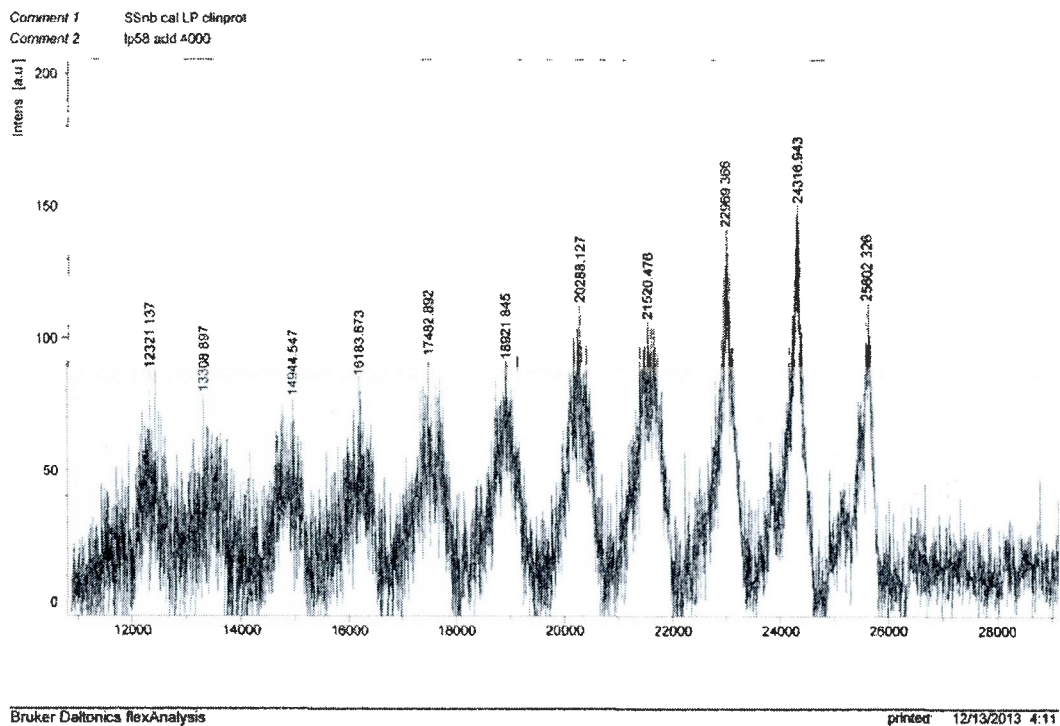


Figure S88. MALDI TOF spectrum of compound 24.

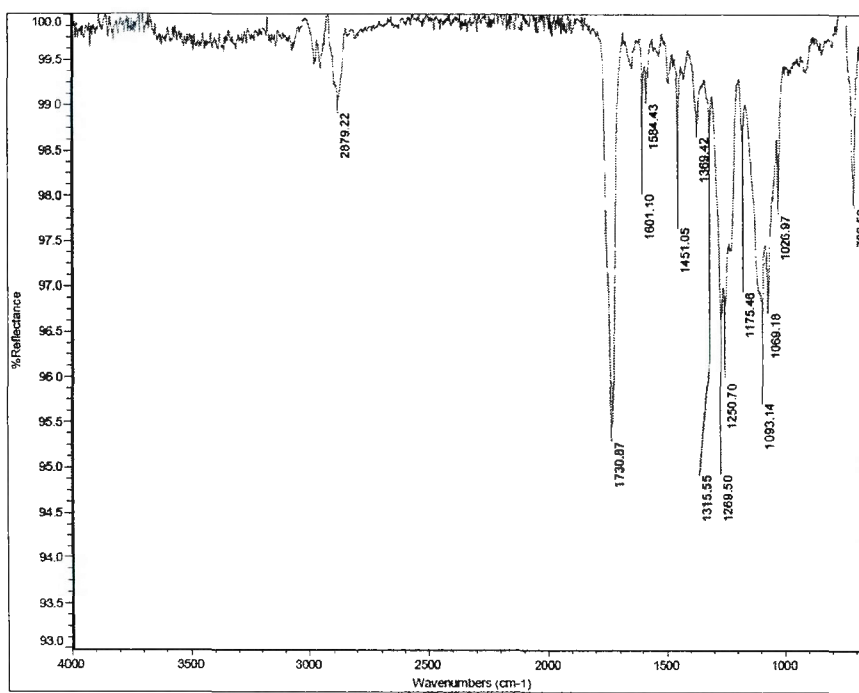
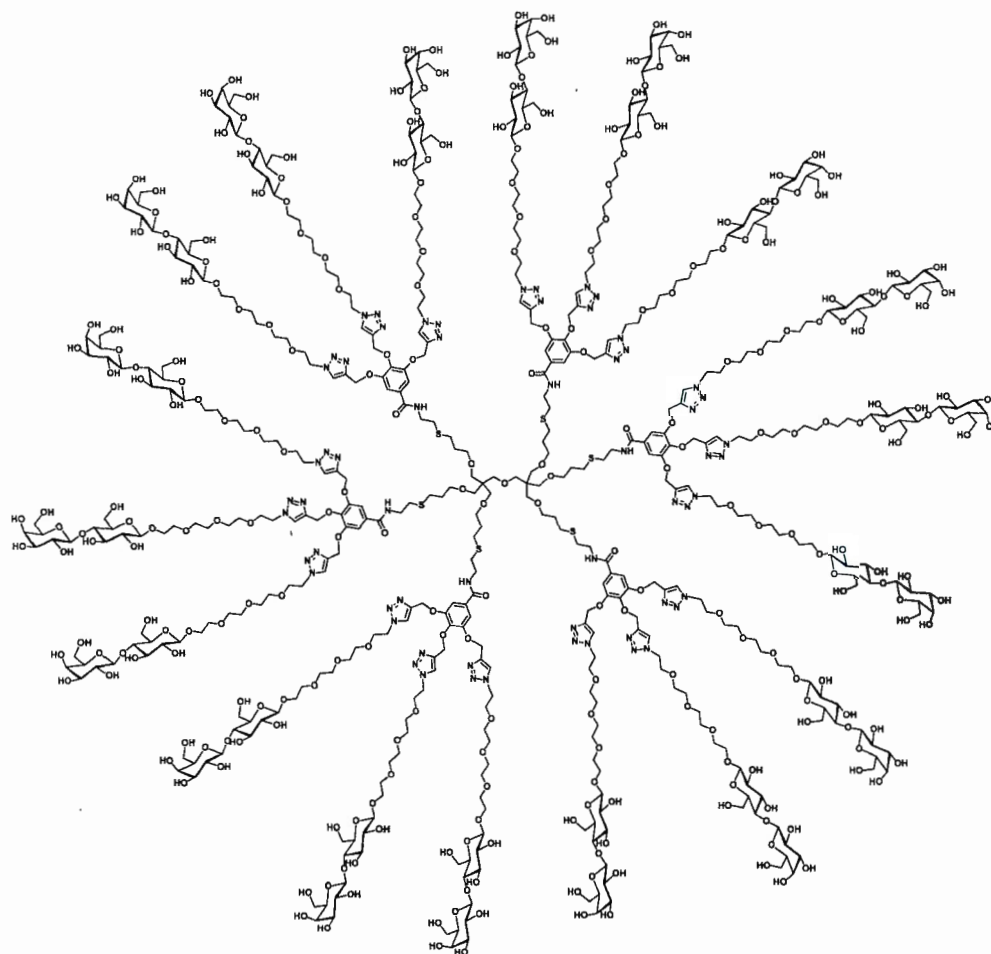


Figure S89. IR spectrum of compound 24.



Synthesis of compound 25: To a stirring solution of compound 24 (100mg, 3.93 μ mol) in MeOH (3mL), was slowly added a 1M solution of MeONa/MeOH to adjust the pH to 9-10. The reaction mixture was left stirring overnight. The reaction pH was adjusted to 6 with H⁺ resin and the solvent was evaporated. The residue was dissolved in 3mL of water and washed with diethyl ether (3 \times 15ml) to remove the impurities. Aqueous layer was lyophilized to afford 25 (41mg, 3.3 μ mol) as a white solid in a 85% yield.

¹H NMR (600 MHz, D₂O) δ 8.16–7.70 (m, 18H), 7.25–7.1 (m, 12H), 5.15–4.83 (m, 18H), 4.56–4.20 (m, 36H), 4.37–4.20 (m, 67H), 3.86–3.06 (m, 627H), 2.67–2.47 (br s, 12H), 2.45–2.30 (br s, 12H), 1.75–1.45 (br s, 12H).

¹³C{¹H} NMR (151 MHz, D₂O) δ : 168.5, 152.3, 150.4, 139.7, 130.3, 126.4, 107.4, 103.6, 102.8, 79.1, 75.9, 75.3, 74.9, 73.4, 73.1, 72.6, 71.5, 70.2, 70.1, 70.1, 69.2, 69.1, 63.0, 61.6, 60.7, 51.0, 45.9, 40.0, 31.3, 29.4, 28.6.

IR (cm^{–1}): 3695, 3384, 2937, 2843, 1646, 1429, 1347, 1055, and 1032.

MALDI-TOF m/z calc for $C_{496}H_{814}N_{60}O_{283}S_6$, 12361.4 $[M+Na]^+$; found, 12368.4, 12401.9 (Cu adduct); found 12403.5.

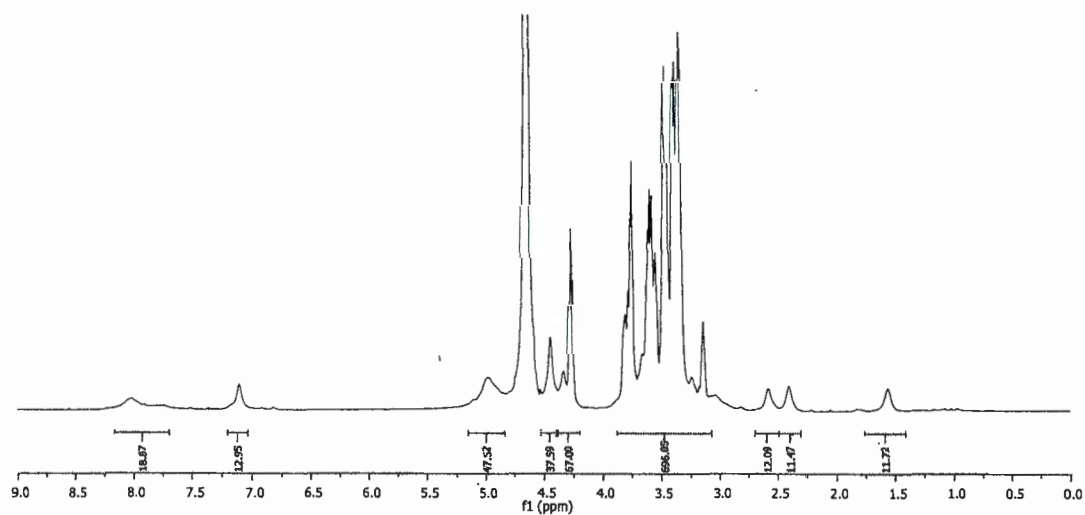


Figure S90. 1H NMR spectrum of compound 25 (600 MHz, D_2O).

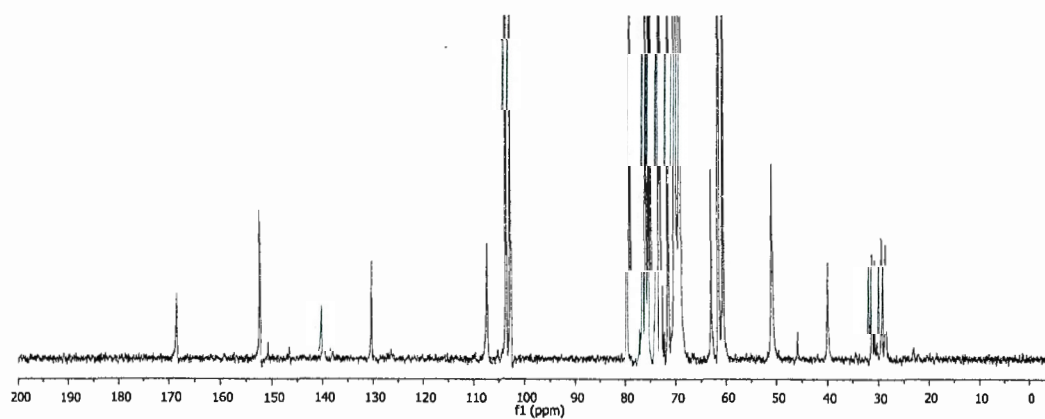


Figure S91. $^{13}C\{^1H\}$ NMR spectrum of compound 25 (151 MHz, D_2O).

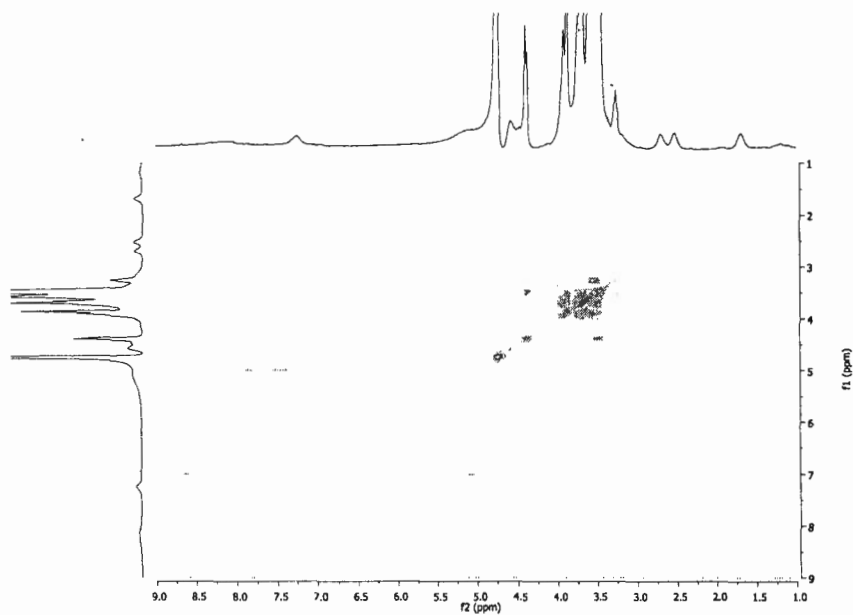
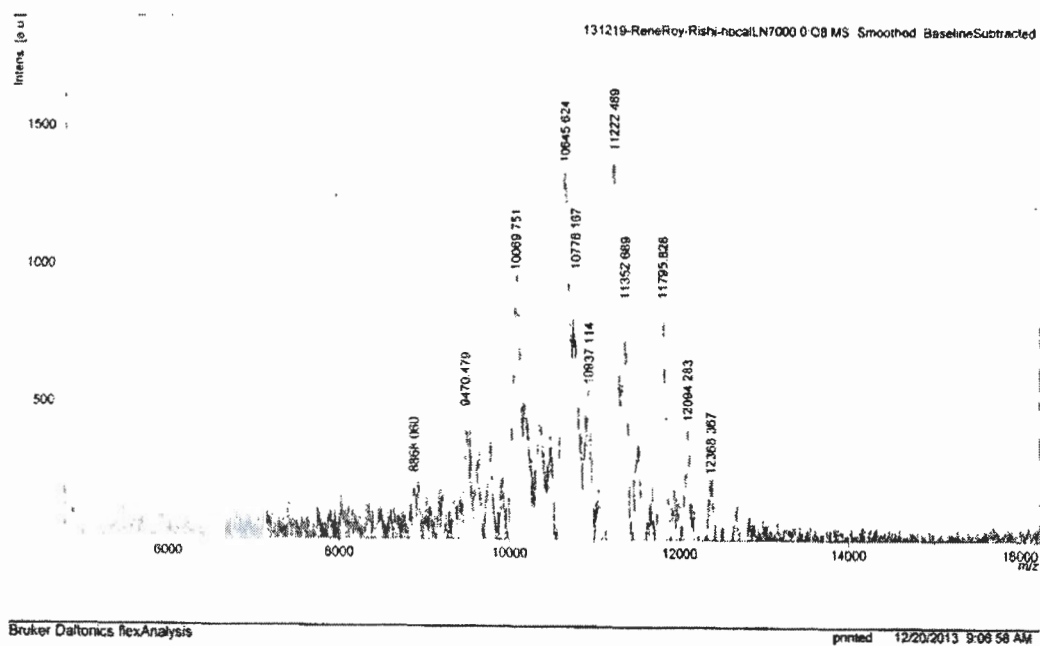


Figure S92. COSY spectrum of compound 25.



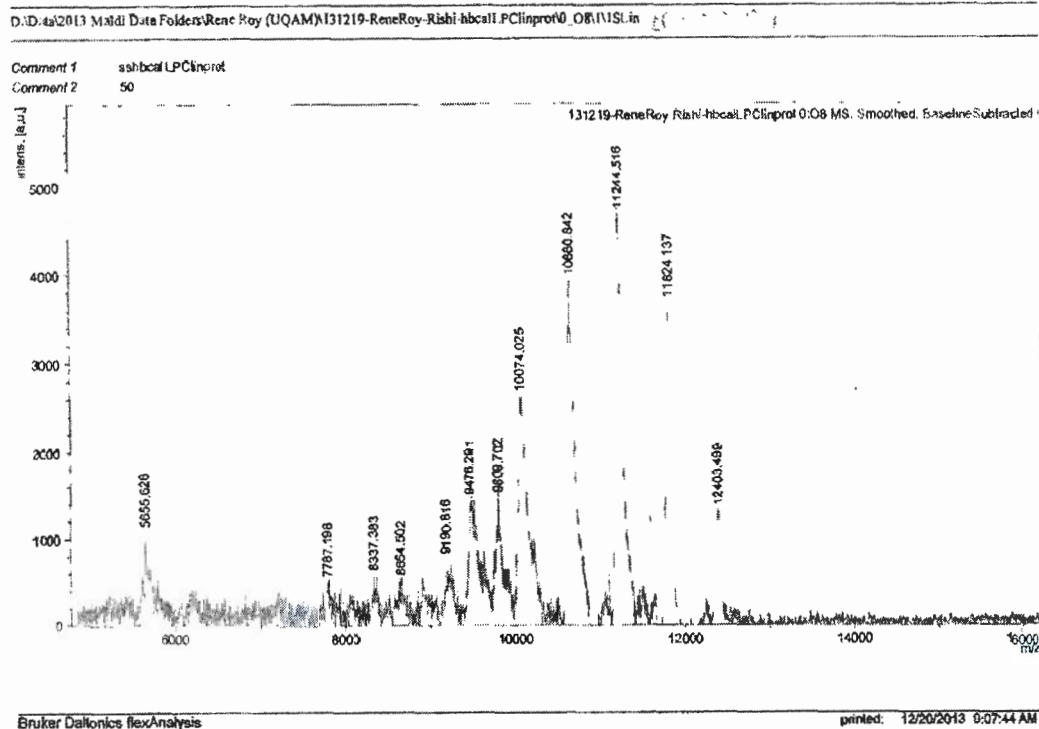


Figure S93. Top: MALDI TOF spectrum of compound **25**, bottom: MALDI-TOF spectrum of compound **25** (Positive mode with Cu)

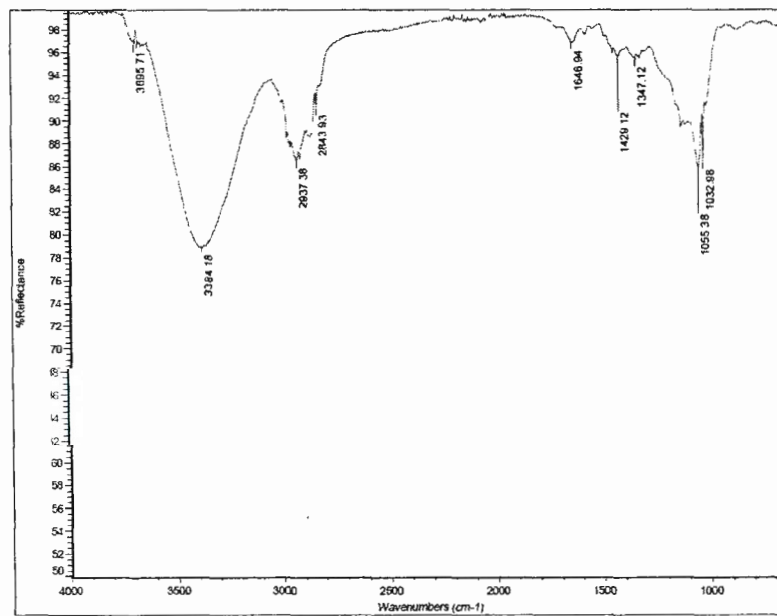


Figure S94. IR spectrum of compound **25**.

4. Surface plasmon resonance (SPR) studies:

The studies were conducted using a Biacore T200 SPR instrument with a CM5 sensor chip. A continuous flow of HEPES buffer (10 mM HEPES and 150 mM NaCl, 2 mM CaCl_2 , pH 7.4) was maintained over the sensor surface at a flow rate of 10 $\mu\text{L}/\text{min}$. The CM5 sensor chip was activated with an injection of a solution containing *N*-ethyl-*N'*-(3-diethylaminopropyl) carbodiimide (EDC) (0.2M) and *N*-hydroxysuccinimide (NHS) (0.05M) for 7 minutes. Lactoside **21** (200 $\mu\text{g}/\text{mL}$) and Et_3N (1 mM) in NaOAc buffer (pH 4.5) was injected over the activated flow cell at flow rate of 10 $\mu\text{L}/\text{min}$ for 2 minute to achieve a ~ 230 RU immobilization. The immobilization procedure was completed by an injection of ethanolamine hydrochloride (1M) (70 μL), followed by a flow of the buffer (100 $\mu\text{L}/\text{min}$), in order to eliminate physically adsorbed compounds. Ethanol amine alone was used in one of the flow-cell as a reference. The solutions of pre-incubated (1 hr) mixtures of glycodendrimers or monomers (with the various concentrations) and a PA-IL lectin (1.5 μM) in running HEPES buffer are passed over flow cells of the galactoside and ethanol amine (Association: 3 min and dissociation: 3 min). The sensor chip was regenerated with the serial injections of D-lactose (0.25 M, 3 min), buffer (3 min), D-lactose (0.25 M, 3 min) and buffer (3 min). For each inhibition assay, PA-IL lectin (1.5 μM) without inhibitor was injected to observe the full adhesion of the lectin onto the sugar-coated surface (0% inhibition). Response units from the surface of lactoside were subtracted from the surface of ethanol amine to eliminate non-specific interactions, as well as, bulk change in RU due to variation in refractive index of the medium. The primary subtracted sensorgrams were analyzed by 1:1 Langmuir model fitting, using the BIAevaluation software. For IC_{50} evaluation, the response units at the equilibrium was considered as the amount of lectin bound to the sugar surface in the presence of a defined concentration of inhibitor. Inhibition curves were obtained by plotting the percentage of inhibition against the inhibitor concentration (on a

logarithmic scale) by using Origin 7.0 software (OriginLab Corp.) and IC_{50} values were extracted from a sigmoidal fit of the inhibition curve.

SPR Sensorgram:

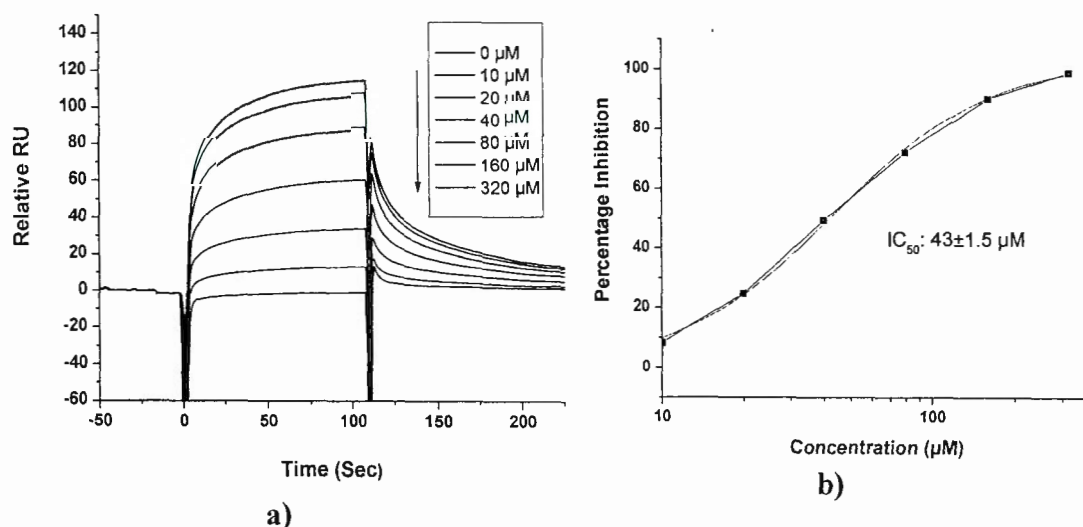


Figure S95. (a) Sensorgrams obtained by injection of PA-IL ($1.5 \mu M$) incubated with different concentrations of **18** varying from $10 \mu M$ (top curve) to $320 \mu M$ (bottom curve) on the surface of immobilized lactoside **21**. (b) The inhibitory curve for the **18**. IC_{50} value was extracted from the sigmoidal fit of the inhibition curve.

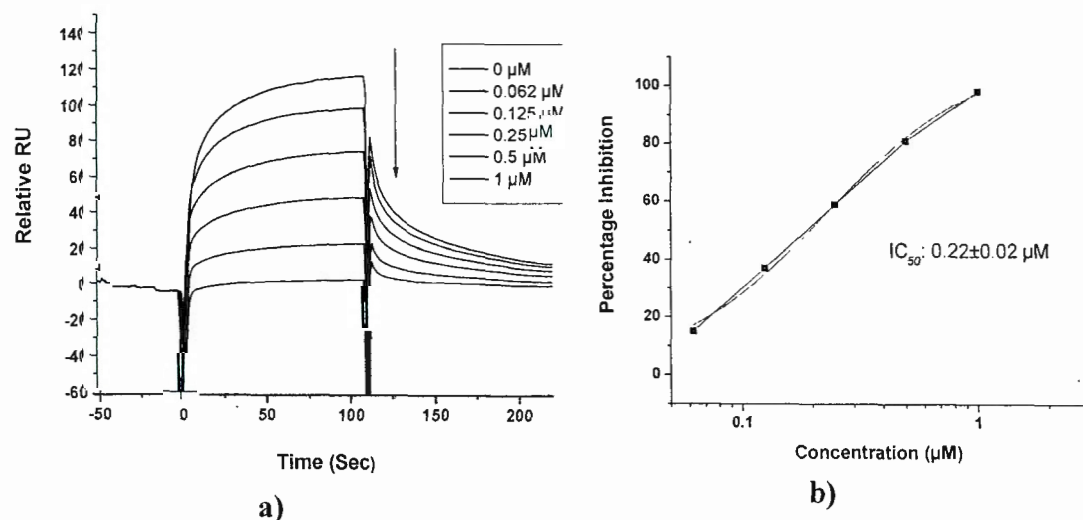


Figure S96. (a) Sensorgrams obtained by injection of PA-IL ($1.5 \mu M$) incubated with different concentrations of dendrimer **8** varying from $0.062 \mu M$ (top curve) to $1 \mu M$

(bottom curve) on the surface of immobilized lactoside **21**. (b) The inhibitory curve for the dendrimer **8**. IC_{50} value was extracted from the sigmoidal fit of the inhibition curve.

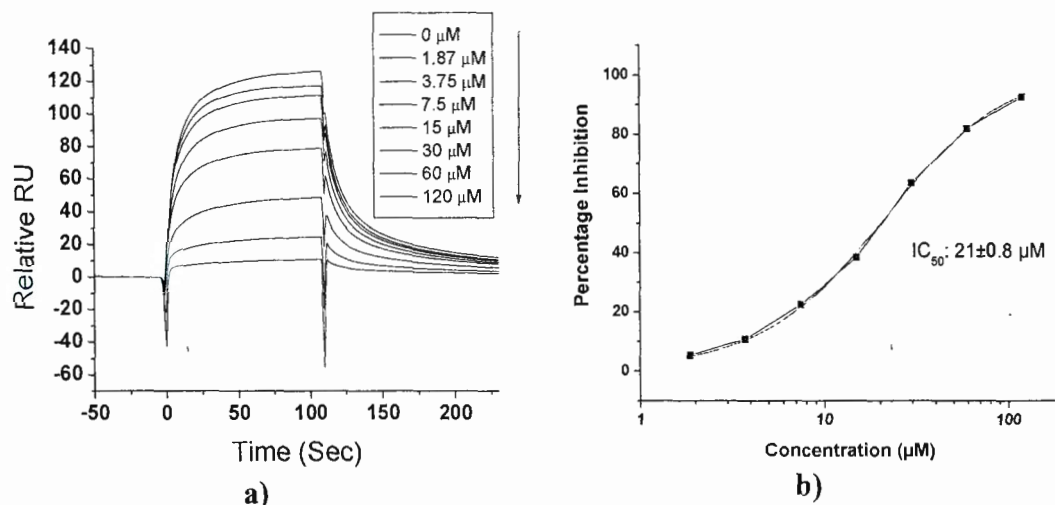


Figure S97. (a) Sensorgrams obtained by injection of PA-IL (1.5 μ M) incubated with different concentrations of **19** varying from 1.87 μ M (top curve) to 120 μ M (bottom curve) on the surface of immobilized lactoside **21**. (b) The inhibitory curve for the **19**. IC_{50} value was extracted from the sigmoidal fit of the inhibition curve.

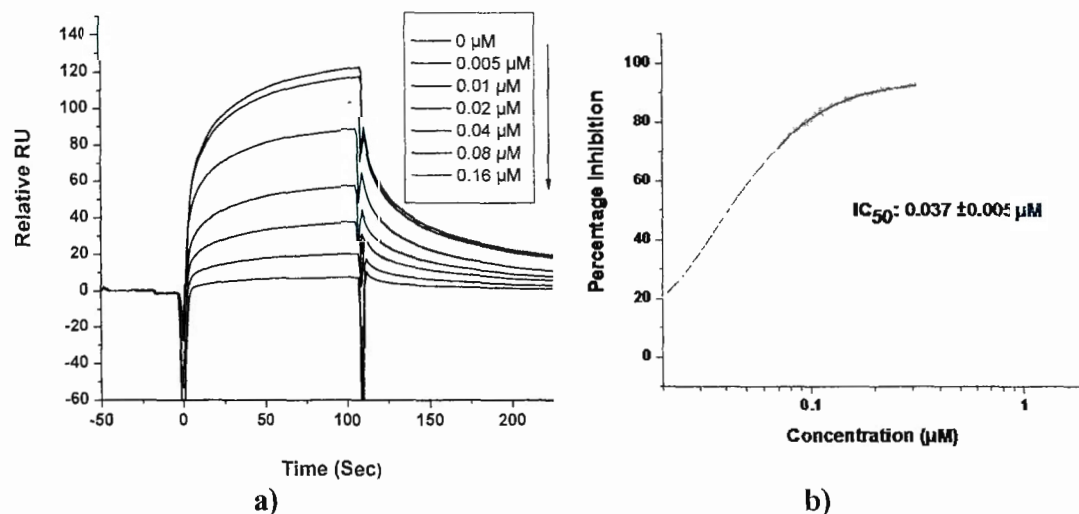


Figure S98. (a) Sensorgrams obtained by injection of PA-IL (1.5 μ M) incubated with different concentrations of glycodendrimer **23** varying from 0.005 μ M (top curve) to 0.16 μ M (bottom curve) on the surface of immobilized lactoside **21**. (b) The

inhibitory curve for the glycodendrimer **23**. IC_{50} value was extracted from the sigmoidal fit of the inhibition curve.

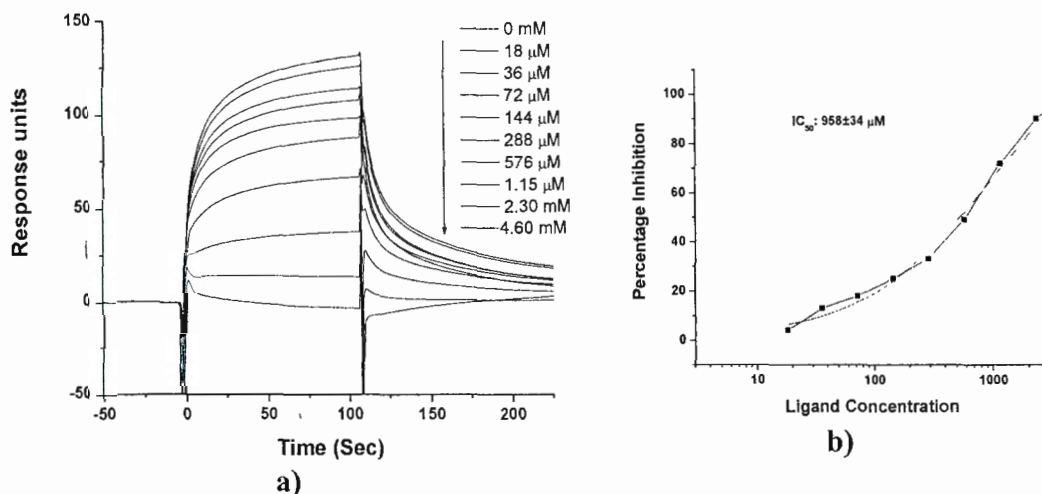


Figure S99. (a) Sensorgrams obtained by injection of PA-IL (1.5 μM) incubated with different concentrations of **20** varying from 18 μM (top curve) to 4.60 mM (bottom curve) on the surface of immobilized lactoside **21**. (b) The inhibitory curve for **20**. IC_{50} value was extracted from the sigmoidal fit of the inhibition curve.

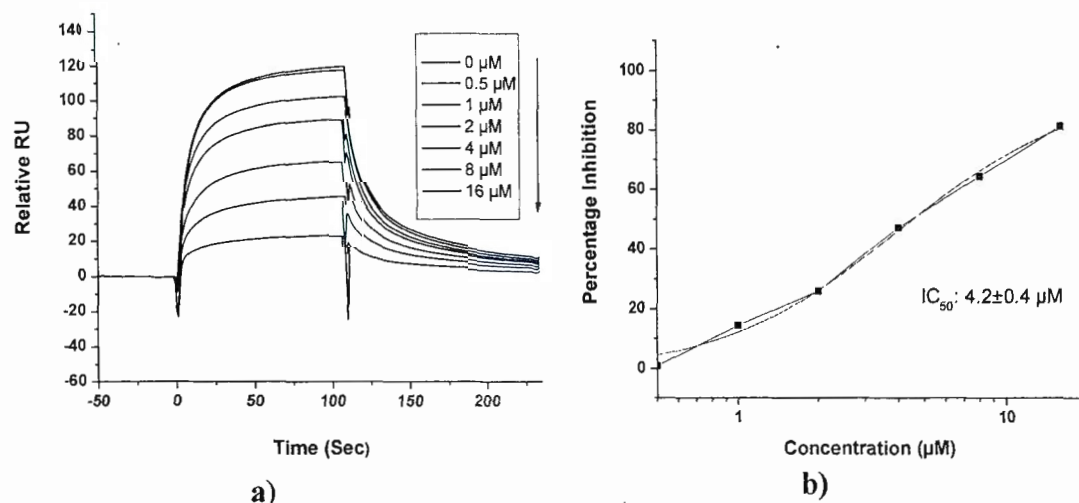


Figure S100. (a) Sensorgrams obtained by injection of PA-IL (1.5 μM) incubated with different concentrations of dendrimer **25** varying from 0.5 μM (top curve) to 16 μM (bottom curve) on the surface of immobilized lactoside **21**. (b) The inhibitory curve for the dendrimer **25**. IC_{50} value was extracted from the sigmoidal fit of the inhibition curve.

APPENDIX C

SUPPORTING INFORMATION-CHAPTER 4: A FAST TRACK STRATEGY
TOWARD HIGHLY FUNCTIONALIZED DENDRIMERS WITH DIFFERENT
STRUCTURAL LAYERS: "ONION PEEL APPROACH"

1. Materials and methods:

All reactions in organic medium were performed in standard oven dried glassware under an inert atmosphere of nitrogen using freshly distilled solvents. CH_2Cl_2 and DMF were distilled from CaH_2 and ninhydrin respectively, and kept over molecular sieves. Solvents and reagents were deoxygenated when necessary by purging with nitrogen. All reagents were used as supplied without prior purification unless otherwise stated, and obtained from Sigma-Aldrich Chemical Co. Ltd. Reactions were monitored by analytical thin-layer chromatography (TLC) using silica gel 60 F254 precoated plates (E. Merck) and compounds were visualized by 254 nm light, a mixture of iodine/silica gel and/or mixture of ceric ammonium molybdate solution (100 ml H_2SO_4 , 900 ml H_2O , 25g $(\text{NH}_4)_6\text{Mo}_7\text{O}_{24}\cdot\text{H}_2\text{O}$, 10g $\text{Ce}(\text{SO}_4)_2$) and subsequent development by gentle warming with a heat-gun. Purifications were performed by flash column chromatography using silica gel from Silicycle (60 Å, 40-63 μm) with the indicated eluent.

^1H NMR and ^{13}C $\{^1\text{H}\}$ NMR spectra were recorded at 300 or 600 MHz and 75 or 150 MHz, respectively, on a Bruker spectrometer (300 MHz) and Varian spectrometer (600 MHz). All NMR spectra were measured at 25°C in indicated deuterated solvents. Proton and carbon chemical shifts (δ) are reported in ppm and coupling constants (J) are reported in Hertz (Hz). The resonance multiplicity in the ^1H NMR spectra are described as "s" (singlet), "d" (doublet), "t" (triplet), "quint" (quintuplet) and "m" (multiplet) and broad resonances are indicated by "br". Residual protic solvent of CDCl_3 (^1H , δ 7.27 ppm; ^{13}C , δ 77.0 ppm (central resonance of the triplet)), D_2O (^1H , δ 4.79 ppm and 30.9 ppm for CH_3 of Acetone for ^{13}C spectra, MeOD (^1H , δ 3.31 ppm and ^{13}C , δ 49.0 ppm. 2D Homonuclear correlation ^1H - ^1H COSY experiments were used to confirm NMR peak assignments. Gel Permeation Chromatography (GPC) was performed using Chloroform and THF as the eluent, at 40°C with a 1 ml/min flow rate on a Viscotek VE 2001 GPCmax (SEC System) with Wyatt DSP/Dawn EOS and refractive index RI/LS system as detectors. 2 PLGel mixed B LS (10 μm , 300×7.5 mm) and LS-MALLS detection with performances verified with polystyrene 100 kDa and 2000 kDa were used to determine the number-average molecular weight (M_n) and polydispersity index (M_w/M_n). Calculations were performed with Zimm Plot (model). Fourier transform infrared (FTIR) spectra were obtained with Thermo-scientific, Nicolet model 6700 equipped with ATR. The

absorptions are given in wave numbers (cm^{-1}). Accurate mass measurements (HRMS) were performed on a LC-MSD-TOF instrument from Agilent Technologies in positive electrospray mode. Either protonated molecular ions $[\text{M}+\text{nH}]^{n+}$ or adducts $[\text{M}+\text{nX}]^{n+}$ ($\text{X} = \text{Na}, \text{K}, \text{NH}_4$) were used for empirical formula confirmation. MALDI-TOF experiments were performed on an Autoflex III from Bruker Smarteam in linear positive mode (Mass Spectrometry Laboratory (McGill University)) to afford adducts $[\text{M}+\text{nX}]^{n+}$ ($\text{X} = \text{Na}, \text{K}$ or Li). DLS experiments were carried out at ambient temperature using a Zeta sizer nano S-90 from Malvern instruments equipped with 4mW He-Ne Laser 633 nm and avalanche photodiode positioned at 90° to the beam. The Non-Negatively constrained Least Squares (NNLS) algorithm was used to generate raw intensity vs particle size data for a single measurement. A Gaussian curve was fitted to estimate the average particle size and coefficient of variation, defined as the ratio of standard deviation to mean particle size. Polydispersity is calculated from a cumulants analysis of the dynamic light scattering intensity autocorrelation function and is a measure of the deviation of the correlation function from the initial slope.

NMR diffusion experiments: NMR diffusion measurements were performed at 25°C on a Bruker Avance III HD (Bruker BioSpin Ltd., Milton, ON, Canada) operating at a frequency of 599.95 MHz for ^1H using a 5 mm broadband z-gradient temperature-regulated probe. The measurement of the diffusion rate (D) allows calculating the solvodynamic diameter of a molecule.¹ The application of the Stokes-Einstein equation gives an estimate of the diameter of the molecule.

Stokes-Einstein equation: $D = K_B T / 6\pi\eta r_s$

D : Diffusion rate ($\text{m}^2 \cdot \text{s}^{-1}$); K_B : Boltzmann's constant ($k_B = 1.38 \times 10^{-23} \text{ m}^2 \cdot \text{kg} \cdot \text{s}^{-2} \cdot \text{K}^{-1}$); T : Temperature (K) ($T = 298.15 \text{ K}$); η : solvent viscosity in Pa s; r_s : Solvodynamic radius of the species.

2. Synthetic protocols and characterization:

A. General procedure for the microwave-assisted copper catalyzed reactions:

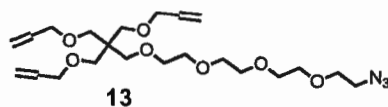
An acetylene terminated dendrimer (1eq) and azide terminated building block (1.5 eq per acetylene) were suspended in a 3:1 mixture of tetrahydrofuran (THF) and water (5ml/mmol) in a 5 ml glass vial equipped with a small magnetic stirring bar. To this was added the copper sulphate (0.5 eq /acetylene) and sodium ascorbate (0.5 eq /acetylene), and the vial was tightly sealed with an aluminum/Teflon® crimp top. The mixture was then irradiated for 5h at 50°C using an irradiation power of 100 W. After

completion of the reaction, the vial was cooled to 25°C by gas jet cooling before it was opened. The solvent was then removed and dichloromethane (DCM) was added to reaction mixture. Organic layer was washed a few times with saturated solution of ethylenediaminetetraacetic acid (EDTA) till the green color of copper disappeared followed by washing with brine. The organic layer was dried using anhydrous sodium sulphate, filtered and finally solvent was evaporated. The crude mixture was purified using silica gel column chromatography to provide pure desired compounds in good yields.

B. General procedure for the microwave-assisted thiol-ene reactions:

An alkene terminated dendrimer (1eq) and 1- thioglycerol (5 eq per alkene) were suspended in methanol (0.5ml) in a 5 ml glass vial equipped with a small magnetic stirring bar. To this was added AIBN (10 mol% /acetylene) and the vial was tightly sealed with an aluminum/Teflon® crimp top. The mixture was then irradiated for 6h at 90°C using an irradiation power of 100 W. After completion of the reaction, the vial was cooled to 25°C by gas jet cooling before it was opened. Solvent was removed and diethyl ether was added to the reaction mixture. The precipitates formed were washed few times with diethyl ether to remove excess of 1- thioglycerol and disulfide. Crude product was then completely dissolved in minimum volume of methanol, diluted with 4 ml water and loaded in the dialysis bag of 1000 cut-off. Dialysis was performed for 12 h changing water every 3h interval.

Note: For dialysis, all dendrimers were first dissolved completely in minimum volume of methanol and added to dialysis bag which already contained milli-Q water because none of dendrimers was soluble in water.



Synthesis of compound 13: To a stirred solution of 3-(allyloxy)-2,2-bis((allyloxy)methyl)propan-1-ol **11** (1000 mg, 3.9 mmol) in dry DMF, added powdered NaH (60% in oil, 280 mg, 11.7 mmol) in portions at 0°C under N₂ environment. The reaction mixture was stirred for 10-15 minutes followed by the slow addition of 2-(2-(2-(2-azidoethoxy)ethoxy)ethoxy)ethyl 4-methylbenzenesulfonate **12** (1600 mg, 4.29 mmol) dissolved in minimum volume of DMF. The reaction mixture was allowed to come to room temperature. Upon completion, reaction was quenched at 0°C with saturated NH₄Cl solution followed by the addition of DCM (100 ml) The organic layer was washed few times with cold

water to get rid of DMF. It was dried with anhydrous sodium sulphate, filtered and concentrated in *vacuo*. The purification by column chromatography was performed and the desired product **13** was isolated using 25% EtOAc in hexanes as colourless oil in 80% yield.

^1H NMR (300 MHz, CDCl_3) δ 5.89 (ddt, $J = 17.2, 10.5, 5.3$ Hz, 3H), 5.36 – 5.03 (m, 6H), 3.95 (dt, $J = 5.3, 1.5$ Hz, 6H), 3.74 – 3.55 (m, 14H), 3.47 (d, $J = 8.4$ Hz, 8H), 3.43 – 3.36 (m, 2H).

^{13}C $\{^1\text{H}\}$ NMR (75 MHz, CDCl_3) δ 135.2, 115.97, 72.1, 70.97, 70.7, 70.6, 70.5, 70.2, 69.9, 69.2, 50.60, 45.36.

HRMS (ESI^+) m/z calc. For $\text{C}_{22}\text{H}_{39}\text{N}_3\text{O}_7$, 457.5610; Found, 458.2848 $[\text{M} + \text{H}]^+$, 475.3112 $[\text{M} + \text{NH}_4]^+$.

I.R (cm^{-1}): 2866, 2102, 1478, 1349, 1288, 1091, 992, 923.

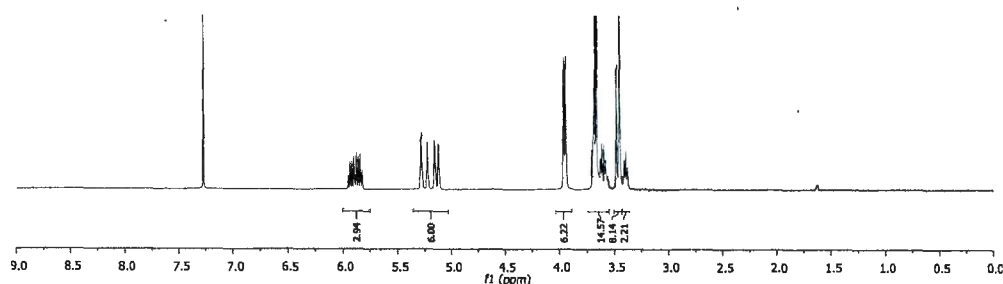


Figure S1. ^1H NMR spectrum of compound **13** (CDCl_3 , 300 MHz).

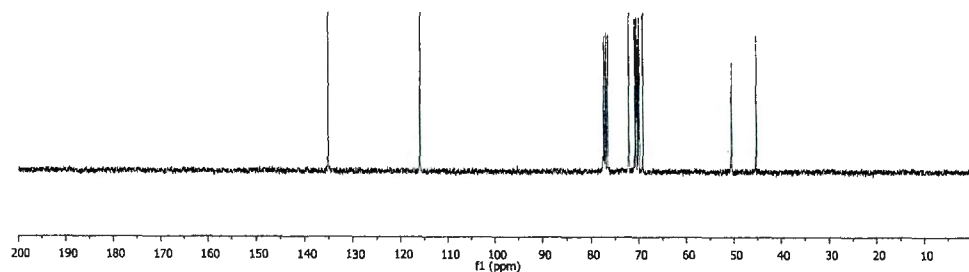


Figure S2. $^{13}\text{C}\{^1\text{H}\}$ NMR of compound **13** (CDCl_3 , 75 MHz).

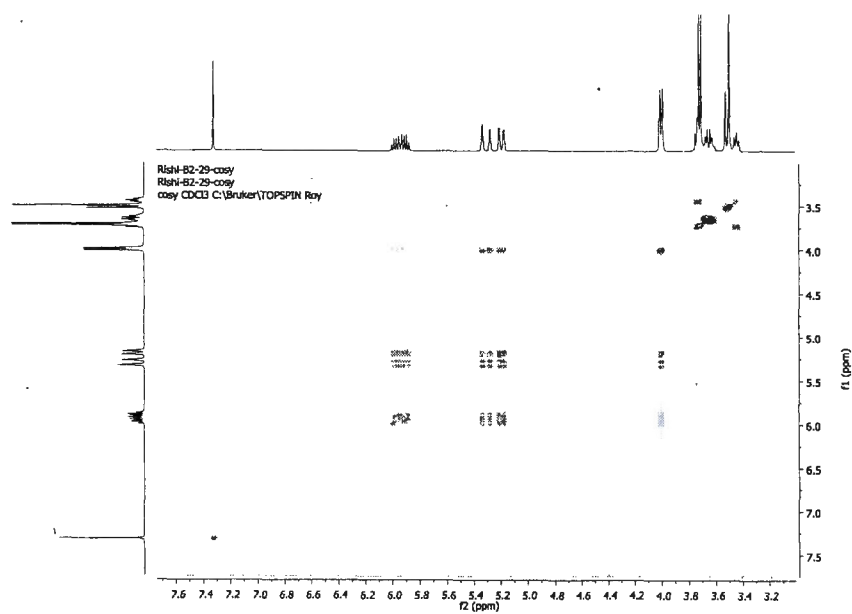


Figure S3. COSY spectrum of compound 13.

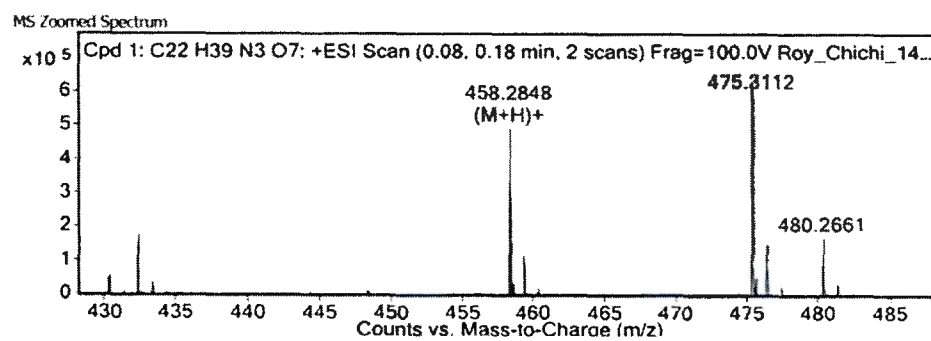


Figure S4. HRMS (ESI⁺) spectrum of compound 13.

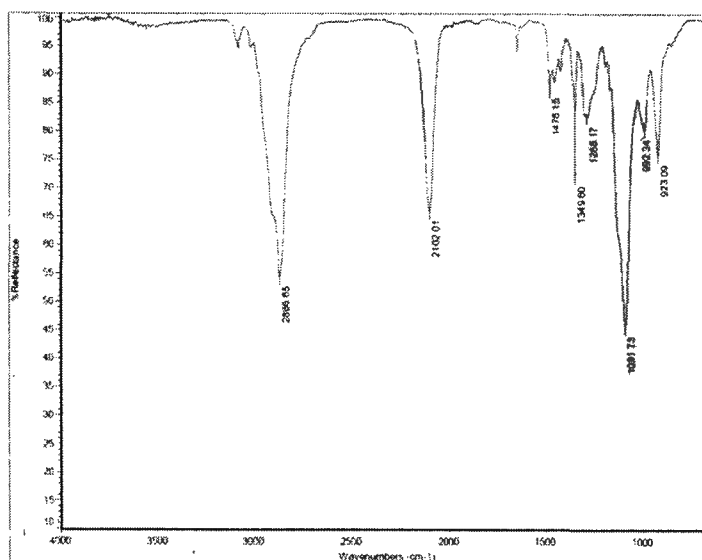
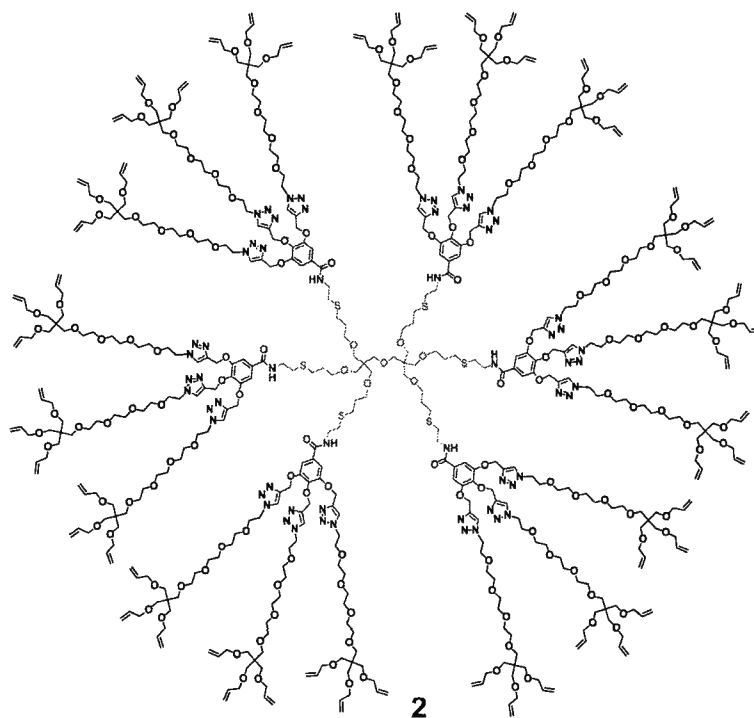


Figure S5. IR spectrum of compound **13**.



Synthesis of compound 2: A mixture of propargyl terminated dendrimer **1** (30 mg, 0.0117 mmol, 1eq), compound **13** (144 mg, 0.315 mmol, 27 eq.), CuSO₄·5H₂O (26 mg, 0.1053 mmol, 9 eq.) and sodium ascorbate (21 mg, 0.1053 mmol, 9 eq.) was

reacted together following the procedure A and was purified by column chromatography (4% MeOH in DCM as eluent) to yield compound **2** as a colourless oil in 78% yield.

^1H NMR (600 MHz, CDCl_3) δ 7.92 (s, 12H), 7.84 (s, 6H), 7.25 (s, 12H), 5.93 – 5.80 (m, 54H), 5.26 – 5.07 (m, 152H), 4.51 (dt, $J = 34.4$, 5.2 Hz, 38H), 3.93 (d, $J = 5.3$ Hz, 112H), 3.86 (dt, $J = 25.9$, 5.3 Hz, 38H), 3.63 – 3.53 (m, 226H), 3.46 (s, 40H), 3.43 (s, 112H), 3.37 (s, 12H), 2.77 (br s, 12H), 2.65 (t, $J = 6.8$ Hz, 12H), 1.85 (d, $J = 6.0$ Hz, 12H).

$^{13}\text{C}\{^1\text{H}\}$ NMR (75 MHz, CDCl_3) δ 166.7, 152.0, 144.0, 143.2, 140.0, 135.2, 134.7, 130.0, 124.7, 124.5, 116.5, 116.0, 107.1, 72.3, 72.1, 72.0, 70.9, 70.5, 70.4, 70.3, 70.1, 69.7, 69.3, 69.2, 66.2, 62.9, 50.1, 49.9, 45.6, 45.3, 39.6, 31.3, 29.7, 28.5.

(MALDI-TOF) m/z : calculated for $\text{C}_{532}\text{H}_{850}\text{N}_{60}\text{O}_{157}\text{S}_6$: 10791.1392, found: 10814.3920 $[\text{M}+\text{Na}]^+$

I.R (cm^{-1}) 3705, 3680, 2981, 2937, 2922, 2865, 2844, 1454, 1426, 1346, 1098, 1054, 1033, 1012.

GPC (CHCl_3) $M_n = 10770$ g/mol. $M_w/M_n = 1.08$

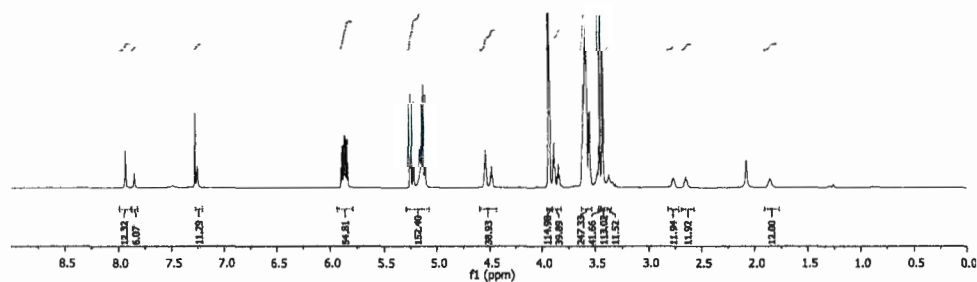


Figure S6. ^1H NMR spectrum of compound **2** (CDCl_3 , 600 MHz).

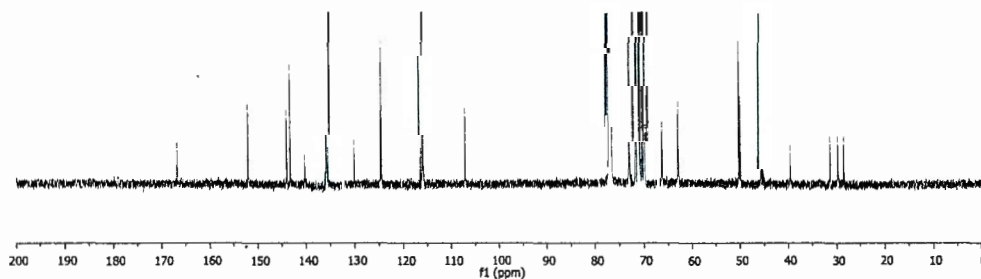


Figure S7. $^{13}\text{C}\{^1\text{H}\}$ NMR of compound **2** (CDCl_3 , 75 MHz)

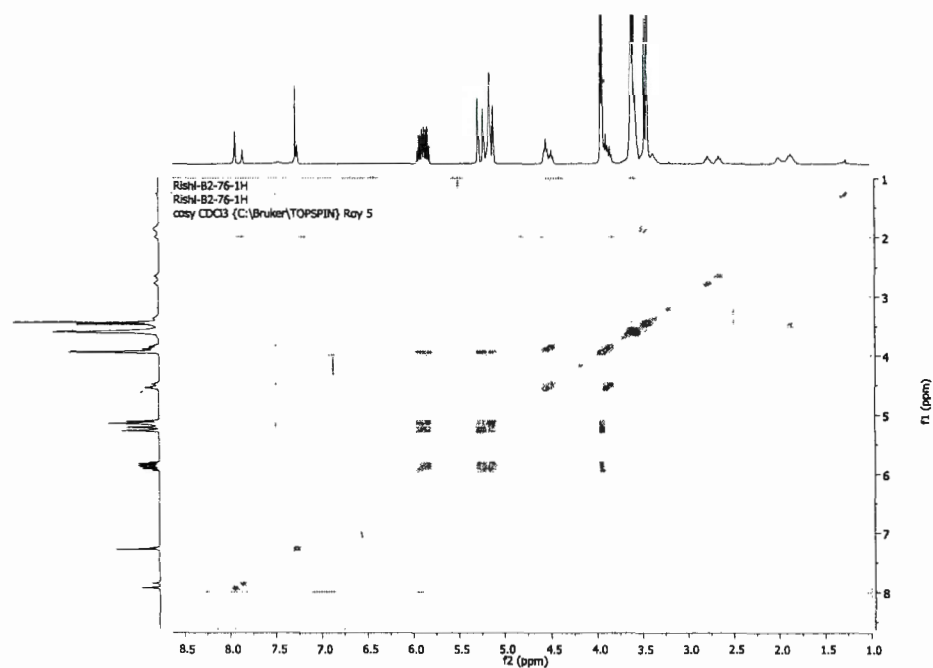


Figure S8. COSY spectrum of compound 2

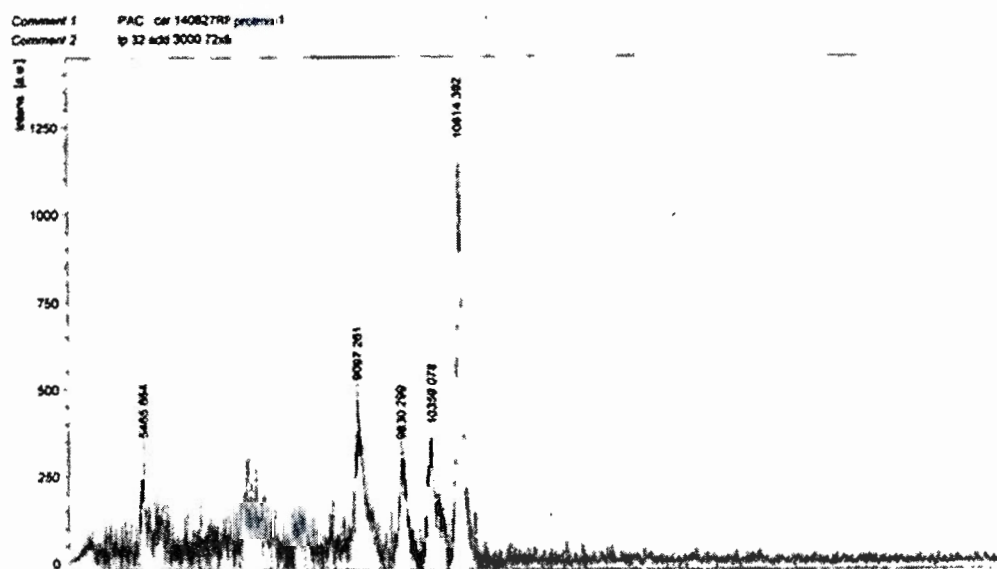
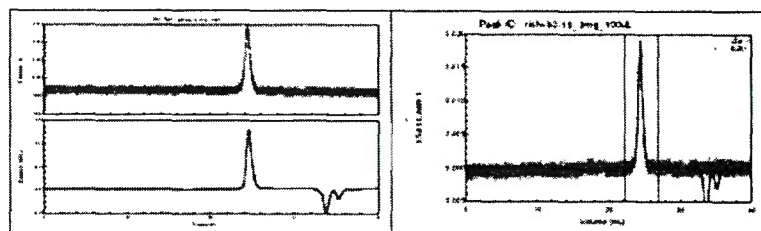


Figure S9. MALDI-TOF spectrum of compound 2



COLLECTION INFORMATION

Collection time : Wed Aug 21, 2002 03:01 PM Est (heure d'été)
 Instrument type : DAWN EOS
 Cell type : XS
 Laser wavelength : 690.0 nm
 Solvent name : water
 Solvent RI : 1.330
 Calibration constants
 DAWN : 6.1620e-06
 AUX1 : 3.5650e-04
 AUX2 : 1.0000e-06
 Flow rate : 1.000 mL/min
 Collection interval : 0.200 sec
 Number of slices : 6400

Volume (mL) : 22.520 = 46.867
 Slices (used) : 1096 (735)
 A2 (mol/mL.g) : 0.000e+00
 Fit degree : 1
 Injected Mass (g) : 2.0000e-06
 dn/dc (mL.g) : 0.074
 Polydispersity(Mw/Mn) : 1.044±0.143 (15%)
 Polydispersity(Mz/Mn) : 1.442±0.491 (46%)

Molar Mass Moments (g/mol)
 Mn : 1.077e+04 (84)
 Mw : 1.166e+04 (12%)
 Mz : 1.597e+04 (45%)

Figure S10. GPC traces of compound 2

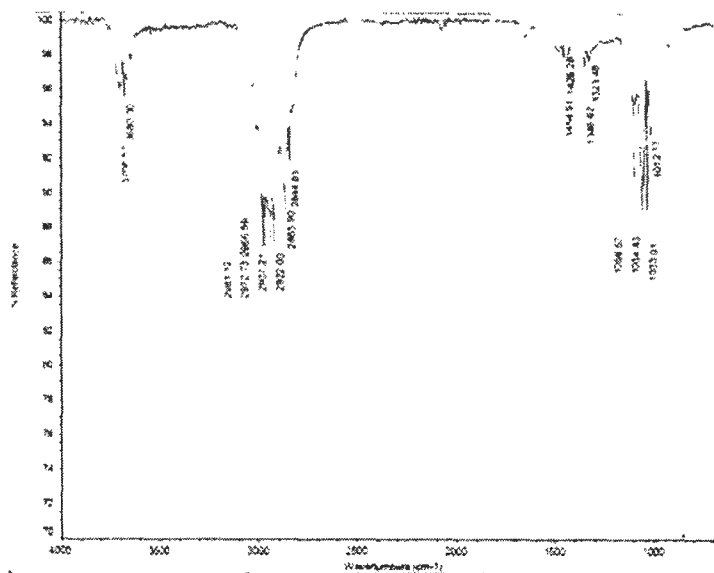
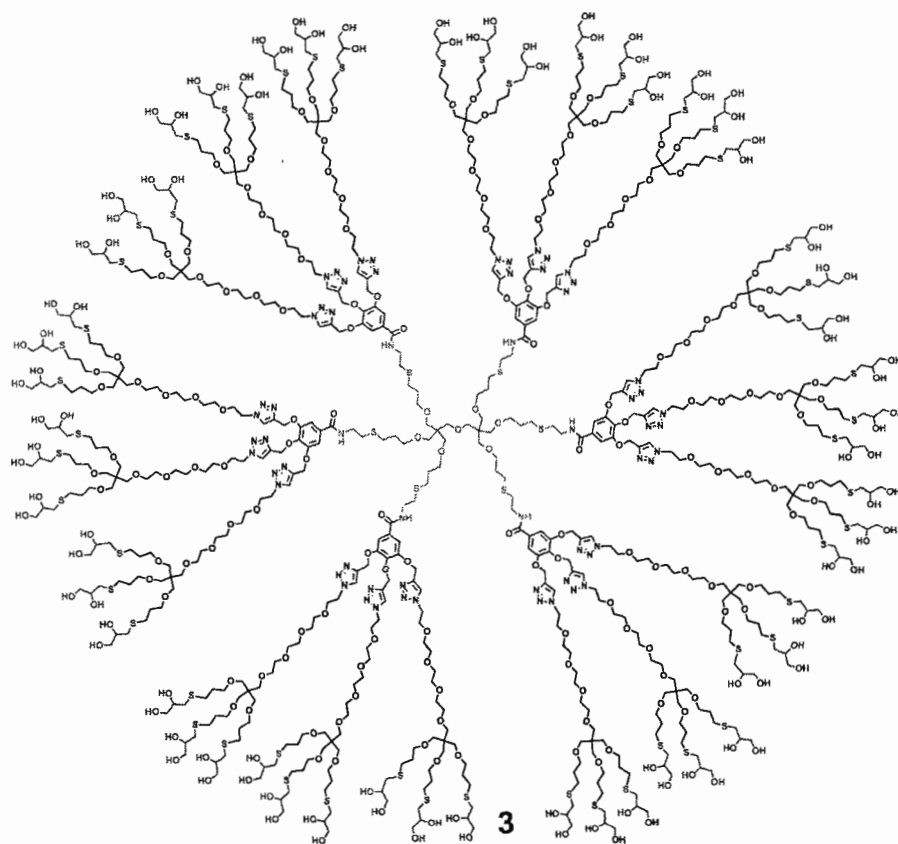


Figure S11. IR spectrum of compound 2.



Synthesis of compound 3: Alkene terminated dendrimer **2** (65 mg, 0.006 mmol, 1eq), 1-thioglycerol (0.139 ml, 1.62 mmol, 270 eq.), and AIBN (5.3 mg, 0.0324 mmol, 5.4 eq.) were reacted together following the procedure B and was purified by dialysis to yield compound **3** as a colourless oil in 85% yield.

^1H NMR (300 MHz, MeOD) δ 8.52 (br s, 6H), 8.17 (s, 12H), 7.92 (s, 6H), 7.34 (s, 12H), 5.16 (d, J = 26.5 Hz, 46H), 4.57 (d, J = 28.4 Hz, 38H), 3.95 – 3.33 (m, 798H), 2.79 – 2.47 (m, 244H), 1.93 – 1.72 (m, 120H).

$^{13}\text{C}\{^1\text{H}\}$ NMR (151 MHz, MeOD) δ 168.7, 153.5, 145.2, 144.4, 141.4, 131.2, 129.4, 126.6, 126.5, 108.4, 77.6, 73.2, 73.1, 72.8, 72.2, 71.6, 71.5, 71.4, 71.1, 71.0, 70.9, 70.5, 70.3, 66.9, 66.0, 63.8, 51.5, 51.4, 49.8, 46.8, 46.7, 41.2, 36.4, 35.2, 35.1, 32.1, 31.0, 30.7, 30.4, 29.6, 19.1.

HRMS (ESI $^+$) m/z calc. For $\text{C}_{694}\text{H}_{1282}\text{N}_{60}\text{O}_{265}\text{S}_{60}$, 16631.7479; Found: 16631.7480.

I.R (cm^{-1}) 3349, 2920, 2870, 1643, 1425, 1227, 1094, 1032.

Differential light scattering Hydrodynamic diameter: 5.70 nm

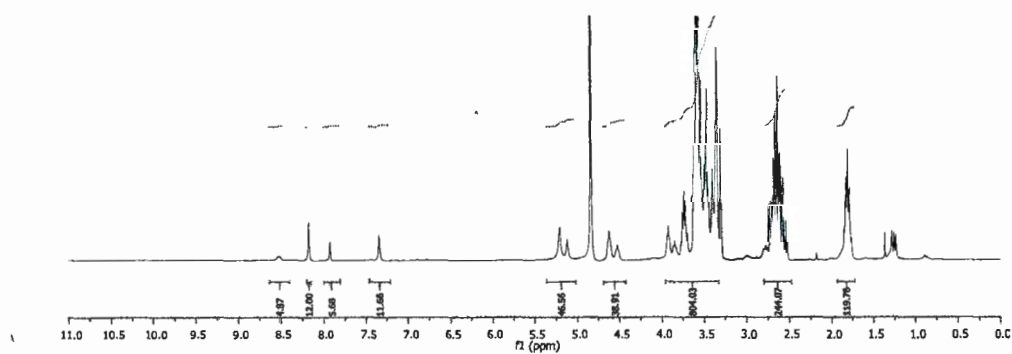


Figure S12. ^1H NMR spectrum of compound **3** (CD_3OD , 300 MHz)

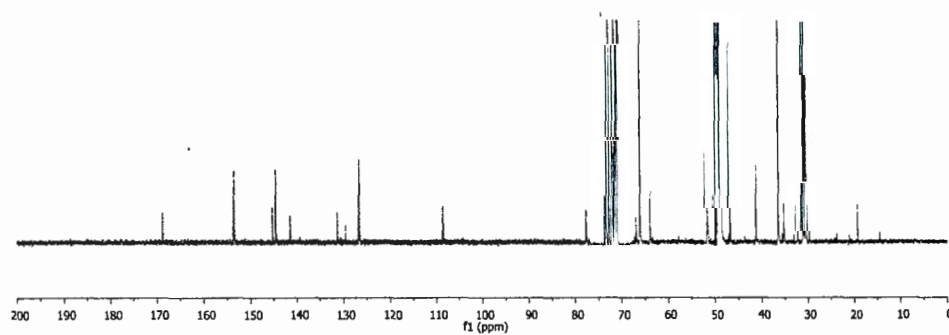


Figure S13. ^{13}C $\{^1\text{H}\}$ NMR. of compound **3** (CD_3OD , 151 MHz)

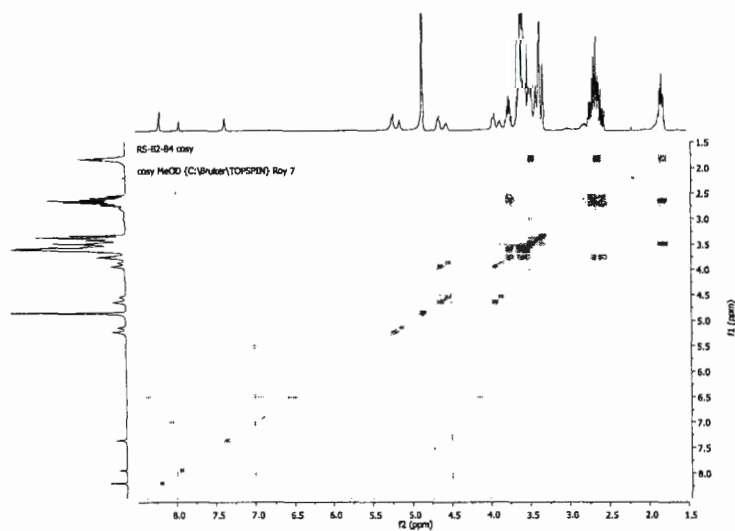


Figure S14. COSY spectrum of compound **3**.

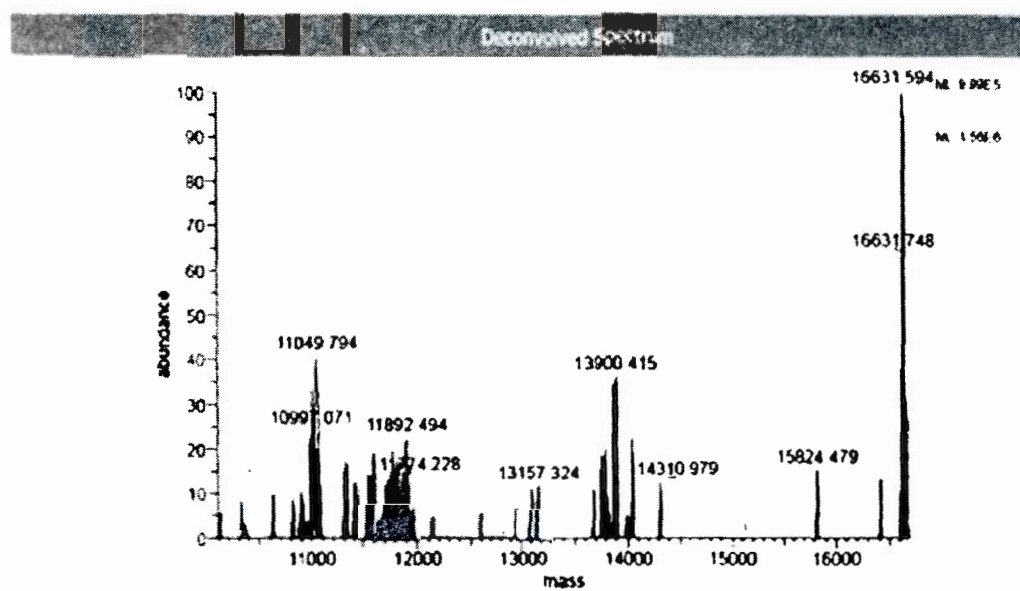


Figure S15. HRMS (ESI⁺) spectrum of compound 3.

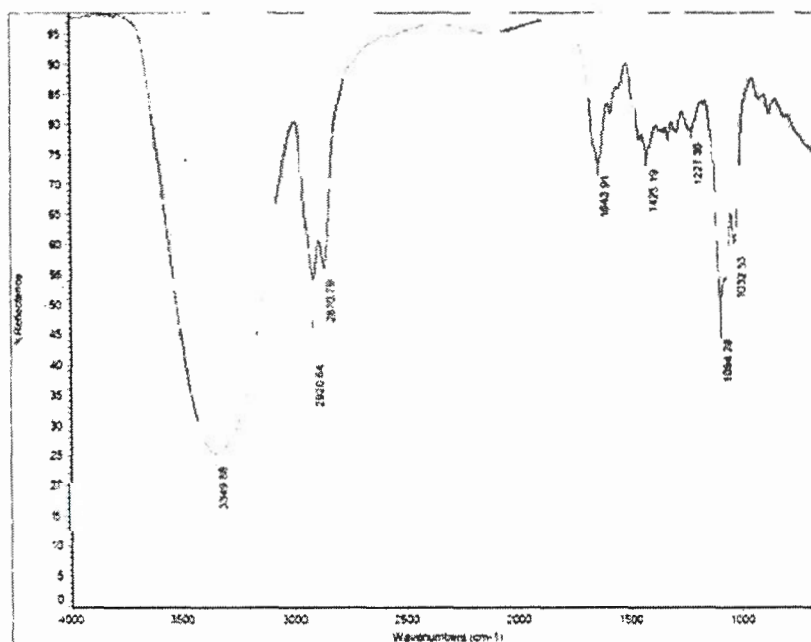


Figure S16. IR spectrum of compound 3.

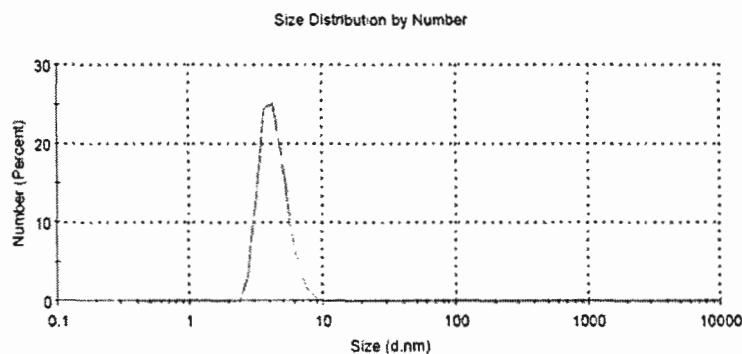
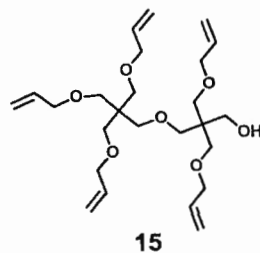


Figure S17. DLS size distribution of dendrimer 3 in methanol at 25°C.



Synthesis of compound 15: Dipentaerythritol **14** (1.5 g, 5.9 mmol) was suspended in DMSO (22 ml) followed by addition of Sodium hydroxide solution (40% in water, 16 ml) slowly. The mixture was stirred at room temperature for 30 minutes. Allyl bromide (5.2 ml, 57.3 mmol) was added drop wise. The reaction mixture was stirred at room temperature for 16 h. It was diluted with diethyl ether (150 ml), washed with water (25 ml) and brine (25 ml), and dried over MgSO_4 . The solvent was evaporated and the crude was passed through a column of silica gel with hexane-ethyl acetate mixtures (0-30% ethyl acetate) as eluent to obtain pure pentaallyl dipentaerythritol **15** in 40% yield along with tetraallyl derivative in 49% yield.

^1H NMR (300 MHz, CDCl_3) δ 5.88 (ddd, $J = 22.6, 10.6, 5.4$ Hz, 5H), 5.34 – 5.09 (m, 10H), 4.03 – 3.89 (m, 10H), 3.71 (d, $J = 6.3$ Hz, 2H), 3.48 (s, 4H), 3.44 (d, $J = 6.2$ Hz, 10H), 3.04 (t, $J = 6.3$ Hz, 1H).

$^{13}\text{C}\{^1\text{H}\}$ NMR (75 MHz, CDCl_3) δ 135.17, 134.90, 116.43, 72.42, 71.11, 70.69, 69.63, 66.18, 45.40, and 45.10.

IR (cm^{-1}) 3502, 3079, 2979, 2866, 1754, 1646, 1478, 1420, 1350, 1265, 1089, 991, 922.

HRMS (ESI^+) m/z calc, 454.5968; found, 455.30 $[M + \text{H}]^+$.

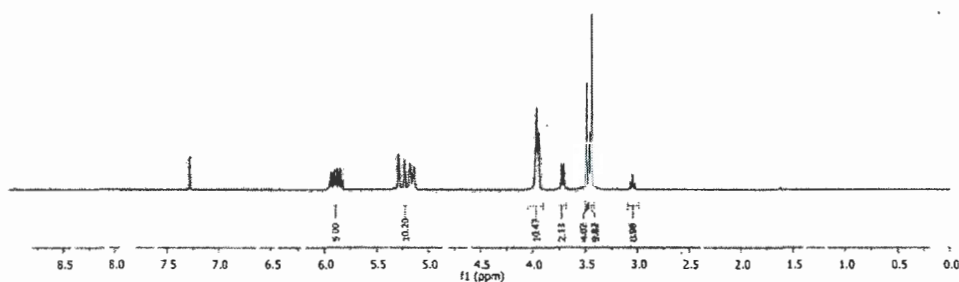


Figure S18. ^1H NMR spectrum of compound **15** (CDCl_3 , 300 MHz).

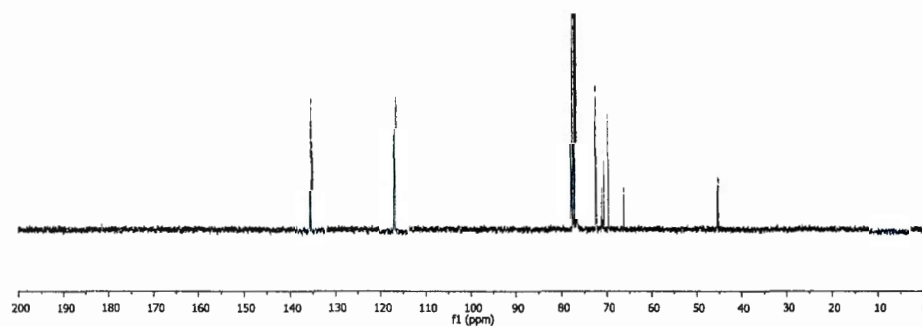


Figure S19. ^{13}C $\{^1\text{H}\}$ NMR of compound **15** (CDCl_3 , 75 MHz).

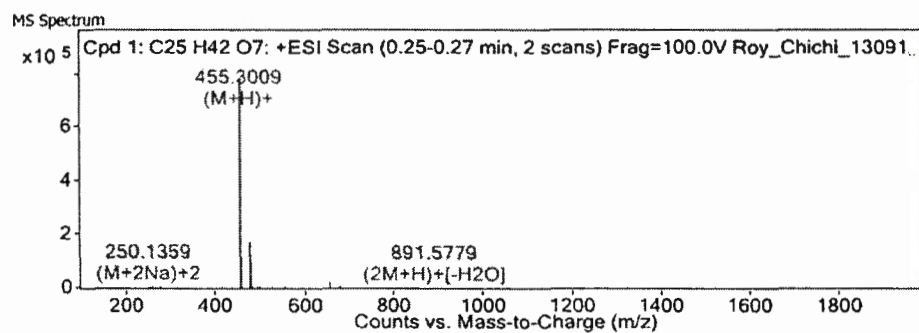


Figure S20. HRMS (ESI^+) spectrum of compound **15**.

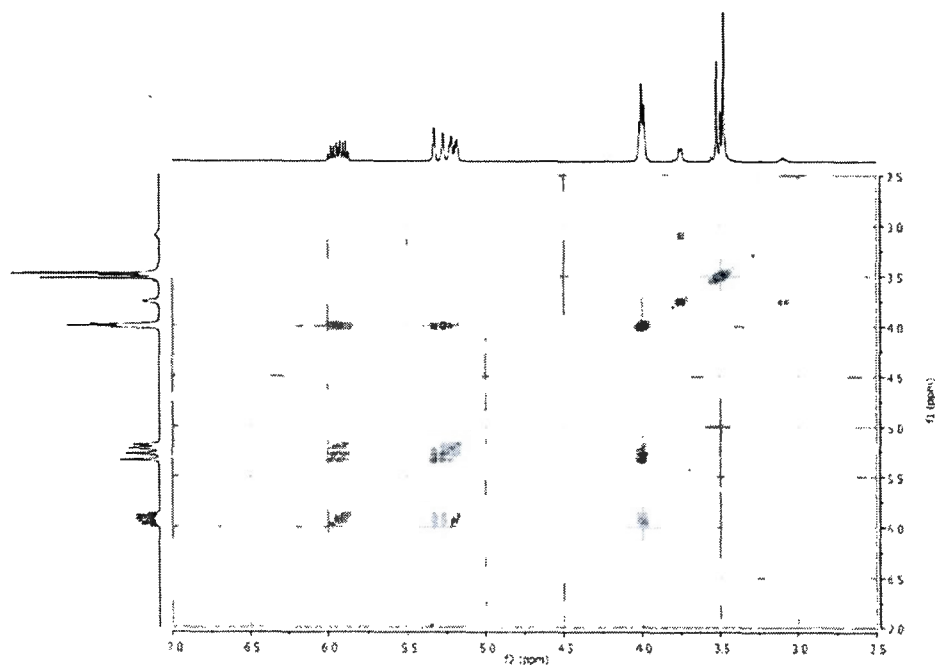


Figure S21. COSY spectrum of compound 15.

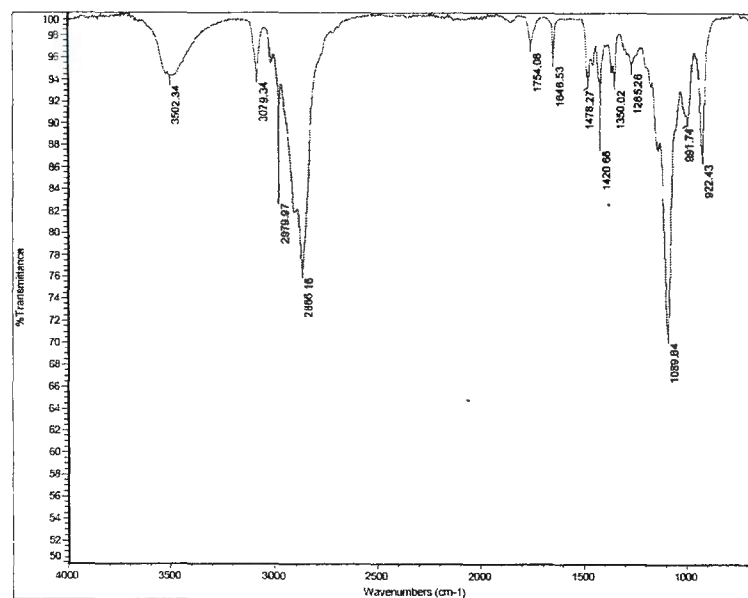
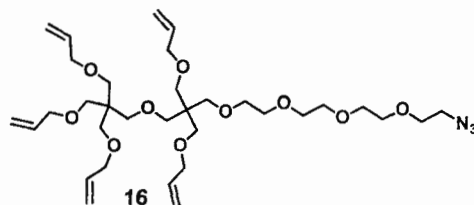


Figure S22. IR spectrum of compound 15.



Synthesis of compound 16: To a solution of 3-(allyloxy)-2-((3-(allyloxy)-2,2-bis((allyloxy)methyl)propoxy)methyl)-2-((allyloxy)methyl)propan-1-ol (**15**) (800 mg, 1.76 mmol) in DMF (10ml) at 0°C sodium hydride (60% in oil, 500 mg, 12.5 mmol) was added. The mixture was stirred at 0°C for 15 min followed by addition of 2-(2-(2-azidoethoxy)ethoxy)ethoxyethyl 4-methylbenzenesulfonate (**12**) (8.54 mg, 2.29 mmol) dissolved in DMF (2ml). The mixture was stirred at 0°C for 1 h and RT for 10 minutes. Reaction was quenched with saturated NH₄Cl solution and extracted with EtOAc (50 ml) followed with brine wash. The organic layer was separated, dried and crude mixture was purified with column chromatography. Desired compound **16** was obtained using 25% EtOAc: hexane as eluent in 68% yield.

¹H NMR (300 MHz, CDCl₃) δ 5.96 – 5.80 (m, 5H), 5.19 (ddd, *J* = 13.8, 11.4, 1.3 Hz, 10H), 4.02 – 3.88 (m, 10H), 3.67 (d, *J* = 5.4 Hz, 10H), 3.64 – 3.53 (m, 4H), 3.47 – 3.37 (m, 18H).

¹³C{¹H} NMR (75 MHz, CDCl₃) δ 135.1, 115.9, 72.1, 70.9, 70.5, 70.2, 70.1, 69.9, 69.3, 50.5, 45.5, 45.4.

HRMS (ESI⁺) *m/z* calc. For C₃₃H₅₇N₃O₁₀, 655.8198; Found, 656.4104 [M + H]⁺, 673.4368 [M + NH₄]⁺.

I.R (cm⁻¹) 2865, 2102, 1646, 1478, 1452, 1420, 1349, 1288, 1085, 989, 919.

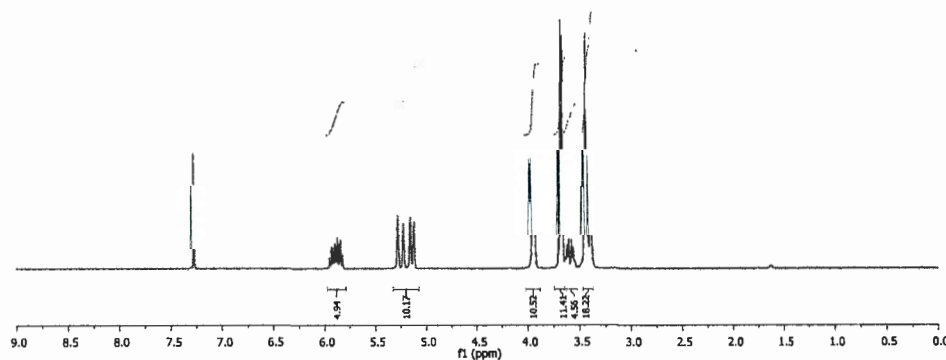


Figure S23. ¹H NMR spectrum of compound **16** (CDCl₃, 300 MHz).

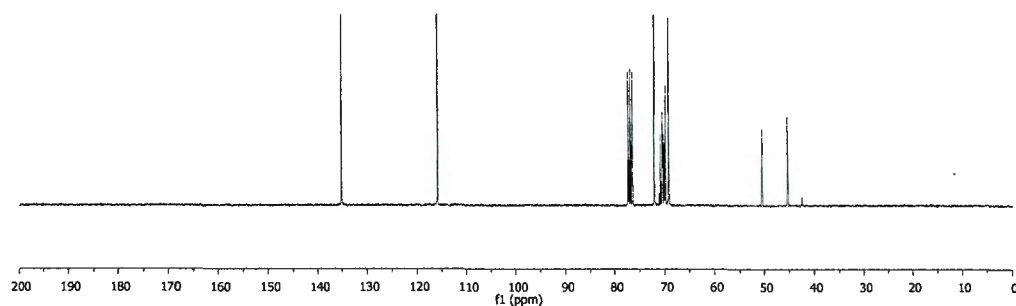


Figure S24. $^{13}\text{C} \{^1\text{H}\}$ NMR of compound 16 (CDCl_3 , 75 MHz).

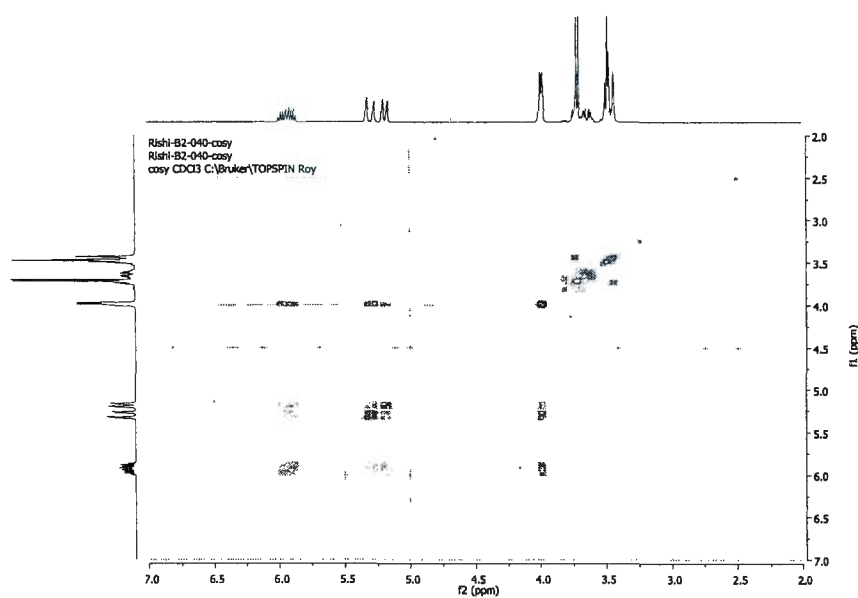


Figure S25. COSY spectrum of compound 16.

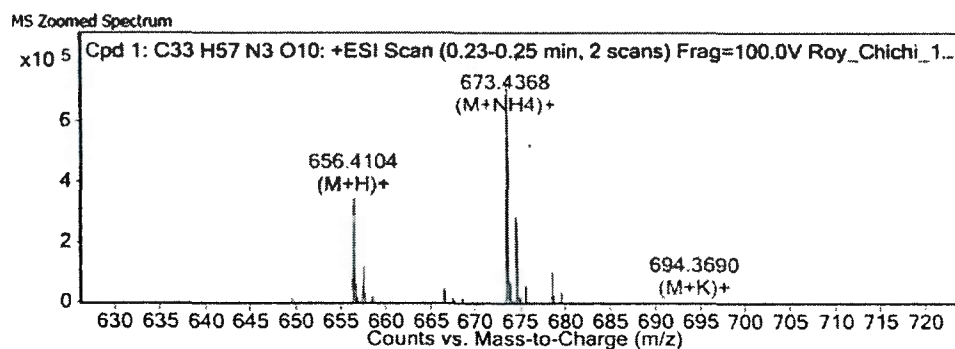


Figure S26. HRMS (ESI^+) spectrum of compound 16.

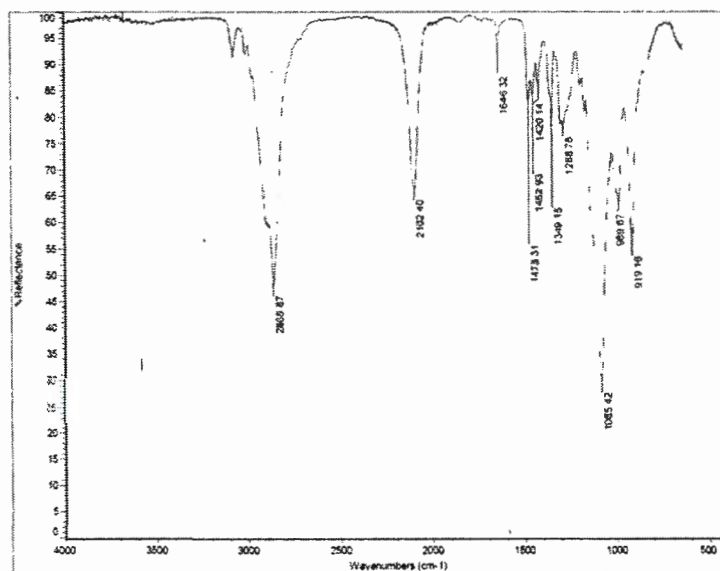
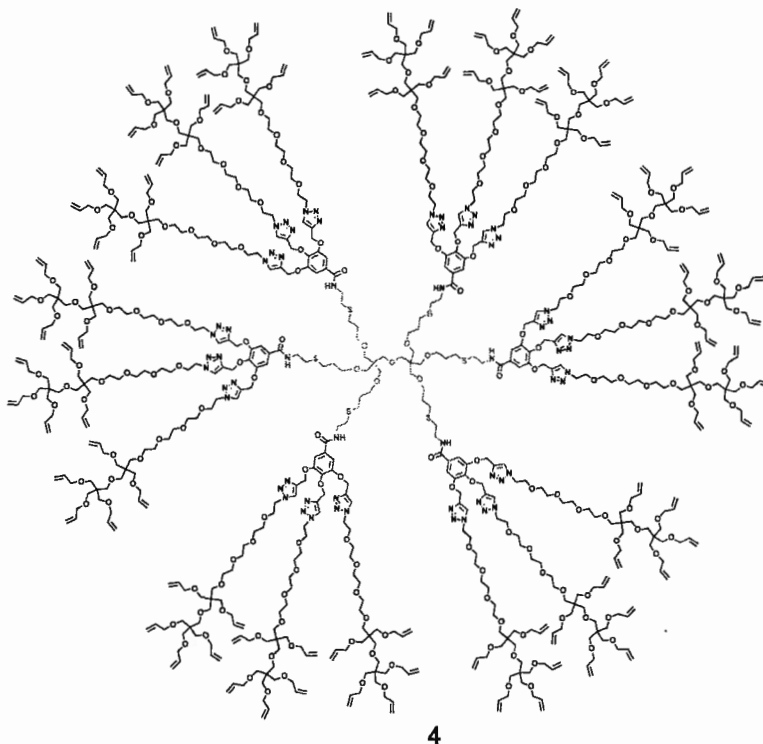


Figure S27. IR spectrum of compound 16.



Synthesis of compound 4: Propargyl terminated dendrimer **1** (30 mg, 0.0117 mmol, 1eq), compound **16** (207 mg, 0.31 mmol, 27 eq.), $\text{CuSO}_4 \cdot 5\text{H}_2\text{O}$ (26 mg, 0.1053 mmol, 9 eq.) and sodium ascorbate (21 mg, 0.1053 mmol, 9 eq.) were reacted

together following the procedure A and was purified by column chromatography (4% MeOH in DCM as eluent) to yield compound **4** as a colourless oil in 71% yield.

^1H NMR (300 MHz, CDCl_3): δ 7.91 (s, 12H), 7.84 (s, 6H), 7.24 (s, 12H), 5.94 – 5.80 (m, 90H), 5.28 – 5.25 (m, 45H), 5.22 – 5.19 (m, 40H), 5.15 – 5.09 (m, 110H), 4.60 – 4.43 (m, 36H), 3.95 – 3.86 (m, 220H), 3.64 – 3.52 (m, 244H), 3.45 – 3.34 (m, 315H), 2.77 (s, 12H), 2.65 (s, 12H), 2.10 – 1.76 (m, 24H).

^{13}C $\{^1\text{H}\}$ NMR (151 MHz, CDCl_3): δ 166.7, 152, 144, 143.2, 140.2, 135.2, 130.1, 124.7, 124.6, 124.4, 116, 107.1, 72.2, 70.9, 70.9, 70.5, 70.4, 70.3, 70.02, 70, 69.7, 69.30, 66.2, 62.9, 50.1, 49.9, 45.5, 45.3, 39.6, 31.3, 29.7, 28.5.

I.R (cm^{-1}) 3800, 3664, 3647, 2980, 2971, 2929, 1462, 1381, 1250, 1151, 1077, 956.

(MALDI-TOF) m/z : calculated for $\text{C}_{730}\text{H}_{1174}\text{N}_{60}\text{O}_{211}\text{S}_6$: 14359.7980, found: 14385.100 $[\text{M}+\text{Na}]^+$

GPC (CHCl_3): M_n = 14490 g/mol. M_w/M_n = 1.20

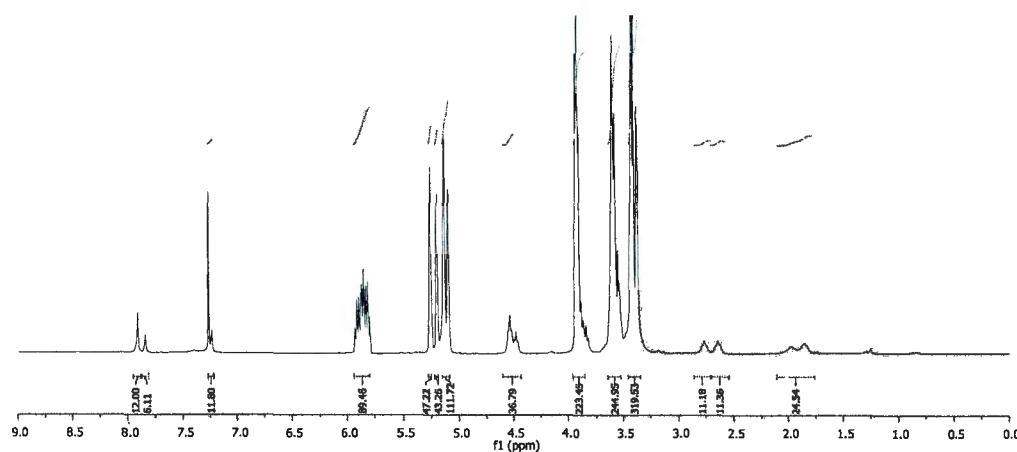


Figure S28. ^1H NMR spectrum of compound **4** (CDCl_3 , 300 MHz).

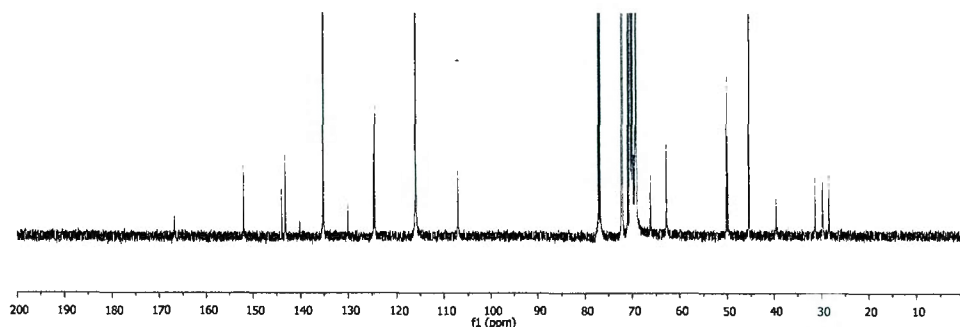


Figure S29. $^{13}\text{C}\{^1\text{H}\}$ NMR of compound **4** (CDCl_3 , 151 MHz).

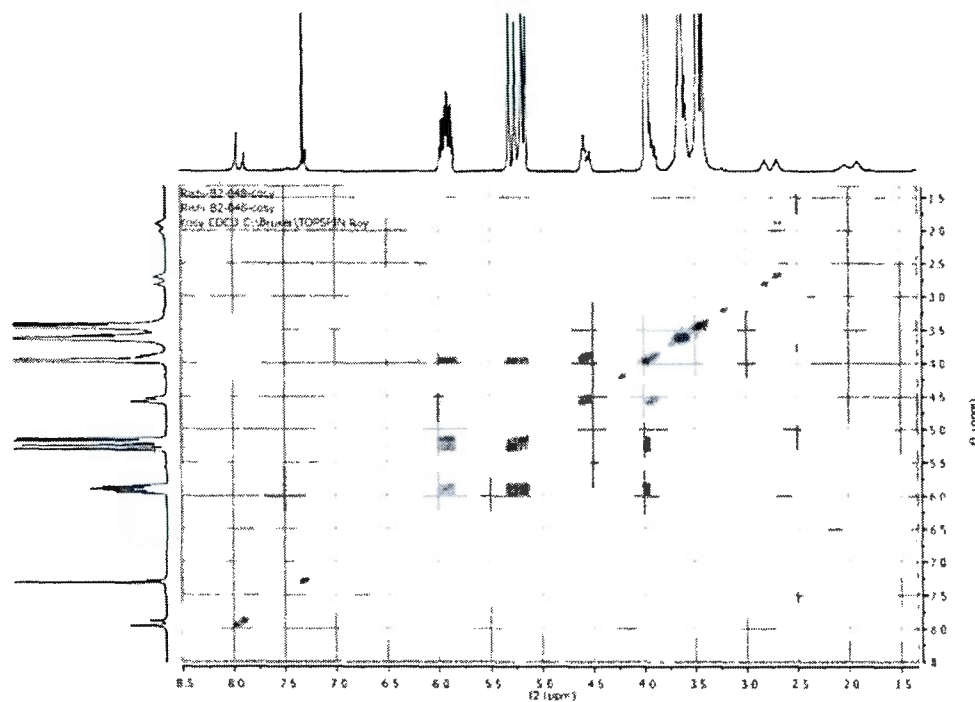
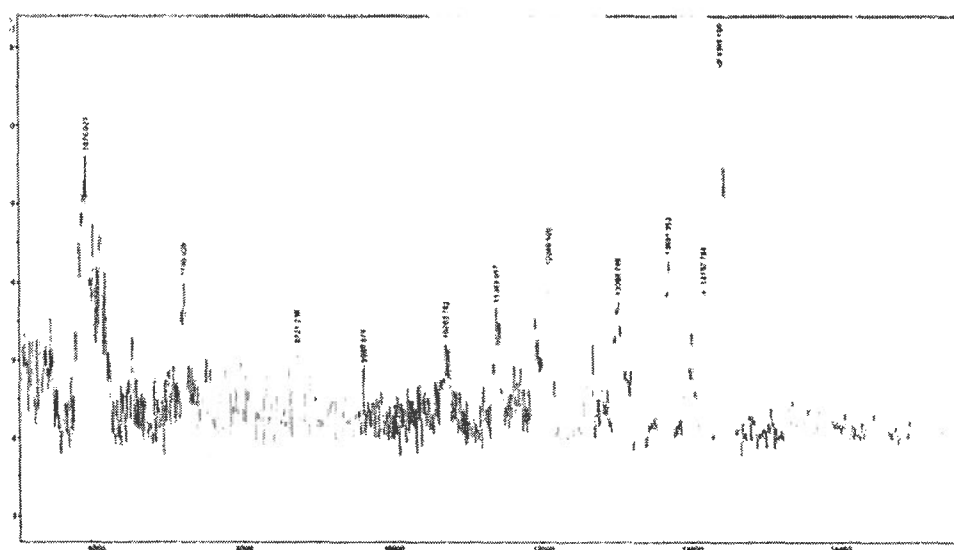
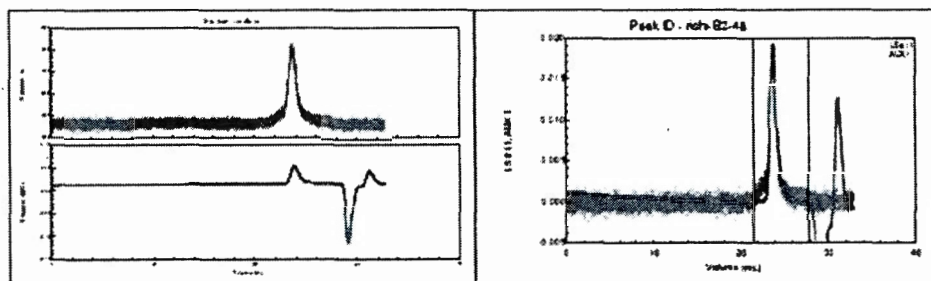


Figure S30. COSY spectrum of compound 4.





COLLECTION INFORMATION

Collection time : Thu Jun 06, 2002 03:32 AM Est (heure d'été)
 Instrument type : DAWN EOS
 Cell type : K5
 Laser wavelength : 690.0 nm
 Solvent name : chloroform
 Solvent RI : 1.439
 Calibration constants
 DAWN : 8.7600e-06
 AUX1 : 2.7500e-04
 AUX2 : 1.0000e-04
 Flow rate : 1.000 mL/min
 Collection interval : 0.250 sec
 Number of slices : 7843

Figure S32. GPC traces of compound 4.

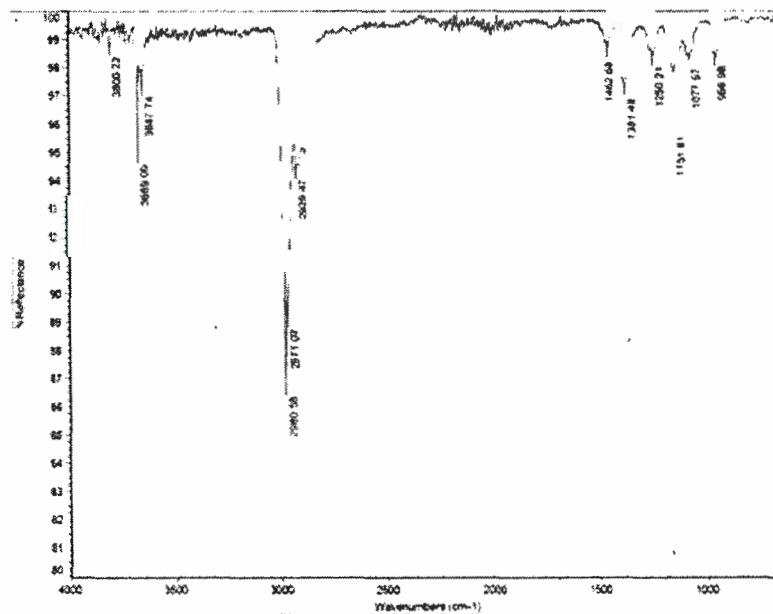
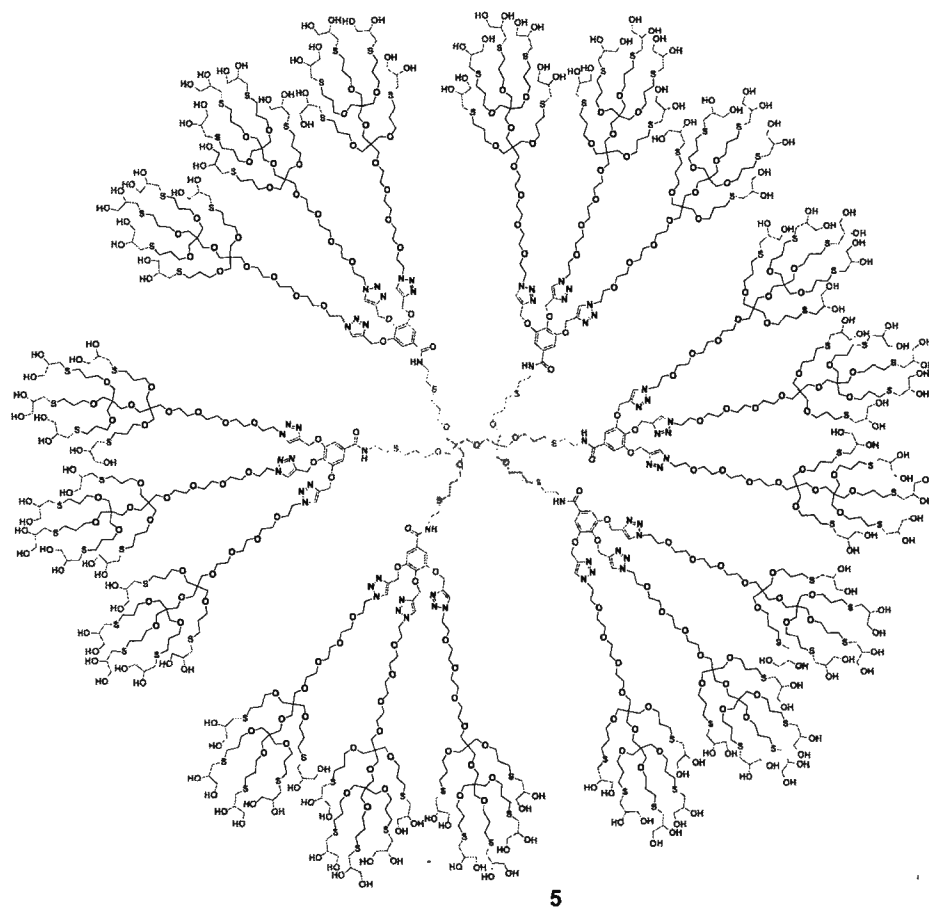


Figure S33. IR spectrum of compound 4.



Synthesis of compound 5: Allyl terminated dendrimer **4** (35 mg, 0.0024 mmol, 1eq), 1- thioglycerol (0.093 ml, 1.08 mmol, 450 eq.), and AIBN (7mg, 0.043, 18 eq.) were reacted together following the procedure B and was purified by dialysis to yield compound as a colourless oil in 82% yield.

^1H NMR (300 MHz, CD_3OD) δ 8.18 (br s, 12H), 7.92 (br s, 6H), 7.36 (br s, 12H), 5.18 (d, $J = 30.4$ Hz, 40H), 4.59 (d, $J = 28.8$ Hz, 30H), 3.99 – 3.36 (m, 1068H), 2.75 – 2.53 (m, 370H), 1.91 – 1.76 (m, 180H).

^{13}C $\{^1\text{H}\}$ NMR (151 MHz, CD_3OD) δ 168.7, 153.5, 145.2, 144.4, 141.5, 131.2, 126.5, 108.4, 77.7, 73.8, 73.2, 72.8, 72.3, 71.9, 71.7, 71.6, 71.5, 71.3, 70.9, 70.4, 69.9, 66.0, 64.4, 63.8, 51.5, 51.4, 47.0, 41.2, 36.3, 35.2, 35.1, 33.0, 32.1, 31.5, 31.0, 30.8, 30.7, 30.5, 29.7, 23.7, 19.3, 14.4.

I.R (cm^{-1}) 3707, 3680, 3396, 2980, 2966, 2936, 2922, 2865, 1101, 1056, 1032, 1015.

HRMS (ESI^+) m/z calc. for $\text{C}_{1001}\text{H}_{1898}\text{N}_{60}\text{O}_{391}\text{S}_{96}$: 24110.1882, found: 24124.9040

Differential light scattering Hydrodynamic diameter: 8.221 (nm) .

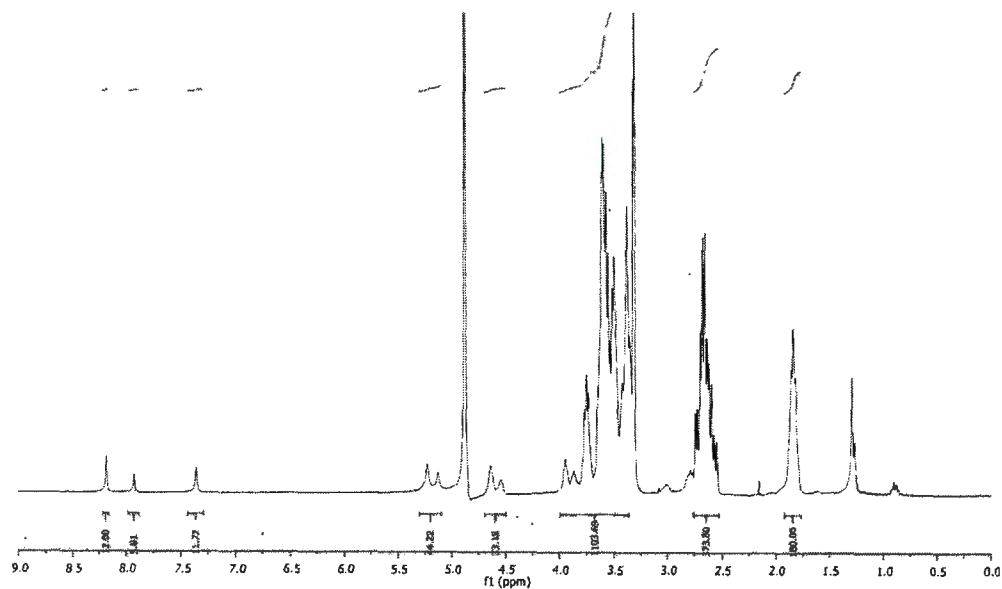


Figure S34. ^1H NMR spectrum of compound **5** (CD_3OD , 300 MHz).

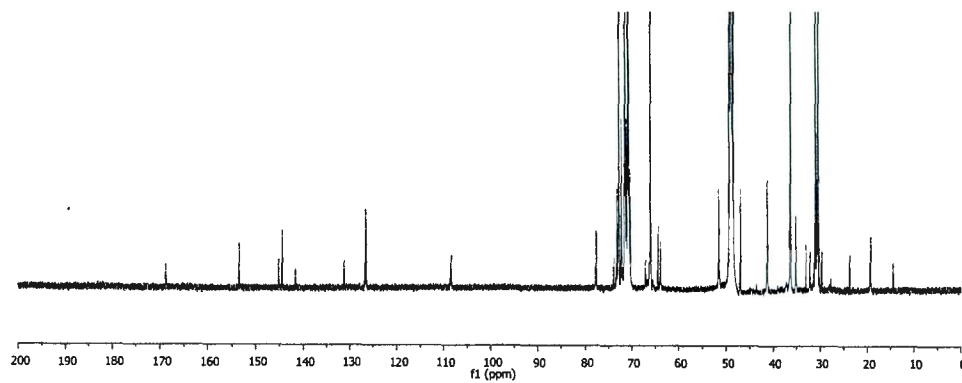


Figure S35. ^{13}C $\{^1\text{H}\}$ NMR of compound **5** (CD_3OD , 151 MHz).

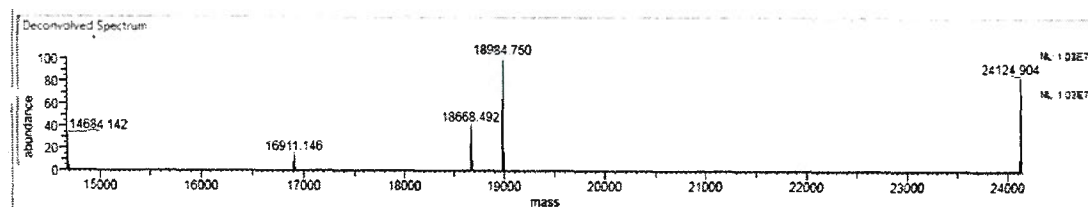


Figure S36. HRMS (ESI^+) spectrum of compound **5**.

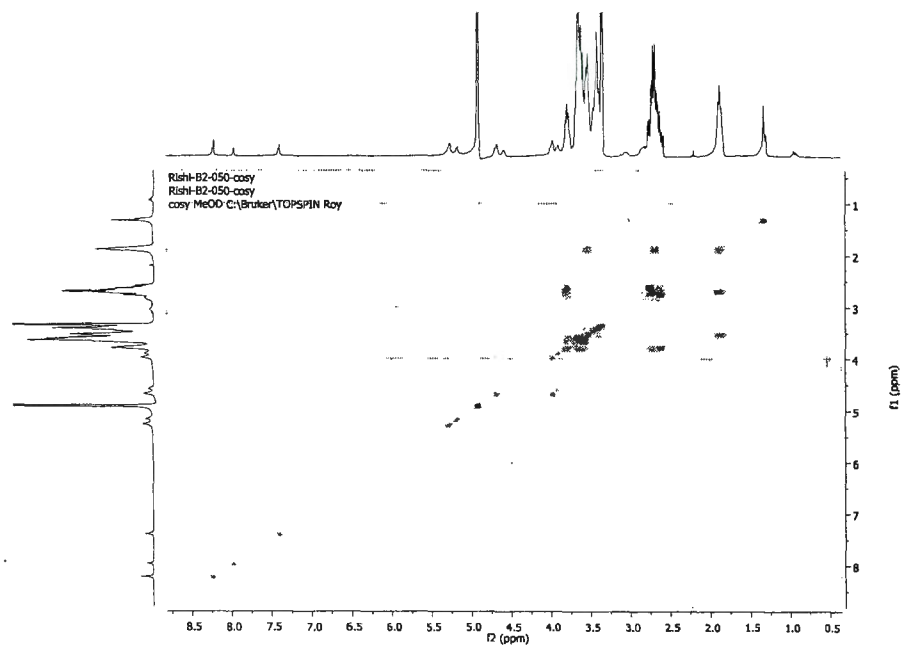


Figure S37. COSY spectrum of compound 5.

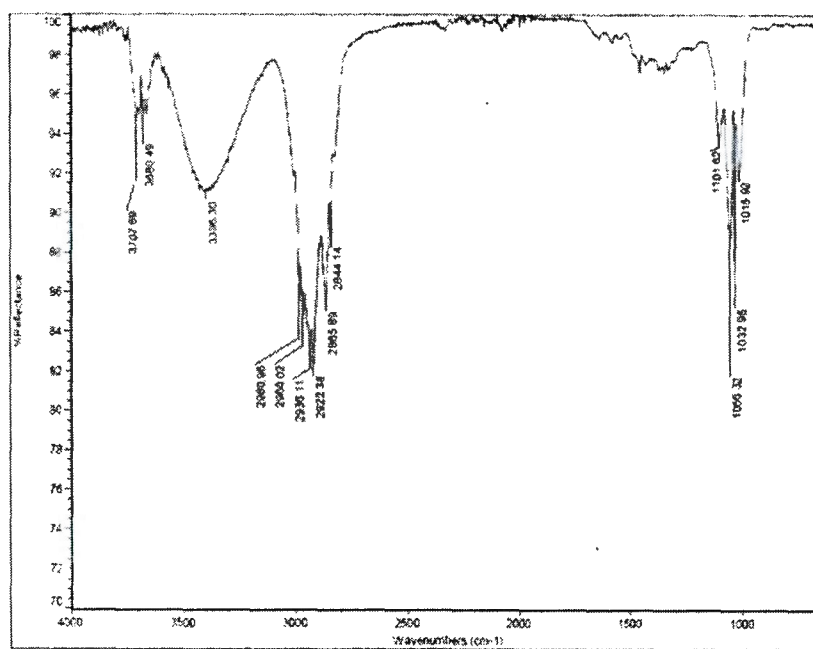


Figure S38. IR spectrum of compound 5.

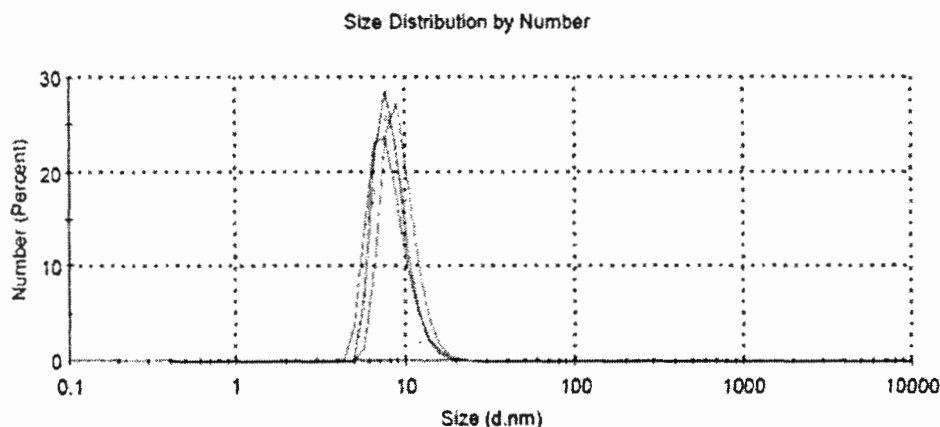
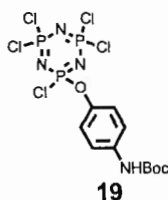


Figure S39. DLS size distribution of dendrimer **5** in methanol at 25°C.



Synthesis of compound **19**: Recrystallized hexachlorocyclotriphosphazene **17** (200.0 mg, 0.0575 mmol, 2.0 eq.) and Boc protected p-aminophenol **18** (60.2 mg, 0.0287 mmol, 1.0 eq.) were dissolved in 25 ml of anhydrous THF. Under nitrogen atmosphere, CS_2CO_3 (187.4 mg, 0.5750 mmol, 2.0 eq.) was added and the mixture was stirred at reflux temperature (66°C) for 6 hours. The solution was filtered and washed with DCM. The filtrate was concentrated under reduced pressure. Column chromatography on silica (DCM/Hexanes 1:9 to 7:3) afforded the desired compound **19** (75.0 mg, 0.0144 mmol, 50%) as a colorless oil.

^1H NMR (CDCl_3 , 300 MHz): δ ppm 7.40 (d, 2H, $J = 9.0$ Hz), 7.18 (d, 2H, $J = 9.0$ Hz), 6.62 (s, 1H), 1.52 (s, 9H).

^{13}C $\{^1\text{H}\}$ NMR (CDCl_3 , 75 MHz): δ ppm 152.5, 144.4, 137.0, 121.8, 119.5, 80.9, 28.3.

^{31}P NMR (CDCl_3 , 121.5 MHz): δ ppm 22.4 (d, 2P, $2J(\text{P},\text{P}) = 59.3$ Hz, PCl_2), 12.8 (t, 1P, $2J(\text{P},\text{P}) = 59.3$ Hz, P-O).

HRMS (ESI $^+$) m/z calc. for $\text{C}_{11}\text{H}_{14}\text{Cl}_5\text{N}_4\text{O}_3\text{P}_3 = 540.8614$ $[\text{M}+\text{Na}]^+$; found 540.8628.

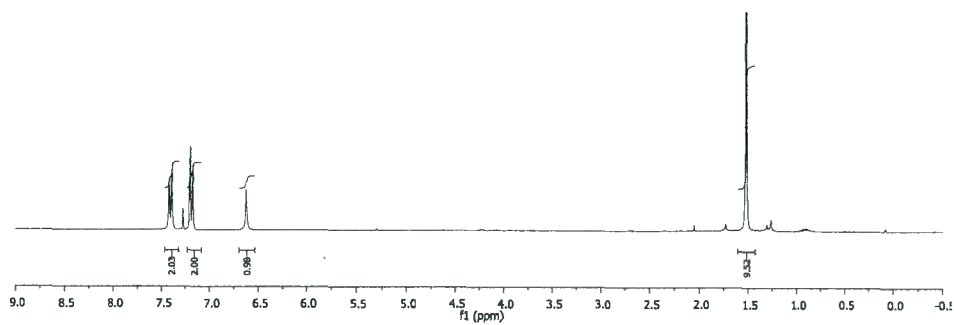


Figure 40. ^1H NMR spectrum of compound **19** (CDCl_3 , 300 MHz).

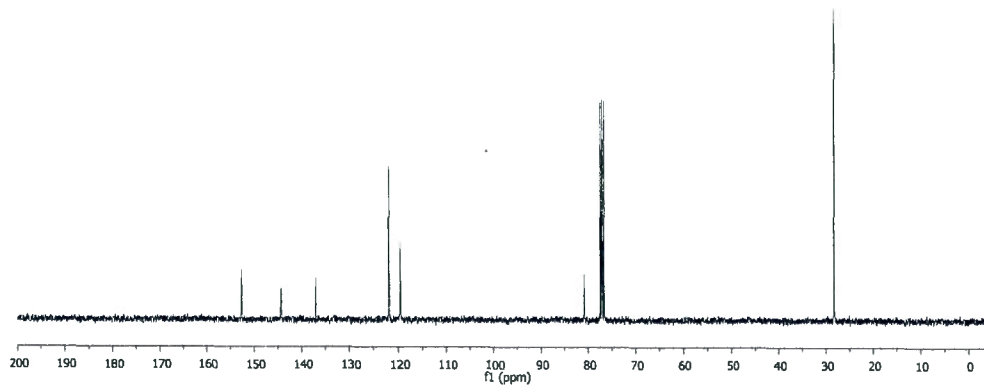


Figure S41. $^{13}\text{C}\{^1\text{H}\}$ NMR of compound **19** (CDCl_3 , 75 MHz).

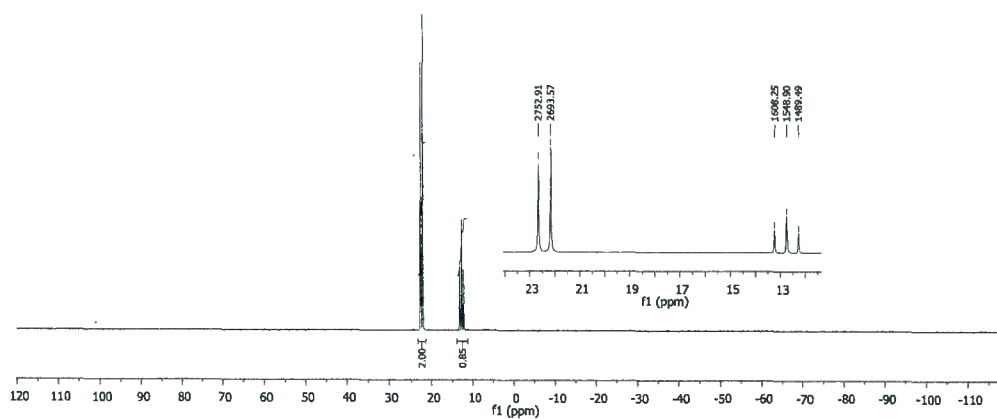


Figure S42. ^{31}P NMR spectrum of compound **19** (CDCl_3 , 122 MHz).

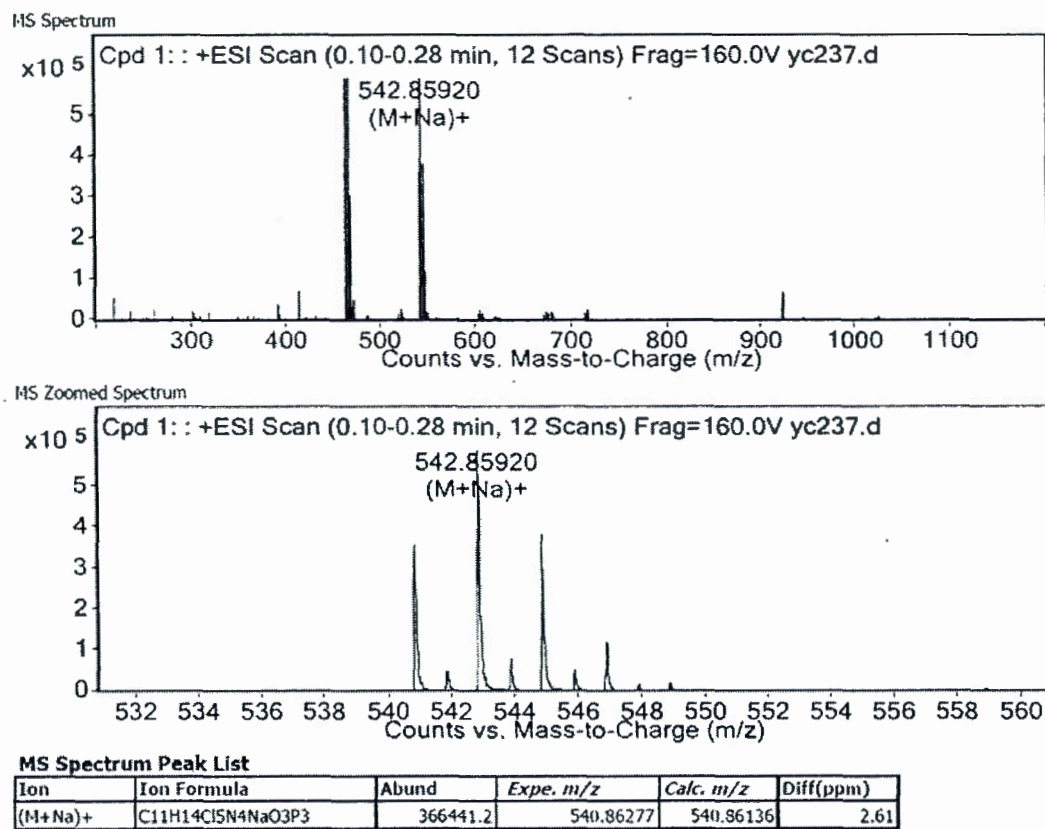
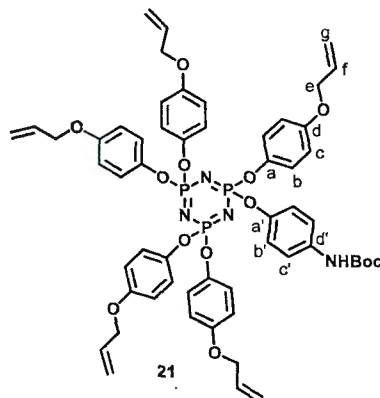


Figure S43. HRMS (ESI⁺) spectrum of compound 19.



Synthesis of compound 21: To Boc protected amine monofunctionalized cyclotriphosphazene (**19**) (240 mg, 0.46 mmol, 1 eq) and p-allyloxyphenol **20** (692.1 mg, 4.6 mmol, 10 eq) in THF (40 ml) was added dry cesium carbonate (2.3 g, 6.9 mmol, 15 eq). The solution was stirred and refluxed for 16h. Upon completion, reaction mixture was diluted with EtOAc (50 ml) and washed with brine and water. The mixture was dried with anhydrous Na₂SO₄, filtered and evaporated under reduced pressure. Silica gel column chromatography was performed (Hexane/AcOEt 5% to 25%) to obtain pure desired compound **21** in 88% yield. *R_f* = 0.57, Hex/AcOEt 65:35

¹H NMR (CDCl₃, 300 MHz): δ 7.16 (d, 2H, ³J_{c',b'} = 8.9 Hz, H-c'), 6.84-6.79 (m, 12H, H-b', H-c), 6.71-6.67 (m, 10H, H-b), 6.41 (s, 1H, NH), 6.11-5.97 (m, 5H, H-f), 5.44-5.37 (m, 5H, H-g), 5.30-5.26 (m, 5H, *J* = 1.3 Hz, *J* = 10.5 Hz, H-g), 4.49-4.45 (m, 10H, H-e), 1.51 (s, 9H, Boc).

¹³C {¹H} NMR (CDCl₃, 75 MHz): δ 155.6, 152.7, 144.4, 135.2, 133.3, 133.2, 121.9, 121.5, 119.5, 117.8, 115.2, 80.6, 76.7, 69.2, 28.4.

³¹P NMR (CDCl₃, 75 MHz): 9.89 (t, *J* = 15.9 Hz, 3P).

HRMS (ESI⁺) *m/z* calc. for C₅₆H₅₉N₄O₁₃P₃, 1089.3364 [M+H]⁺, found 1089.3372.

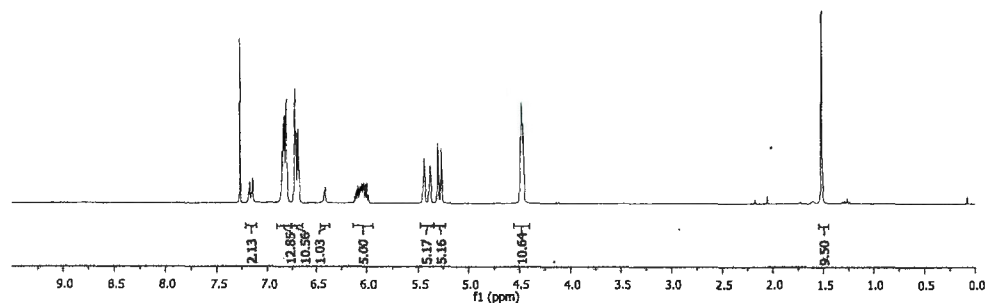


Figure S44. ¹H NMR spectrum of compound **21** (CDCl₃, 300 MHz).

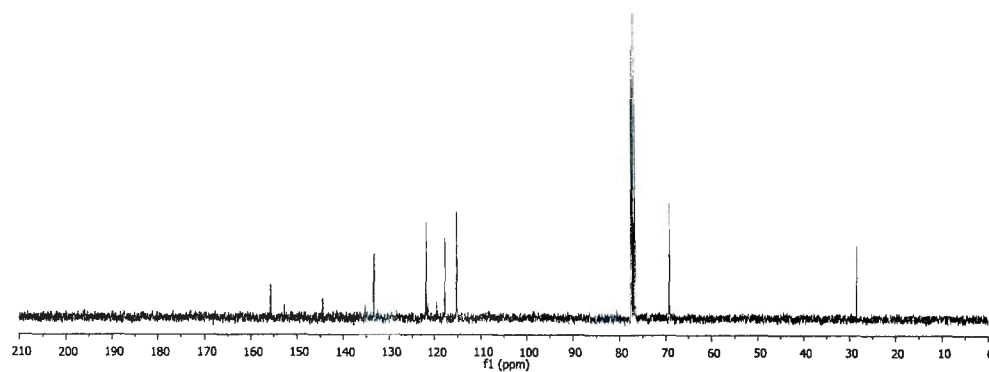


Figure S45. $^{13}\text{C}\{^1\text{H}\}$ NMR of compound **21** (CDCl_3 , 75 MHz).

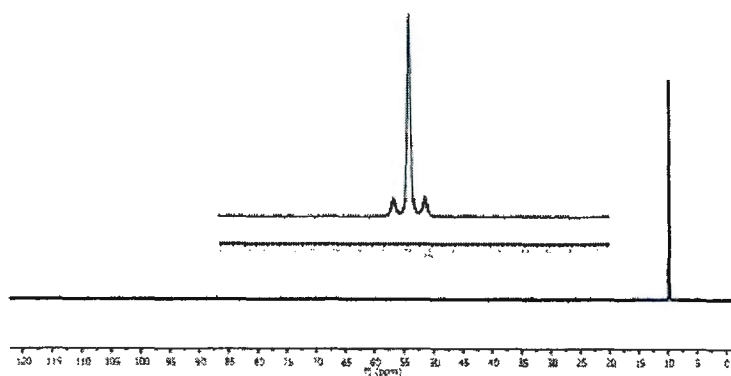


Figure S46. ^{31}P NMR spectrum of compound **21** (CDCl_3 , 122 MHz).

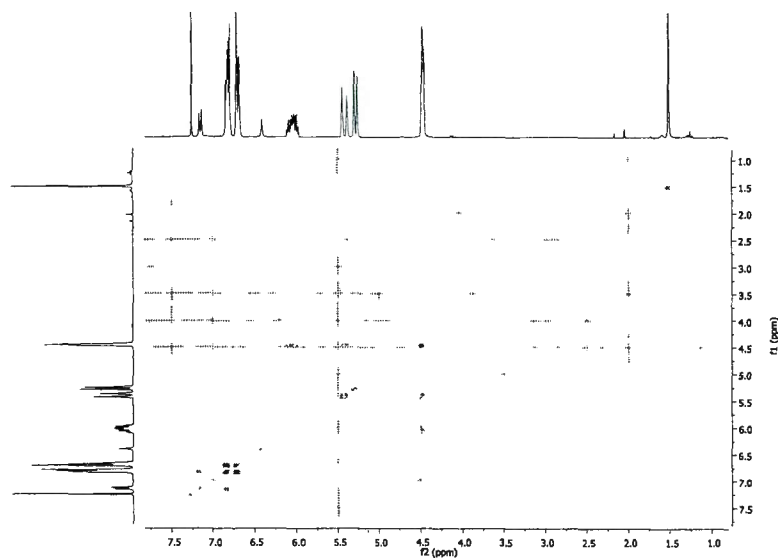


Figure S47. COSY spectrum of compound 21.

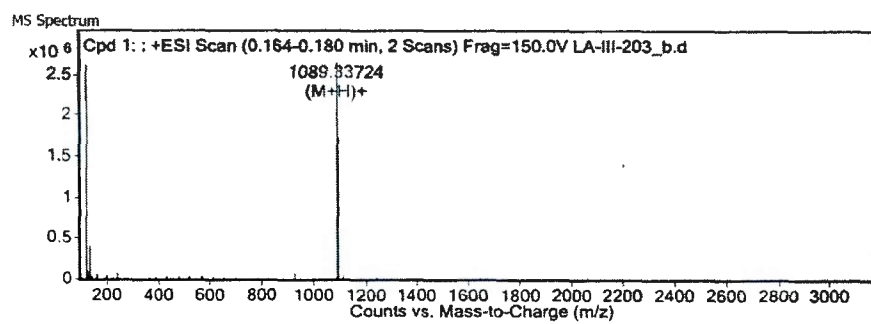
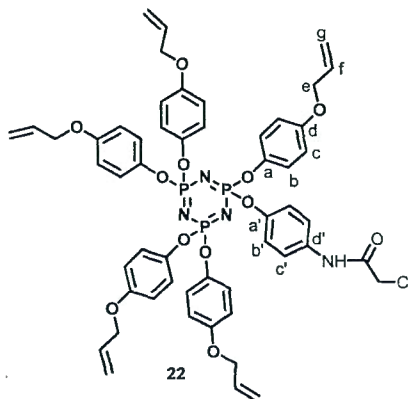


Figure S48. HRMS (ESI^+) spectrum of compound 21.



Synthesis of compound 22: To a stirring solution of compound **21** (294 mg, 0.27 mmol) in 3ml DCM at 0°C was added TFA (4ml) and the reaction mixture was stirred for 4h at room temperature. Upon completion solvent was removed followed by co-evaporation with toluene 3-4 times. Reaction mixture was dried under vacuum. To the TFA salt was added DIPEA (, 1.3 mmol, 4.8 eq) and DCM (3 ml) followed by addition of chloroacetyl chloride (85 μ L, 1.1 mmol, 4 eq) slowly. The solution was stirred at room temperature overnight. After 16 h, the reaction mixture was evaporated, diluted with EtOAc (50 ml) and washed with HCl (1M) and water. The mixture was dried with anhydrous Na₂SO₄, filtered and evaporated under reduced pressure. Purification by silica gel column (Hexane/ EtOAc 10% to 40%) afforded desired compound **22** (220.8 mg, 76%).

R_f = 0.32, Hex/AcOEt 65:35

¹H NMR (300 MHz, CDCl₃) : δ 8.19 (s, 1H, NH), 7.36 (d, 2H, ³*J*_{c',b'} = 8.9 Hz, H-c'), 6.92-6.81 (m, 12H, H-b', H-c), 6.75-6.70 (m, 10H, H-b), 6.10-5.99 (m, 5H, H-f), 5.45-5.39 (dd, 5H, *J* = 1.9 Hz, *J* = 10 Hz, H-g) 5.31-5.28 (dd, *J* = 1.4 Hz, *J* = 17.2 Hz, 5H, H-g), 4.49-4.47 (m, 10H, H-e), 4.18 (s, 2H, CH₂Cl).

¹³C {¹H } NMR (CDCl₃, 75 MHz): δ = 163.7, 155.7, 147.8, 144.3, 133.3, 133.2, 121.9, 121.6, 121.2, 117.8, 115.3, 115.2, 76.7, 69.2, 69.2, 42.9.

³¹P NMR (CDCl₃, 121.5 MHz): 9.89 (t, *J* = 19.9 Hz, 3P).

HRMS (ESI⁺) *m/z* calc. for C₅₃H₅₂ClN₄O₁₂P₃, 1065.2556 [M+H]⁺, found 1065.2561, [M+Na]⁺, 1087.2388 found.

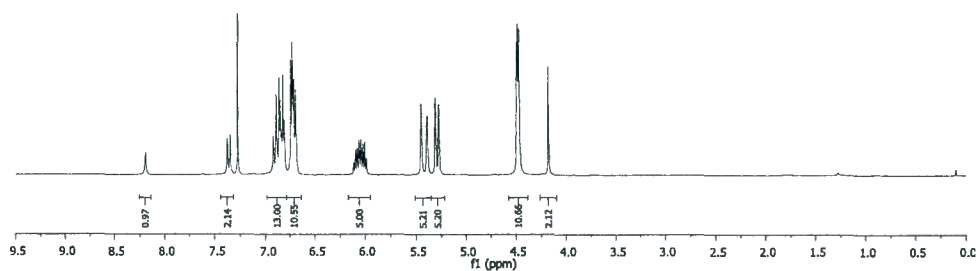


Figure S49. ^1H NMR spectrum of compound **22** (CDCl_3 , 300 MHz).

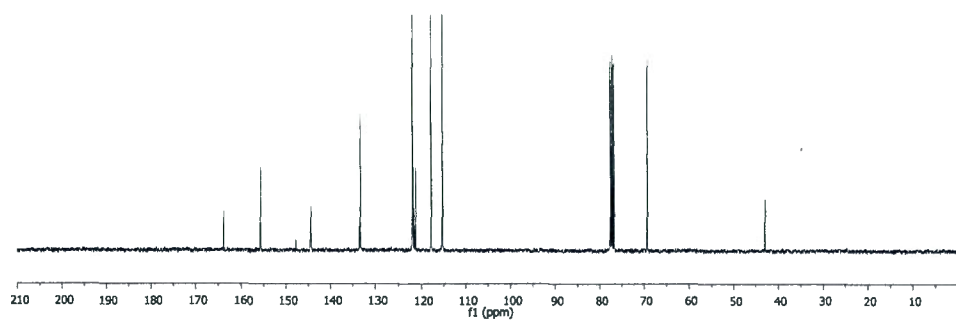


Figure S50. ^{13}C $\{^1\text{H}\}$ NMR of compound **22** (CDCl_3 , 75 MHz).

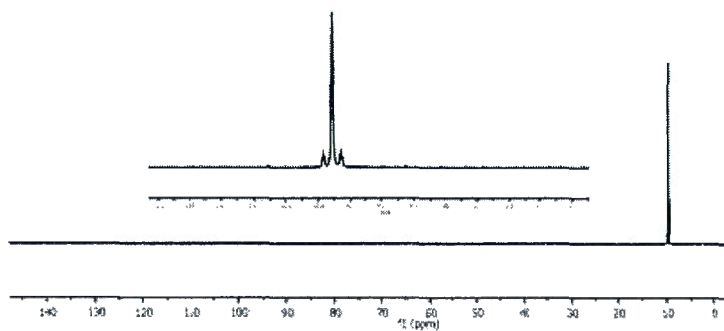


Figure S51. ^{31}P NMR spectrum of compound **22** (CDCl_3 , 122 MHz).

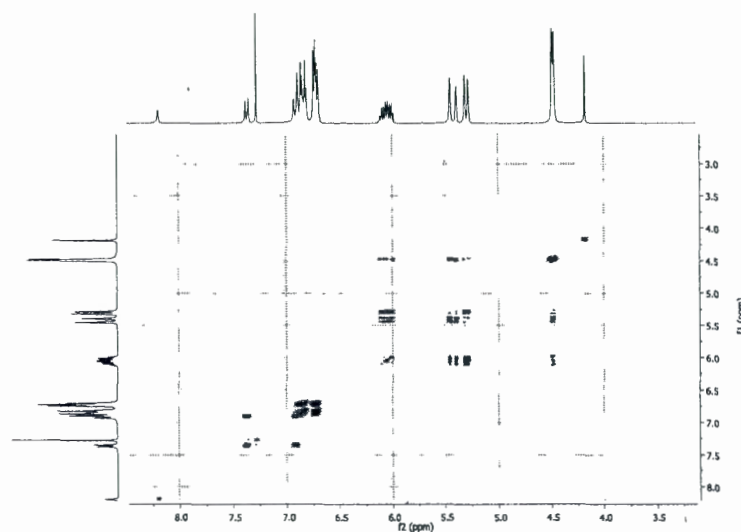


Figure S52. COSY spectrum of compound 22.

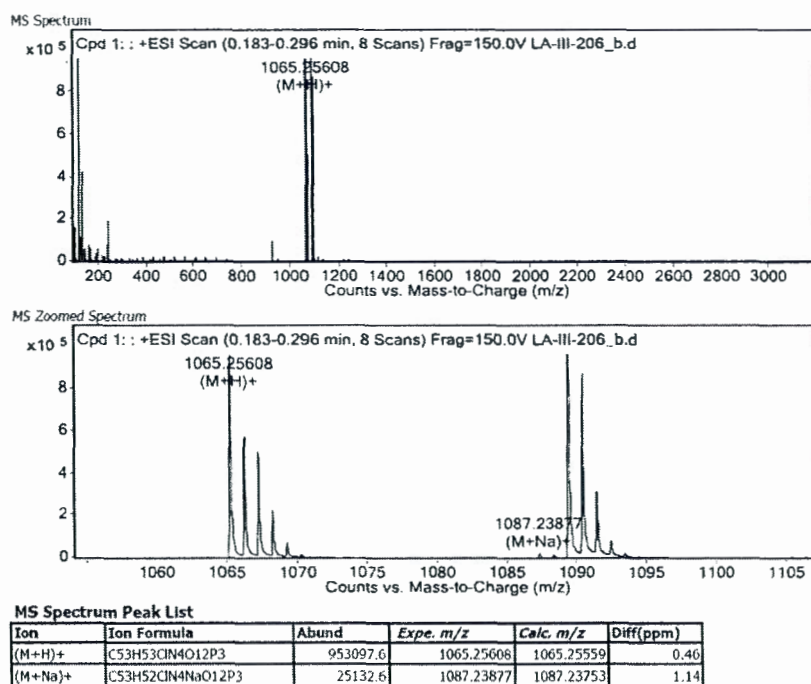


Figure S53. HRMS (ESI⁺) spectrum of compound 22.

Rf= 0.84, DCM/MeOH96:4

¹³C {¹H} NMR (CDCl₃, 75 MHz): δ 163.7, 155.7, 147.8, 144.3, 133.3, 133.2, 121.9, 121.6, 121.2, 117.8, 115.3, 115.2, 76.7, 69.2, 69.2, 42.9.

³¹P NMR (CDCl₃, 121.5 MHz): 9.89 (t, *J*=19.9 Hz, 3P).

HIRMS (ESI⁺) *m/z* calc. for C₅₃H₅₂ClN₄O₁₂P₃, 1072.2960 [M+H]⁺, found 1072.2971.

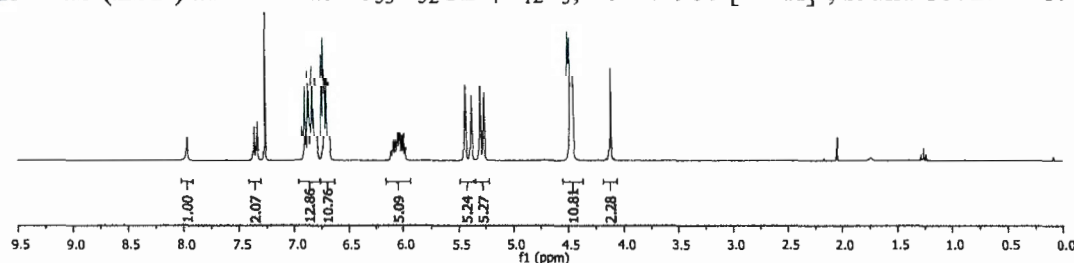


Figure S54. ^1H NMR spectrum of compound **23** (CDCl_3 , 300 MHz).

MS Spectrum

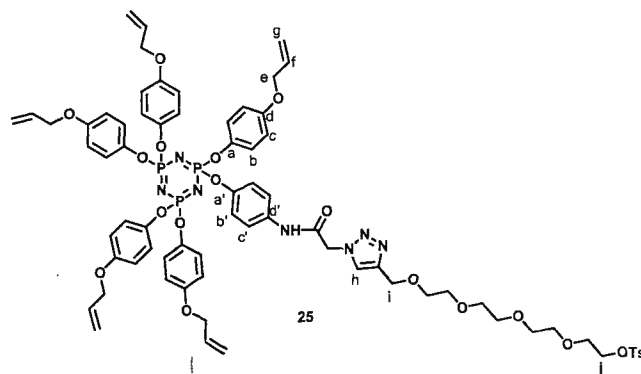
Cpd 1: : +ESI Scan (0.204-0.220 min, 2 Scans) Frag=150.0V LA-III-207_b.d

1072.29705
(M+H)⁺

536.65242
(M+2H)²⁺

Counts vs. Mass-to-Charge (m/z)

Figure S57. ^{31}P NMR spectrum of compound **23** (CDCl_3 , 122 MHz).



Synthesis of compound 25: 3,6,9,12-tetraoxapentadec-14-yn-1-yl 4-methylbenzenesulfonate **24** (75.0 mg, 0.19 mmol, 1.3 eq.) and compound **23** (160.3 mg, 0.15 mmol, 1.0 eq) were dissolved in a THF/H₂O 1:1 mixture (3 mL). Sodium ascorbate (88.7 mg, 0.45 mmol, 3.0 eq) and CuSO₄ 5H₂O (111.8 mg, 0.45 mmol, 3.0 eq) were added. The solution was stirred and heated at 55 °C overnight. The reaction mixture was diluted with EtOAc (50 ml) and washed twice with saturated aqueous ammonium chloride (2 × 75 ml) and water (50 ml). The mixture was dried with anhydrous Na₂SO₄, filtered and evaporated under reduced pressure. Crude reaction mixture was purified using silica gel column (DCM/MeOH 100:0 to 94:6) which afforded desired compound **25** (139.6 mg, 64%).

R_f = 0.31, DCM/MeOH 96:4

¹H NMR (300 MHz, CDCl₃) : δ 8.73 (s, 1H, NH), 7.81 (s, 1H, H-triazole), 7.73 (d, 2H, *J*=8.3 Hz, H-c'), 7.37 (d, 2H, *J*=8.9 Hz, H-aromTos) 7.26 (d, 2H, *J*=8.1 Hz, H-aromTos), 6.90-6.64 (m, 22H, H-b', H-c, H-b), 6.08-5.93 (m, 5H, H-f), 5.42-5.33 (m, 5H, H-g) 5.28-5.18 (m, 7H, H-g, CH₂-triazole), 4.65 (s, 2H, H-i), 4.45-4.42 (m, 10H, H-e), 4.11-4.07 (m, 2H, H-j), 3.68-3.52 (m, 14H, OCH₂CH₂O), 2.38 (s, 3H, CH₃).

¹³C {¹H} NMR (CDCl₃, 75 MHz) : δ 163.4, 155.7, 155.6, 147.4, 145.3, 145.0, 144.3, 134.3, 133.3, 133.2, 132.8, 130.0, 128.0, 124.9, 121.9, 121.4, 121.1, 117.7, 115.3, 115.2, 76.8, 70.7, 70.6, 70.6, 70.5, 70.5, 69.8, 69.4, 69.2, 68.8, 64.5, 53.2, 21.7.

³¹P NMR (CDCl₃, 121.5 MHz): 9.76 (t, *J*=18.1 Hz, 3P).

HRMS (ESI+) *m/z* calc. for C₇₁H₇₈N₇O₁₉P₃S, 1458.4359 [M+H]⁺, found 1458.4384.

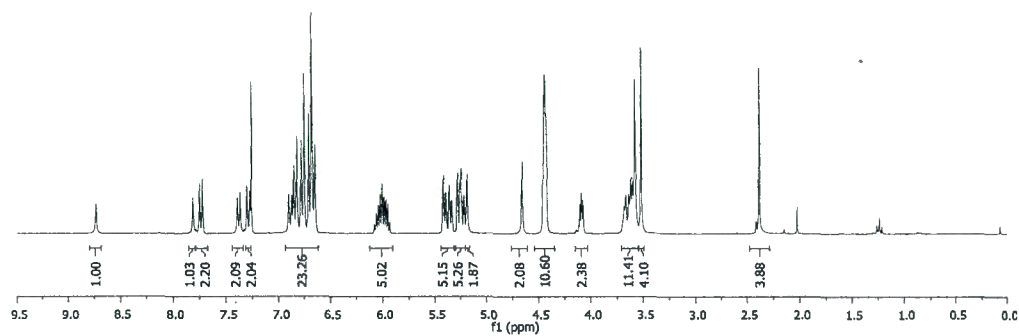


Figure S58. ^1H NMR spectrum of compound **25** (CDCl_3 , 300 MHz).

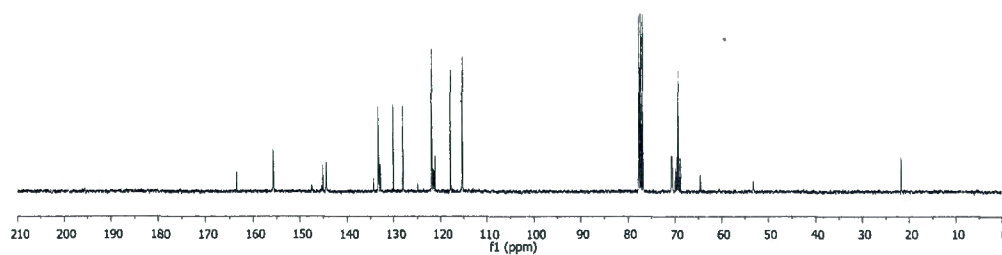


Figure S59. ^{13}C $\{^1\text{H}\}$ NMR of compound **25** (CDCl_3 , 75 MHz).

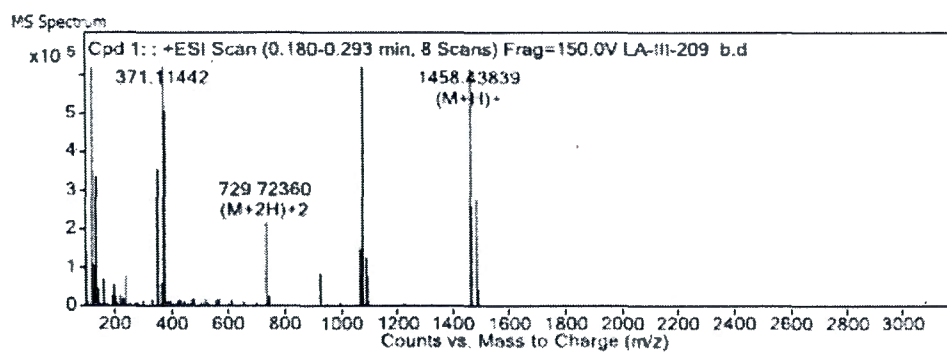


Figure S60. HRMS (ESI^+) spectrum of compound **25**.

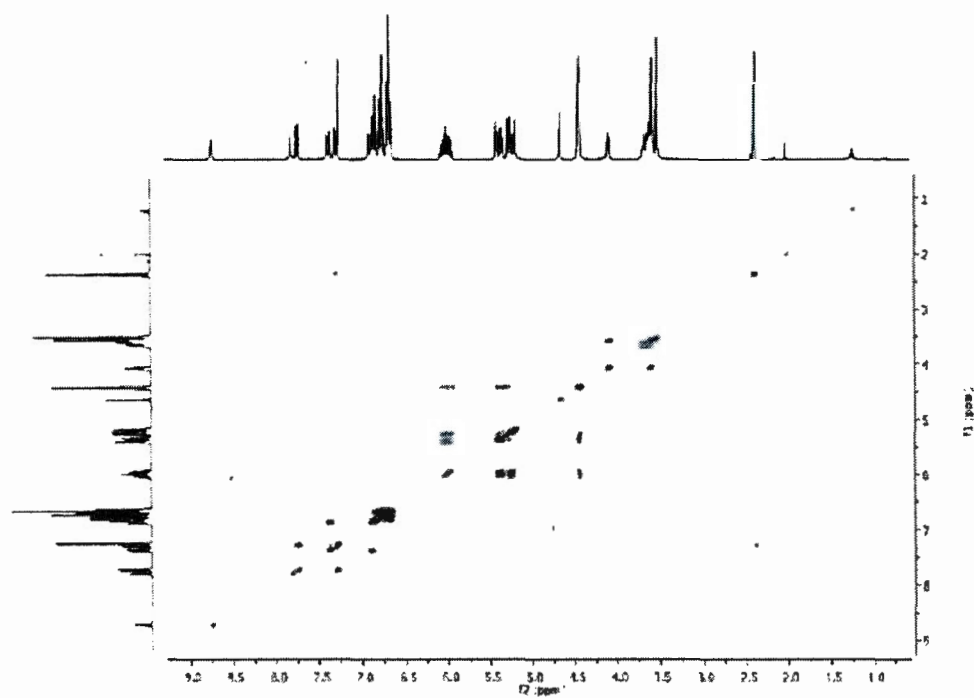


Figure S61. COSY spectrum of compound **25**.

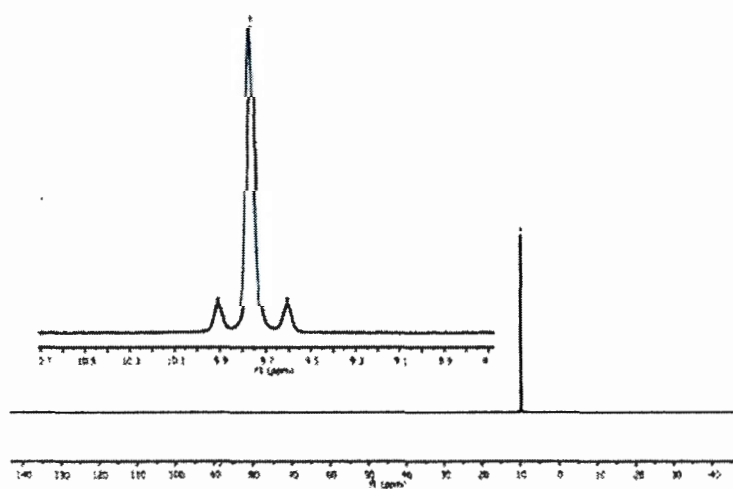


Figure S62. ³¹P NMR spectrum of compound **25** (CDCl₃, 122 MHz).

$R_f = 0.31$, DCM/MeOH 96:4

¹³C {¹H }NMR (75 MHz, CDCl₃) δ 163.4, 155.7, 155.6, 147.3, 145.2, 144.4, 144.3, 134.3, 133.3, 133.2, 124.9, 121.8, 121.5, 121.1, 117.8, 115.3, 115.2, 76.8, 70.6, 70.6, 70.0, 69.9, 69.2, 69.2, 64.5, 53.1, 50.6.

³¹P NMR (121.5 MHz, CDCl₃) 9.75 (t, *J*=18.0 Hz, 3P).

HRMS (ESI⁺) *m/z* calc. for C₆₄H₇₁N₁₀O₁₆P₃, 1329.4335 [M+H]⁺, found 1329.4361.

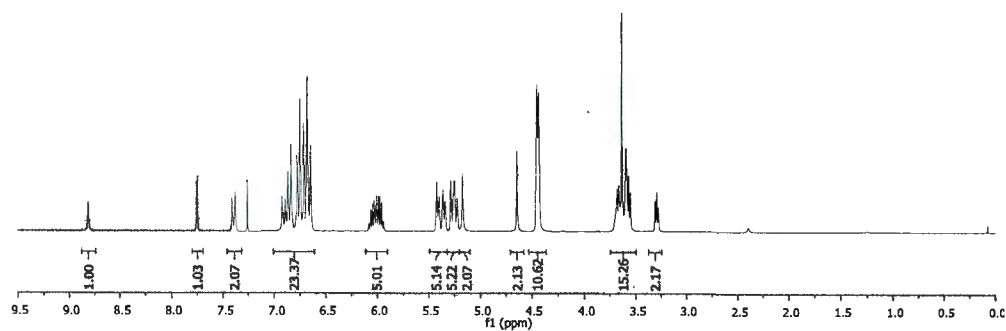


Figure S63. ^1H NMR spectrum of compound **26** (CDCl_3 , 300 MHz).

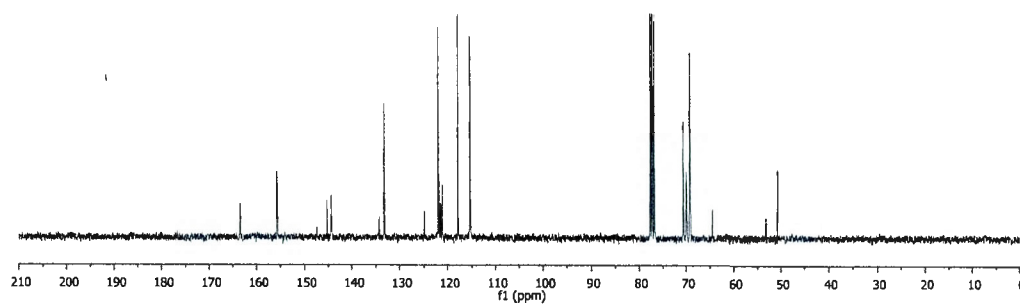


Figure S64. ^{13}C $\{^1\text{H}\}$ NMR of compound **26** (CDCl_3 , 75 MHz).

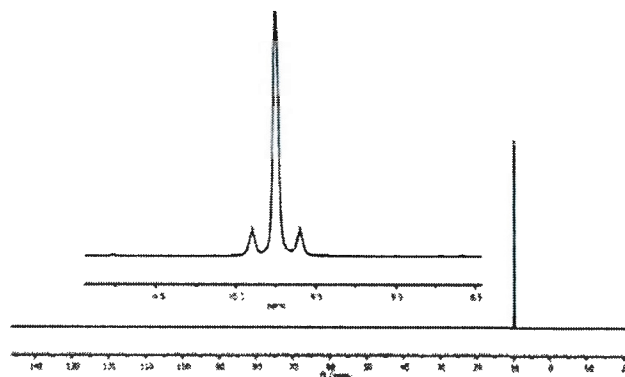


Figure S65. ^{31}P NMR spectrum of compound **26** (CDCl_3 , 122 MHz).

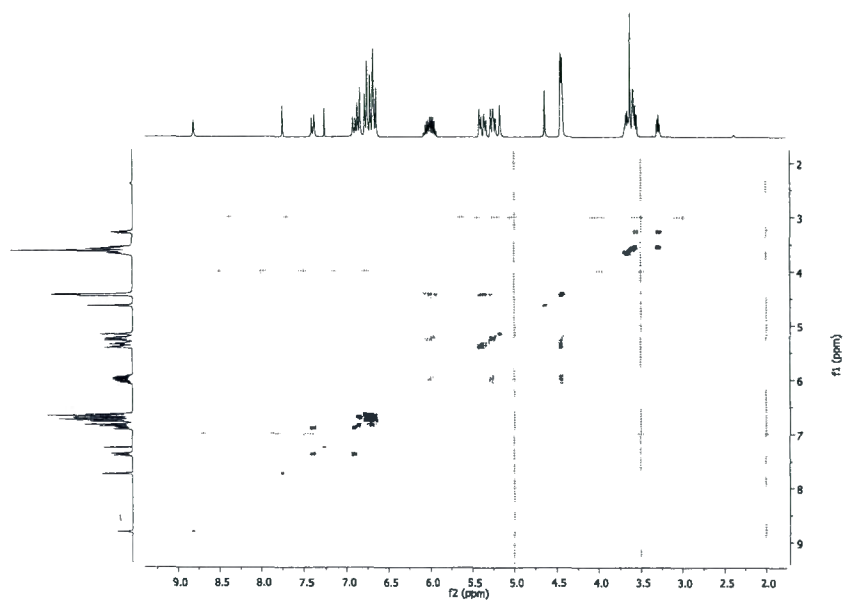


Figure S66. COSY spectrum of compound 26.

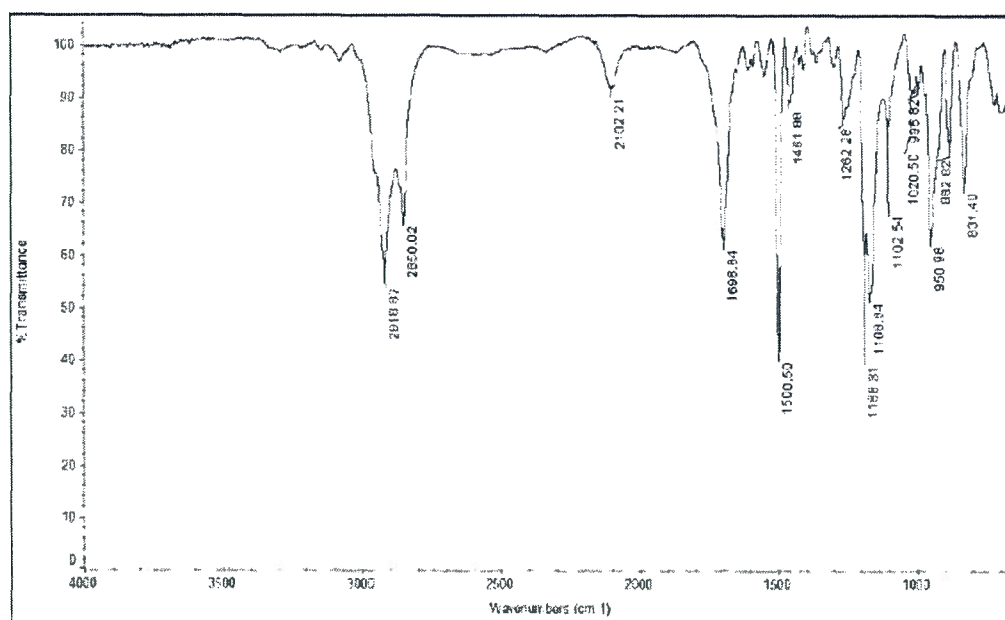


Figure S67. I.R. spectrum of compound 26.

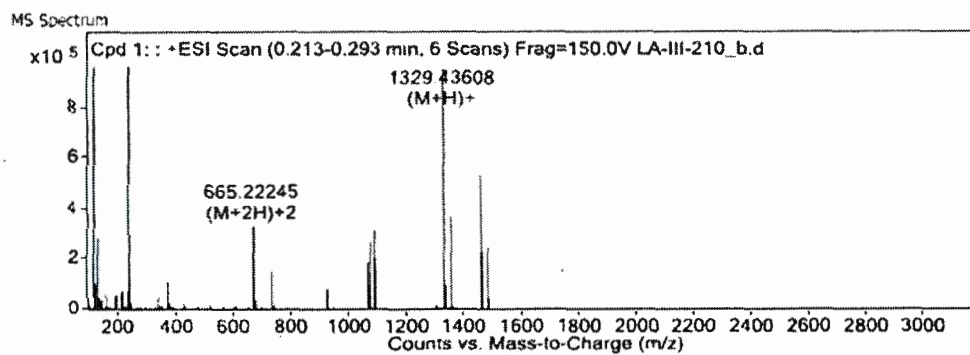
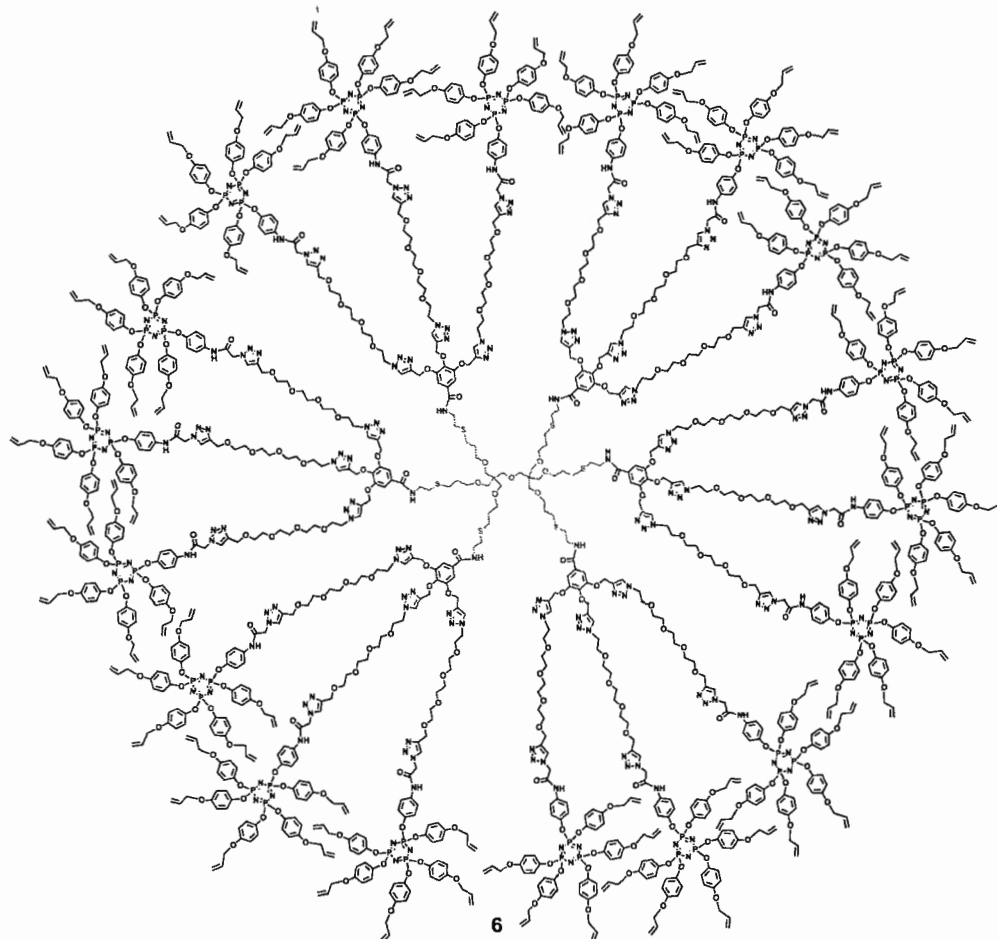


Figure S68. HRMS (ESI⁺) spectrum of compound 26.



Synthesis of compound 6: Propargyl terminated dendrimer **1** (5 mg, 0.0019 mmol, 1eq), compound **26** (94 mg, 0.070 mmol, 36 eq.), CuSO₄·5H₂O (9 mg, 0.0351 mmol,

18 eq.) and sodium ascorbate (7 mg, 0.0351 mmol, 18 eq.) were reacted together following the procedure A and was purified by column chromatography (4% MeOH in DCM as eluent) to yield compound **6** as a colourless oil in 50% yield.

^1H NMR (300 MHz, CDCl_3) δ 9.63 (s, 12H), 7.88 (d, $J = 29.3$ Hz, 18H), 7.73 (s, 18H), 7.56 – 7.42 (m, 36H), 7.07 – 6.44 (m, 396H), 6.10 – 5.88 (m, 90H), 5.52 – 4.94 (m, 244H), 4.67 – 4.13 (m, 260H), 3.80 – 3.20 (m, 302H), 2.71 (d, $J = 41.5$ Hz, 30H), 1.79 (s, 12H).

^{13}C $\{^1\text{H}\}$ NMR (151 MHz, CDCl_3) δ 167.6, 163.7, 155.5, 147.1, 144.6, 144.2, 134.7, 130.8, 128.7, 125.0, 121.7, 121.2, 120.9, 117.6, 117.5, 115.2, 115.1, 106.9, 71.3, 70.3, 69.6, 69.0, 68.1, 64.1, 52.8, 50.2, 38.7, 31.9, 30.3, 29.6, 28.9, 23.7, 22.9, 22.6, 20.3, 14.0, 10.9.

^{31}P NMR (122 MHz, CDCl_3) δ 9.70 (s).

I.R (cm^{-1}) 3708, 3680, 2980, 2922, 2865, 2844, 1702, 1552, 1501, 1455, 1426, 1295, 1262, 1189, 1170, 1103, 1054, 1032, 1011, 953, 884, 834.

MALDI-TOF m/z : calculated for $\text{C}_{1288}\text{H}_{1426}\text{N}_{186}\text{O}_{319}\text{P}_{54}\text{S}_6$: 26481.1320, found: 26249.7870.

GPC (THF): $M_n = 26350$ g/mol. $M_w/M_n = 1.03$

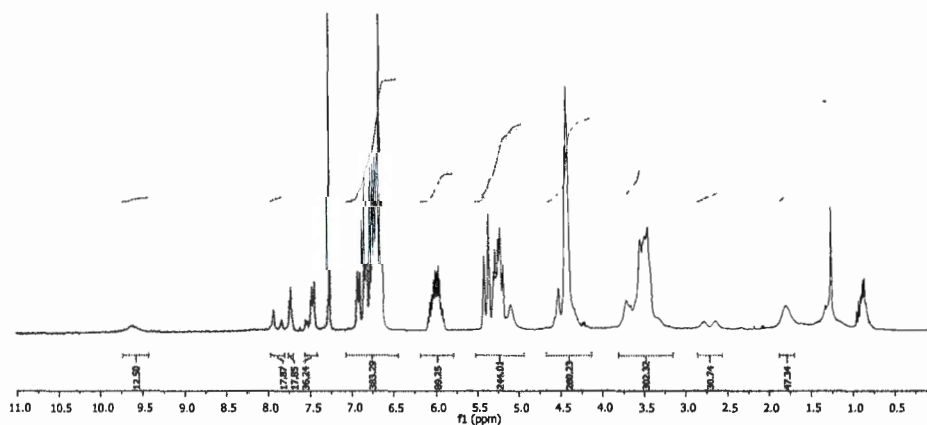


Figure S69. ^1H NMR spectrum of compound **6** (CDCl_3 , 300 MHz).

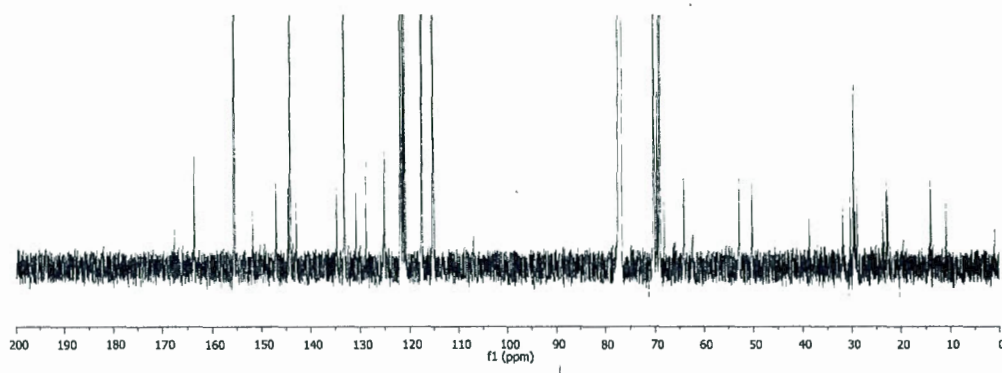


Figure S70. $^{13}\text{C} \{^1\text{H}\}$ NMR of compound **6** (CDCl_3 , 151 MHz).

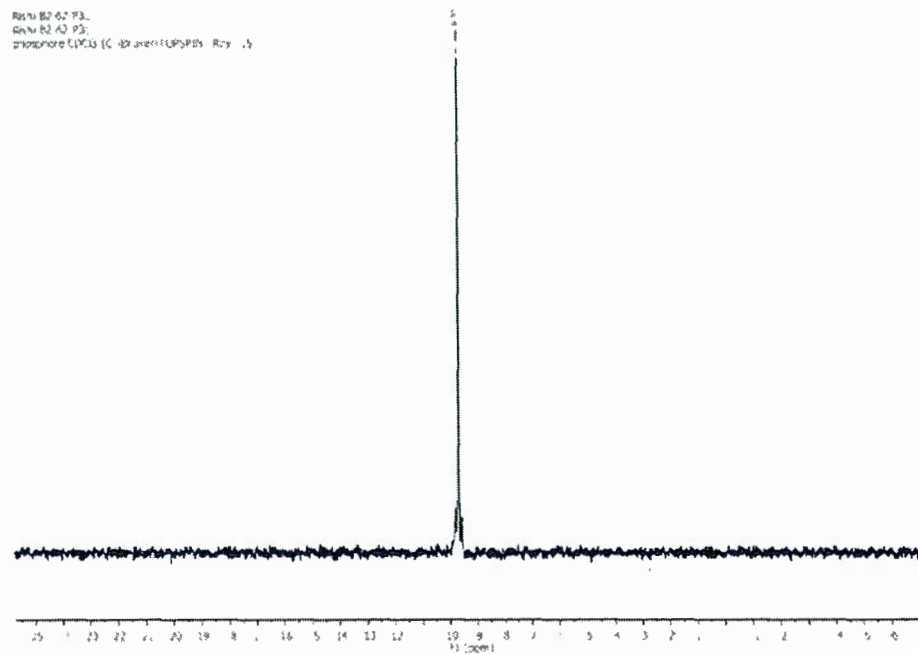


Figure S71. ^{31}P NMR spectrum of compound **6** (CDCl_3 , 122 MHz).

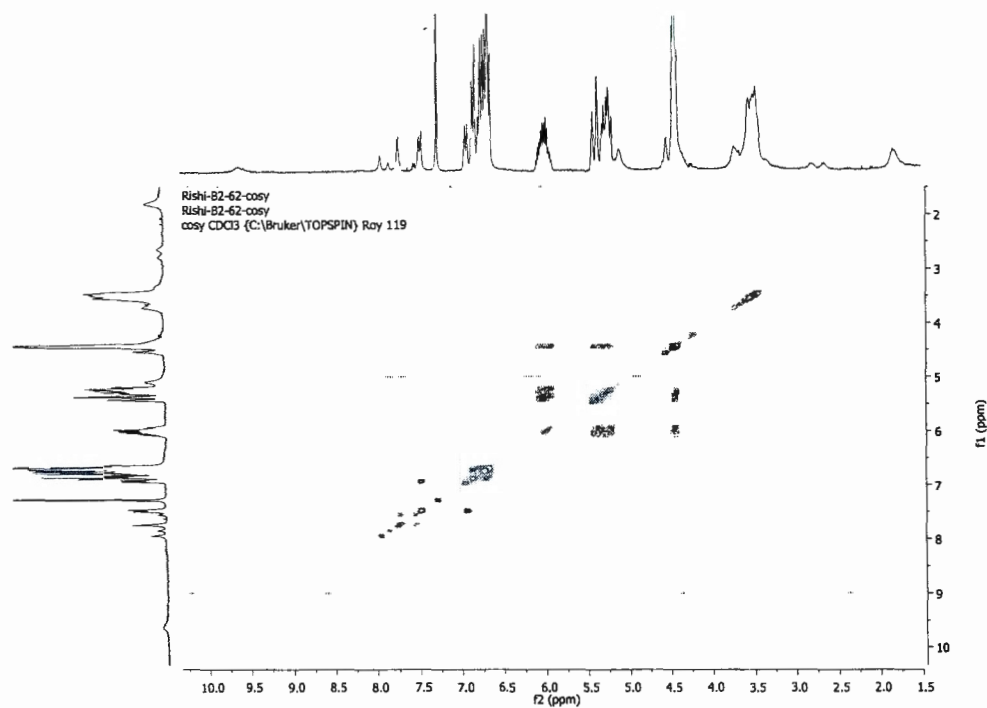


Figure S72. COSY spectrum of compound 6.

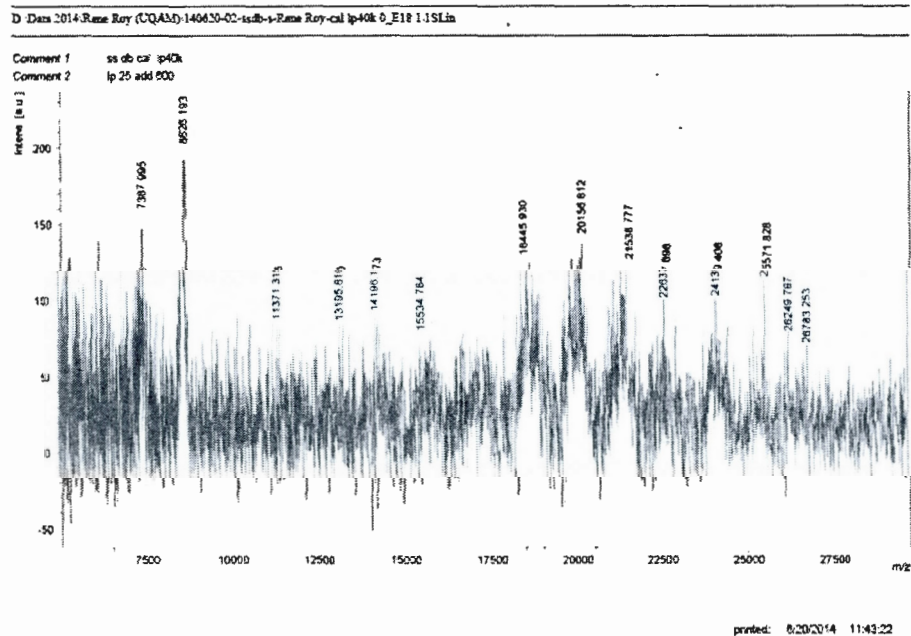
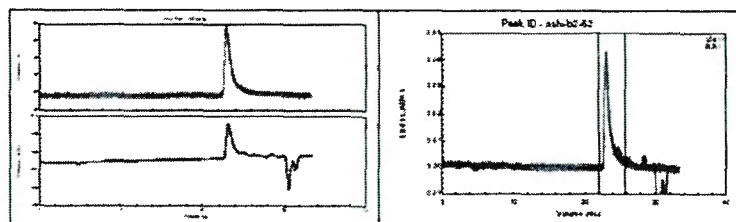


Figure S73. MALDI-TOF spectrum of compound 6.



COLLECTION INFORMATION

Collection time : Wed May 06, 2003 04:29 PM Est (heure d'été)
 Instrument type : EASN 802
 Cell type : F3
 Laser wavelength : 690.0 nm
 Solvent name : THF
 Solvent RI : 1.401
 Calibration constants
 DAWN : 4.7600e-04
 AUX1 : 2.8000e-04
 AUX2 : 1.0000e-04
 Flow rate : 1.000 mL/min
 Collection interval : 0.250 sec
 Number of slices : 7949

Volume (mL) : 22.104 - 25.725
 Slices (used) : 970 (767)
 A2 (mol mL/g²) : 0.000e+00
 Fit degree : 1
 Injected Mass (g) : 1.1100e-04
 dn/dc (mL/g) : 0.098
 Polydispersity(Mw: Mn) : 1.030±0.132 (13%)
 Polydispersity(Mz: Mn) : 1.058±0.237 (22%)

Molar Mass Moments (g/mol)

Mn : 2.635e+04 (9%)
 Mw : 2.713e+04 (9%)
 Mz : 2.747e+04 (20%)

Figure S74. GPC traces of compound 6.

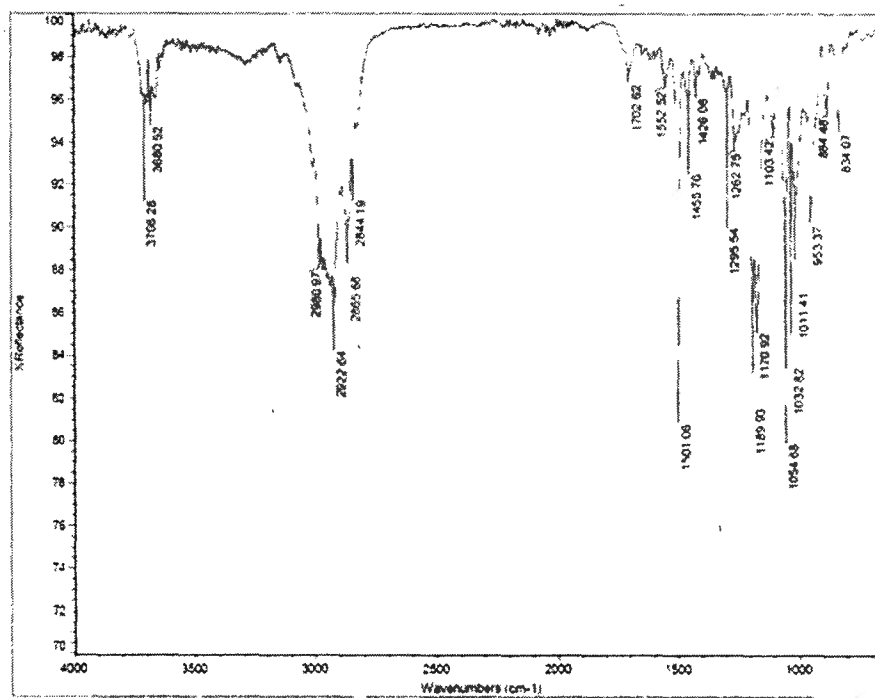
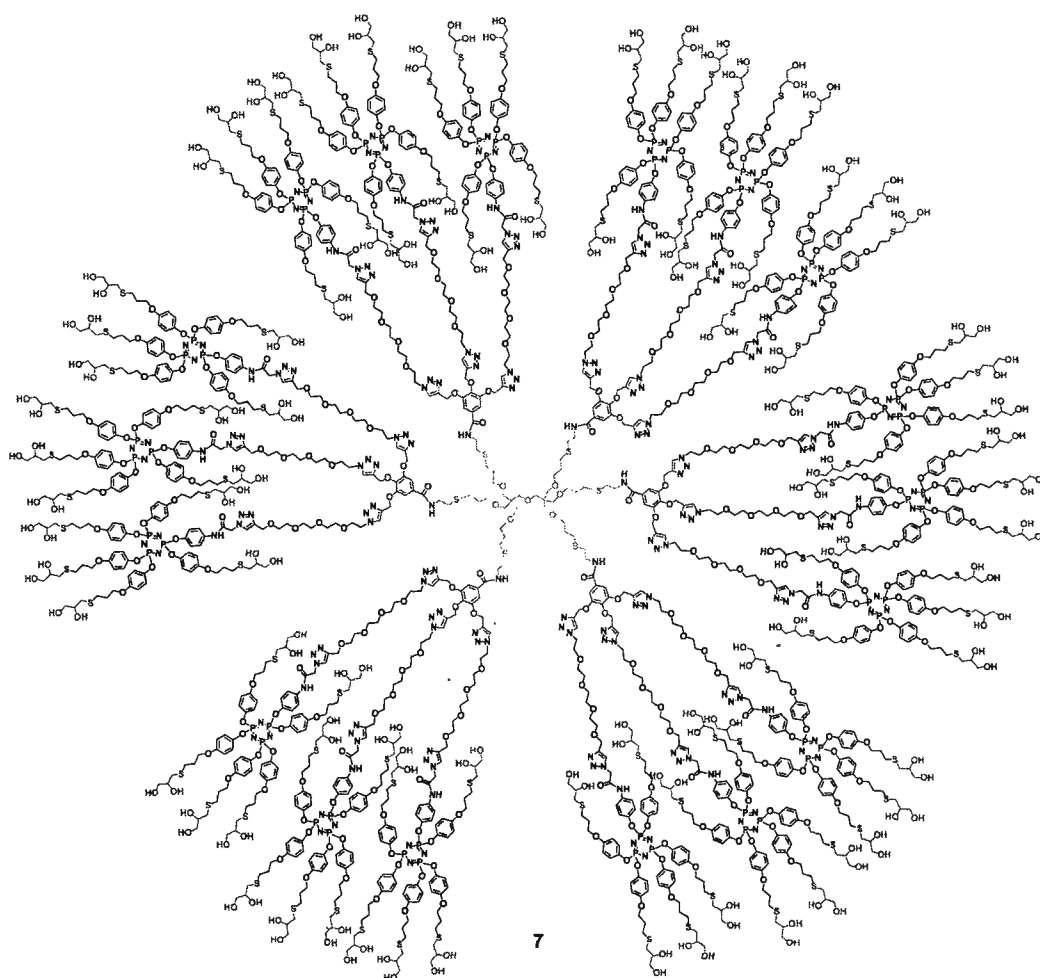


Figure S75. IR spectrum of compound 6.



Synthesis of compound 7: Alkene terminated dendrimer **6** (20 mg, 0.00075 mmol, 1eq), 1- thioglycerol (0.040 ml, 0.4725 mmol, 630 eq.), and AIBN (3.7 mg, 0.0225, 30 eq.) were reacted together following the procedure B and was purified by dialysis to yield compound **7** as a colourless oil in 75% yield.

^1H NMR (300 MHz, MeOD): δ 7.94 – 7.84 (m, 36H), 7.50 – 7.40 (m, 36H), 6.73 (s, 396H), 5.25 (d, J = 36.8 Hz, 460H), 4.55 (brs, 233H), 3.9 – 2.6 (m, 793), 2.07 (s, 192H).

^{13}C $\{^1\text{H}\}$ NMR (151 MHz, MeOD): δ 185.2, 157.4, 145.2, 122.9, 122.6, 122.4, 122.3, 120.7, 116.9, 116.2, 81.4, 72.9, 72.8, 72.7, 71.9, 67.8, 65.9, 64.5, 63.6, 54.1, 53.8, 50.5, 50.4, 44.2, 41.7, 39.6, 39.2, 38.5, 37.3, 37.0, 36.8, 36.2, 35.9, 34.7, 33.6, 33.5, 30.6, 30.5, 30.1, 28.2, 23.6.

^{31}P NMR (243 MHz, MeOD): δ 10.39, 10.34, 10.24, 10.19.

MALDI-TOF m/z: calculated for $C_{1558}H_{2146}N_{186}O_{499}P_{54}S_{96}$: 36215.4798, found: 37226.6720.

Differential light scattering Hydrodynamic diameter: 1.955nm

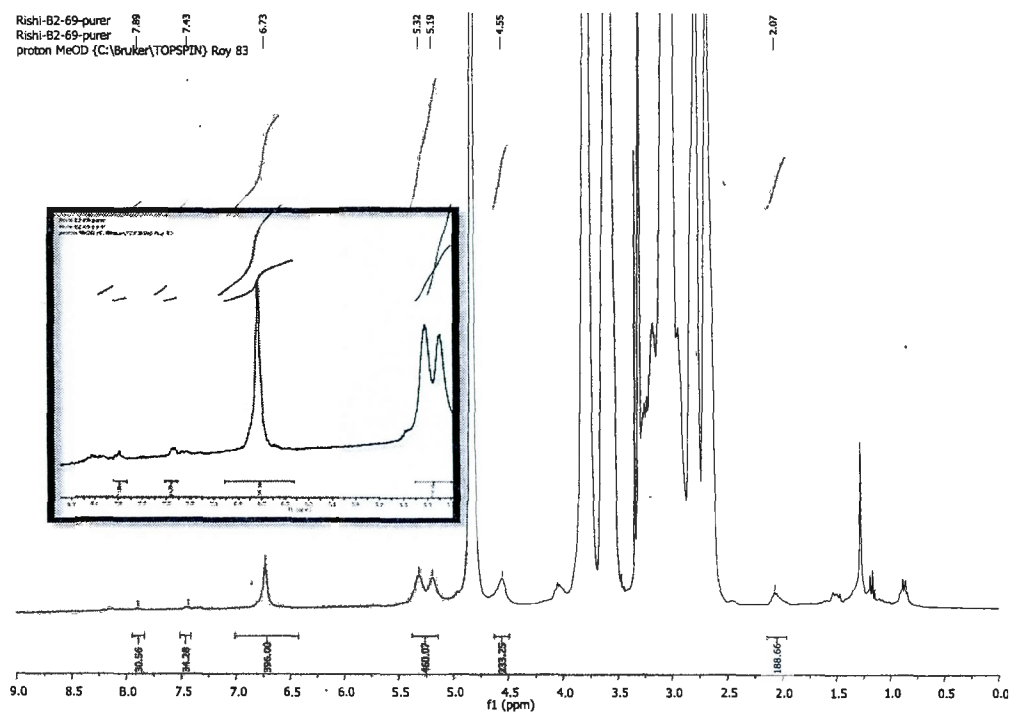


Figure S76. ^1H NMR spectrum of compound **7** (CD₃OD, 300 MHz).

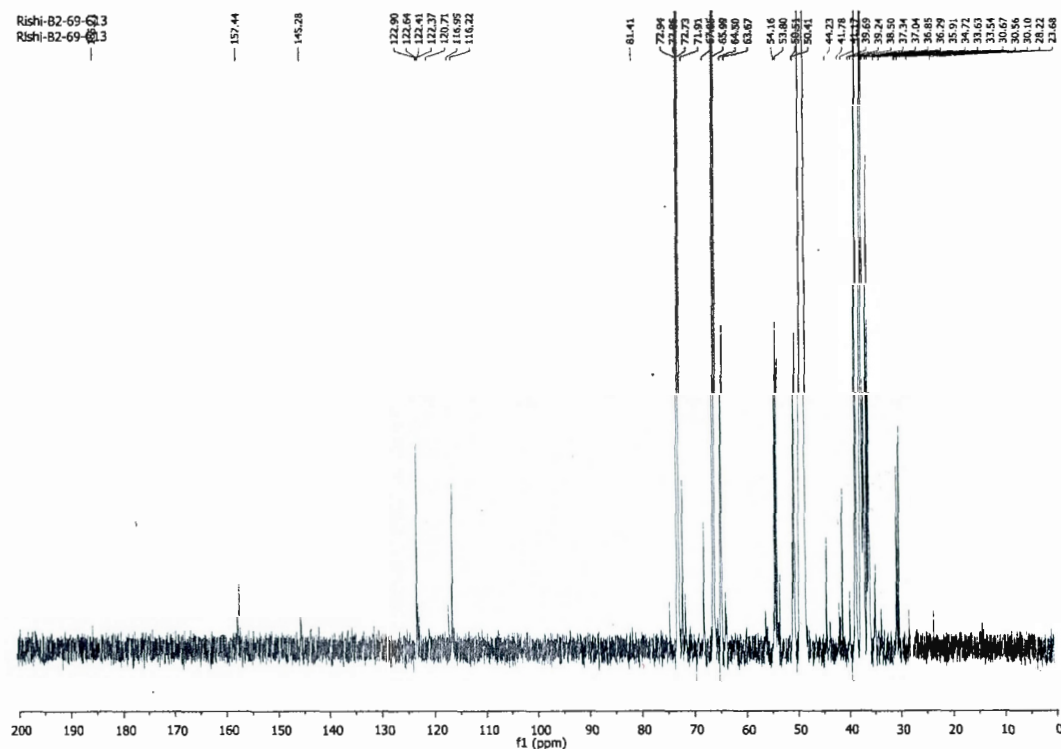


Figure S77. $^{13}\text{C} \{^1\text{H}\}$ NMR of compound 7 (CD_3OD , 151 MHz).

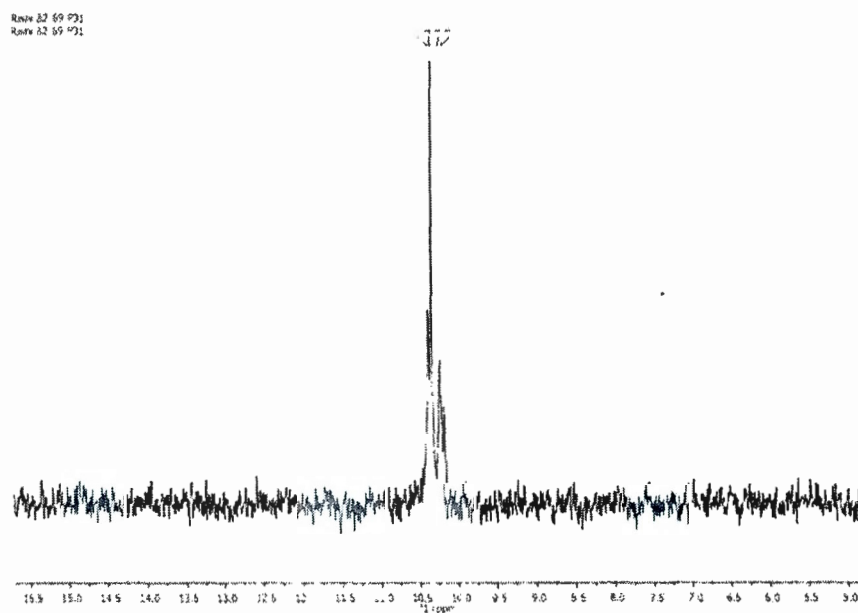


Figure S78 ^{31}P NMR spectrum of compound 7 (CD_3OD , 243 MHz)

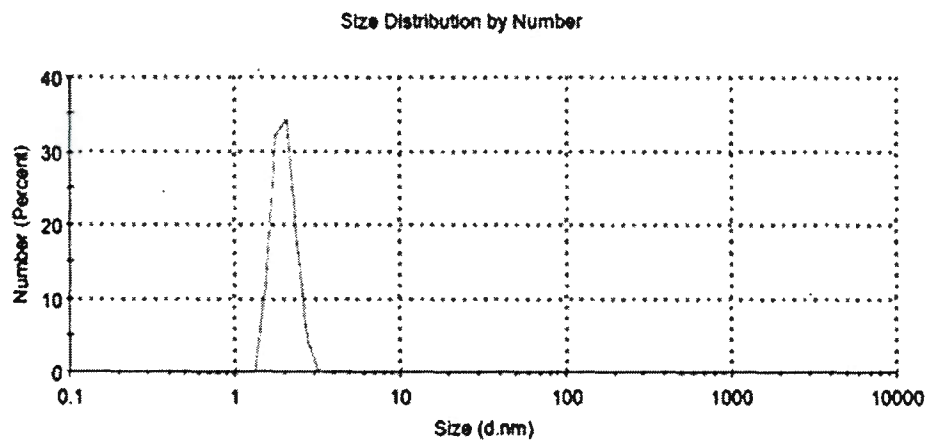


Figure S79. DLS size distribution of dendrimer 7 in methanol at 25°C

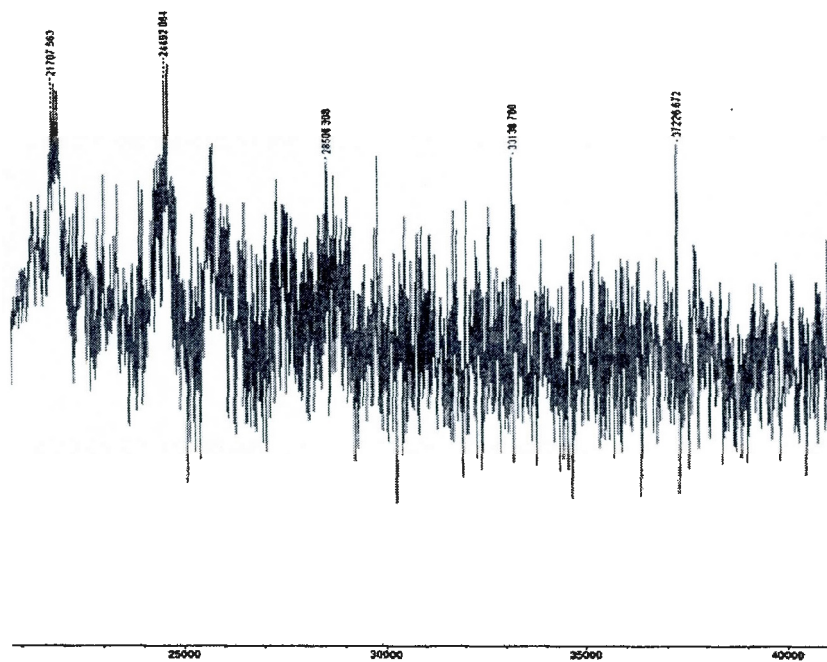
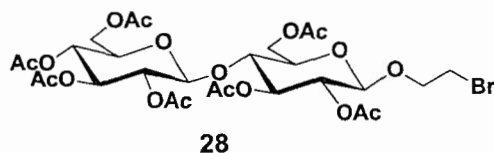


Figure S80. MALDI-TOF spectrum of compound 7.



Synthesis of compound 28: Cellobiose octaacetate **27** (1.5g, 0.0021 moles) was dissolved in DCM (20 ml) followed by the addition of 2-bromoethanol (0.31 ml, 0.0044 moles). The reaction mixture was cooled to 0°C and BF₃·etherate (0.8 ml, 0.0064 moles) was added dropwise. The mixture was then stirred at 0°C for 4 h. It was allowed to come to room temperature and stirred for additional 2 h. The mixture was diluted with DCM (100 ml) and washed with aq. NaHCO₃ (3X30ml) and brine. The organic layer was dried and evaporated. The crude was purified by flash chromatography over silica gel (eluent hexane: DCM: Toluene: Ethyl acetate, 1:1:1:2) to provide **28**. (Yield: 43%).

¹H NMR (600 MHz, CDCl₃) δ 5.22 – 5.10 (m, 2H), 5.06 (t, J = 9.7 Hz, 1H), 4.92 (t, J = 9 Hz 2H), 4.52 (dt, J = 15.1, 4.5 Hz, 3H), 4.36 (dd, J = 12.4, 4.3 Hz, 1H), 4.12–4.01 (m, 2H), 4.04 (dd, J = 12.4, 1.4 Hz, 1H), 3.85 – 3.73 (m, 2H), 3.65 (ddd, J = 9.9, 3.8, 1.9 Hz, 1H), 3.60 (dd, J = 9.9, 4.9 Hz, 1H), 3.48–3.39 (m, 2H), 2.14 – 1.95 (m, 21H).

¹³C {¹H} NMR (151 MHz, CDCl₃) δ 170.44 (s), 170.4, 170.2, 170.1, 169.7, 169.6, 169.2, 168.9, 100.8, 100.7, 76.3, 72.8, 72.7, 72.2, 71.9, 71.5, 71.2, 69.7, 67.6, 61.4, 29.8, 20.8, 20.7, 20.6, 20.5.

HRMS (ESI⁺) *m/z* calc. For C₂₈H₃₉BrO₁₈, 743.5025 found, 762.1631 [M + NH₄]⁺.

I.R (cm⁻¹) 3712, 3705, 3680, 3667, 2981, 2972, 2892, 2865, 2843, 2825, 1743, 1365, 1261, 1216, 1052, 1032, 1017.

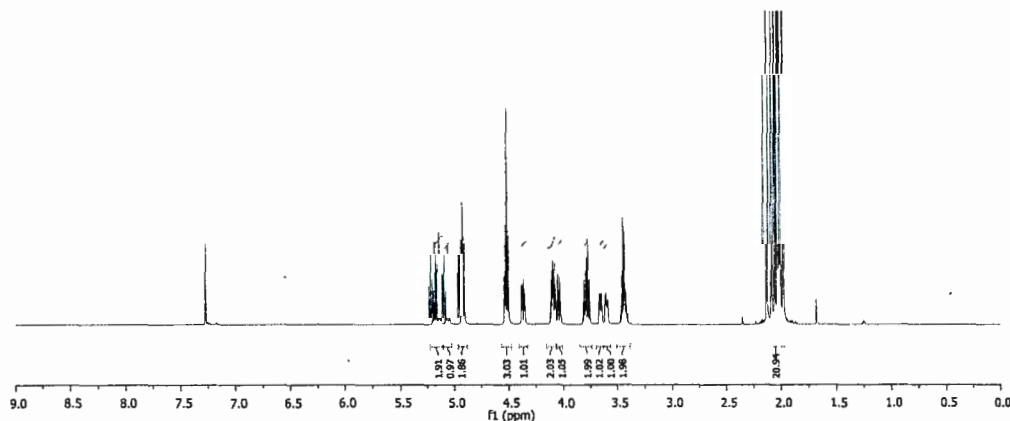


Figure S81. ¹H NMR spectrum of compound **28** (CDCl₃, 300 MHz).

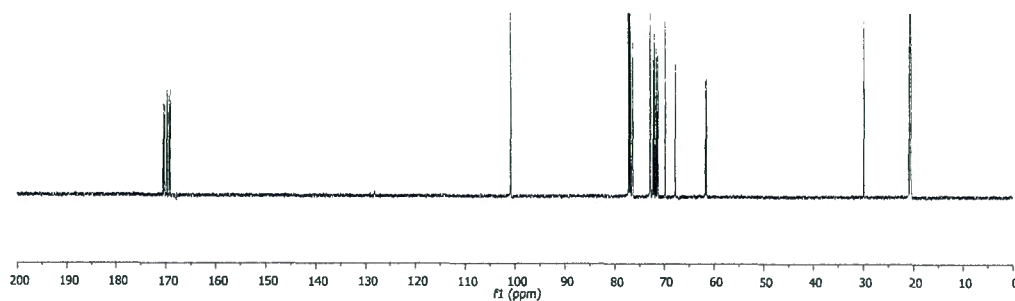


Figure S82. $^{13}\text{C} \{^1\text{H}\}$ NMR of compound **28** (CDCl_3 , 151 MHz).

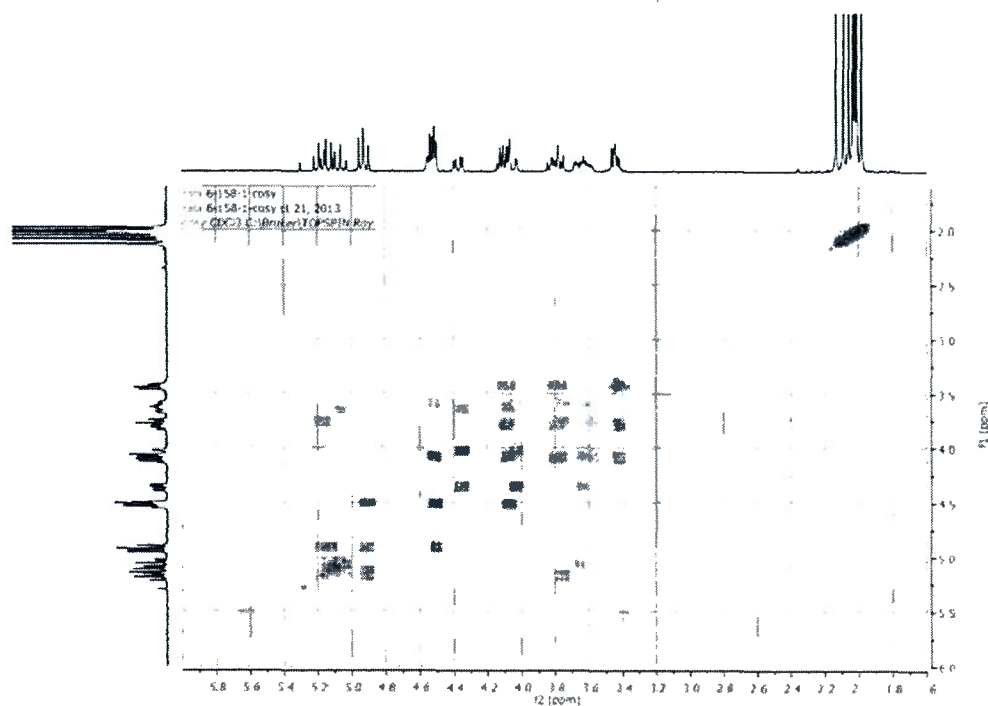


Figure S83. COSY spectrum of compound **28**.

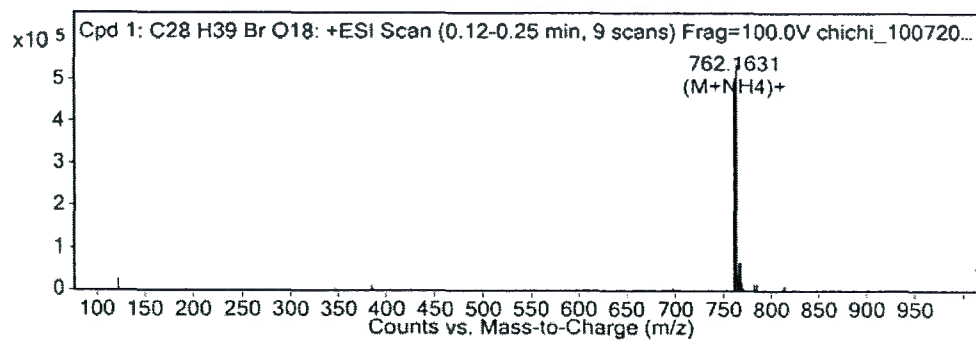


Figure S84. HRMS (ESI^+) spectrum of compound **28**.

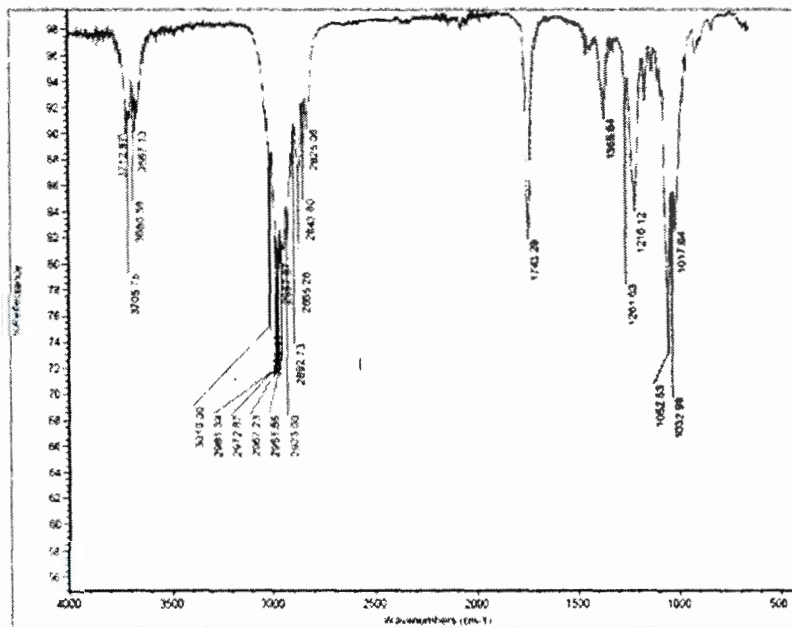
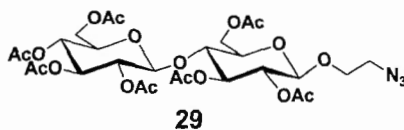


Figure S85. IR spectrum of compound 28.



Synthesis of compound 29: A mixture of heptaacetyl-1-(2-bromoethyl)- cellobiose **28** (500 mg, 0.67 mmol) and sodium azide (152 mg, 2.33 mmol) in DMF (5ml) was kept at 70°C for 4 hrs. The mixture was cooled, diluted with EtOAc, washed with H₂O (2X10ml) and brine. The organic layer was dried with anhydrous sodium sulphate, filtered and evaporated. The crude was recrystallized from DCM: hexane mixture and pure azide **29** was obtained in 92% yield.

¹H NMR (600 MHz, CDCl₃) δ 5.22 – 5.13 (m, 2H), 5.08 (t, *J* = 9, 1H), 4.98 – 4.90 (m, 2H), 4.60 – 4.50 (m, 3H), 4.38 (dd, *J* = 12.5, 3.3 Hz, 1H), 4.13 – 4.02 (m, 2H), 4.03 – 3.96 (m, 1H), 3.80 (t, *J* = 9.5 Hz, 1H), 3.71 – 3.64 (m, 2H), 3.61 (dd, *J* = 9.9, 4.7 Hz, 1H), 3.52 – 3.44 (m, 1H), 3.27 (dt, *J* = 13.4, 3.4 Hz, 1H), 2.17 – 1.96 (m, 21H).

¹³C {¹H} NMR (151 MHz, CDCl₃) δ 170.4, 170.24, 169.7, 169.6, 169.2, 169, 100.7, 100.5, 76.3, 72.9, 72.7, 72.4, 71.9, 71.5, 71.3, 68.6, 67.7, 61.6, 61.5, 50.4, 20.8, 20.6, 20.5.

HRMS (ESI⁺) *m/z* calc. For C₂₈H₃₉N₃O₁₈, 705.6186; found, 723.2585 [M + NH₄]⁺.

I.R (cm^{-1}) 2963, 2105, 1432, 1366, 1165, 1130, 1035, 906, 731.

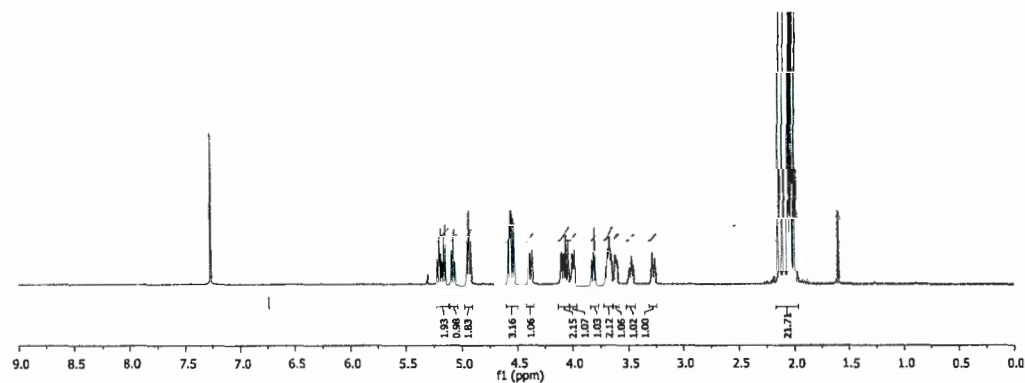


Figure S86. ^1H NMR spectrum of compound **29** (CDCl_3 , 300 MHz).

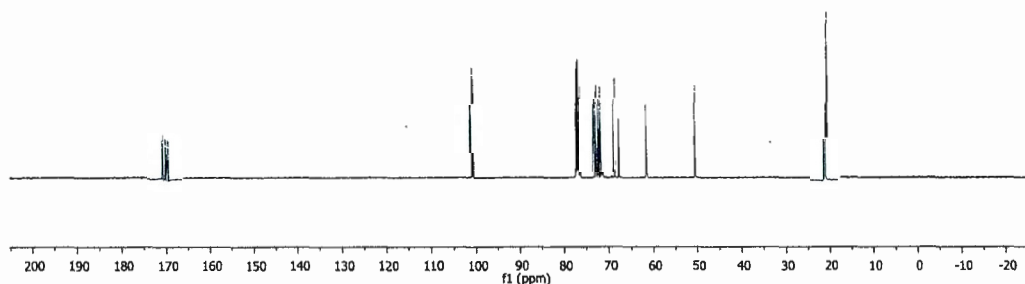


Figure S87. ^{13}C $\{^1\text{H}\}$ NMR of compound **29** (CDCl_3 , 151 MHz).

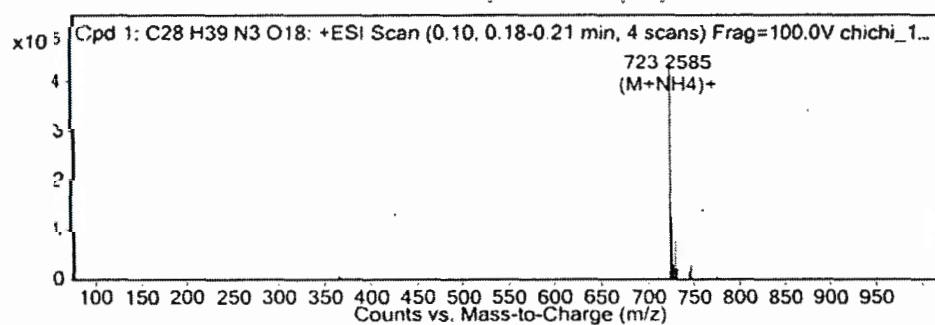


Figure S88. HRMS (ESI^+) spectrum of compound **29**.

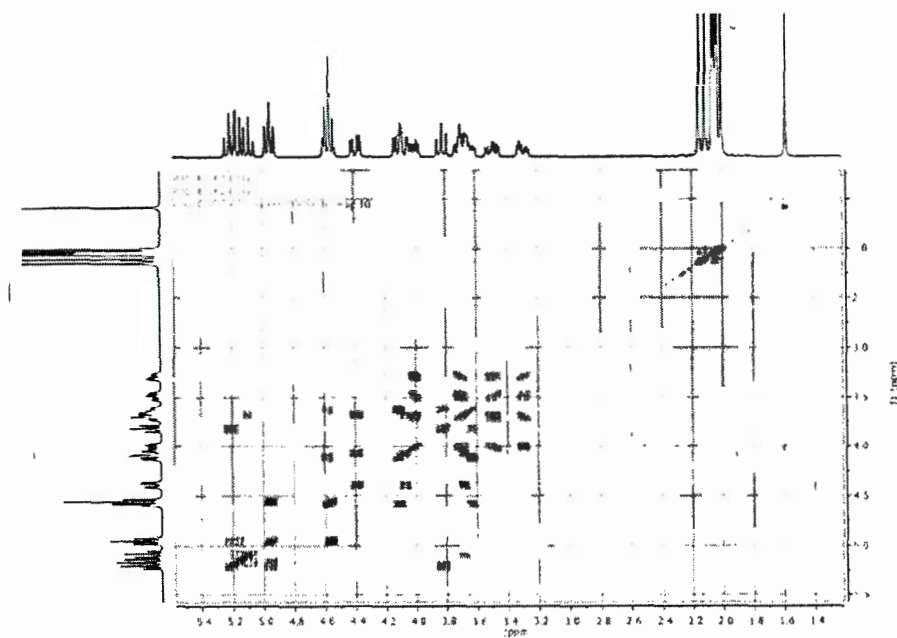


Figure S89. COSY spectrum of compound 29.

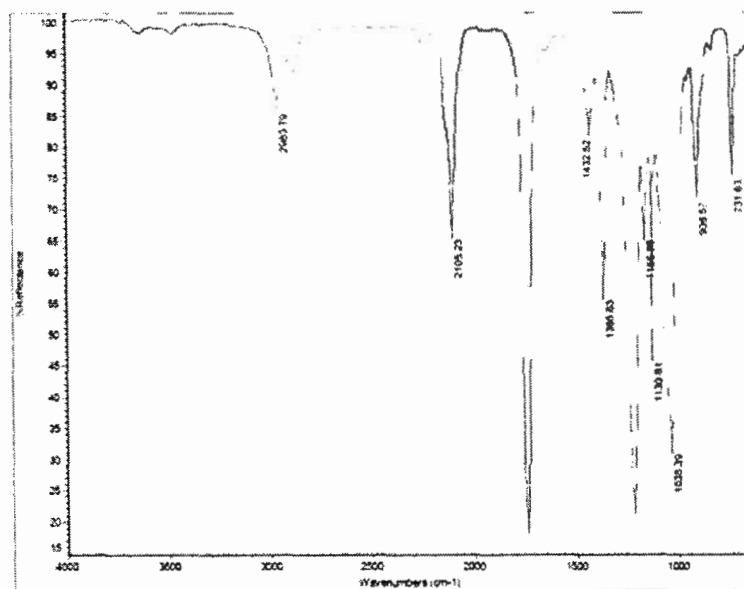
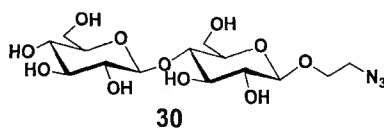


Figure S90. IR spectrum of compound 29.



Synthesis of compound 30: To a solution of heptaacetyl-1(2-azidoethyl) cellobioside **29** (520 mg, 0.74 mmol) in methanol was added 1M NaOMe until pH 9-10 was reached. It was allowed to stir at room temperature for 5h. Acidic resin (IR-120) was added to make pH 5-6 and solution was filtered through cotton bed and evaporated to yield **30** in 90% yield.

^1H NMR (300 MHz, D_2O) δ 4.53 (dd, $J = 7.9, 5.9$ Hz, 2H), 4.11 – 3.23 (m, 16H).

^{13}C $\{^1\text{H}\}$ NMR (75 MHz, D_2O) δ 110.4, 103.2, 102.8, 79.2, 76.6, 76.1, 75.4, 74.92, 73.8, 73.5, 70.1, 69.2, 61.2, 60.6, 51.1.

HRMS (ESI^+) m/z calc. For $\text{C}_{14}\text{H}_{25}\text{N}_3\text{O}_{11}$, 411.3618; found, 434.1396 $[\text{M} + \text{Na}]^+$.

I.R (cm^{-1}) 3345, 2114, 1639, 1032.

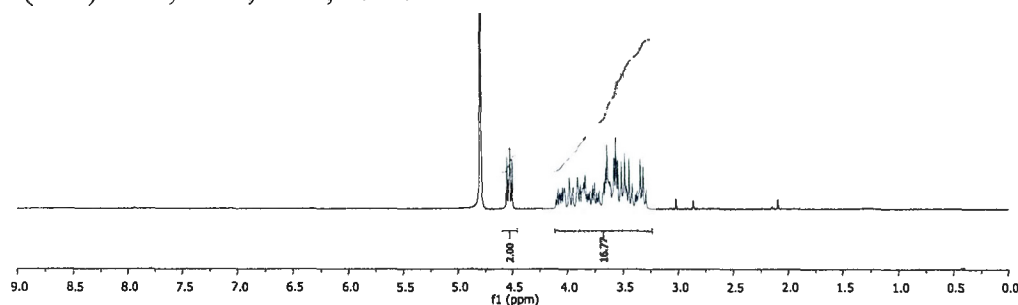


Figure S91. ^1H NMR spectrum of compound **30** (D_2O , 300 MHz).

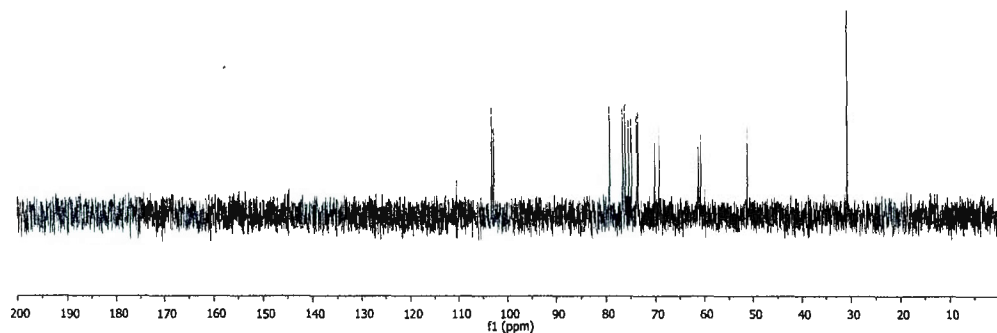


Figure S92. ^{13}C $\{^1\text{H}\}$ NMR of compound **30** (D_2O , 75 MHz).

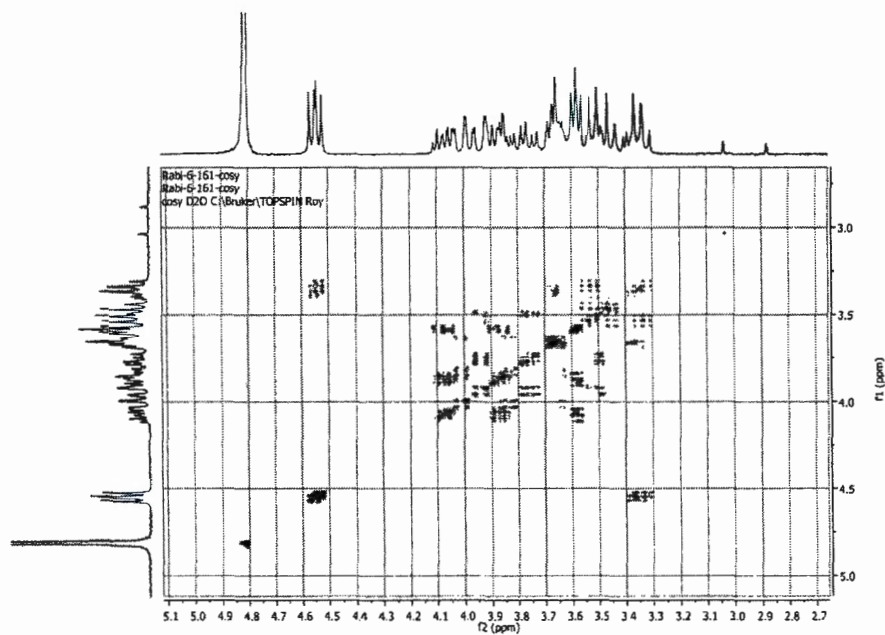


Figure S93. COSY spectrum of compound 30.

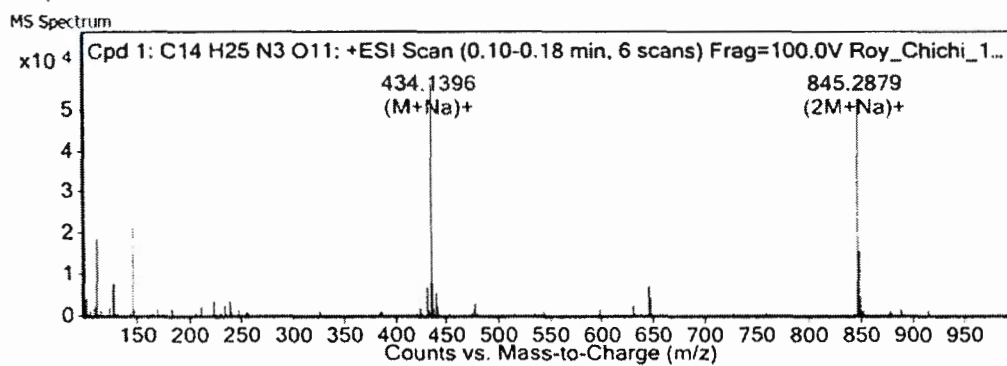


Figure S94. HRMS (ESI⁺) spectrum of compound 30.

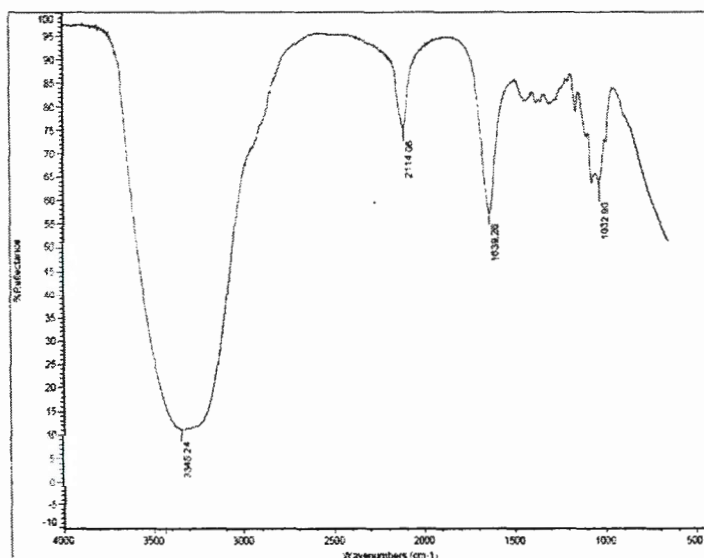
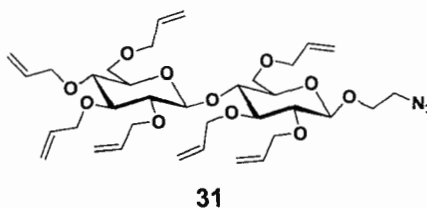


Figure S95. IR spectrum of compound **30**.



Synthesis of compound 31: To a solution of 1-(2-azidoethyl) cellobioside **30** (268 mg, 0.387 mmol) in DMF (10ml) at 0°C sodium hydride (60% in oil, 500 mg, 12.5 mmol) was added. The mixture was stirred at 0°C for 15 min followed by addition of allyl bromide (1.4 ml, 16.2 mmol) dropwise. The mixture was stirred at 0°C for 1 h and at RT for 10 minutes. Reaction was quenched with saturated NH₄Cl sol. and extracted with EtOAc (50 ml) followed with brine wash. The organic layer was separated, dried and evaporated. The crude mixture was purified with column chromatography. The desired compound **31** was obtained using 20% EtOAc: hexane as eluent in 89% yield.

¹H NMR (300 MHz, CDCl₃) δ 6.07 – 5.79 (m, 7H), 5.35 – 5.04 (m, 14H), 4.49 – 3.89 (m, 17H), 3.85 – 3.58 (m, 6H), 3.56 – 3.19 (m, 8H), 3.17 – 3.07 (t, J = 18 Hz, 1H).

¹³C {¹H} NMR (151 MHz, CDCl₃) δ 136, 135.2, 135.1, 135, 134.9, 134.8, 134.6, 116.8, 116.7, 116.6, 116.4, 116.3, 115.7, 84.4, 82.4, 81.8, 81, 77.3, 77.2, 75, 74.7, 74.2, 74, 73.8, 73.7, 73.5, 72.3, 72.1, 68.6, 68.1, 68, 50.9

HRMS (ESI⁺) m/z calc. For C₃₅H₅₃N₃O₁₁, 691.8088; found, 709.4022 [M + NH₄]⁺, 730.3342 [M + K]⁺.

I.R (cm⁻¹) 3680, 3078, 2919, 2866, 2103, 1646, 1457, 1420, 1346, 1305, 1120, 994, 918.

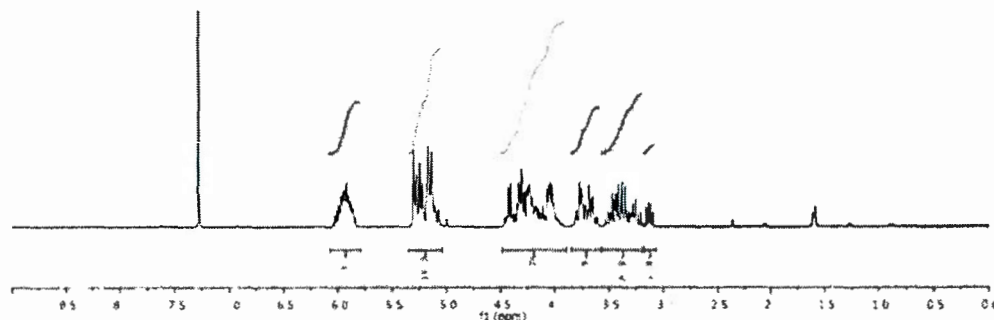


Figure S96. ¹H NMR spectrum of compound **31** (CDCl₃, 300 MHz).

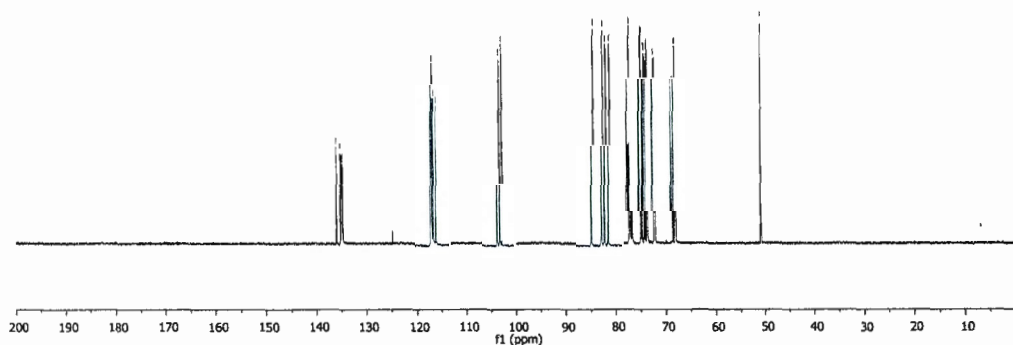


Figure S97. ¹³C {¹H} NMR of compound **31** (CDCl₃, 151 MHz).

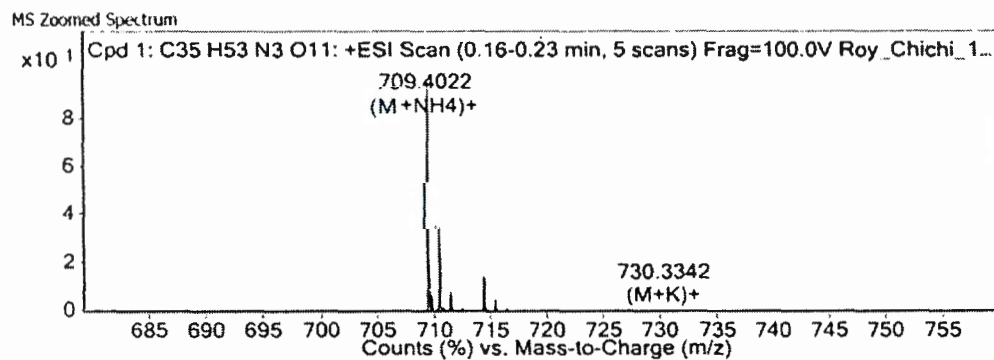
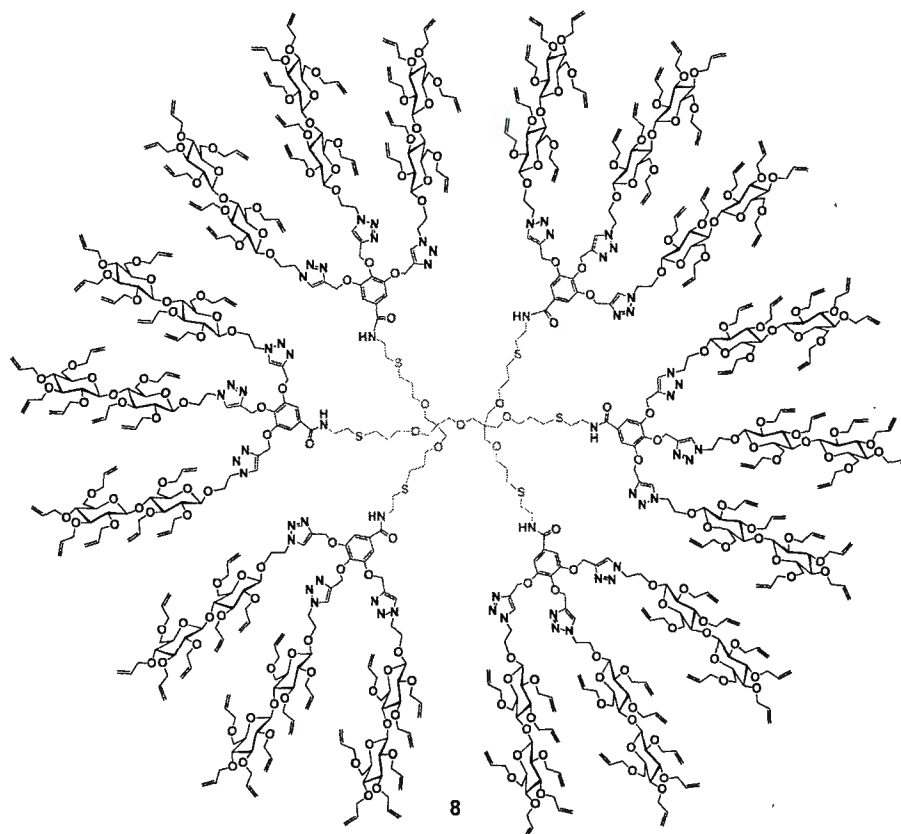


Figure S98. HRMS (ESI⁺) spectrum of compound **31**.

Figure S100. IR spectrum of compound **31**.



Synthesis of compound 8: Propargyl terminated dendrimer **1** (10 mg, 0.0039 mmol, 1 eq), compound **31** (72 mg, 0.105 mmol, 27 eq.), CuSO₄·5H₂O (9 mg, 0.0351 mmol, 9 eq.) and sodium ascorbate (7 mg, 0.0351 mmol, 9 eq.) were reacted together following the procedure A and was purified by column chromatography (4% MeOH in DCM as eluent) to yield compound **8** as a colourless oil in 76% yield.

¹H NMR (300 MHz, CDCl₃) δ 8.01 – 7.88 (m, 18H), 7.30 (br s, 12H), 6.04 – 5.69 (m, 126H), 5.32 – 4.98 (m, 272H), 4.68 – 3.03 (m, 638H), 2.85 (br s, 12H), 2.70 (br s, 12H), 1.87 (br s, 12H).

¹³C {¹H} NMR (151 MHz, CDCl₃) δ 166.6, 151.8, 144.0, 143.3, 135.9, 135.2, 134.9, 134.8, 134.5, 129.9, 124.6, 116.8, 116.7, 116.5, 116.3, 115.8, 115.7, 107.1, 103.0, 102.7, 84.4, 82.4, 81.8, 80.7, 74.9, 74.7, 74.2, 74.0, 73.6, 73.5, 73.4, 72.3, 72.0, 68.6, 68.4, 68.0, 67.9, 67.5, 62.5, 50.2, 45.5, 39.3, 34.6, 31.5, 29.6, 25.2, 22.5, 14.0, 11.3.

IR (cm⁻¹) 3648, 3403, 3080, 2980, 2971, 2918, 1647, 1459, 1379, 1261, 1072, 925.

MALDI-TOF m/z: calculated for C₇₆₆H₁₁₀₂N₆₀O₂₂₉S₆: 15007.6007, found: 15011.0180

GPC (CHCl₃): M_n = 15140 g/mol. M_w/M_n = 1.07

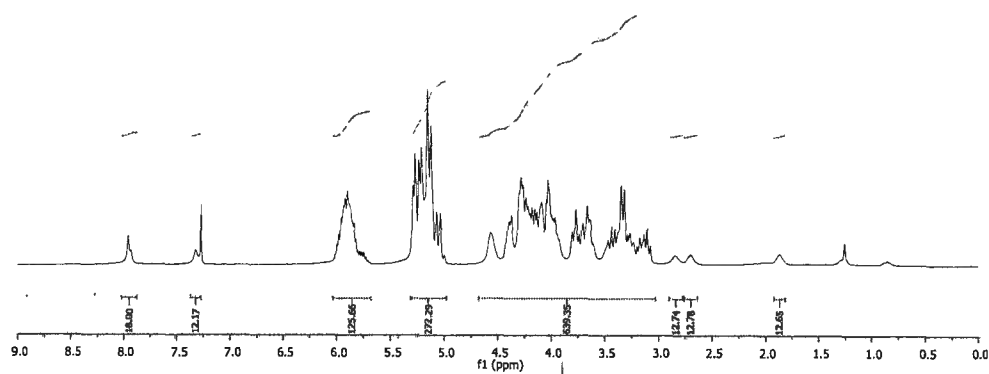


Figure S101. ^1H NMR spectrum of compound **8** (CDCl_3 , 300 MHz).

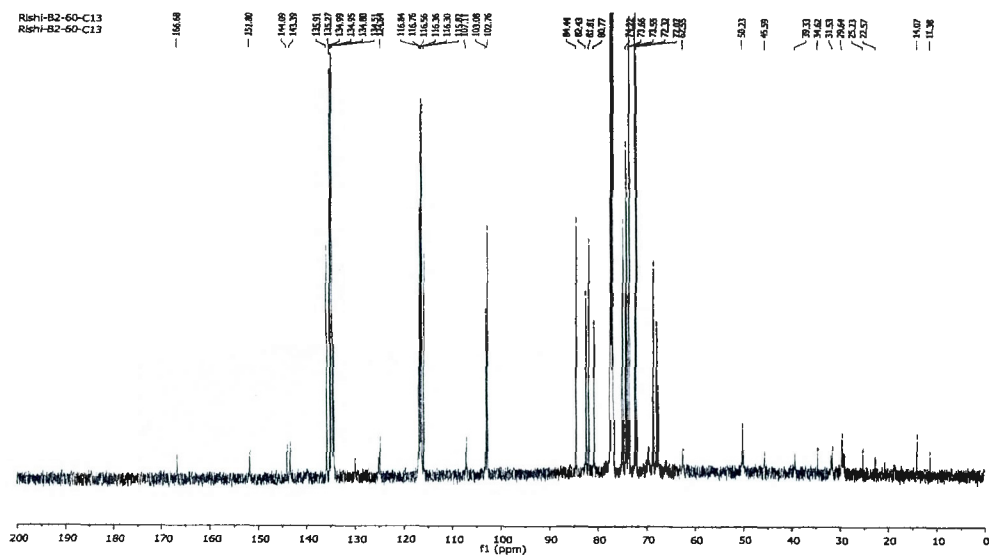


Figure S102. ^{13}C $\{^1\text{H}\}$ NMR of compound **8** (CDCl_3 , 151 MHz).

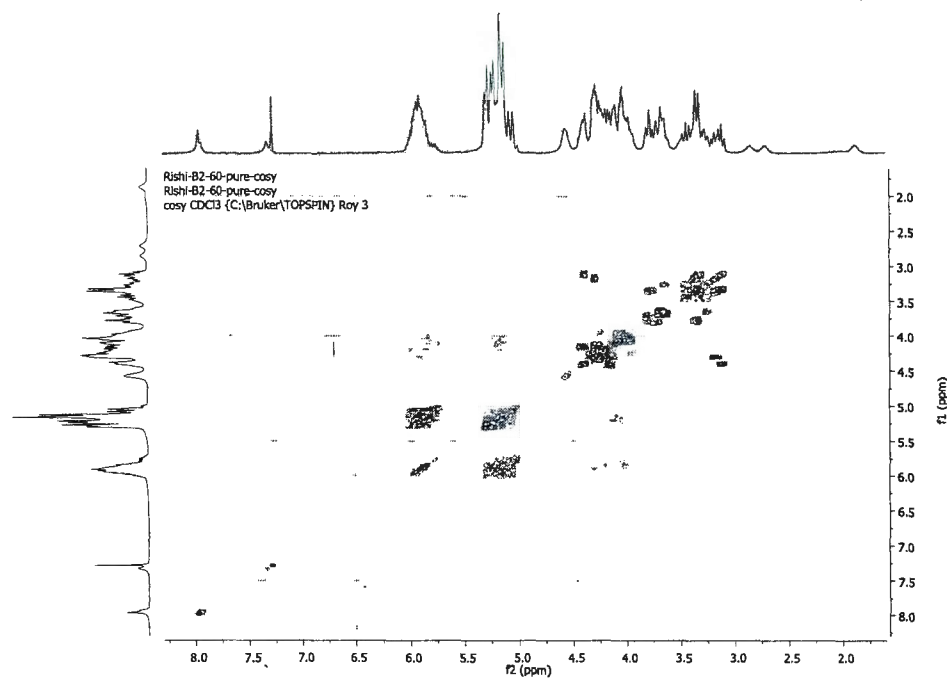


Figure S103. COSY spectrum of compound 8.

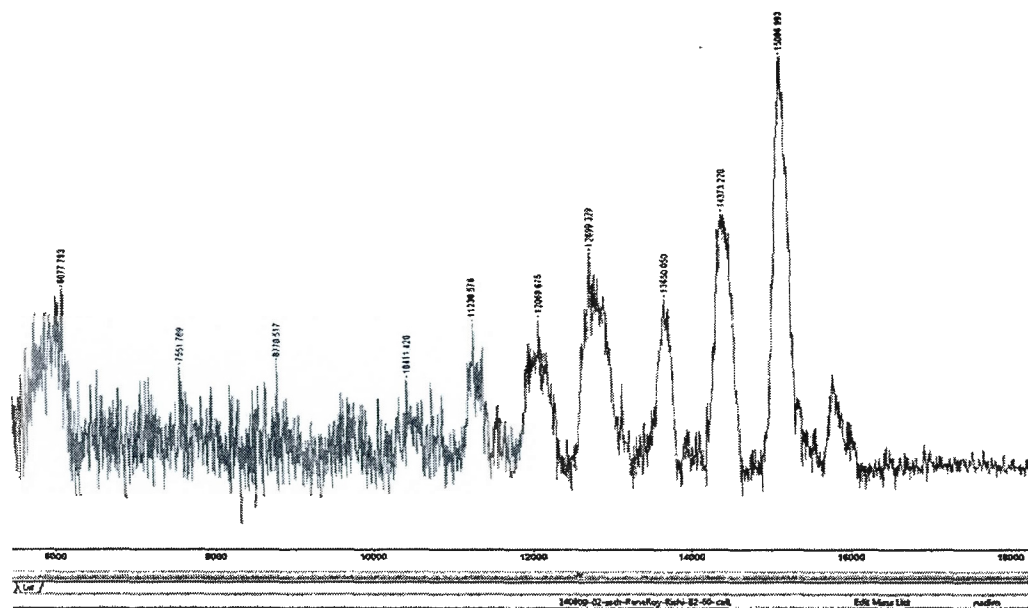


Figure S104. MALDI-TOF spectrum of compound 8.

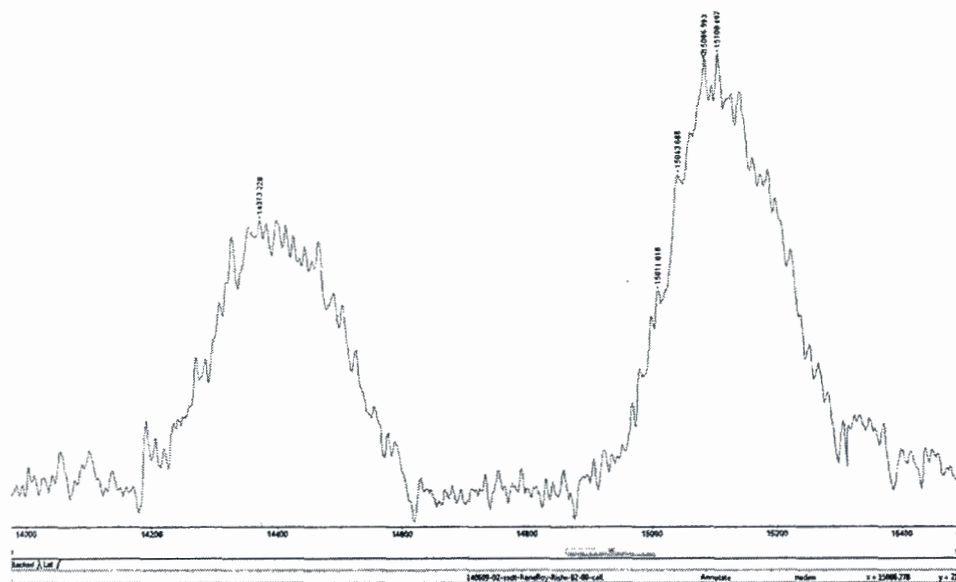
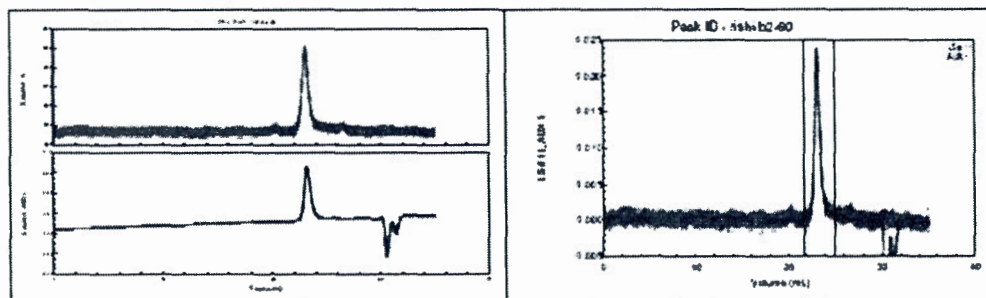


Figure S105. MALDI-TOF expanded spectrum of compound 8.



Volume (mL) : 21.567 - 24.973
 Slices (used) : 813 (698)
 A2 (mol mL/g²) : 0.000e+00
 Fit degree : 1
 Injected Mass (g) : 1.3600e-04
 dn/dc (mL/g) : 0.079
 Polydispersity (Mw/Mn) : 1.074±0.152 (14%)
 Polydispersity (Mz/Mn) : 1.400±0.490 (35%)

Molar Mass Moments (g/mol)

Mn : 1.514e+04 (9%)
 Mw : 1.626e+04 (10%)
 Mz : 2.120e+04 (33%)

R.M.S. Radius Moments (nm)

Rn : 23.2 (73%)
 Rw : 23.8 (72%)
 Rz : 25.8 (70%)

COLLECTION INFORMATION

Collection time : Wed May 08,
 Instrument type : DAWN EOS
 Cell type : K5
 Laser wavelength : 690.0 nm
 Solvent name : CHCl3
 Solvent RI : 1.446
 Calibration constants
 DAWN : 8.7600e-06
 AUX1 : 2.8000e-04
 AUX2 : 1.0000e-04
 Flow rate : 1.000 mL/min
 Collection interval : 0.250 sec
 Number of slices : 8400

Figure S106. GPC traces of compound 8.

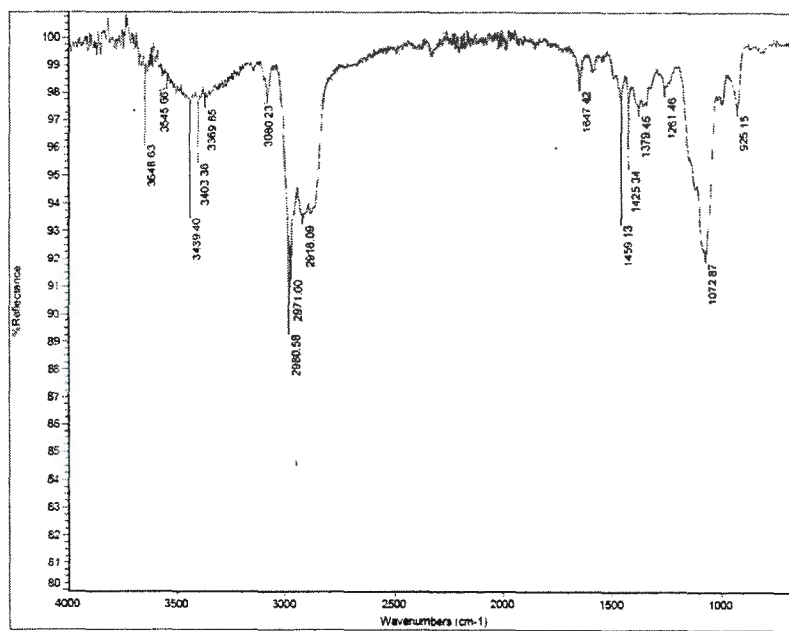
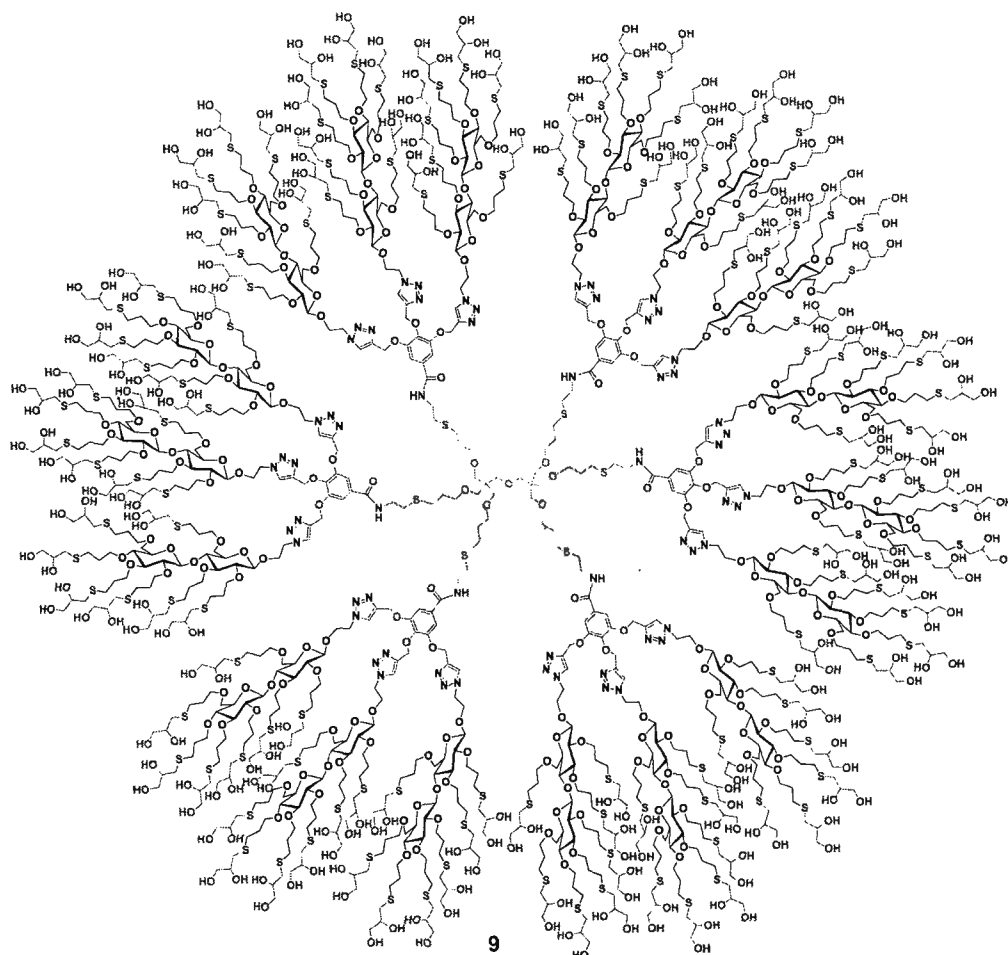


Figure S107. IR spectrum of compound 8.



Synthesis of compound 9: Allyl terminated dendrimer **8** (25 mg, 0.0016 mmol, 1eq), 1- thioglycerol (0.096 ml, 1.4mmol, 882 eq.), and AIBN (4 mg, 0.020, 12.6 eq.) were reacted together following the procedure B and was purified by dialysis to yield compound **9** as a colourless oil in 85% yield.

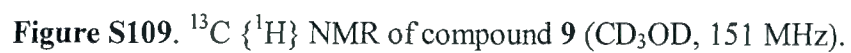
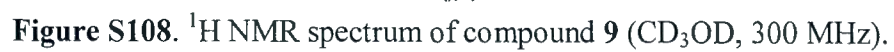
^1H NMR (600 MHz, MeOD) δ 8.16 (br s, 12H), 7.92 (br s, 6H), 7.30 (br s, 6H), 5.35 – 4.95 (m, 48H), 4.69 – 4.47 (m, 40H), 4.43 – 2.17 (m, 1308H), 2.07 – 1.40 (m, 208H), 1.35 – 1.05 (m, 34H).

^{13}C $\{^1\text{H}\}$ NMR (151 MHz, MeOD) δ 153.5, 144.3, 126.4, 104.4, 103.8, 86.2, 83.9, 82.8, 79.3, 77.6, 76.2, 73.2, 72.8, 71.9, 71.0, 70.9, 66.1, 65.3, 49.4, 49.2, 49.0, 48.8, 48.7, 48.5, 43.5, 36.3, 36.3, 31.8, 31.5, 31.0, 30.5, 30.4, 23.7, 21.2, 19.3, 17.9.

I.R (cm^{-1}) 3707, 3694, 3680, 3377, 2981, 2937, 2922, 2866, 2843, 1050, 1033, 1013.

(MALDI-TOF) m/z : calculated for $\text{C}_{1146}\text{H}_{2118}\text{N}_{60}\text{O}_{481}\text{S}_{132}$: 28667.7725, found: 28690.0370. $[\text{M}+\text{Na}]^+$.

Differential light scattering Hydrodynamic diameter: 6.980nm



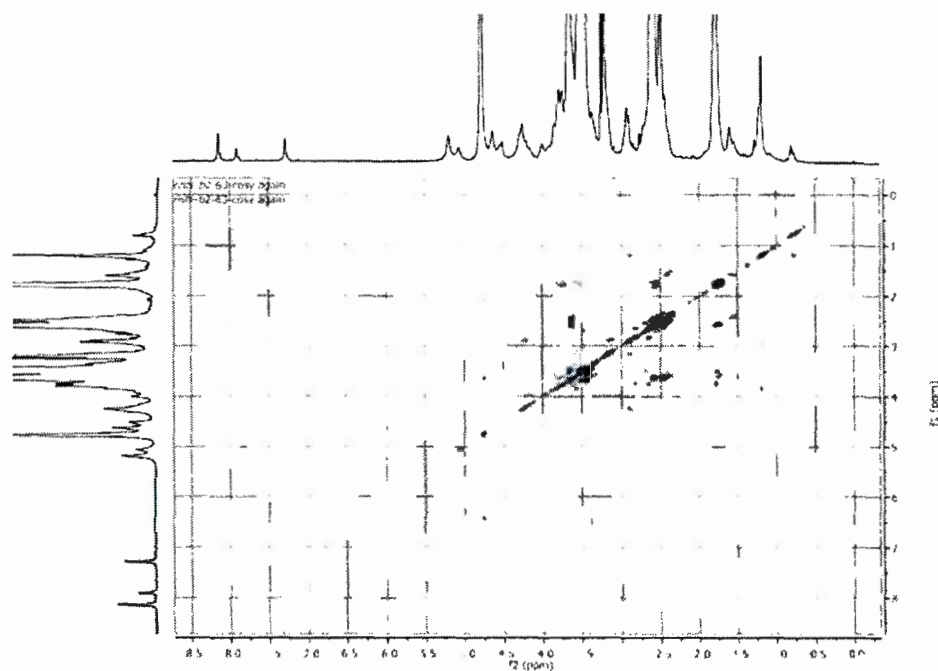


Figure S110. COSY spectrum of compound 9.

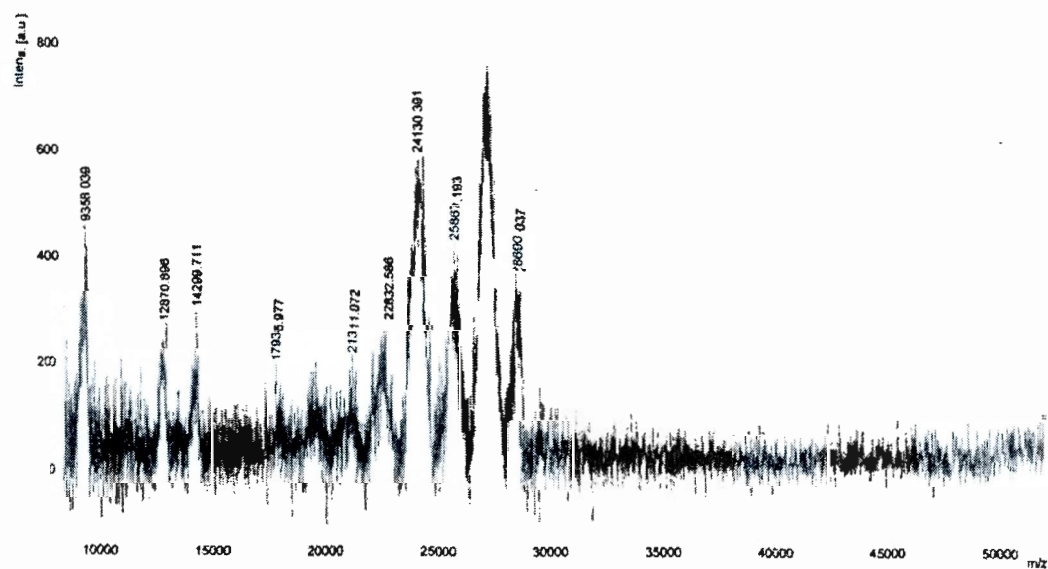


Figure S111. MALDI-TOF expanded spectrum of compound 9.

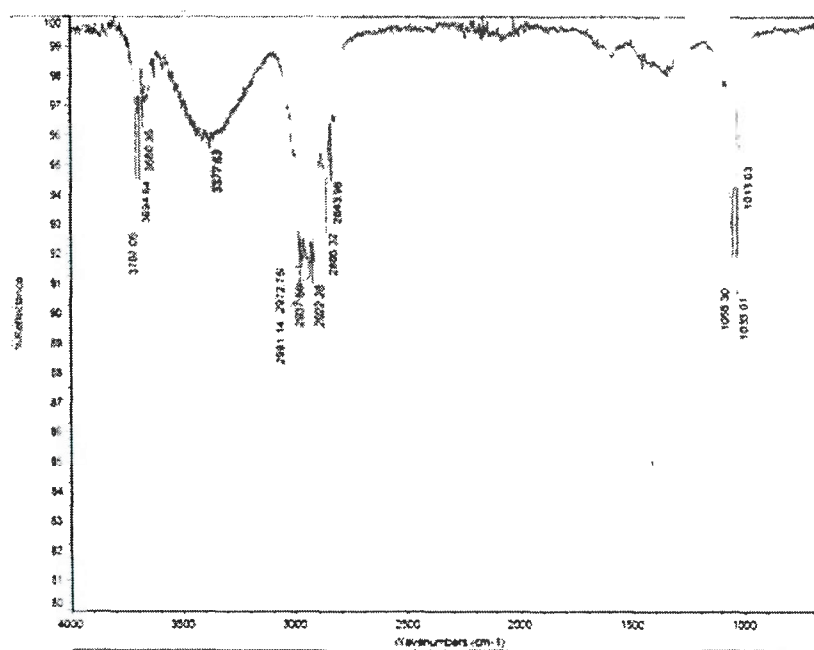


Figure S112. IR spectrum of compound 9.

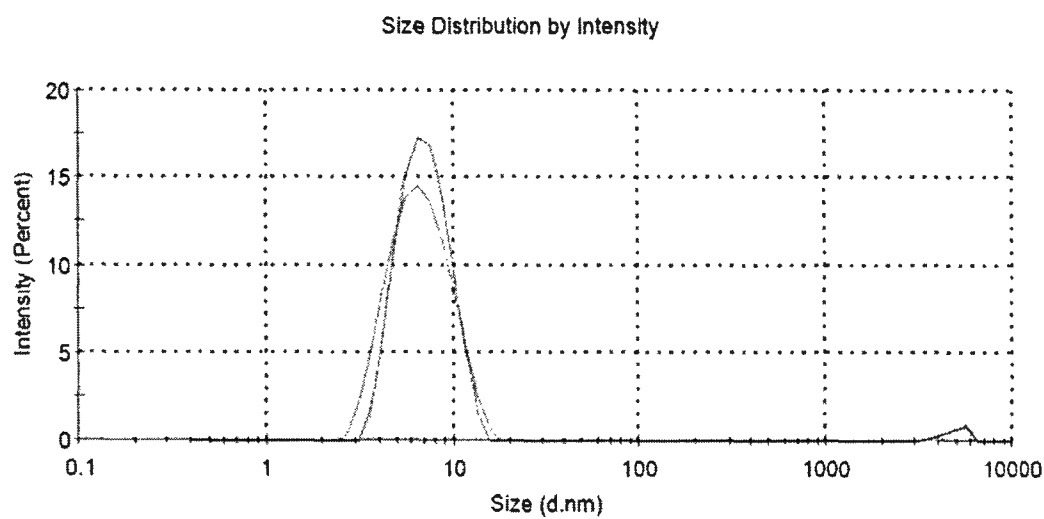


Figure S113. DLS size distribution of dendrimer 9 in methanol at 25°C.

Biological Experiments:

Cell culture and treatment. The HepG2, U251N and MCF-7 human cell lines were originally obtained from the American Type Culture Collection. HepG2 cells were cultured in Minimum Essential Medium (Invitrogen); U251N and MCF-7 cells were cultured in Dulbecco's Modified Eagle's Medium (Invitrogen). All media were supplemented with 10% (v/v) fetal bovine serum (Invitrogen), 2 mM L-glutamine, 100 IU/mL penicillin, 100 µg/mL streptomycin (Invitrogen), and 1% non-essential amino acids. Cells were maintained at 37°C with 5% CO₂.

Confluent HepG2, U251N and MCF-7 cells cultures were detached using 0.05% trypsin-EDTA (Invitrogen), seeded at 20,000 cells per well in 96-well plates (Sarstedt), and cultured for 24h before treatment. Cells were treated with dendrimers at increasing concentrations (1 nM, 10 nM, 50 nM, 100 nM, 500 nM, 1 µM, 5 µM, and 10 µM) for 24h. Dendrimers were dissolved in dimethyl sulfoxide (DMSO; Sigma-Aldrich), and in-well DMSO concentrations were kept below 0.3%. Vehicle controls were included in each experiment.

MTT assay. After treatment, media was refreshed with serum-deprived media, and thiazolyl blue tetrazolium (Sigma-Aldrich) was added for an in-well concentration of 0.5 mg/mL. Cells were incubated for 30 minutes at 37°C to allow for the formation of formazan crystals, following which the medium was removed and 100 µL/well of DMSO was added to dissolve the formazan. Absorbance was measured at 595 nm using an Asys UVM 340 microplate reader (Biochrom).

Cell viability assay. After treatment, media was removed and cells were washed twice with phosphate buffered saline (PBS). Cells were fixed using 4% paraformaldehyde for 15 minutes, labelled with 10 µM Hoechst 33342 (Sigma-Aldrich) for 10 minutes, then washed and stored in PBS. Imaging of cell nuclei fluorescently labelled with Hoechst was performed using an Operetta high-throughput imaging platform (Perkin Elmer). Image analysis and cell counting was done in the Columbus Analysis platform (Perkin Elmer).

Statistical analysis. Each experiment was performed three times and each treatment was included in sixplicate. The student's *t*-test with Bonferroni correction was used to find significant differences between treatments (*p* values < 0.01 were considered significant).

Reference:

1. Diaz, M. D.; Berger, S. *Carbohydr. Res.* **2000**, *329*, 1–5.